NASA/TP—2015-216046

Detailed Results From the Flame Extinguishment Experiment (FLEX) March 2009 to December 2011

Daniel L. Dietrich
Glenn Research Center, Cleveland, Ohio

Paul V. Ferkul, Victoria M. Bryg, and M. Vedha Nayagam
National Center for Space Exploration Research, Glenn Research Center, Cleveland, Ohio

Michael C. Hicks
Glenn Research Center, Cleveland, Ohio

Forman A. Williams
University of California, San Diego, La Jolla, California

Frederick L. Dryer
Princeton University, Princeton, New Jersey

Benjamin D. Shaw
University of California, Davis, Davis, California

Mun Y. Choi
University of Connecticut, Storrs, Connecticut

C. Thomas Avedisian
Cornell University, Ithaca, New York

November 2015

NASA STI Program . . . in Profile

Since its founding, NASA has been dedicated to the advancement of aeronautics and space science. The NASA Scientific and Technical Information (STI) Program plays a key part in helping NASA maintain this important role.

The NASA STI Program operates under the auspices of the Agency Chief Information Officer. It collects, organizes, provides for archiving, and disseminates NASA's STI. The NASA STI Program provides access to the NASA Technical Report Server—Registered (NTRS Reg) and NASA Technical Report Server—Public (NTRS) thus providing one of the largest collections of aeronautical and space science STI in the world. Results are published in both non-NASA channels and by NASA in the NASA STI Report Series, which includes the following report types:

- TECHNICAL PUBLICATION. Reports of completed research or a major significant phase of research that present the results of NASA programs and include extensive data or theoretical analysis. Includes compilations of significant scientific and technical data and information deemed to be of continuing reference value. NASA counter-part of peer-reviewed formal professional papers, but has less stringent limitations on manuscript length and extent of graphic presentations.

- TECHNICAL MEMORANDUM. Scientific and technical findings that are preliminary or of specialized interest, e.g., "quick-release" reports, working papers, and bibliographies that contain minimal annotation. Does not contain extensive analysis.

- CONTRACTOR REPORT. Scientific and technical findings by NASA-sponsored contractors and grantees.

- CONFERENCE PUBLICATION. Collected papers from scientific and technical conferences, symposia, seminars, or other meetings sponsored or co-sponsored by NASA.

- SPECIAL PUBLICATION. Scientific, technical, or historical information from NASA programs, projects, and missions, often concerned with subjects having substantial public interest.

- TECHNICAL TRANSLATION. English-language translations of foreign scientific and technical material pertinent to NASA's mission.

For more information about the NASA STI program, see the following:

- Access the NASA STI program home page at http://www.sti.nasa.gov

- E-mail your question to help@sti.nasa.gov

- Fax your question to the NASA STI Information Desk at 757-864-6500

- Telephone the NASA STI Information Desk at 757-864-9658

- Write to:
  NASA STI Program
  Mail Stop 148
  NASA Langley Research Center
  Hampton, VA 23681-2199

NASA/TP—2015-216046

Detailed Results From the Flame Extinguishment Experiment (FLEX) March 2009 to December 2011

Daniel L. Dietrich
Glenn Research Center, Cleveland, Ohio

Paul V. Ferkul, Victoria M. Bryg, and M. Vedha Nayagam
National Center for Space Exploration Research, Glenn Research Center, Cleveland, Ohio

Michael C. Hicks
Glenn Research Center, Cleveland, Ohio

Forman A. Williams
University of California, San Diego, La Jolla, California

Frederick L. Dryer
Princeton University, Princeton, New Jersey

Benjamin D. Shaw
University of California, Davis, Davis, California

Mun Y. Choi
University of Connecticut, Storrs, Connecticut

C. Thomas Avedisian
Cornell University, Ithaca, New York

National Aeronautics and
Space Administration

Glenn Research Center
Cleveland, Ohio 44135

November 2015

Level of Review: This material has been technically reviewed by expert reviewer(s).

Available from

NASA STI Program
Mail Stop 148
NASA Langley Research Center
Hampton, VA 23681-2199

National Technical Information Service
5285 Port Royal Road
Springfield, VA 22161
703-605-6000

This report is available in electronic form at http://www.sti.nasa.gov/ and http://ntrs.nasa.gov/

Contents

Detailed Results From the Flame Extinguishment Experiment (FLEX) March 2009 to December 2011

Daniel L. Dietrich
National Aeronautics and Space Administration
Glenn Research Center
Cleveland, Ohio 44135

Paul V. Ferkul, Victoria M. Bryg, and M. Vedha Nayagam
National Center for Space Exploration Research
Glenn Research Center
Cleveland, Ohio 44135

Michael C. Hicks
National Aeronautics and Space Administration
Glenn Research Center
Cleveland, Ohio 44135

Forman A. Williams
University of California, San Diego
La Jolla, California 92093

Frederick L. Dryer
Princeton University
Princeton, New Jersey 08544

Benjamin D. Shaw
University of California, Davis
Davis, California 95616

Mun Y. Choi
University of Connecticut
Storrs, Connecticut 06269

C. Thomas Avedisian
Cornell University
Ithaca, New York 14853

Executive Summary

The Flame Extinguishment Experiment (FLEX) program is a continuing set of experiments on droplet combustion, performed employing the Multi-User Droplet Combustion Apparatus (MDCA), inside the chamber of the Combustion Integrated Rack (CIR), which is located in the Destiny module of the International Space Station (ISS). This report describes the experimental hardware, the diagnostic equipment, the experimental procedures, and the methods of data analysis for FLEX. It also presents the results of the first 284 tests performed. The intent is not to interpret the experimental results but rather to make them available to the entire scientific community for possible future interpretations.

The apparatus for the FLEX experiments was transported to the ISS and installed late in 2009. It includes canisters for fuel storage, two opposed-needle syringes for injecting fuel to form a droplet, two opposed hot-wire igniters for initiating combustion, and a long, fine fiber that can be used to tether the droplet and move it at a programmable low velocity through the gas in the chamber. The combustion history is recorded photographically, with a visible-light color camera that views the entire field, a backlit camera that highlights the droplet to determine its diameter accurately as a function of time during burning, and a camera with a filter centered at 310 nm, intended to record emissions from excited hydroxyl radicals produced in the flame (Low Light Level Ultra-Violet, LLUV), thereby providing a measure of the flame diameter. Although the ISS crew must change the fuel canisters and the gas bottles needed to establish the atmosphere in the combustion chamber, each droplet-burning experiment is run remotely from the Telescience Support Center at the NASA Glenn Research Center in

Cleveland, Ohio. During periodically scheduled experiment intervals, about 4 to 10 droplets are burned in this remote operation, with use made mainly of the color camera to guide the procedure, which involves a number of manual steps.

In addressing the experimental procedures and data analysis, this report details the methods, data downlink, and format, and it provides error estimates. The results include histories of droplet diameters obtained from the backlit camera and histories of flame diameters obtained from both the hydroxyl-filter camera and the color camera. Both flame diameter measurements are of the outer edge of the flame, and the diameters in the color-camera images are the smaller of the two, approximately three-fourths of the LLUV results. Average burning-rate constants for each burn also are reported, as are extinction diameters, for the cases where the flame extinguished at a finite droplet size. Both radiative and diffusive extinctions occurred during the testing.

The fuels studied in these experiments were methanol and n-heptane. The droplets had initial diameters between 2 and 5 mm, and they were burned in oxidizing atmospheres at ambient temperature and various pressures between 0.70 and 3.05 atm, over ranges of dilution of oxygen with nitrogen, with carbon dioxide, and with mixtures thereof. Most of the tests were conducted at pressures between 0.7 and 1 atm, and many of the tests were in air. A principle objective was to determine the limiting oxygen index (LOI), the oxygen percentage below which combustion would not occur. This objective reflected the FLEX focus on investigating fire safety in spacecraft. Observed LOI values for these fuels appear to be slightly lower than initially expected. Besides documenting both radiative extinction at higher dilutions and diffusive extinctions at lower dilutions for both fuels, the results exhibited disruptive extinctions and provided information pertinent to soot production for heptane. The continuing experiments are providing additional data for these two fuels, as well as droplet-combustion data for other fuels, and NASA intends to catalog these data in similar reports.

1.0 Introduction

The spherically symmetrical combustion of a liquid fuel droplet in a quiescent ambient gaseous oxidizing atmosphere is a classical problem in combustion research, having been addressed first more than 50 years ago by Godsave (1952), Hall and Diederichsen (1953), and Spalding (1952, 1953). Numerous reviews of the subject are now available in the literature, among them those of Wise and Agoston (1958), Williams (1973), Faeth (1977), Law (1982), Sirignano (1983), and Choi and Dryer (2001). An advantage of spherical symmetry is that only one spatial dimension enters the description of the combustion process, so that one-dimensional (spherically symmetrical) time-dependent conservation equations apply. This greatly facilitates both computational and theoretical descriptions of the problem, thereby enhancing understanding of experimental results, which becomes much more difficult, uncertain, and inaccurate in multidimensional situations. Natural convection, however, destroys the spherical symmetry of combustion in normal gravity, as was quite evident in the earliest experiments of Hall and Diederichsen (1953) and Goldsmith (1956). Kumagai and Isoda (1956) were the first to realize that microgravity experiments afforded the opportunity to achieve spherical symmetry—a fact that NASA has taken advantage of in fundamental combustion investigations for a number of years (Williams, 1981; Dietrich et al., 1996; Nayagam et al., 1998).

The Flame Extinguishment Experiment (FLEX) is a droplet combustion experiment performed on the International Space Station (ISS). FLEX is the first experiment in the multipurpose facility developed at the NASA Glenn Research Center—the Combustion Integrated Rack (CIR). The CIR provides the combustion chamber, most of the diagnostics, the gas-mixing system, and the primary interface between the ISS and the ground controllers at Glenn. The Multi-User Droplet Combustion Apparatus (MDCA) is the hardware that deploys and ignites the liquid fuel droplets and provides some of the diagnostics. The MDCA is located in the CIR combustion chamber, but it communicates through the CIR to ground controllers at Glenn.

The purpose of this report is to detail and permanently archive the results of a subset of the FLEX experiments, namely those occurring between March 2009 and the end of December 2011. It is not intended to interpret the data from those experiments or to draw any scientific conclusions; that will occur through future NASA reports and peer-reviewed journal articles that reference this report. The next section provides a brief description of the experimental hardware and test procedures. This is followed by a section that provides details of the data analysis. The last two sections provide details of the experimental results.

2.0 Experiment Setup

The FLEX experiments are conducted on the ISS in the combustion chamber of the CIR facility—a multipurpose facility dedicated to combustion experiments. The CIR, a large rack-level experiment in the Destiny module, was developed at Glenn. The FLEX experiments were the first experiments to be conducted in the CIR.

2.1 Experimental Hardware

The CIR facility (Fig. 1), described in detail elsewhere (Banu, 2008), consists of a 90-liter combustion chamber that can operate at pressures of approximately 0 to 9 atm. Although the chamber can operate at a working pressure of 9 atm, the maximum pressure for a given experiment is frequently much

Figure 1.—Astronaut Mike Fincke to the left of the Combustion Integrated Rack (CIR) facility shortly after it was installed in the Destiny module of the International Space Station (ISS).

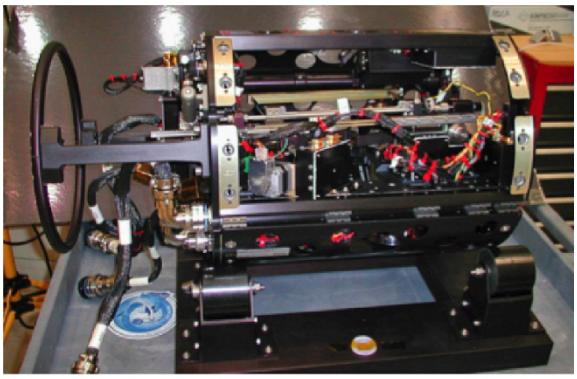

Figure 2.—Multi-User Droplet Combustion Apparatus (MDCA) with hardware installed in the Combustion Integrated Rack (CIR).

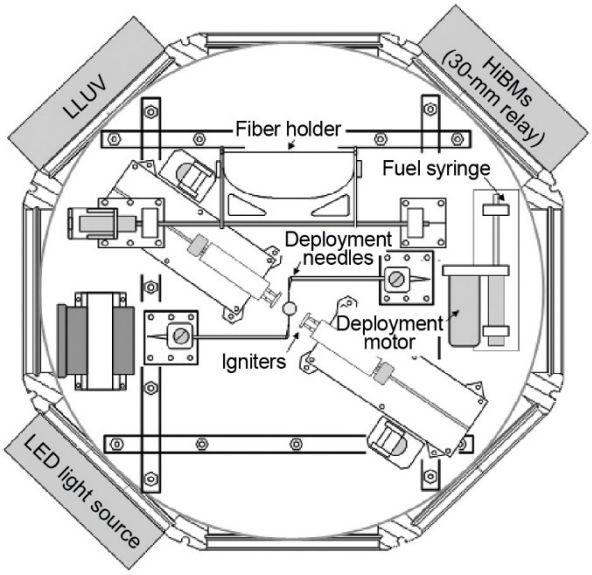

Figure 3.—Multi-User Droplet Combustion Apparatus (MDCA) looking down from the top, with hardware installed in the Combustion Integrated Rack (CIR).

less than that depending on a rigorous (and very conservative) safety analysis. For the FLEX experiments, this analysis reduced the maximum working pressures to approximately 3 atm. The interior of the CIR chamber contains the mechanical, fluid, and electrical interfaces necessary to mount experiment-specific hardware inside the chamber.

The CIR facility can accurately control the ambient environment inside the chamber. This capability is provided by the Fuel and Oxidizer Mixing Apparatus (FOMA). The FOMA consists of gas bottles, a connection for ISS nitrogen connected through a series of valves, pressure transducers, and mass flow controllers to the combustion chamber. The contents of the chamber can be evacuated via a vacuum pump connected to the ISS overboard vent.

The hardware for the FLEX experiments, the MDCA, is pictured in Figure 2 and shown schematically in Figure 3. The MDCA facility, which is described in detail elsewhere (Robbins and Shinn, 2010), is based on the design of the space shuttle Droplet Combustion Experiment (DCE, Nayagam et al., 1998). The MDCA can deploy both free and fiber-supported droplets in a quiescent microgravity environment.

Stainless-steel tubes with 250-µm outside diameters and specially treated ends are used for the deployment. Each needle is connected via flexible Teflon (DuPont) tubing to a fuel reservoir, or cartridge, which consists of a gas-tight syringe connected to a remotely actuated, gas-tight solenoid valve. The crew can easily replace the two reservoirs mounted in the MDCA during nominal operations. For the experiments reported herein, each reservoir contained one of the experiment fuels—heptane or methanol. The amount of fuel put in the syringe was a function of the detailed safety analysis, approximately 2.5 ml for methanol and 1.25 ml for heptane.

During each FLEX test, the syringe assembly dispensed the fluid between the horizontally opposed needles. The needles then slowly stretched to a distance slightly smaller than the distance where the fluid would pull off one of the needles. Just before ignition, the needles rapidly retracted, ideally leaving a motionless droplet floating in the middle of the CIR combustion chamber.

Once the needles retracted, the control computer energized two hot-wire igniters located 180° to each other and in the same plane as the deployment needles. After a preset time, the control computer deenergized the igniters and activated the linear motors to retract them away from the droplet.

The MDCA also performed tests with fiber-supported droplets, either for cases where the drift velocity of the droplets exceeded values acceptable to the science team or for tests where the science team wished to examine the effect of a subbuoyant convective flow on the combustion process. For fiber-supported tests, the procedure was exactly the same, except that the droplets were deployed on a small 80-μm support fiber. For tests with translation, after ignition, the control computer translated the fiber (in the direction parallel to the orientation of the fiber) at a prescribed speed and for a prescribed time duration.

2.2 Experiment Diagnostics

The primary diagnostics for the FLEX experiment were provided by the CIR facility and are described in detail elsewhere (Banu, 2008). They included a backlit view of the droplet and an orthogonal view of the flame. The illumination for the backlit view was a laser diode source and a collimating optical system. They provided monochromatic illumination with a center wavelength between 650 to 660 nm. The laser diode operated below the lasing threshold current and thus acted as a noncoherent illumination source. The image system for the backlit view was the High-Bit-Depth Multispectral (HiBMs) imaging package. The HiBMs package had a telemetric imaging optical system and a high-resolution 12-bit output digital camera.

Almost all of the tests reported herein[1] used the full 1024 by 1024 array with a fixed field of view (FOV) of approximately 30 mm on a side. The images used the full 12-bit output and a framing rate of approximately 30 frames per second (fps). The HiBMs package, when used in conjunction with the illumination package, can measure the droplet size as a function of time and the soot volume fraction for soot-producing flames (i.e., heptane for the tests described in this report).

The CIR also provided a LLUV package to image the chemiluminescence from hydroxyl ($OH^{\bullet}$) emissions from the burning droplet. The LLUV package was a 1024 by 1024 monochrome frame-transfer charged-coupled device (CCD) array with 12-bit digital imaging capability. The CCD array was directly coupled to an 18-mm Gen II–UV microchannel plate intensifier to provide maximum response at short wavelengths. The intensifier included intensifier and gating control that allowed varied exposure times depending on the expected brightness of the flames. The LLUV also had a spectral notch filter integrated to image the chemiluminescence at 310 nm (the filter had a 10-nm full width at half maximum (FWHM) bandwidth). Ground control of the LLUV enabled pretest setting of the gain, pixel binning, and gate to optimally image the flames surrounding the droplets. All of the tests reported herein used the 2 by 2 binned (512 by 512) array with a fixed FOV of approximately 50 mm on a side. The framing rate for the majority of the tests was 30 fps, with a smaller number at 15 fps as an attempt to improve flame contrast for very dim flames. The intensifier gain did vary somewhat over the tests in this report.

The MDCA provided two diagnostics: a color camera and radiometers. The color camera provided a visual overview of the FLEX experiments. This camera view was augmented with illumination from a white-light-emitting diode (LED) located on the MDCA inside the CIR chamber. This camera had a zoom lens that provided a closeup view of the needles and droplet during droplet formation. The white LED was turned on at this time to allow the operator to see the droplet formation process. Immediately prior to droplet deployment and ignition, the camera zoomed out and the white LED turned off to provide an overview of the combustion process. The FOV of this camera was approximately 110 by 90 mm. This view, which provided flame size, shape, and color information, was downlinked to the ground during nominal test point operations.

The MDCA provided two radiometers: a broadband radiometer to detect the total radiative output of the flame and a radiometer with a filter to examine the emission from the water vapor. For the tests reported herein, these radiometers were not sensitive enough to provide reliable quantitative information about flame radiometric output, so the data are not reported. A replacement radiometer package will be available for future FLEX tests.

2.3 Experimental Procedures

During nominal operations, there was very little crew involvement in the FLEX experiments. The FLEX experiments required crew time to replace gas bottles, fuel reservoirs, and fiber assemblies during nominal operations. Crew time also was required during malfunction operations to diagnose hardware and replace damaged components. Finally, immediately prior to

[1]The exception is the first few "engineering" test points that used ISS cabin air as the ambient. The primary purpose of these tests was an engineering evaluation of the integrated hardware. These tests used a camera configuration that was slightly different.

test-point operations, the crew removed the alignment guides to the Passive Rack Isolation System (PaRIS). PaRIS isolated the CIR from the lower level, higher frequency vibrations or g-jitter of the ISS to provide a cleaner gravitational environment for the FLEX experiments. The CIR rack had accelerometer heads to monitor the gravitational (g) and vibrational environment during testing. For all of the experiments in this report, the g-environment was low enough that buoyant flow could be considered to be negligible; however, g-jitter was evident when the droplet began to move in a particular direction and potentially out of the camera FOV (particularly with the HiBMs).

Once the fuel reservoirs and gas bottles were in place and the alignment guides removed, the test operations began. Personnel at the Telescience Support Center (TSC) at Glenn controlled all functions of the FLEX experiments. Test-point operations typically required three operators, two controlling the functions of the CIR, and one dedicated to the MDCA. In addition, for most tests a representative of the science team was present to help make any necessary real-time decisions regarding the testing. The sequence for test-point operations follows:

(1) **Activate the CIR.** The CIR operators activated the rack and performed all housekeeping necessary for test-point operations.

(2) **Operate the FOMA.** The CIR operators operated the FOMA to fill the CIR chamber to the appropriate ambient pressure **and** gas composition. During these operations, the CIR and ground computers recorded in detail the pressure history during the fill and evacuation procedures so that the actual chamber composition could be computed a posteriori.

(3) **Activate the MDCA.** Once the ambient environment was set, the MDCA was activated. The MDCA console operator at the TSC then performed all necessary housekeeping on the MDCA to prepare for test-point operations. All commands to and from the MDCA passed through the CIR computers.

(4) **Open the fuel valve and purge line.** Typically, all the fuel in the fuel lines **between** the reservoir and needle tip had evaporated. The MDCA operator then slowly dispensed fuel (advances the linear stepper motor attached to the fuel syringe containing the fuel) until fuel visually appeared from the fuel needle.

(5) **Perform the test-point operation.**

(a) **Dispense the fuel droplet.** The MDCA operator slowly dispensed fuel to form a droplet of the appropriate size. In theory, the operator could just advance the stepper motor the theoretical amount to dispense the fuel volume for a given droplet size. In practice, however, the MDCA operator used the stepper motor counts as a guide and estimated the appropriate droplet size (with consultation from the science team). The needles were together at this point, and the dispensed fuel bridged the small gap between the needles.

(b) **Stretch the fuel droplet.** The MDCA operator slowly moved the needles apart to a distance slightly smaller than that where the fuel would spontaneously pull off. This distance was a function of the fuel type and fuel volume and was performed manually according to the judgment of the MDCA operator.

(c) **Burn the droplet.** The MDCA computer could perform steps (1) to (5)(b) in a preprogrammed manner. Early testing, however, showed that manual operation was more efficient. Consequently, for these tests, once the droplet had the appropriate stretch, the MDCA operator zoomed out the color camera, turned off the illumination from the LED (the backlight for the HiBMs, however, remained on), and turned over control to the MDCA onboard computer. The MDCA computer then performed the following steps in a rapid progression:

(i) **Start data recording.** The CIR HiBMs and LLUV and the MDCA color camera began recording images.

(ii) **Deploy the droplet.** The needles were rapidly and simultaneously retracted.

(iii) **Ignite the droplet.** The small hot-wire igniters located nearly orthogonal to the deployment needles and close to the droplet (a ground-controllable distance) were turned on for a preset time and power level (a ground-controllable voltage).

(iv) **Retract the igniter.** The igniters were turned off and rapidly retracted a relatively large distance from the droplet.

(v) **Stop data recording.** The CIR and MDCA cameras stopped recording data after a preset time (typically on the order of 40 s).

(6) **Conduct posttest operations.** The CIR and MDCA operators then performed a number of housekeeping operations to prepare for the next test-point operations (if necessary). If another test was to be performed in the same ambient environment, the circulation fan located in the chamber was turned on for a brief period of time (approximately 1 min) to mix the gases uniformly inside the chamber.

Figure 4 shows sequence (1) to (6) as recorded by the HiBMs, LLUV, and MDCA color cameras. Figure 4(a) (HiBMs and MDCA color cameras only) shows the droplet stretched between the fuel needles just before the automated sequence was run. Figure 4(b) (HiBMs only) shows the droplet immediately after the deployment needles had retracted. The

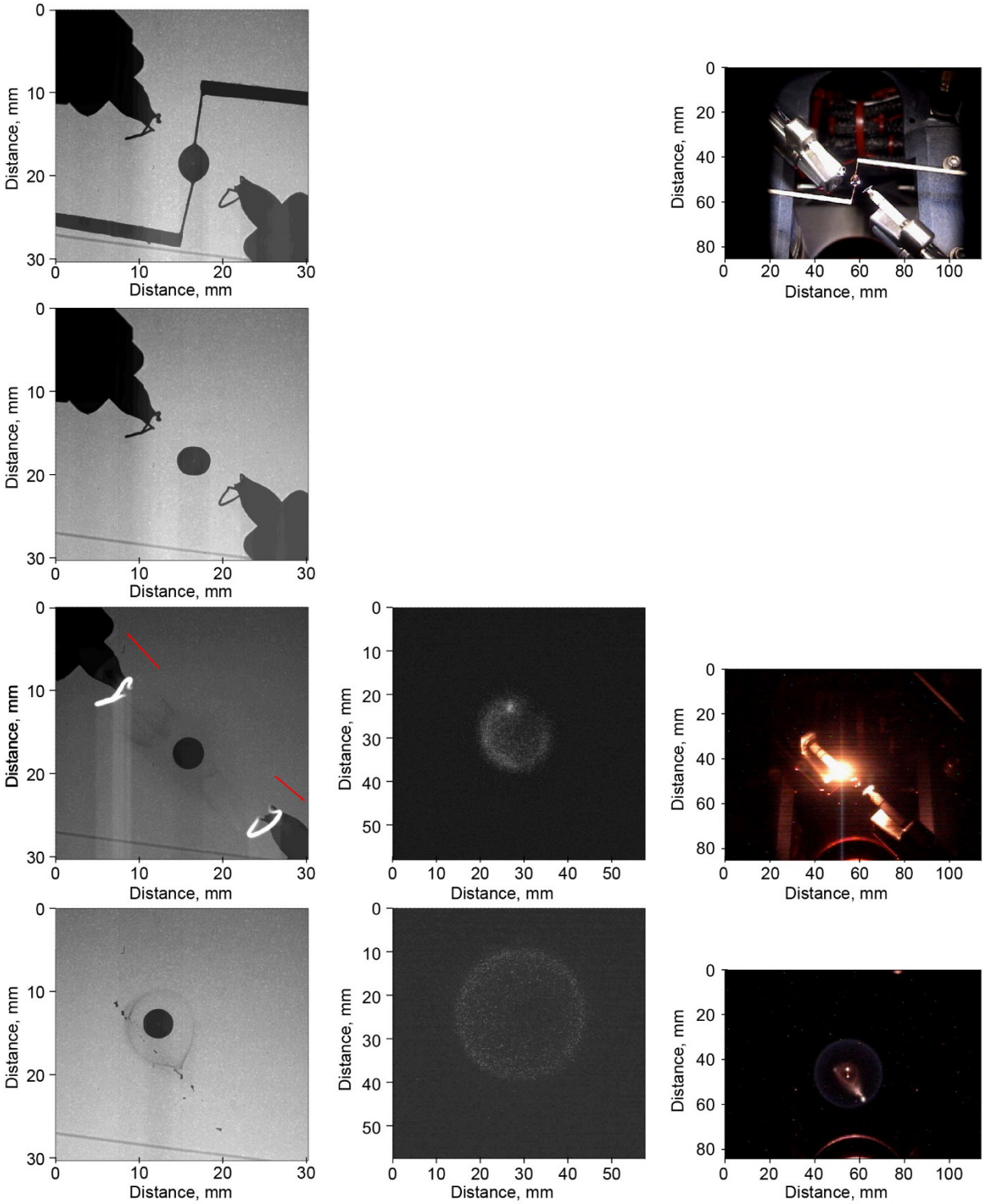

Figure 4.—Test sequence as recorded by the High-Bit-Depth Multispectral (HiBMs) (left), Low Light Level Ultra-Violet (LLUV) (center), and Multi-User Droplet Combustion Apparatus (MDCA) color (right) cameras. The chamber illumination for the MDCA color camera turns off when the needles retract. The sequence shows (from top to bottom) the droplet stretched between the needles, droplet deployment, ignition, and an image during the burn. This test is a heptane droplet burning in a cabin air (0.21/0.79 O_2/N_2 mole fraction), 1.0-atm ambient environment. Each row of images is from the same instant of time. Missing images for the LLUV and MDCA color cameras are dark-field images.

droplet in this image is misshaped by the needle retraction but assumes the expected spherical shape within approximately 1 s. Figure 4(c) shows the views from all three cameras during ignition.

Given the large size of the CIR chamber and the need to minimize resource utilization, the chamber atmosphere was frequently reused. The ambient atmosphere in this report was that computed from the downlink from the pressure and temperature data during the FOMA operations and corrected for the fuel vaporized, oxygen consumed, and carbon dioxide and water vapor produced during test-point operations.

2.4 Experiment Data Downlink and Format

The CIR diagnostics systems can store the camera data for several on-orbit tests. The exact number depends on the length of recording, the recording format (binned versus unbinned on the cameras), and other factors. Typically after one or two test-point days, there is a dedicated time to transfer the data between CIR computers and then downlink the image data from the ISS to ground computers at the NASA Johnson Space Center. From Johnson, the data are eventually transferred to the servers at the TSC at Glenn. This process typically takes approximately 24 hr for three to six test points. The data from the CIR cameras is compressed, and once at the TSC, the CIR staff decompresses and transfers the raw data to the science team.

The data transferred to the FLEX science team for analysis consist of a number of text files that contain the following information:

(1) HiBMs camera settings
(2) LLUV camera settings
(3) MDCA color camera settings (two files)
(4) CIR chamber and pressure data
(5) Radiometer data
(6) CIR facility settings
(7) MDCA settings
(8) Test comments for any anomalies encountered (e.g., missing data) during the acquisition, transfer, and downlink process

In addition, there are text files for each camera that include the image number, the image name, and the time of acquisition for each camera image. Each frame from the HiBMs and LLUV cameras is stored as a 12-bit tagged-image file format (TIFF) image, and each frame from the color camera is stored as a bitmap (BMP) image.

This represents a large amount of data, much of it unnecessary for scientific analysis of the FLEX data. For this report, the FLEX science team extracted a small subset of the total downlinked data—only that which was important for scientific analysis.

3.0 Data Analysis

The three camera views are the primary data for the FLEX experiments. The backlit HiBMs view of the droplet provides the droplet size and droplet dynamics as a function of time. This camera operated at full resolution (1024 by 1024 pixels) and 30 fps for all but the first few tests documented in this report. The images provided to the FLEX team are 12-bit grayscale images scaled to 16-bit images. The droplet appears as a dark object on a light background. The images from this view also allow the determination of the soot volume fraction surrounding the droplet for tests that produce soot. Those data are not detailed in this report, but will be available elsewhere (e.g., Suh et al., 2011).

The LLUV view provides the flame chemiluminescence from $OH^{\bullet}$ as a function of time. The viewing window for the LLUV camera became dirty or smudged early in the FLEX testing. For the majority of tests in this report, this contamination showed up as asymmetries in the LLUV view. This coupled with the very dim flames added to the uncertainty in the flame measurements. The flame sizes documented in this report are the dimensions of the flame directly from the TIFF images. No effort was made to perform the deconvolution to determine the peak radial location of $OH^{\bullet}$ chemiluminescence (e.g., Marchese et al., 1996) because of the asymmetrical noisy images that resulted from the smudged window.

The color camera provided a direct view of the combustion process. This view provided the size and dynamics of the visual flame as a function of time. The following subsections provide detailed descriptions of the analysis of each view.

3.1 HiBMS Image Analysis

3.1.1 Procedure

The images were analyzed in a semiautomatic manner by using the commercially available image-processing packages, Image J (National Institutes of Health, 2011) or Igor Pro (http://www.wavemetrics.com). Analysis of the HiBMs images proceeded as follows:

(1) **Determine which frames to analyze.** The droplets were typically deployed with some residual velocity. In addition, g-jitter caused the droplet to drift. In a significant number of tests, the droplet drifted out of the HiBMs FOV (and sometimes back into the FOV) before recording stops. This stage involved identifying the frames where the droplet was within the FOV.

(2) **Crop the image to limit the region to analyze.**

(3) **Despeckle the image to reduce noise.**

(4) **Adjust the contrast and set the segmentation value.** This is the value that set the threshold between the background and the object (droplet). It varied from test to test because the

background intensity varied between tests. The value was set manually to optimally distinguish between the droplet and background for the entire test. Detailed analysis of a single test showed that within reasonable limits the threshold value had little impact on the droplet size and, thus, was not a major source of error.

(5) **Fill holes and manually remove stray objects.** If there was a bright spot in the middle of the droplet, this step made that region the same average intensity as the surrounding droplet. This step also involved manually removing stray objects that might interfere with the droplet size measurement.

(6) **Measure the area, center of mass, and perimeter of the flame in the image.** The measurement was converted to a flame size using the appropriate scale factor (32.5 pixels/mm) for most of the tests herein.

(7) **Perform steps 2 through 6 for each image identified in step 1.**

3.1.2 Error Analysis

The error or uncertainty in the measurement of droplet diameter comes from a few sources. The first is the spatial resolution of the camera. The FOV for the HiBMs is 30.25 mm^2. For all but the first few tests, the HiBMs operated at full frame (not binned), or 1024 by 1024 pixels. Therefore, the minimum spatial resolution was ±29.5 μm.

There was additional uncertainty in estimating the appropriate segmentation value, especially since the background gray level in the HiBMs view was not spatially uniform. The FLEX science team performed extensive ground testing in the functionally identical (to the CIR HiBMs on the ISS) Ground Interface Unit (GIU) HiBMs system with precision spheres of known size. This testing provided the guidelines for setting the appropriate threshold (segmentation) value to determine the edge of the droplet.

Also, it was obvious that there was noise in the image that could contribute to the uncertainty in droplet size. The uncertainty as a result of these last two sources was greatly reduced by measuring the projected area (as opposed to a single spatial dimension) of the droplet. As a result, we estimated the uncertainty in the droplet size to be ±50 μm.

3.2 LLUV Image Analysis

3.2.1 Procedure

The flame size is much more difficult to measure than the droplet size. The flames are quite dim, and as a result, there is a significant amount of noise in the LLUV images. The damage to the window in the CIR chamber for the LLUV camera made the noise worse for the tests in this report. There was also ambiguity in the flame definition, the peak in flame temperature, the peak in $OH^•$ emission, or the outer edge of $OH^•$ emission. The damage to the CIR window, coupled with the very dim images, precluded the deconvolution of the LLUV images (e.g., Marchese et al., 1996) to get the radial distribution of the $OH^•$ chemiluminescence. The flame dimension detailed in this report represents the outer edge of the $OH^•$ chemiluminescence.

The image sequences were analyzed in a semiautomatic manner using the commercially available image-processing packages, Image J (National Institutes of Health, 2011) or Igor Pro (http://www.wavemetrics.com). Analysis of the LLUV images proceeded as follows.

(1) **Determine which frames to analyze.**

(2) **Perform a gaussian blur to reduce the noise in the image.**

(3) **Remove outliers.** This process removed any pixel values that were near saturation. These values were not from the flame but were a result of the intensifier on the LLUV camera.

(4) **Adjust the contrast, and set the threshold value.** This was the value that set the threshold between the background and the object (flame). The value was manually set to optimally distinguish between the flame and the background for an individual image. For some tests a constant threshold value could be used for the entire test. For others the threshold value was a function of the flame luminosity with brighter flames using a higher threshold value. The segmentation (threshold) value was typically relatively low (compared with the maximum in an image) and, therefore, represented a very dim part of the flame or the very outer edge of the flame. The value is likely somewhat larger than a flame diameter based on the dimension of maximum temperature or $OH^•$ chemiluminescence.

(5) **Fill holes, and manually remove stray objects.** There was a darker region inside the flame, and this "hole" was included in the area measurement of the flame.

(6) **Measure the area, center of mass, and perimeter of the droplet in the image.** The measurement was converted to a droplet size using the appropriate scale factor (8.86 pixels/mm for most of the tests herein).

(7) **Perform steps 2 through 6 for each image identified in step 1.**

3.2.2 Error Analysis

The error or uncertainty in the measurement of flame diameter is more difficult to determine than the droplet size measurement. The FOV for the LLUV is 57.8 mm^2. For all of the tests in this report, the LLUV operated with 2 by 2 binning or a resolution of 512 by 512 pixels. Therefore, the minimum spatial resolution was ±113 μm.

There is additional uncertainty in estimating the appropriate segmentation value. The value represents the outer edge of the

flame and likely overestimates a measure based on the maximum radial intensity. Also, it is obvious that there is noise in the image that can contribute to the uncertainty in flame size. The uncertainty as a result of these last two sources was greatly reduced by measuring the projected area (as opposed to a single spatial dimension) of the flame. As a result, we estimated the uncertainty in the flame size to be ±200 μm.

3.3 Multi-User Droplet Combustion Apparatus Color Camera Analysis

3.3.1 Procedure

The procedure to measure the flame size from the MDCA color camera was almost identical to that used on the LLUV images. The flames were also quite dim, and as a result, there is a significant amount of noise in the color camera images. There also is ambiguity as to the definition of the flame. The flame dimension detailed in this report represents the outer edge of the visible flame.

The image sequences were analyzed in a semiautomatic manner using the commercially available image-processing packages, Image J (National Institutes of Health, 2011) or Igor Pro (http://www.wavemetrics.com). The analysis used on the MDCA color camera images follows.

(1) **Determine which frames to analyze.**

(2) **Crop the image so that it contains only the flame.**

(3) **Remove outliers.** This process removed any pixel values that were near saturation. These values were not from the flame but were a result of the intensifier on the LLUV camera.

(4) **Adjust the contrast and set the segmentation value.** This is the value that sets the threshold between the background and the object (flame). It was constant throughout the test but varied from test to test. The value was set manually to optimally distinguish between the flame and background for the entire test. The segmentation (threshold) value was typically relatively low and therefore represented a very dim part of the flame or the very outer edge of the flame. The value was likely somewhat larger than a flame diameter based on the dimension of the maximum temperature or $OH^{\bullet}$ chemiluminescence.

(5) **Fill holes and manually remove stray objects.** There was a darker region inside the flame, and this "hole" was included in the area measurement of the flame.

(6) **Measure the area, center of mass, and perimeter of the droplet in the image.** The measurement was converted to a droplet size using the appropriate scale factor (6.87 pixels/mm for most of the tests herein).

(7) **Perform steps 2 through 6 for each image identified in step 1.**

3.3.2 Error Analysis

The error or uncertainty in the measurement of the flame diameter is more difficult to determine than the droplet size measurement. The FOV for the LLUV is 93.2 mm wide, and the video camera has standard National Television System Committee (NTSC) resolution, or 640 by 480 pixels. Therefore, the minimum spatial resolution is ±146 μm.

There is additional uncertainty in estimating the appropriate segmentation value. The value represents the outer edge of the flame and likely overestimates a measure based on maximum radial intensity. Also, it is obvious that there is noise in the image that can contribute to the uncertainty in flame size. The uncertainty as a result of these last two sources was greatly reduced by measuring the projected area (as opposed to a single spatial dimension) of the flame. As a result, we estimated the uncertainty in the flame size to be ±250 μm.

4.0 Experimental Results

4.1 Test Matrix—March 2009 through December 2011

This report documents the results of the FLEX experiments from March 2009 through December 2011. The tests were conducted in numerical order, so there was a small amount of accumulated carbon dioxide, water vapor, and fuel vapor. Table I outlines the first tests, which were performed in cabin air on the ISS. The ambient gas composition on the ISS is nominally that of air (0.21 oxygen mole fraction, 0.005 carbon dioxide mole fraction, balance nitrogen) at 1.0-atm pressure. Once filled, the atmosphere was not changed for any of these tests. These tests were not part of the nominal FLEX test matrix, but were performed to determine the proper operation of the CIR and MDCA integrated systems. The tests do, however, provide scientifically relevant data, so the results are reported in this document.

Table II provides details for the next series of tests, which were in high-pressure, carbon-dioxide-enriched ambient environments. These tests were next in sequence in order to optimize the use of limited on-orbit gas resources. During these tests, however, the engineering and science teams noticed that the fuel system did not respond well to cycling from high to low pressures. As a result, after only a few tests were conducted in these ambient environments, the teams decided to change the order of the tests in the test matrix.

After the test matrix was reordered, the FLEX experiments focused on low-pressure (≤1-atm), nitrogen-diluted, ambient environments. Table III provides details for the initial tests, which focused on ambient conditions with higher oxygen mole

TABLE I.—FLEX TEST MATRIX FOR TESTS CONDUCTED IN CABIN AIR
[Droplet not supported by a fiber; tests conducted in ambient air—0.21 oxygen mole fraction, 0.005 carbon dioxide mole fraction, 0.79 nitrogen mole fraction (balance) at 1.0-atm pressure.]

Test	Date	Fuel	Initial droplet diameter, D_0, mm	Pressure, P, atm
001	Mar. 5, 2009	Methanol	1.80	1.00
002	Mar. 5, 2009	Methanol	2.00	1.00
003	Mar. 5, 2009	Methanol	1.71	1.01
004	Mar. 31, 2009	Methanol	2.19	1.00
005	Mar. 31, 2009	Methanol	1.95	1.00
006	Mar. 31, 2009	Methanol	2.90	1.00
007	Apr. 10, 2009	Heptane	1.91	1.00
008	Apr. 10, 2009	Heptane	2.89	1.00
009	Apr. 10, 2009	Heptane	3.00	1.00

TABLE II.—FLEX TEST MATRIX FOR TESTS CONDUCTED IN HIGH-PRESSURE, CARBON-DIOXIDE-ENRICHED AMBIENT ENVIRONMENTS
[Droplet not supported by a fiber; 0.21 oxygen mole fraction, 0.700 carbon dioxide mole fraction, 0.090 nitrogen mole fraction.]

Test	Date	Fuel	Initial droplet diameter, D_0, mm	Pressure, P, atm
010	May 22, 2009	Methanol	3.88	3.05
011	May 22, 2009	Methanol	3.02	3.05
012	May 22, 2009	Heptane	3.09	3.05
013	June 25, 2009	Methanol	2.72	2.73
014	June 29, 2009	Methanol	3.71	2.70
015	June 29, 2009	Methanol	4.43	2.72
016	June 29, 2009	Methanol	1.80	2.73
017	July 1, 2009	Methanol	2.81	2.03
018	July 1, 2009	Heptane	2.92	2.04

TABLE III.—FLEX TEST MATRIX FOR THE TESTS CONDUCTED IN NITROGEN-DILUTED AMBIENT ENVIRONMENTS, INCLUDING TESTS IN ENVIRONMENTS WITH HIGHER OXYGEN MOLE FRACTIONS

Test	Date	Fuel	Initial droplet diameter, D_0, mm	Fiber	Pressure, P, atm	Mole fraction of oxygen	Mole fraction of nitrogen
019	Aug. 26, 2009	Heptane	3.43	No	0.71	0.400	0.600
020	Oct. 24, 2009	Methanol	3.46	No	.71	.400	.600
021	Oct. 24, 2009	Methanol	3.49	No	.71	.400	.600
022	Oct. 24, 2009	Methanol	3.55	No	.71	.400	.600
023	Oct. 24, 2009	Heptane	3.18	No	.71	.400	.600
024	Oct. 24, 2009	Heptane	4.0	No	.71	.400	.600
025	Nov. 9, 2009	Methanol	2.65	No	.71	.300	.700
026	Nov. 9, 2009	Methanol	3.70	No	.71	.300	.700
027	Nov. 9, 2009	Heptane	4.00	No	.71	.300	.700
028	Nov. 9, 2009	Heptane	3.46	No	.71	.300	.700
029	Nov. 13, 2009	Methanol	2.65	No	1.01	.300	.700
030	Nov. 13, 2009	Methanol	3.32	No	1.01	.300	.700
031	Nov. 13, 2009	Heptane	3.51	No	1.01	.300	.700
032	Nov. 13, 2009	Heptane	3.08	No	1.01	.300	.700
037	Jan. 7, 2010	Methanol	3.41	Yes	.70	.337	.662
038	Jan. 7, 2010	Methanol	3.51	Yes	.70	.337	.661
039	Jan. 7, 2010	Heptane	2.91	Yes	.70	.336	.661
040	Jan. 8, 2010	Methanol	3.77	Yes	.70	.297	.699
041	Jan. 8, 2010	Methanol	3.33	Yes	.70	.297	.699
042	Jan. 8, 2010	Heptane	3.02	Yes	.70	.298	.700
043	Jan. 8, 2010	Heptane	3.02	Yes	.70	.298	.700
044	Jan. 11, 2010	Methanol	3.52	Yes	1.01	.298	.697
045	Jan. 11, 2010	Methanol	2.46	Yes	1.01	.298	.697
052	Jan. 11, 2010	Heptane	3.64	Yes	1.01	.297	.697

fractions. As testing progressed, however, the science team noticed a propensity for the droplets to burn disruptively and not exhibit flame extinction (at a finite-sized droplet diameter). The latter half of the test matrix focused on lower oxygen mole fraction ambient environments where both diffusive and radiative extinction occurred; these results are detailed in Table IV for methanol and in Table V for heptane. The tests in the lower oxygen mole fraction ambient environments started at the maximum ambient oxygen mole fraction, 0.21 (at 1-atm pressure). Testing proceeded as the ambient gas in the chamber was gradually diluted with increasing amounts of nitrogen until the limit where quasi-steady burning was not observed. This limit represented the limiting oxygen index (LOI), identification of which was one of the primary objectives of the FLEX experiments. Typically in a given ambient environment, tests were conducted with both fuels (on different test days) over a small range of droplet sizes (typically 3 to 4 mm). In many cases, tests with fiber-supported droplets and a brief translation of the fiber were conducted in addition to the quiescent, free-floating droplet tests.

TABLE IV.—FLEX TEST MATRIX FOR METHANOL TESTS CONDUCTED IN NITROGEN-DILUTED AMBIENT ENVIRONMENTS, INCLUDING TESTS IN ENVIRONMENTS WITH LOWER OXYGEN MOLE FRACTIONS (BELOW 0.21)

Test	Date	Initial droplet diameter, D_0, mm	Fiber	Pressure, P, atm	Mole fraction of oxygen	Mole fraction of nitrogen
033	Nov. 27, 2009	2.72	No	1.01	0.210	0.790
034	Nov. 27, 2009	3.95	No	1.01	.210	.790
036	Dec. 15, 2009	2.45	No	0.71	.210	.790
046	Jan. 12, 2010	2.88	Yes	1.01	.209	.786
048	Jan. 12, 2010	3.68	Yes	1.01	.209	.786
054	Jan. 12, 2010	3.61	No	0.71	.197	.796
055	Jan. 29, 2010	3.52	Yes	0.71	.197	.795
058	Feb. 4, 2010	3.73	No	1.02	.176	.816
059	Feb. 4, 2010	3.08	No	1.01	.176	.816
060	Feb. 4, 2010	3.57	Yes	1.02	.176	.816
061	Feb. 4, 2010	3.77	Yes	1.02	.176	.815
065	Mar. 19, 2010	3.44	No	1.01	.146	.846
066	Mar. 19, 2010	2.63	No	1.01	.146	.845
067	Mar. 19, 2010	4.01	No	1.01	.146	.845
068	Mar. 19, 2010	2.45	No	1.01	.146	.845
071	Mar. 19, 2010	2.26	No	1.01	.146	.845
075	Mar. 29, 2010	2.56	Yes	1.01	.135	.854
076	Mar. 29, 2010	3.29	Yes	1.01	.135	.854
077	Mar. 29, 2010	3.41	No	1.01	.135	.854
078	Mar. 29, 2010	2.69	No	1.01	.135	.854
082	Apr. 19, 2010	2.93	No	1.01	.126	.870
083	Apr. 19, 2010	3.60	No	1.02	.125	.869
084	Apr. 19, 2010	2.43	No	1.01	.126	.869
085	Apr. 19, 2010	2.49	No	1.01	.126	.869
086	Apr. 19, 2010	3.10	Yes	1.01	.126	.869
087	Apr. 19, 2010	2.66	Yes	1.01	.126	.869

TABLE V.—FLEX TEST MATRIX FOR HEPTANE TESTS CONDUCTED IN NITROGEN-DILUTED AMBIENT ENVIRONMENTS, INCLUDING TESTS IN ENVIRONMENTS WITH LOWER OXYGEN MOLE FRACTIONS (BELOW 0.21)

Test	Date	Initial droplet diameter, D_0, mm	Fiber	Pressure, P, atm	Mole fraction of oxygen	Mole fraction of nitrogen
035	Nov. 27, 2009	3.91	No	1.01	0.210	0.790
047	Jan. 12, 2010	3.42	No	1.01	.209	.786
049	Jan. 19, 2010	3.58	Yes	1.01	.208	.786
050	Jan. 19, 2010	3.69	Yes	1.01	.208	.786
051	Jan. 19, 2010	2.45	Yes	1.01	.208	.786
053	Jan. 12, 2010	3.4	No	1.01	.209	.786
056	Jan. 29, 2010	3.64	No	.72	.196	.795
057	Jan. 29, 2010	3.17	Yes	.72	.196	.794
062	Mar. 11, 2010	3.48	No	1.00	.175	.815
063	Mar. 11, 2010	2.28	No	1.01	.175	.815
064	Mar. 11, 2010	2.74	Yes	1.01	.175	.815
069	Mar. 19, 2010	1.29	Yes	1.01	.145	.845
070	Mar. 23, 2010	1.30	No	1.01	.145	.845
073	Mar. 23, 2010	4.72	No	1.00	.145	.845
074	Mar. 23, 2010	1.53	Yes	1.01	.145	.845
079	Mar. 30, 2010	3.06	No	1.01	.134	.853
080	Mar. 30, 2010	4.00	Yes	1.01	.134	.853
081	Mar. 30, 2010	2.40	Yes	1.01	.134	.853

Following the completion of the nitrogen-diluted ambient test matrix, testing proceeded with carbon-dioxide-diluted ambient environments. These tests also began at the highest oxygen mole fraction ambient environment; then increasing amounts of CO_2 were added while the ambient pressure was maintained constant. Testing concluded when quasi-steady burning was not observed, again the determination of the LOI. This also represented the minimum carbon dioxide mole fraction required to extinguish or prevent the spread of a flame. The tests were conducted in a 1.0-atm, 0.21 oxygen mole fraction (initially) ambient environment and a 0.70-atm, 0.30 oxygen mole fraction (initially) ambient environment. These two ambient environments represent the nominal environment on the ISS and the extravehicular activity (EVA) pre-breathe environment on the ISS and the maximum proposed oxygen mole fraction on future exploration vehicles. Table VI (for methanol) and Table VII (for heptane) detail the test matrices in the nominally 0.7-atm ambient environment. These tests start at a relatively high carbon dioxide mole fraction (0.15) to minimize the testing in higher oxygen mole fraction ambient environments. Table VIII details the test matrix in the 1.0-atm ambient environment.

TABLE VI.—FLEX TEST MATRIX FOR METHANOL TESTS CONDUCTED IN 0.70-atm CARBON-DIOXIDE-DILUTED AMBIENT ENVIRONMENTS

Test	Date	Initial droplet diameter, D_0, mm	Fiber	Pressure, P, atm	Mole fraction of oxygen	Mole fraction of carbon dioxide	Mole fraction of nitrogen
088	May 5, 2010	3.08	No	0.71	0.250	0.150	0.600
089	May 5, 2010	3.79	No	.71	.250	.150	.600
090	May 6, 2010	3.65	Yes	.71	.250	.150	.600
091	May 5, 2010	3.59	Yes	.71	.250	.150	.600
097	June 16, 2010	4.29	No	.70	.240	.200	.560
098	June 21, 2010	3.67	No	.71	.230	.250	.520
099	June 21, 2010	4.34	No	.70	.230	.250	.520
104	June 16, 2010	3.66	No	.70	.240	.200	.560
105	June 16, 2010	4.35	Yes	.70	.240	.200	.560
106	June 21, 2010	3.16	Yes	.71	.230	.250	.520
107	June 16, 2010	3.25	Yes	.70	.240	.200	.560
108	June 21, 2010	3.82	Yes	.71	.230	.250	.520
109	Aug. 31, 2010	3.62	No	.71	.211	.299	.490
110	Aug. 31, 2010	2.88	No	.71	.211	.299	.490
111	Aug. 31, 2010	3.38	Yes	.71	.211	.299	.490
112	Sept. 1, 2010	4.02	Yes	.70	.211	.299	.490
113	Sept. 1, 2010	4.26	No	.70	.200	.350	.450
114	Sept. 1, 2010	3.28	No	.70	.200	.350	.450
115	Sept. 1, 2010	4.03	Yes	.71	.200	.350	.450
116	Sept. 1, 2010	3.15	Yes	.71	.200	.350	.450
121	Sept. 8, 2010	4.33	No	.69	.180	.400	.420
122	Sept. 8, 2010	3.57	No	.70	.180	.400	.420
123	Sept. 8, 2010	4.13	Yes	.70	.180	.400	.420
124	Sept. 8, 2010	3.57	Yes	.70	.180	.400	.420
125	Sept. 13, 2010	3.70	No	.71	.170	.450	.380
126	Sept. 13, 2010	2.89	No	.71	.170	.450	.380
127	Sept. 13, 2010	3.20	Yes	.71	.170	.450	.380
128	Sept. 13, 2010	2.93	Yes	.71	.170	.450	.380
140	Nov. 4, 2010	4.05	No	.70	.146	.500	.354
141	Nov. 4, 2010	2.94	No	.70	.146	.500	.354
142	Nov. 4, 2010	1.88	No	.70	.146	.500	.354
143	Nov. 4, 2010	2.33	No	.70	.146	.500	.354
147	Sept. 13, 2010	3.13	No	.71	.170	.450	.380

TABLE VII.—FLEX TEST MATRIX FOR HEPTANE TESTS CONDUCTED IN 0.70-atm CARBON-DIOXIDE-DILUTED AMBIENT ENVIRONMENTS

Test	Date	Initial droplet diameter, D_0, mm	Fiber	Pressure, P, atm	Mole fraction of oxygen	Mole fraction of carbon dioxide	Mole fraction of nitrogen
092	June 14, 2010	3.46	No	0.71	0.250	0.150	0.600
093	June 15, 2010	2.61	Yes	.71	.250	.150	.600
094	June 15, 2010	3.59	No	.70	.240	.200	.560
095	June 15, 2010	3.77	Yes	.70	.240	.200	.560
096	June 15, 2010	2.30	Yes	.70	.240	.200	.560
100	June 29, 2010	4.27	No	.71	.230	.250	.520
101	June 29, 2010	3.87	Yes	.71	.230	.250	.520
102	June 29, 2010	3.69	No	.70	.210	.300	.490
103	June 29, 2010	4.05	Yes	.70	.210	.300	.490
117	Sept. 6, 2010	3.89	No	.70	.200	.350	.450
118	Sept. 6, 2010	3.11	Yes	.70	.200	.350	.450
119	Sept. 7, 2010	2.68	Yes	.70	.180	.400	.420
120	Sept. 7, 2010	2.53	Yes	.70	.180	.400	.420
129	Sept. 17, 2010	3.43	No	.71	.170	.450	.380
130	Sept. 17, 2010	3.02	Yes	.71	.170	.450	.380

TABLE VIII.—FLEX TEST MATRIX FOR TESTS CONDUCTED IN 1.0-atm CARBON-DIOXIDE-DILUTED AMBIENT ENVIRONMENTS

[Droplets not supported by a fiber.]

Test	Date	Fuel	Initial droplet diameter, D_0, mm	Pressure, P, atm	Mole fraction of oxygen	Mole fraction of carbon dioxide	Mole fraction of nitrogen
148	Nov. 18, 2010	Heptane	2.66	1.01	0.200	0.050	0.750
149	Nov. 18, 2010	Heptane	2.37	1.01	.200	.050	.750
150	Nov. 18, 2010	Heptane	3.26	1.01	.200	.050	.750
151	Dec. 8, 2010	Methanol	3.90	1.00	.180	.150	.670
152	Dec. 8, 2010	Methanol	3.41	1.01	.180	.150	.670
153	Dec. 8, 2010	Methanol	2.80	1.01	.180	.150	.670
154	Dec. 9, 2010	Heptane	3.76	1.00	.180	.150	.670
155	Dec. 9, 2010	Heptane	2.84	1.01	.180	.150	.670
156	Dec. 9, 2010	Heptane	2.30	1.01	.180	.150	.670
157	Dec. 9, 2010	Heptane	2.02	1.01	.180	.150	.670
158	Dec. 14, 2010	Methanol	4.31	1.00	.160	.250	.590
159	Dec. 14, 2010	Methanol	3.78	1.01	.160	.250	.590
160	Dec. 14, 2010	Methanol	2.71	1.01	.160	.250	.590
161	Dec. 14, 2010	Methanol	2.81	1.01	.160	.250	.590
162	Dec. 28, 2010	Methanol	3.79	1.00	.153	.298	.549
163	Dec. 28, 2010	Methanol	3.07	1.01	.153	.298	.549
164	Dec. 28, 2010	Methanol	2.59	1.01	.153	.298	.549
165	Dec. 28, 2010	Methanol	2.69	1.01	.153	.298	.549
166	Dec. 9, 2010	Heptane	2.19	1.01	.180	.150	.670

4.2 Analyzed Data

The digital image data from the FLEX experiments yielded a wealth of information regarding the combustion of liquid fuel droplets in quiescent and subbuoyant flow (achieved by translating the fiber) microgravity environments. The data archived in this report include the following:

(1) Droplet size as a function of time
(2) LLUV flame size as a function of time
(3) Color camera flame size as a function of time

The video records also provide qualitative information of the combustion process including, but not limited to,

(1) Droplet shape as a function of time
(2) Qualitative sooting propensity as a function of time
(3) Flame shape and flame dynamics as a function of time
(4) Disruptive burning
(5) Droplet/fiber interactions
(6) Postcombustion vaporization and vapor cloud formation

In an effort to document and archive the results from the FLEX experiments, all data for (1) to (6) are archived in this report. Appendix A gives the detailed results of the experiments. The data are also available electronically as text files and compressed video recordings of the HiBMs and color camera views.

5.0 Observations and Discussion

5.1 General Observations

The primary objective for this report was to detail and archive the results from the FLEX experiments from March 2009 to December 2010. Appendix B presents the detailed results for the droplet size (droplet diameter squared) and flame sizes (from both the LLUV and color camera views) as functions of time. These results, along with the raw experiment data, are available from the NASA Physical Science Informatics data repository (psi.nasa.gov, registration required).

In each test, there is a clear ambiguity in the droplet size during ignition (after deployment and before the igniters withdraw). This was the result of the broadband glow from the igniters changing the discrimination between the droplet and the background. This was especially present from the FLEX–001 test to the FLEX–009 test. For these tests, the shutter speed (integration time of the array) was 1/30 s (inverse of the framing rate). After the FLEX–009 test, the shutter speed decreased to a much smaller value (1/1000 s) with a corresponding increase in the illumination level. This minimized the image distortion caused by the igniters and the broadband flame radiation (from soot for heptane), resulting in more accurate droplet size data.

The great majority of the tests were of free-floating droplets (no support tether). For these tests, the droplets were rarely completely motionless; they had some residual velocity from deployment and ignition and then drifted more as a result of the residual acceleration of the spacecraft (g-jitter). As a result of this, the droplets did drift out of the FOV of one (typically the HiBMs) or more of the CIR cameras. For tests where the droplet drifted out of the FOV of the camera, the data end abruptly (e.g., the droplet regression during the FLEX–011 test). This does not correspond to the end of the test, just to the end of the data from that particular view (note that the flame histories continue during the FLEX–011 test). For a minority of tests, the droplet drifted out of the HiBMs FOV as a result of the deployment, ignition, and/or g-jitter. However, it then actually drifted back into the FOV. In this case, there is a gap in the history of that view (e.g., the droplet history for the FLEX–013 test). The sharp decline in the droplet size on either side of that gap corresponds to the time when the droplet (usually) or flame (rarely) was partially in and partially out of the FOV.

For some tests, some of the CIR cameras failed to record data for a portion of the test, and for other tests, none of the test was recorded. These show up in the plots in Appendix A as either missing traces or gaps in the data (e.g., the FLEX–024 test, for which the HiBMs failed to record any data).

The detailed data plots in Appendix B show two different measurements of flame diameter, one from the LLUV camera and the other from the color camera. For almost all of the tests, the diameter measured by the LLUV is larger than that measured by the color camera. The flame diameters from the color camera are typically about three-fourths of those from the LLUV camera. This discrepancy is not unusual and is a result of the LLUV being sensitive to the $OH^{\bullet}$ chemiluminescence, which typically peaks outside of the visible flame. For heptane tests, where there is significant soot luminosity (which is not visible in the LLUV, but dominates the color camera), the discrepancy is even larger because the peak of the soot luminosity is typically inside the blue flame envelope.

5.2 Fuel Needle Contamination

During the assembly of the MDCA hardware, a conformal coating was applied to the fuel-dispensing needles. The product was applied in two layers, a primer (Dow Corning 1204) and a conformal coat (Dow Corning 3140 RTV (MIL–A–46146) coating). Subsequent testing showed that the coating can both dissolve and “flake” off in both methanol and heptane. When this occurred, the deployed fuel droplet was clearly not pure but contained an unknown amount of the conformal coating. Once this problem was discovered, the mitigation was to prepare and fly new uncoated needles. All tests subsequent to these (to be reported in the future) will not have contamination. From extensive testing, careful analysis of the experimental data, comparison with space-based data from uncontaminated

needles, numerical modeling efforts, and ground-based testing, we can make the following assertions about the experimental data reported herein:

(1) Burning-rate constants were average, and the droplet history was minimally influenced by the contaminant. The contaminant was likely present in trace amounts and was a very low volatility compound. Because methanol and heptane are relatively high volatility fuels, the droplet regression history was dominated by the fuel not by the contaminant.

(2) The flame size and flame history were similarly minimally influenced by the contaminant.

(3) In the few tests where unusual features were observed in the flame view, such as minor disruptions and visual "sparklers," these features were probably influenced, and possibly caused, by the presence of the contaminant.

(4) Disruptive extinction of methanol is probably due to the presence of the contaminant.

(5) Disruptive extinction of heptane may be due to the presence of the contaminant. Subsequent tests with clean needles and fuel, however, also exhibited disruptive extinction at small droplet sizes, so no conclusion can be drawn regarding disruptive burning for heptane in the tests reported herein.

(6) The diffusive extinction droplet diameters (smaller diameters) for methanol (where there is no disruption) were minimally influenced by the presence of the contaminant.

(7) Radiative extinction droplet diameters (larger diameters) were not influenced by the presence of the contaminant.

(8) Distorted droplets (e.g., the HiBMs video from the FLEX–088 test) for methanol droplet burning (approximately four tests) are probably the result of the contaminant.

6.0 Conclusions

Histories of droplet and flame diameters, as well as burning-rate constants and extinction diameters, were obtained in Flame Extinguishment Experiment (FLEX) program experiments performed on the International Space Station for methanol and n-heptane droplets with initial diameters between 2 and 5 mm. Burning was done in oxidizing atmospheres at ambient temperature and at various pressures between 0.70 and 3.05 atm, over ranges of dilution of oxygen with nitrogen, oxygen with carbon dioxide, and mixtures thereof. The experimental methods and data analysis procedures are reported here, and the results are presented and catalogued. More than 100 useful combustion histories were obtained. These extensive experimental results are not interpreted here; the intent is merely to make the data readily available for future scientific interpretation.

Glenn Research Center
National Aeronautics and Space Administration
Cleveland, Ohio, November 21, 2015

Appendix A.—Detailed Experimental Results

This appendix provides a detailed listing of all the results of the Flame Extinguishment Experiment (FLEX) tests from March 2009 through December 2010. In addition to the data printed in this section, electronic data files are available with the detailed results on the digital video disc (DVD) addendum.

A.1 Summary Data

The following list explains the column headings in Table IX:

FLEX test—number used by the FLEX science team

FLEX identifier—used by the Combustion Integrated Rack (CIR) engineering team

Test date—date the test was performed

Test time—time the test was performed (Greenwich Mean Time, GMT)

Fuel—fuel used for the test: methanol (CH_3OH) or heptane (C_7H_{16})

Actual D_0—initial droplet diameter or droplet diameter at time zero where time zero is the time when the igniters are turned ON

Burning rate—average burning rate constant from a linear fit of the droplet diameter squared versus time from shortly after ignition to extinction

Visible flame extinction diameter—droplet diameter at the time the visible flame extinguished, where "-" indicates flame extinction did not occur either because the droplet burned to completion or because a droplet disruption ended the test. For cases where the droplet left the HiBMs field of view (FOV) before extinction, we did estimate (extrapolate the burning history) to determine the extinction droplet diameter if there was sufficient burning history and the length of time to extrapolate was not that long. If the droplet was not in the HiBMS FOV for enough time, the extinction droplet diameter is not listed.

Notes—specific observations for a particular test, as explained in the notes at the bottom of the table

Fiber—Yes or No depending on whether a support fiber was in place for the tests

P—absolute ambient pressure

O_2—ambient oxygen mole fraction from detailed records of the chamber fill, recirculation, filter, and combustion history

CO_2—ambient carbon dioxide mole fraction from detailed records of the chamber fill, recirculation, filter, and combustion history

N_2—ambient nitrogen mole fraction from detailed records of the chamber fill, recirculation, filter, and combustion history

H_2O—ambient water vapor mole fraction from detailed records of the chamber fill, recirculation, filter, and combustion history

Heptane—ambient heptane (C_7H_{16}) vapor mole fraction from detailed records of the chamber fill, recirculation, filter, and combustion history

Methanol—ambient methanol (CH_3OH) vapor mole fraction from detailed records of the chamber fill, recirculation, filter, and combustion history

A.2 Experiment Results

Table IX summarizes the data.

TABLE IX.—RESULTS BY TEST NUMBER AND FLEX IDENTIFIER

FLEX		Test		Fuel	Ambient pressure, mmHg	Initial ambient composition, mole fraction				Droplet initial diameter, mm	Visible flame extinction diameter, mm	Burning rate, mm^2/s	Burn time, s	Test end
Test	Identifier	Date	Greenwich mean time			O_2	N_2	CO_2	He					
FLEX–001	20CAL08	3/5/09	17:22:03	Methanol	757.7	0.21	0.79	0	0	1.69	0.89	0.52	4.3	Disruption
FLEX–002	20CAL10	3/5/09	19:20:06	Methanol	762	.21	.79	0	0	1.86	.94	.6	5	Extinction
FLEX–003	20CAL12	3/5/09	21:17:46	Methanol	764.2	.21	.79	0	0	1.61	.92	.58	3.2	Extinction
FLEX–004	30CAL02	3/31/09	17:16:18	Methanol	760	.21	.79	0	0	2.06	–	.6	7.64	Extinction
FLEX–005	30CAL03	3/31/09	19:00:48	Methanol	760	.21	.79	0	0	1.92	.81	.48	6.34	Extinction
FLEX–006	40CAL01	3/31/09	20:05:49	Methanol	760	.21	.79	0	0	2.54	1.53	.51	9.6	Extinction
FLEX–007	20CAL13	4/10/09	13:26:11	Heptane	761.3	.21	.79	0	0	1.87	–	.67	5.3	Disruption
FLEX–008	30CAL06	4/10/09	18:07:15	Heptane	762.4	.21	.79	0	0	2.95	–	.79	14.8	Disruption
FLEX–009	30CAL07	4/10/09	–	Heptane	760	.21	.79	0	0	–	–	–	–	Disruption
FLEX–010	256F002	5/22/09	14:53:27	Methanol	2319.7	.21	.09	.7	0	3.86	–	.37	13.6	Extinction
FLEX–011	256R001	5/22/09	15:33:47	Methanol	2318.8	.21	.09	.7	0	3.03	–	.4	16.5	Extinction
FLEX–012	264F003	5/22/09	19:23:35	Heptane	2319.9	.21	.09	.7	0	2.74	–	–	–	Disruption
FLEX–013	256R002	6/25/09	15:33:05	Methanol	2074.2	.21	.09	.7	0	2.59	–	.49	10.8	Extinction
FLEX–014	256F007	6/29/09	12:26:06	Methanol	2055.6	.21	.09	.7	0	3.7	–	–	11.3	Extinction
FLEX–015	256F008	6/29/09	13:56:06	Methanol	2066.6	.21	.09	.7	0	4.42	–	–	23.1	Extinction
FLEX–016	256F009	6/29/09	15:34:58	Methanol	2072.1	.21	.09	.7	0	1.66	1	.53	3.4	Extinction
FLEX–017	240R003	7/1/09	12:28:41	Methanol	1545.7	.21	.09	.7	0	2.67	–	–	2.4	Disruption
FLEX–018	248F001	7/1/09	16:28:56	Heptane	1553.8	.21	.09	.7	0	2.74	1.77	.61	8.1	Extinction
FLEX–019	196F001	8/26/09	19:07:28	Heptane	539.1	.34	.66	0	0	3.39	–	.9	4.2	Disruption
FLEX–020	192F001	10/24/09	14:09:04	Methanol	539.5	.34	.66	0	0	3.4	1.56	.53	17.4	Completion
FLEX–021	192F002	10/24/09	15:15:24	Methanol	540.6	.34	.66	0	0	3.49	.95	.66	17.8	Disruption
FLEX–022	192F003	10/24/09	15:39:48	Methanol	540.5	.34	.66	0	0	3.5	–	.65	18.2	Disruption
FLEX–023	196F002	10/24/09	18:29:53	Heptane	541.8	.34	.66	0	0	3.01	–	.73	13.1	Disruption
FLEX–024	196F003	10/24/09	19:44:04	Heptane	542.8	.34	.66	0	0	–	–	–	–	Disruption
FLEX–025	191R001	11/9/09	11:42:23	Methanol	537.3	.3	.7	0	0	2.6	.59	.65	10.3	Completion
FLEX–026	191F001	11/9/09	11:59:59	Methanol	538.4	.3	.7	0	0	3.63	.4	.62	22.2	Disruption
FLEX–027	195F001	11/9/09	14:04:11	Heptane	540.7	.3	.7	0	0	3.87	–	.64	23.8	Disruption
FLEX–028	195F002	11/9/09	14:56:05	Heptane	539.7	.3	.7	0	0	3.36	–	.64	17.3	Disruption
FLEX–029	178R001	11/13/09	13:11:23	Methanol	766.9	.3	.7	0	0	2.57	–	.74	10.4	Completion
FLEX–030	178F001	11/13/09	14:03:46	Methanol	769.2	.3	.7	0	0	3.26	1.32	.59	15.6	Extinction
FLEX–031	182F001	11/13/09	18:33:39	Heptane	770.5	.3	.7	0	0	3.39	–	.85	18.4	Disruption

FLEX		Test		Fuel	Ambient pressure, mmHg	Initial ambient composition, mole fraction				Droplet initial diameter, mm	Visible flame extinction diameter, mm	Burning rate, mm^2/s	Burn time, s	Test end
Test	Identifier	Date	Greenwich mean time			O_2	N_2	CO_2	He					
FLEX–032	182F002	11/13/09	19:04:33	Heptane	771	.3	.7	0	0	3.07	–	.68	14	Completion
FLEX–033	177R002	11/27/09	10:02:15	Methanol	764.5	.21	.79	0	0	2.62	1.25	.48	11.4	Extinction
FLEX–034	177F001	11/27/09	11:15:38	Methanol	767.7	.21	.79	0	0	3.89	2	.44	27.3	Extinction
FLEX–035	181F001	11/27/09	13:01:24	Heptane	768.1	.21	.79	0	0	3.85	3.34	.43	8.9	Extinction
FLEX–036	190R002	12/15/09	10:39:35	Methanol	539	.2	.8	0	0	2.4	1.67	.45	7.1	Extinction
FLEX–037	220R001	1/7/10	19:08:46	Methanol	534.3	.34	.66	0	0	3.31	–	.72	10.7	Disruption
FLEX–038	220R002	1/7/10	19:20:38	Methanol	534.4	.34	.66	0	0	3.59	–	.71	15.3	Disruption
FLEX–039	224F001	1/7/10	21:51:19	Heptane	534.9	.34	.66	0	0	2.91	0	.8	9.9	Disruption
FLEX–040	219R001	1/8/10	5:02:52	Methanol	535.1	.3	.7	0	0	3.77	–	.62	19.2	Disruption
FLEX–041	219F001	1/8/10	4:41:55	Methanol	534.3	.3	.7	0	0	3.35	–	.65	14.1	Disruption
FLEX–042	223F001	1/8/10	1:02:04	Heptane	535	.3	.7	0	0	2.92	–	.58	11.3	Disruption
FLEX–043	223F002	1/8/10	3:16:16	Heptane	534.9	.3	.7	0	0	2.97	0	.78	11.4	Disruption
FLEX–044	206F001	1/11/10	10:33:22	Methanol	766.8	.3	.7	0	0	3.49	–	.63	16.6	Disruption
FLEX–045	206R001	1/11/10	10:54:25	Methanol	768.3	.3	.7	0	0	2.42	1.01	.73	6.6	Extinction
FLEX–046	205R001	1/12/10	13:14:25	Methanol	769.5	.21	.79	0	0	2.78	1.08	.54	13.1	Disruption
FLEX–047	209F001	1/12/10	15:48:17	Heptane	770.1	.21	.79	0	0	3.36	–	.5	17.1	Completion
FLEX–048	205F001	1/12/10	12:14:55	Methanol	768.7	.21	.79	0	0	3.66	–	.27	23.5	Disruption
FLEX–049	209F003	1/19/10	9:09:16	Heptane	764.9	.21	.79	0	0	3.46	2.78	.59	8.6	Extinction
FLEX–050	209F004	1/19/10	14:08:17	Heptane	770.1	.21	.79	0	0	3.57	2.98	.52	8.4	Extinction
FLEX–051	209F005	1/19/10	16:38:35	Heptane	771.4	.21	.79	0	0	2.41	0	.65	8.2	Completion
FLEX–052	210F002	1/11/10	13:46:44	Heptane	771.1	.3	.7	0	0	3.53	0	.7	18.3	Disruption
FLEX–053	209F002	1/12/10	16:29:37	Heptane	770.2	.21	.79	0	0	–	–	–	18.5	Disruption
FLEX–054	190F003	1/29/10	11:27:01	Methanol	541.4	.2	.8	0	0	3.56	–	.41	29	Extinction
FLEX–055	218F001	1/29/10	16:06:50	Methanol	542.6	.2	.8	0	0	3.37	2.39	.46	20.5	Disruption
FLEX–056	194F001	1/29/10	19:13:22	Heptane	544.1	.2	.79	0	0	3.56	3.04	.44	7.9	Completion
FLEX–057	303F001	1/29/10	19:50:16	Heptane	544.4	.2	.79	0	0	3.1	2.49	.54	6.8	Extinction
FLEX–058	176F001	2/4/10	2:32:01	Methanol	773.3	.18	.82	0	0	3.69	–	.42	29.1	Extinction
FLEX–059	176R001	2/4/10	0:26:28	Methanol	769.2	.18	.82	0	0	2.93	1.39	.43	17.7	Extinction
FLEX–060	204F001	2/4/10	3:26:05	Methanol	773.7	.18	.82	0	0	3.43	–	.45	23.2	Extinction
FLEX–061	204R001	2/4/10	3:52:39	Methanol	774.1	.18	.82	0	0	3.68	2	.41	25.7	Extinction
FLEX–062	301F001	3/11/10	21:37:48	Heptane	761.8	.18	.82	0	0	3.43	3.17	.39	4.8	Extinction
FLEX–063	301F002	3/11/10	23:07:51	Heptane	767.6	.18	.81	0	0	2.15	0	.51	9.6	Completion
FLEX–064	302F001	3/11/10	22:12:39	Heptane	764.6	.18	.81	0	0	2.69	2.07	.6	5.5	Extinction
FLEX–065	189R001	3/19/10	8:42:53	Methanol	765.9	.15	.85	0	0	3.37	–	.4	24.3	Extinction

FLEX		Test		Fuel	Ambient pressure, mmHg	Initial ambient composition, mole fraction				Droplet initial diameter, mm	Visible flame extinction diameter, mm	Burning rate, mm^2/s	Burn time, s	Test end
Test	Identifier	Date	Greenwich mean time			O_2	N_2	CO_2	He					
FLEX–066	189F001	3/19/10	9:26:45	Methanol	766.8	.15	.85	0	0	2.52	1.32	.38	12.9	Extinction
FLEX–067	189F002	3/19/10	10:17:06	Methanol	767.7	.15	.85	0	0	3.97	3.3	.36	14.4	Extinction
FLEX–068	189R003	3/19/10	12:04:45	Methanol	768.8	.15	.84	0	0	2.38	1.29	.39	10.7	Extinction
FLEX–069	193R002	3/23/10	10:23:00	Heptane	767.1	.14	.84	0	0	1.1	0	.94	1.3	Completion
FLEX–070	193F001	3/23/10	7:25:43	Heptane	761	.15	.84	0	0	4.67	4.6	.41	1.6	Extinction
FLEX–071	189R002	3/19/10	11:19:22	Methanol	768.3	.15	.84	0	0	2.25	–	.4	8.4	Extinction
FLEX–072	193R001	3/23/10	9:06:37	Heptane	765.2	.15	.84	0	0	1.13	–	.52	2.5	Completion
FLEX–073	193F001	3/23/10	7:25:43	Heptane	761	.15	.84	0	0	4.64	4.58	.56	1.5	Extinction
FLEX–074	221F001	3/23/10	9:44:36	Heptane	765.9	.15	.84	0	0	1.33	–	.77	2.3	Completion
FLEX–075	203R002	3/29/10	21:06:40	Methanol	770.8	.13	.85	0	0	2.54	1.78	.37	9.1	Extinction
FLEX–076	203F001	3/29/10	19:24:36	Methanol	769.5	.13	.85	0	0	3.21	2.78	.37	8.9	Extinction
FLEX–077	175R001	3/29/10	18:39:20	Methanol	768.4	.14	.85	0	0	3.33	2.91	.34	8.5	Extinction
FLEX–078	175F001	3/29/10	17:49:23	Methanol	766	.14	.85	0	0	2.66	1.66	.35	12.9	Extinction
FLEX–079	179F001	3/30/10	0:40:16	Heptane	768.1	.13	.85	0	0	2.92	2.86	.25	1.5	Extinction
FLEX–080	207F001	3/30/10	2:29:19	Heptane	770	.13	.85	0	0	–	–	–	1	Extinction
FLEX–081	207F002	3/30/10	3:59:28	Heptane	770.2	.13	.85	0	0	–	–	–	1.5	Extinction
FLEX–082	304F001	4/19/10	17:19:17	Methanol	764.6	.13	.87	0	0	2.84	2.39	.35	7.5	Extinction
FLEX–083	304F002	4/19/10	21:18:05	Methanol	772	.12	.87	0	0	–	–	–	5.45	Extinction
FLEX–084	304R001	4/19/10	17:51:24	Methanol	767.2	.12	.87	0	0	2.35	1.42	.35	10.8	Extinction
FLEX–085	304R002	4/19/10	20:12:58	Methanol	771.2	.12	.87	0	0	2.4	1.77	.35	9.3	Extinction
FLEX–086	305F002	4/19/10	19:16:37	Methanol	770	.12	.87	0	0	3.07	2.56	.35	9	Extinction
FLEX–087	305F003	4/19/10	20:38:54	Methanol	771.2	.12	.87	0	0	2.64	1.92	.38	9.3	Extinction
FLEX–088	053R001	5/5/10	22:37:54	Methanol	537.5	.25	.6	.15	0	3.01	–	.53	14.8	Disruption
FLEX–089	053F001	5/5/10	22:19:33	Methanol	537.4	.25	.6	.15	0	3.7	–	.51	24	Disruption
FLEX–090	141R001	5/6/10	0:07:51	Methanol	539.2	.25	.6	.15	0	3.62	–	.53	20.1	Disruption
FLEX–091	141F001	5/5/10	23:10:01	Methanol	538.3	.25	.6	.15	0	3.51	–	.51	18	Disruption
FLEX–092	061F002	6/14/10	22:54:56	Heptane	536.3	.25	.6	.15	0	3.41	–	.55	21.7	Disruption
FLEX–093	149F001	6/15/10	0:32:31	Heptane	537.3	.25	.6	.15	0	2.48	0	.71	8.3	Disruption
FLEX–094	C08H101	6/15/10	2:10:43	Heptane	533.6	.24	.56	.2	0	3.53	2.76	.51	10.1	Extinction
FLEX–095	C08H201	6/15/10	3:22:41	Heptane	534.4	.24	.56	.2	0	3.6	3.04	.58	8	Extinction
FLEX–096	C08H301	6/15/10	4:37:39	Heptane	534.4	.24	.56	.2	0	–	–	–	5.2	Disruption
FLEX–097	C08M101	6/16/10	22:43:35	Methanol	534.2	.23	.56	.2	0	4.25	2.6	.45	26.5	Completion
FLEX–098	C09M201	6/21/10	14:21:26	Methanol	537.1	.23	.52	.25	0	3.64	1.74	.47	22.9	Extinction
FLEX–099	C09M101	6/21/10	12:57:34	Methanol	535	.23	.52	.25	0	4.28	2.32	.42	33	Extinction
FLEX–100	C09H101	6/29/10	8:30:46	Heptane	536.7	.23	.52	.25	0	4.14	3.98	.34	6.1	Extinction

FLEX		Test		Fuel	Ambient pressure, mmHg	Initial ambient composition, mole fraction				Droplet initial diameter, mm	Visible flame extinction diameter, mm	Burning rate, mm^2/s	Burn time, s	Test end
Test	Identifier	Date	Greenwich mean time			O_2	N_2	CO_2	He					
FLEX–101	C09H201	6/29/10	9:38:10	Heptane	538.7	.23	.52	.25	0	3.88	3.45	.5	6.5	Extinction
FLEX–102	C10H101	6/29/10	11:21:09	Heptane	534.2	.21	.49	.3	0	3.57	3.43	.33	4.2	Extinction
FLEX–103	C10H201	6/29/10	11:56:02	Heptane	534.3	.21	.49	.3	0	4	3.88	.35	3.2	Extinction
FLEX–104	C08M201	6/16/10	23:04:00	Methanol	534.1	.23	.56	.2	0	3.6	1.58	.49	23.2	Extinction
FLEX–105	C08M301	6/16/10	23:29:19	Methanol	534.6	.23	.56	.2	0	4.17	2	.47	30.7	Disruption
FLEX–106	C09M401	6/21/10	15:52:51	Methanol	538.3	.23	.52	.25	0	3.08	1.75	.51	14.1	Disruption
FLEX–107	C08M401	6/16/10	23:51:26	Methanol	535	.23	.56	.2	0	3.18	–	.52	15.1	Disruption
FLEX–108	C09M301	6/21/10	15:35:57	Methanol	538.3	.23	.52	.25	0	3.75	–	.47	24.3	Completion
FLEX–109	C10M102	8/31/10	5:38:01	Methanol	536.5	.21	.49	.3	0	3.56	1.92	.42	–	Extinction
FLEX–110	C10M201	8/31/10	7:16:40	Methanol	537	.21	.49	.3	0	2.83	1.57	.45	13	Extinction
FLEX–111	C10M303	8/31/10	8:58:24	Methanol	536.9	.21	.49	.3	0	3.37	2.1	.45	16.4	Completion
FLEX–112	C10M401	9/1/10	15:27:44	Methanol	530.7	.21	.49	.3	0	3.99	2.35	.43	25.2	Completion
FLEX–113	C11M101	9/1/10	19:17:58	Methanol	534.6	.2	.45	.35	0	4.2	2.85	.49	18.2	Extinction
FLEX–114	C11M201	9/6/10	19:14:22	Methanol	0	.2	.45	.35	0	3.23	1.68	.42	18.9	Extinction
FLEX–115	C11M301	9/1/10	20:40:16	Methanol	535.8	.2	.45	.35	0	3.97	2.61	.41	22.9	Extinction
FLEX–116	C11M401	9/1/10	20:57:41	Methanol	536.3	.2	.45	.35	0	3.16	1.57	.46	16.9	Extinction
FLEX–117	C11H101	9/6/10	18:14:53	Heptane	531.1	.2	.45	.35	0	3.84	3.77	.25	2.4	Extinction
FLEX–118	C11H201	9/6/10	19:14:22	Heptane	532.8	.2	.44	.35	0	3.03	2.93	.38	2.5	Extinction
FLEX–119	C12H103	9/7/10	1:50:01	Heptane	532.6	.18	.42	.4	0	2.6	2.48	.37	1.3	Extinction
FLEX–120	C12H201	9/7/10	1:08:26	Heptane	532.5	.18	.42	.4	0	2.45	2.39	.38	1.43	Extinction
FLEX–121	C12M101	9/8/10	19:21:31	Methanol	526.3	.18	.42	.4	0	4.25	3.92	.34	8	Extinction
FLEX–122	C12M201	9/8/10	21:44:37	Methanol	531.2	.18	.42	.4	0	3.46	2.58	.41	13.9	Extinction
FLEX–123	C12M301	9/8/10	22:16:51	Methanol	532	.18	.42	.4	0	4.13	3.79	.35	8.7	Extinction
FLEX–124	C12M401	9/8/10	22:45:54	Methanol	532.4	.18	.42	.4	0	2.87	2.74	.3	2.4	Extinction
FLEX–125	C13M103	9/13/10	21:07:02	Methanol	537.2	.17	.38	.45	0	3.63	3.37	.35	5.7	Extinction
FLEX–126	C13M201	9/13/10	18:11:39	Methanol	536.1	.17	.38	.45	0	2.8	1.84	.4	11.7	Extinction
FLEX–127	C13M301	9/13/10	19:22:49	Methanol	536.7	.17	.38	.45	0	3.22	2.53	.38	11	Extinction
FLEX–128	C13M401	9/13/10	19:49:24	Methanol	537.3	.17	.38	.45	0	2.91	–	.39	11.5	Extinction
FLEX–129	C13H102	9/17/10	1:32:49	Heptane	536.2	.17	.38	.45	0	3.33	3.34	.33	.55	Extinction
FLEX–130	C13H201	9/17/10	3:55:59	Heptane	537.2	.17	.38	.45	0	2.91	2.89	.05	.6	Extinction
FLEX–131	C21H101	10/6/10	11:28:52	Heptane	763.9	.24	.56	.2	0	1.72	.52	.61	4.9	Disruption
FLEX–132	C21H201	10/6/10	12:59:06	Heptane	765.2	.24	.56	.2	0	2.63	.53	.6	12.4	Disruption
FLEX–133	C21H301	10/6/10	13:59:59	Heptane	766.7	.24	.56	.2	0	3.25	.55	.56	19	Disruption
FLEX–134	C21H401	10/6/10	14:57:06	Heptane	767.2	.24	.56	.2	0	3.66	2.88	.56	9.2	Extinction
FLEX–135	C21H501	10/6/10	16:22:15	Heptane	768.2	.24	.56	.2	0	2.78	0	.59	10.8	Completion

FLEX		Test		Fuel	Ambient pressure, mmHg	Initial ambient composition, mole fraction				Droplet initial diameter, mm	Visible flame extinction diameter, mm	Burning rate, mm^2/s	Burn time, s	Test end
Test	Identifier	Date	Greenwich mean time			O_2	N_2	CO_2	He					
FLEX–136	C21H302	10/6/10	17:30:58	Heptane	768.1	.24	.56	.2	0	3.08	–	.51	17	Completion
FLEX–137	C21H303	10/6/10	17:53:35	Heptane	768.2	.24	.56	.2	0	3.13	–	.55	17.5	Disruption
FLEX–138	C21H304	10/6/10	18:08:43	Heptane	768.6	.24	.56	.2	0	–	–	–	–	Disruption
FLEX–139	C21H305	10/6/10	19:09:45	Heptane	768	.24	.56	.2	0	1.75	–	.63	5.4	Disruption
FLEX–140	C14M101	11/4/10	16:52:39	Methanol	533.5	.15	.35	.5	0	3.98	3.95	.2	1.3	Extinction
FLEX–141	C14M201	11/4/10	18:07:51	Methanol	534.1	.15	.35	.5	0	2.86	2.73	.3	2.3	Extinction
FLEX–142	C14M301	11/4/10	19:11:39	Methanol	534.5	.15	.35	.5	0	1.86	1.48	.39	3.4	Extinction
FLEX–143	C14M302	11/4/10	20:19:22	Methanol	534.7	.15	.35	.5	0	2.25	2.06	.36	2.7	Extinction
FLEX–144	C01M101	11/16/10	9:42:08	Methanol	761.9	.2	.75	.05	0	3.53	1.53	.45	23.8	Extinction
FLEX–145	C01M201	11/16/10	10:21:24	Methanol	763.5	.2	.75	.05	0	3.33	1.61	.45	20	Extinction
FLEX–146	C01M301	11/16/10	10:54:23	Methanol	765.5	.2	.75	.05	0	4.35	1.95	.41	39.2	Extinction
FLEX–147	C13M102	9/13/10	17:35:49	Methanol	535.7	.17	.38	.45	0	3.02	2.49	.4	7.8	Extinction
FLEX–148	C01H101	11/18/10	8:39:27	Heptane	764.4	.2	.75	.05	0	2.58	1.15	.54	11.8	Disruption
FLEX–149	C01H201	11/18/10	9:25:38	Heptane	766.2	.2	.75	.05	0	2.21	.82	.53	8.9	Disruption
FLEX–150	C01H302	11/18/10	10:17:02	Heptane	767.6	.2	.75	.05	0	3.18	2.54	.46	8	Extinction
FLEX–151	C03M101	12/8/10	18:31:22	Methanol	762.5	.18	.67	.15	0	3.86	–	.36	31.3	Completion
FLEX–152	C03M201	12/8/10	20:10:32	Methanol	765	.18	.67	.15	0	3.33	1.23	.43	23.2	Extinction
FLEX–153	C03M301	12/8/10	21:08:17	Methanol	765.6	.18	.67	.15	0	2.78	1.19	.42	15.7	Extinction
FLEX–154	C03H101	12/9/10	16:02:14	Heptane	762.3	.18	.67	.15	0	3.7	3.6	.34	2.2	Extinction
FLEX–155	C03H201	12/9/10	17:49:08	Heptane	764.9	.18	.67	.15	0	2.73	2.52	.39	2.7	Extinction
FLEX–157	C03H401	12/9/10	19:12:27	Heptane	765.7	.18	.67	.15	0	1.34	.45	.48	3.2	Completion
FLEX–158	C05M101	12/14/10	13:41:00	Methanol	762.1	.16	.59	.25	0	4.24	3.96	.3	7.6	Extinction
FLEX–159	C05M201	12/14/10	14:30:46	Methanol	764.4	.16	.59	.25	0	3.7	3.22	.37	10.1	Extinction
FLEX–160	C05M301	12/14/10	15:17:59	Methanol	765.5	.16	.59	.25	0	2.71	1.34	.38	14.9	Extinction
FLEX–161	C05M401	12/14/10	17:51:58	Methanol	767.6	.16	.59	.25	0	2.77	1.52	.38	14.8	Extinction
FLEX–162	C06M101	12/28/10	11:41:39	Methanol	763.3	.15	.54	.32	0	3.72	3.5	.28	6	Extinction
FLEX–163	C06M201	12/28/10	12:05:23	Methanol	764.4	.15	.53	.32	0	3.05	2.54	.37	8.5	Extinction
FLEX–164	C06M301	12/28/10	13:00:43	Methanol	765.9	.15	.53	.32	0	2.59	1.63	.37	11.6	Extinction
FLEX–165	C06M401	12/28/10	13:36:43	Methanol	766.1	.15	.53	.32	0	2.59	1.79	.42	8.9	Extinction
FLEX–166	C03H302	12/9/10	18:51:34	Heptane	765.4	.18	.67	.15	0	1.96	1.39	.54	3.9	Extinction
FLEX–167	C07M101	1/12/11	21:56:45	Methanol	760.8	.14	.5	.36	0	3.22	3.08	.28	3.4	Extinction
FLEX–168	C07M201	1/12/11	22:11:40	Methanol	761.6	.14	.5	.36	0	2.32	1.84	.37	5.9	Extinction
FLEX–169	C15M101	1/18/11	12:54:25	Methanol	763.4	.21	.64	.15	0	3.03	1.57	.48	15.6	Disruption
FLEX–170	C15M201	1/18/11	14:19:29	Methanol	766.1	.21	.64	.15	0	3.05	1.28	.51	16.7	Extinction
FLEX–171	C15M301	1/18/11	15:58:46	Methanol	766.7	.21	.64	.15	0	3.53	1.59	.46	23.6	Extinction

FLEX		Test		Fuel	Ambient pressure, mmHg	Initial ambient composition, mole fraction				Droplet initial diameter, mm	Visible flame extinction diameter, mm	Burning rate, mm^2/s	Burn time, s	Test end
Test	Identifier	Date	Greenwich mean time			O_2	N_2	CO_2	He					
FLEX–172	C03H501	2/21/11	17:56:40	Heptane	759.9	.18	.67	.15	0	3.74	3.68	.35	2.8	Extinction
FLEX–173	C03H601	2/21/11	19:07:48	Heptane	762	.18	.67	.15	0	2.4	1.96	.46	4.4	Extinction
FLEX–174	C03H701	2/21/11	19:17:37	Heptane	762.1	.18	.67	.15	0	1.35	.47	.5	3.6	Disruption
FLEX–175	C08H502	2/21/11	22:15:54	Heptane	531.7	.24	.56	.2	0	2.5	.21	.56	11.2	Disruption
FLEX–176	C08H601	2/21/11	22:43:37	Heptane	532.1	.24	.56	.2	0	2.88	–	.55	15.6	Disruption
FLEX–177	C08M501	4/18/11	20:27:36	Methanol	536.9	.24	.56	.2	0	4.53	–	.46	38.2	Extinction
FLEX–178	C08M601	4/18/11	20:52:24	Methanol	537	.24	.56	.2	0	3.02	1.35	.52	14.5	Extinction
FLEX–179	C09H501	4/20/11	17:56:25	Heptane	533.6	.23	.52	.25	0	3.32	2.61	.5	8.9	Extinction
FLEX–180	C09H601	4/20/11	18:22:58	Heptane	534.4	.23	.52	.25	0	2.07	.48	.57	7.5	Disruption
FLEX–181	C02H101	4/20/11	20:00:24	Heptane	758.4	.19	.71	.1	0	3.4	3.13	.41	4.5	Extinction
FLEX–182	C02H201	4/20/11	21:14:08	Heptane	759.1	.19	.71	.1	0	2.48	1.68	.49	7	Extinction
FLEX–183	C02H202	4/20/11	21:26:02	Heptane	759	.19	.71	.1	0	1.64	.49	.54	5.1	Disruption
FLEX–184	C09M501	8/8/11	13:14:11	Methanol	534.4	.23	.52	.25	0	3.72	–	.53	26.2	Extinction
FLEX–185	C09M502	8/8/11	13:30:14	Methanol	535.1	.23	.52	.25	0	3.42	–	.51	15.8	Extinction
FLEX–186	C09M601	8/8/11	13:42:04	Methanol	535.2	.23	.52	.25	0	2.8	1.33	.51	12.7	Extinction
FLEX–187	C09M701	8/8/11	14:52:15	Methanol	536.2	.23	.52	.25	0	2.47	1.21	.52	9.2	Extinction
FLEX–188	C02M101	8/8/11	16:16:48	Methanol	758	.19	.71	.1	0	3.38	1.29	.47	21.8	Extinction
FLEX–189	C02M201	8/8/11	17:49:19	Methanol	758.1	.19	.71	.1	0	2.47	1.08	.46	11	Extinction
FLEX–190	C03M501	8/9/11	10:53:21	Methanol	761.2	.18	.67	.15	0	3.77	1.78	.42	30.5	Extinction
FLEX–191	C03M601	8/9/11	12:28:41	Methanol	764.6	.18	.67	.15	0	2.74	.95	.5	14	Extinction
FLEX–192	C03M701	8/9/11	12:46:53	Methanol	765.3	.18	.67	.15	0	1.76	.81	.46	5.5	Extinction
FLEX–193	C04M101	8/9/11	17:07:27	Methanol	759.5	.17	.63	.2	0	3.46	–	.39	21.8	Extinction
FLEX–194	C04M201	8/9/11	18:26:45	Methanol	759.1	.17	.63	.2	0	2.77	1.27	.4	15.6	Extinction
FLEX–195	C04H101	8/17/11	22:31:20	Heptane	752	.17	.63	.2	0	3.76	3.71	.29	1.6	Extinction
FLEX–196	C04H201	8/17/11	22:53:58	Heptane	752.5	.17	.63	.2	0	2.9	2.79	.36	1.9	Extinction
FLEX–197	C01H501	8/18/11	0:24:31	Heptane	758.4	.2	.75	.05	0	3.06	2.28	.52	8.9	Extinction
FLEX–198	C01H601	8/18/11	1:38:10	Heptane	759.8	.2	.75	.05	0	3.04	2.33	.49	8.1	Extinction
FLEX–199	C01H701	8/18/11	1:55:56	Heptane	760.1	.2	.75	.05	0	2.12	.13	.53	8.7	Disruption
FLEX–200	C01M501	8/24/11	15:07:47	Methanol	754	.2	.75	.05	0	3.37	.98	.49	21	Extinction
FLEX–201	C01M602	8/24/11	15:56:17	Methanol	756.1	.2	.75	.05	0	2.57	1.13	.47	11.7	Extinction
FLEX–202	C01M603	8/24/11	16:18:58	Methanol	756.9	.2	.75	.05	0	2.4	1.05	.48	10.2	Extinction
FLEX–203	N01M101	8/24/11	21:05:01	Methanol	760.2	.21	.79	0	0	3.3	1.42	.47	19.5	Extinction
FLEX–204	N01M201	8/24/11	21:58:36	Methanol	761.6	.21	.79	0	0	2.75	1.11	.52	12.8	Extinction
FLEX–206	N01H101	8/29/11	19:04:50	Heptane	756.5	.21	.79	0	0	3.56	–	.43	23.9	Disruption

FLEX		Test		Fuel	Ambient pressure, mmHg	Initial ambient composition, mole fraction				Droplet initial diameter, mm	Visible flame extinction diameter, mm	Burning rate, mm^2/s	Burn time, s	Test end
Test	Identifier	Date	Greenwich mean time			O_2	N_2	CO_2	He					
FLEX–207	N01H102	8/29/11	19:21:49	Heptane	757.3	.21	.79	0	0	3.58	–	.42	24	Disruption
FLEX–208	N01H201	8/29/11	20:28:30	Heptane	760.2	.21	.79	0	0	2.96	.47	.5	17.1	Disruption
FLEX–209	N01H202	8/29/11	21:54:40	Heptane	762.7	.21	.79	0	0	2.72	1.13	.54	11.5	Completion
FLEX–210	N01H301	8/29/11	22:19:47	Heptane	762.9	.21	.79	0	0	2.92	–	.69	12.8	Completion
FLEX–211	N02H101	8/29/11	23:36:18	Heptane	759.8	.16	.84	0	0	3.34	3.18	.34	3.4	Extinction
FLEX–212	N02H201	8/29/11	23:51:11	Heptane	759.8	.16	.84	0	0	–	–	–	–	Extinction
FLEX–214	N02H203	8/30/11	0:58:06	Heptane	759.9	.16	.84	0	0	2.52	2.13	.42	4.5	Extinction
FLEX–215	N03H101	9/1/11	19:44:42	Heptane	764	.15	.85	0	0	2.55	2.31	.37	3.4	Extinction
FLEX–216	N03H201	9/1/11	21:02:30	Heptane	766.2	.15	.85	0	0	1.77	.33	.47	6.7	Completion
FLEX–217	N04H101	9/1/11	22:54:16	Heptane	759.8	.14	.86	0	0	4.16	4.15	.24	1.6	Extinction
FLEX–218	N04H201	9/1/11	23:17:17	Heptane	759.9	.14	.86	0	0	1.83	–	.39	3.8	Extinction
FLEX–219	N04M101	9/8/11	17:00:27	Methanol	757.6	.14	.86	0	0	3.5	–	.3	26	Extinction
FLEX–220	N04M201	9/8/11	17:21:15	Methanol	758.3	.14	.86	0	0	2.67	1.27	.38	15.6	Extinction
FLEX–221	N05M101	9/8/11	19:00:48	Methanol	759.4	.13	.87	0	0	3.46	2.96	.36	9.5	Extinction
FLEX–222	N05M201	9/8/11	20:24:20	Methanol	760.6	.13	.87	0	0	2.75	1.46	.35	16.3	Extinction
FLEX–223	N06M101	9/9/11	13:09:53	Methanol	761.6	.12	.88	0	0	2.6	2.09	.36	6.9	Extinction
FLEX–224	N06M201	9/9/11	13:28:43	Methanol	761.9	.12	.88	0	0	1.94	1.05	.35	7.8	Extinction
FLEX–225	N06M202	9/9/11	14:26:07	Methanol	763.7	.12	.88	0	0	1.84	1.04	.38	6	Extinction
FLEX–226	H01M102	9/9/11	17:41:47	Methanol	759.2	.2	.75	0	.05	2.91	1.12	.51	14.4	Extinction
FLEX–227	H01M104	9/9/11	18:27:14	Methanol	759.6	.2	.75	0	.05	–	–	–	~6	Extinction
FLEX–229	H01H102	9/13/11	11:55:40	Heptane	755.3	.2	.75	0	.05	2.25	–	.57	~9	Completion
FLEX–230	H01H103	9/13/11	12:22:18	Heptane	756.5	.2	.75	0	.05	2.3	–	.58	9.8	Disruption
FLEX–231	H02M101	9/21/11	22:28:54	Methanol	753.4	.19	.71	0	.1	2.78	–	.57	12.5	Extinction
FLEX–232	H03M101	9/22/11	0:02:52	Methanol	759.2	.18	.67	0	.15	2.79	1.3	.51	12.5	Extinction
FLEX–233	H03M201	9/22/11	0:44:55	Methanol	760.3	.18	.67	0	.15	2.95	1.67	.53	11.7	Extinction
FLEX–234	N01H401	9/23/11	23:18:09	Heptane	767.4	.21	.79	0	0	3.32	1.37	.52	17.5	Extinction
FLEX–235	N01H502	9/24/11	0:06:41	Heptane	768.1	.21	.79	0	0	2.39	–	.57	10.6	Disruption
FLEX–236	N01H601	9/24/11	1:06:33	Heptane	769.2	.21	.79	0	0	3.65	2.85	.57	9.6	Extinction
FLEX–237	H02H101	9/24/11	2:44:09	Heptane	758.8	.19	.71	0	.1	2.59	–	.54	12	Disruption
FLEX–238	H03H101	9/27/11	12:08:14	Heptane	763.7	.18	.67	0	.15	3.52	3.28	.41	4.1	Extinction
FLEX–239	H03H201	9/27/11	13:00:54	Heptane	765.9	.18	.67	0	.15	2.3	–	.49	9.1	Completion
FLEX–240	H03H202	9/27/11	13:25:07	Heptane	766.5	.18	.67	0	.15	2.27	–	.51	8.6	Completion
FLEX–241	H04H101	9/27/11	15:00:33	Heptane	759.3	.17	.63	0	.2	2.85	2.6	.46	3.2	Extinction

FLEX		Test		Fuel	Ambient pressure, mmHg	Initial ambient composition, mole fraction				Droplet initial diameter, mm	Visible flame extinction diameter, mm	Burning rate, mm^2/s	Burn time, s	Test end
Test	Identifier	Date	Greenwich mean time			O_2	N_2	CO_2	He					
FLEX–242	H04H201	9/27/11	15:12:24	Heptane	759.3	.17	.63	0	.2	2.12	1.39	.59	4.5	Extinction
FLEX–243	H04H302	9/27/11	16:18:19	Heptane	759.6	.17	.63	0	.2	–	–	–	1.7	Disruption
FLEX–244	H04H303	9/27/11	16:40:04	Heptane	759.8	.17	.63	0	.2	1.61	–	.91	2.7	Completion
FLEX–245	H04M101	10/1/11	0:34:58	Methanol	754.2	.17	.63	0	.2	2.99	–	.49	9.1	Extinction
FLEX–246	H04M202	10/1/11	1:21:41	Methanol	757	.17	.63	0	.2	2.9	1.42	.51	13.1	Extinction
FLEX–247	H05M102	10/1/11	2:58:40	Methanol	759.9	.16	.59	0	.25	3.4	2.79	.51	7.9	Extinction
FLEX–248	H05M202	10/1/11	4:26:52	Methanol	761	.16	.59	0	.25	–	–	–	5	Extinction
FLEX–249	H05H103	10/5/11	14:58:32	Heptane	757.9	.16	.59	0	.25	1.49	.69	.6	2.9	Extinction
FLEX–250	H06M102	10/7/11	12:12:14	Methanol	755.6	.15	.55	0	.3	3.67	3.47	.43	3.6	Extinction
FLEX–251	H06M201	10/7/11	13:00:56	Methanol	756.7	.15	.55	0	.3	2.52	2.06	.56	4	Extinction
FLEX–252	H07M101	10/7/11	14:25:42	Methanol	759.2	.14	.51	0	.35	2.44	2.26	.56	1.5	Extinction
FLEX–253	H07M202	10/7/11	15:06:17	Methanol	759.8	.14	.51	0	.35	1.88	1.73	.58	1	Extinction
FLEX–254	H08M101	10/11/11	12:11:56	Methanol	763.5	.13	.47	0	.4	3.56	3.54	.51	.3	Extinction
FLEX–255	H10H101	10/12/11	20:16:43	Heptane	534	.24	.56	0	.2	3.78	2.52	.72	12.2	Extinction
FLEX–256	H11H101	10/12/11	21:58:55	Heptane	532.2	.23	.52	0	.25	2.8	.12	.71	11.4	Completion
FLEX–257	H10M101	11/18/11	14:48:10	Methanol	534.3	.24	.56	0	.2	2.82	1.03	.62	11.2	Extinction
FLEX–258	H10M102	11/18/11	15:19:28	Methanol	534.6	.24	.56	0	.2	2.79	1.53	.7	8.1	Disruption
FLEX–259	H11M101	11/18/11	16:59:20	Methanol	531.7	.23	.52	0	.25	2.45	.86	.6	8.3	Extinction
FLEX–260	H11M102	11/18/11	17:51:23	Methanol	531.8	.23	.52	0	.25	2.61	–	.73	6.3	Disruption
FLEX–261	H12M101	11/18/11	18:53:50	Methanol	531.9	.21	.49	0	.3	3.22	–	.56	10.4	Extinction
FLEX–262	H12M102	11/18/11	21:29:35	Methanol	531.2	.21	.49	0	.3	3.25	1.78	.65	12.1	Extinction
FLEX–263	H12M201	11/18/11	21:53:16	Methanol	531.2	.21	.49	0	.3	2.67	1.42	.7	7.6	Extinction
FLEX–264	H12H101	11/22/11	13:04:17	Heptane	529.6	.21	.49	0	.3	3.23	2.33	.67	7.5	Extinction
FLEX–265	H12H201	11/22/11	15:49:36	Heptane	529	.21	.49	0	.3	2.86	.71	.7	11	Extinction
FLEX–266	H13H101	11/22/11	20:40:42	Heptane	532.5	.2	.45	0	.35	3.69	3.32	.61	4.3	Extinction
FLEX–267	H13H201	11/22/11	20:58:21	Heptane	532	.2	.45	0	.35	3.08	1.69	.67	5.4	Extinction
FLEX–268	H13M102	11/28/11	13:13:31	Methanol	527.6	.2	.45	0	.35	3.87	2.24	.6	17.4	Extinction
FLEX–269	H13M201	11/28/11	13:24:55	Methanol	527.9	.2	.45	0	.35	2.95	1.5	.63	10.6	Extinction
FLEX–270	H14M101	11/28/11	15:07:28	Methanol	532.4	.18	.42	0	.4	3.5	2.67	.59	7.8	Extinction
FLEX–271	H14M201	11/28/11	15:35:38	Methanol	532.9	.18	.42	0	.4	2.7	1.92	.63	5.9	Extinction
FLEX–272	H14M202	11/28/11	15:54:09	Methanol	533.2	.18	.42	0	.4	1.84	1.3	.62	2.3	Extinction
FLEX–273	H14H101	11/30/11	8:39:18	Heptane	528	.18	.42	0	.4	2.27	1.64	.71	3.5	Extinction
FLEX–274	H14H201	11/30/11	9:49:07	Heptane	530.3	.18	.42	0	.4	1.86	.84	.77	3.5	Extinction
FLEX–275	H15H101	11/30/11	11:30:51	Heptane	532.2	.17	.38	0	.45	2.22	1.86	.76	1.9	Extinction

FLEX		Test		Fuel	Ambient pressure, mmHg	Initial ambient composition, mole fraction				Droplet initial diameter, mm	Visible flame extinction diameter, mm	Burning rate, mm^2/s	Burn time, s	Test end
Test	Identifier	Date	Greenwich mean time			O_2	N_2	CO_2	He					
FLEX–276	H15H201	11/30/11	12:09:00	Heptane	532.5	.17	.38	0	.45	1.61	.91	1.06	1.4	Completion
FLEX–277	H15M102	12/5/11	22:54:10	Methanol	530.4	.17	.38	0	.45	2.79	2.3	.63	4	Extinction
FLEX–278	H15M201	12/5/11	23:39:04	Methanol	531.5	.17	.38	0	.45	2.68	2.31	.66	2.9	Extinction
FLEX–279	H19H101	12/8/11	22:29:44	Heptane	764.7	.21	.64	0	.15	3.54	2.91	.55	7.6	Extinction
FLEX–280	H19H201	12/8/11	23:41:45	Heptane	766.2	.21	.64	0	.15	2.82	.73	.65	11.7	Extinction

Appendix B.—Droplet and Flame Sizes

Figures 5 to 280 show the results of each experiment. These figures show the droplet diameter squared and the flame diameter (for both the Low Light Level Ultra-Violet (LLUV) and Multi-User Droplet Combustion Apparatus (MDCA) color camera) as functions of time. Time zero in the plots corresponds to when the igniter was energized. This time came from data files downlinked from the CIR after a test. The data for each test are also available in a text file associated with this report.

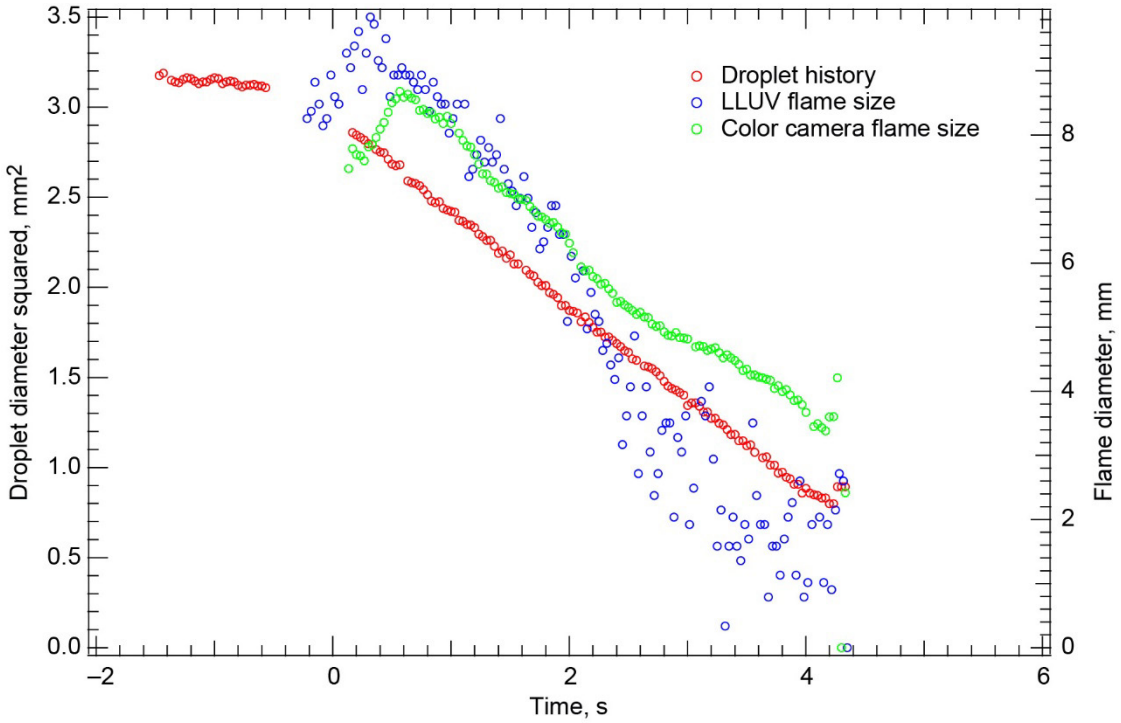

Figure 5.—Test FLEX–001. Free-floating methanol droplet burning in a cabin air (0.21/0.79 O_2/N_2), 1.0-atm ambient environment. This was the first FLEX test. The droplet remained in the fields of view (FOVs) of all the cameras for the entire test. Because the Low Light Level Ultra-Violet (LLUV) camera settings were not optimal, the LLUV data are not reliable. The droplet probably disrupted at the end of the test coincident with flame extinction. The igniters were too bright and overexposed the High-Bit-Depth Multispectral (HiBMs) images during ignition, so the droplet diameter could not be measured accurately.

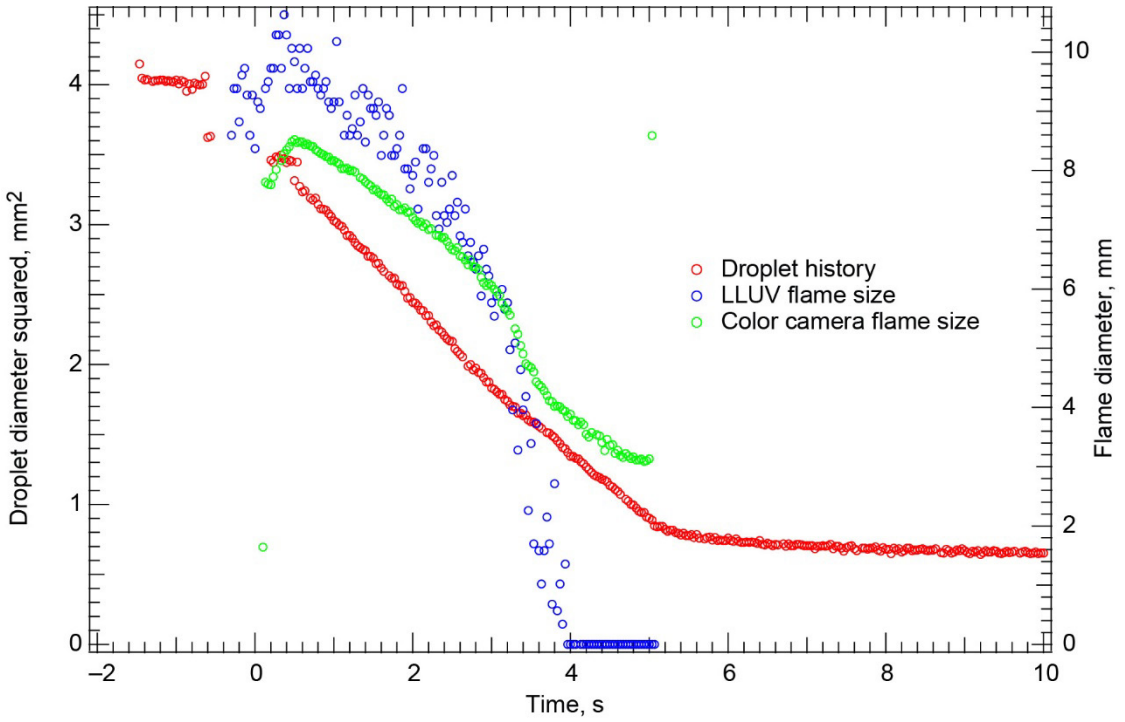

Figure 6.—Test FLEX–002. Free-floating methanol droplet burning in a cabin air (0.21/0.79 O_2/N_2), 1.0-atm ambient environment. The droplet remained in the fields of view (FOVs) of all the cameras for the entire test and extinguished diffusively. Because this was a calibration run, the Low Light Level Ultra-Violet (LLUV) setting was not optimal. Consequently, the LLUV flame data are not reliable, especially near the end of the test. The droplet did not disrupt, but clearly something happened to the flame near the end of the test.

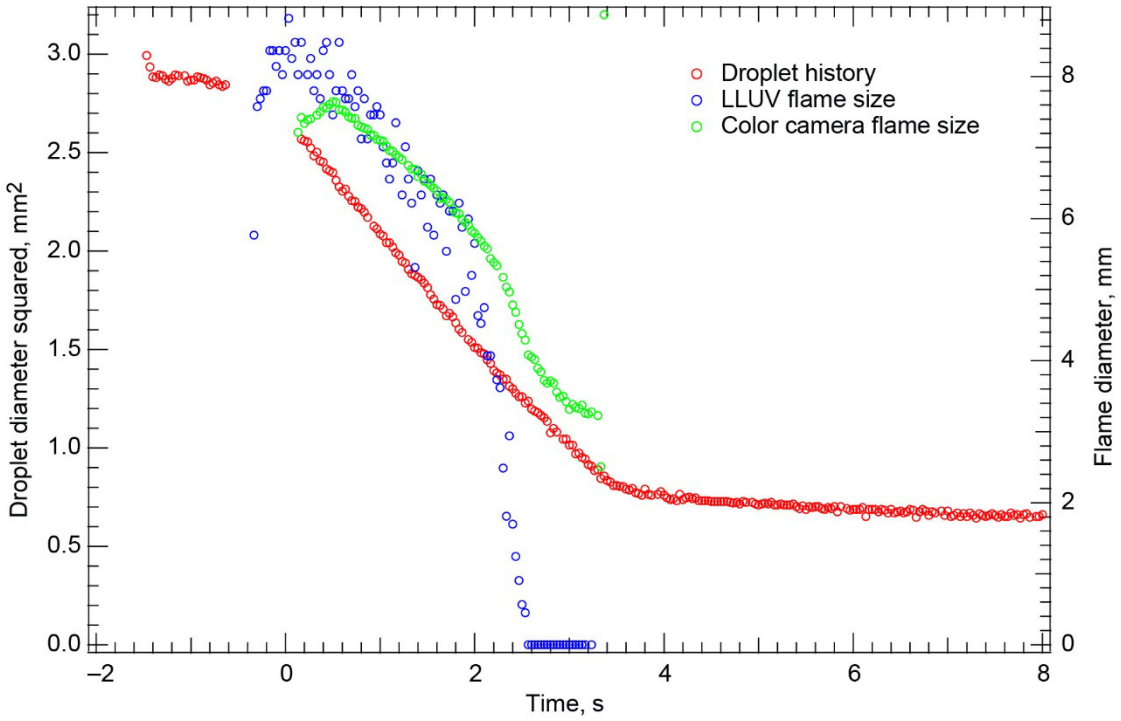

Figure 7.—Test FLEX–003. Free-floating methanol droplet burning in a cabin air (0.21/0.79 O_2/N_2), 1.0-atm ambient environment. The droplet remained in the fields of view (FOVs) of all the cameras for the entire test. Because this was a calibration run, the Low Light Level Ultra-Violet (LLUV) setting was not optimal as indicated by the flame being very difficult to see and measure (especially near the end of the test).

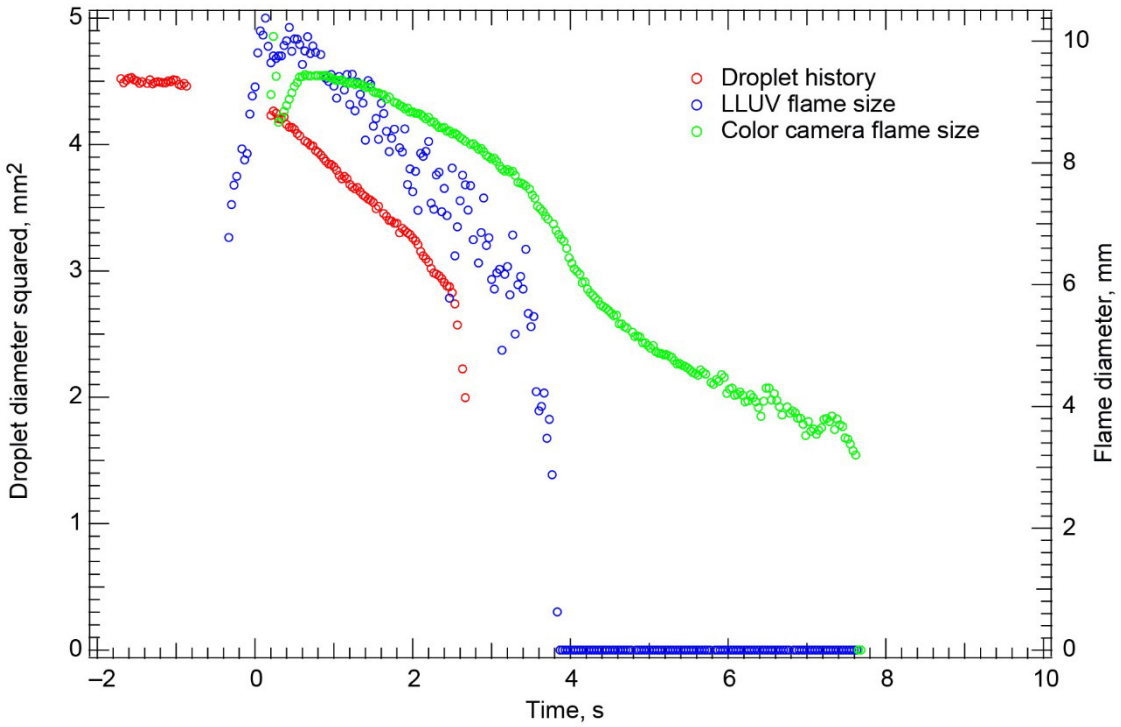

Figure 8.—Test FLEX–004. Free-floating methanol droplet burning in a cabin air (0.21/0.79 O_2/N_2), 1.0-atm ambient environment. The droplet drifted south in the High-Bit-Depth Multispectral (HiBMs) field of view (FOV) after deployment and ignition, leaving the HiBMs FOV one-third of the way through the burn. There was some evidence of flame disruption before the flame extinguished, but it was difficult to judge from the color camera images. This was a calibration test point. The igniter overwhelmed the HiBMs and made measuring the droplet impossible until the igniters moved out of the FOV. The Low Light Level Ultra-Violet (LLUV) setting was not optimal, and the flame nearly disappeared from the LLUV halfway through the burn, coincident with when the color camera showed a noticeable change in the flame behavior.

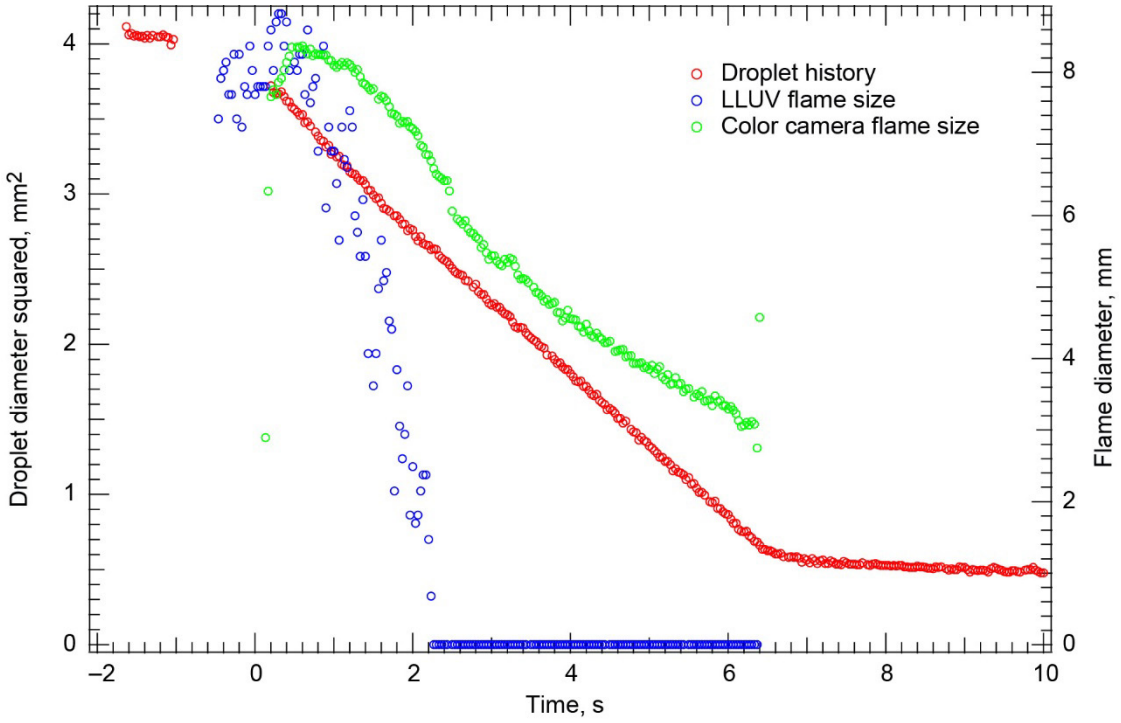

Figure 9.—Test FLEX–005. Free-floating methanol droplet burning in a cabin air (0.21/0.79 O_2/N_2), 1.0-atm ambient environment. The droplet remained in the fields of view (FOVs) of all the cameras. Because this was a calibration run, the Low Light Level Ultra-Violet (LLUV) settings were not optimal. Consequently, halfway through the burn the flame became undetectable in the LLUV. There was no evidence of disruptive burning near extinction. The flame, however, seemed to shrink quickly after ignition—maybe because of a small bubble burst.

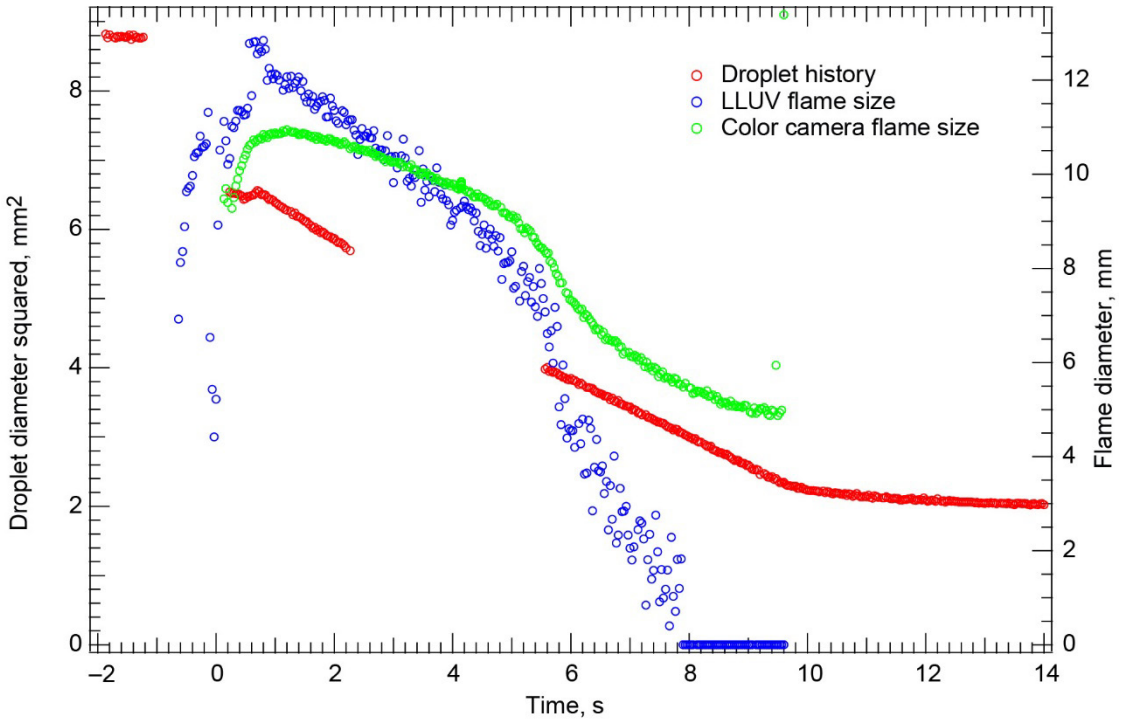

Figure 10.—Test FLEX–006. Free-floating methanol droplet burning in a cabin air (0.21/0.79 O_2/N_2), 1.0-atm ambient environment. The droplet was misshapen on the needles before it stretched and deployed. Ignition imparted a significant drift velocity on the droplet to the east. This could be due to a small air bubble that distorted the droplet and then popped when the igniters turned on. The droplet drifted out of the High-Bit-Depth Multispectral (HiBMs) field of view (FOV) and then drifted back in the FOV. The flame extinguished without disruption. This was a calibration test. Because the Low Light Level Ultra-Violet (LLUV) settings were not optimized for these tests, late in the flame lifetime the flame was not discernable in the LLUV.

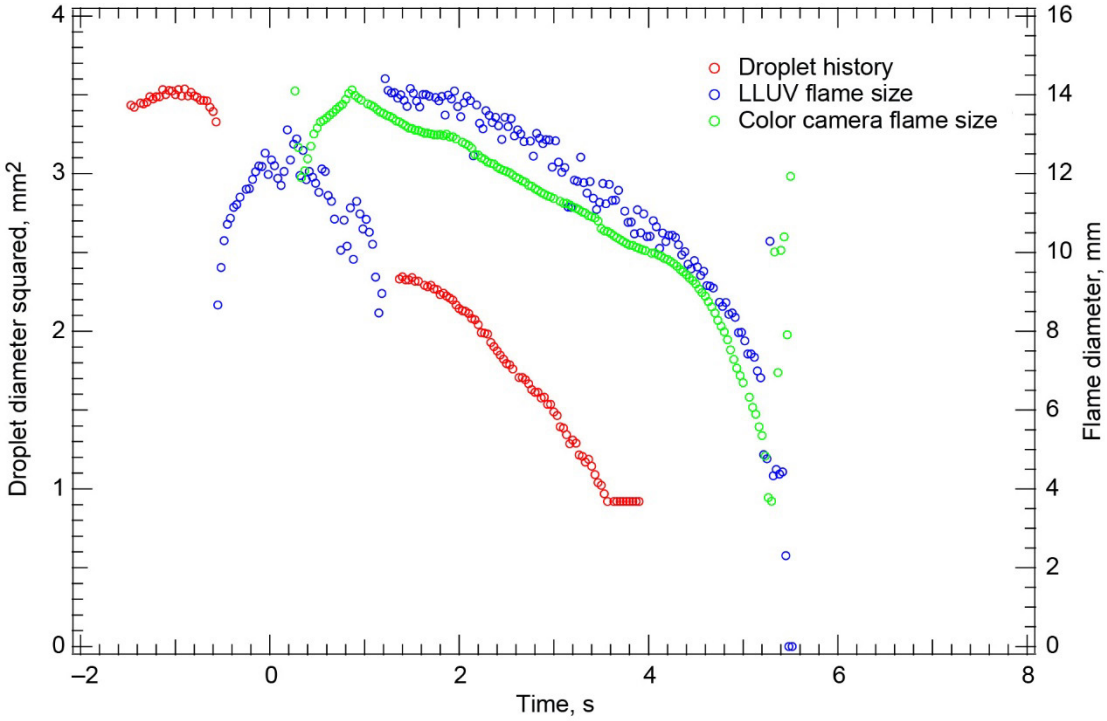

Figure 11.—Test FLEX−007. Free-floating heptane droplet burning in a cabin air (0.21/0.79 O_2/N_2), 1.0-atm ambient environment. The droplet deployed and ignited with little residual velocity and remained within the High-Bit-Depth Multispectral (HiBMs) field of view (FOV) for the entire test. The droplet burned with a very luminous flame that obscured the droplet in the HiBMs for a large portion of the test. The droplet burned to a small droplet size and then disrupted. The last part of the droplet history was obscured by the luminous flame.

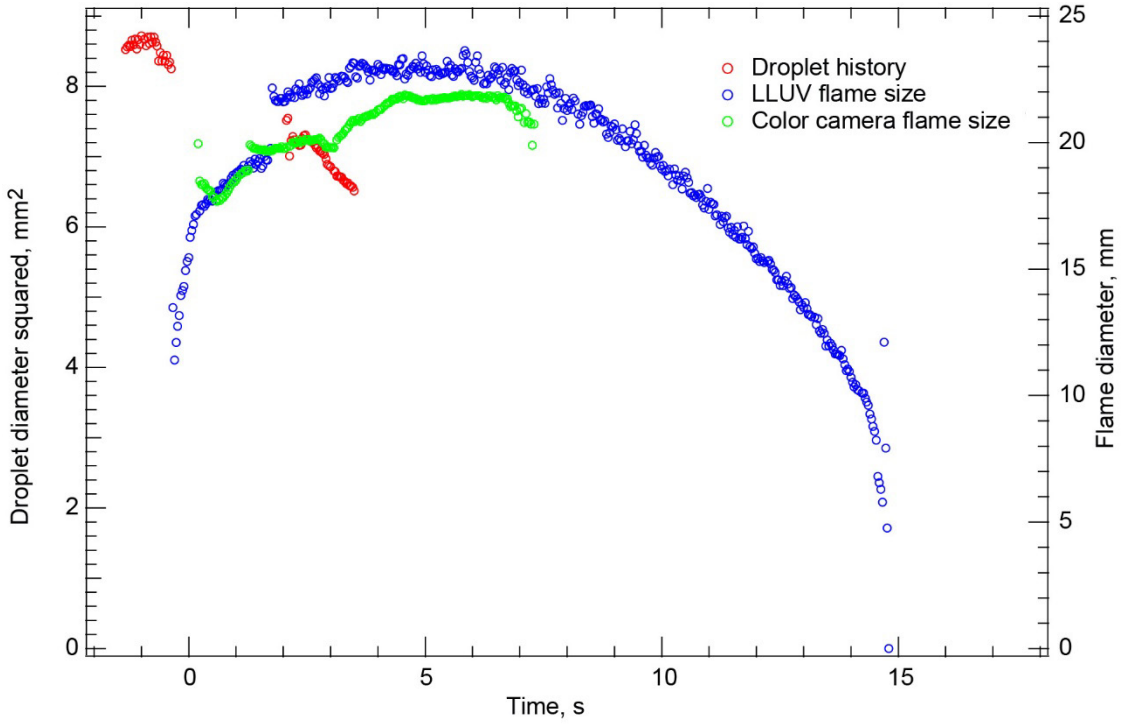

Figure 12.—Test FLEX−008. Free-floating heptane droplet burning in a cabin air (0.21/0.79 O_2/N_2), 1.0-atm ambient environment. The droplet drifted southeast out of the High-Bit-Depth Multispectral (HiBMs) field of view (FOV) a few seconds after the igniter was withdrawn. Significant sooting was apparent in the HiBMs. The droplet also drifted out of the color camera FOV. It remained in the Low Light Level Ultra-Violet (LLUV) FOV for the entire burn. There is a lot of noise in the droplet diameter data because of the soot, but the LLUV showed that the droplet disrupted at the end of the burn.

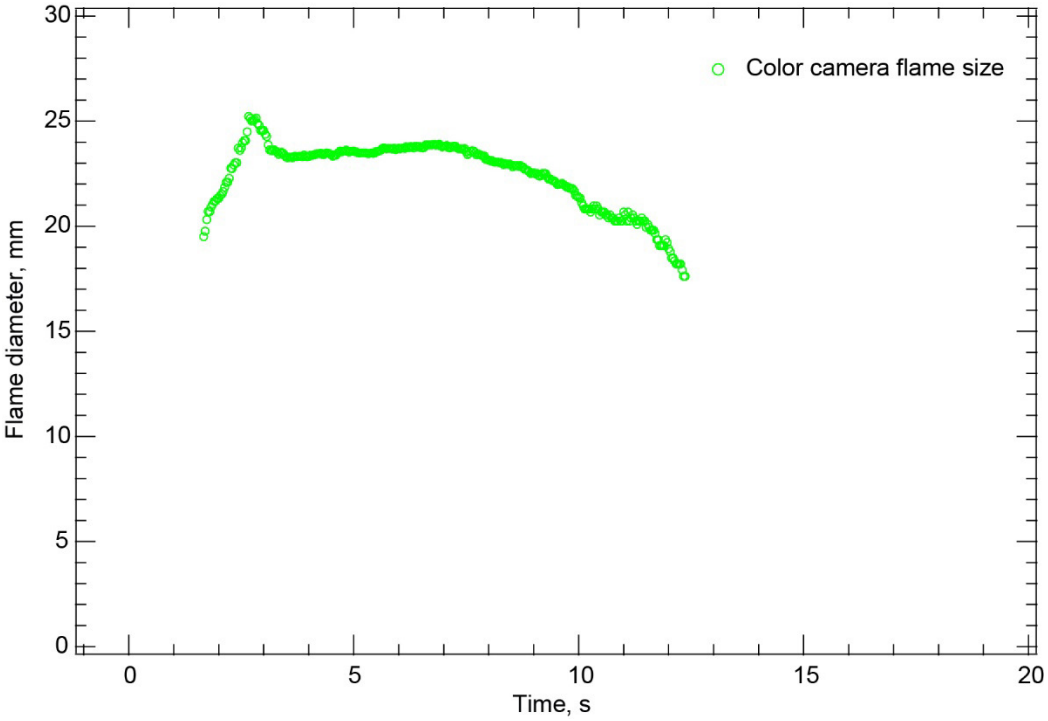

Figure 13.—Test FLEX−009. Free-floating heptane droplet burning in a cabin air (0.21/0.79 O_2/N_2), 1.0-atm ambient environment. The deployment was very poor, and the droplet drifted out of the fields of view (FOVs) of all the cameras very shortly after deployment and ignition. No Image Processing and Storage Unit (IPSU) data were downlinked for this test. The color camera analysis was from the downlinked video.

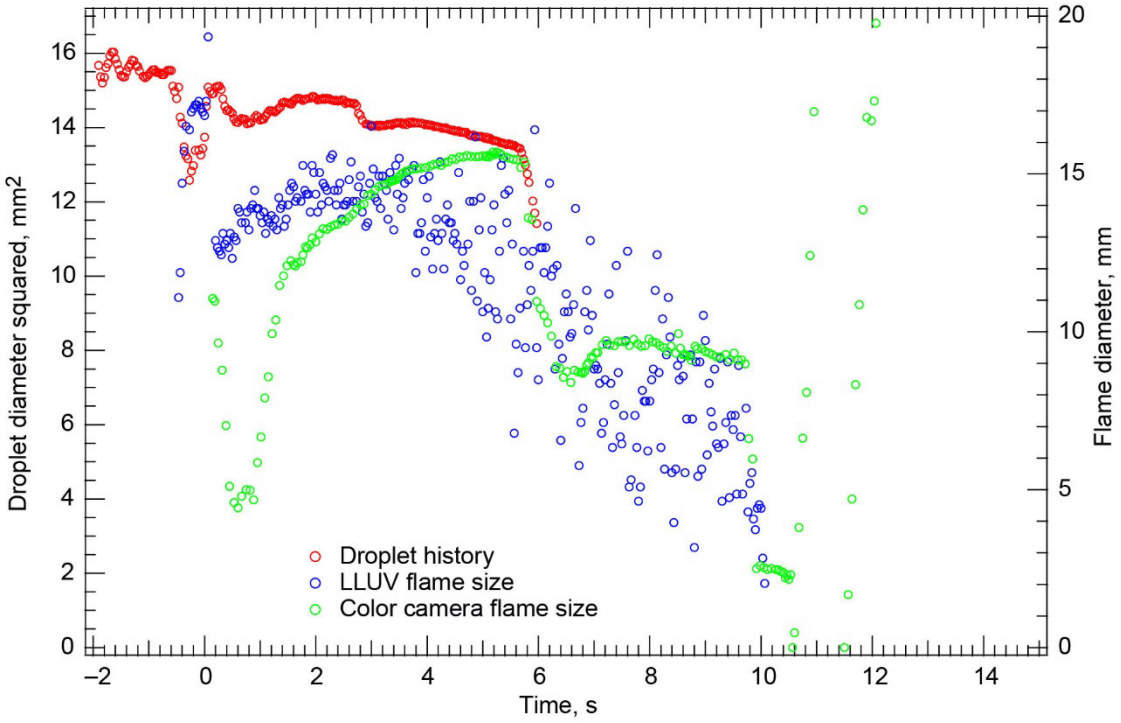

Figure 14.—Test FLEX−010. Free-floating methanol droplet burning in a 0.21/0.09/0.70 $O_2/N_2/CO_2$, 3.0-atm ambient environment. The droplet drifted southeast after deployment, hit the igniter, changed direction, and quickly moved west out of the fields of view (FOVs) of the High-Bit-Depth Multispectral (HiBMs), Low Light Level Ultra-Violet (LLUV), and color camera. The HiBMs produced a saturated image that influenced the droplet size measurement. In addition, the HiBMs backlight was too strong, and the droplet size measurement was a function of which “quad-slice” the droplet was in the HiBMs image. Because the droplet was in the HiBMs FOV for only a short time, no burning rate constant or extinction droplet diameter is reported.

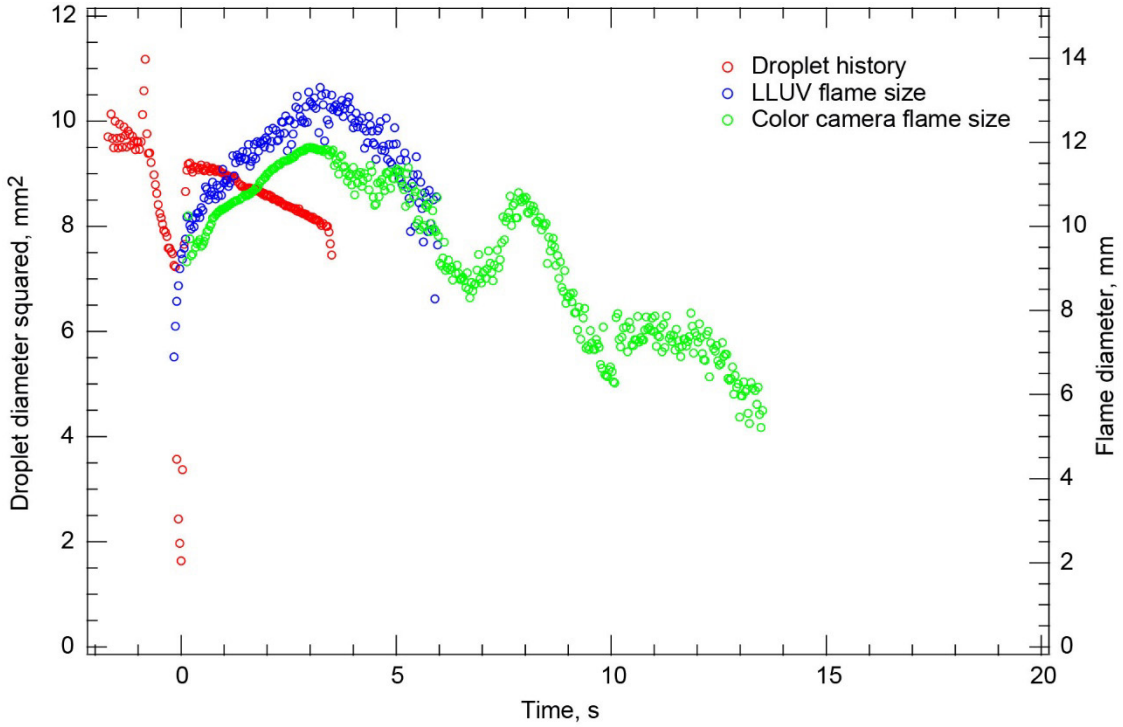

Figure 15.—Test FLEX−011. Free-floating methanol droplet burning in a 0.21/0.09/0.70 $O_2/N_2/CO_2$, 3.0-atm ambient environment. The droplet drifted southeast in the High-Bit-Depth Multispectral (HiBMs) field of view (FOV) after deployment, hit the lower igniter, and then drifted very quickly to the east and out of the HiBMs FOV. The HiBMs and illumination settings were not correct, so the igniters obscured the droplet. Also the background was near saturation, so the droplet size is a function of the "quadrant slice" of the HiBMs image that it was in. The droplet drifted out of the Low Light Level Ultra-Violet (LLUV) FOV, but it remained in the color camera FOV most of the time.

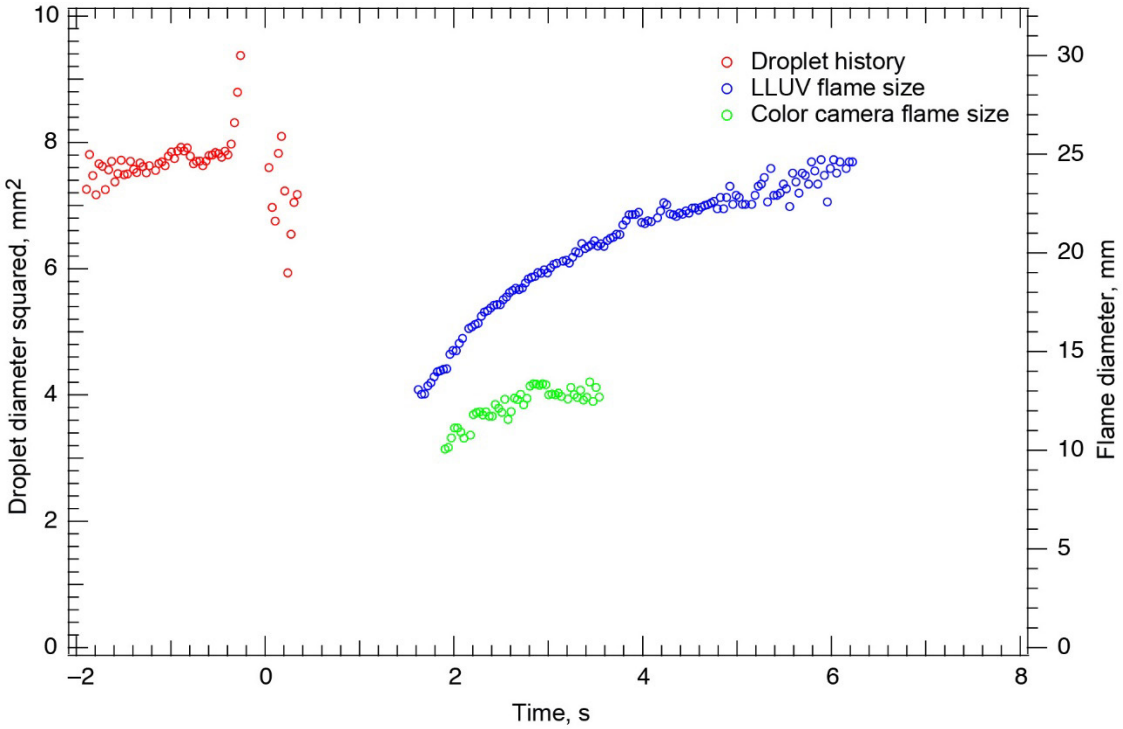

Figure 16.—Test FLEX−012. Free-floating heptane droplet burning in a 0.21/0.09/0.70 $O_2/N_2/CO_2$, 3.0-atm ambient environment. The deployment was very poor. The droplet drifted toward the upper igniter in the High-Bit-Depth Multispectral (HiBMs) field of view (FOV) after deployment, hooked around the igniter, and got hit by the igniter when the igniter was withdrawn. That propelled the droplet rapidly out of the HiBMs FOV. The droplet left the FOVs of all the cameras before burning to a presumed extinction. The flame was very luminous and yellow, with significant sooting present in the HiBMs.

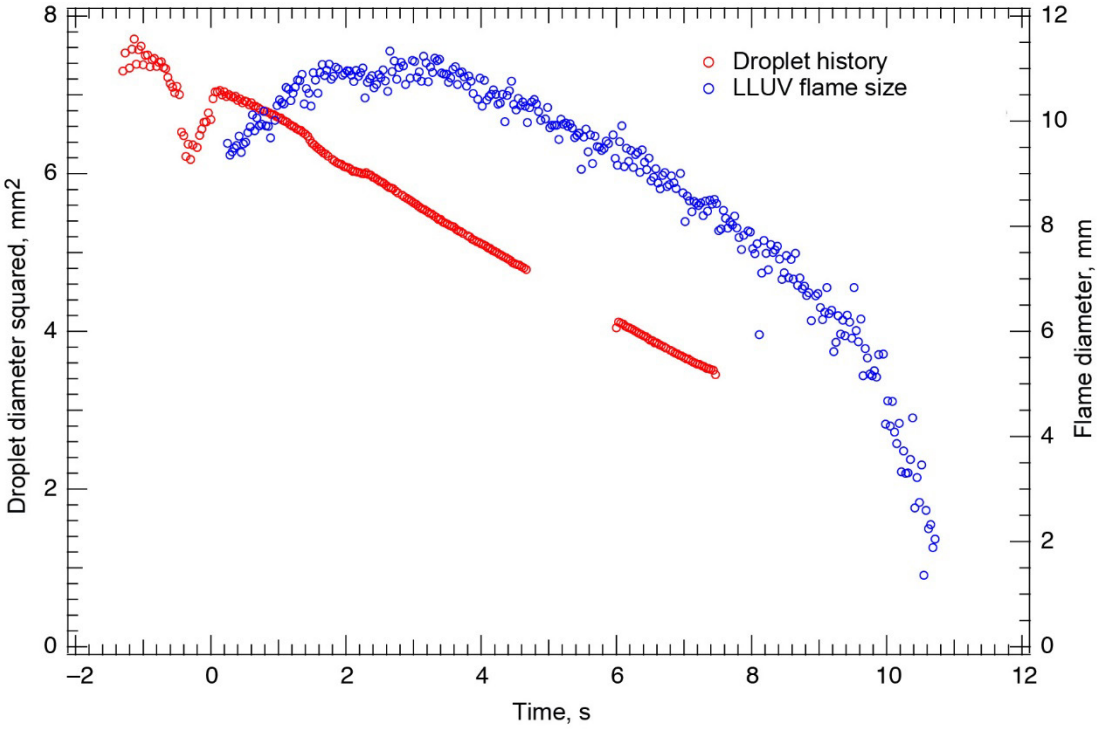

Figure 17.—Test FLEX−013. Free-floating methanol droplet burning in a 0.21/0.09/0.70 $O_2/N_2/CO_2$, 3.0-atm ambient environment. The droplet drifted west in the High-Bit-Depth Multispectral (HiBMs) field of view (FOV), hit the igniter, drifted southeast after the igniter was withdrawn, and left the FOV. It reappeared for a short time before disappearing again. The glow from the igniter influenced the droplet size measurement early, the HiBMs and illumination package settings were not good enough for reliable droplet size measurements. Because the droplet was not in the HiBMs FOV for enough of the test, no extinction droplet diameter is reported. The color camera Image Processing and Storage Unit (IPSU) did not record any images after deployment.

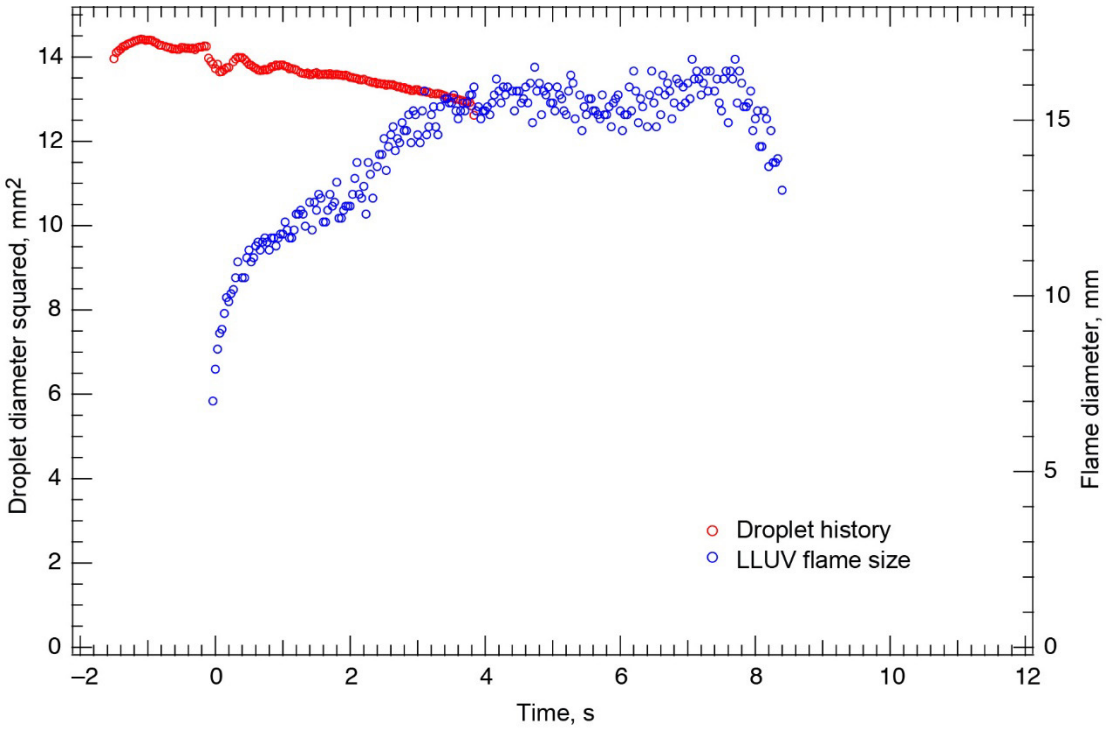

Figure 18.—Test FLEX−014. Free-floating methanol droplet burning in a 0.21/0.09/0.70 $O_2/N_2/CO_2$, 3.0-atm ambient environment. The droplet drifted significantly to the northwest in the High-Bit-Depth Multispectral (HiBMs) after deployment and ignition (ignition did not change the motion visually). Then the droplet quickly drifted out of the field of view (FOV) of the HiBMs. The color camera Image Processing and Storage Unit (IPSU) did not record any images for this test. The droplet also drifted north out of the Low Light Level Ultra-Violet (LLUV) FOV before the flame extinguished. Because the droplet was within the HiBMs FOV for only a limited time, no burning rate or extinction droplet diameter is reported.

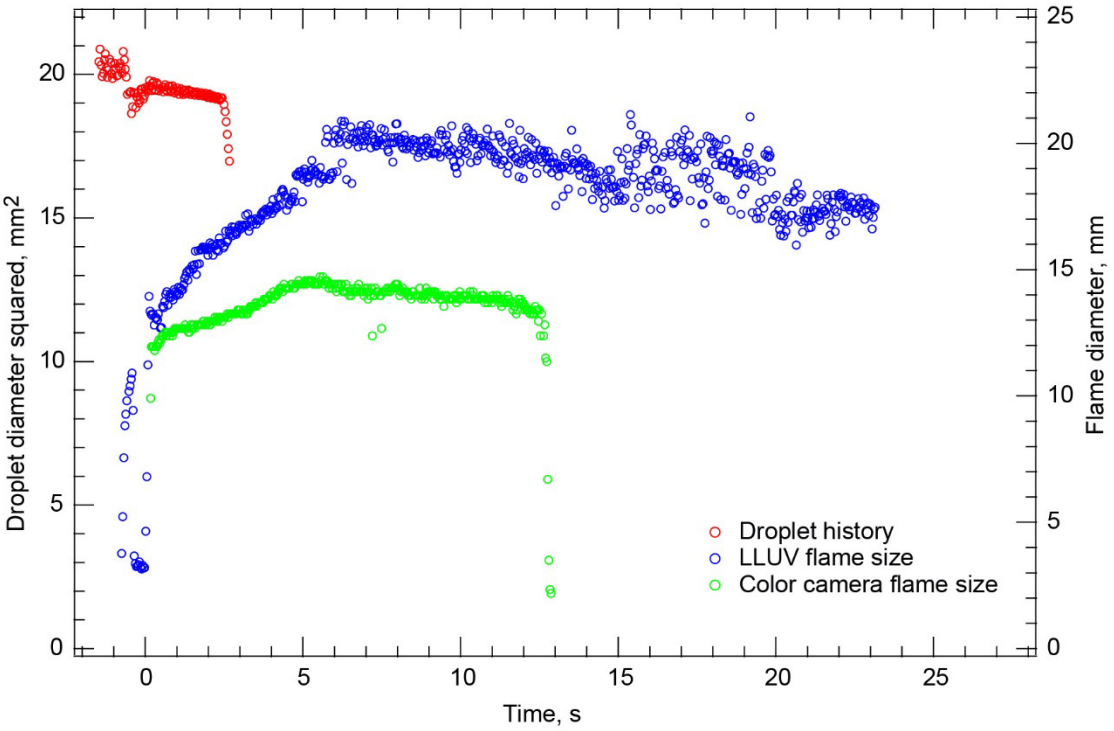

Figure 19.—Test FLEX−015. Free-floating methanol droplet burning in a 0.21/0.09/0.70 $O_2/N_2/CO_2$, 3.0-atm ambient environment. After ignition, the droplet quickly drifted north and out of the High-Bit-Depth Multispectral (HiBMs) field of view (FOV). Because the droplet was in the HiBMs FOV for only a short time, no burning rate constant is reported. The droplet did not drift out of the FOV of the Low Light Level Ultra-Violet (LLUV), but the Image Processing and Storage Unit (IPSU) data for the LLUV ended before the flame extinguished. The droplet drifted northeast and out of the color camera FOV before the flame extinguished. In the color camera view, the flame was visibly brighter in the direction of the translation, an indication that the convective motion was impacting the flame behavior significantly.

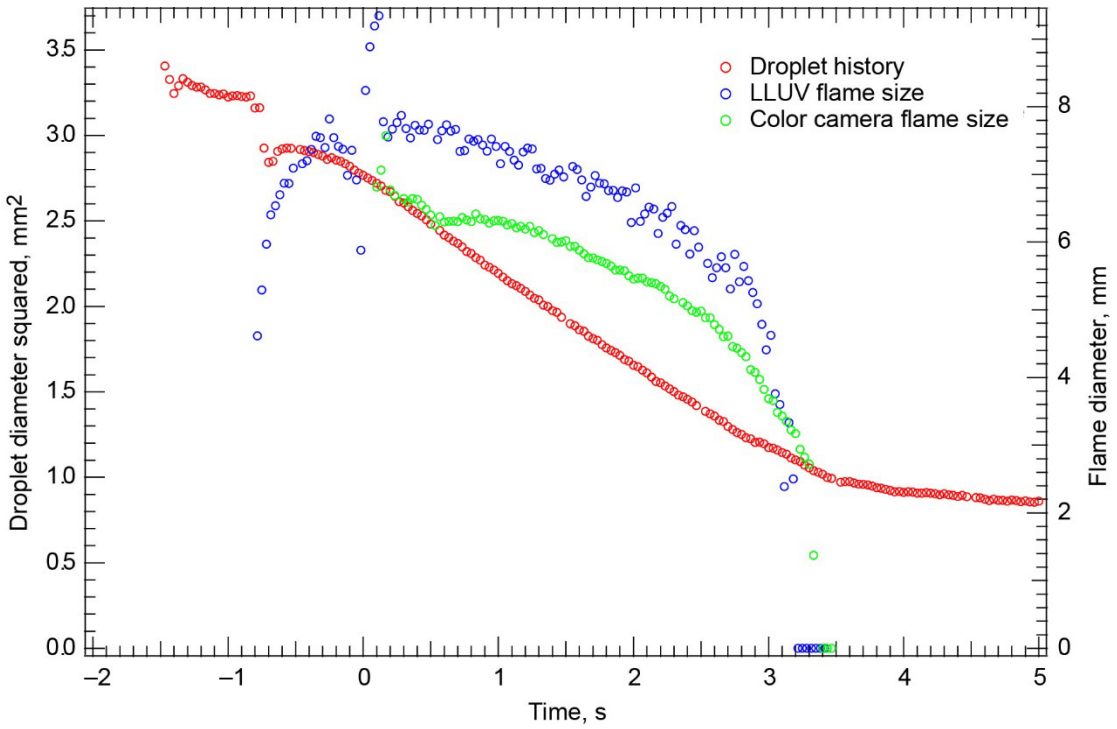

Figure 20.—Test FLEX−016. Free-floating methanol droplet burning in a 0.21/0.09/0.70 $O_2/N_2/CO_2$, 3.0-atm ambient environment. The droplet drifted and hit the igniter before the igniter was withdrawn. Then the droplet drifted slowly west in the High-Bit-Depth Multispectral (HiBMs) field of view (FOV), but it remained in the FOVs of all the cameras for the entire test. There was significant translation in the HiBMs FOV during the test.

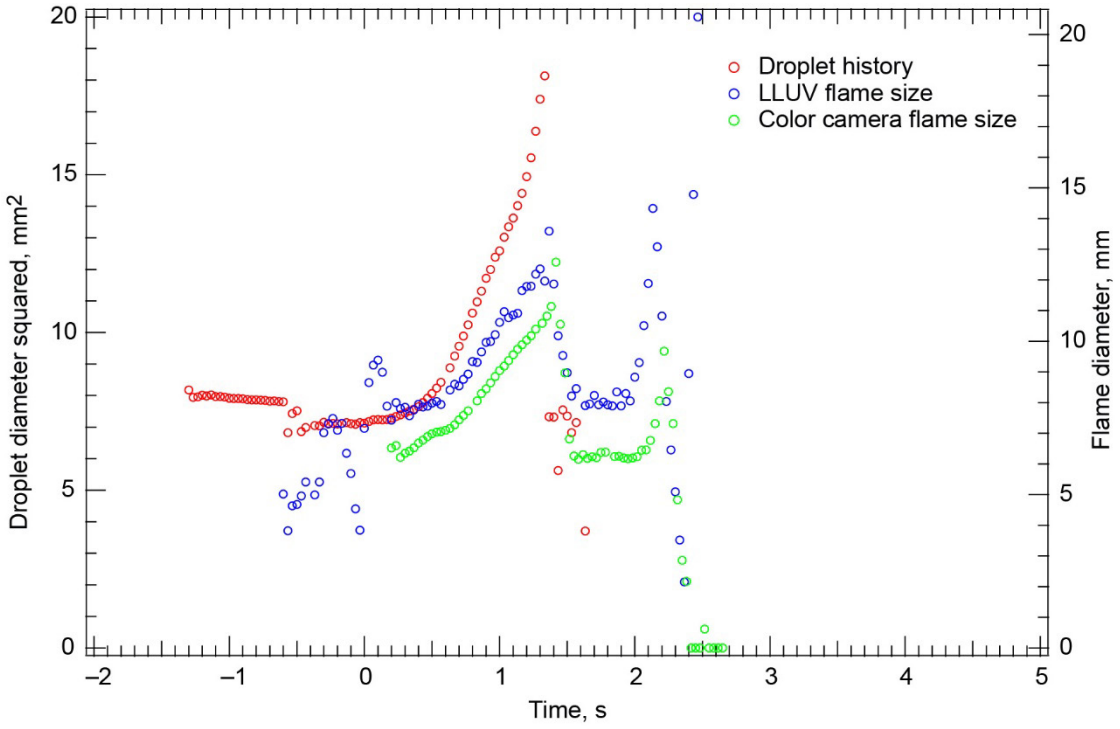

Figure 21.—Test FLEX−017. Free-floating methanol droplet burning in a 0.21/0.09/0.70 $O_2/N_2/CO_2$, 3.0-atm ambient environment. The droplet drifted east in the High-Bit-Depth Multispectral (HiBMs) field of view (FOV) after deployment, hit the igniter, and then drifted north. The droplet immediately began to grow, disrupted, and finally shattered, causing the flame to extinguish. This behavior was probably due to a gas bubble being trapped in the droplet after deployment.

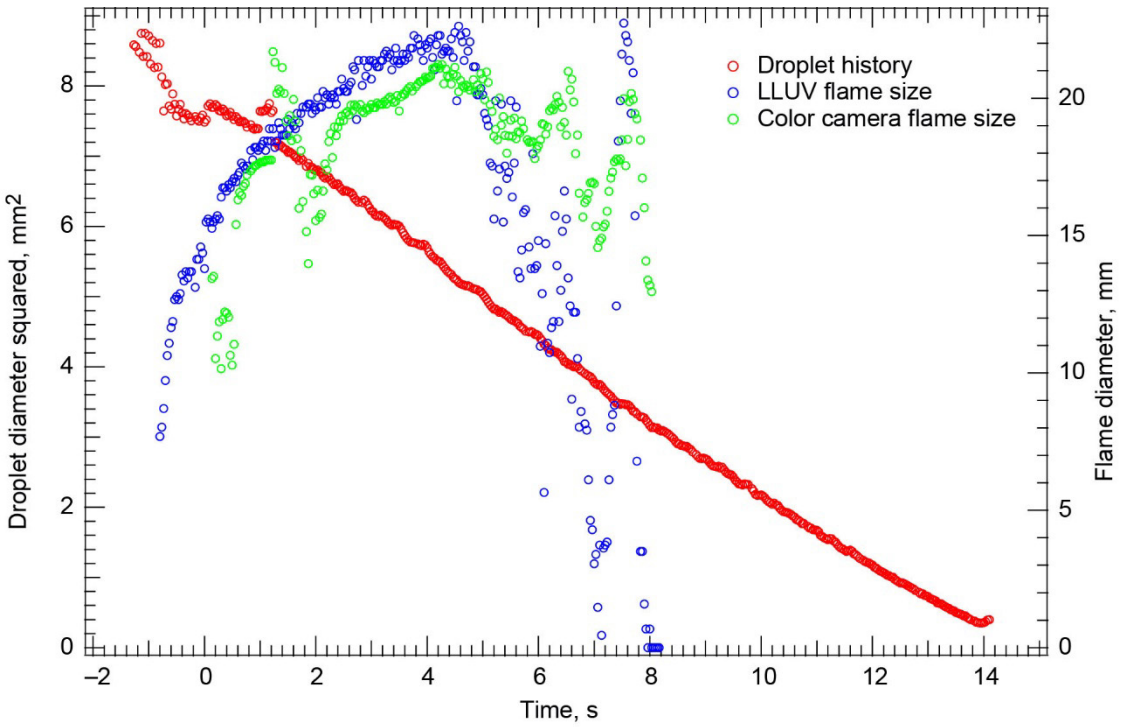

Figure 22.—Test FLEX−018. Free-floating heptane droplet burning in a 0.21/0.09/0.70 $O_2/N_2/CO_2$, 2.0-atm ambient environment. There was a luminous yellow flame immediately after ignition, with the High-Bit-Depth Multispectral (HiBMs) view showing significant soot formation. Then the luminous flame disappeared, and a dim blue flame surrounded the droplet. The flame oscillated and then appeared to extinguish in both the Low Light Level Ultra-Violet (LLUV) and color camera fields of view (FOVs). However, the droplet continued to vaporize vigorously, and the radiometer did not settle to its baseline value. There was “hazing” around the droplet in the HiBMs FOV during combustion, almost like there was significant internal liquid motion. The droplet disrupted after it drifted out of the HiBMs FOV. There probably was cool flame burning after the visible flame extinguished.

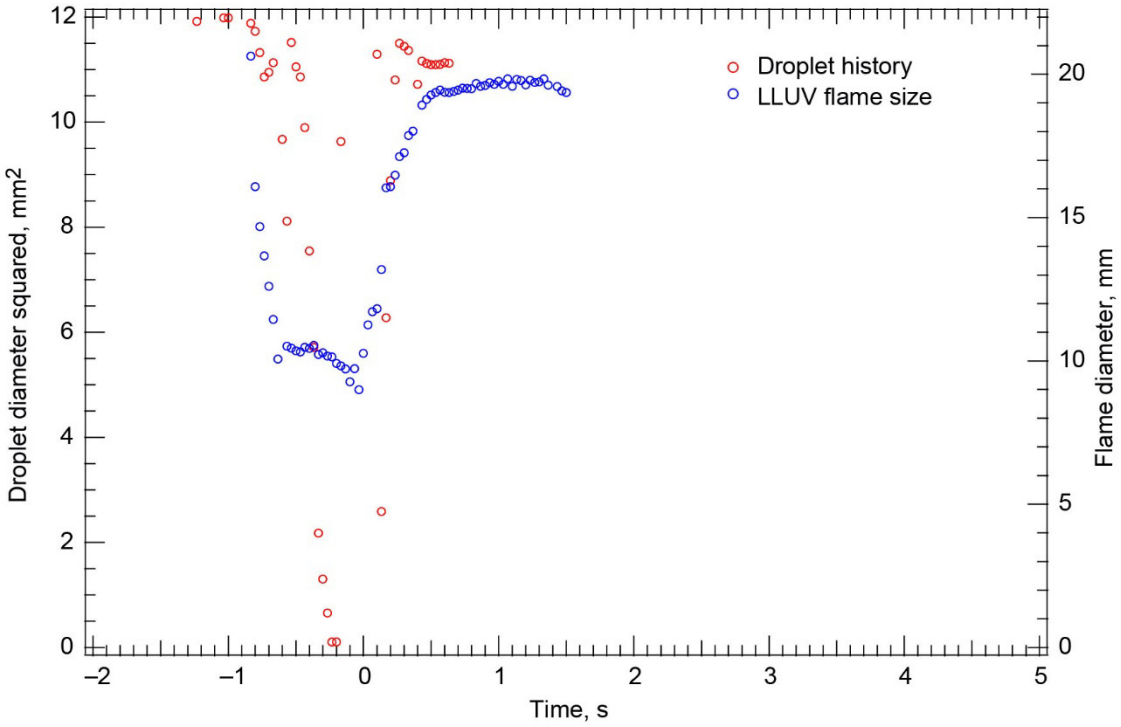

Figure 23.—Test FLEX−019. Free-floating heptane droplet burning in a 0.34/0.66 O_2/N_2, 0.70-atm ambient environment. The droplet was almost motionless after deployment, but after the igniters began to heat, a large impulse moved the droplet southwest and quickly out of High-Bit-Depth Multispectral (HiBMs) field of view (FOV). The droplet was nearly out of the FOV when the igniters began to move away from the droplet. There was significant sooting with large aggregates, so the data from this test are not reliable.

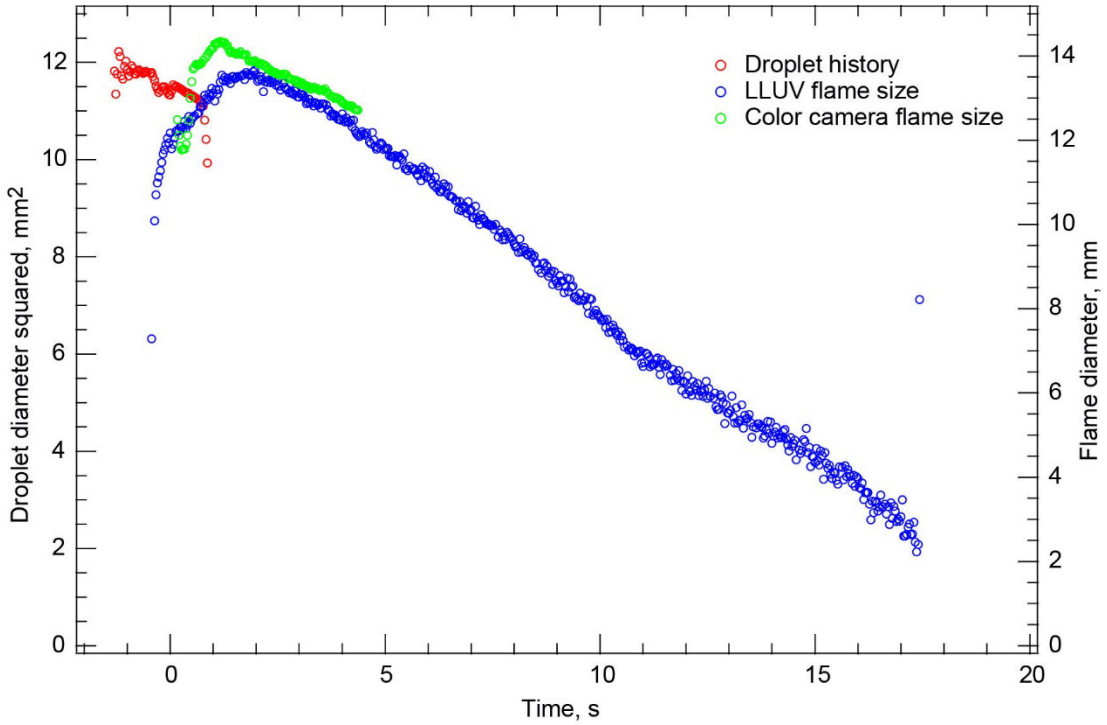

Figure 24.—Test FLEX−020. Free-floating methanol droplet burning in a 0.34/0.66 O_2/N_2, 0.70-atm ambient environment. The droplet drifted south in the High-Bit-Depth Multispectral (HiBMs) field of view (FOV) after deployment and ignition. It was in the HiBMs FOV for only a short time, and it drifted quickly out of the color camera FOV. It remained in the Low Light Level Ultra-Violet (LLUV) FOV for the entire burn and seemed to burn to either a very small extinction droplet size or completion.

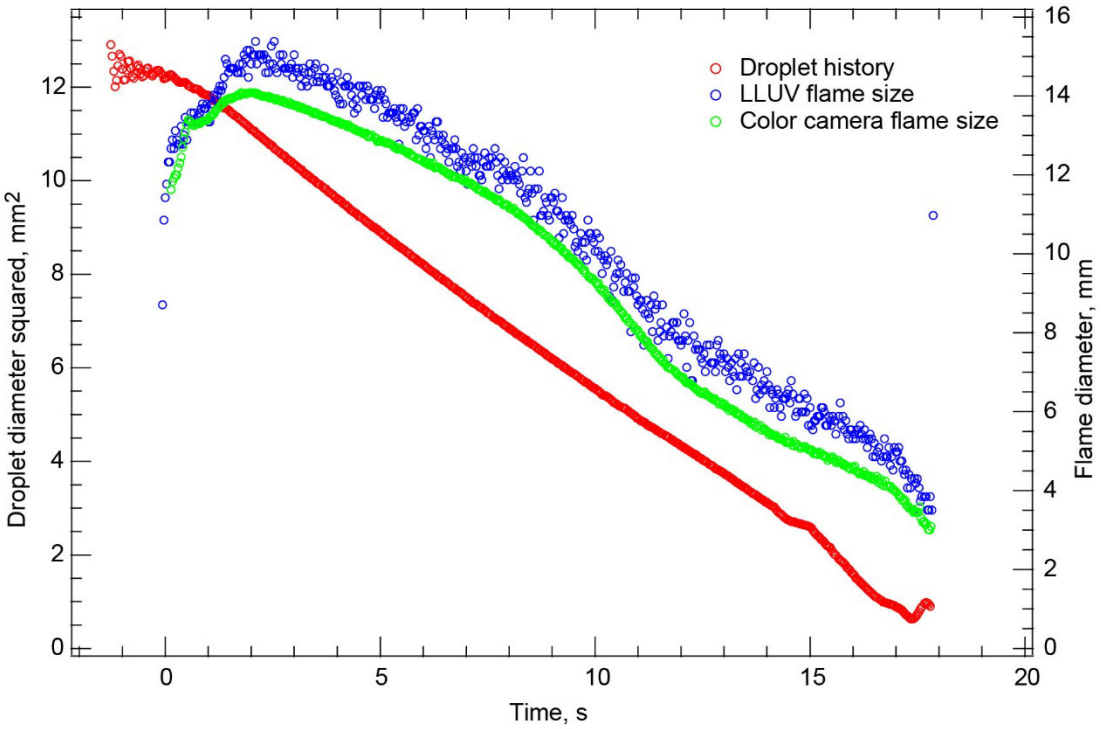

Figure 25.—Test FLEX−021. Free-floating methanol droplet burning in a 0.34/0.66 O_2/N_2, 0.70-atm ambient environment. This was the first successful test after switching from the high-CO_2, high-pressure ambient environments, where we had significant deployment problems. The droplet had a high burning rate and remained in the High-Bit-Depth Multispectral (HiBMs) field of view (FOV) for the entire test. Before the flame extinguished, the droplet distorted. Eventually, the droplet shattered coincident with flame extinction.

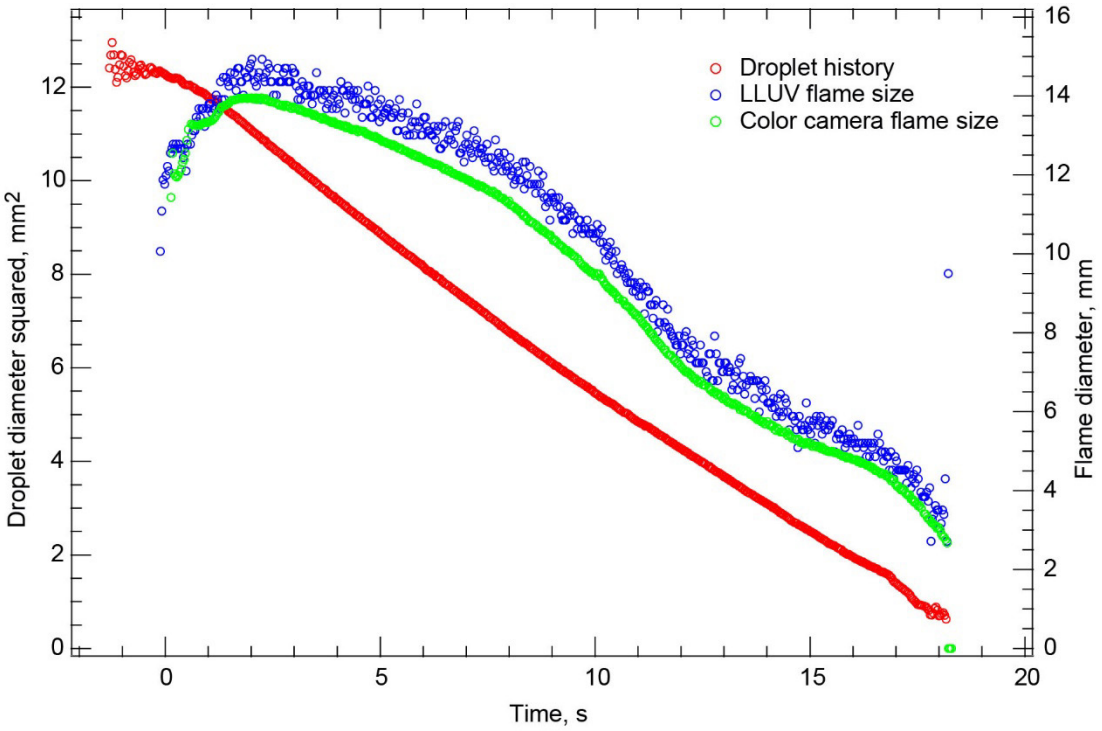

Figure 26.—Test FLEX−022. Free-floating methanol droplet burning in a 0.34/0.66 O_2/N_2, 0.7-atm ambient environment. The droplet remained in the High-Bit-Depth Multispectral (HiBMs) field of view (FOV) for the entire test and drifted slowly south-southeast during the test. The droplet began to change shape, and it became almost oblong with a pointed end (shown in the video) before disrupting. The disruption was coincident with flame extinction.

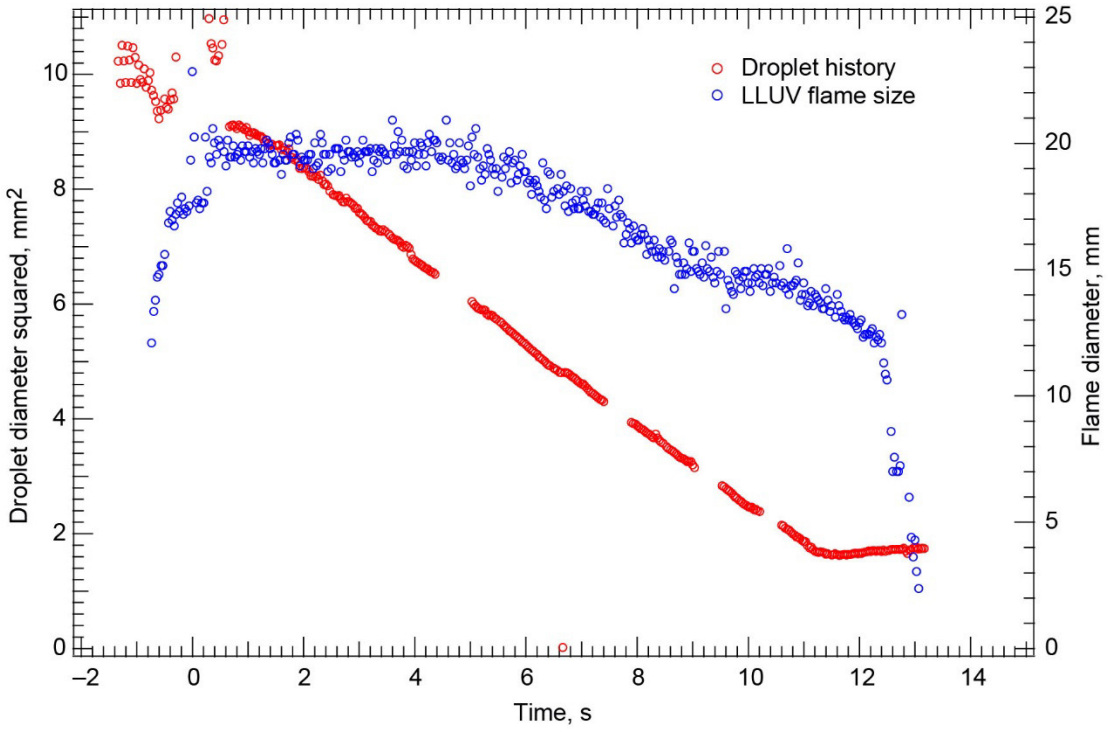

Figure 27.—Test FLEX−023. Free-floating heptane droplet burning in a 0.37/0.66 O_2/N_2, 0.70-atm ambient environment. The droplet drifted south in the High-Bit-Depth Multispectral (HiBMs) field of view (FOV) after deployment and ignition. It drifted partially out of the FOV, but then it drifted back in. Throughout the test, there was significant sooting with large agglomerates.

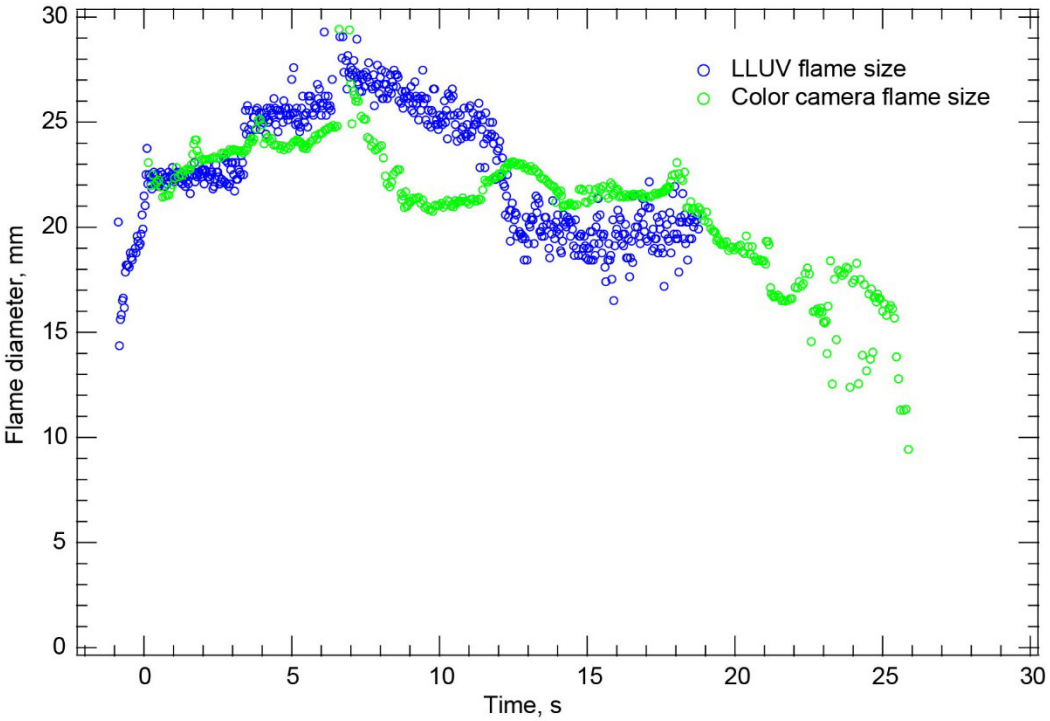

Figure 28.—Test FLEX−024. Free-floating heptane droplet burning in a 0.34/0.66 O_2/N_2, 0.70-atm ambient environment. The High-Bit-Depth Multispectral (HiBMs) Image Processing and Storage Unit (IPSU) did not record any images for this test. There appeared to be a needle fire. The color camera and Low Light Level Ultra-Violet (LLUV) IPSUs stopped recording before the test was complete. In addition, the LLUV images were recorded at 8-bit depth (instead of 12-bit depth), which resulted in more uncertainty in the LLUV flame size measurements.

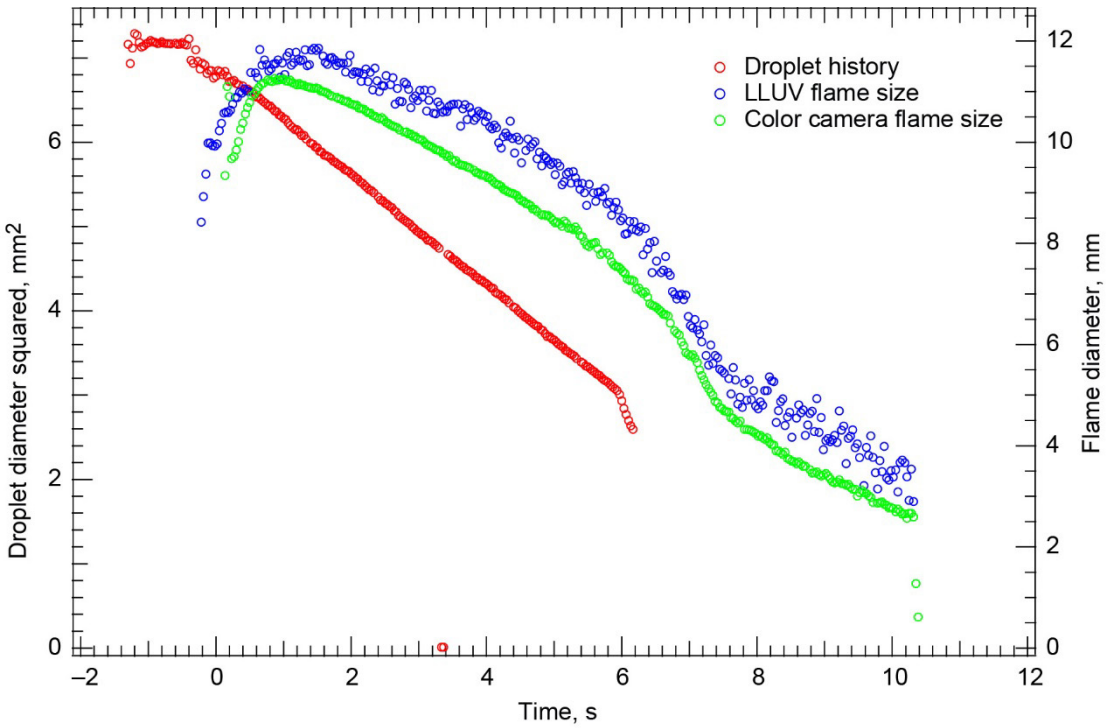

Figure 29.—Test FLEX−025. Free-floating methanol droplet burning in a 0.30/0.70 O_2/N_2, 0.7-atm ambient environment. The droplet drifted south in the High-Bit-Depth Multispectral (HiBMs) field of view (FOV) after deployment and ignition, leaving the FOV halfway through the burn before burning to near completion.

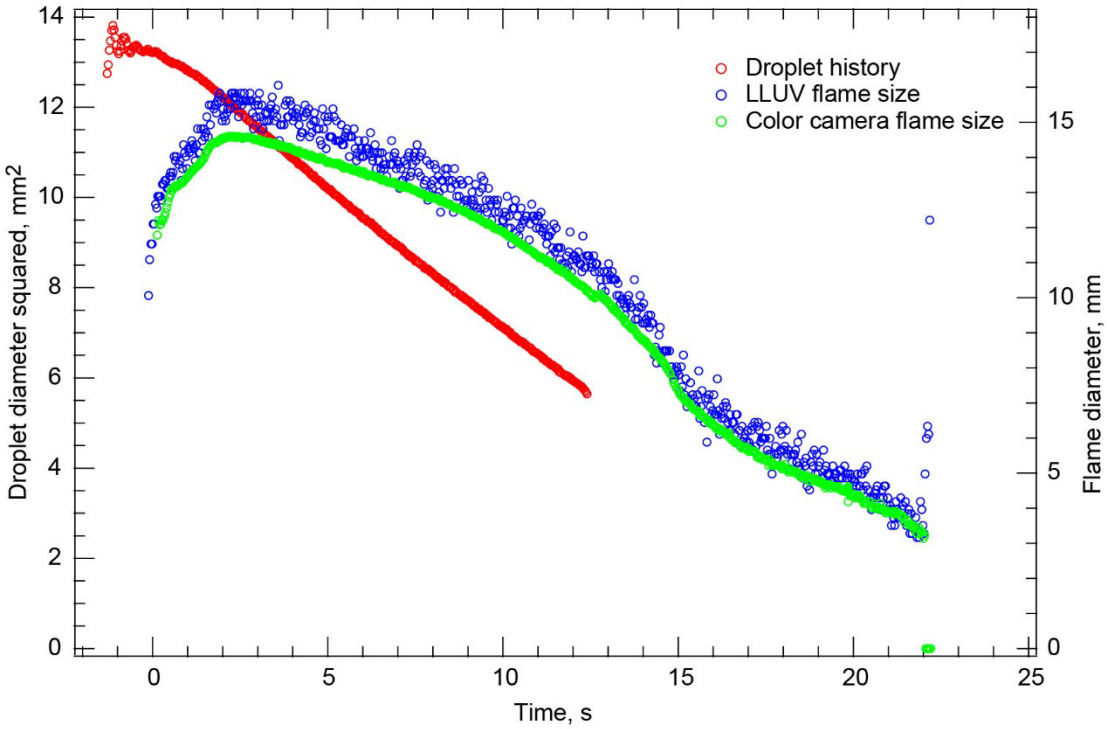

Figure 30.—Test FLEX−026. Free-floating methanol droplet burning in a 0.30/0.80 O_2/N_2, 0.70-atm ambient environment. The droplet drifted northwest out of the High-Bit-Depth Multispectral (HiBMs) field of view (FOV) about halfway through the burn. The droplet appeared to burn to completion or a very small size before it disrupted, causing the flame to extinguish.

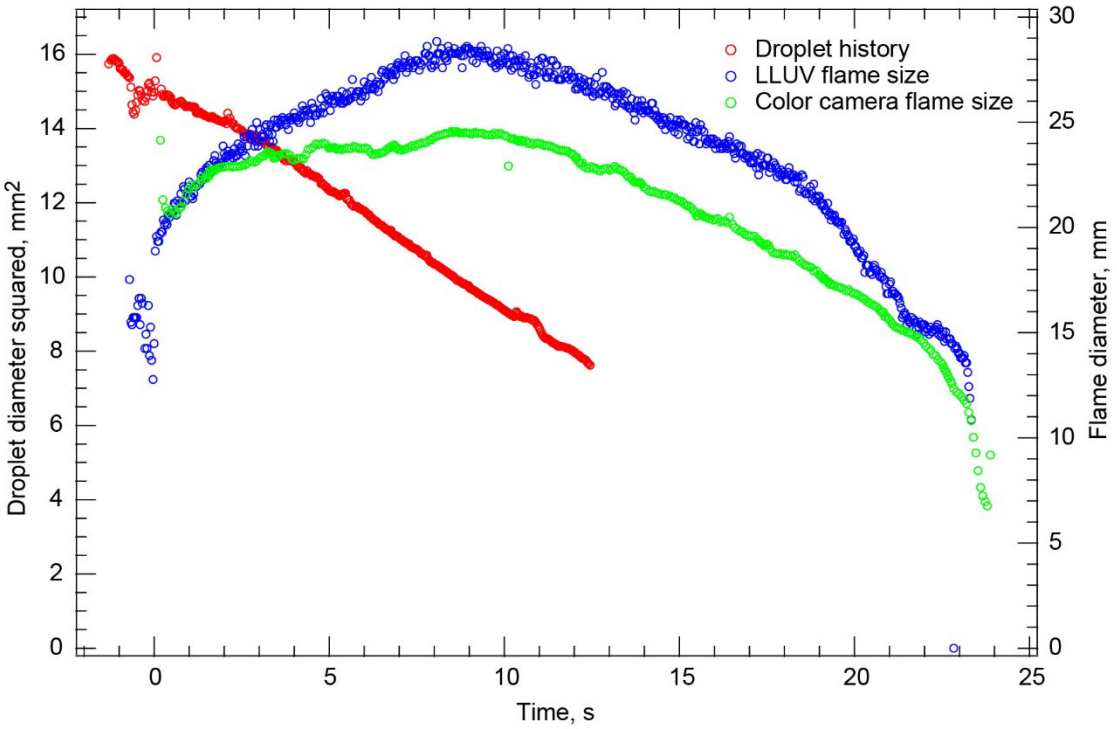

Figure 31.—Test FLEX−027. Free-floating heptane droplet burning in a 0.30/0.70 O_2/N_2, 0.7-atm ambient environment. The droplet drifted west in the High-Bit-Depth Multispectral (HiBMs) field of view (FOV) after deployment and ignition, and it drifted out of the FOV two-thirds of the way through the test. Initially luminous yellow, the flame dimmed to blue relatively quickly about one-third of the way through the burn. There was significant sooting with large soot agglomerates present throughout the burn. The droplet disrupted coincident with flame extinction.

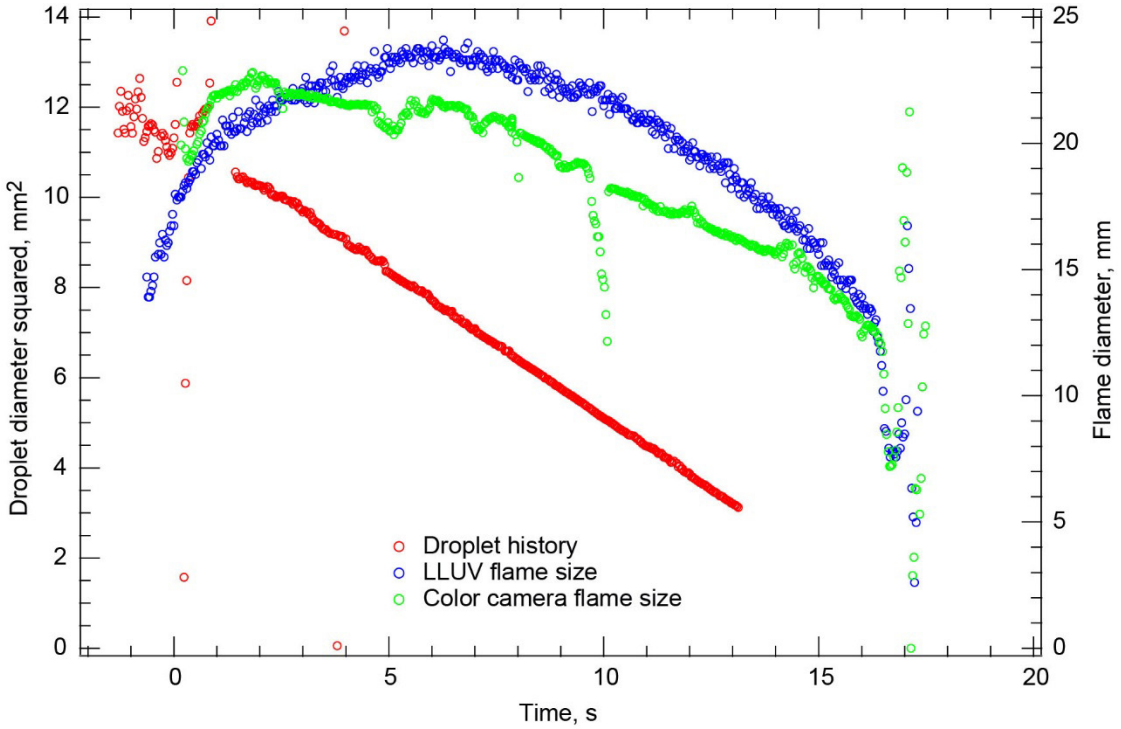

Figure 32.—Test FLEX−028. Free-floating heptane droplet burning in a 0.30/0.70 O_2/N_2, 0.7-atm ambient environment. The droplet drifted north in the High-Bit-Depth Multispectral (HiBMs) field of view (FOV) after deployment and ignition and out of the FOV approximately two-thirds of the way through the burn. A bright, luminous flame persisted throughout the droplet lifetime. There was significant sooting with large soot agglomerates present throughout the burn. The droplet disrupted coincident with flame extinction.

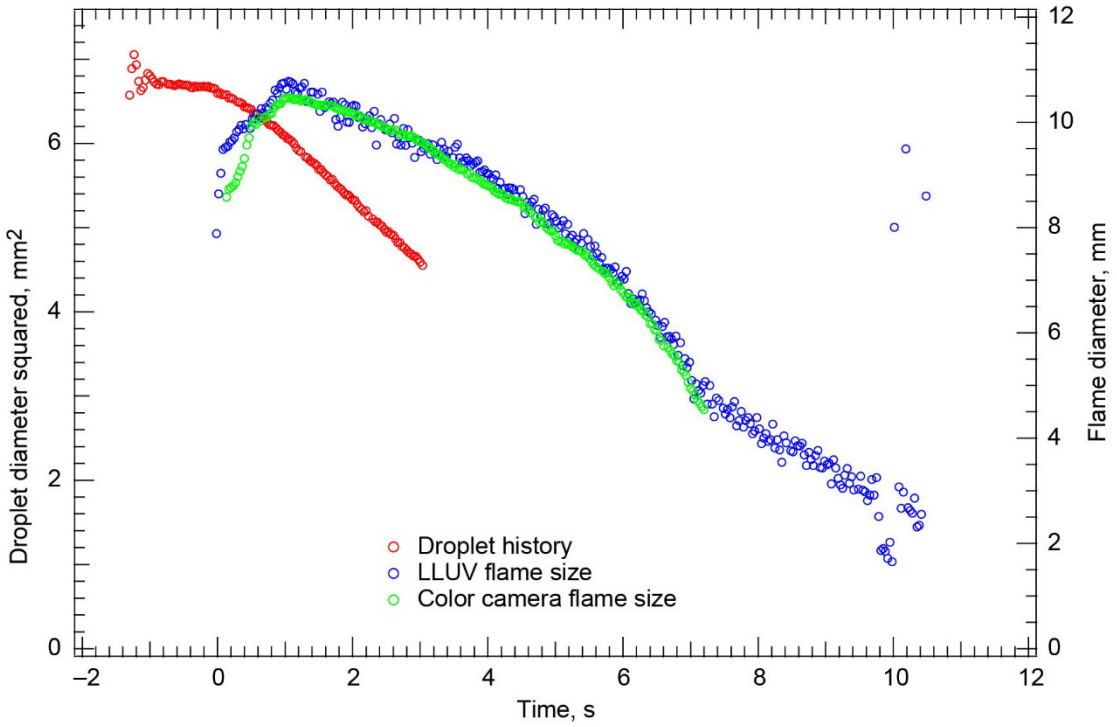

Figure 33.—Test FLEX−029. Free-floating methanol droplet burning in a 0.360/0.80 O_2/N_2, 1.0-atm ambient environment. The droplet drifted south out of the High-Bit-Depth Multispectral (HiBMs) field of view (FOV) about one-third of the way through the test. The droplet also drifted out of the color camera FOV before the flame extinguished. The droplet remained in the Low Light Level Ultra-Violet (LLUV) FOV for the entire test and the droplet did not appear to disrupt when the flame extinguished. From the extrapolated droplet history and the duration of the burn, the droplet burned to completion or to a very small droplet size.

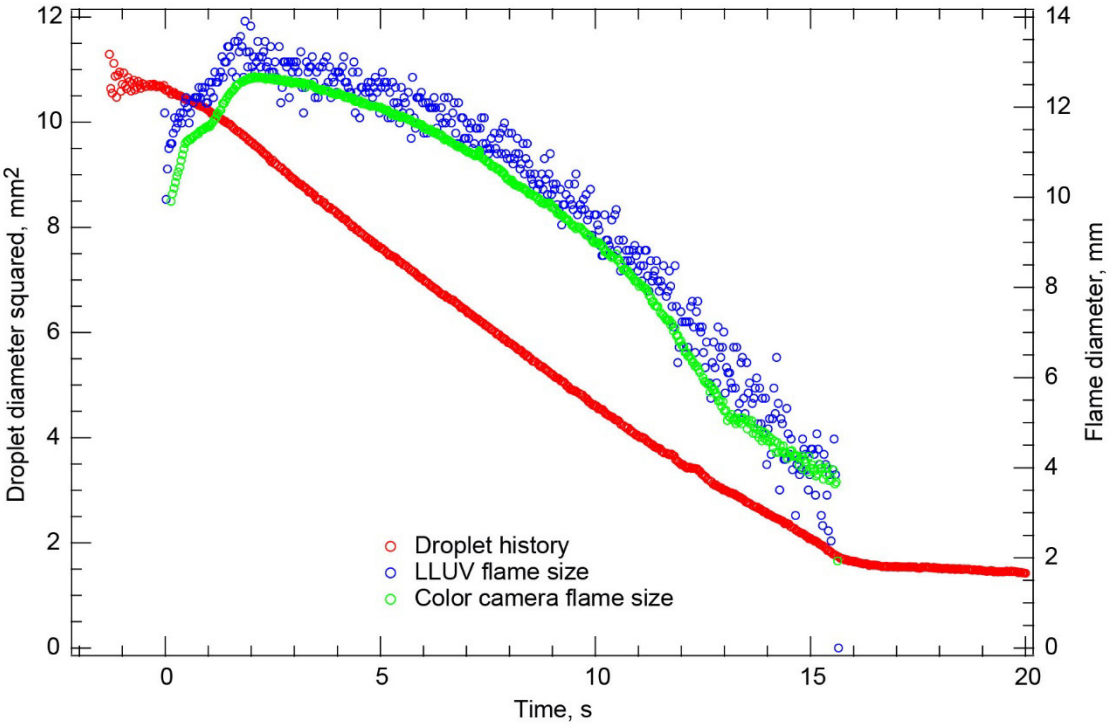

Figure 34.—Test FLEX−030. Free-floating methanol droplet burning in a 0.30/0.70 O_2/N_2, 1.0-atm ambient environment. The droplet remained in the fields of view (FOVs) of all the cameras for the entire test. The droplet drifted south, east, and then north in the High-Bit-Depth Multispectral (HiBMs) FOV. Coincident with flame extinction, the droplet became almost football shaped. The oblong-shaped droplet with a pointed end remained stationary for several seconds until the recording ended. The actual extinction diameter is reported, but it may be influenced by the shape change.

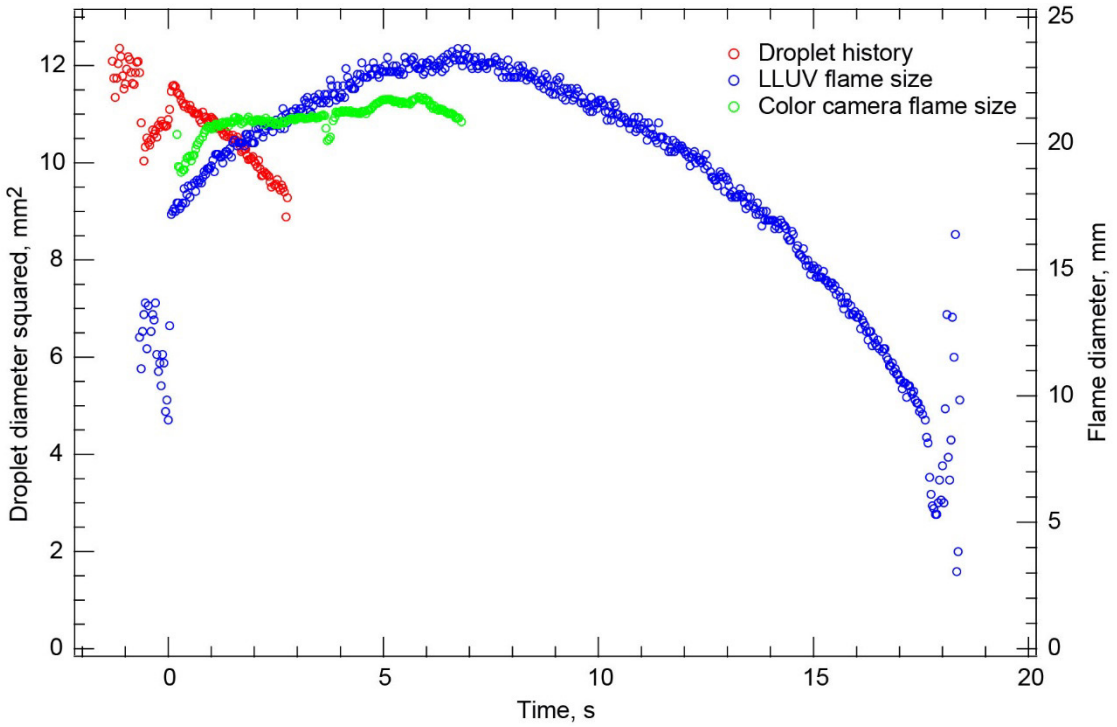

Figure 35.—Test FLEX−031. Free-floating heptane droplet burning in a 0.30/0.70 O_2/N_2, 1.0-atm ambient environment. The droplet drifted south in the High-Bit-Depth Multispectral (HiBMs) field of view (FOV) and left the FOV shortly after the igniter was withdrawn. There was significant sooting, and a large soot shell surrounded the droplet. The droplet drifted out of the color camera FOV, but it remained in the Low Light Level Ultra-Violet (LLUV) FOV. The droplet burned to disruption at a small size.

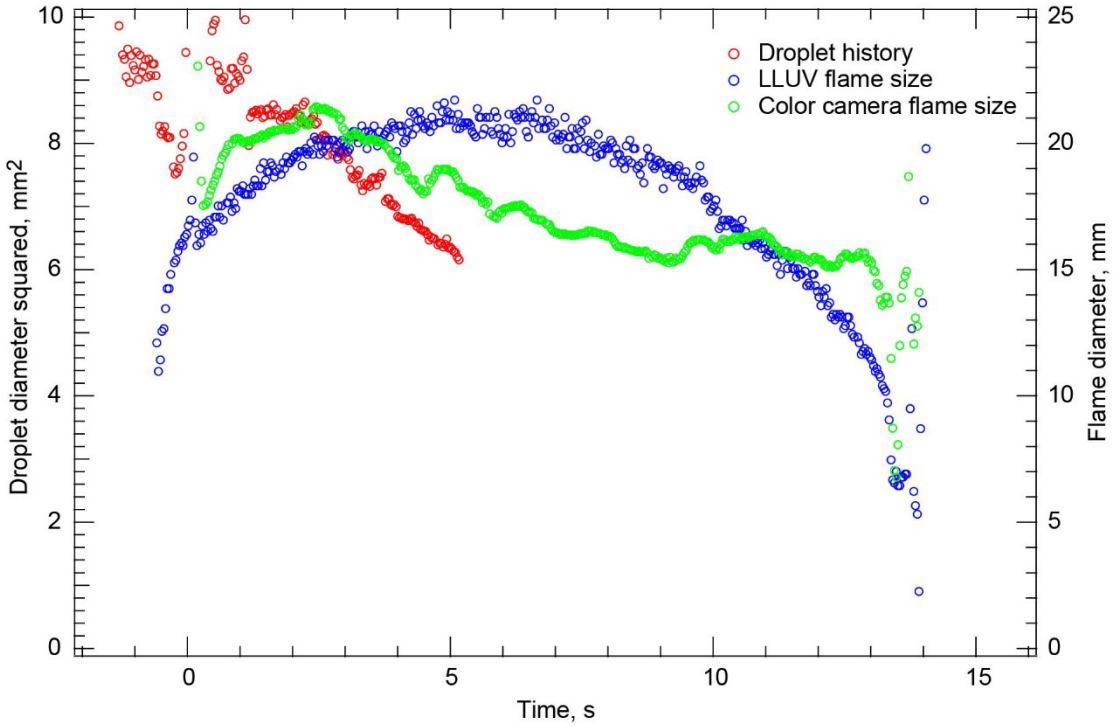

Figure 36.—Test FLEX−032. Free-floating heptane droplet burning in a 0.30/0.70 O_2/N_2, 1.0-atm ambient environment. There was significant sooting with large agglomerates throughout the test. A very luminous flame persisted throughout the droplet lifetime until disruptive extinction. The droplet drifted northwest out of the High-Bit-Depth Multispectral (HiBMs) field of view (FOV) one-third of the way through the test. It remained in the Low Light Level Ultra-Violet (LLUV) and color camera FOVs for the entire test. The significant sooting made accurate measurement of the droplet size difficult.

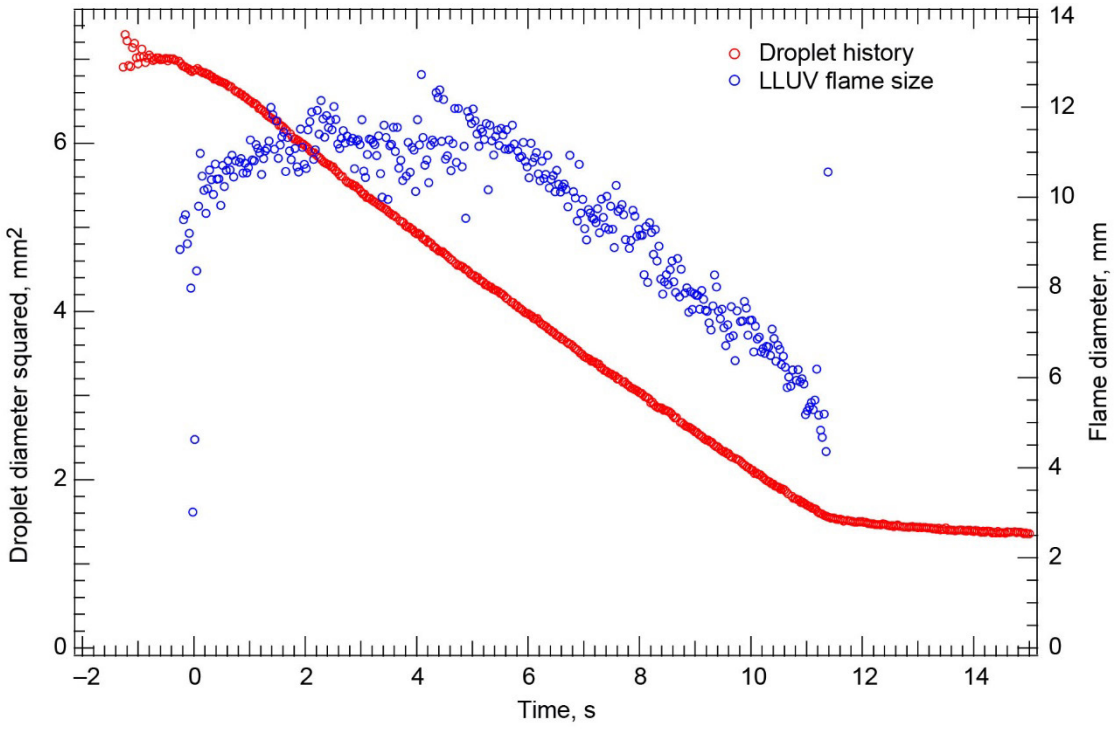

Figure 37.—Test FLEX−033. Free-floating methanol droplet burning in a 0.21/0.79 O_2/N_2, 1.0-atm ambient environment. The droplet drifted slightly north and then east in the High-Bit-Depth Multispectral (HiBMs) field of view (FOV). It eventually left the HiBMs FOV, but that was well after the flame extinguished. The color camera Image Processing and Storage Unit (IPSU) did not record any images after deployment.

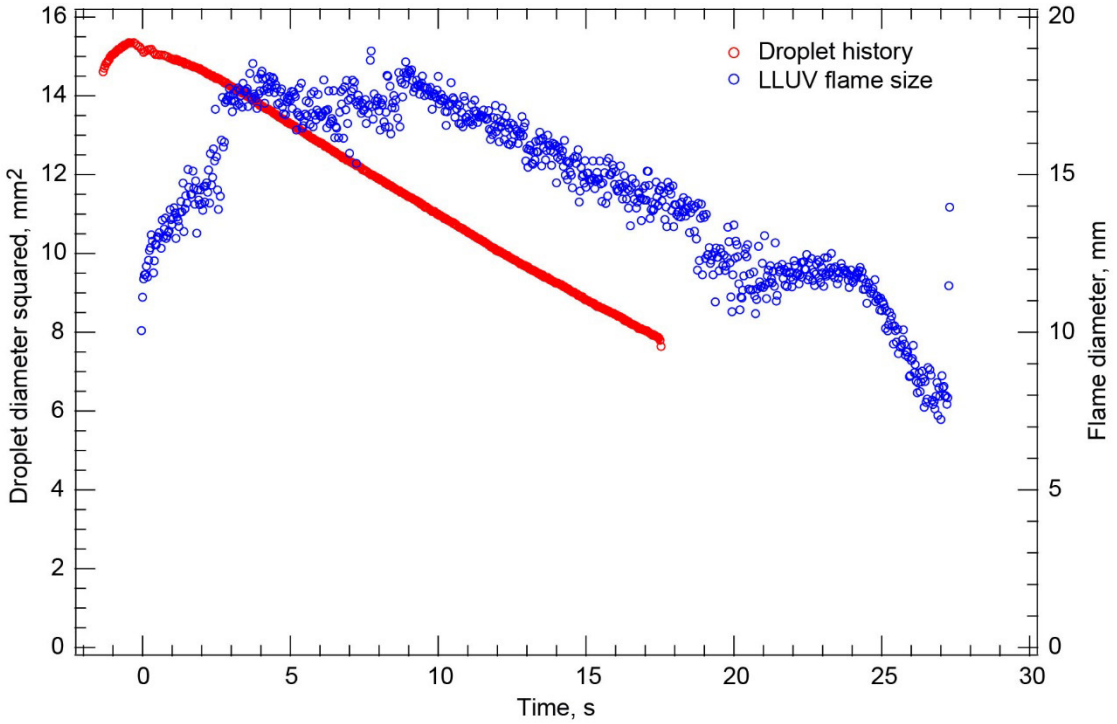

Figure 38.—Test FLEX−034. Free-floating methanol droplet burning in a cabin air (0.21/0.79 O_2/N_2, 1.0-atm) ambient environment. The droplet was almost motionless after deployment and ignition. It slowly drifted north in the High-Bit-Depth Multispectral (HiBMs) field of view (FOV), then began to move north much quicker and out of the HiBMs FOV about halfway through the test. The color camera Image Processing and Storage Unit (IPSU) did not record any images for this test. It is not clear from the Low Light Level Ultra-Violet (LLUV) whether the droplet disrupted coincident with flame extinction. Because the droplet was out of the HiBMs FOV for a long time near visible flame extinction, no extinction droplet diameter is reported.

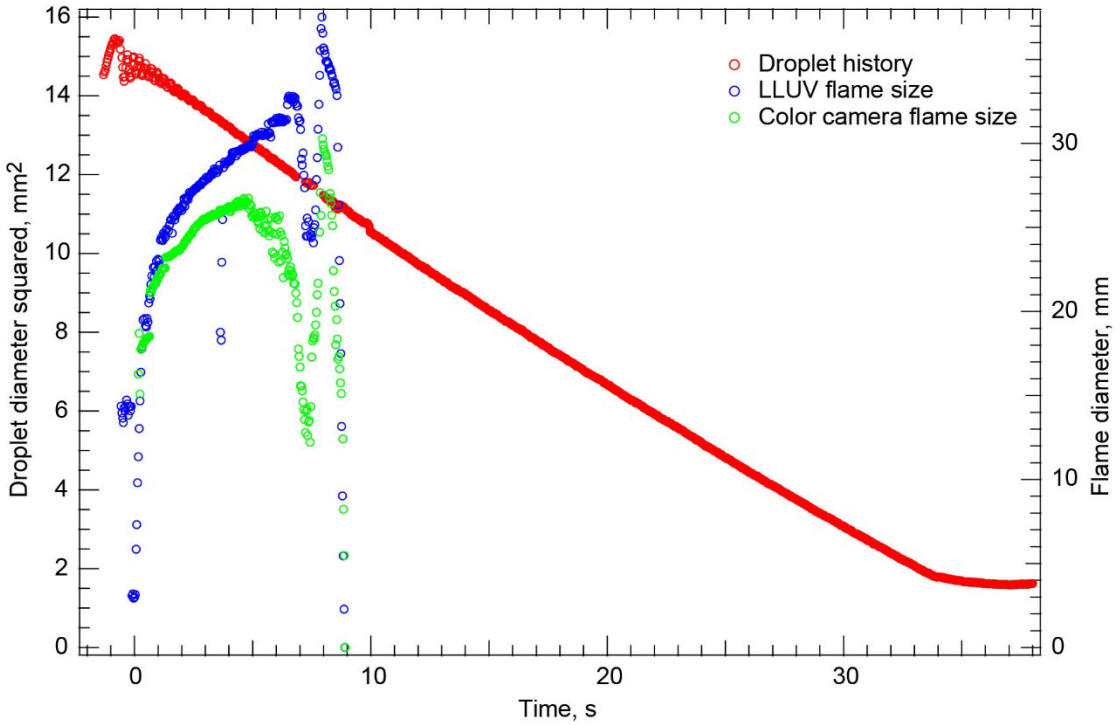

Figure 39.—Test FLEX−035. Free-floating heptane droplet in a cabin air (0.21/0.79 O_2/N_2), 1.0-atm ambient environment. The droplet remained in the High-Bit-Depth Multispectral (HiBMs) field of view (FOV) for the entire test including a long time after the visible flame extinguished. The flame oscillated before the visible flame extinguished, and this was apparent in both the Low Light Level Ultra-Violet (LLUV) and color camera. After the flame extinguished, the droplet vaporized very vigorously with droplet-diameter-squared versus time behavior that was nearly perfectly linear. The vaporization rate was only slightly lower than the burning rate constant before the flame extinguished. The droplet vaporization rate then plateaued coincident with the formation of a very large vapor cloud. This behavior is indicative of cool flame burning and extinction.

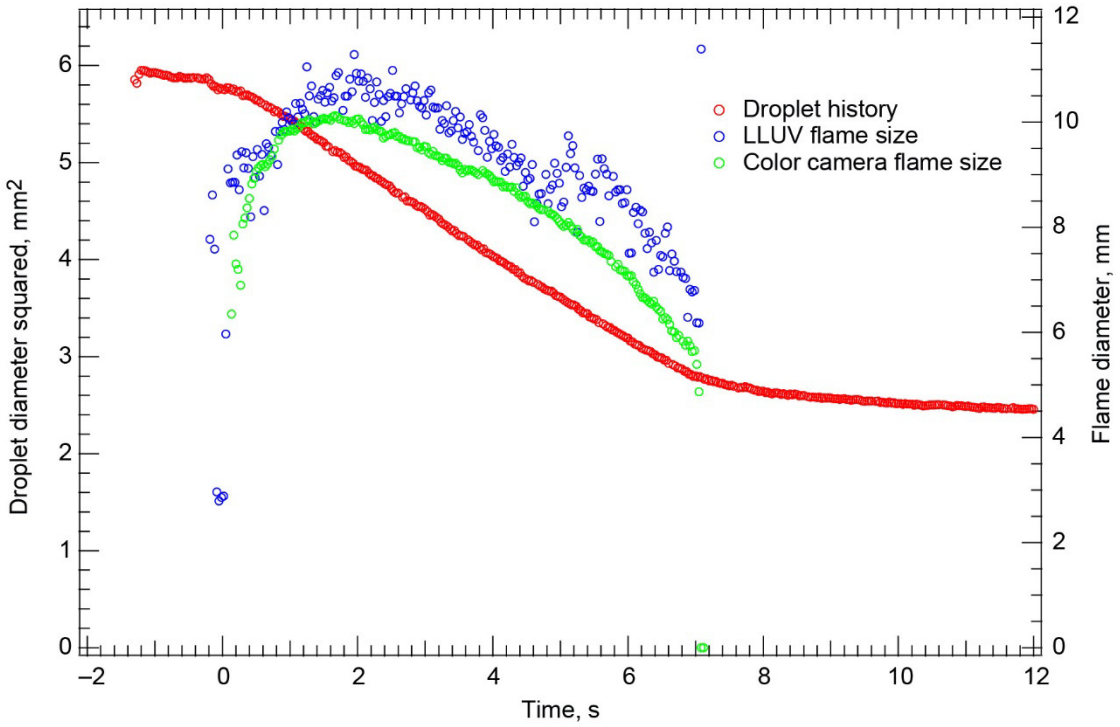

Figure 40.—Test FLEX−036. Free-floating methanol droplet burning in a cabin air (0.21/0.79 O_2/N_2), 0.70-atm ambient environment. The droplet remained in the High-Bit-Depth Multispectral (HiBMs) field of view (FOV) for the entire burn and for several seconds after the flame extinguished. The droplet did not distort or disrupt.

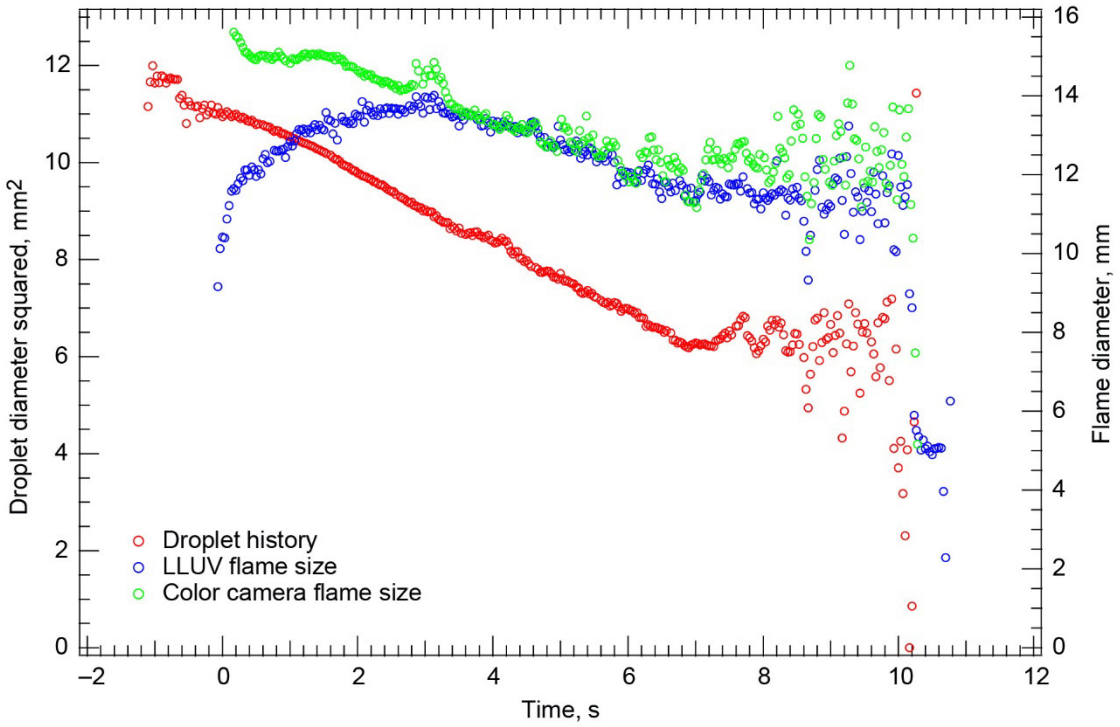

Figure 41.—Test FLEX−037. Fiber-supported methanol droplet translating approximately 3 mm/s and burning in a 0.34/0.66 O_2/N_2, 0.7-atm ambient environment. The droplet remained within the High-Bit-Depth Multispectral (HiBMs) field of view (FOV) for the entire test. After ignition and the start of translation, there was significant transverse motion. There was a lot of scatter in the droplet history because of the motion of the droplet on the fiber. The color camera showed a bright flame with ***a lot*** of sparklers throughout the burn. The transverse droplet motion became more severe toward the end of the test, with the droplet deforming. The flame extinguished when a complete disruption tore the droplet off the fiber.

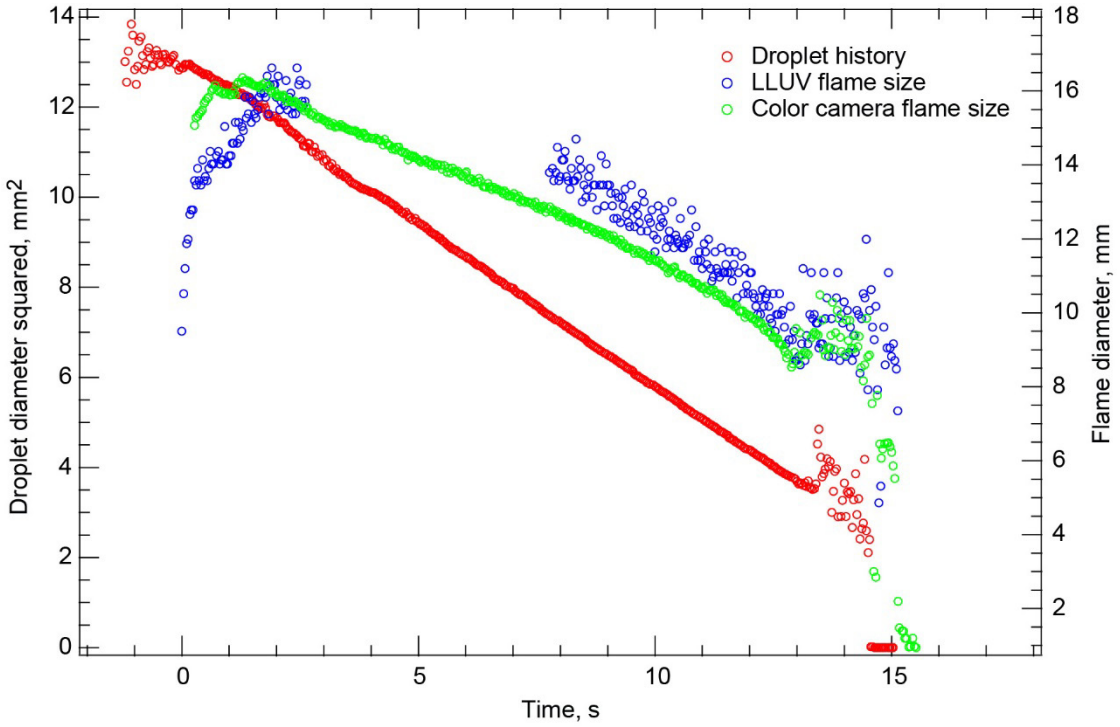

Figure 42.—Test FLEX−038. Fiber-supported methanol droplet translating and burning in a 0.34/0.66 O_2/N_2, 0.7-atm ambient environment. The burn was very smooth, with little motion of the droplet relative to the fiber for most of the test. About 80 percent of the way through the burn, the droplet began to vibrate transversely on the fiber. The vibrations grew in magnitude until the droplet disrupted and disintegrated, extinguishing the flame and leaving no fuel droplet on the fiber. The Low Light Level Ultra-Violet (LLUV) Image Processing and Storage Unit (IPSU) stopped recording for about one-half of the test (in the middle).

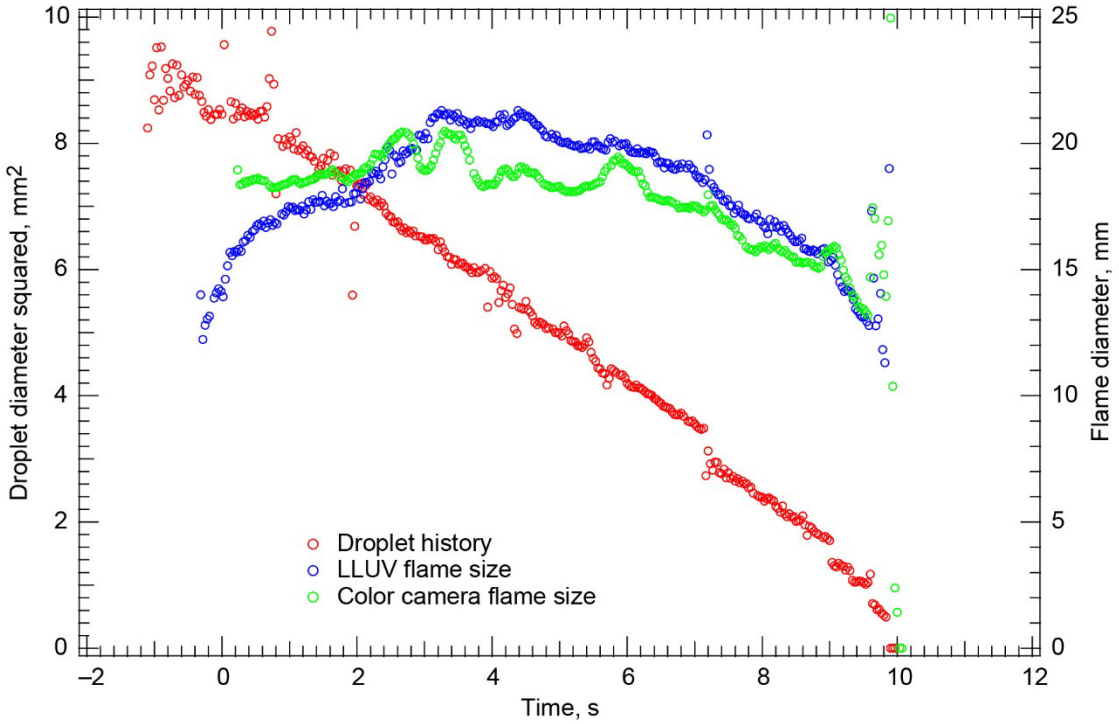

Figure 43.—Test FLEX−039. Fiber-supported heptane droplet translating 3 mm/s and burning in a 0.34/0.66 O_2/N_2, 0.70-atm ambient environment. There were significant transverse and axial oscillations on the fiber during the entire burn, but the droplet remained within the High-Bit-Depth Multispectral (HiBMs) field of view (FOV) for the entire test. There also was significant sooting with large aggregates throughout the test. The sooting was so severe that the threshold intensity for droplet discrimination had to be reduced to get reasonable droplet size measurements. The flame was bright yellow and very luminous throughout the entire test. A disruption dislocated the droplet from fiber coincident with flame extinction.

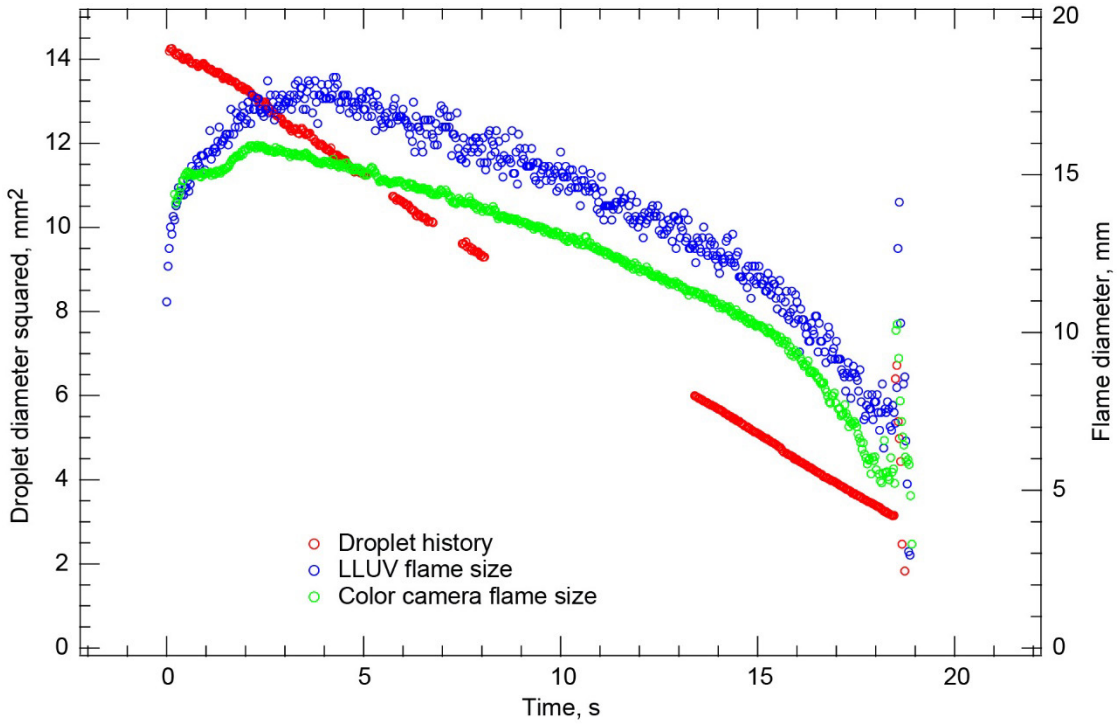

Figure 44.—Test FLEX−040. Fiber-supported methanol droplet translating 3 mm/s and burning in a 0.30/0.70 O_2/N_2, 0.7-atm ambient environment. The droplet had some transverse oscillations after ignition, but they diminished relatively quickly. During and after translation, the droplet oscillated axially. It moved east into and partially out of the High-Bit-Depth Multispectral (HiBMs) field of view (FOV). Then the droplet stopped moving both transversely and axially and burned smoothly—eventually shrinking until it was fully in the HiBMs FOV. Near the end of the test, the droplet again began to oscillate on the fiber and disrupted, dislodging from the fiber and causing the flame to extinguish.

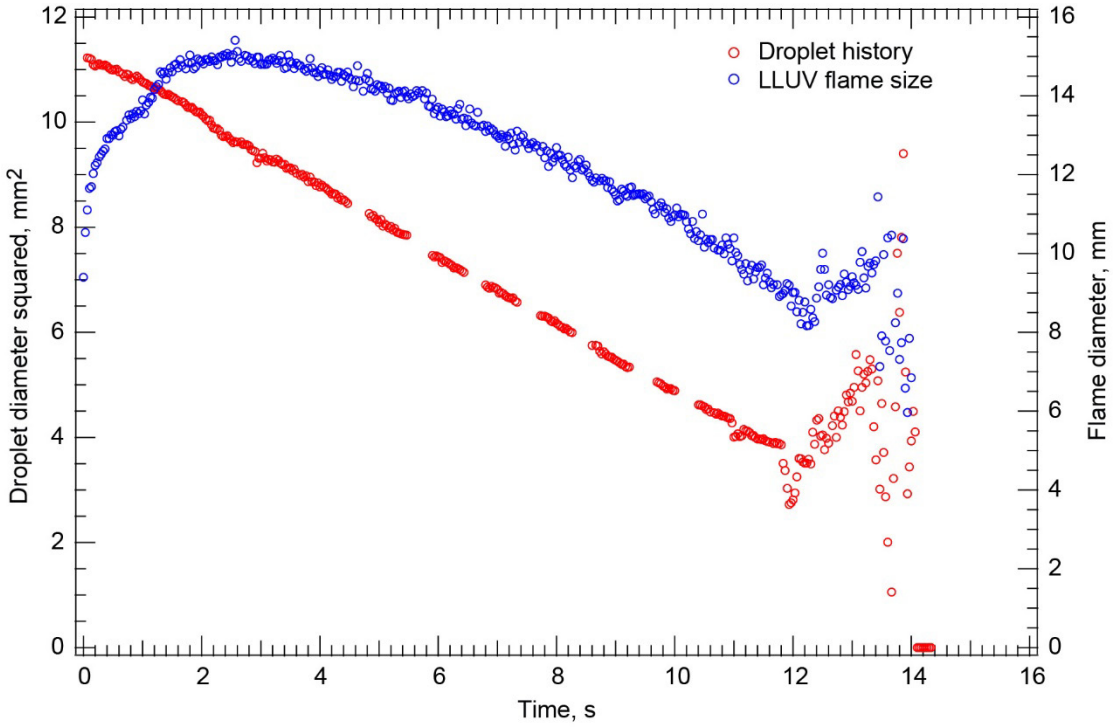

Figure 45.—Test FLEX−041. Fiber-supported methanol droplet translating 3 mm/s and burning in a 0.30/0.70 O_2/N_2, 0.7-atm ambient environment. The droplet had significant axial oscillations during and after the start and stop of fiber translation. The droplet drifted in and partially out of the High-Bit-Depth Multispectral (HiBMs) field of view (FOV). At the end of the test, the droplet swelled, disrupted, and became dislodged from the fiber coincident with flame extinction. The dislodged droplet did burn as it drifted away. The color camera Image Processing and Storage Unit (IPSU) did not record any images after deployment.

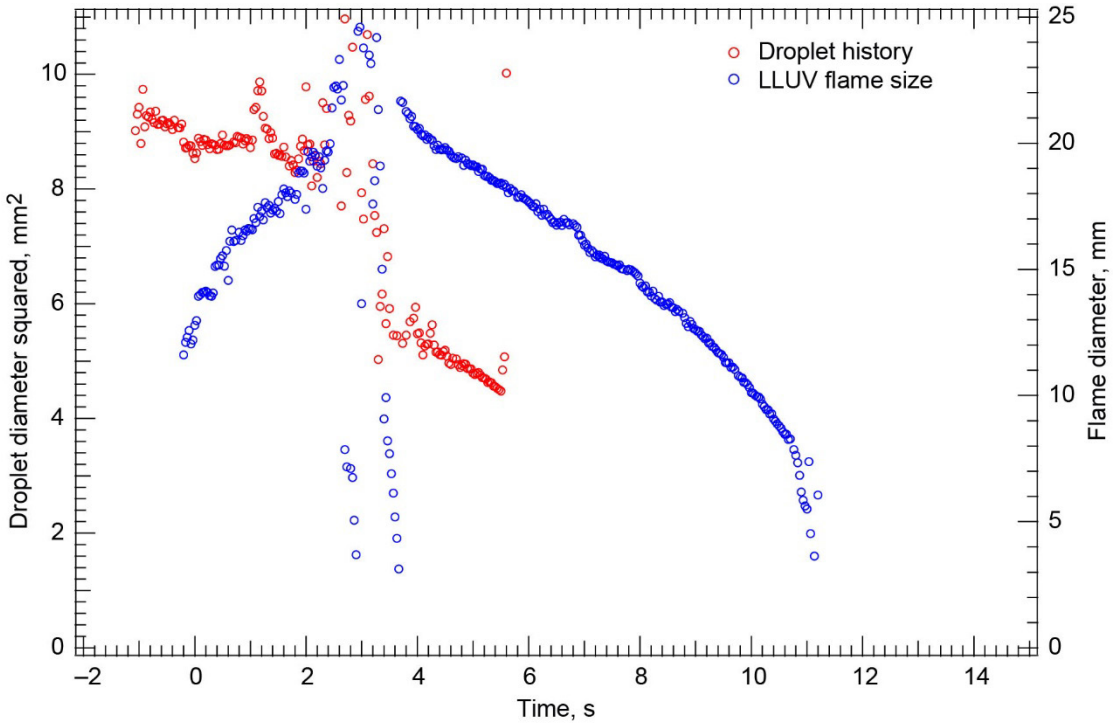

Figure 46.—Test FLEX−042. Fiber-supported heptane droplet burning in a 0.30/0.70 O_2/N_2, 0.70-atm ambient environment. The droplet was sooted relatively heavily immediately after ignition. Shortly after ignition, the droplet began to distort severely, periodically expelling small droplets of fuel that continued to burn. A large disruption completely dislodged the droplet from the fiber. Afterward, the droplet drifted north in the High-Bit-Depth Multispectral (HiBMs) field of view (FOV), then south (after another disruption). It then burned relatively cleanly to disruption at a small size. The burning rate constant was that during the relatively clean period after the droplet was dislodged from the fiber. The color camera Image Processing and Storage Unit (IPSU) did not record any images after deployment.

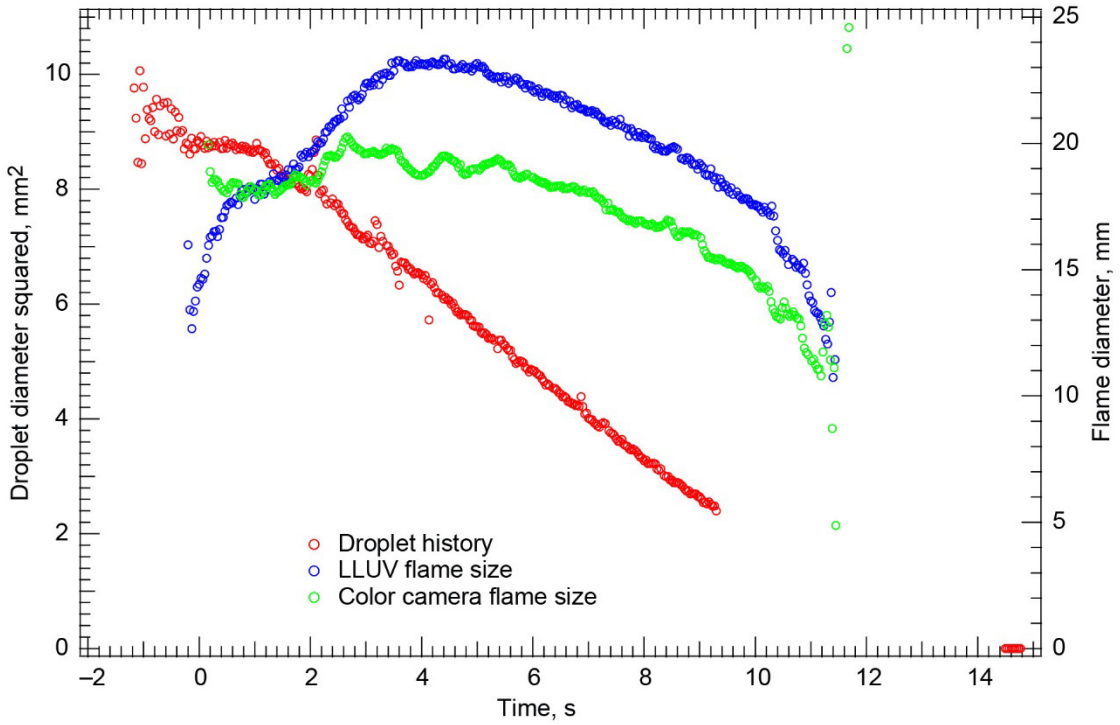

Figure 47.—Test FLEX−043. Fiber-supported heptane droplet translating 3 mm/s and burning in a 0.30/0.70 O_2/N_2, 0.7-atm ambient environment. There was significant sooting, but the droplet remained in the High-Bit-Depth Multispectral (HiBMs) field of view (FOV) for the entire test until it disrupted and dislodged from the fiber. There was significant oscillatory axial motion on the fiber during the entire test.

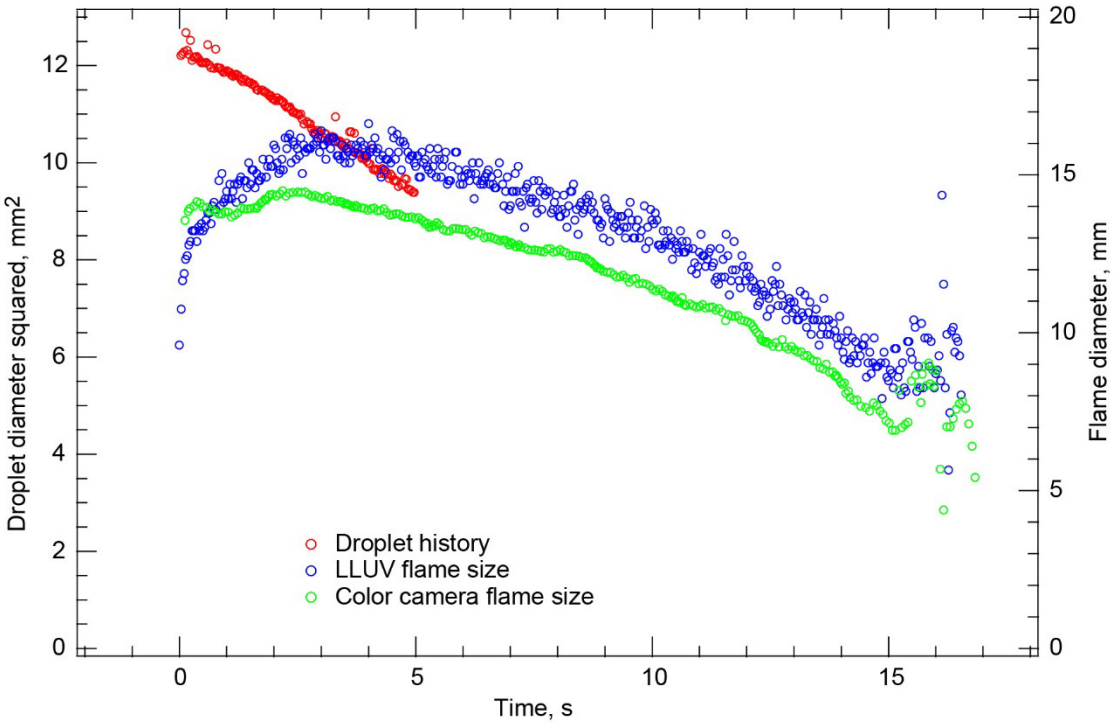

Figure 48.—Test FLEX−044. Fiber-supported methanol droplet translating 3 mm/s and burning in a 0.30/0.70 O_2/N_2, 1.0-atm ambient environment. Transverse motion that began after deployment persisted throughout the test. In addition, there was significant oscillatory axial motion during the translation that persisted after the fiber stopped translating. The droplet drifted axially out of the High-Bit-Depth Multispectral (HiBMs) field of view (FOV) about one-third of the way through the burn. Significant “sparkling” was evident in the color camera but was not visible in the HiBMs or Low Light Level Ultra-Violet (LLUV). The droplet disrupted and dislodged from the fiber coincident with flame extinction.

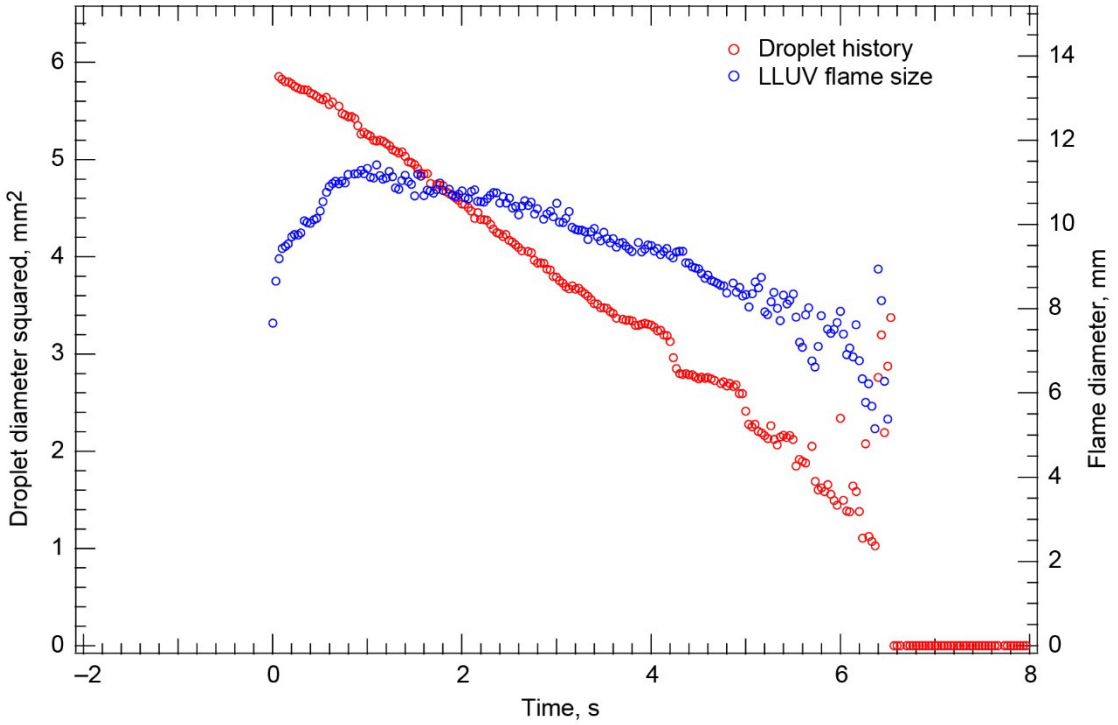

Figure 49.—Test FLEX−045. Fiber-supported methanol droplet translating 3 mm/s and burning in a 0.30/0.70 O_2/N_2, 1.0-atm ambient environment. The droplet remained in the High-Bit-Depth Multispectral (HiBMs) field of view (FOV) for the entire test. There was some axial and transverse droplet motion from deployment until the end of the test, and there was some droplet swelling or shape change before disruption. The color camera Image Processing and Storage Unit (IPSU) did not record any images after deployment, so the extinction droplet diameter is that when the droplet disrupted and became dislodged from the fiber coincident with flame extinction.

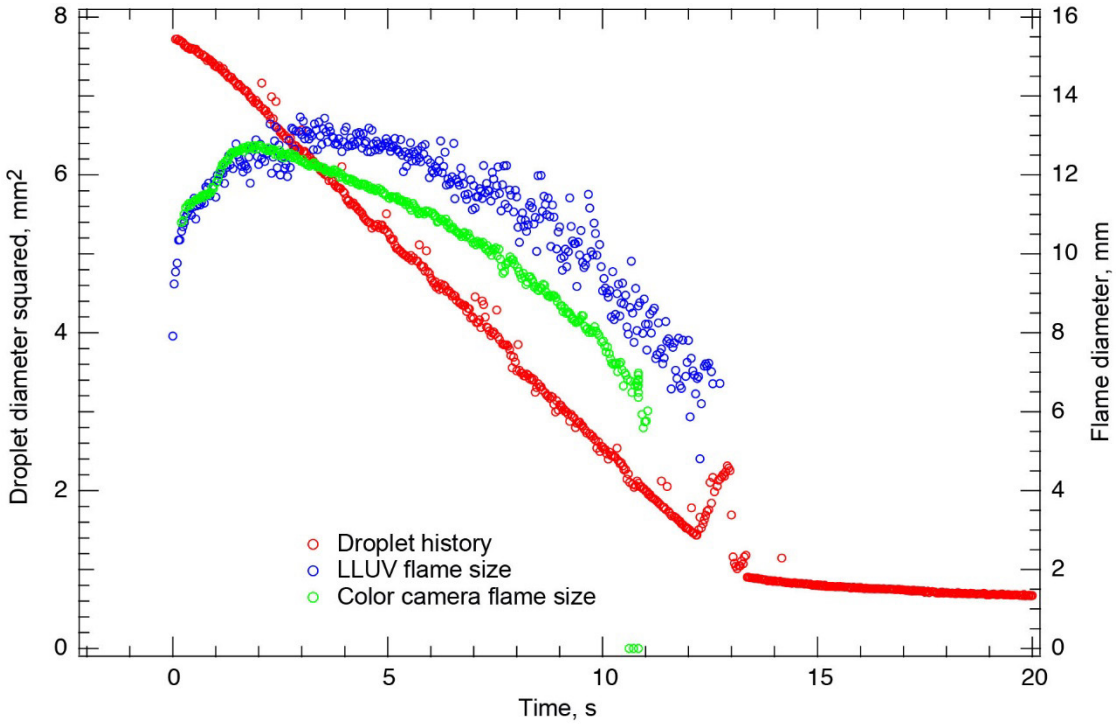

Figure 50.—Test FLEX−046. Fiber-supported methanol droplet burning in a cabin air (0.21/0.79 O_2/N_2), 1.0-atm ambient environment. The droplet remained in the High-Bit-Depth Multispectral (HiBMs) field of view (FOV) for the entire test. There was significant oscillatory axial motion during the most of the test, but at the very end, the droplet became stationary and there was some deformation, growth, and shape change. A small disruption occurred coincident with flame extinction.

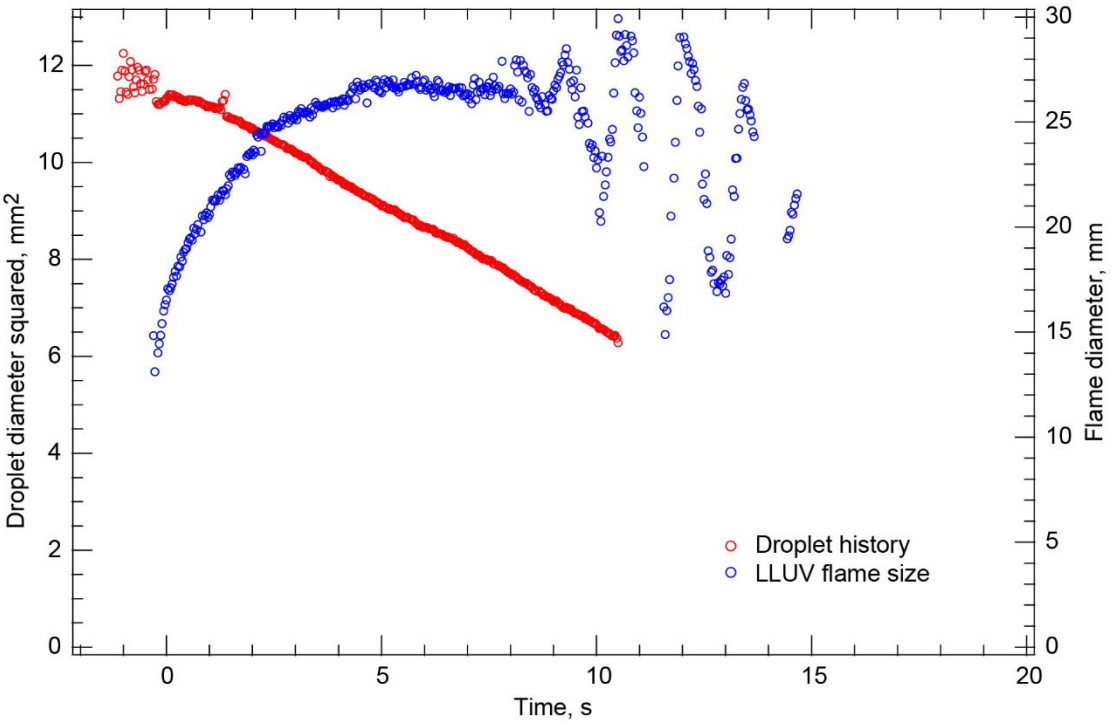

Figure 51.—Test FLEX−047. Free-floating heptane droplet burning in a cabin air (0.21/0.79 O_2/N_2), 1.0-atm ambient environment. The droplet drifted east out of the High-Bit-Depth Multispectral (HiBMs) field of view (FOV) about halfway through the test. The droplet oscillated for several seconds before the droplet left the FOVs of all the cameras. It left the Low Light Level Ultra-Violet (LLUV) FOV last, oscillating as it translated south out of the FOV. The radiometer showed that the flame persisted even after the droplet left the FOV. Extrapolating the burning history to when the radiometer indicated extinction (with large error bars) showed that the droplet burned nearly to extinction. There was no evidence of disruptive burning in any of the camera views. The color camera did not capture the flame history correctly because it did not zoom out.

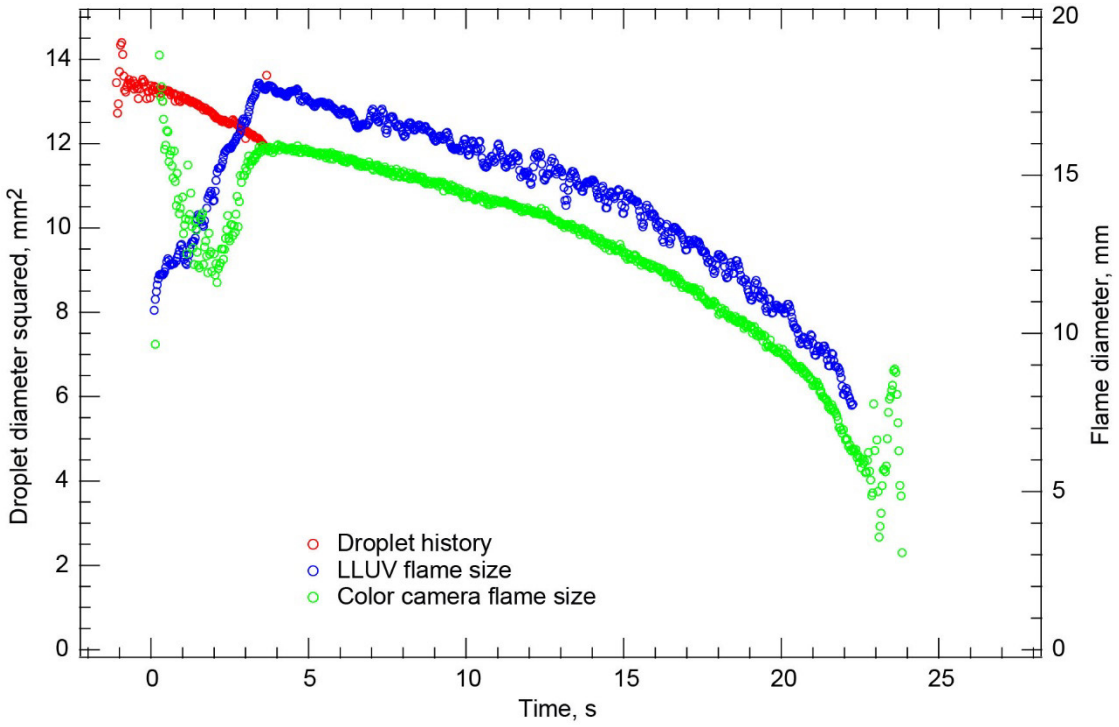

Figure 52.—Test FLEX−048. Fiber-supported methanol droplet translating 3 mm/s and burning in a cabin air (0.21/0.79 O_2/N_2), 1.0-atm ambient environment. The droplet drifted east after the start of translation and out of the High-Bit-Depth Multispectral (HiBMs) field of view (FOV) about one-fifth of the way through the test. The flame remained within the FOVs of the Low Light Level Ultra-Violet (LLUV) and color camera for the entire test. There was disruptive burning at the end of the test.

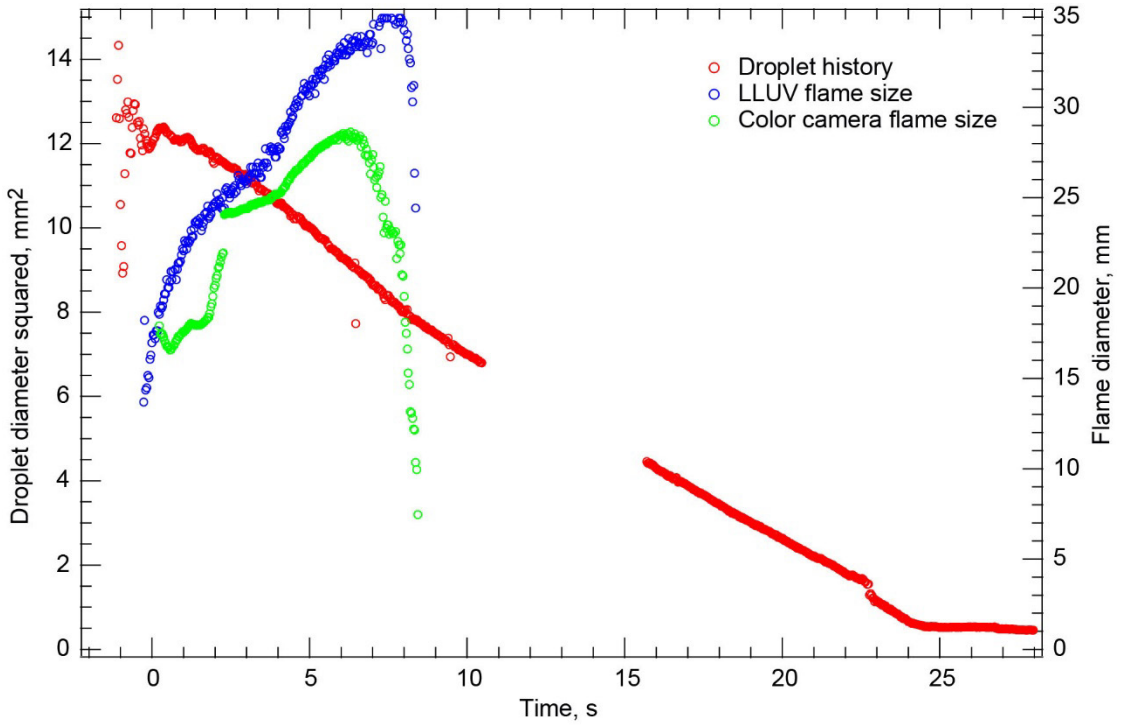

Figure 53.—Test FLEX−049. Fiber-supported heptane droplet translating 3 mm/s and burning in a cabin air (0.21/0.79 O_2/N_2), 1-atm ambient environment. The High-Bit-Depth Multispectral (HiBMs) Image Processing and Storage Unit (IPSU) stopped recording for a few seconds, which resulted in a gap in the droplet history. The droplet oscillated on the fiber throughout the test, with the amplitude and frequency changing. There also was some unusual gas-phase recirculation evident from soot particle motion. The droplet vaporized vigorously after the visible flame extinguished, and a large vapor cloud formed near the end of the recording period. This is evidence of cool flame burning and extinction following visible flame extinction.

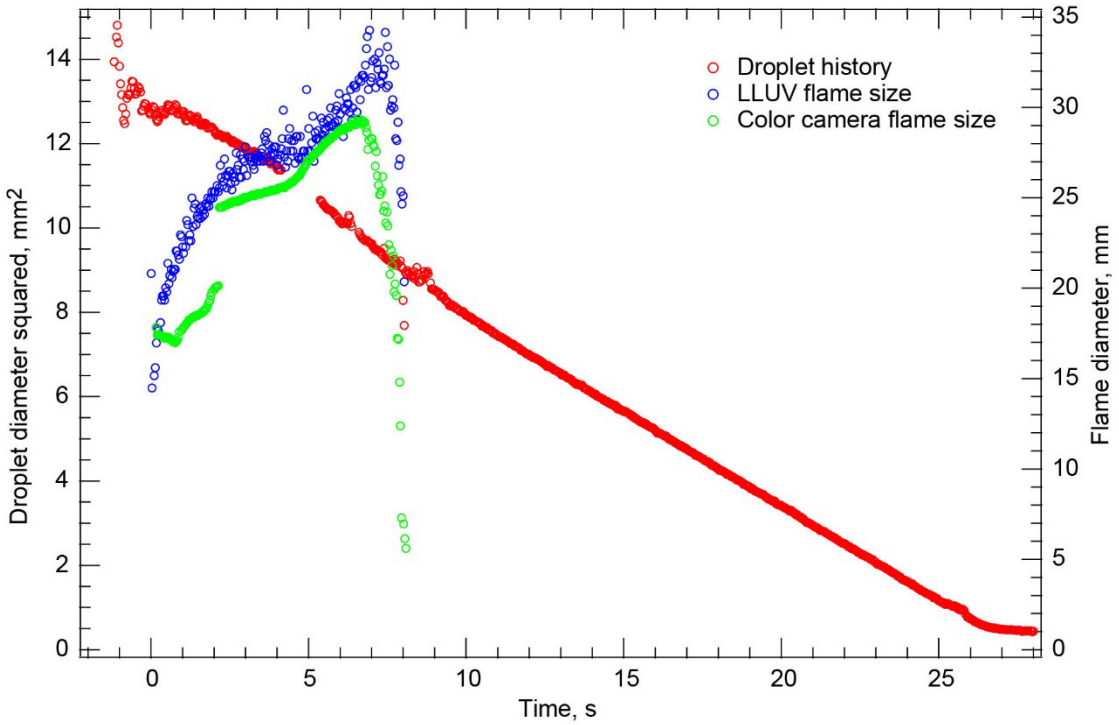

Figure 54.—Test FLEX−050. Fiber-supported heptane droplet translating 3 mm/s and burning in a cabin air (0.21/0.79 O_2/N_2), 1-atm ambient environment. There were moderate transverse oscillations on the fiber throughout the test, and unique circulation patterns in the gas phase were evident from the soot motion. The droplet continued to vaporize linearly after the visible flame extinguished, and a large vapor cloud formed nearly coincident with a plateau in the droplet history. This is evidence of cool flame burning and extinction following visible flame extinction.

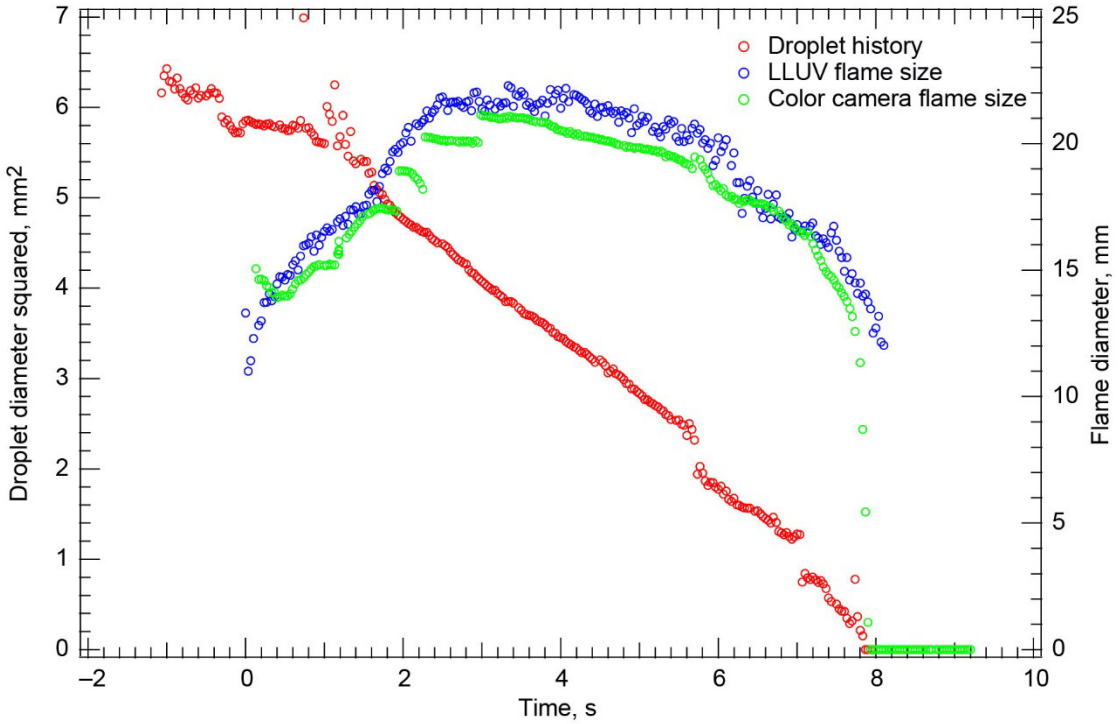

Figure 55.—Test FLEX−051. Fiber-supported heptane droplet burning in a cabin air (0.21/0.79 O_2/N_2), 1.0-atm ambient environment. The droplet remained in the High-Bit-Depth Multispectral (HiBMs) field of view (FOV) for the entire test, and it burned to completion. The flame was very luminous flame initially, but it disappeared abruptly halfway through the burn. The droplet had significant transverse oscillations on the fiber, but it never dislodged.

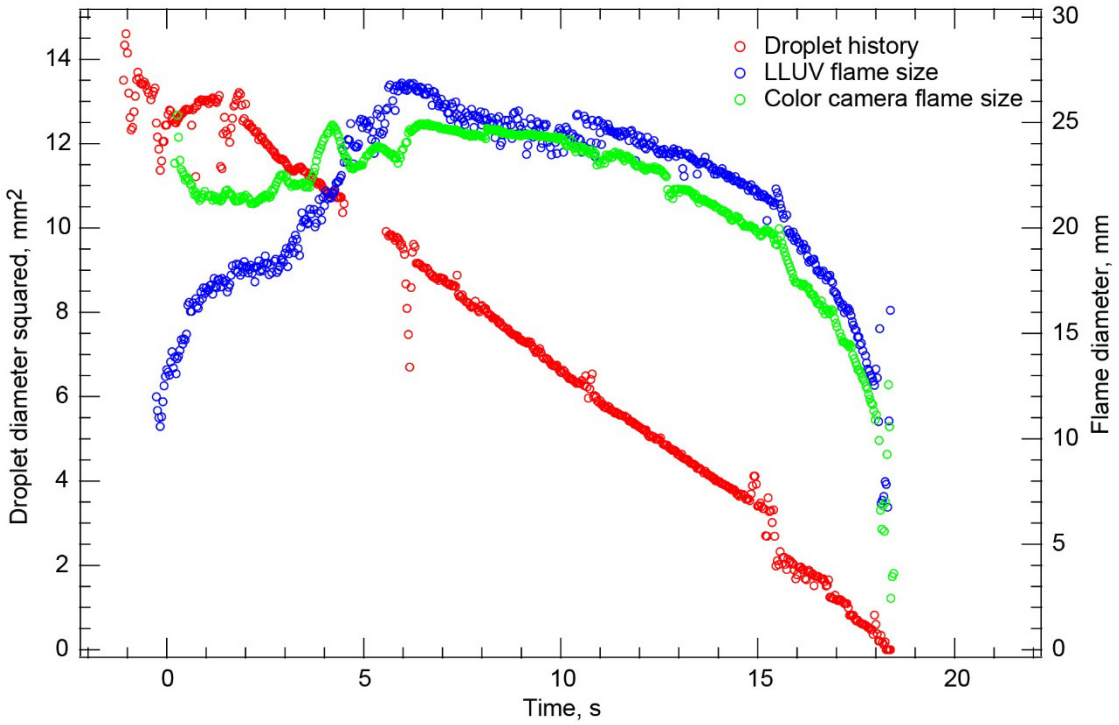

Figure 56.—Test FLEX−052. Fiber-supported heptane droplet translating 3 mm/s and burning in a 0.30/0.70 O_2/N_2, 1.0-atm ambient environment. The droplet oscillated significantly on the fiber throughout the burn. There also was significant sooting, with large agglomerates stuck to the fiber (which created scatter in the droplet history). The droplet drifted partially out of the High-Bit-Depth Multispectral (HiBMs) field of view (FOV) for a short time before moving back in. Late in the test, significant oscillations, shape changes, and ejection of material from the droplet ended with a disruption.

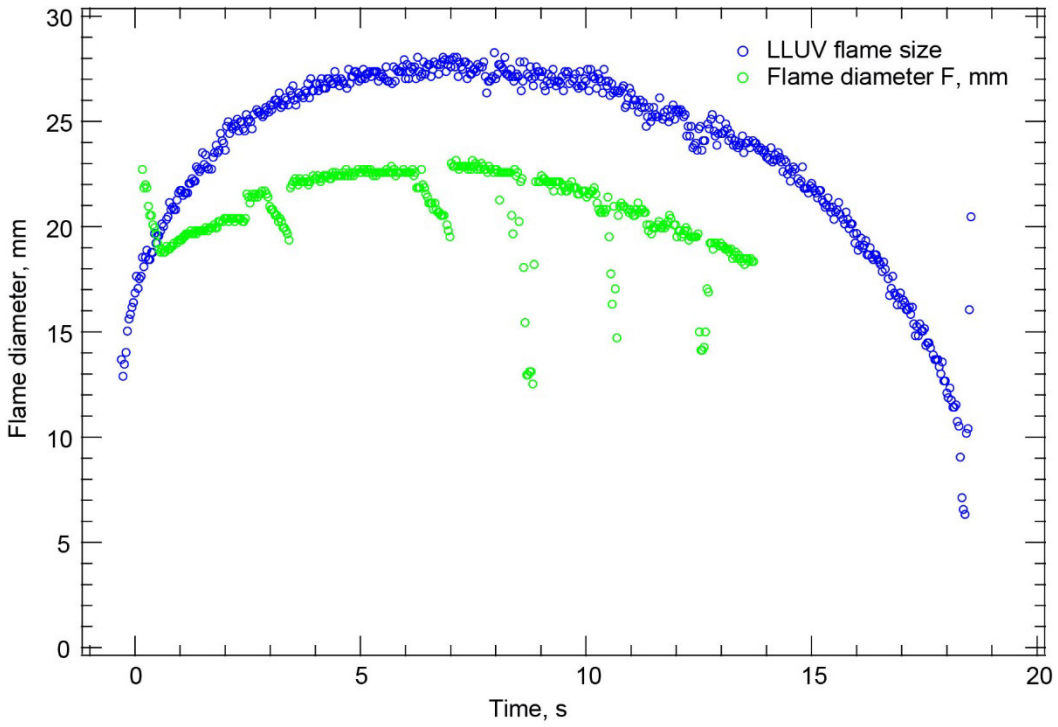

Figure 57.—Test FLEX−053. Fiber-supported heptane droplet burning in a cabin air (0.21/0.79 O_2/N_2), 1.0-atm ambient environment. There were no High-Bit-Depth Multispectral (HiBMs) data for this test. There was poor alignment between the needle and the droplet, and the droplet did not deploy on the fiber. It drifted north in the color camera field of view (FOV) after deployment and ignition and out of the FOV before the end of the test. However, the droplet remained in the Low Light Level Ultra-Violet (LLUV) FOV for the entire test. The discrepancy in the flame size between the LLUV and color camera was due to the flame being much brighter at the leading edge than at the trailing edge, which resulted in some of the flame being cropped from the color camera images during analysis.

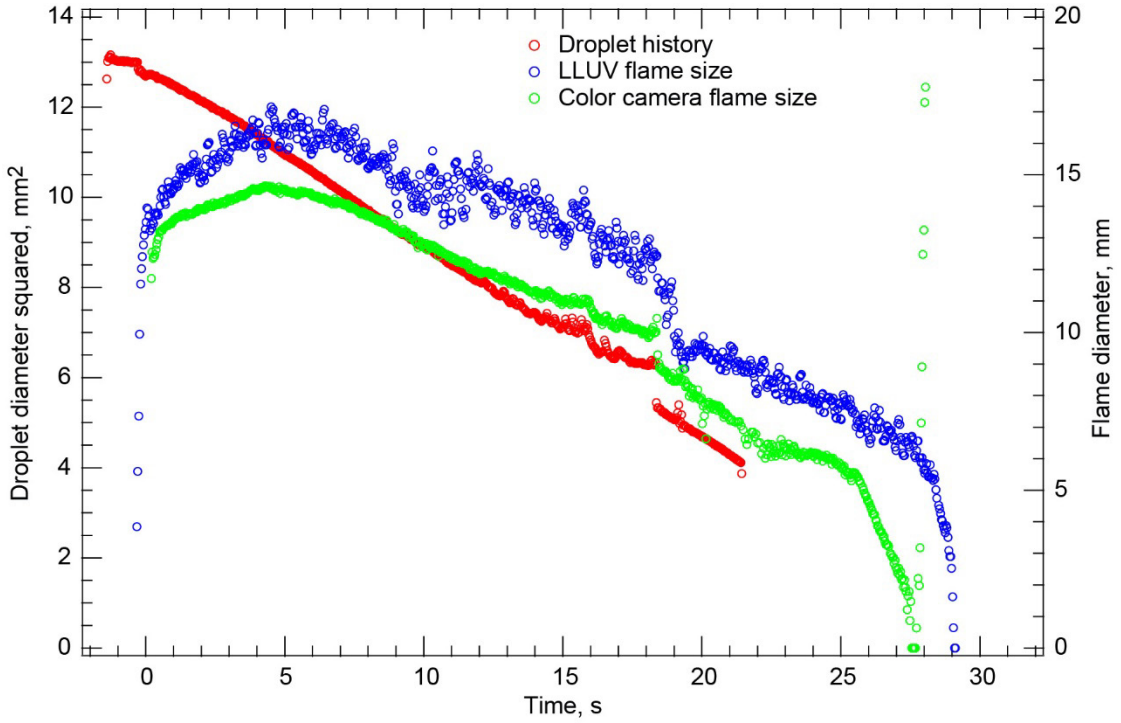

Figure 58.—Test FLEX−054. Free-floating methanol droplet burning in a 0.20/0.80 O_2/N_2, 0.7-atm ambient environment. The droplet had almost no residual motion after ignition. About halfway through the test, the droplet began to move abruptly north-northeast and then quickly changed direction to the northeast. The droplet left the High-Bit-Depth Multispectral (HiBMs) field of view (FOV) after the second change in direction. The color camera views indicate that there may have been some small gas bubbles in the droplet. There also was some distortion in the droplet history right before the droplet changed direction. This could have been due to the expanding gas bubbles distorting the droplet, then bursting and imparting a momentum to the droplet. The burning rate constant and flame standoff data are for the portion of the test before the disruption and change in direction. Because the droplet was in the HiBMs FOV for only a limited time and because there were disruptions in the droplet during the burn, no extinction droplet diameter is reported.

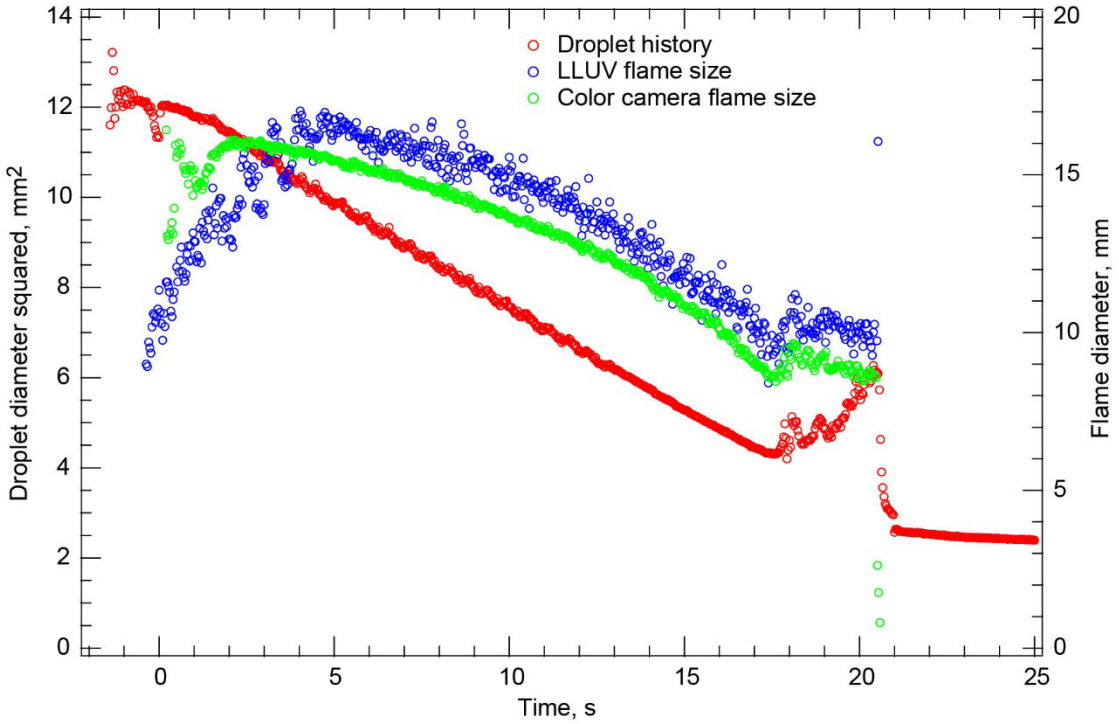

Figure 59.—Test FLEX−055. Fiber-supported methanol droplet translating 3 mm/s and burning in a 0.20/0.80 O_2/N_2, 0.7-atm ambient environment. The droplet remained in the High-Bit-Depth Multispectral (HiBMs) field of view (FOV) for the entire test. After the start of translation, the droplet oscillated rapidly between the spots where the flame impinged on the fiber. The periodic noise in the droplet history was caused by the oscillation, which stopped approximately halfway through the test. The droplet then grew and had a small disruption (coincident with flame extinction) that left a small residual droplet on the fiber.

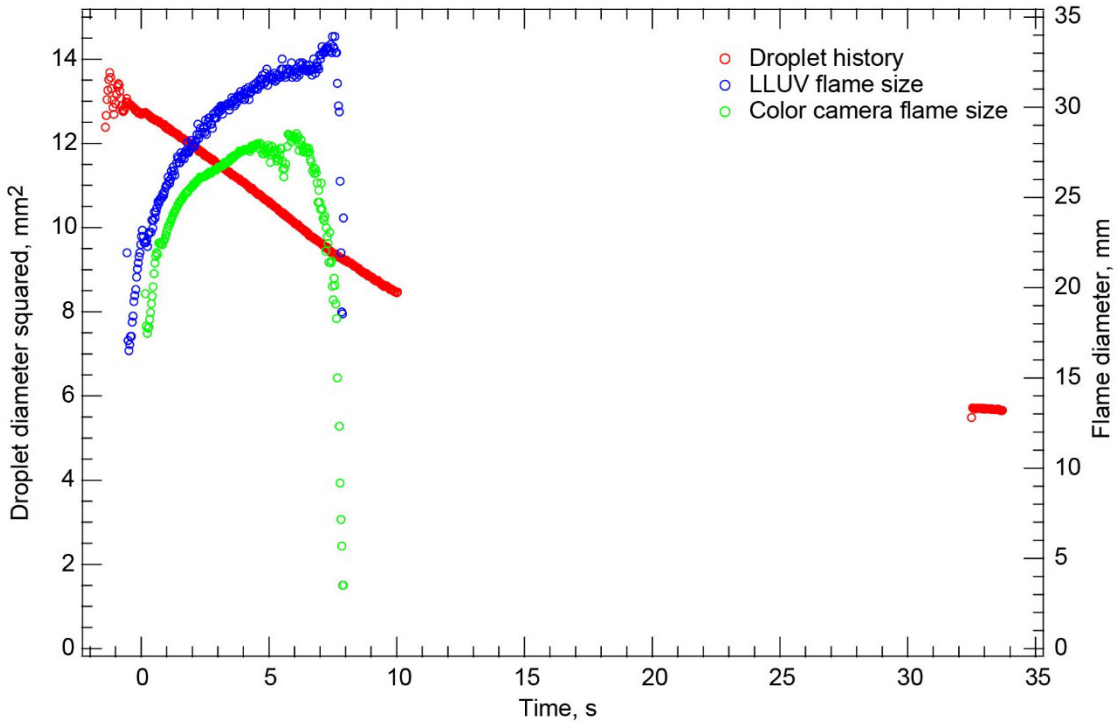

Figure 60.—Test FLEX−056. Free-floating heptane droplet burning in a 0.20/0.80 O_2/N_2, 0.70-atm ambient environment. The droplet drifted east after ignition and left the High-Bit-Depth Multispectral (HiBMs) field of view (FOV) shortly after the visible flame extinguished. The droplet reentered the HiBMs FOV from the east a few seconds prior to the stop of video recording. A vapor cloud formed in the color camera view approximately 20 s after the visible flame extinguished. It is not clear whether cool flame burning and extinction occurred for this test.

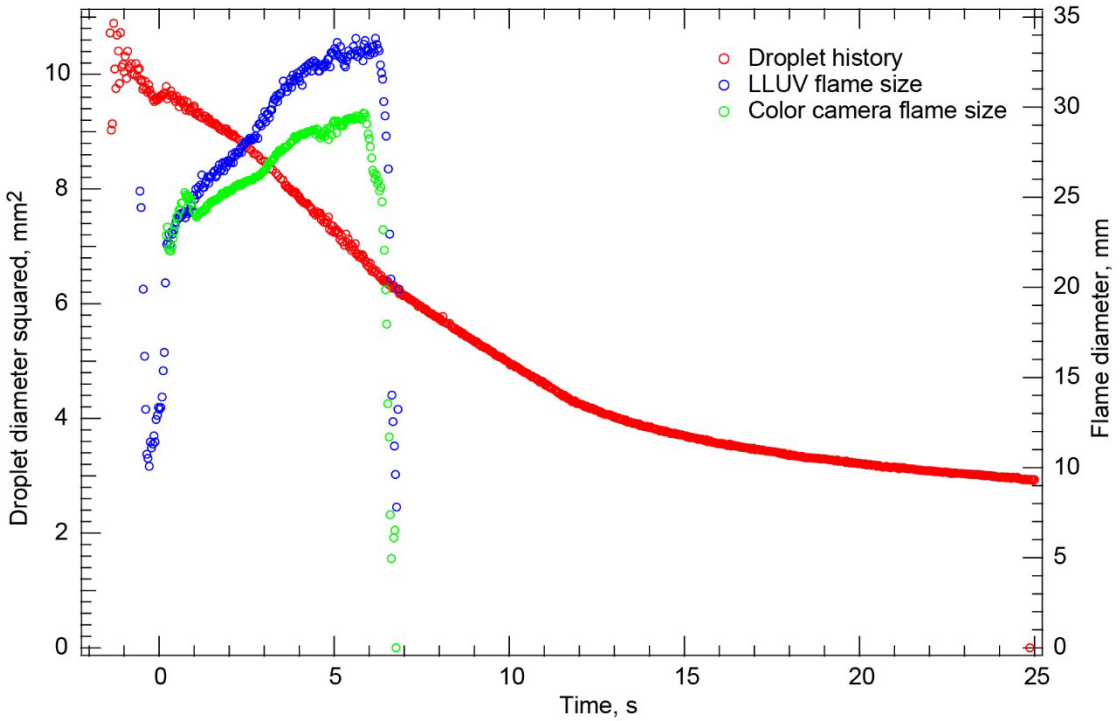

Figure 61.—Test FLEX−057. Fiber-supported heptane droplet translating 3 mm/s and burning in a 0.20/0.80 O_2/N_2, 0.70-atm ambient environment. There were moderate transverse and axial oscillations on the fiber after deployment, during the entire visible flame, and after the visible flame extinguished. The flame extinguished after the translation stopped, with the trailing edge of the flame visibly weaker and extinguishing first. There were unusual, recirculating flow patterns in the High-Bit-Depth Multispectral (HiBMs) fuel from soot that moved toward the droplet, accelerated circumferentially in a short arc, and then moved radially toward the flame and back again. A small vapor cloud formed in the color camera view approximately 20 s after the visible flame extinguished. It is not clear whether cool flame burning and extinction was present in this test.

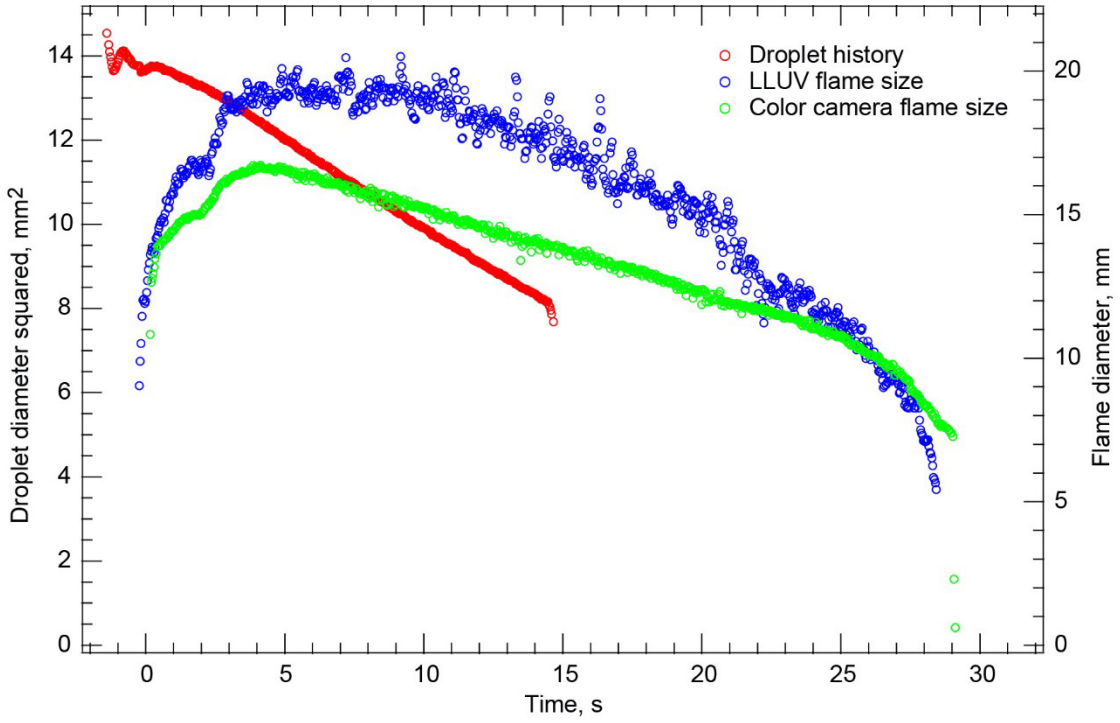

Figure 62.—Test FLEX−058. Free-floating methanol droplet burning in a 0.18/0.82 O_2/N_2, 1.0-atm ambient environment. The droplet drifted slowly east out of the High-Bit-Depth Multispectral (HiBMs) field of view (FOV), accelerating slowly before leaving the FOV. The droplet remained in the FOVs of the Low Light Level Ultra-Violet (LLUV) and color camera for the entire test, and there was no disruption. Because the droplet was not in the HiBMs FOV for the majority of the burning history, no extinction droplet diameter is reported.

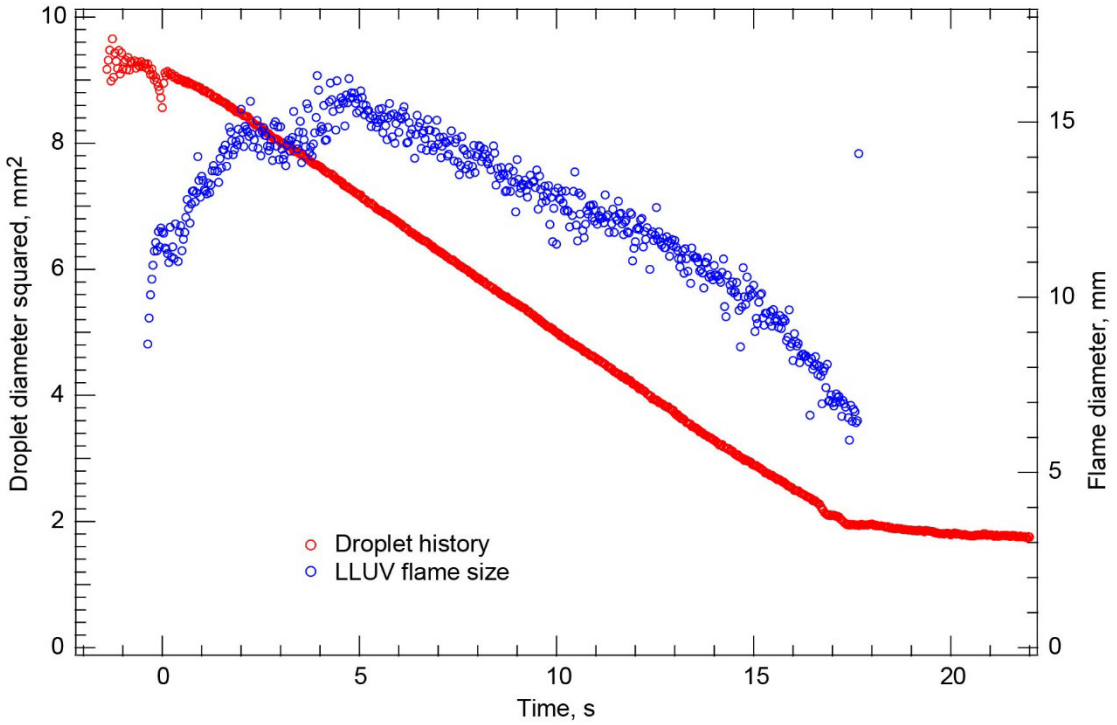

Figure 63.—Test FLEX−059. Free-floating methanol droplet burning in a 0.18/0.82 O_2/N_2, 1.0-atm ambient environment. The droplet remained in the High-Bit-Depth Multispectral (HiBMs) field of view (FOV) for the entire test, drifting north after deployment, stopping, drifting southwest to the corner of the FOV, and then drifting north to the middle west of the FOV. The color camera Image Processing and Storage Unit (IPSU) did not record any images for this test.

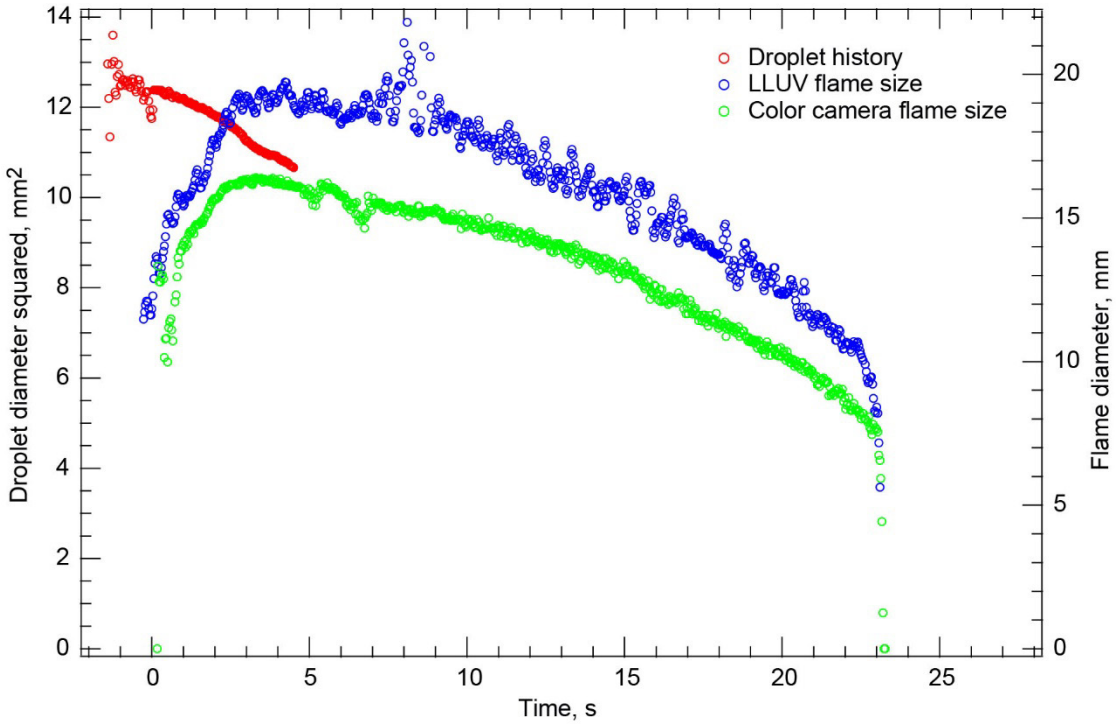

Figure 64.—Test FLEX−060. Fiber-supported methanol droplet translating 3 mm/s and burning in a 0.18/0.82 O_2/N_2, 1.0-atm ambient environment. The droplet moved east in the High-Bit-Depth Multispectral (HiBMs) field of view (FOV) with translation and continued to move east along the fiber and out of the FOV after the translation stopped. It also drifted partially out of the Low Light Level Ultra-Violet (LLUV) FOV. The droplet then oscillated between the regions where the flame impinged on the fiber for several seconds before becoming quiescent and burning until the flame extinguished, presumably diffusively. There was no apparent disruption at or near flame extinction.

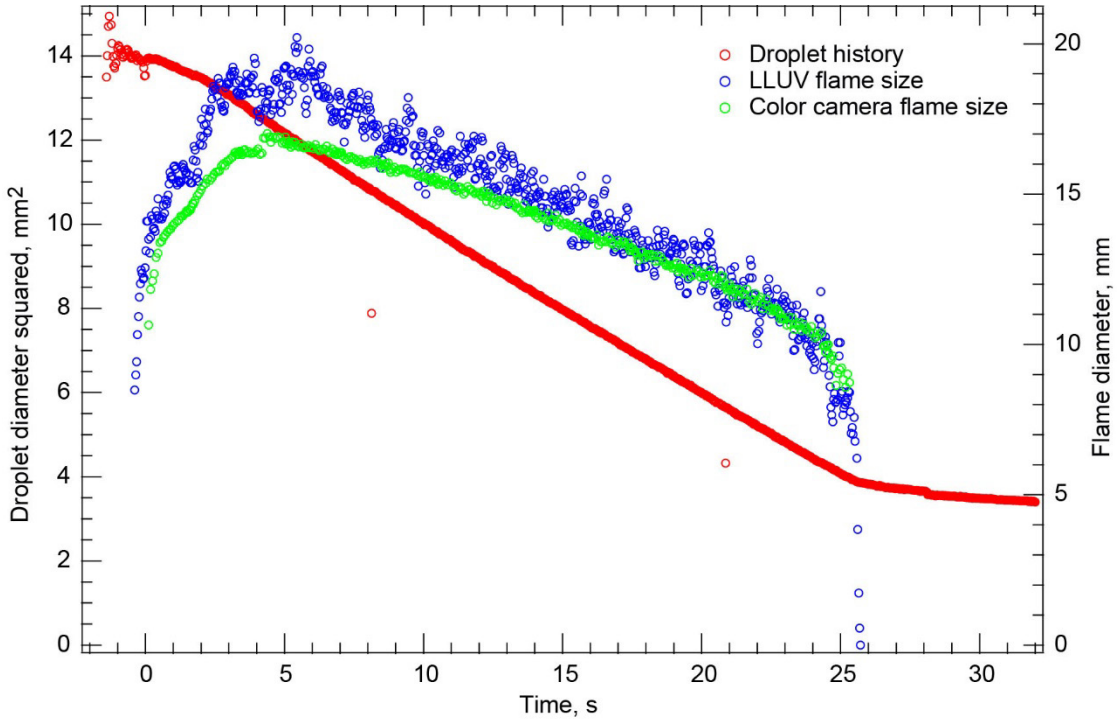

Figure 65.—Test FLEX−061. Fiber-supported methanol droplet with no translation and burning in a 0.18/0.82 O_2/N_2, 1.0-atm ambient environment. The droplet remained stationary on the fiber and within the High-Bit-Depth Multispectral (HiBMs) field of view (FOV) for the entire test. The flame was very dim in both the Low Light Level Ultra-Violet (LLUV) and color camera views.

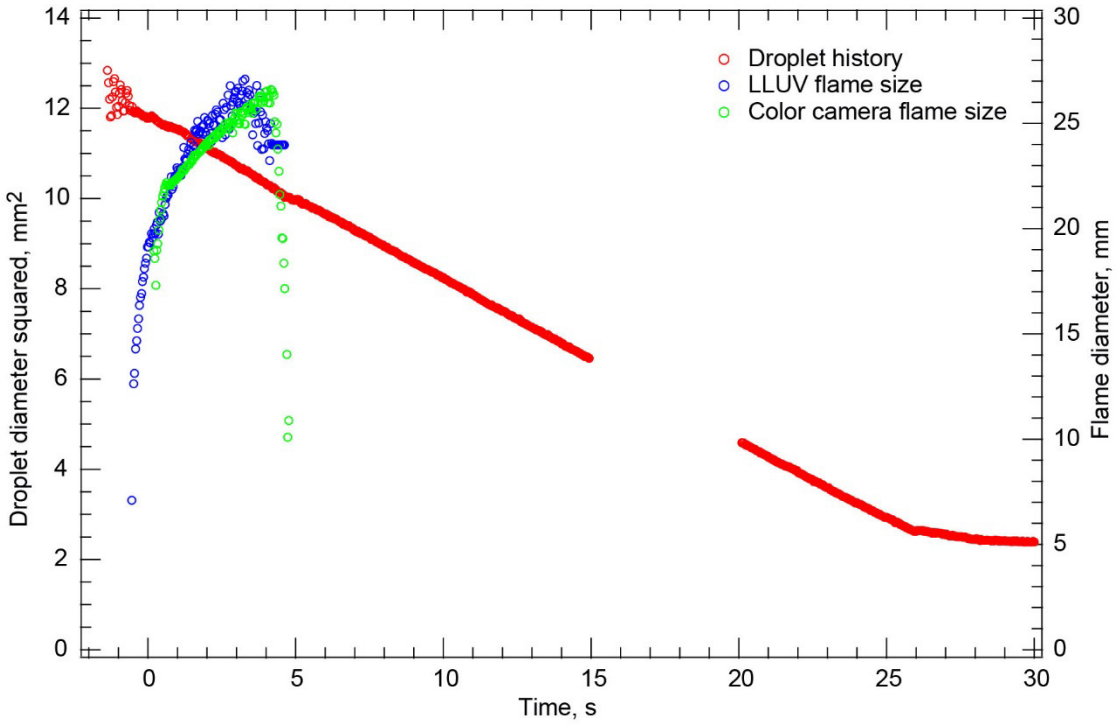

Figure 66.—Test FLEX−062. Free-floating heptane droplet burning in a 0.18/0.82 O_2/N_2, 1.0-atm ambient environment. The droplet was nearly motionless after deployment and ignition and remained in the fields of view (FOVs) of all the cameras for the entire test. The High-Bit-Depth Multispectral (HiBMs) Image Processing and Storage Unit (IPSU) stopped recording images for a short time after the visible flame extinguished. After the visible flame extinguished, there was continued rapid vaporization and a large vapor cloud formed. This is indicative of cool flame burning and extinction following visible flame extinction.

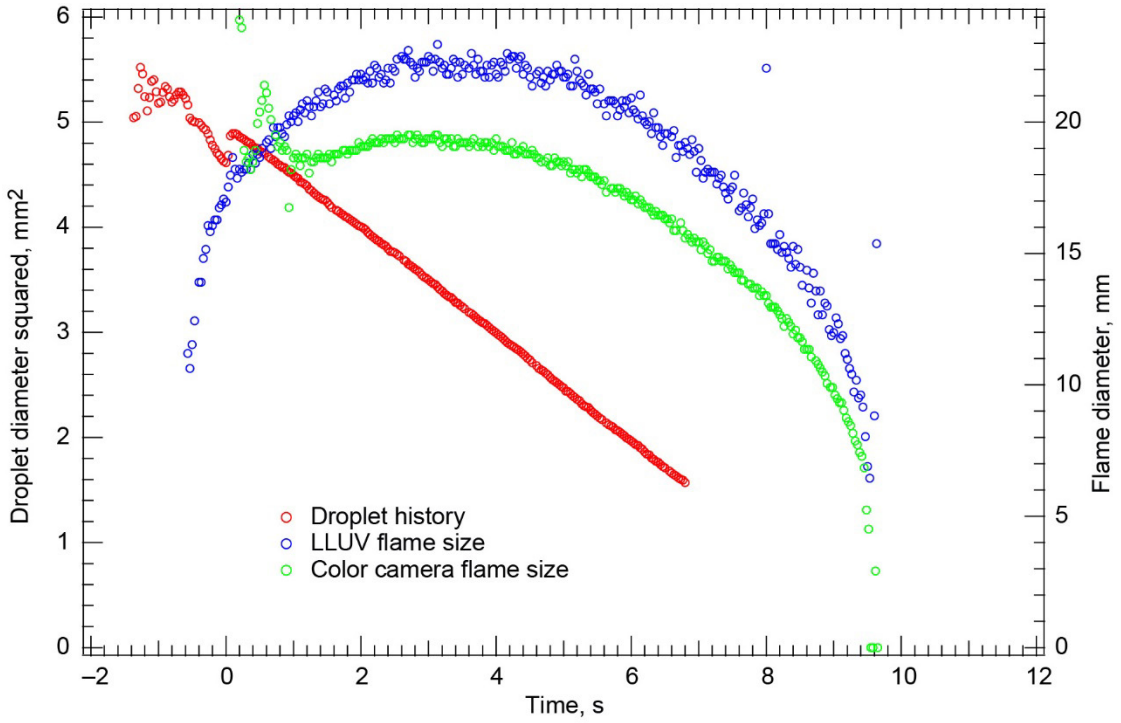

Figure 67.—Test FLEX−063. Free-floating heptane droplet burning in a 0.18/0.82 O_2/N_2, 1.0-atm ambient environment. The droplet drifted north in the High-Bit-Depth Multispectral (HiBMs) field of view (FOV) after deployment and ignition and out of the FOV two-thirds of the way through the test. There was a small disruption near the end of the test. Extrapolating the droplet history using the average burning rate constant resulted in a very small extinction droplet size, indicating that the droplet burned essentially to completion.

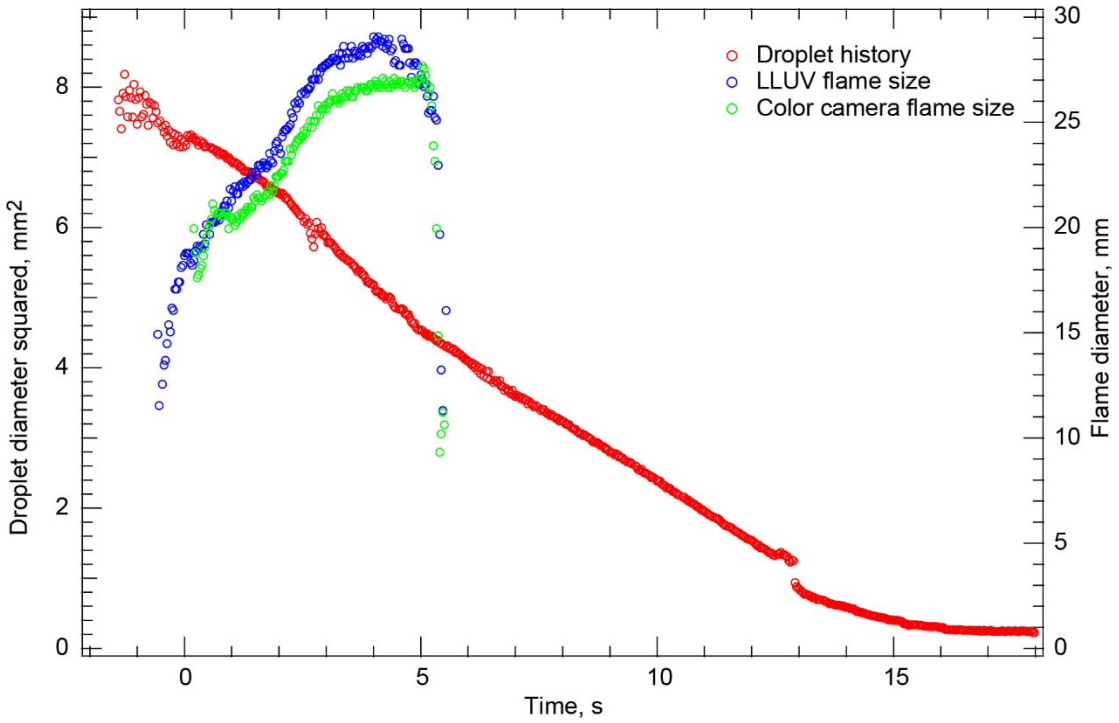

Figure 68.—Test FLEX−064. Fiber-supported heptane droplet translating 3 mm/s (for approximately 4 s) and burning in a 0.18/0.82 O_2/N_2, 1.0-atm ambient environment. The droplet had moderate transverse oscillations and remained within the High-Bit-Depth Multispectral (HiBMs) field of view (FOV) for the entire test. The flame grew and became dim blue. During translation, the leading edge of the flame was bright and the fiber glowed brightly. The trailing edge of the flame was much dimmer and the fiber did not glow. After the translation stopped, the flame extinguished and the droplet vaporized significantly. A small disruption very late in the droplet lifetime left a small residual droplet on the fiber. The behavior after the visible flame extinguished is indicative of cool flame burning and extinction.

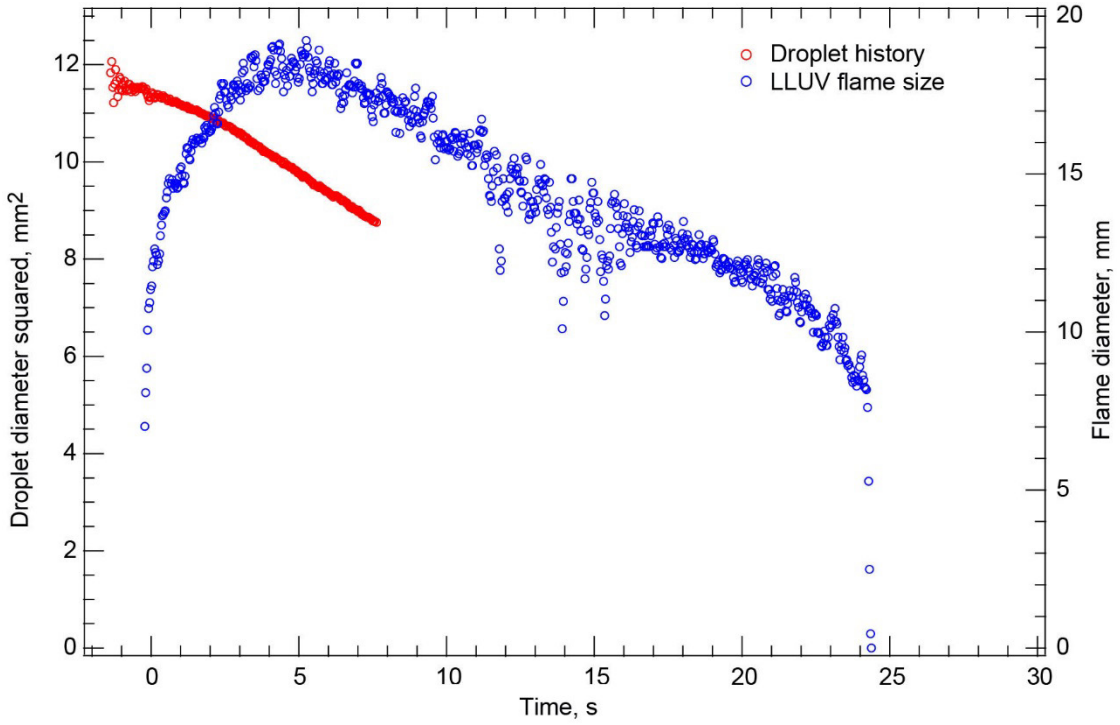

Figure 69.—Test FLEX−065. Free-floating methanol droplet burning in a 0.15/0.85 O_2/N_2, 1.0-atm ambient environment. The droplet drifted south-southeast and out of the High-Bit-Depth Multispectral (HiBMs) field of view (FOV) before the end of the test. The color camera Image Processing and Storage Unit (IPSU) did not record any images for this test. The Low Light Level Ultra-Violet (LLUV) showed a very long burn with a flame that appeared to get a little bit brighter for a short period of time. Because the droplet was out of the HiBMs FOV for most of the droplet lifetime, no extinction droplet diameter is reported.

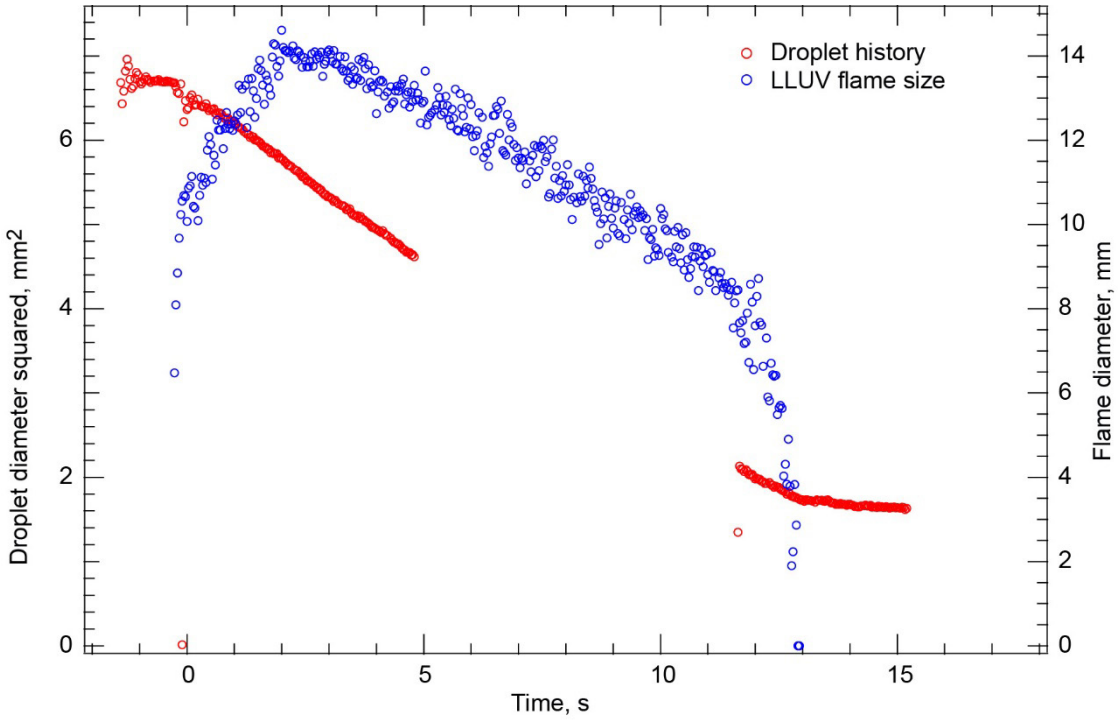

Figure 70.—Test FLEX−066. Free-floating methanol droplet burning in a 0.15/0.85 O_2/N_2, 1.0-atm ambient environment. The droplet drifted southeast and out of the High-Bit-Depth Multispectral (HiBMs) field of view (FOV), but then it drifted back into the FOV for a few seconds before the flame extinguished. During ignition, the droplet changed shape when some material was apparently ejected. The droplet shape oscillated immediately after this. The color camera Image Processing and Storage Unit (IPSU) did not record any images for this test.

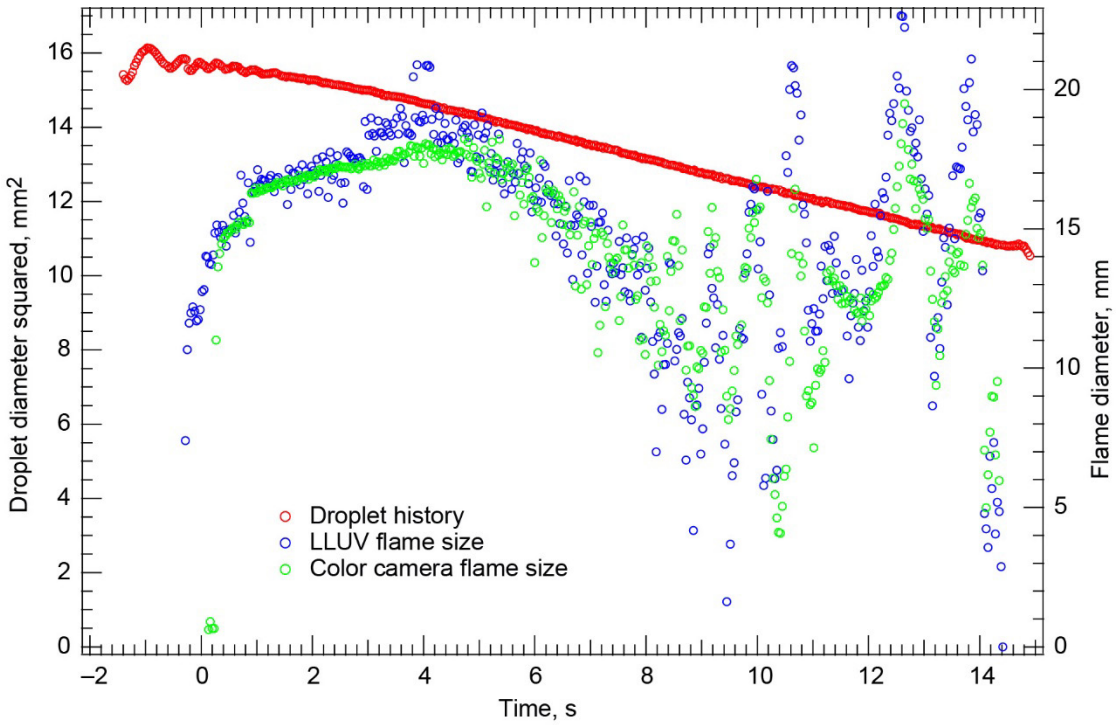

Figure 71.—Test FLEX−067. Free-floating methanol droplet burning in a 0.15/0.85 O_2/N_2, 1.0-atm ambient environment. The flame oscillated significantly before the flame extinguished. After the flame extinguished, the droplet drifted slowly east and then southeast and out of the High-Bit-Depth Multispectral (HiBMs) field of view (FOV).

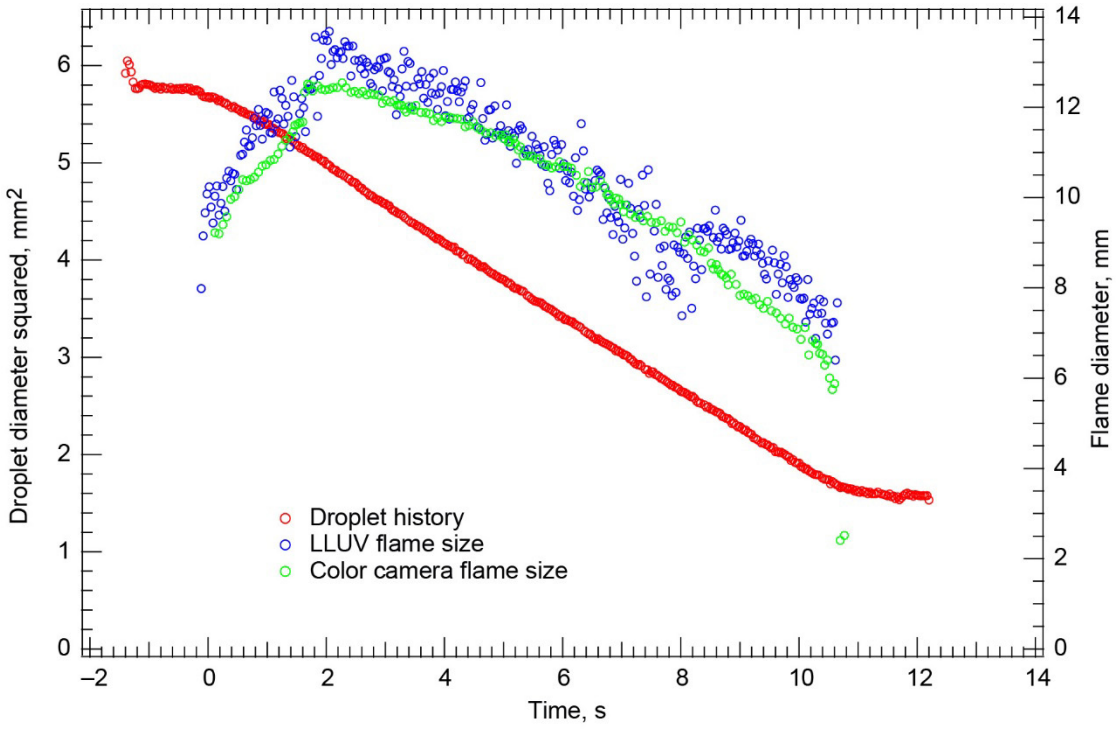

Figure 72.—Test FLEX−068. Free-floating methanol droplet burning in a 0.15/0.85 O_2/N_2, 1.0-atm ambient environment. The droplet drifted slowly to the north, turned south, then drifted slowly before accelerating out of the field of view (FOV) right after the visible flame extinguished.

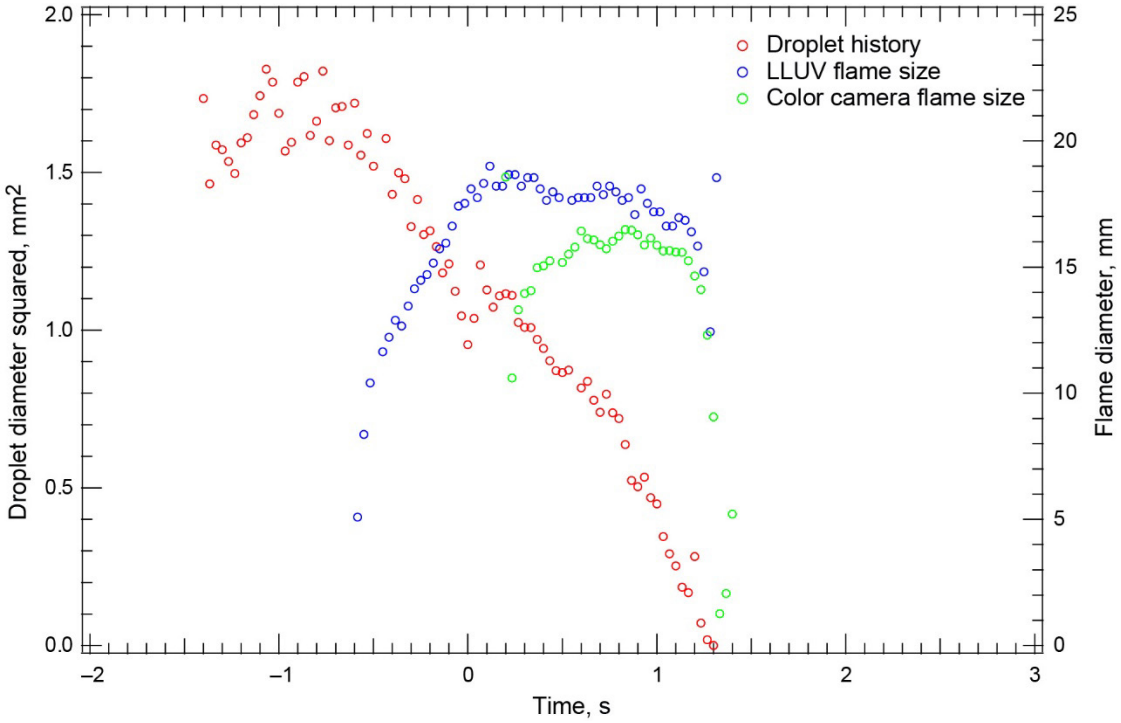

Figure 73.—Test FLEX−069. Fiber-supported heptane droplet with no translation burning in a 0.15/0.85 O_2/N_2, 1.0-atm ambient environment. There was significant droplet motion during the entire very short burn, and there appeared to be some visible distortions where the droplet edge intersected the fiber. This small droplet had significant motion on the fiber, which had a marked influence on the burning characteristics.

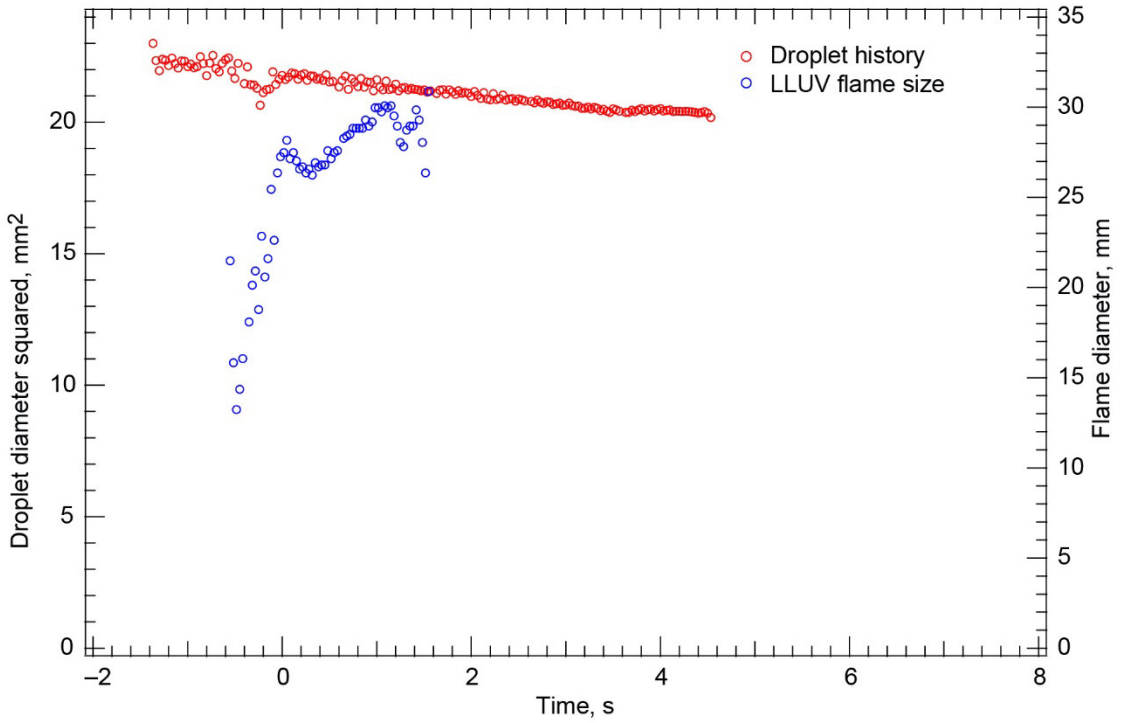

Figure 74.—Test FLEX−070. Free-floating heptane droplet burning in a 0.15/0.85 O_2/N_2, 1.0-atm ambient environment. Extra fuel was dispensed after the automated sequence started. After deployment, the droplet drifted northwest in the High-Bit-Depth Multispectral (HiBMs) field of view (FOV), hit the upper igniter, and quickly drifted southeast and out of the HiBMs FOV. The post deployment/ignition velocity was quite high, approximately 8 mm/s. The color camera Image Processing and Storage Unit (IPSU) did not record any images after deployment. It is not known whether there was cool flame burning and extinction for this test.

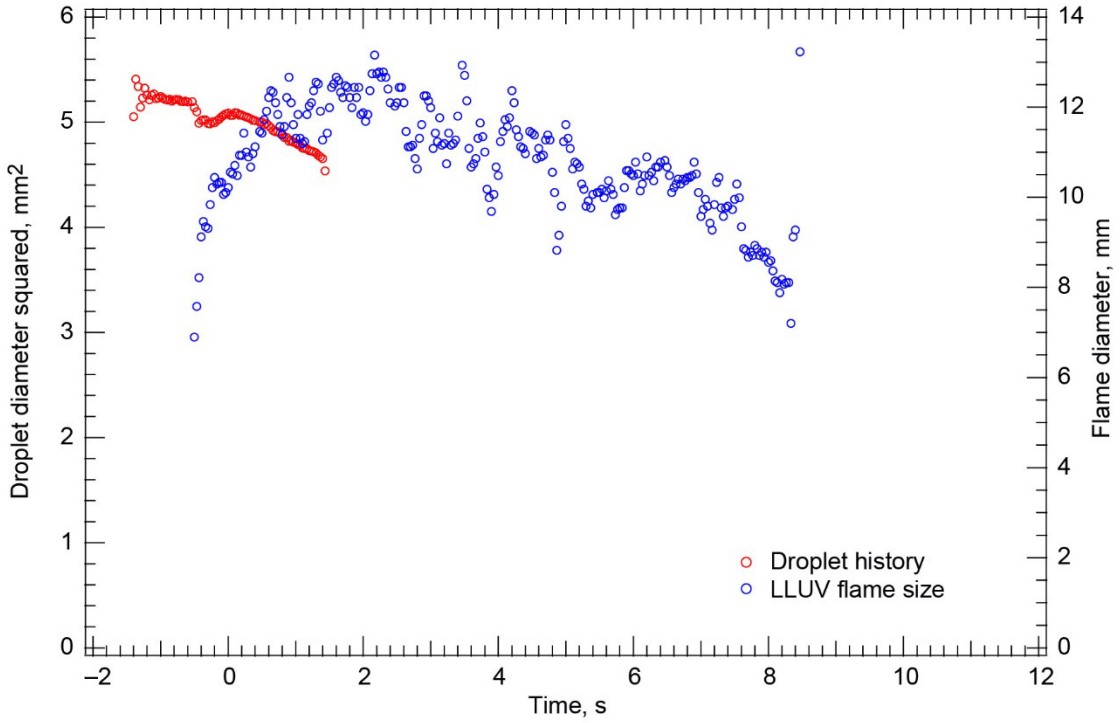

Figure 75.—Test FLEX−071. Free-floating methanol droplet burning in a 0.15/0.85 O_2/N_2, 1.0-atm ambient environment. The droplet had a high drift velocity to the north after deployment. It hit the igniter and then continued to move to the north-northwest after ignition at approximately 7 to 8 mm/s. It left the High-Bit-Depth Multispectral (HiBMs) field of view (FOV) relatively quickly and well before the flame extinguished. Because the droplet was out of the HiBMs FOV for most of the burn, no extinction droplet diameter is reported. The color camera Image Processing and Storage Unit (IPSU) did not record any images after deployment.

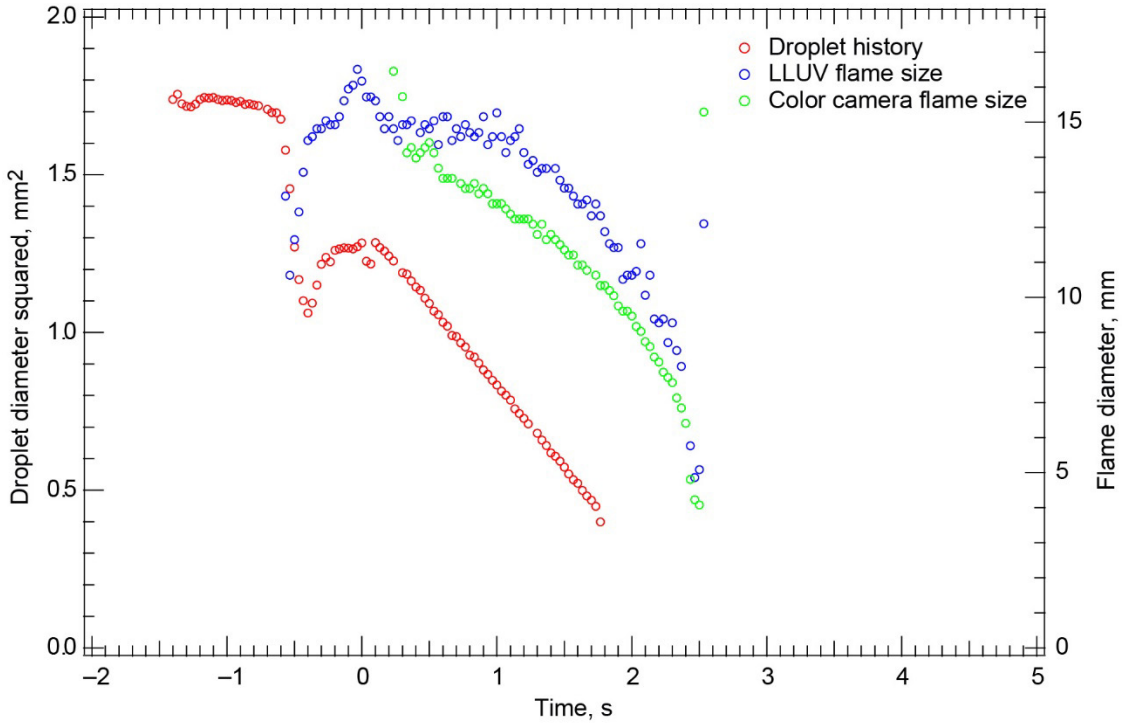

Figure 76.—Test FLEX−072. Free-floating heptane droplet burning in a 0.15/0.85 O_2/N_2, 1.0-atm ambient environment. This was a very small droplet, smaller than would be typically recommended to burn in the apparatus. The droplet drifted north-northwest in the High-Bit-Depth Multispectral (HiBMs) field of view (FOV) after deployment and ignition with a significant (7 to 8 mm/s) velocity, and it left the FOV before the test was complete. The droplet burned with a dim blue flame to completion without disruption. After ignition, there was only a little luminous region. This may have been due to a small bubble burst during ignition (indicated by the droplet history).

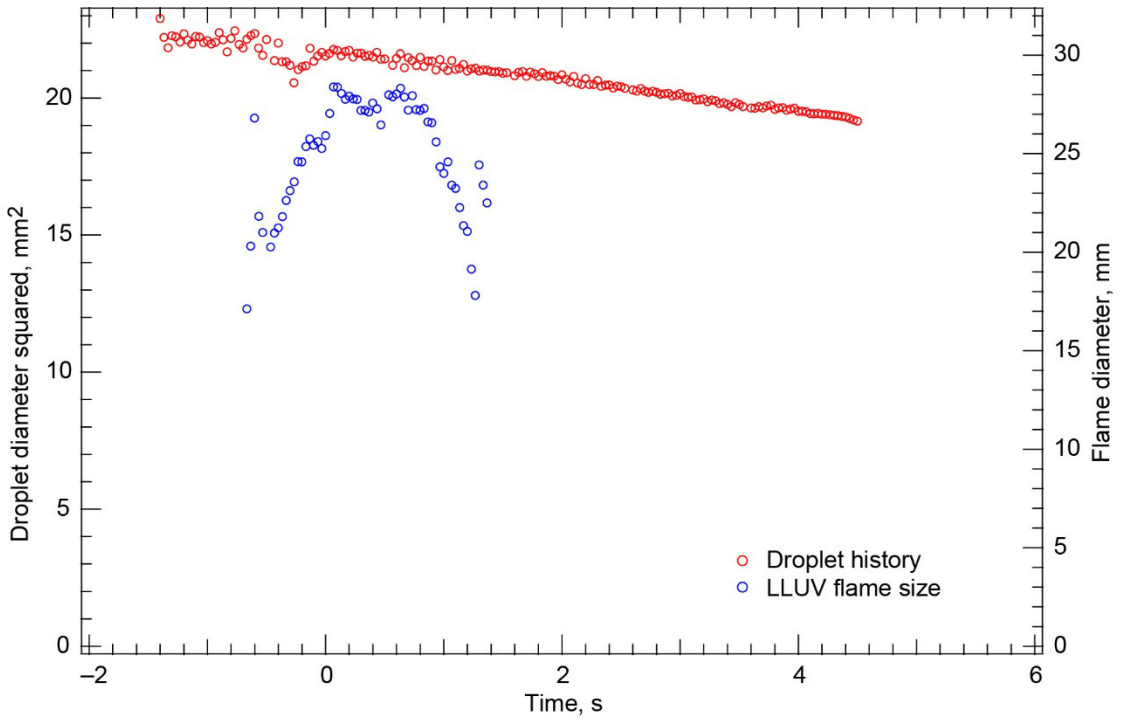

Figure 77.—Test FLEX−073. Free-floating heptane droplet burning in a 0.15/0.85 O_2/N_2, 1.0-atm ambient environment. There was an error in the automated test sequence, and the Multi-User Droplet Combustion Apparatus (MDCA) dispensed fuel before deployment. The result was a very large droplet, much larger than intended. The droplet drifted northwest in the High-Bit-Depth Multispectral (HiBMs) field of view (FOV) after deployment, then it hit the igniter and began to drift southeast and quickly out of the FOV. The droplet lifetime was very short with the flame extinguishing only a few seconds after the igniter was withdrawn. The color camera Image Processing and Storage Unit (IPSU) did not record any images after deployment, and there is not enough evidence to know whether this test exhibited cool flame burning and extinction after the visible flame extinguished.

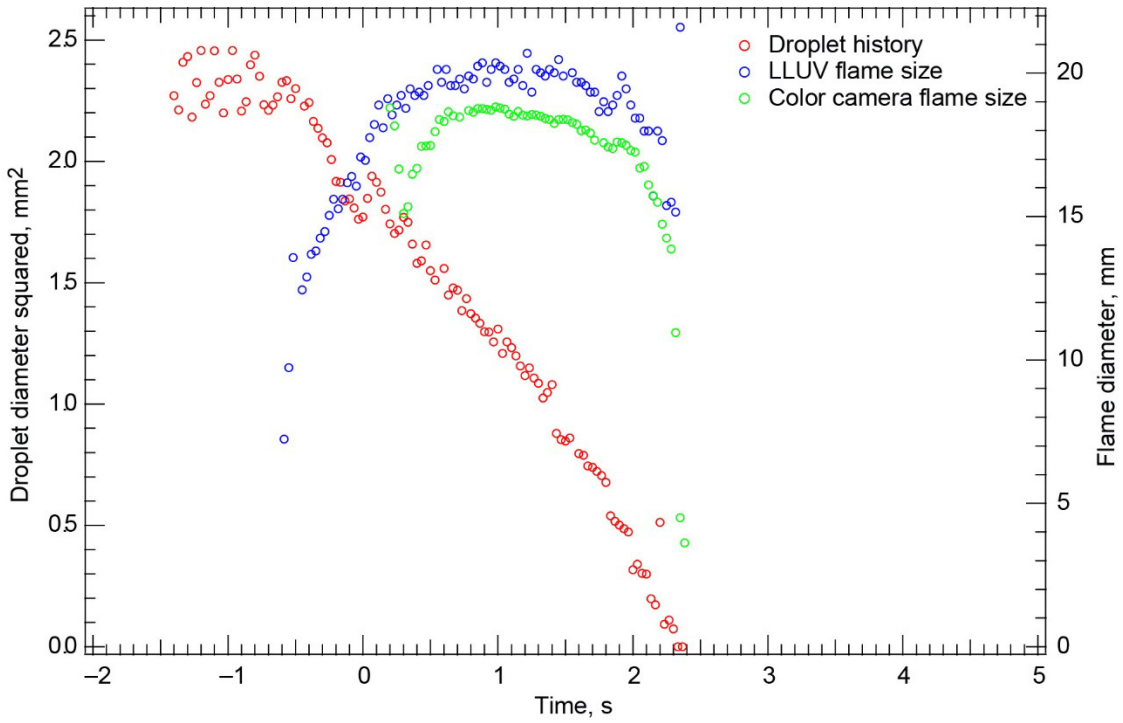

Figure 78.—Test FLEX−074. Fiber-supported heptane droplet burning in a 0.15/0.85 O_2/N_2, 1.0-atm ambient environment. The droplet oscillated significantly on the fiber after deployment and throughout the burn. The oscillations caused the droplet to become misshapen and caused large errors and scatter in the droplet size measurements. This was a very short burn and, although there was not a large disruption, the oscillations compromised the test data.

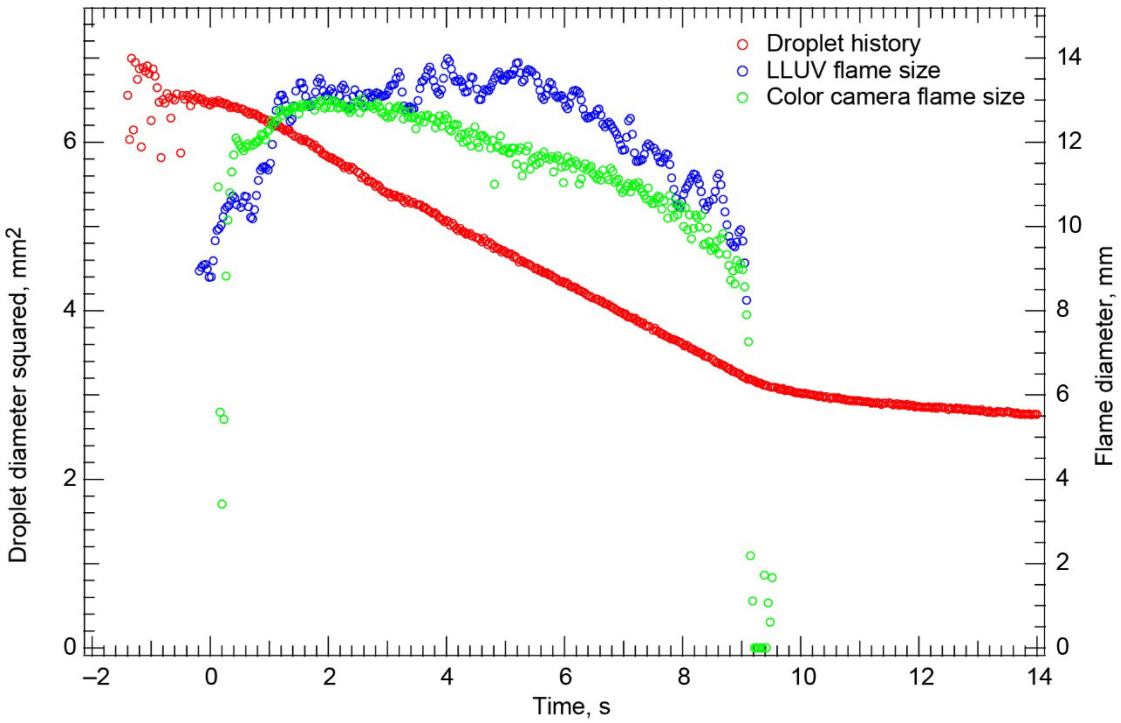

Figure 79.—Test FLEX−075. Fiber-supported methanol droplet translating 3 mm/s and burning in a 0.13/0.85 O_2/N_2, 1.0-atm ambient environment. After deployment, there was some transverse, but no axial, motion along the fiber. The transverse motion persisted throughout the test, but it stopped after the flame extinguished. There was no axial motion relative to the fiber; that is, the droplet started and stopped with the start and stop of the fiber. There also was no disruption during this test.

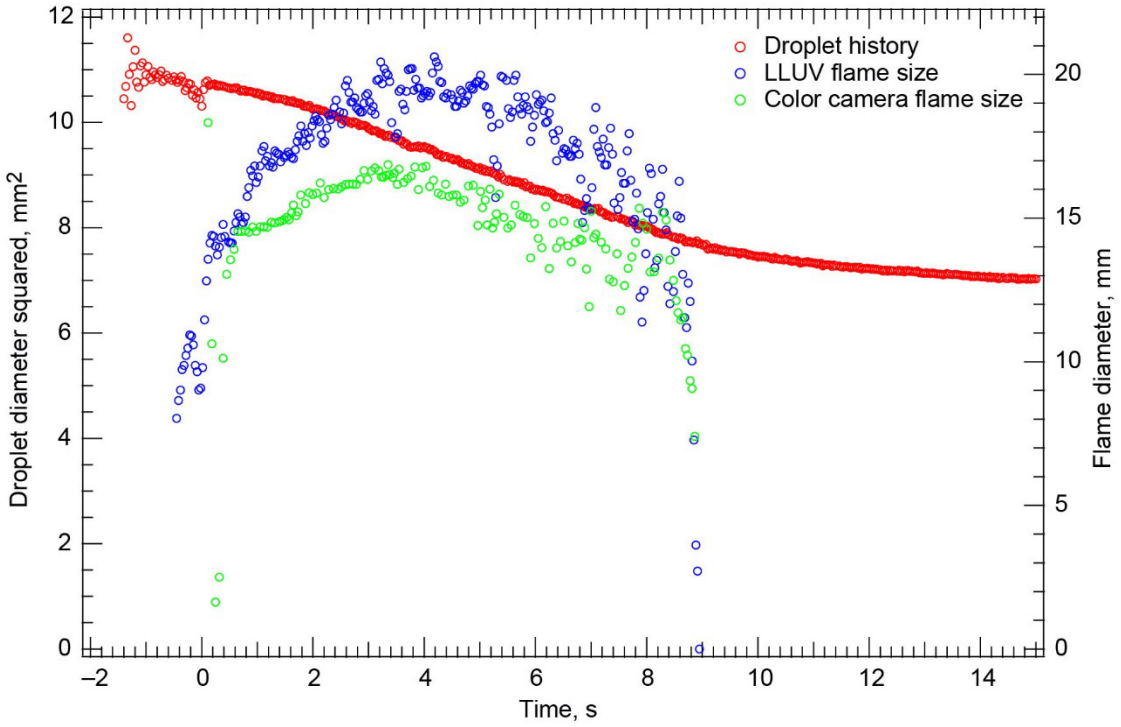

Figure 80.—Test FLEX−076. Fiber-supported methanol droplet burning in a 0.14/0.86 O_2/N_2, 1.0-atm ambient environment. The droplet oscillated axially on the fiber throughout the flame lifetime, only becoming quiescent after the visible flame extinguished.

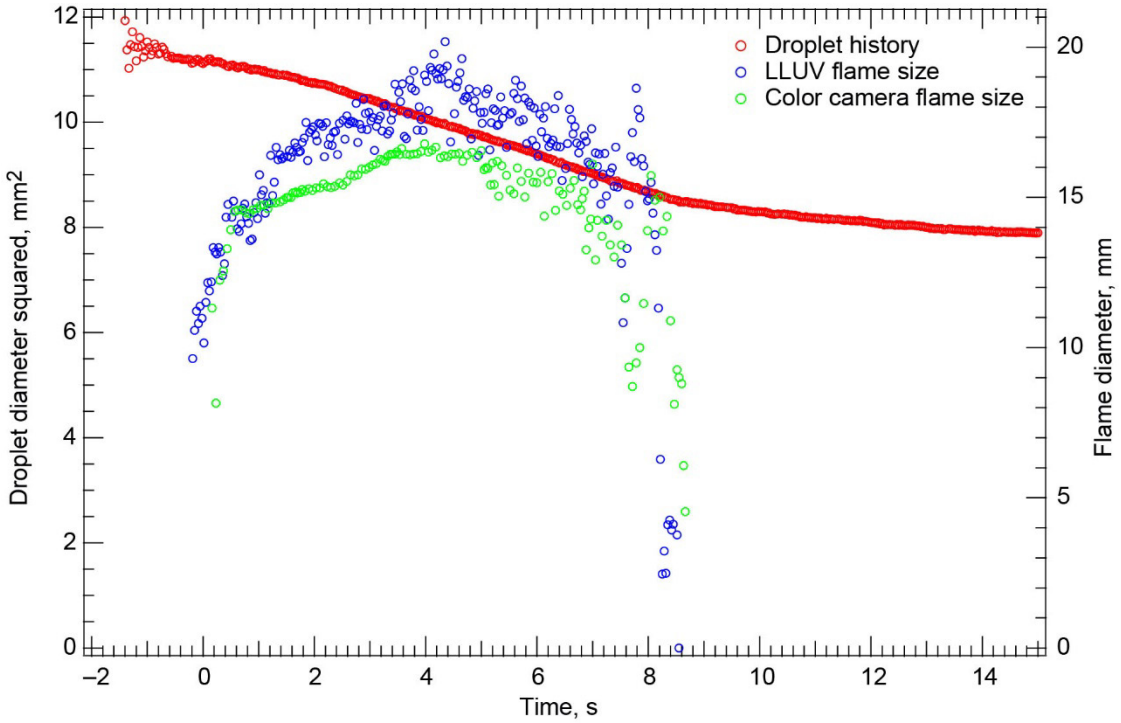

Figure 81.—Test FLEX−077. Free-floating methanol droplet burning in a 0.14/0.85 O_2/N_2, 1.0-atm ambient environment. There was very little droplet motion after deployment and ignition (it only moved a few millimeters during the entire test).

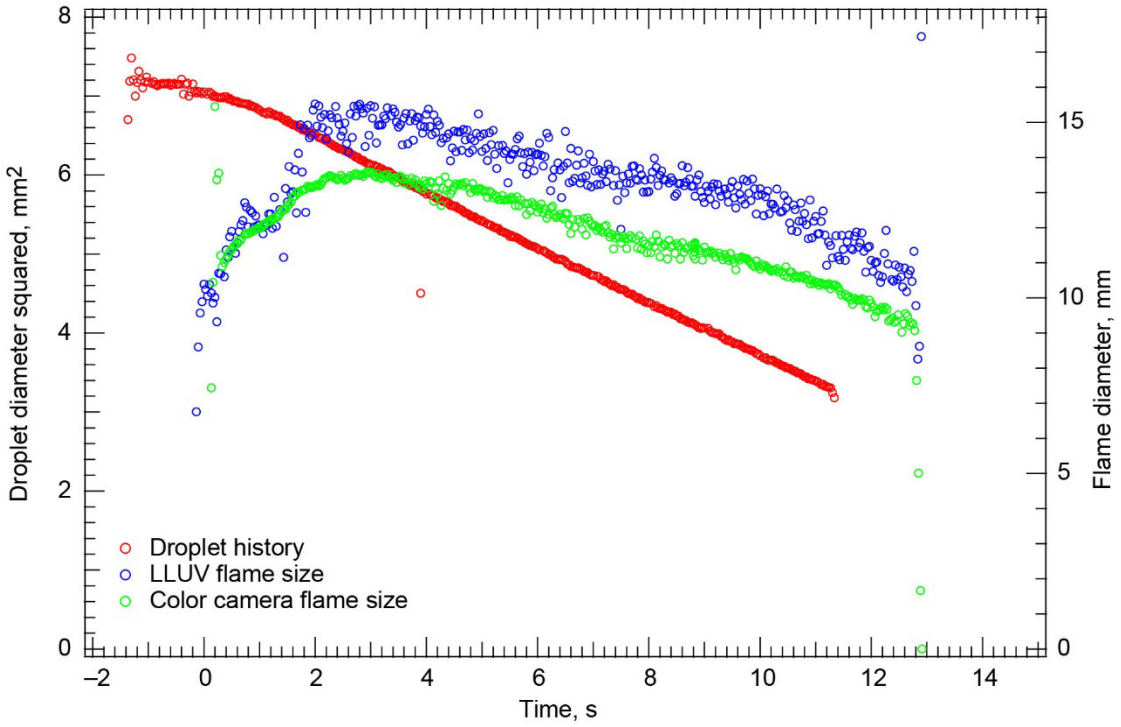

Figure 82.—Test FLEX−078. Free-floating methanol droplet burning in a 0.14/0.85 O_2/N_2, 1.0-atm ambient environment. There was very little droplet motion after ignition. Halfway through the burn, the droplet began to drift east at approximately 3 mm/s. It drifted out of the High-Bit-Depth Multispectral (HiBMs) field of view (FOV) just before the flame extinguished. The extinction droplet diameter was extrapolated from the droplet history and the measured average burning rate constant just prior to when the droplet left the HiBMs FOV.

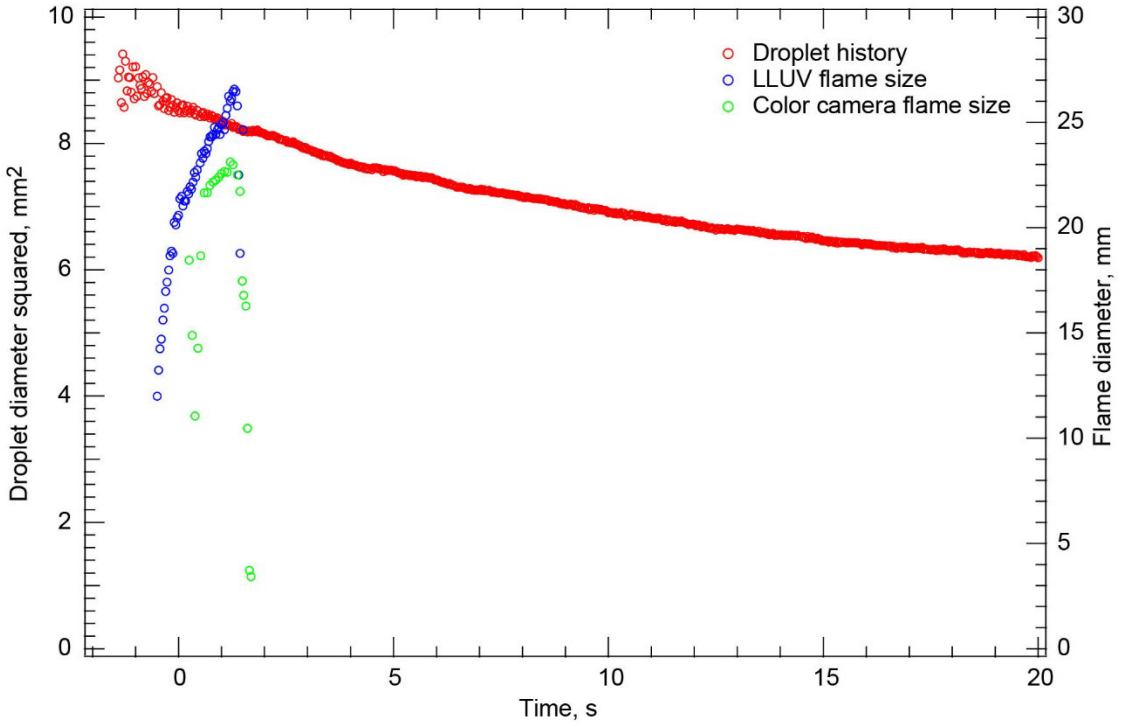

Figure 83.—Test FLEX−079. Free-floating heptane droplet burning in a 0.13/0.85 O_2/N_2, 1.0-atm ambient environment. This very short burn was entirely transient. The ambient environment was probably below the quasi-steady flammability limit. A small vapor cloud formed shortly after the visible flame extinguished, which may be indicative of cool flame burning and extinction following hot flame extinction.

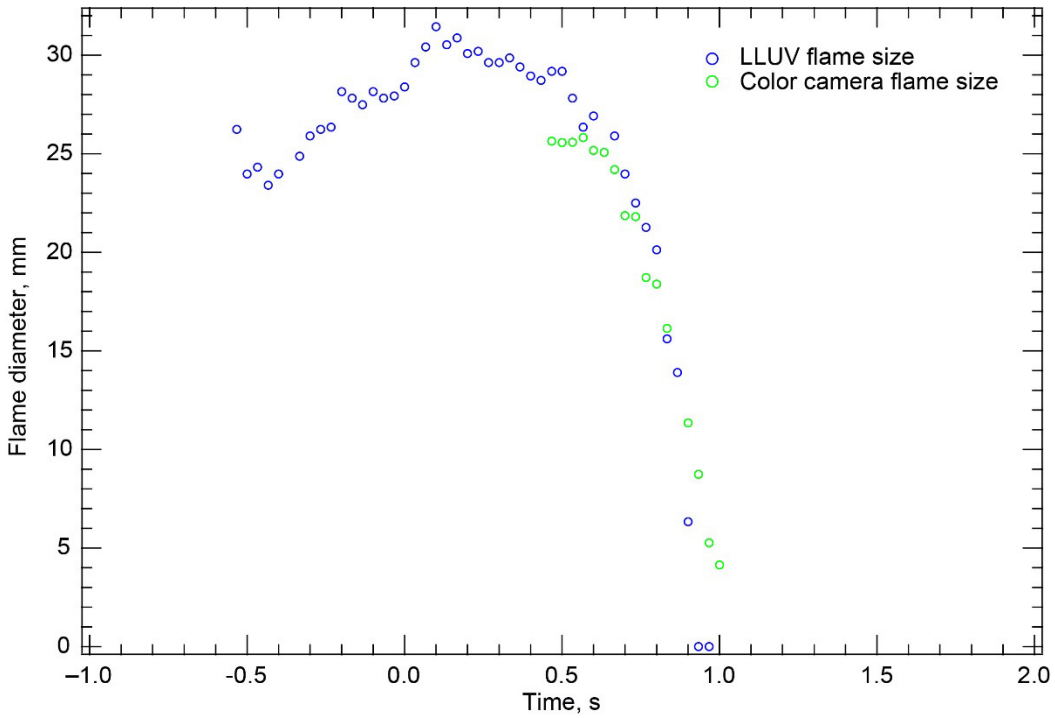

Figure 84.—Test FLEX−080. Fiber-supported heptane droplet translating 3 mm/s and burning in a 0.13/0.87 O_2/N_2, 1.0-atm ambient environment. The High-Bit-Depth Multispectral (HiBMs) Image Processing and Storage Unit (IPSU) did not record any images for this test. This test had a very short flame lifetime, with the flame extinguishing before the droplet began to translate. A small vapor cloud formed sometime after the visible flame extinguished. It is not clear whether there was cool flame burning and extinction following visible flame extinction.

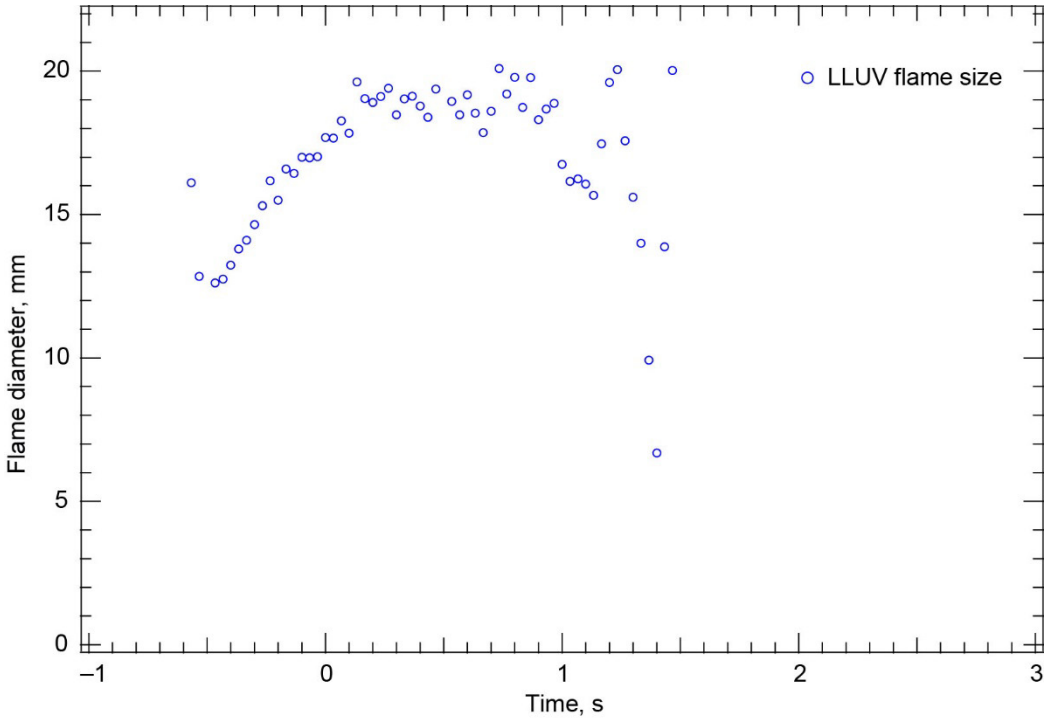

Figure 85.—Test FLEX−081. Fiber-supported heptane droplet burning in a 0.13/0.87 O_2/N_2, 1.0-atm ambient environment. The High-Bit-Depth Multispectral (HiBMs) and color camera Image Processing and Storage Units (IPSUs) did not record any images after deployment. This was a very short burn with almost no burning after the igniter was withdrawn.

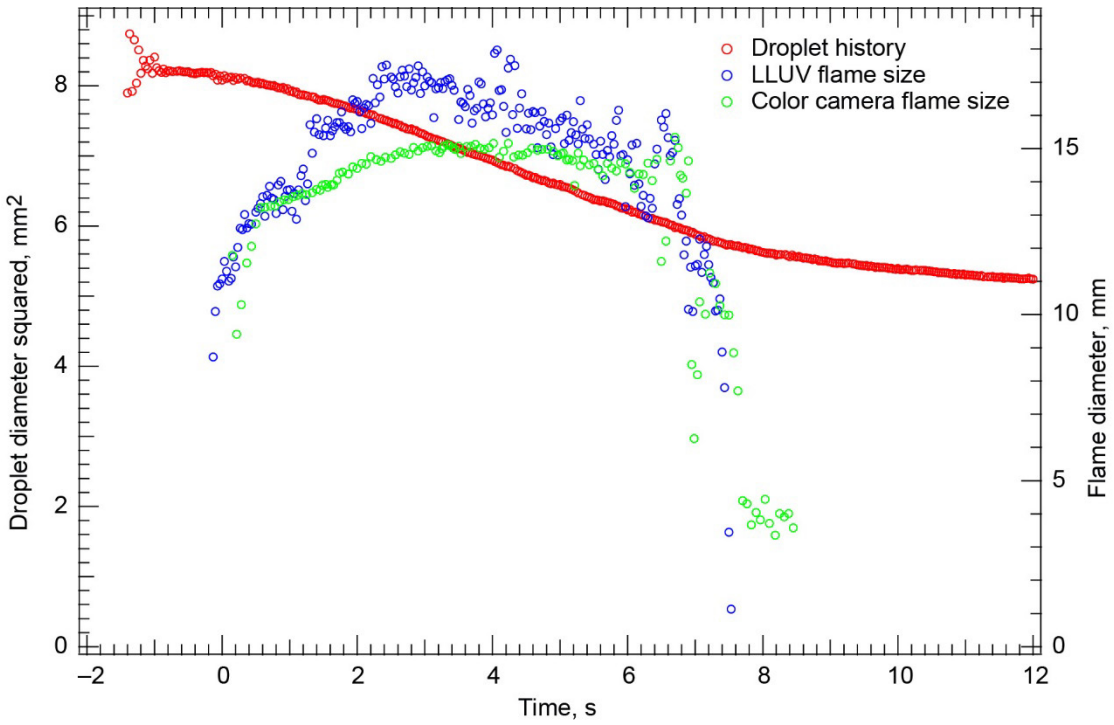

Figure 86.—Test FLEX−082. Free-floating methanol droplet burning in a 0.13/0.87 O_2/N_2, 1.0-atm ambient environment. The deployment and ignition were very good, with almost no residual motion. The droplet did drift south in the High-Bit-Depth Multispectral (HiBMs) field of view (FOV) and then drifted out of the FOV, but not until well after the flame extinguished. This was a very dim flame.

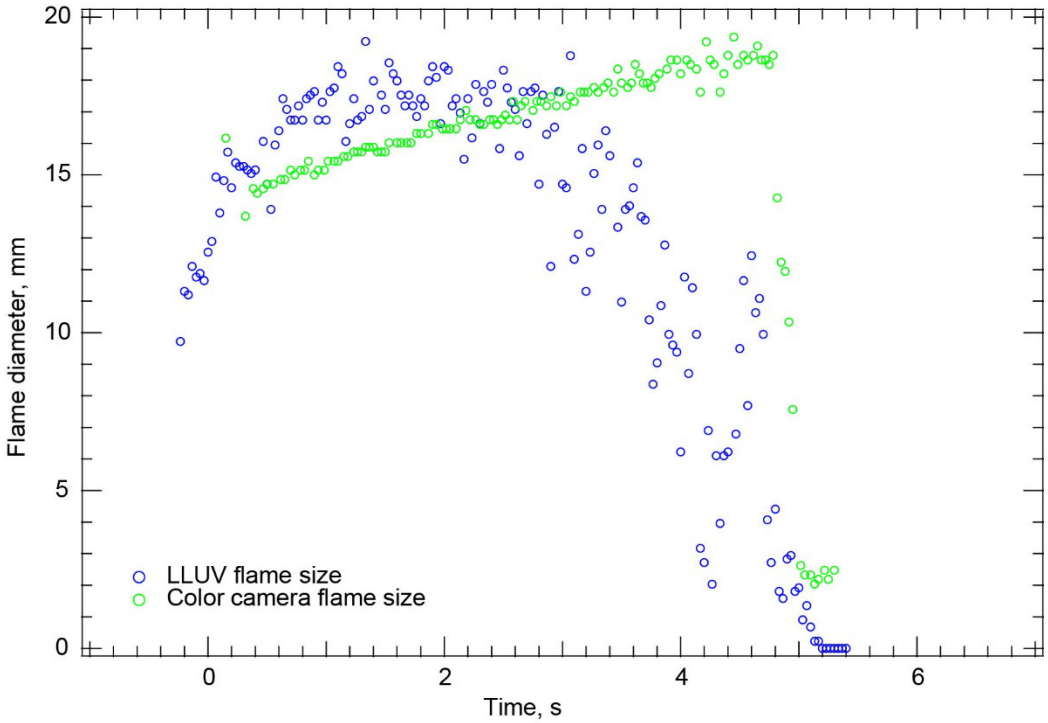

Figure 87.—Test FLEX−083. Free-floating methanol droplet burning in a 0.12/0.88 O_2/N_2, 1.0-atm ambient environment. The High-Bit-Depth Multispectral (HiBMs) Image Processing and Storage Unit (IPSU) did not record any images for this test. The droplet did not drift after deployment and ignition and remained in the fields of view (FOVs) of both the Low Light Level Ultra-Violet (LLUV) and color camera. The flame was very dim and almost undetectable by the LLUV (especially later in the flame lifetime). As a result, the LLUV flame size measurements are not accurate.

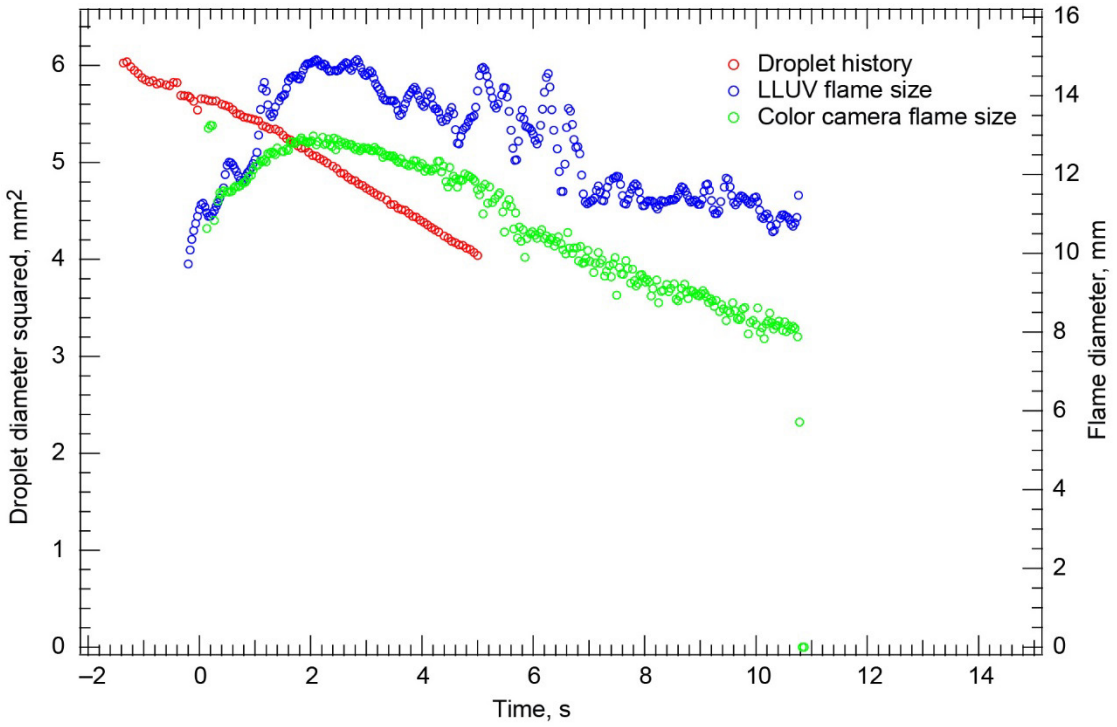

Figure 88.—Test FLEX−084. Free-floating methanol droplet burning in a 0.13/0.87 O_2/N_2, 1.0-atm ambient environment. The droplet drifted north after deployment and ignition (deployment-induced motion) and out of the High-Bit-Depth Multispectral (HiBMs) field of view (FOV) halfway through the test. The flame remained within the Low Light Level Ultra-Violet (LLUV) and color camera FOVs during the entire test. The droplet burned for a long time in this ambient environment. The extinction droplet diameter was based on extrapolating the droplet history using the measured burning rate constant while the droplet was within the HiBMs FOV. The flame was very dim, and the LLUV flame data are not as reliable as for the other tests because of the intensifier noise.

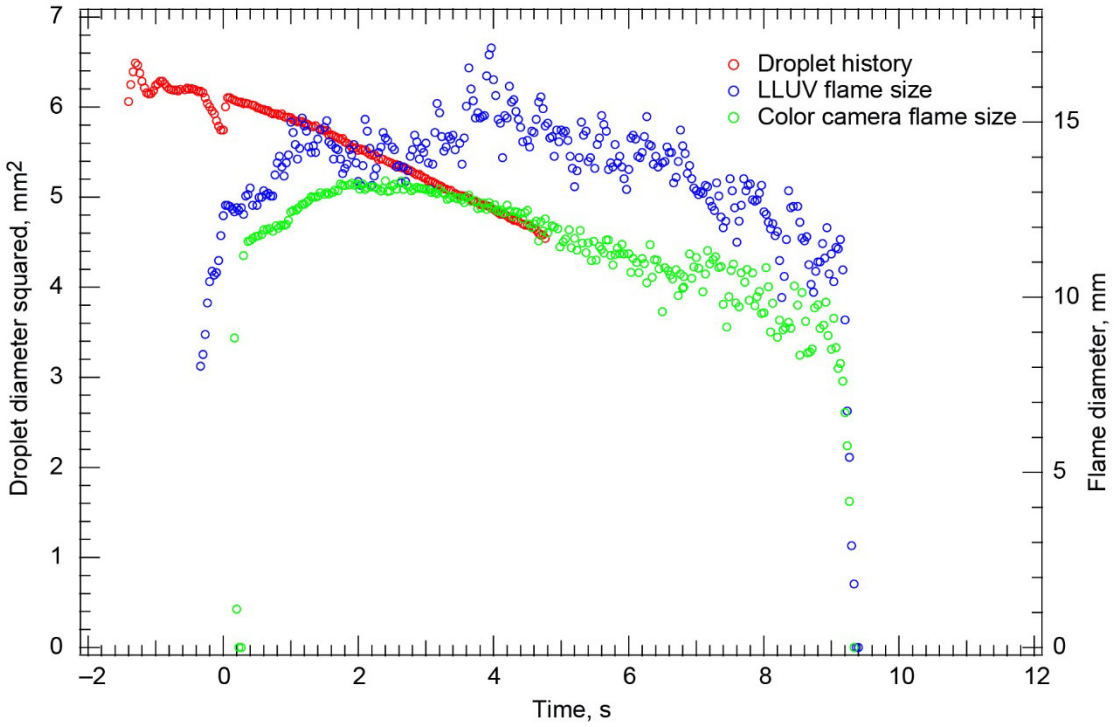

Figure 89.—Test FLEX−085. Free-floating methanol droplet burning in a 0.13/0.87 O_2/N_2, 1.0-atm ambient environment. The droplet drifted northwest in the High-Bit-Depth Multispectral (HiBMs) field of view (FOV) and then drifted out of the FOV about halfway through the test. The flame remained within the Low Light Level Ultra-Violet (LLUV) and color camera FOVs for the entire test. The extinction droplet diameter is based on extrapolating the droplet history using the known burning rate constant from the droplet history until just before the droplet left the HiBMs FOV.

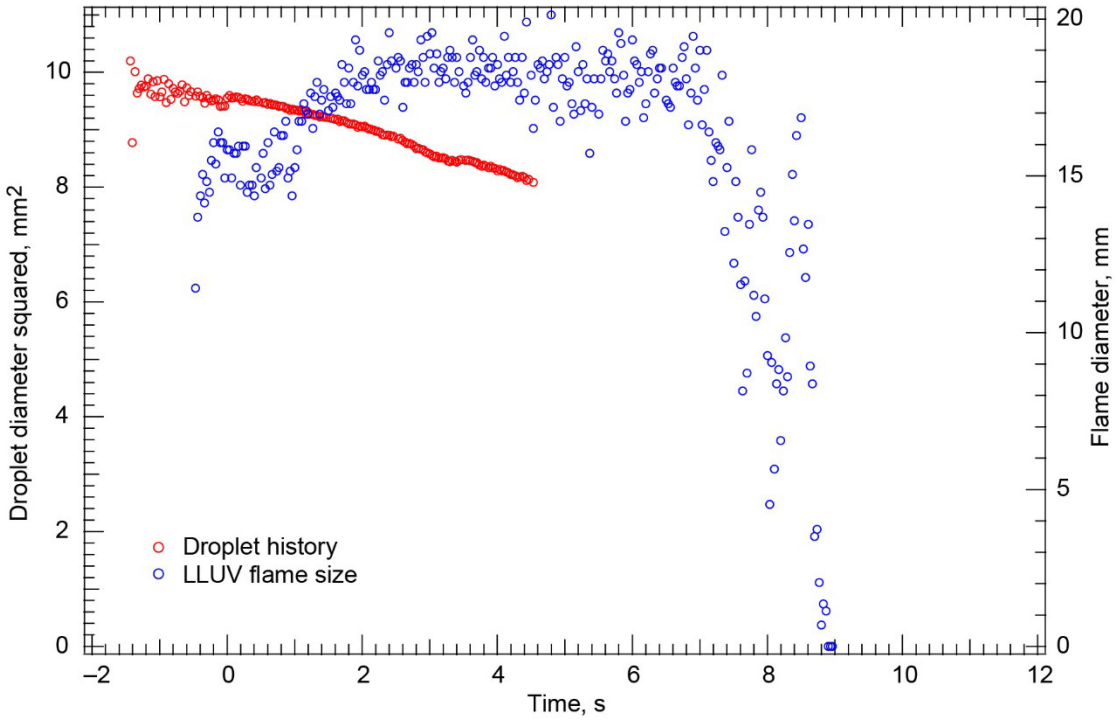

Figure 90.—Test FLEX−086. Fiber-supported methanol droplet translating 3 mm/s and burning in a 0.13/0.87 O_2/N_2, 1.0-atm ambient environment. The droplet oscillated transversely on the fiber throughout the test. It continued to move (relative to the fiber) even after the fiber stopped translating. It drifted out of the High-Bit-Depth Multispectral (HiBMs) field of view (FOV) and to the edge of the Low Light Level Ultra-Violet (LLUV) FOV. Only about half of the test was captured by the HiBMs. The color camera Image Processing and Storage Unit (IPSU) did not record any images after deployment. The extinction droplet diameter was based on extrapolating the droplet history using the measured burning rate constant while the droplet was within the HiBMs FOV (and extinction from the LLUV).

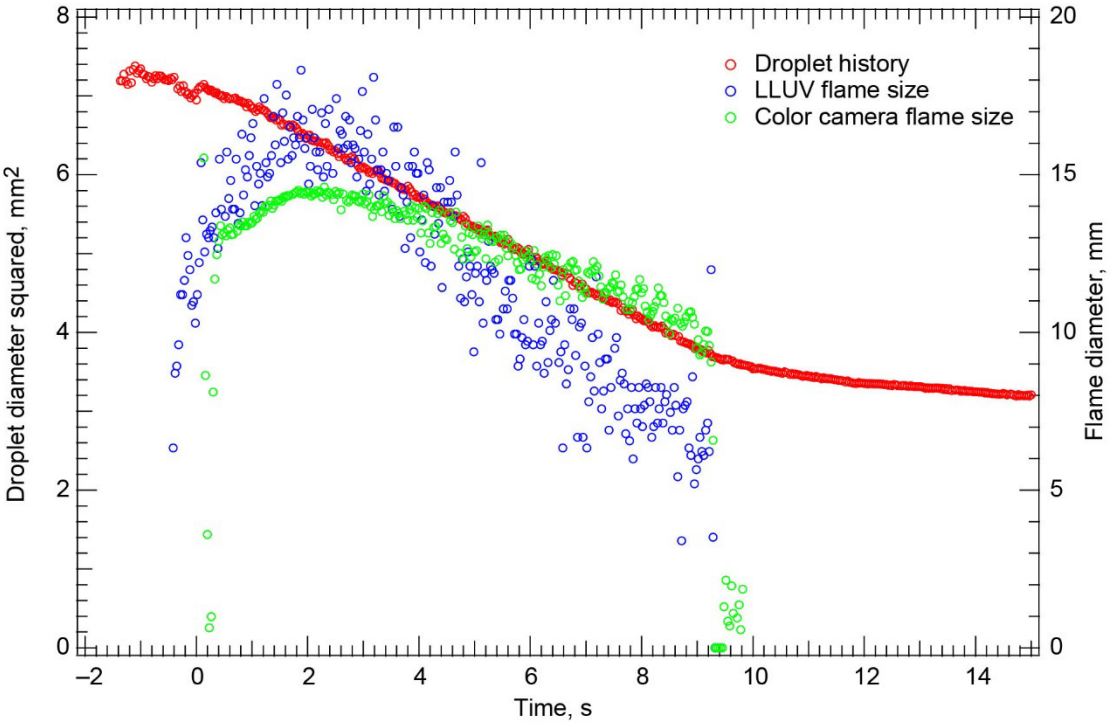

Figure 91.—Test FLEX−087. Fiber-supported methanol droplet with no translation and burning in a 0.13/0.87 O_2/N_2, 1.0-atm ambient environment. Throughout the burn, there were significant axial oscillations along the fiber axis. The oscillations were significant and persistent. The droplet remained within the High-Bit-Depth Multispectral (HiBMs) field of view (FOV) for the entire test, and it burned for a relatively long time in this low-O_2 ambient environment. Because the flame was very dim, the Low Light Level Ultra-Violet (LLUV) flame size measurements are not reliable.

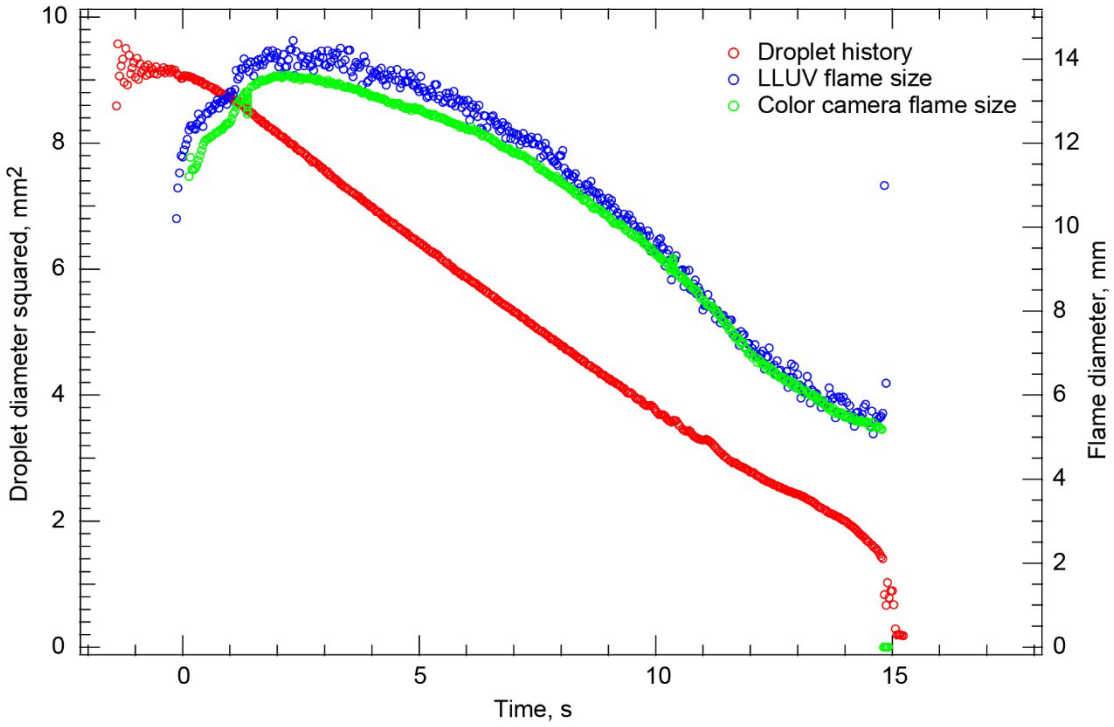

Figure 92.—Test FLEX−088. Free-floating methanol droplet burning in a 0.25/0.60/0.15 $O_2/N_2/CO_2$, 0.70-atm ambient environment. The droplet deployed and ignited with almost no residual motion. It remained within the High-Bit-Depth Multispectral (HiBMs) field of view (FOV) for the entire test. The droplet burned cleanly with a brighter-than-usual blue flame during the entire test. Near the end of the test, the droplet deformed (becoming football shaped). Then the droplet disrupted coincident with flame extinction. The droplet shattered at the end of the test, indicating that it was probably compromised by contamination from the conformal coating on the needle.

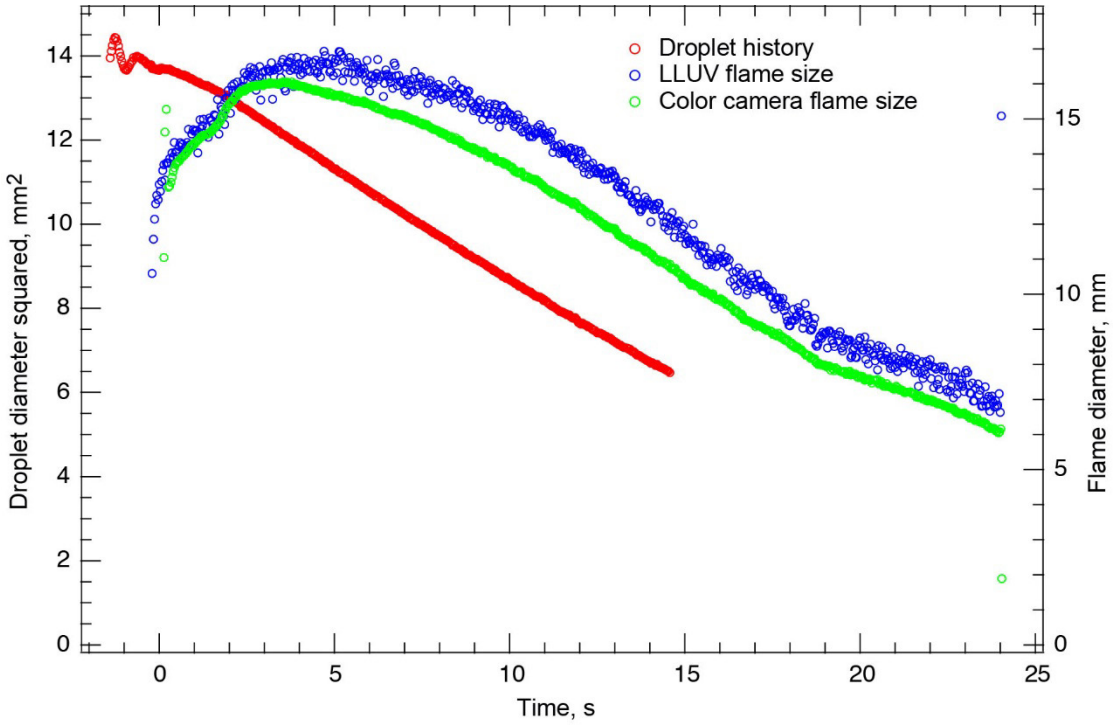

Figure 93.—Test FLEX−089. Free-floating methanol droplet burning in a 0.25/0.60/0.15 $O_2/N_2/CO_2$, 0.70-atm ambient environment. The droplet drifted slowly to the east in the High-Bit-Depth Multispectral (HiBMs) field of view (FOV), then drifted out of the FOV before the test ended. As the droplet was leaving the HiBMs FOV, the liquid began to oscillate slightly. The motion was visible in the color camera view. The flame extinguished abruptly—probably because of disruption.

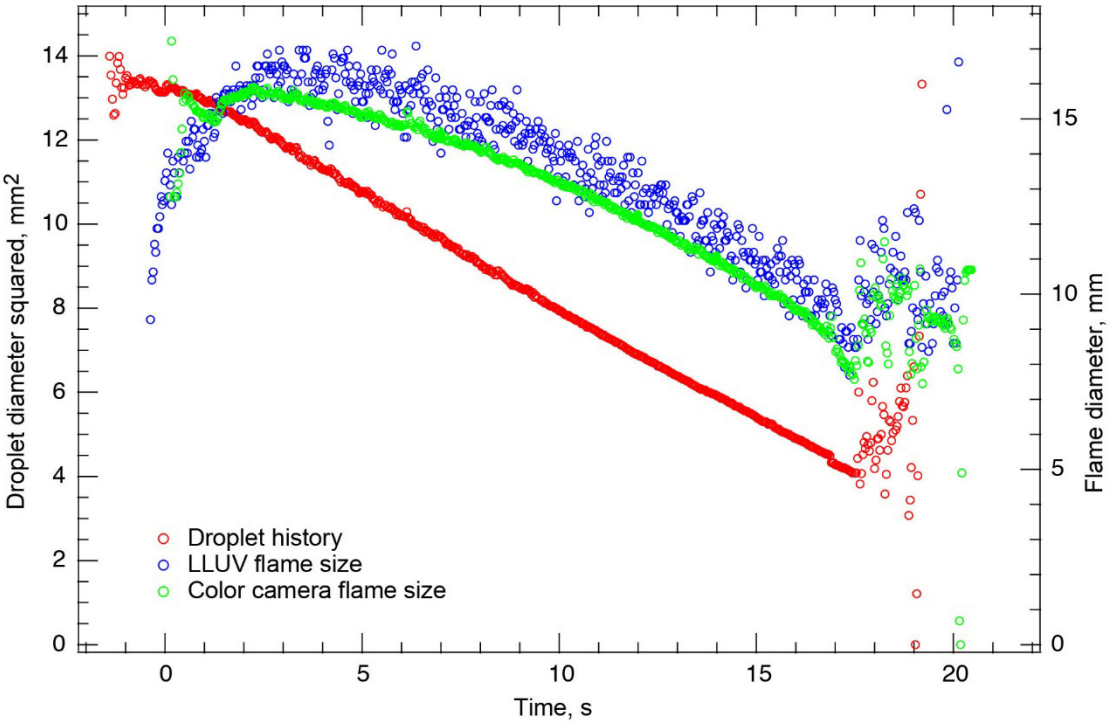

Figure 94.—Test FLEX−090. Fiber-supported methanol droplet with no translation in a 0.25/0.60/0.15 $O_2/N_2/CO_2$, 0.70-atm ambient environment. There were significant axial and transverse oscillations on the fiber after ignition. While the droplet was oscillating on the fiber, “sparklers” were evident on the color camera view. Then the oscillations diminished and the droplet burned cleanly (on the color camera view as well). A few seconds before the flame extinguished, there was a disruption (without dislocation), followed by a complete disruption, dislocation, and flame extinction.

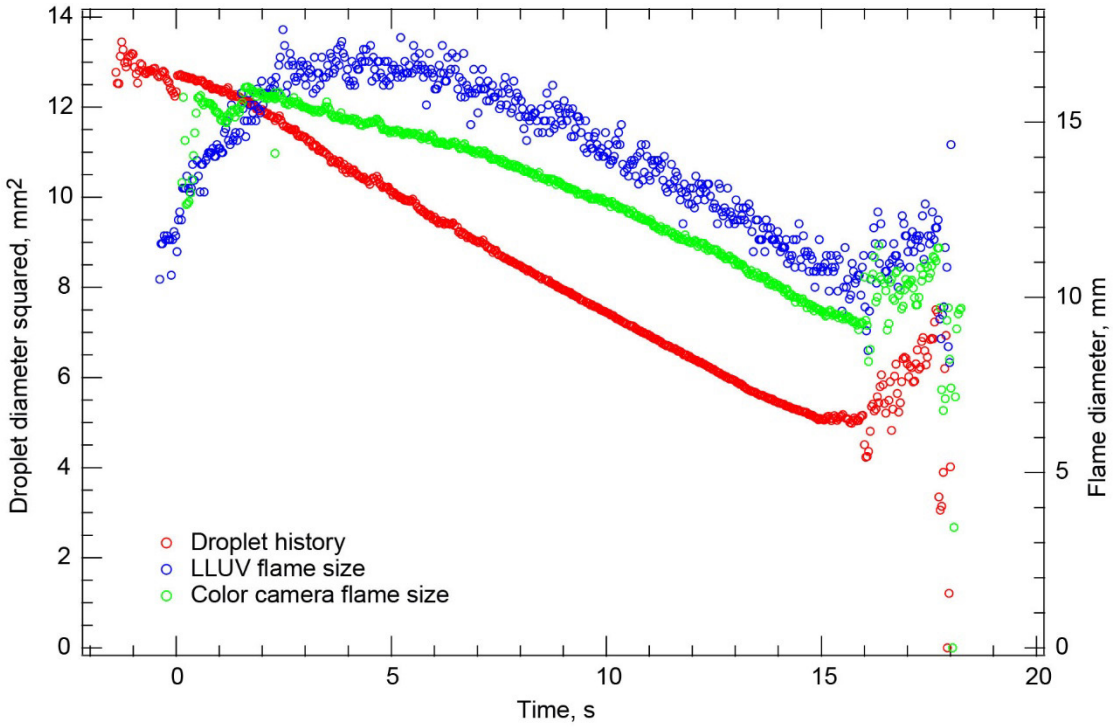

Figure 95.—Test FLEX−091. Fiber-supported methanol droplet translating 3 mm/s and burning in a 0.25/0.60/0.15 $O_2/N_2/CO_2$, 0.70-atm ambient environment. There were moderate axial oscillations on the fiber (lower frequency than for some of the tests with severe oscillations) while the droplet was translating. The oscillations stopped and the droplet burned nicely until the end of the test, when there was a disruption coincident with flame extinction. The increase in droplet size at the end of the test was probably the result of bubble nucleation and growth.

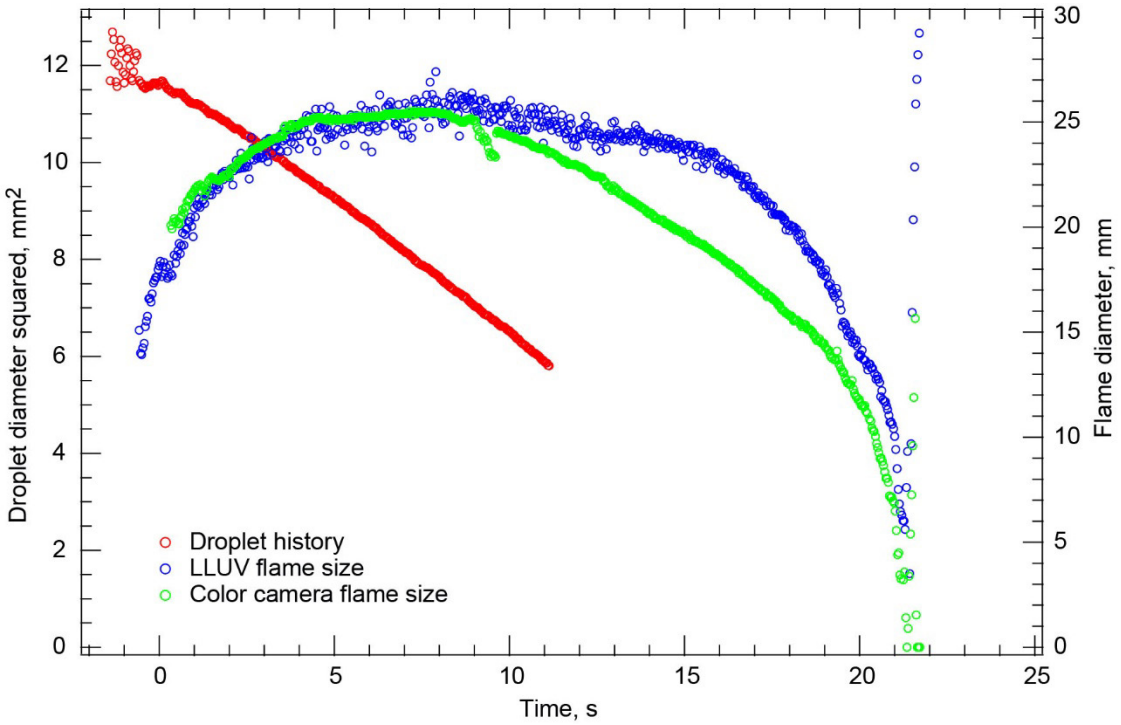

Figure 96.—Test FLEX−092. Free-floating heptane droplet burning in a 0.14/0.86 O_2/N_2, 0.7-atm ambient environment. The droplet drifted north and out of the High-Bit-Depth Multispectral (HiBMs) field of view (FOV) before the burn was complete (about 60 percent of the burn was captured with the HiBMs). The burn looked very clean. The droplet burned for a very long time to a small size, with a disruption that was coincident with flame extinction.

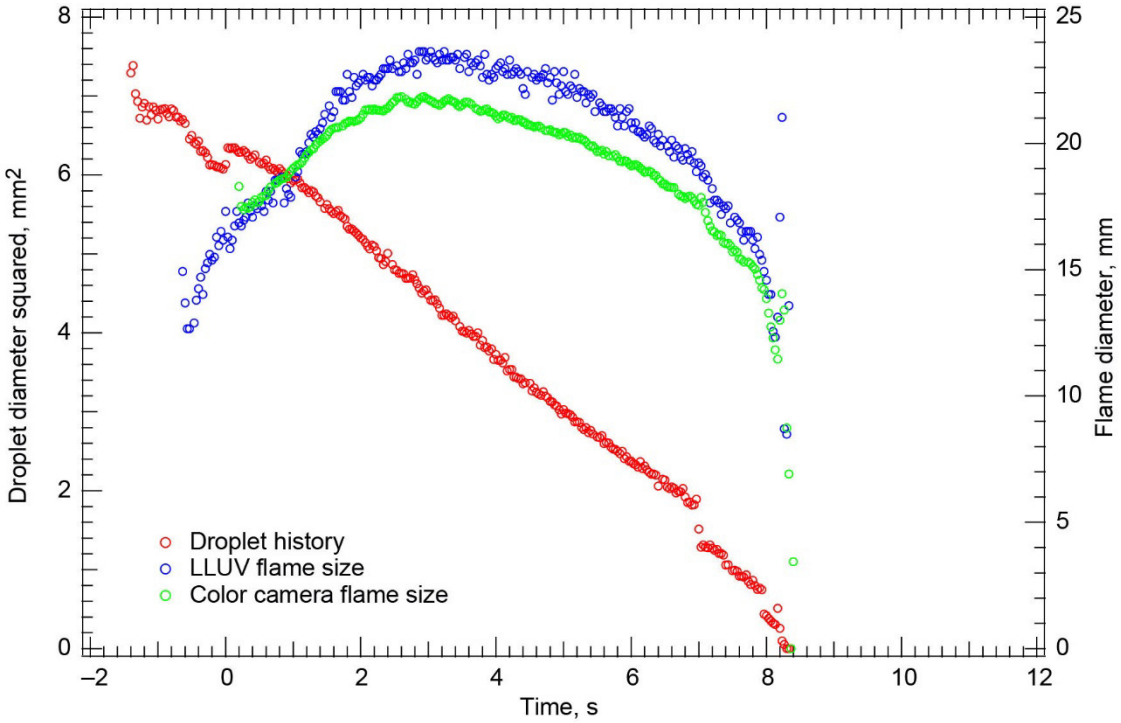

Figure 97.—Test FLEX−093. Fiber-supported heptane droplet translating 3 mm/s and burning in a 0.24/0.56/0.20 $O_2/N_2/CO_2$, 0.70-atm ambient environment. There was a lot of transverse and axial oscillatory motion during the entire droplet burn. The droplet did not leave the High-Bit-Depth Multispectral (HiBMs) field of view (FOV) during the test, but the burning rate was high, probably because of the significant and high-frequency oscillations.

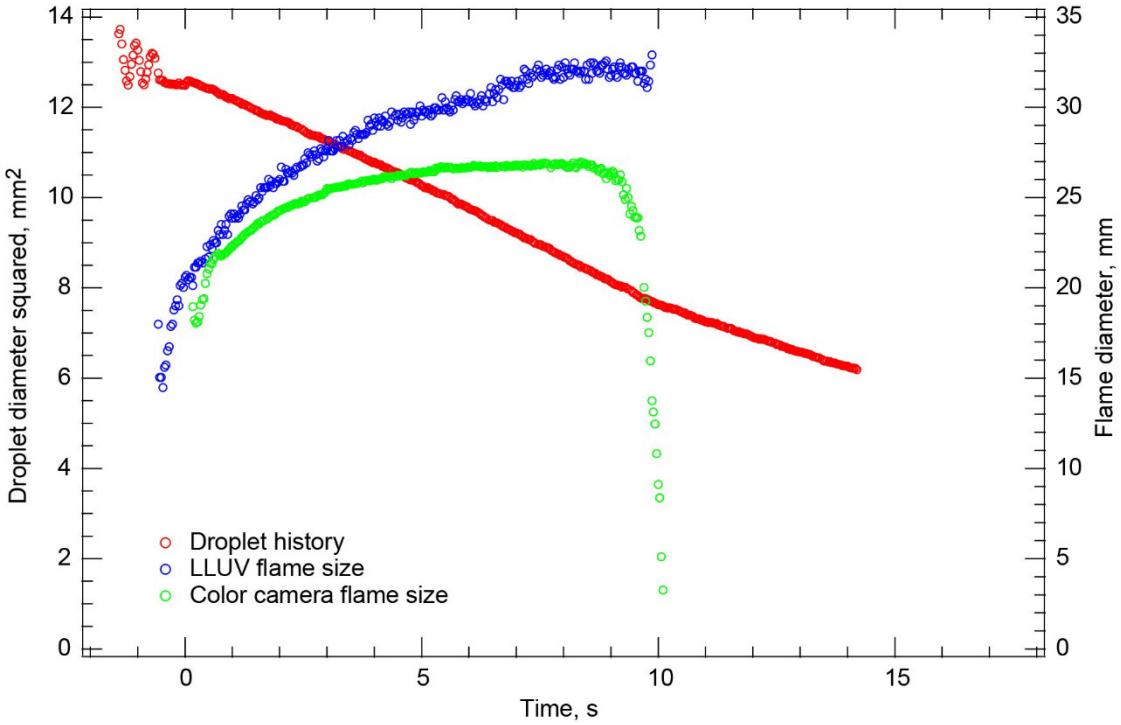

Figure 98.—Test FLEX−094. Free-floating heptane droplet burning in a 0.27/0.56/0.20 $O_2/N_2/CO_2$, 0.70-atm ambient environment. The droplet drifted north after deployment and ignition and out of the High-Bit-Depth Multispectral (HiBMs) field of view (FOV) shortly after the visible flame extinguished. Sometime after the visible flame extinguished, a large vapor cloud formed. This is indicative of cool flame burning and extinction following visible flame extinction.

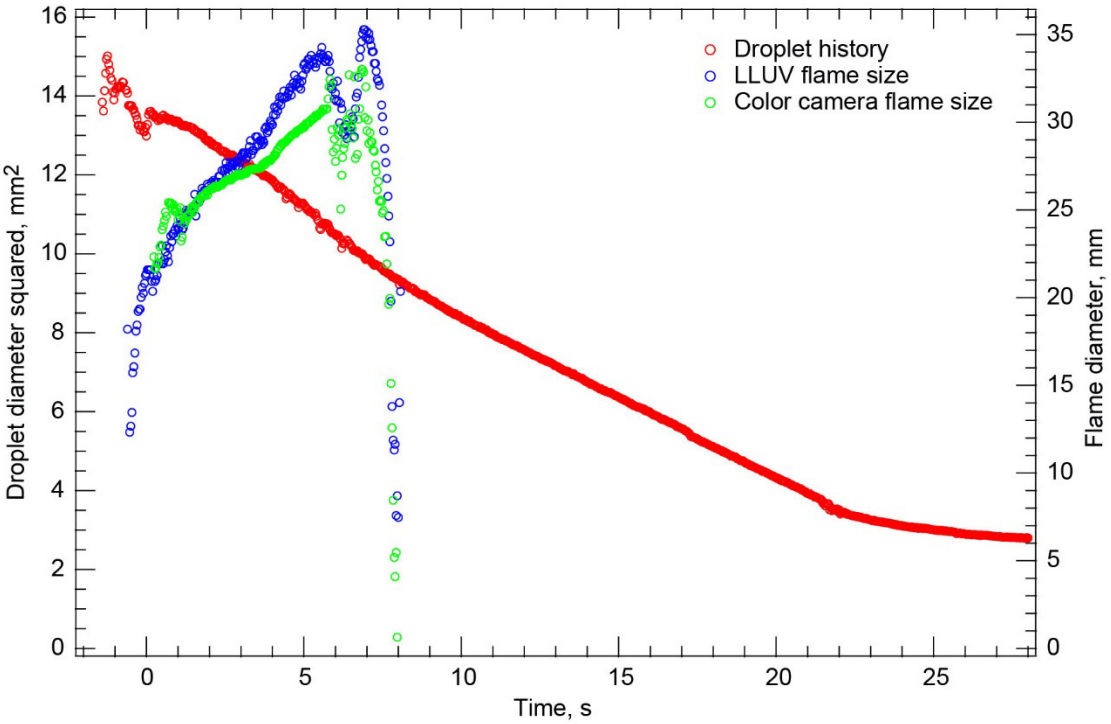

Figure 99.—Test FLEX−095. Fiber-supported heptane droplet translating 3 mm/s (for approximately 4 s) and burning in a 0.24/0.56/0.20 $O_2/N_2/CO_2$, 0.70-atm ambient environment. The droplet had very little axial or transverse oscillation on the fiber, and it remained within the High-Bit-Depth Multispectral (HiBMs) field of view (FOV) for the entire test. Shortly after the fiber translation stopped, the visible flame extinguished, but the droplet continued to vaporize at a relatively high rate. Then there was some axial oscillation on the fiber, followed by a significant reduction in the vaporization rate. The marked decrease in vaporization was coincident with the formation of a large vapor cloud, with a toroidal vapor cloud in the immediate vicinity of the droplet. This is indicative of cool flame burning and extinction following visible flame extinction.

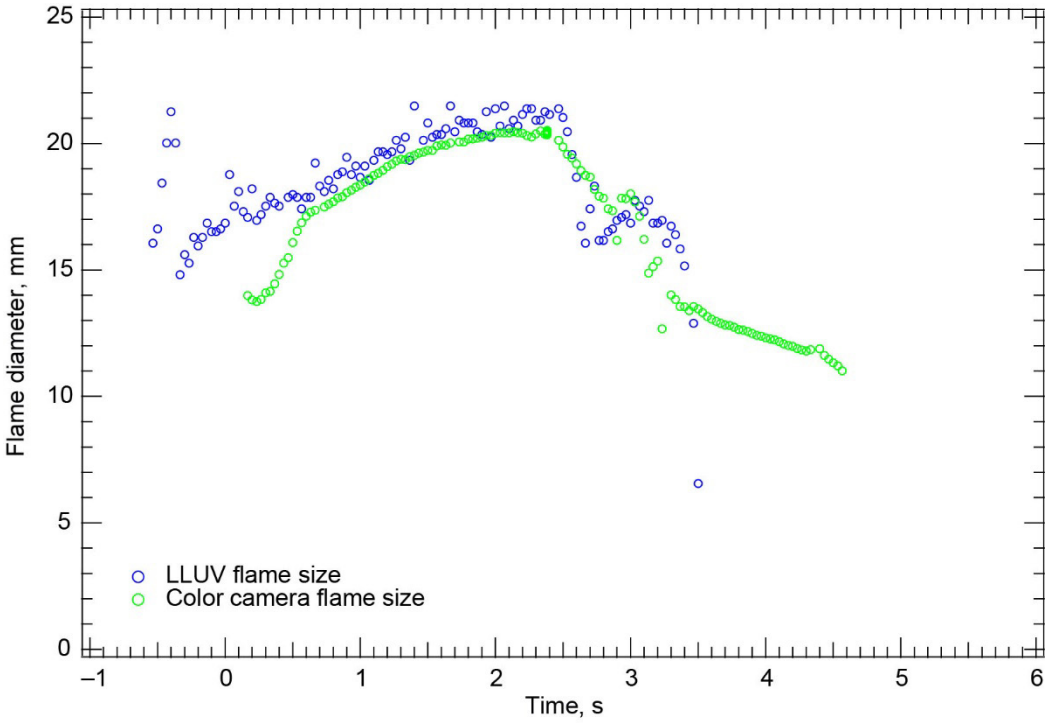

Figure 100.—Test FLEX−096. Fiber-supported heptane droplet burning in a 0.24/0.56/0.20 $O_2/N_2/CO_2$, 1.0-atm ambient environment. The High-Bit-Depth Multispectral (HiBMs) Image Processing and Storage Unit (IPSU) did not record any images for this test. There were significant oscillations on the fiber, so severe that the droplet dislodged from the fiber and drifted south and out of the color camera and Low Light Level Ultra-Violet (LLUV) fields of view (FOVs).

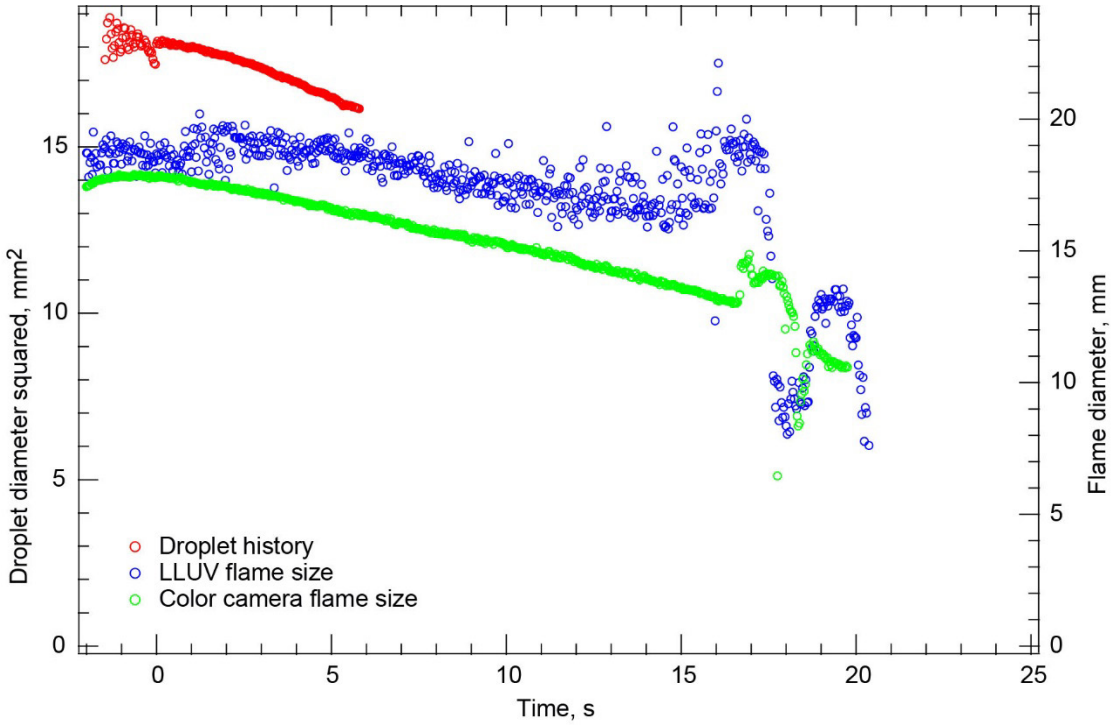

Figure 101.—Test FLEX−097. Free-floating methanol droplet burning in a 0.24/0.56/0.20 $O_2/N_2/CO_2$, 0.70-atm ambient environment. The droplet drifted north with a relatively high velocity in the High-Bit-Depth Multispectral (HiBMs) field of view (FOV) after deployment and ignition, and it drifted out of the FOV shortly after ignition. The droplet appeared to drift close enough to the needle to start a needle fire (also visible on the Low Light Level Ultra-Violet, LLUV). This changed the droplet direction from north to east in the color camera FOV, and it pushed the droplet north in the LLUV FOV. While the needle was still burning, the droplet quickly left the color camera FOV, but it remained in the LLUV FOV, drifting south after deployment and ignition until it left the LLUV FOV before extinction or disruption.

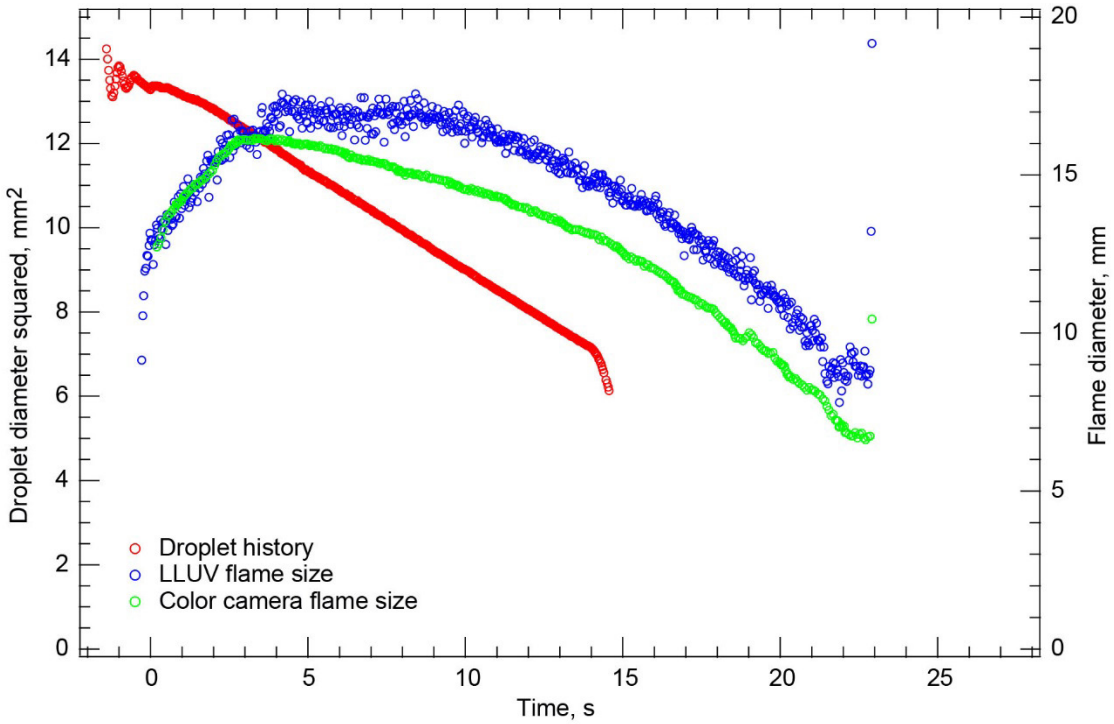

Figure 102.—Test FLEX−098. Free-floating methanol droplet burning in a 0.23/0.52/0.25 $O_2/N_2/CO_2$, 0.70-atm ambient environment. The droplet drifted north in the High-Bit-Depth Multispectral (HiBMs) field of view (FOV) after deployment and ignition, to the edge of the FOV, then east and out of HiBMs FOV before the end of the test. The flame “swirled” a little before extinction in both Low Light Level Ultra-Violet (LLUV) and color camera. The droplet was not in the HiBMs FOV long enough to obtain an accurate estimate of the extinction droplet diameter.

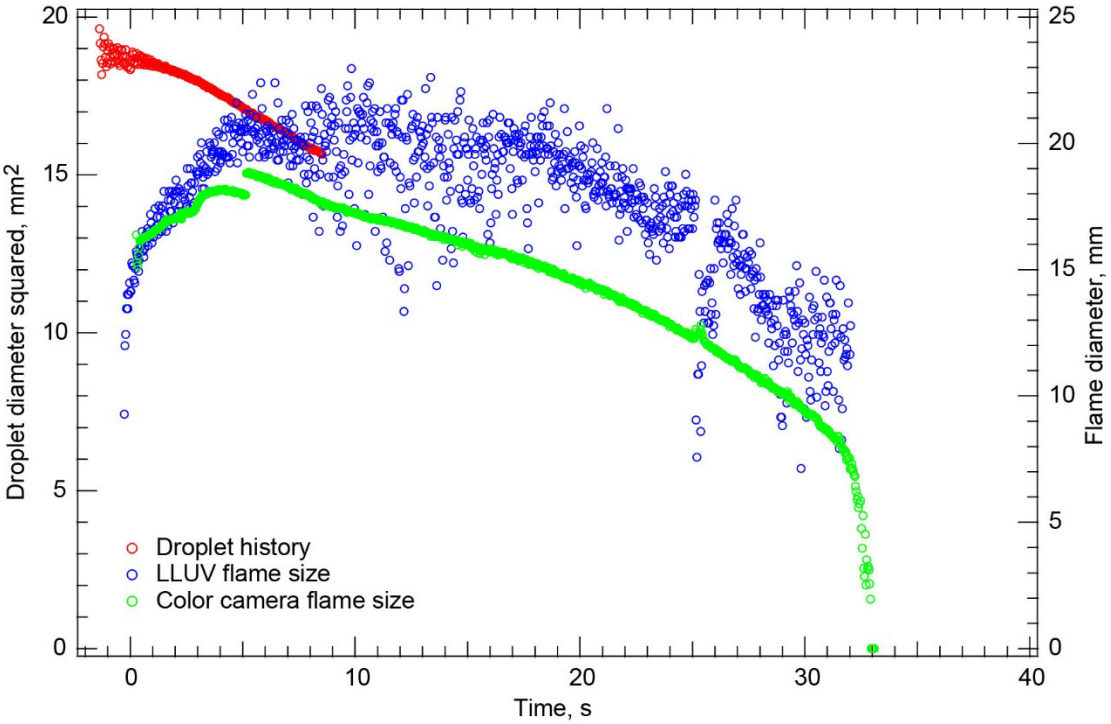

Figure 103.—Test FLEX−099. Free-floating methanol droplet burning in a 0.23/0.52/0.25 $O_2/N_2/CO_2$, 0.70-atm ambient environment. The droplet drifted north and out of the High-Bit-Depth Multispectral (HiBMs) field of view (FOV) after deployment and ignition. It appeared to drift close to the needle (no fire) in the color camera view and was pushed away slightly. It remained in both the Low Light Level Ultra-Violet (LLUV) and color camera FOVs until the flame extinguished. The droplet was not in the HiBMs FOV long enough to obtain a good estimate of the extinction droplet diameter.

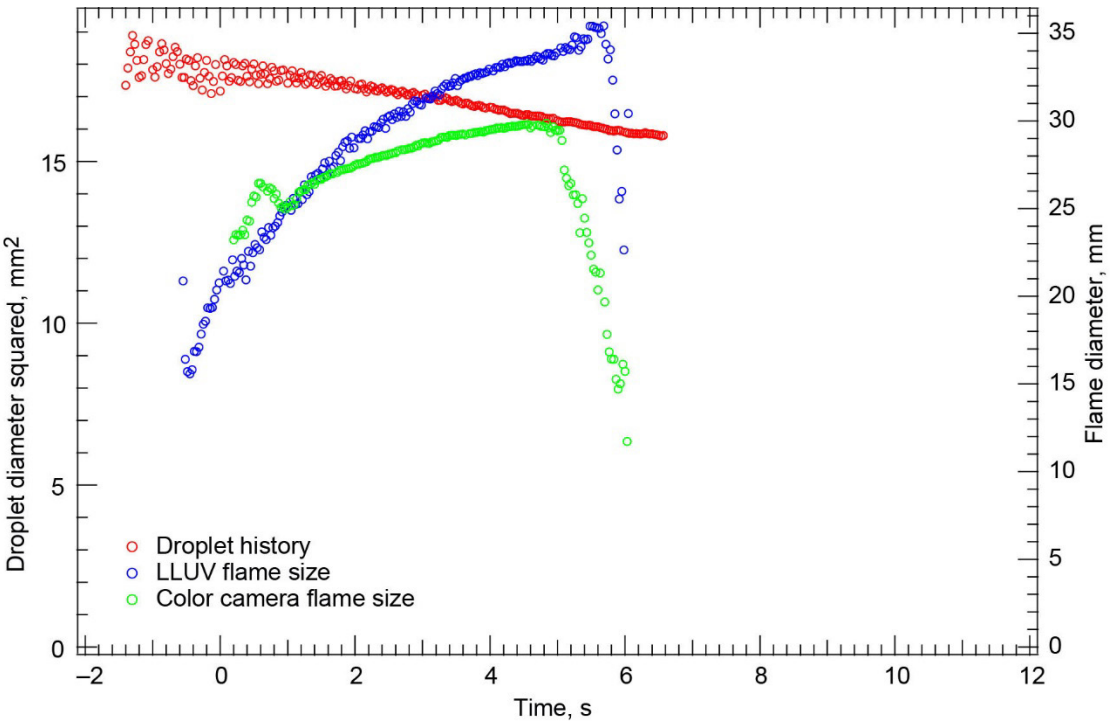

Figure 104.—Test FLEX−100. Free-floating heptane droplet burning in a 0.23/0.52/0.25 $O_2/N_2/CO_2$, 0.70-atm ambient environment. The droplet drifted north after deployment and ignition, and out of High-Bit-Depth Multispectral (HiBMs) field of view (FOV) just after the visible flame extinguished radiatively at a relatively large droplet size. A vapor cloud, which is indicative of cool flame burning and extinction, formed approximately 15 s after the visible flame extinguished.

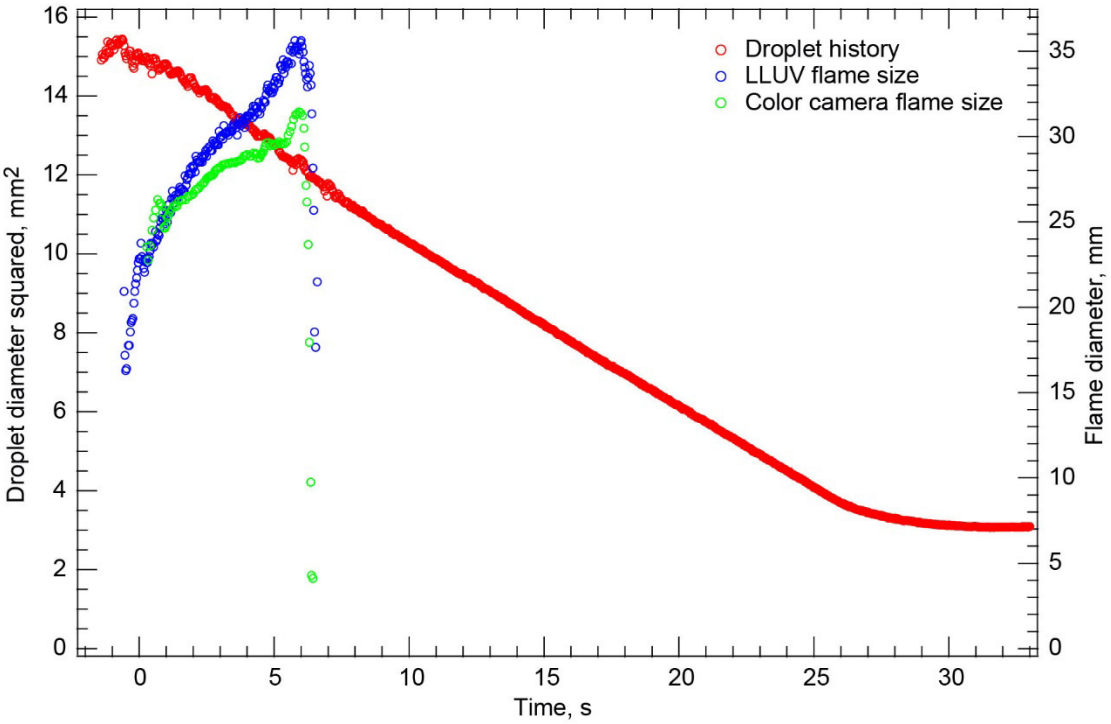

Figure 105.—Test FLEX−101. Fiber-supported heptane droplet translating 3 mm/s (for approximately 4 s) and burning in a 0.23/0.52/0.25 $O_2/N_2/CO_2$, 0.70-atm ambient environment. There was a little axial and transverse oscillation after deployment and ignition and during translation of the fiber, but for most of the burn and postburn, the droplet was relatively quiescent. The droplet remained in the High-Bit-Depth Multispectral (HiBMs) field of view (FOV) for the entire recording of the HiBMs Image Processing and Storage Unit (IPSU). The flame extinguished radiatively, preferentially along the fiber axis. The droplet continued to vaporize at a high rate after the visible flame extinguished. The vaporization then slowed considerably, and a visible vapor cloud formed, which is indicative of cool flame burning and extinction following visible flame extinction.

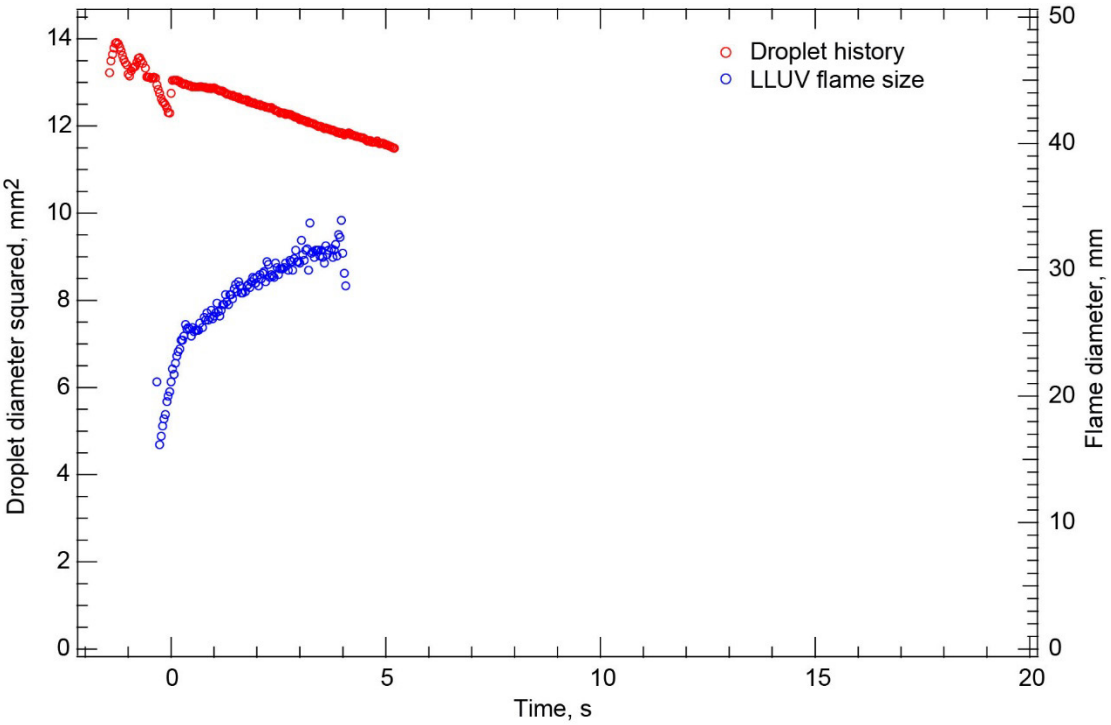

Figure 106.—Test FLEX−102. Free-floating heptane droplet burning in a 0.21/0.49/0.30 $O_2/N_2/CO_2$, 0.70-atm ambient environment. The droplet drifted north in the High-Bit-Depth Multispectral (HiBMs) field of view (FOV) after deployment and ignition and out of the HiBMs FOV shortly after the visible flame extinguished. The color camera Image Processing and Storage Unit (IPSU) failed to record any images after the droplet deployed. The flame extinguished radiatively, and a vapor cloud was visible on the downlink video sometime after the visible flame extinguished. This is indicative of cool flame burning and extinction following visible flame extinction.

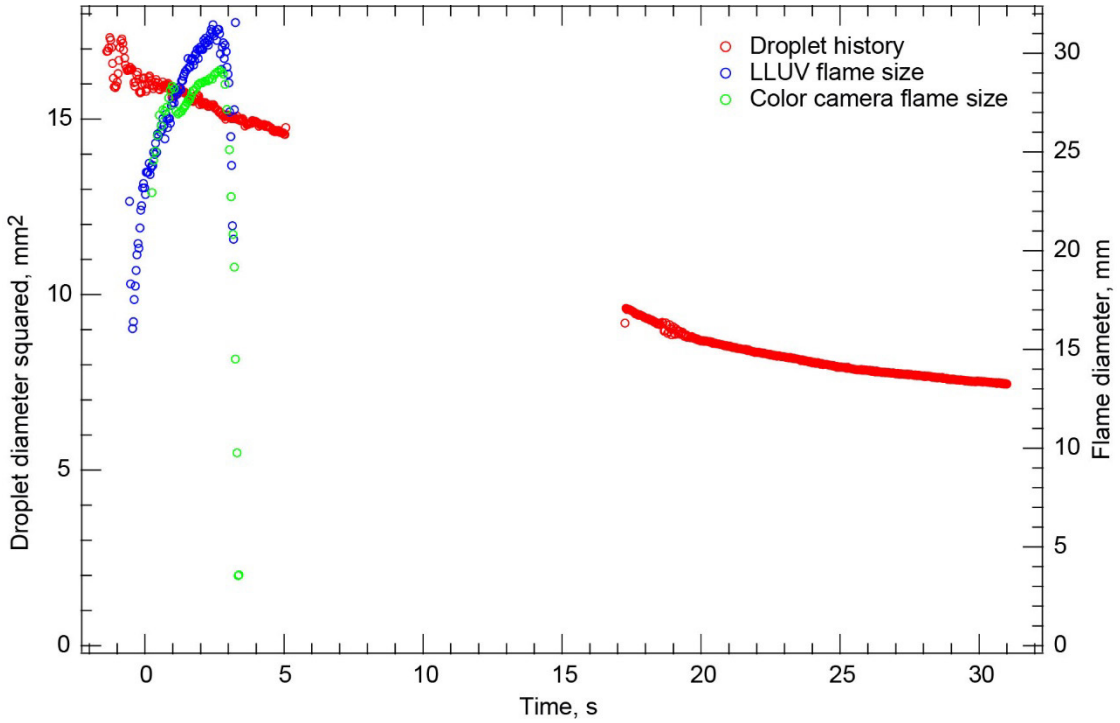

Figure 107.—Test FLEX−103. Fiber-supported heptane droplet translating 3 mm/s and burning in a 0.21/0.49/0.30, 0.70-atm ambient environment. A short time after translation stopped, the droplet moved axially on the fiber and partially out of the High-Bit-Depth Multispectral (HiBMs) field of view (FOV). By the end of the HiBMs Image Processing and Storage Unit (IPSU) recording, it had moved completely back into the HiBMs FOV. A small droplet or debris on the fiber ignited and burned briefly, but it burned out before the flame extinguished radiatively before translation stopped. For a while, the droplet continued to vaporize at a relatively high rate. Then the vaporization rate slowed coincident with the formation of a visible vapor cloud that formed a toroidal ring around the droplet. The background intensity in the HiBMs decreased significantly as the vapor cloud formed. The post-visible-flame-extinction behavior is indicative of cool flame burning and extinction.

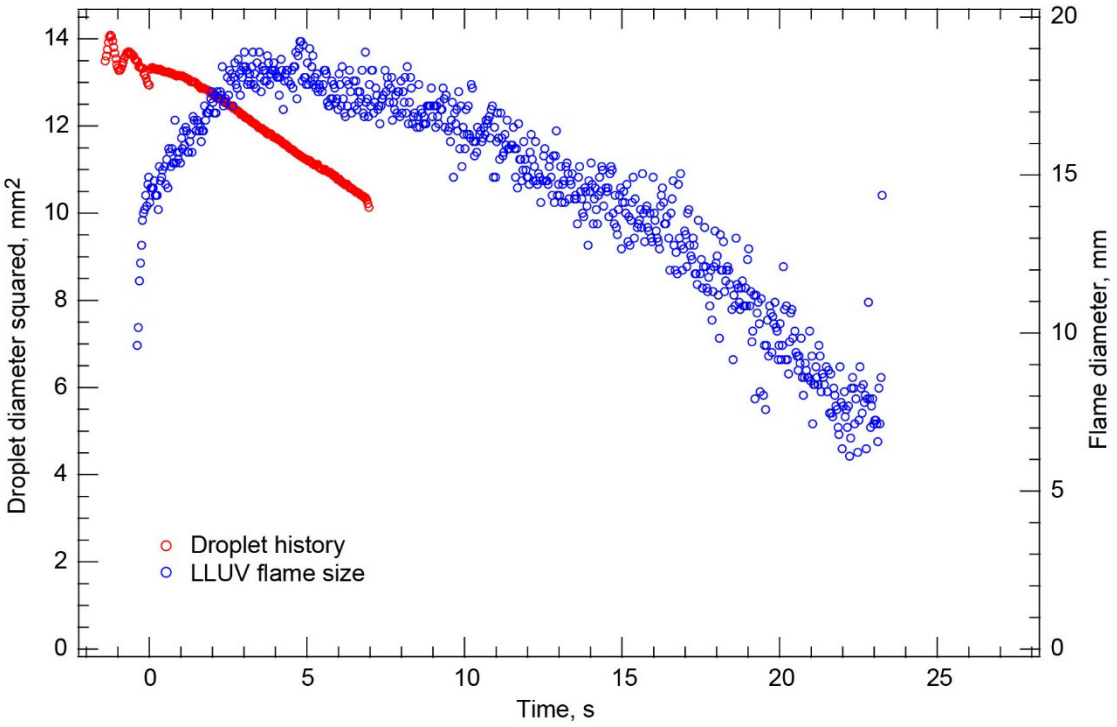

Figure 108.—Test FLEX–104. Free-floating methanol droplet burning in a 0.21/0.49/0.30 $O_2/N_2/CO_2$, 0.70-atm ambient environment. The droplet drifted north after deployment and ignition and out of the High-Bit-Depth Multispectral (HiBMs) field of view (FOV) about one-third of the way through the test. The color camera Image Processing and Storage Unit (IPSU) did not record any images after deployment. The flame extinguished diffusively without disruption. Because the droplet was in the HiBMs FOV for only a short fraction of the burn time, no extinction droplet diameter is reported.

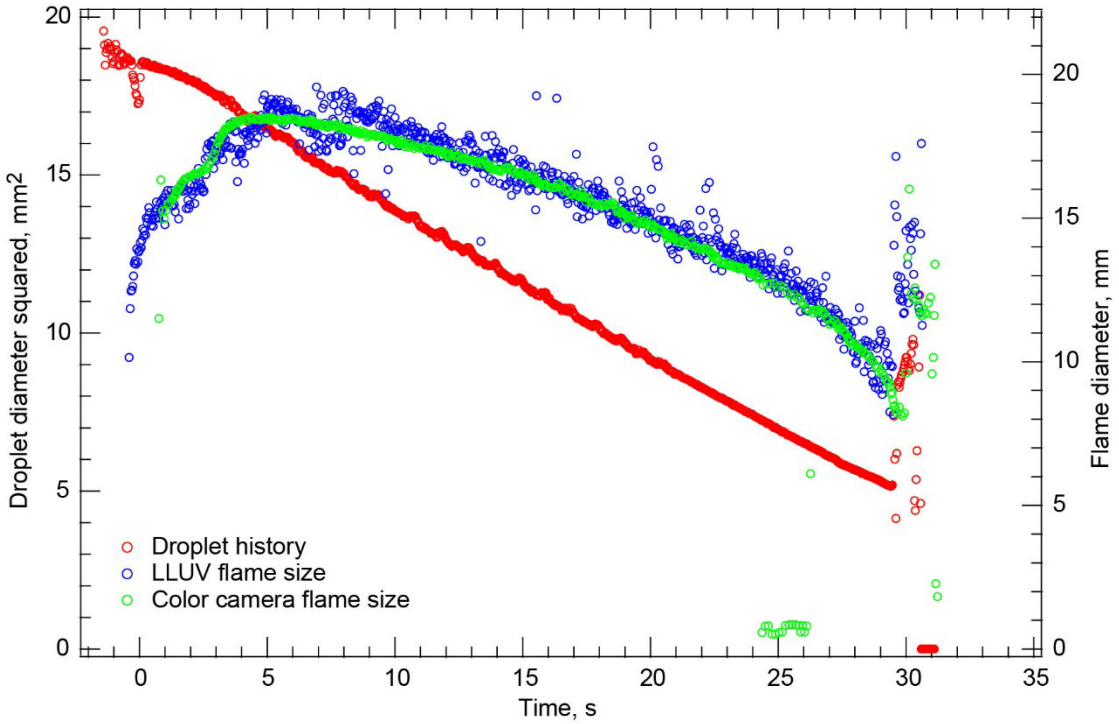

Figure 109.—Test FLEX−105. Fiber-supported methanol droplet translating 3 mm/s and burning in a 0.24/0.56/0.20 $O_2/N_2/CO_2$, 0.70-atm ambient environment. There was significant axial oscillatory motion on the fiber after deployment and ignition that persisted after fiber translation stopped about halfway through the burn. The droplet then burned without axial or transverse motion until it disrupted and dislocated from the fiber coincident with flame extinction.

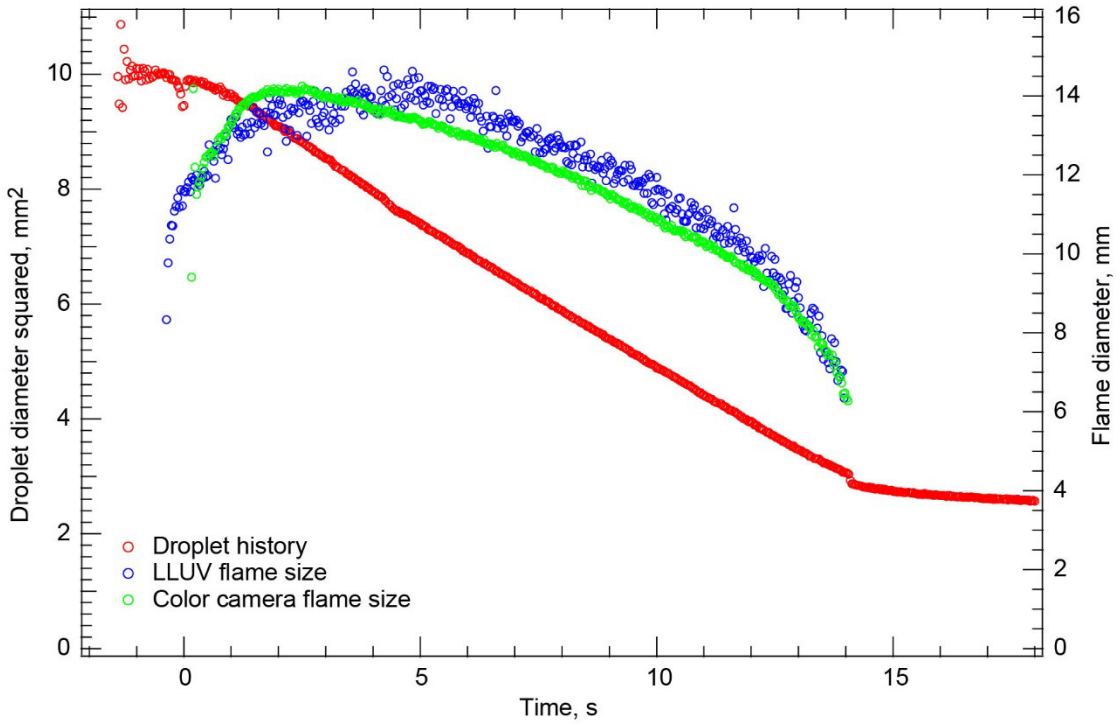

Figure 110.—Test FLEX−106. Fiber-supported methanol droplet translating 3 mm/s and burning in a 0.23/0.52/0.25 $O_2/N_2/CO_2$, 0.70-atm ambient environment. The droplet moved west along the fiber a short distance after deployment and ignition but before translation and then moved east with the fiber during translation. The droplet remained within the High-Bit-Depth Multispectral (HiBMs) field of view (FOV) for the entire test. There was very little motion of the droplet relative to the fiber during the test. However, a small disruption coincident with flame extinction left a slightly smaller droplet on the fiber. The extinction droplet diameter is the droplet diameter just prior to the disruption.

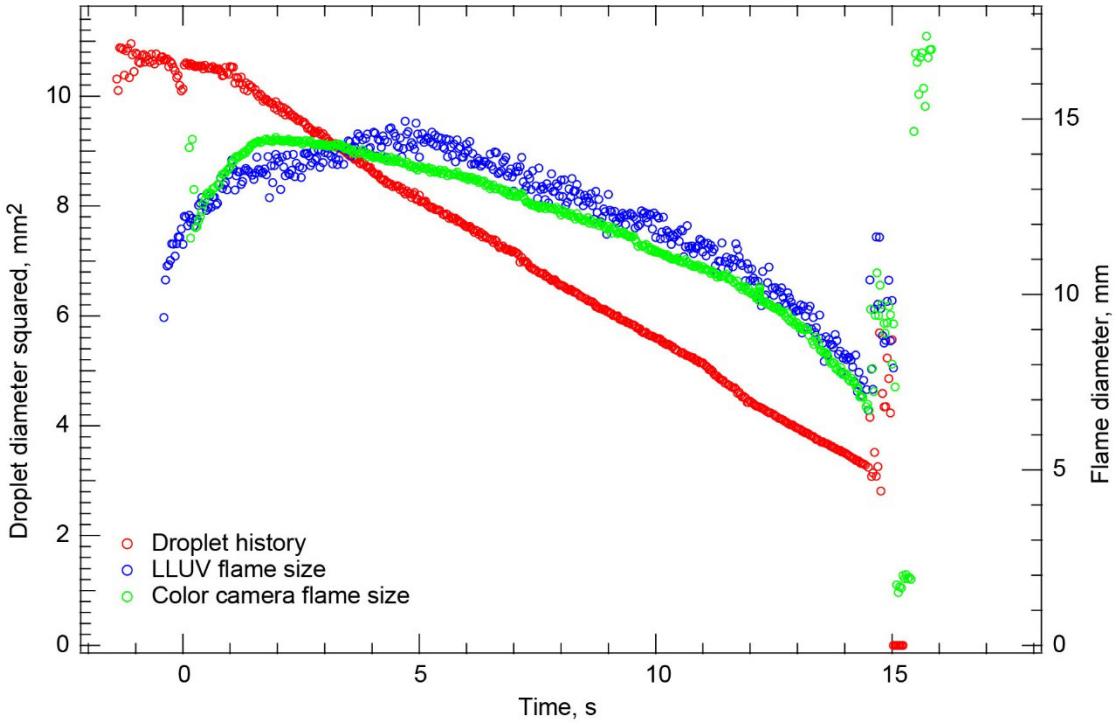

Figure 111.—Test FLEX−107. Fiber-supported methanol droplet translating 3 mm/s and burning in a 0.24/0.56/0.20 $O_2/N_2/CO_2$, 0.70-atm ambient environment. There was not much axial oscillatory motion associated with fiber motion, but there were some transverse oscillations. There was no shape change prior to disruption, which was right around the time of extinction.

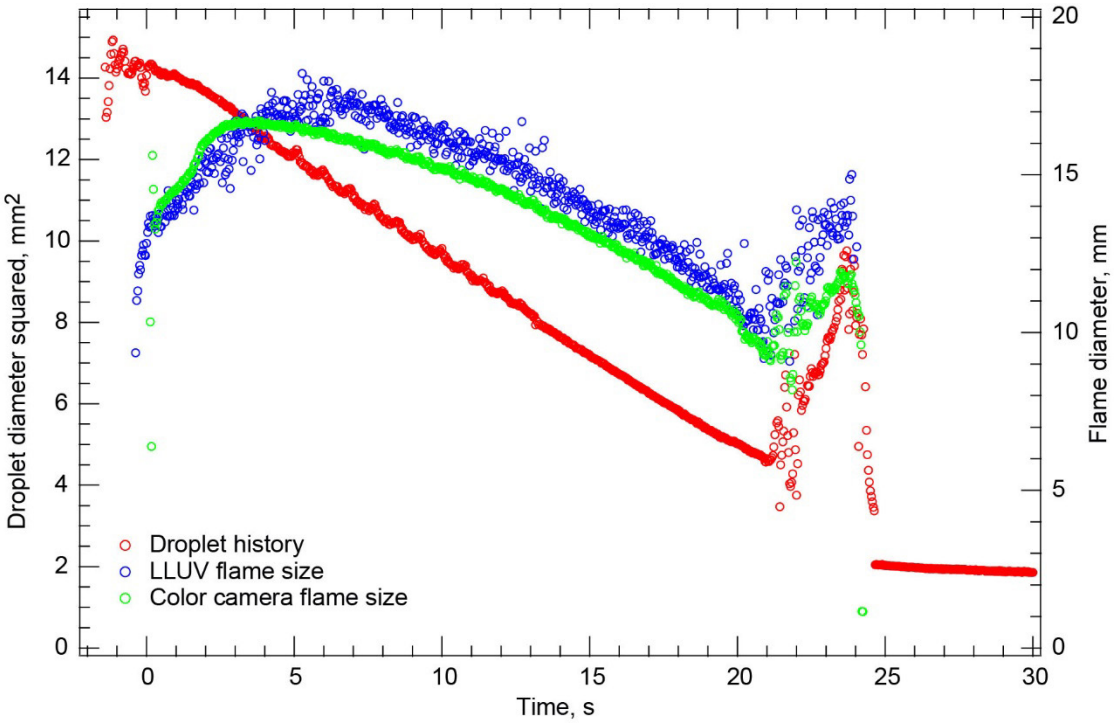

Figure 112.—Test FLEX−108. Fiber-supported methanol droplet translating 3 mm/s and burning in a 0.23/0.52/0.25 $O_2/N_2/CO_2$, 0.70-atm ambient environment. There was significant oscillatory motion of the droplet on the fiber during the burn both before and after the translation. The droplet swelled and eventually disrupted before the flame extinguished, leaving a small residual droplet on the fiber.

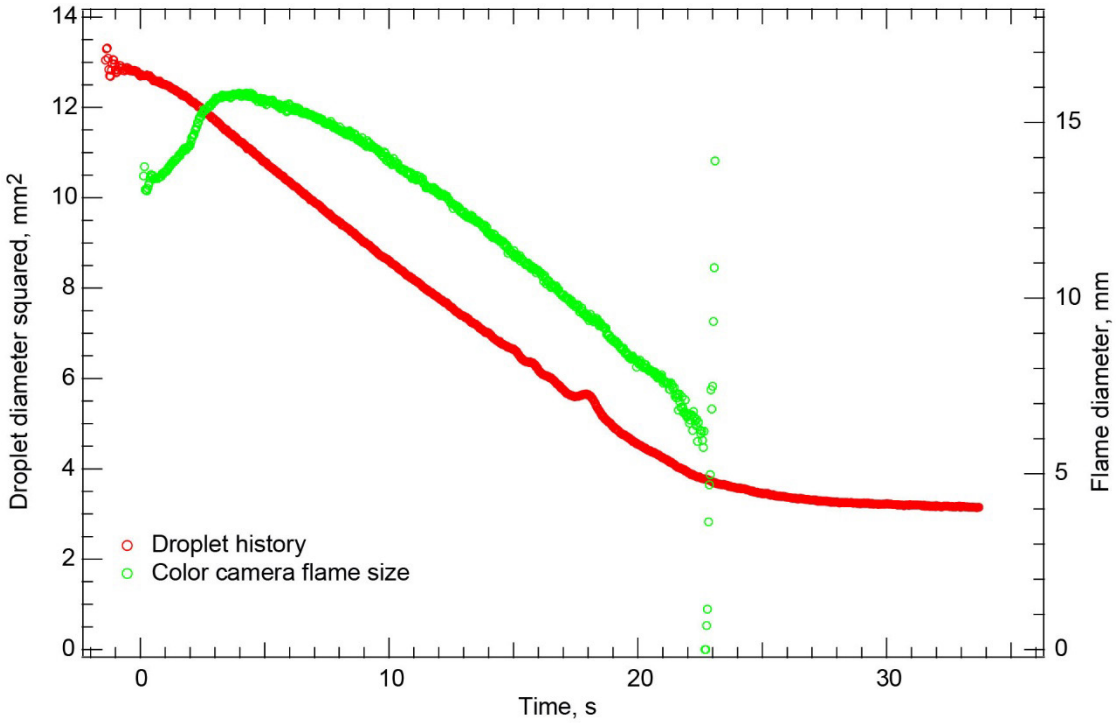

Figure 113.—Test FLEX–109. Free-floating methanol droplet burning in a 0.21/0.49/0.30 $O_2/N_2/CO_2$, 0.70-atm ambient environment. The droplet remained in the High-Bit-Depth Multispectral (HiBMs) and color camera fields of view (FOVs) for the entire Image Processing and Storage Unit (IPSU) recording time (even after the visible flame extinguished). The Low Light Level Ultra-Violet (LLUV) IPSU did not record any images for this test. The droplet deformed (became aspherical) right around the time of extinction and remained misshapen after the flame extinguished. The fuel may have been contaminated during this test.

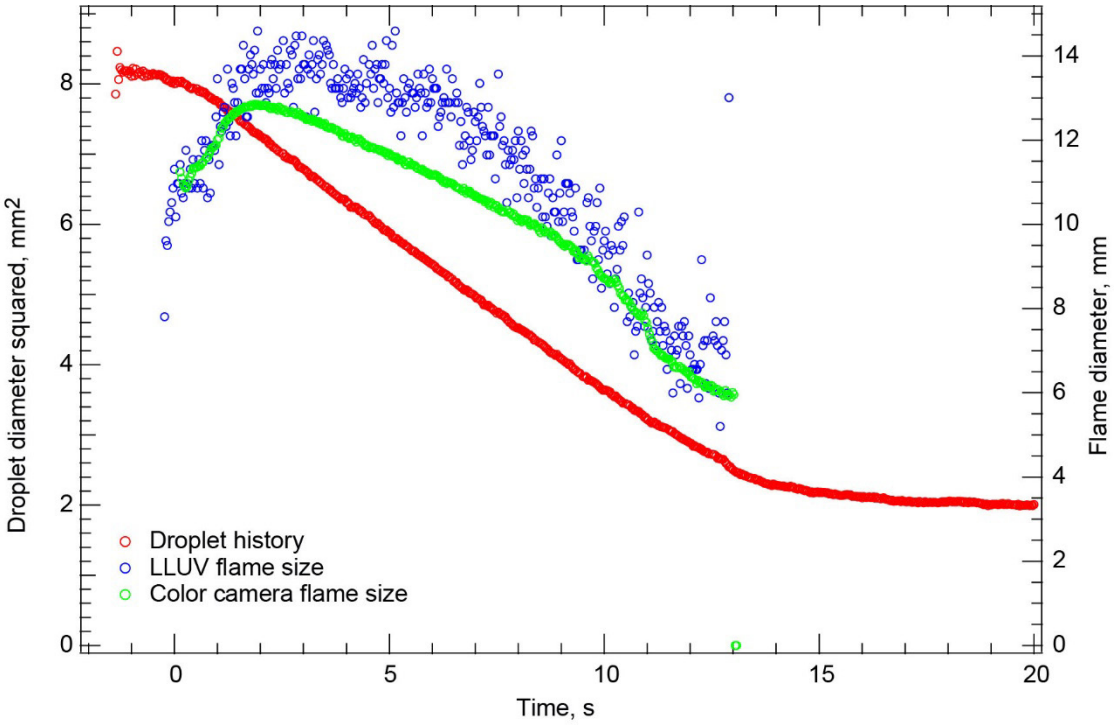

Figure 114.—Test FLEX–110. Free-floating methanol droplet burning in a 0.21/0.49/0.30 $O_2/N_2/CO_2$, 0.70-atm ambient environment. The droplet remained in the fields of view (FOVs) of all cameras, and the flame extinguished radiatively. Because the flame was very dim and there was a smudge on the Combustion Integrated Rack (CIR) Low Light Level Ultra-Violet (LLUV) viewing window, the LLUV data have a lot of noise.

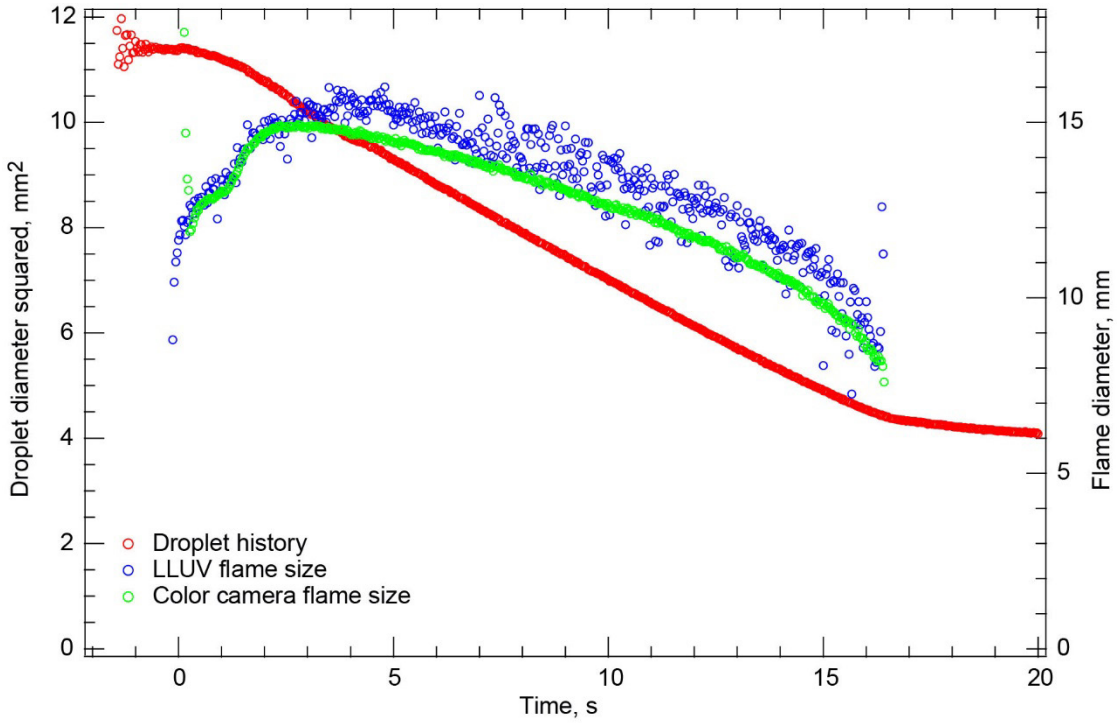

Figure 115.—Test FLEX–111. Fiber-supported methanol droplet burning in a 0.21/0.49/0.30 $O_2/N_2/CO_2$, 0.70-atm ambient environment with fiber translation after ignition. This was an almost ideal fiber-supported test, with almost no oscillation of the droplet. The fiber started and stopped moving with almost no relative motion imparted to the droplet.

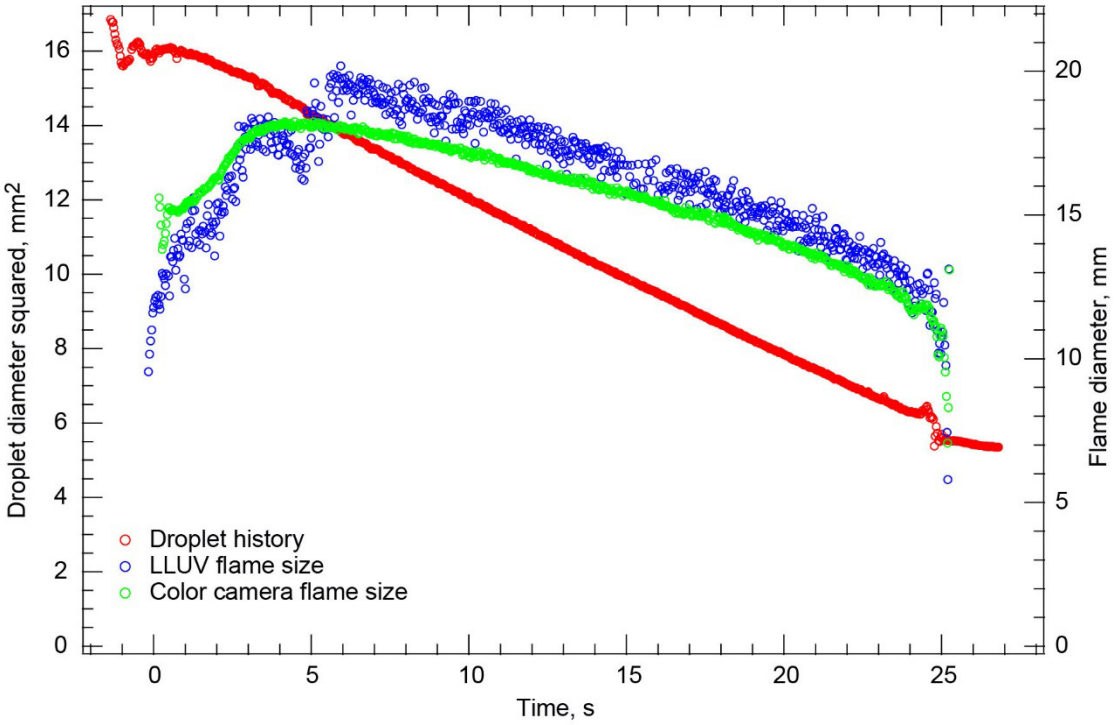

Figure 116.—Test FLEX–112. Fiber-supported methanol droplet burning in a 0.21/0.49/0.30 $O_2/N_2/CO_2$, 0.70-atm ambient environment. There was no fiber translation during this test. The droplet initially moved west in the High-Bit-Depth Multispectral (HiBMs) field of view (FOV) before stopping and then slowly moving back to the center of the image. A little disruption (maybe a small gas bubble popping) occurred near flame extinction coincident with a small satellite droplet being ejected from the droplet.

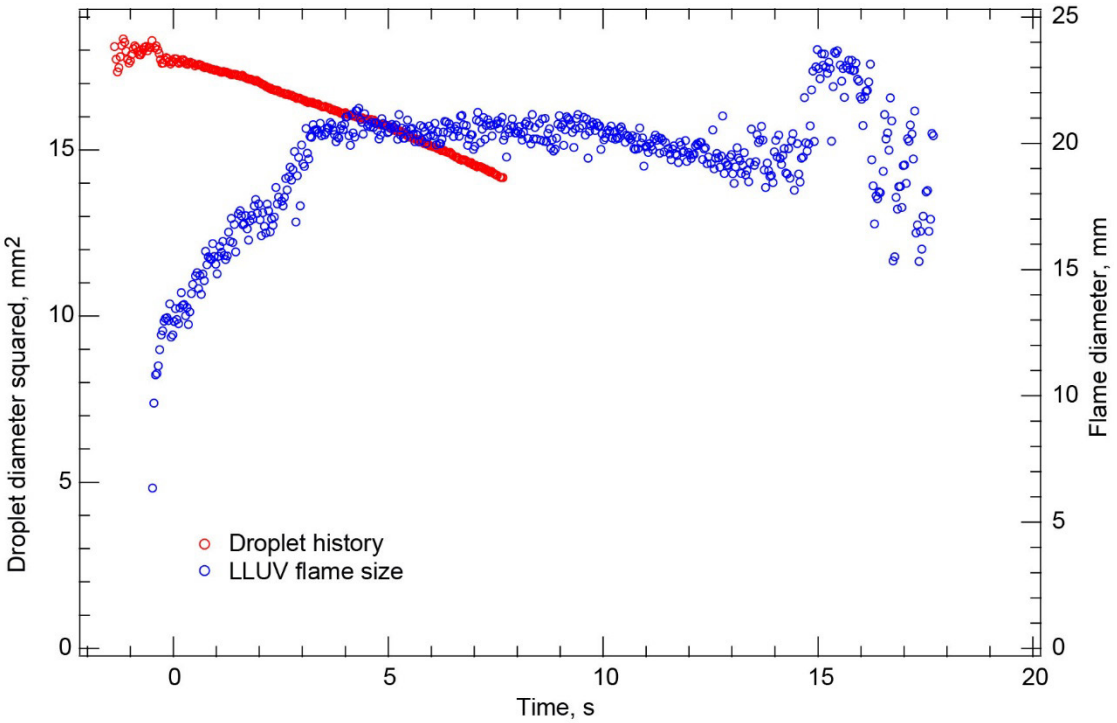

Figure 117.—Test FLEX−113. Free-floating methanol droplet burning in a 0.20/0.45/0.35 $O_2/N_2/CO_2$, 0.70-atm ambient environment. The droplet drifted northwest after deployment in the High-Bit-Depth Multispectral (HiBMs) field of view (FOV), hit the igniter, and then drifted southeast after ignition and out of the FOV approximately 8 s after the igniter was withdrawn. The droplet burned with a very weak relatively steady flame for a long period of time before oscillating before extinction. The extinction droplet diameter is based on an extrapolation of the droplet history to the time of extinction. The measured burning rate constant from just before the droplet left the HiBMs FOV was used in the extrapolation.

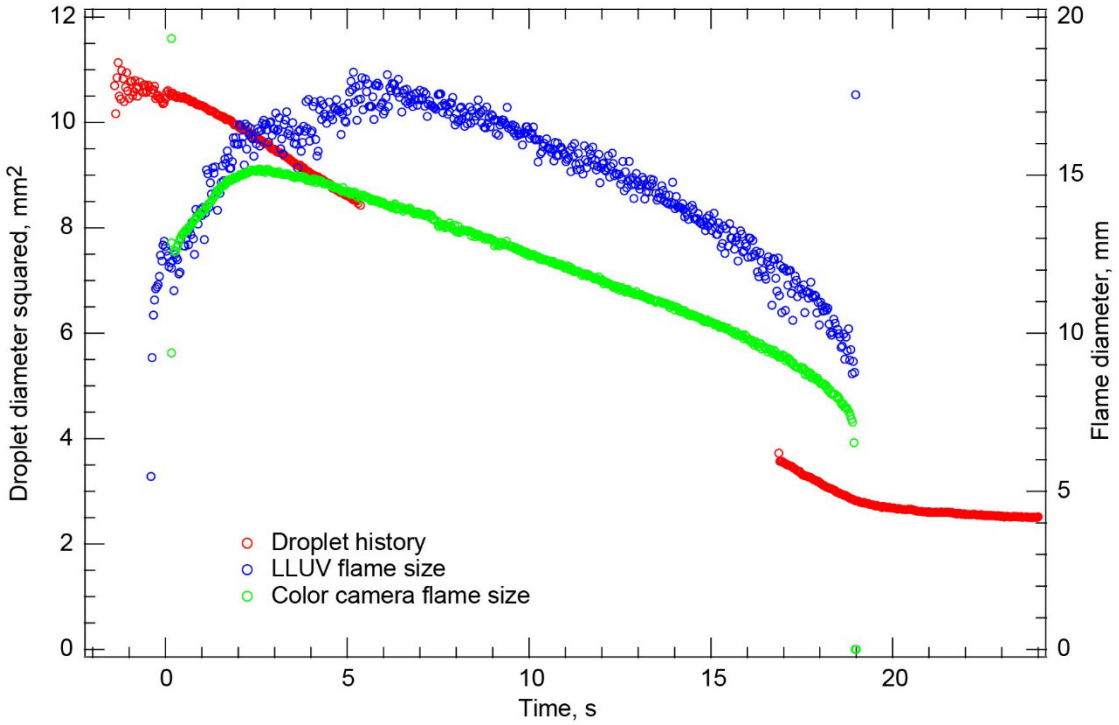

Figure 118.—Test FLEX−114. Free-floating methanol droplet burning in a 0.20/0.45/0.35 $O_2/N_2/CO_2$, 0.70-atm ambient environment. After ignition, the droplet drifted northeast and out of the High-Bit-Depth Multispectral (HiBMs) field of view (FOV). The droplet remained out of the FOV until just before the flame extinguished, when it drifted back into the FOV from the northeast corner.

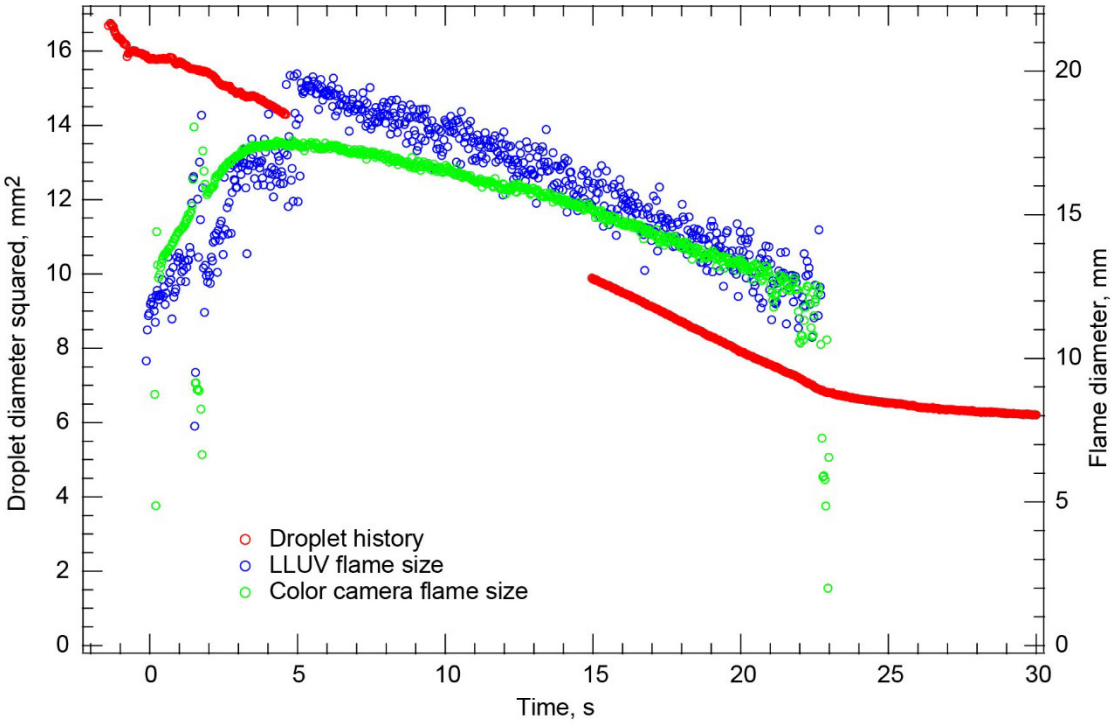

Figure 119.—Test FLEX−115. Fiber-supported methanol droplet translating 3 mm/s and burning in a 0.20/0.45/0.35 $O_2/N_2/CO_2$, 0.70-atm ambient environment. A small residue on the fiber to the west of the droplet ignited a few seconds after the droplet ignited. During translation, this residue burned with a very bright luminous flame for 1 to 2 s. The droplet drifted partially out of the High-Bit-Depth Multispectral (HiBMs) field of view (FOV) after the translation stopped, then it shrank back so that it was completely in the FOV. There appeared to be some oscillations near extinction. The droplet burned without any transverse or axial oscillations along the fiber, and it did not disrupt or deform.

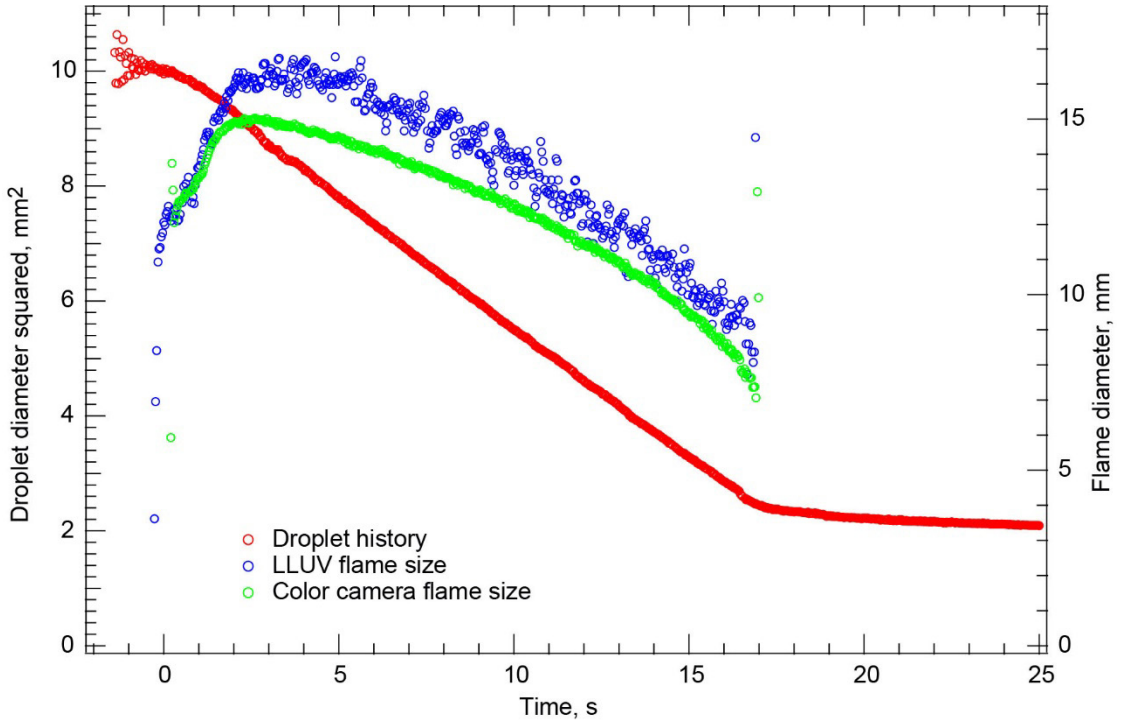

Figure 120.—Test FLEX−116. Fiber-supported methanol droplet (translated for approximately 3 s immediately after ignition) burning in a 0.20/0.45/0.35 $O_2/N_2/CO_2$, 0.70-atm ambient environment. This was a very clean test with very little motion of the droplet on the fiber.

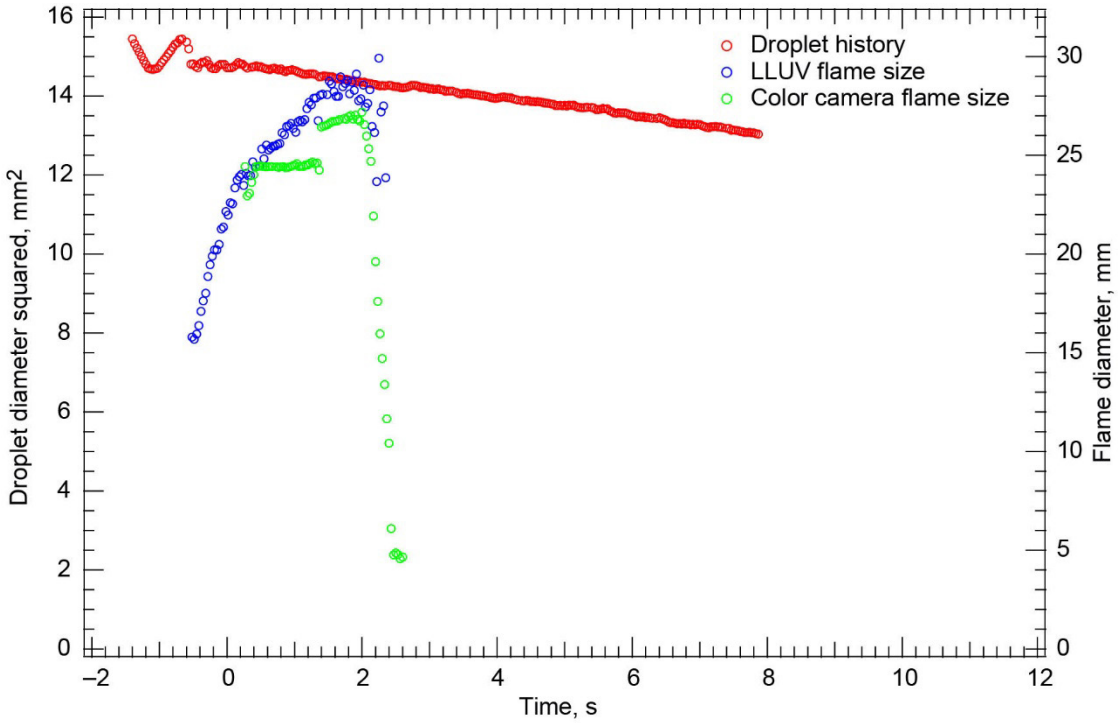

Figure 121.—Test FLEX−117. Free-floating heptane droplet burning in a 0.20/0.45/0.35 $O_2/N_2/CO_2$, 0.70-atm ambient environment. The droplet drifted north in the High-Bit-Depth Multispectral (HiBMs) field of view (FOV) after deployment and ignition and out of the FOV after the visible flame extinguished. The droplet had a very low burning rate constant. A relatively large vapor cloud formed well after the visible flame extinguished, which indicates that there was probably cool flame burning and extinction after visible flame extinction.

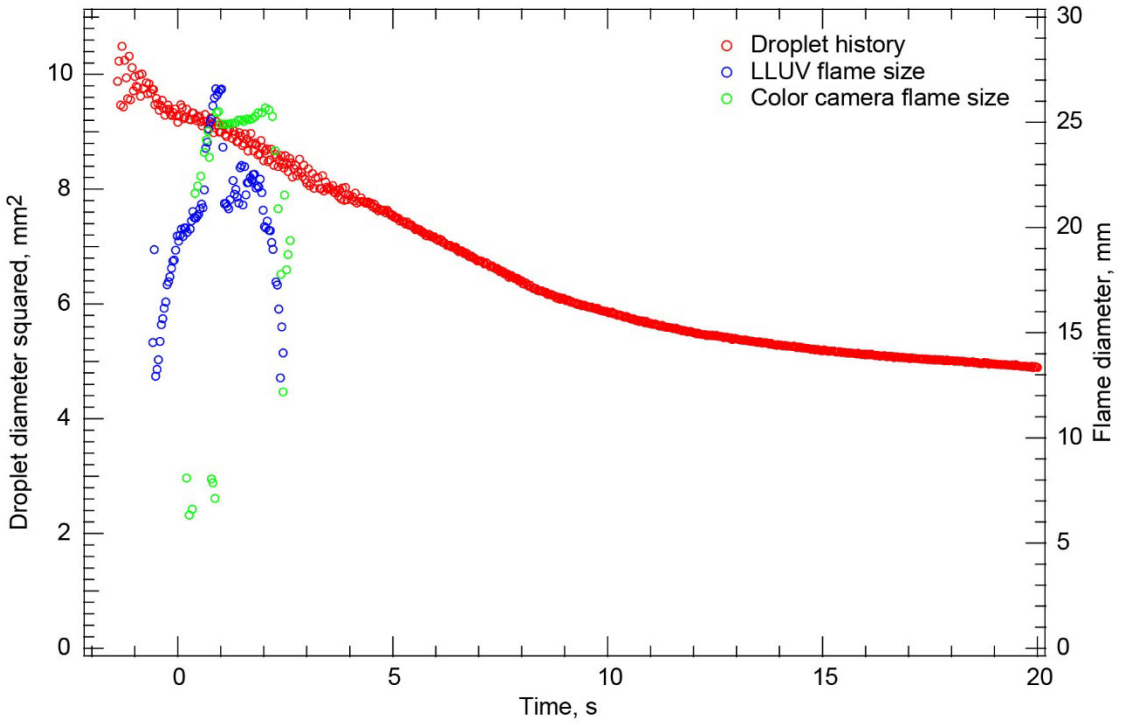

Figure 122.—Test FLEX−118. Fiber-supported heptane droplet burning in a 0.20/0.45/0.25 $O_2/N_2/CO_2$, 0.70-atm ambient environment. The droplet ignited, and shortly after ignition, a small droplet or debris ignited to the west (color camera) or north (Low Light Level Ultra-Violet, LLUV) of the droplet. This small droplet or particle burned for only a short time and was not visible in the High-Bit-Depth Multispectral (HiBMs). The droplet burns for only a short time before the visible flame extinguished radiatively. Rapid vaporization continued, however, and approximately 5 s after the visible flame extinguished, a vapor cloud formed. This is an indication of cool flame burning and extinction following visible flame extinction.

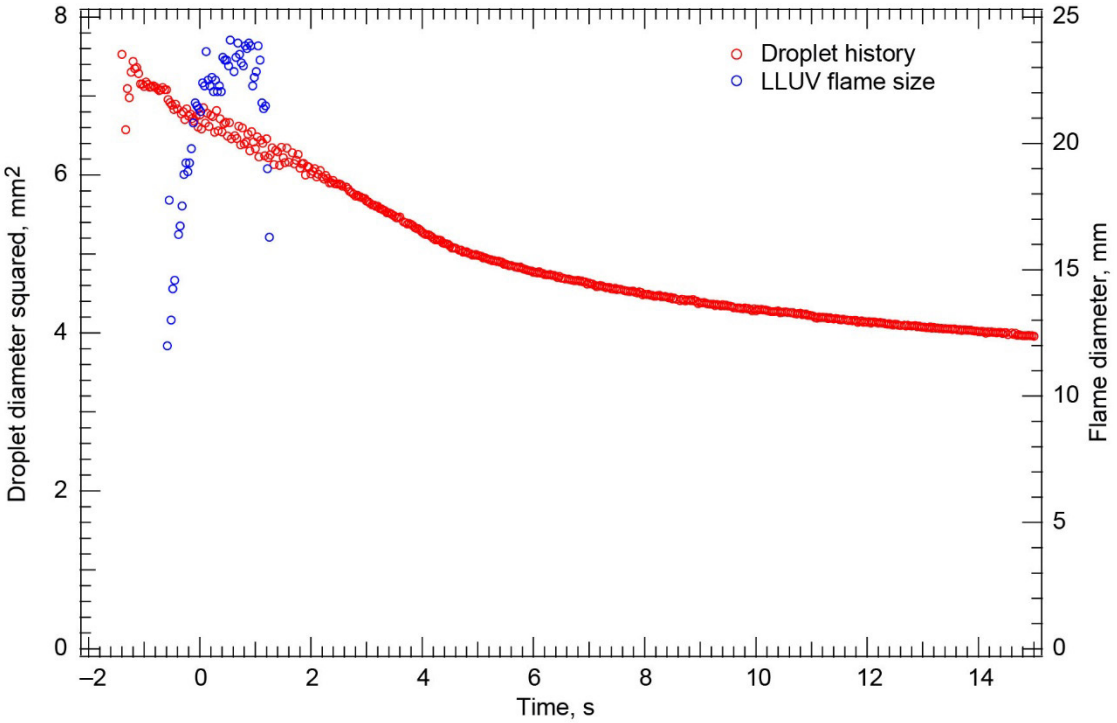

Figure 123.—Test FLEX−119. Fiber-supported heptane droplet burning in a 0.18/0.42/0.40 $O_2/N_2/CO_2$, 0.70-atm ambient environment. After ignition the flame extinguished quickly, probably radiatively. It is quite possible that this ambient condition was below the flammability limit for heptane. The droplet had some unusual oscillations on the fiber during the burn that seemed to disappear for most of the test (after the flame extinguished). The color camera Image Processing and Storage Unit (IPSU) did not record any images for this test. There was a brief period of significant vaporization after the visible flame extinguished; then a small vapor cloud formed. This is indicative of cool flame burning and extinction following visible flame extinction.

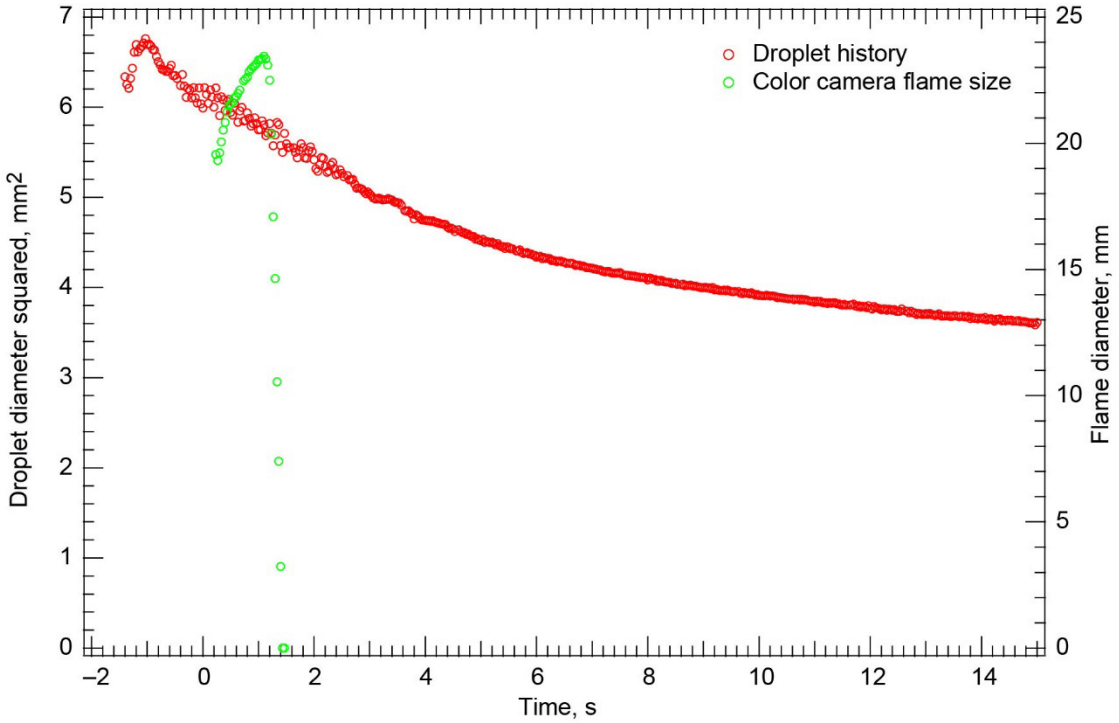

Figure 124.—Test FLEX−120. Fiber-supported heptane droplet with fiber translation burning in a 0.18/0.42/0.40 $O_2/N_2/CO_2$, 0.70-atm ambient environment. The droplet did not oscillate much on the fiber during or after the burn. A small vapor cloud formed after the visible flame extinguished. It is difficult to determine whether there was cool flame burning and extinction from the available data. The Low Light Level Ultra-Violet (LLUV) Image Processing and Storage Unit (IPSU) did not record any images during the burn.

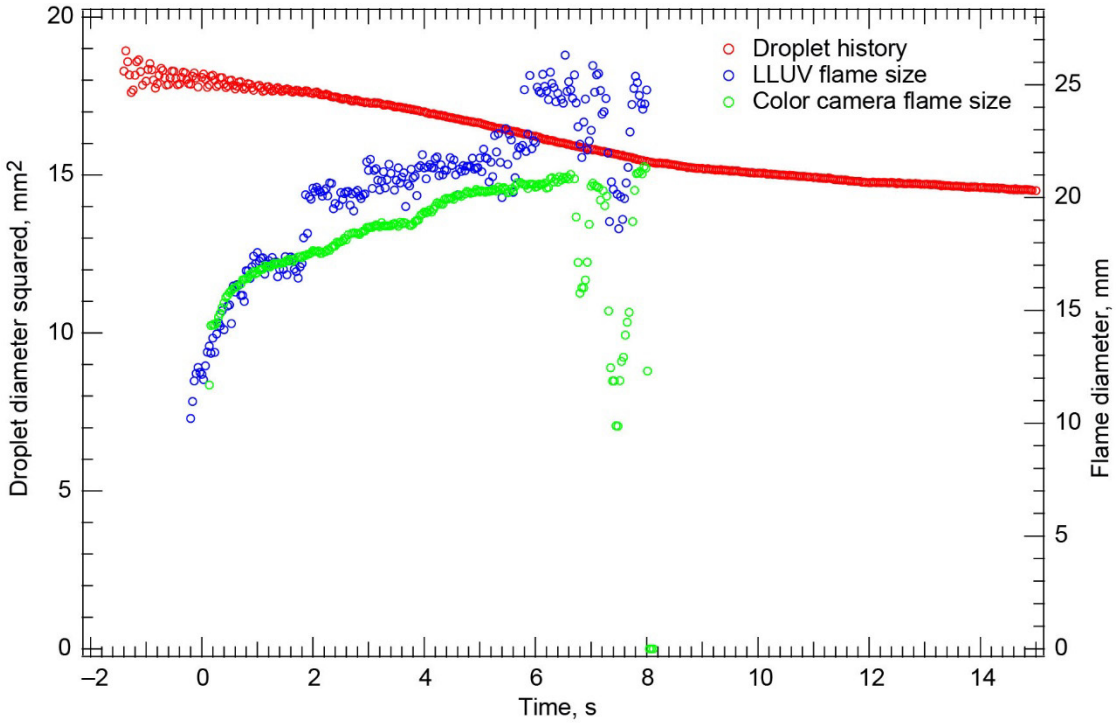

Figure 125.—Test FLEX−121. Free-floating methanol droplet burning in a 0.18/0.42/0.40 $O_2/N_2/CO_2$, 0.70-atm ambient environment. The droplet did not drift at all in any of the camera fields of view (FOVs) after deployment and ignition. The flame oscillated a few times before extinguishing radiatively.

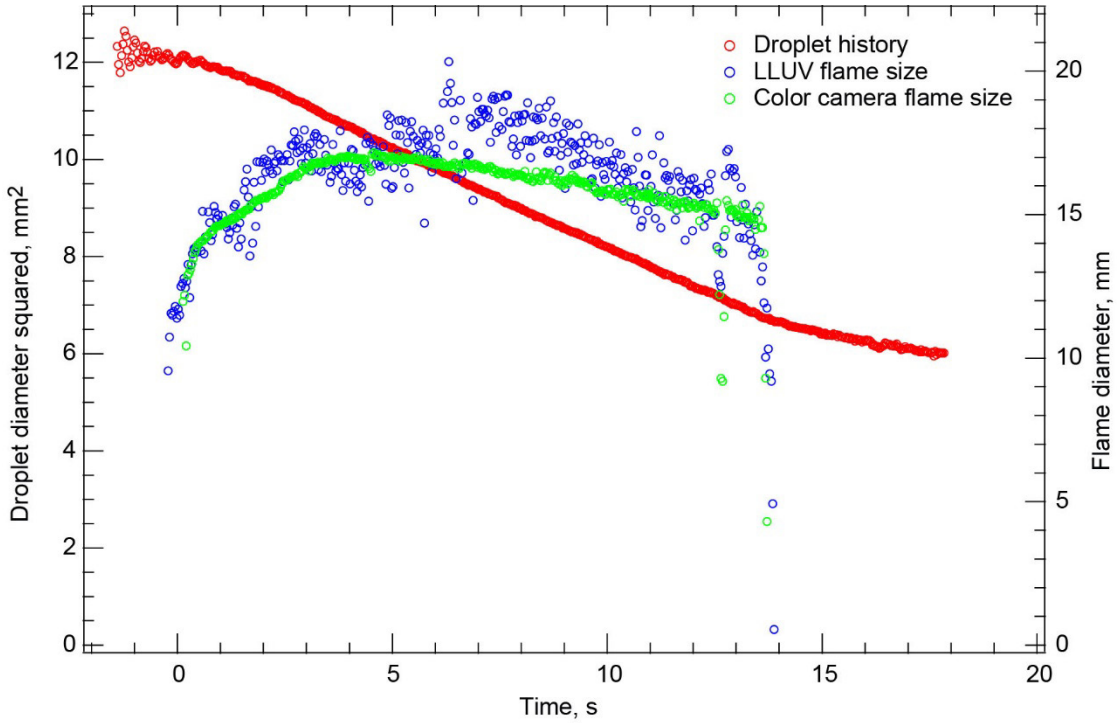

Figure 126.—Test FLEX−122. Free-floating methanol droplet burning in a 0.18/0.42/0.40 $O_2/N_2/CO_2$, 0.7-atm ambient environment. The droplet was almost motionless after deployment and ignition. It then slowly drifted south and eventually out of the High-Bit-Depth Multispectral (HiBMs) field of view (FOV), but this was after the flame extinguished. The droplet burned for about 15 s. Even though the flame appeared to be weak, it persisted for quite a while. This was a nice clean burn with no distortion or disruption. The flame appeared to oscillate radially (primarily in intensity) a few seconds before it extinguished.

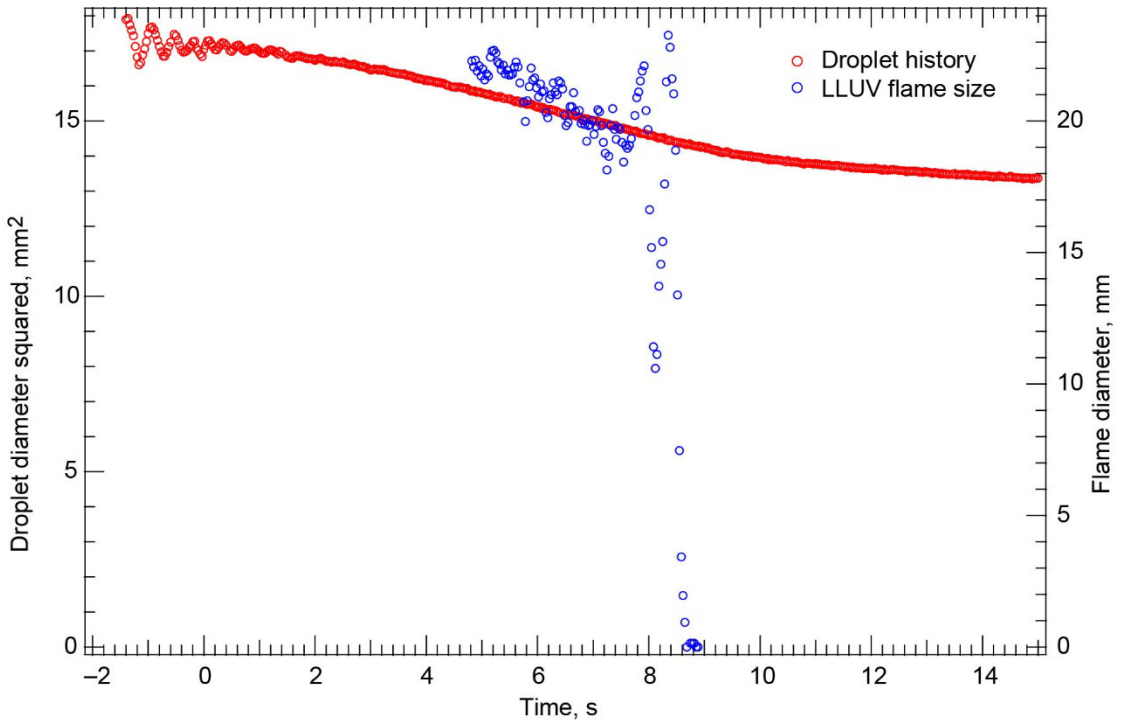

Figure 127.—Test FLEX−123. Fiber-supported methanol droplet burning in a 0.18/0.42/0.40 $O_2/N_2/CO_2$, 0.70-atm ambient environment. There was no fiber translation, and the large droplet appeared to extinguish radiatively. The color camera Image Processing and Storage Unit (IPSU) did not record any images after deployment. The Low Light Level Ultra-Violet (LLUV) IPSU lost data for about 5 s during the test. Also, the Low Light Level Ultra-Violet (LLUV) images were very dim, and it was almost impossible to detect the edges of the flame. In the LLUV view, the flame appeared to be quenched where the flame and fiber met.

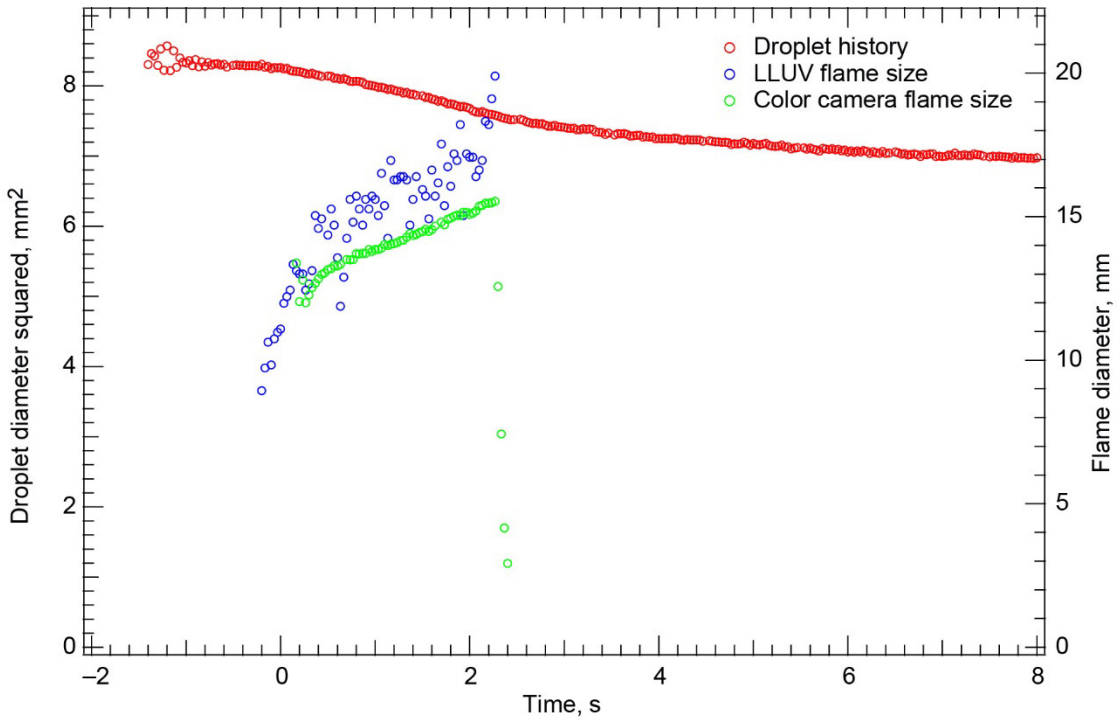

Figure 128.—Test FLEX–124. Free-floating methanol droplet burning in a 0.18/0.42/0.40 $O_2/N_2/CO_2$, 0.70-atm ambient environment. The droplet remained in the fields of view (FOVs) of all the cameras for the entire burn. The droplet burned for only a short time, and the flame probably extinguished radiatively.

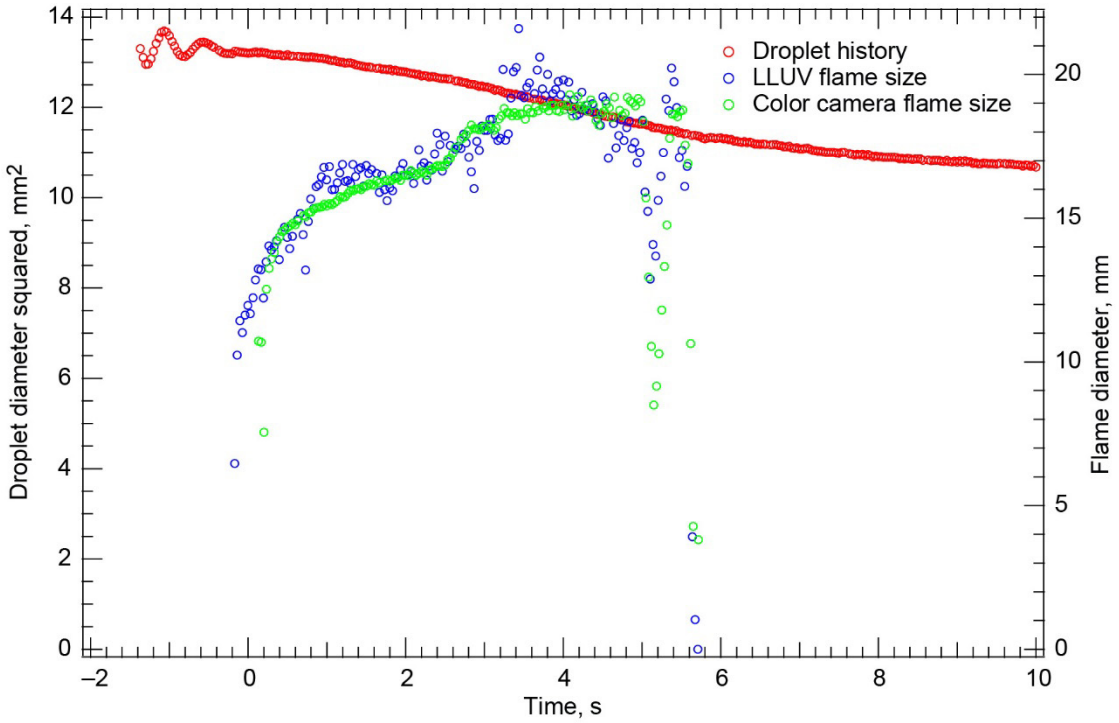

Figure 129.—Test FLEX–125. Free-floating methanol droplet burning in a 0.17/0.38/0.45 $O_2/N_2/CO_2$, 0.70-atm ambient environment. The droplet remained in the fields of view (FOVs) of all cameras after deployment and ignition. The flame oscillated for one or two cycles before extinguishing radiatively. This test was very near, if not below, the flammability limit. Because the flame was barely distinguishable from the background in the Low Light Level Ultra-Violet (LLUV), the color camera flame size data are a bit more reliable than the LLUV data, which have a lot of noise.

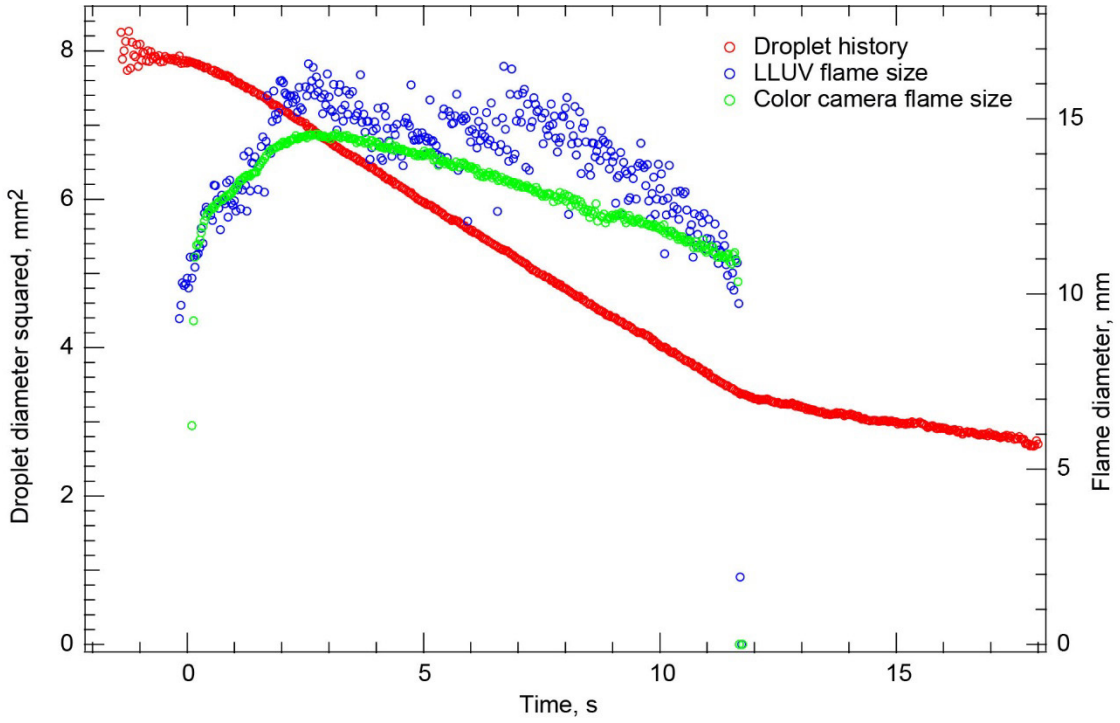

Figure 130.—Test FLEX–126. Free-floating methanol droplet burning in a 0.17/0.38/0.45 $O_2/N_2/CO_2$, 0.70-atm ambient environment. The droplet remained in the fields of view (FOVs) of all cameras after deployment and ignition. The droplet burned a relatively long time and appeared to extinguish diffusively.

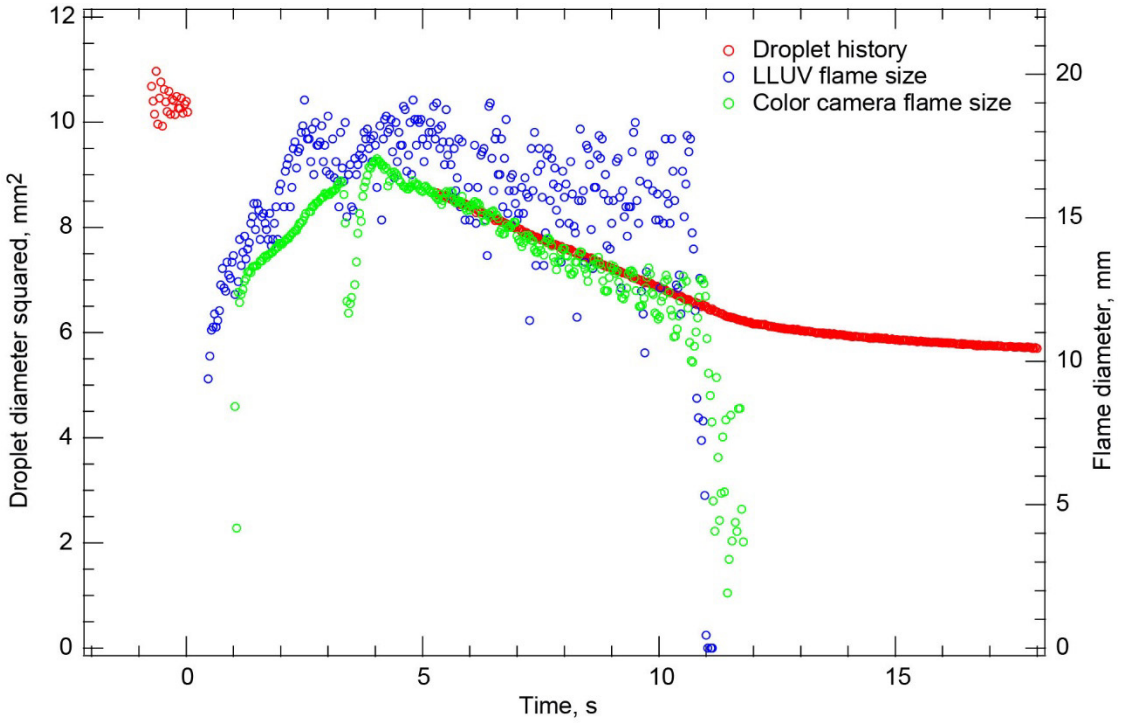

Figure 131.—Test FLEX–127. Fiber-supported methanol with no translation burning in a 0.17/0.38/0.45 $O_2/N_2/CO_2$, 0.70-atm ambient environment. The droplet remained in the High-Bit-Depth Multispectral (HiBMs) field of view (FOV) for the entire test. The flame then became very dim blue and was nearly cylindrical because of flame quenching due to the support fiber. There was little fiber glow (broadband radiation from the heated fiber) after the droplet stopped translating, and the flame measurements from the color camera indicated that the flame size oscillated periodically after the droplet stopped translating. The HiBMs Image Processing and Storage Unit (IPSU) stopped recording for a relatively large block of time: from just before the igniter withdrew to about halfway through the burn.

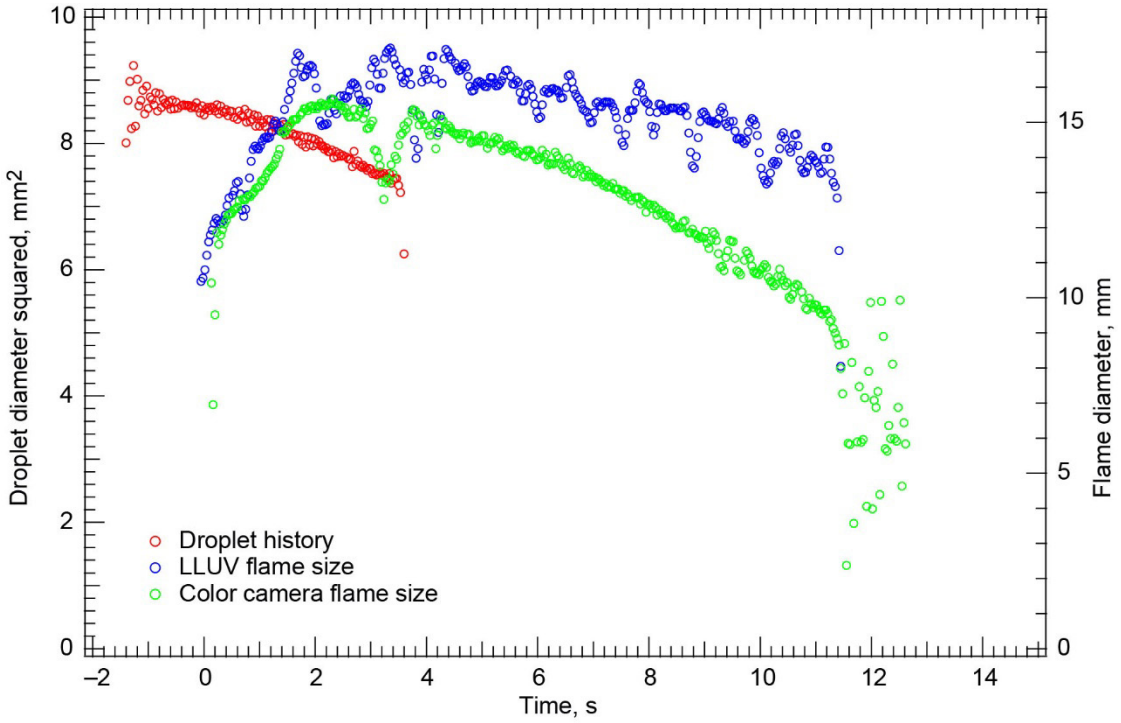

Figure 132.—Test FLEX–128. Fiber-supported methanol droplet burning in a 0.17/0.38/0/45 $O_2/N_2/CO_2$, 0.70-atm ambient environment. Shortly after ignition, the droplet began to move west along the fiber at ~8 mm/s. It left the High-Bit-Depth Multispectral (HiBMs) field of view (FOV) about one-third of the way through the test. The flame was brighter at the leading edge during the translation. When the translation stopped, the flame was quenched by the fiber at both ends, making the flame more cylindrical than spherical. Because the droplet was in the HiBMs FOV for only a short fraction of the burn, no extinction droplet diameter is reported.

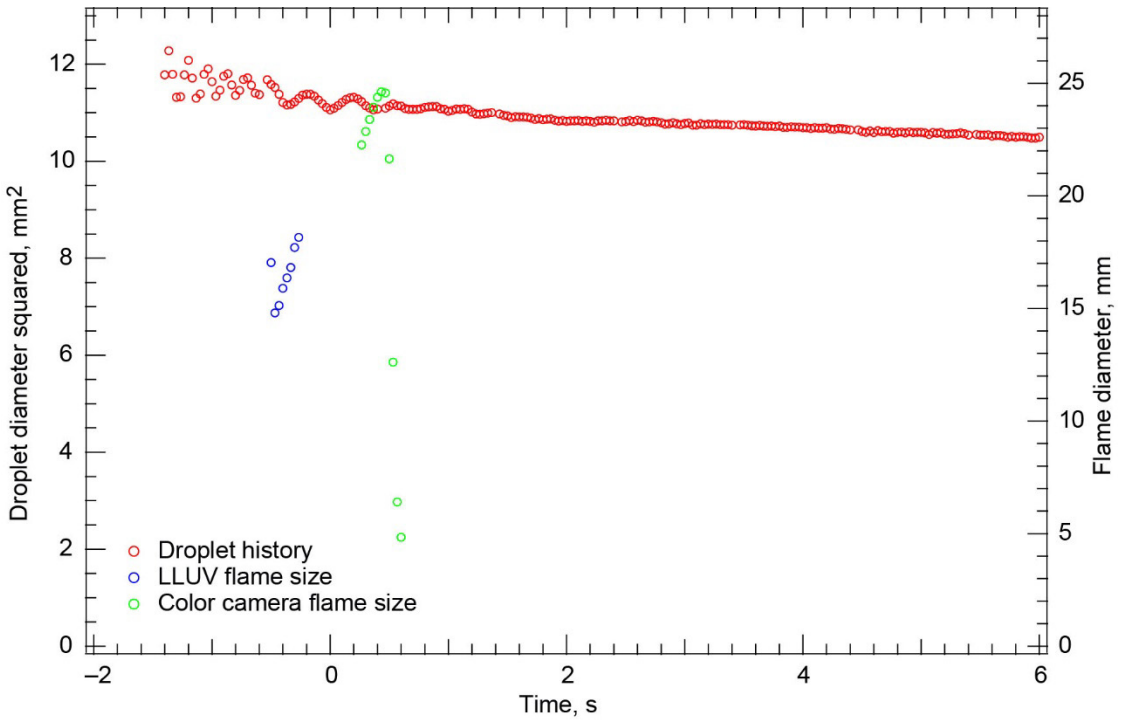

Figure 133.—Test FLEX–129. Free-floating heptane droplet burning in a 0.17/0.38/0.45 $O_2/N_2/CO_2$, 0.70-atm ambient environment. The droplet remained in the fields of view (FOVs) of all the cameras for the very short burn and for a considerable period of time after the visible flame extinguished. The Low Light Level Ultra-Violet (LLUV) stopped recording images for several seconds right around ignition. This was a very short burn with no appreciable vaporization or vapor cloud formation after the visible flame extinguished. There was probably no cool flame or only a very brief cool flame.

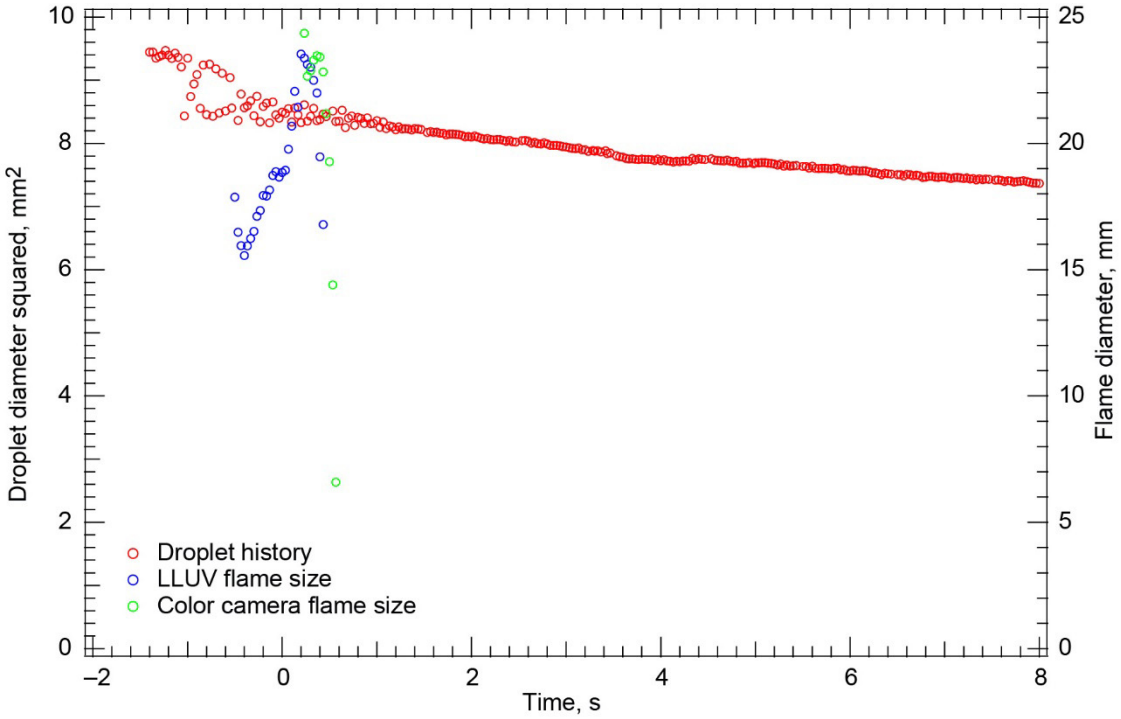

Figure 134.—Test FLEX–130. Fiber-supported heptane droplet translating 3 mm/s and burning in a 0.17/0.38/0.45 $O_2/N_2/CO_2$, 0.7-atm ambient environment. This was a very short burn, and the flame extinguished radiatively very soon after translation began. No vapor cloud formed, and the vaporization rate was quite small after the visible flame extinguished. As a result, there was probably no, or only very brief, cool flame burning.

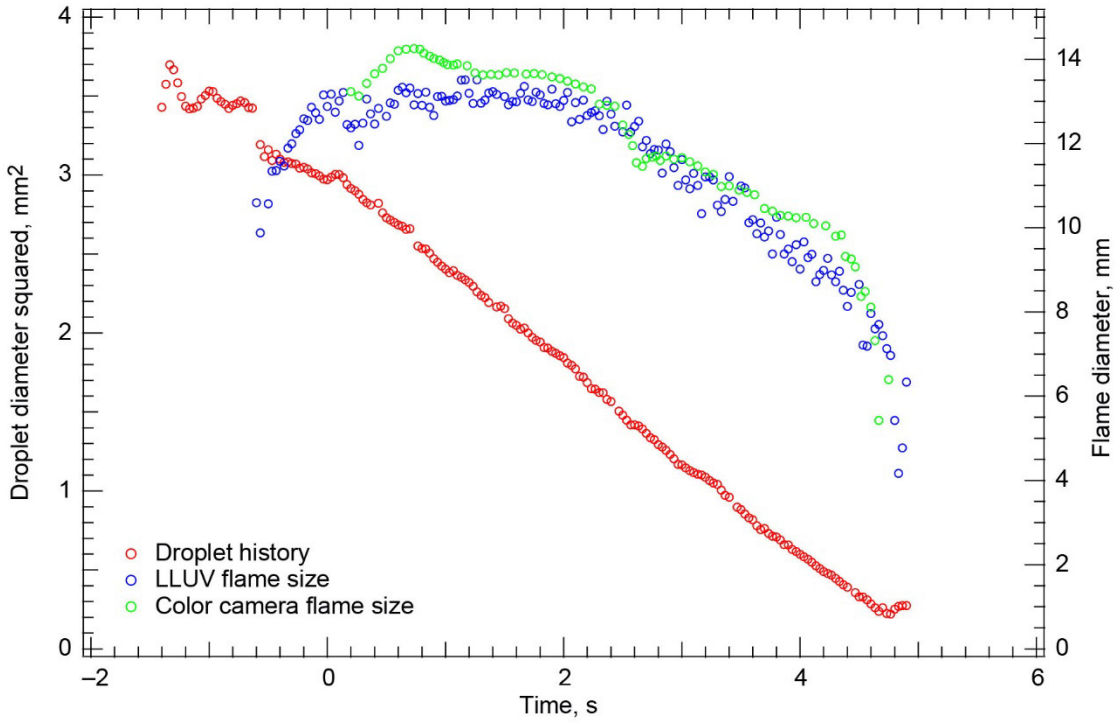

Figure 135.—Test FLEX–131. Free-floating heptane droplet burning in a 0.24/0.56/0.20 $O_2/N_2/CO_2$, 1.0-atm ambient environment. This smaller droplet remained in the fields of view (FOVs) of all the cameras for the entire test. The droplet extinguished disruptively at a small size.

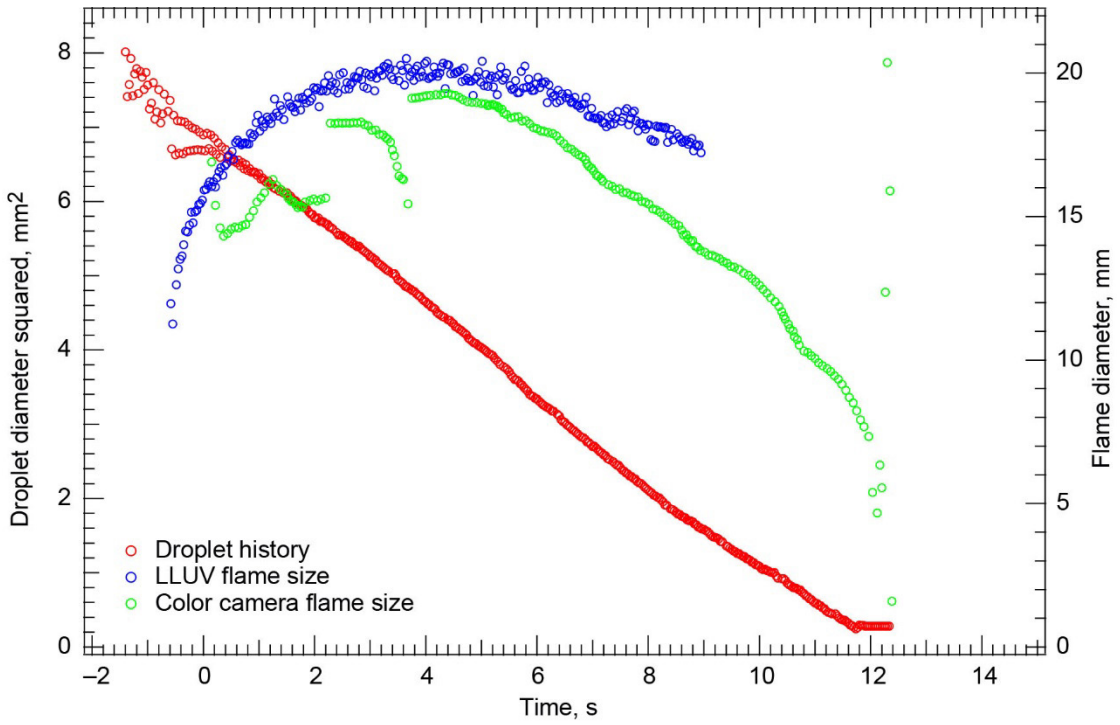

Figure 136.—Test FLEX–132. Free-floating heptane droplet burning in a 0.24/0.56/0.20 $O_2/N_2/CO_2$, 1.0-atm ambient environment. The droplet drifted slowly northeast after ignition, but it remained in the field of view (FOV) for the entire test. The droplet was initially luminous with a bright yellow flame that eventually turned blue with a little yellow and then blue until the end of the test. The droplet burned to a small size before a small disruption when the flame extinguished. The Low Light Level Ultra-Violet (LLUV) Image Processing and Storage Unit (IPSU) stopped recording for about 7 s in the middle of the test.

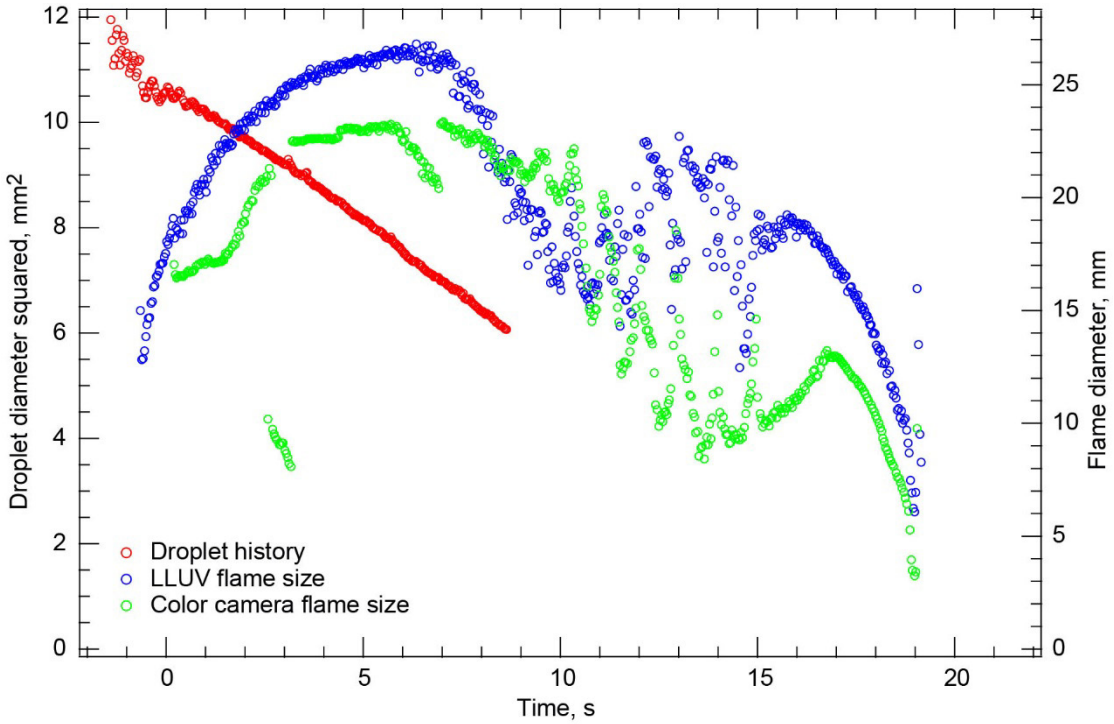

Figure 137.—Test FLEX–133. Free-floating heptane droplet in a 0.24/0.56/0.20 $O_2/N_2/CO_2$, 1.0-atm ambient environment. The droplet drifted northwest and out of the High-Bit-Depth Multispectral (HiBMs) field of view (FOV) before the end of the test (about halfway). After ignition, the droplet flame was luminous, quickly changing to a nearly all blue, dim flame. The flame then began to oscillate for several seconds before becoming stable and brighter. It burned until a small disruption coincident with when the flame extinguished. The extinction droplet diameter is the diameter of the droplet when the flame disrupted; it was estimated from the burning rate constant while the droplet was in the HiBMs FOV and the time of extinction from either the Low Light Level Ultra-Violet (LLUV) or color camera.

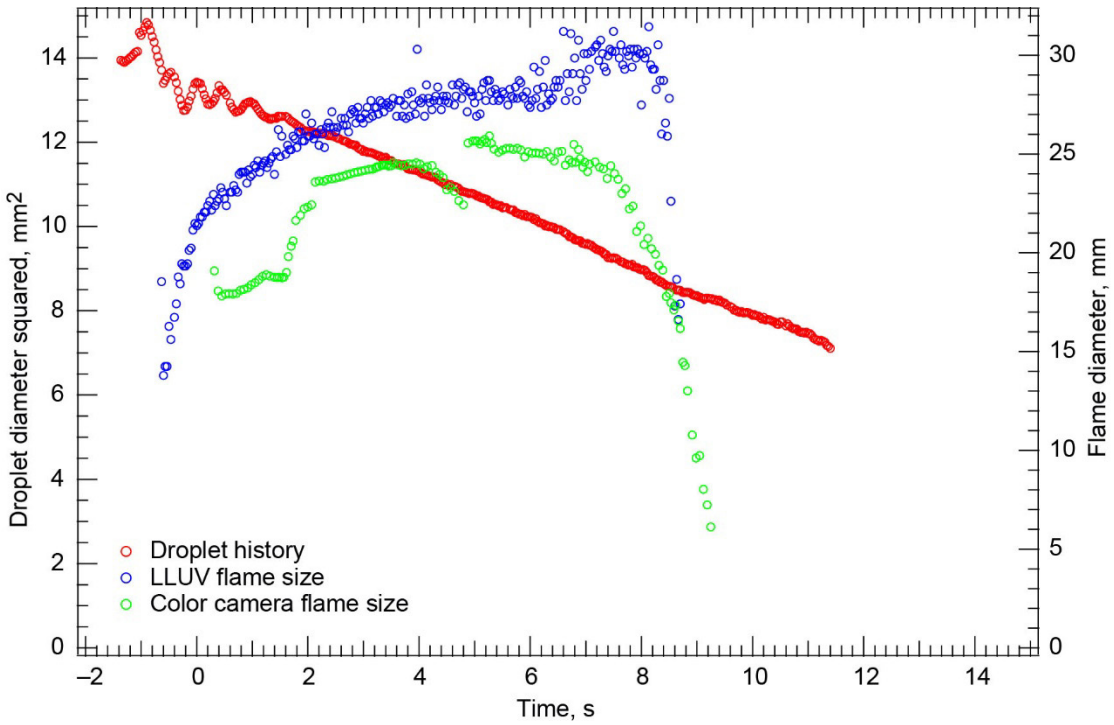

Figure 138.—Test FLEX–134. Free-floating heptane droplet in a 0.24/0.56/0.20 $O_2/N_2/CO_2$, 1.0-atm ambient environment. There were problems with gas bubbles during dispensing, stretching, and deployment. During this test, a small gas bubble burst during ignition and caused the droplet to oscillate. The droplet drifted slowly southeast and out of the High-Bit-Depth Multispectral (HiBMs) field of view (FOV) a few seconds after the flame extinguished radiatively. The droplet continued to vaporize at a relatively high rate after the flame extinguished, although only a few seconds passed before the droplet left the HiBMs FOV. A vapor cloud formed 10 to 20 s after the visible flame extinguished. The post-visible-flame-extinction behavior is indicative of cool flame burning and extinction.

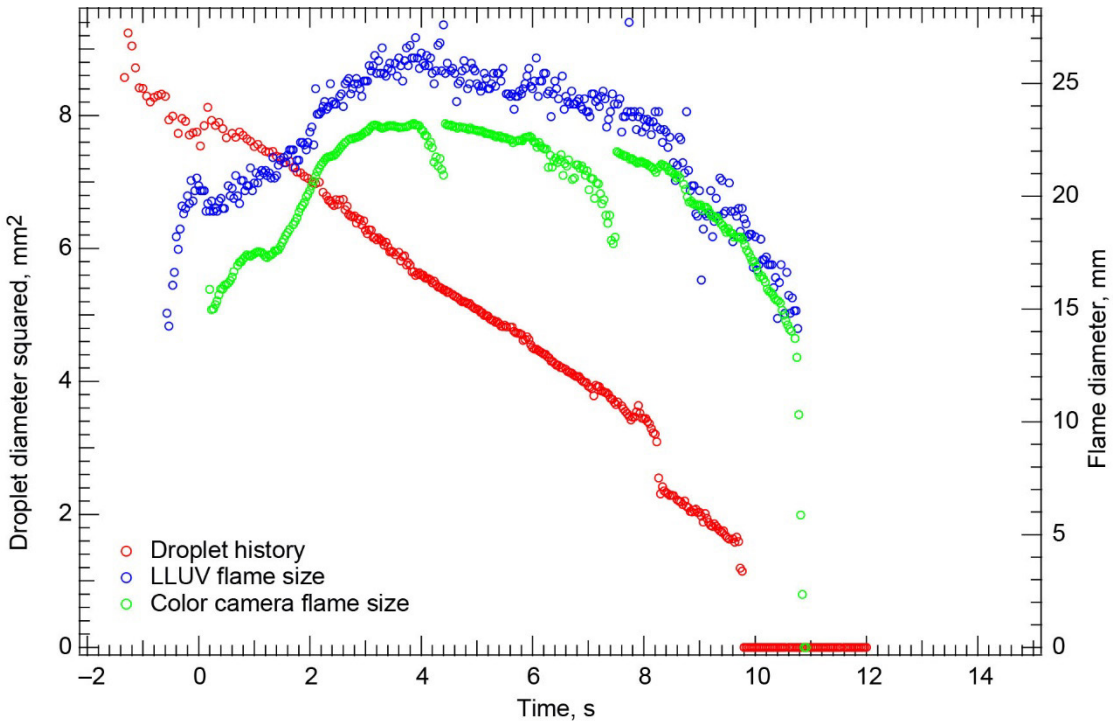

Figure 139.—Test FLEX–135. Fiber-supported heptane droplet with no translation in a 0.24/0.56/0.20 $O_2/N_2/CO_2$, 1.0-atm ambient environment. A small droplet to the west of the main droplet ignited and quickly burned off. There was significant transverse and axial motion of the droplet on the fiber during most of the test. The droplet drifted west on the fiber after deployment; then it stopped and oscillated (irregularly) axially and transversely during the entire burn. The shape changed briefly from spherical when there was a discrete change in droplet size that corresponded to something being ejected from the droplet (visible on the color camera).

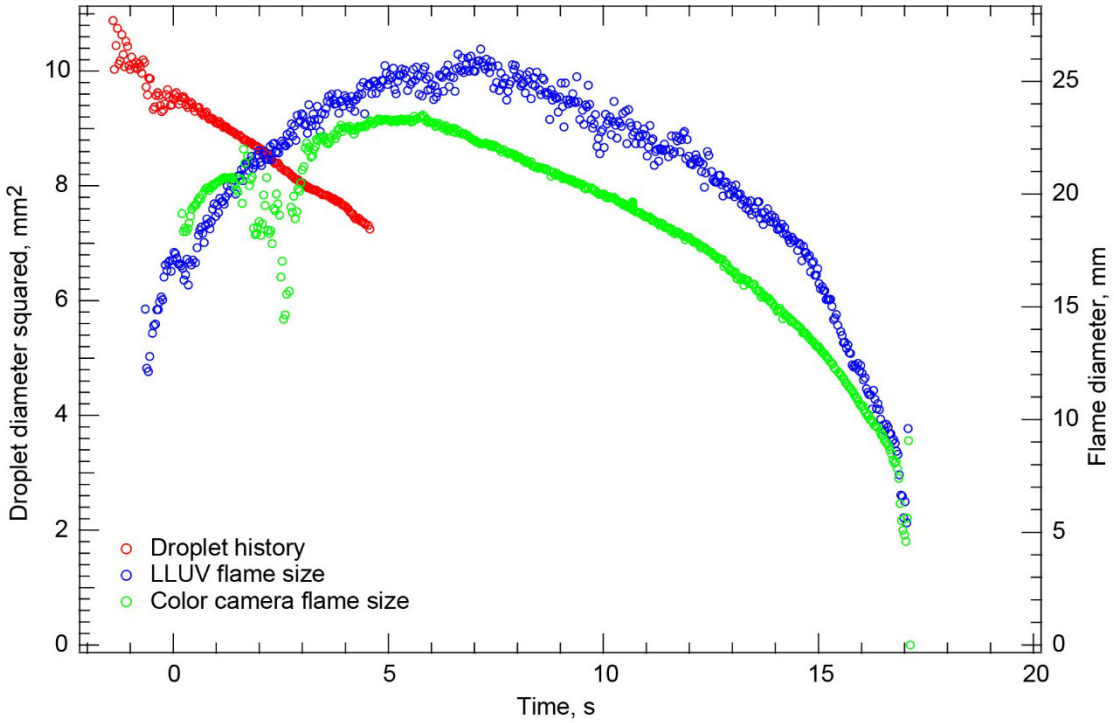

Figure 140.—Test FLEX–136. Free-floating heptane droplet burning in a 0.24/0.56/0.20 $O_2/N_2/CO_2$, 1.0-atm ambient environment. The droplet drifted northwest in the High-Bit-Depth Multispectral (HiBMs) field of view (FOV) after deployment, then it hit the igniter and moved northeast and out of the HiBMs FOV. Because the droplet was in the HiBMs FOV for only a small fraction of the droplet lifetime, no extinction droplet diameter is reported. It is not clear whether the droplet burned to completion or the flame extinguished at a finite droplet size. However, given the ambient conditions and the expected burning behavior, burnout is more likely.

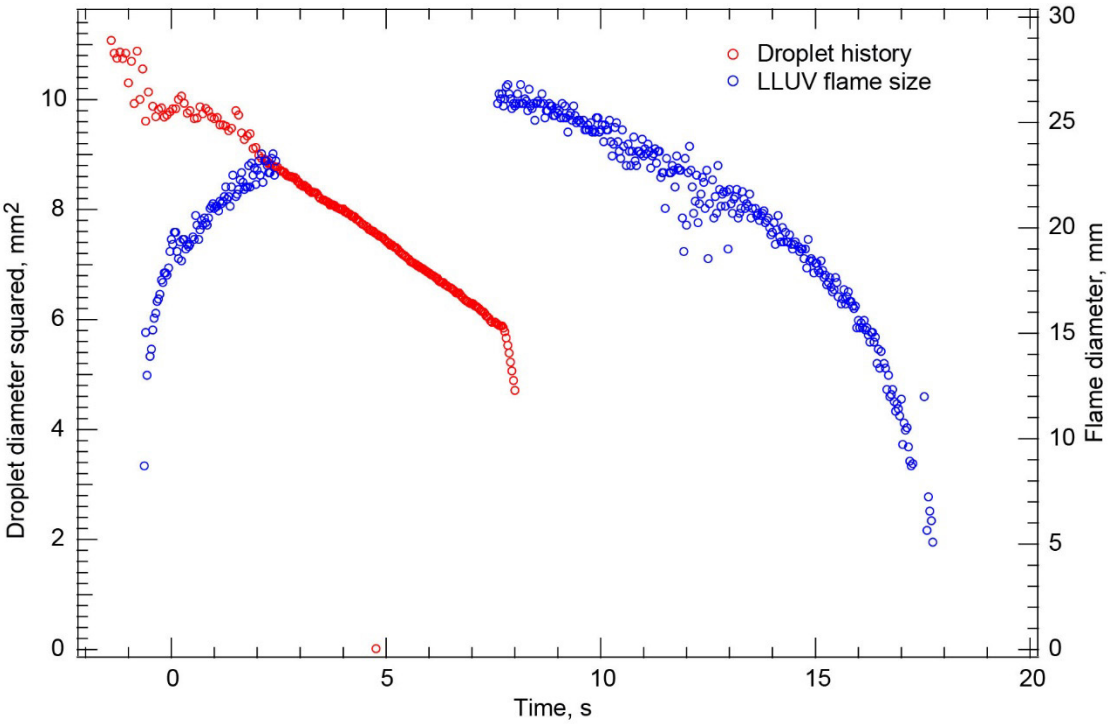

Figure 141.—Test FLEX−137. Free-floating heptane droplet burning in a 0.24/0.56/0.20 $O_2/N_2/CO_2$, 1.0-atm ambient environment. The droplet drifted northwest and out of the High-Bit-Depth Multispectral (HiBMs) field of view (FOV) about halfway through the test. After deployment, there was a disruption (maybe a bubble burst because these droplets had issues with gas bubbles) that caused significant droplet deformation and oscillations. There also was a moderate degree of sooting. The droplet burned to a relatively small size before disruptive extinction. The noise in the beginning of the droplet history was due to soot influencing the droplet size measurement. The color camera Image Processing and Storage Unit (IPSU) failed to record any images after deployment. The Low Light Level Ultra-Violet (LLUV) IPSU stopped recording images for a brief time in the middle of the burn.

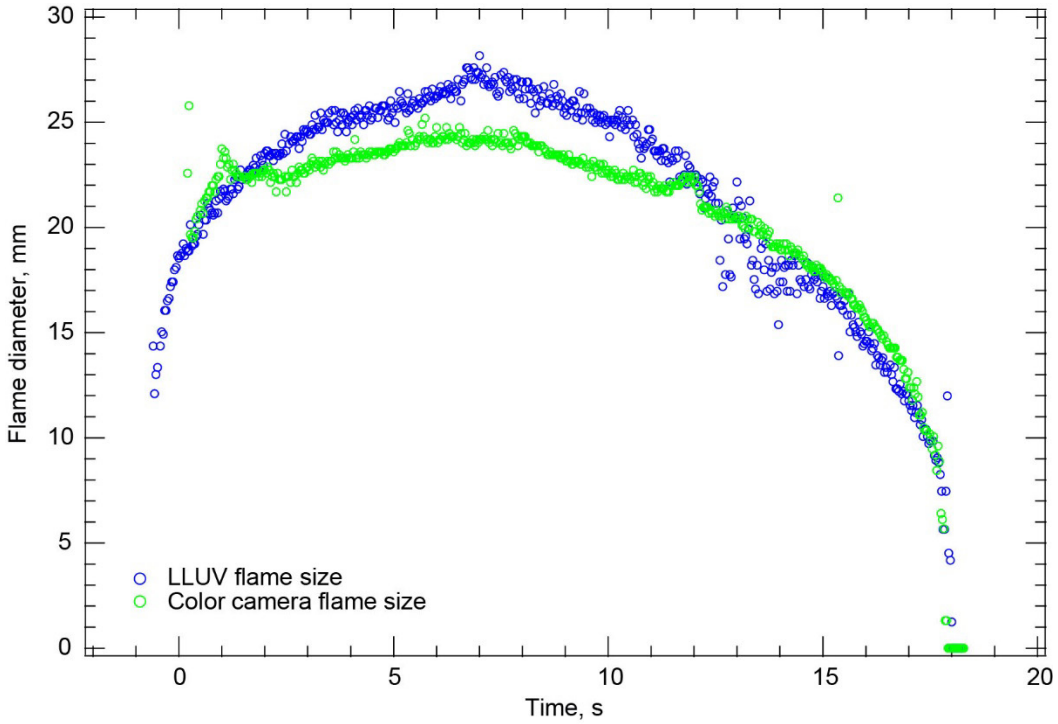

Figure 142.—Test FLEX−138. Free-floating heptane droplet burning in a 0.24/0.56/0.20 $O_2/N_2/CO_2$, 1.0-atm ambient environment. The High-Bit-Depth Multispectral (HiBMs) Image Processing and Storage Unit (IPSU) did not record any images for this test. The flame grew in size initially, became very dim, but then shrank, became brighter, and burned to disruption at a small size.

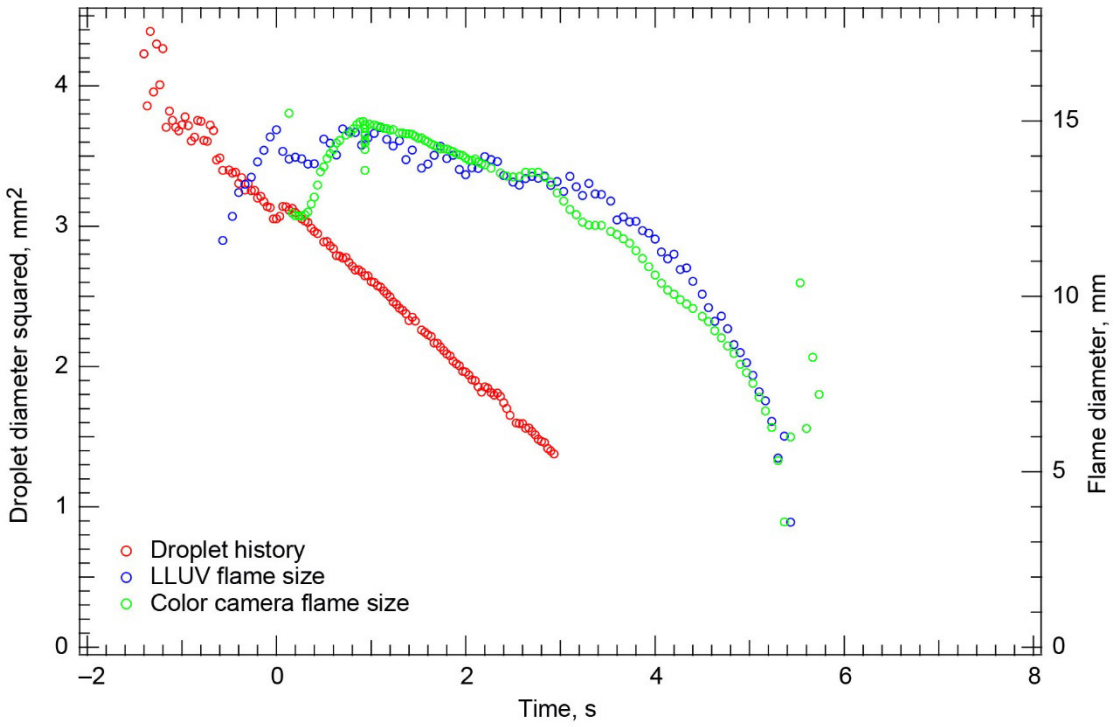

Figure 143.—Test FLEX–139. Free-floating heptane droplet burning in a 0.24/0.56/0.20 $O_2/N_2/CO_2$, 1.0-atm ambient environment. The droplet deformed shortly after deployment, presumably because of a gas bubble that burst. This caused the droplet to drift slowly northeast in the High-Bit-Depth Multispectral (HiBMs). A large flash coincident with ignition caused the droplet to drift southwest at approximately 6 mm/s. The droplet drifted with a constant trajectory until it left the HiBMs field of view (FOV) about halfway through the test. The burning rate was relatively high, and the flame was distorted by the large drift velocity. The droplet burned to a small size, then disrupted when the flame extinguished.

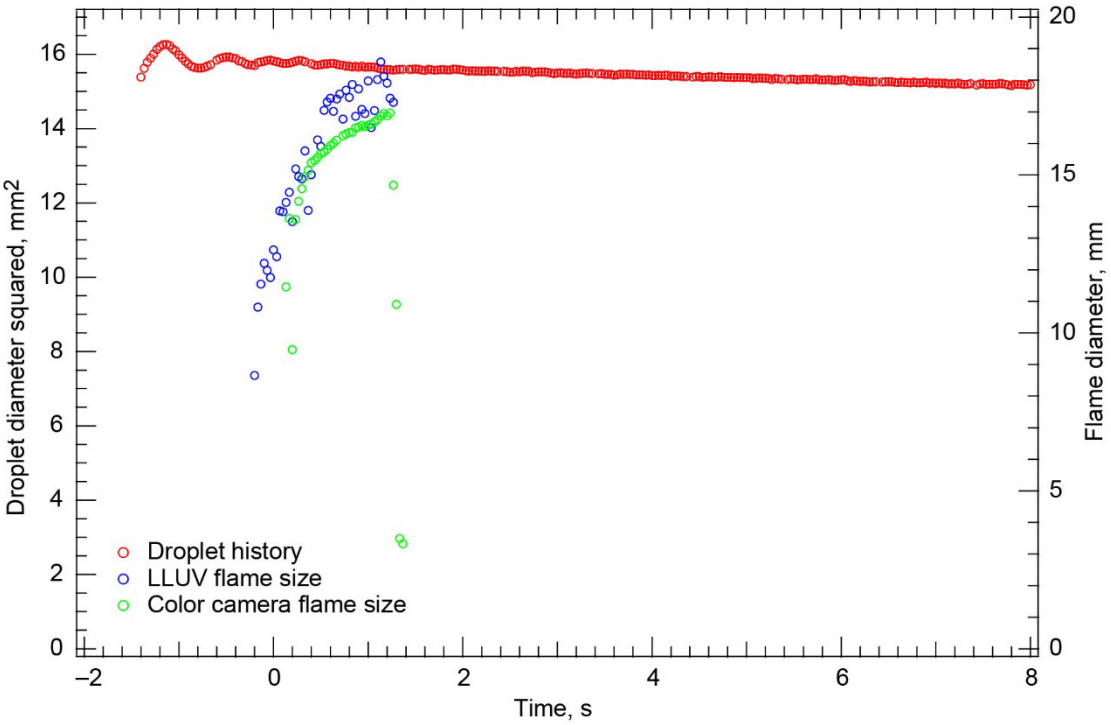

Figure 144.—Test FLEX–140. Free-floating methanol droplet burning in a 0.15/0.35/0.50 $O_2/N_2/CO_2$, 0.70-atm ambient environment. The droplet had a very small drift south after deployment and ignition, but it remained in the High-Bit-Depth Multispectral (HiBMs) field of view (FOV) for the entire recording time. For this very short burn, either the droplet was significantly larger than the radiative extinction limit or the test was completely outside of the quasi-steady flammability boundary.

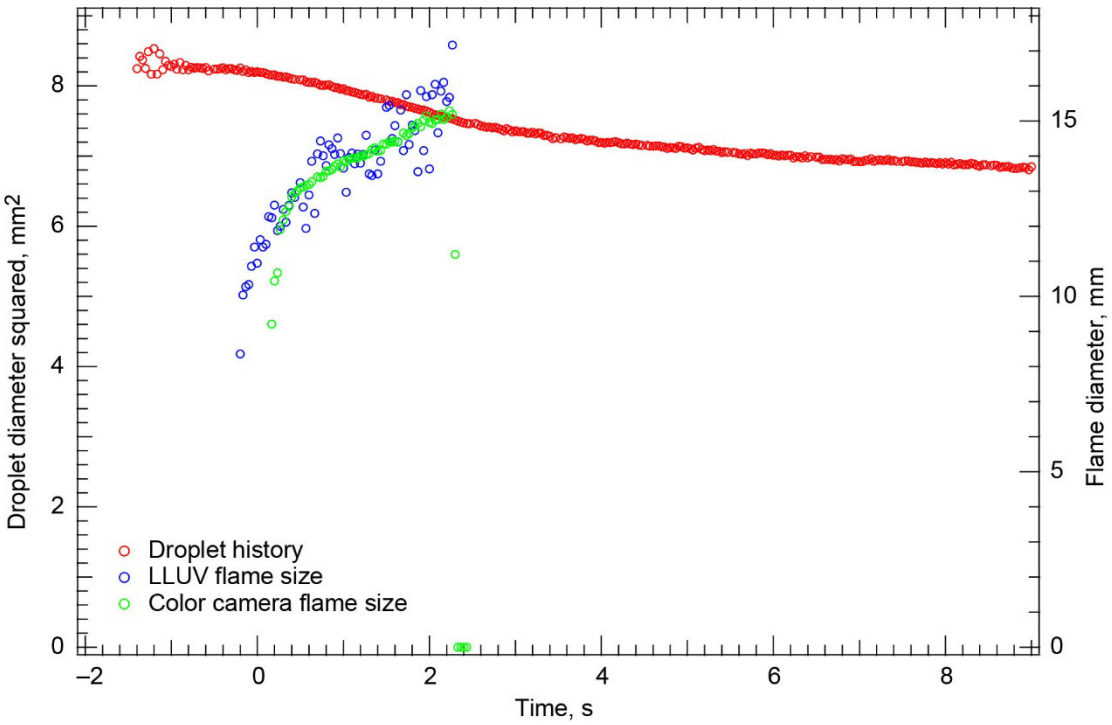

Figure 145.—Test FLEX–141. Free-floating methanol droplet burning in a 0.15/0.35/0.50 $O_2/N_2/CO_2$, 0.70-atm ambient environment. The droplet drifted slowly south, but it remained in the High-Bit-Depth Multispectral (HiBMs) field of view (FOV) for the entire test and well after the flame extinguished. The droplet abruptly left the HiBMs FOV in the video, probably because the HiBMs stopped archiving images for a short time. This very short burn either extinguished radiatively or was completely outside of the quasi-steady flammability boundary.

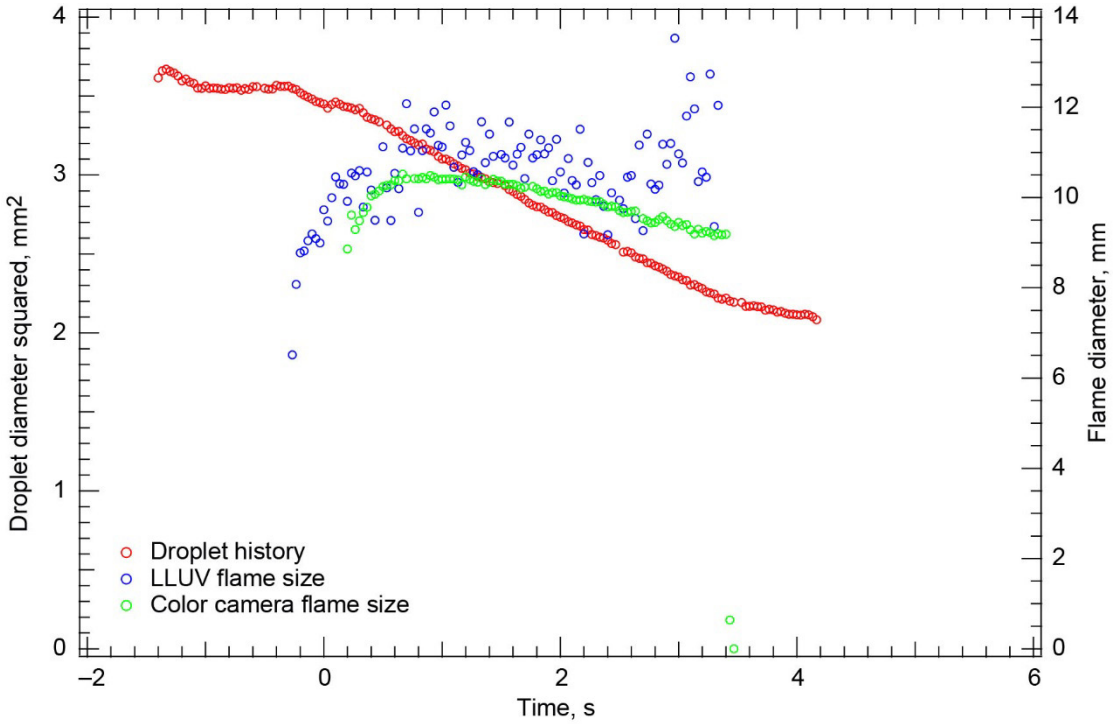

Figure 146.—Test FLEX–142. Free-floating methanol droplet burning in a 0.15/0.35/0.50 $O_2/N_2/CO_2$, 0.70-atm ambient environment. The droplet deployed with a relatively high (~6 mm/s) drift velocity to the northwest. The burn time was relatively short, and the droplet remained in the High-Bit-Depth Multispectral (HiBMs) field of view (FOV) for the entire test.

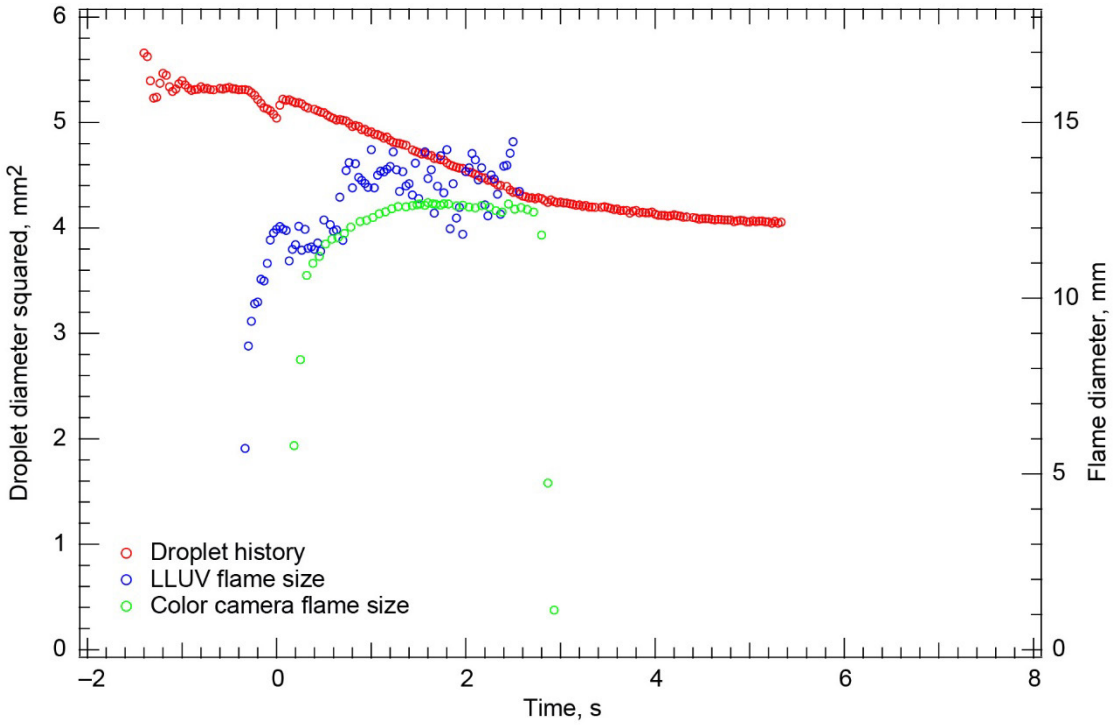

Figure 147.—Test FLEX–143. Free-floating methanol droplet burning in a 0.15/0.35/0.50 $O_2/N_2/CO_2$, 0.70-atm ambient environment. The droplet drifted north after deployment and ignition, and it drifted out of the High-Bit-Depth Multispectral (HiBMs) field of view (FOV) after the flame extinguished. It then drifted back into the HiBMs FOV before Image Processing and Storage Unit (IPSU) recording stopped (thus the gap in the droplet history shown in this figure). This smaller droplet had a very short burn—probably outside of the quasi-steady flammability boundary or, more likely, right at the boundary.

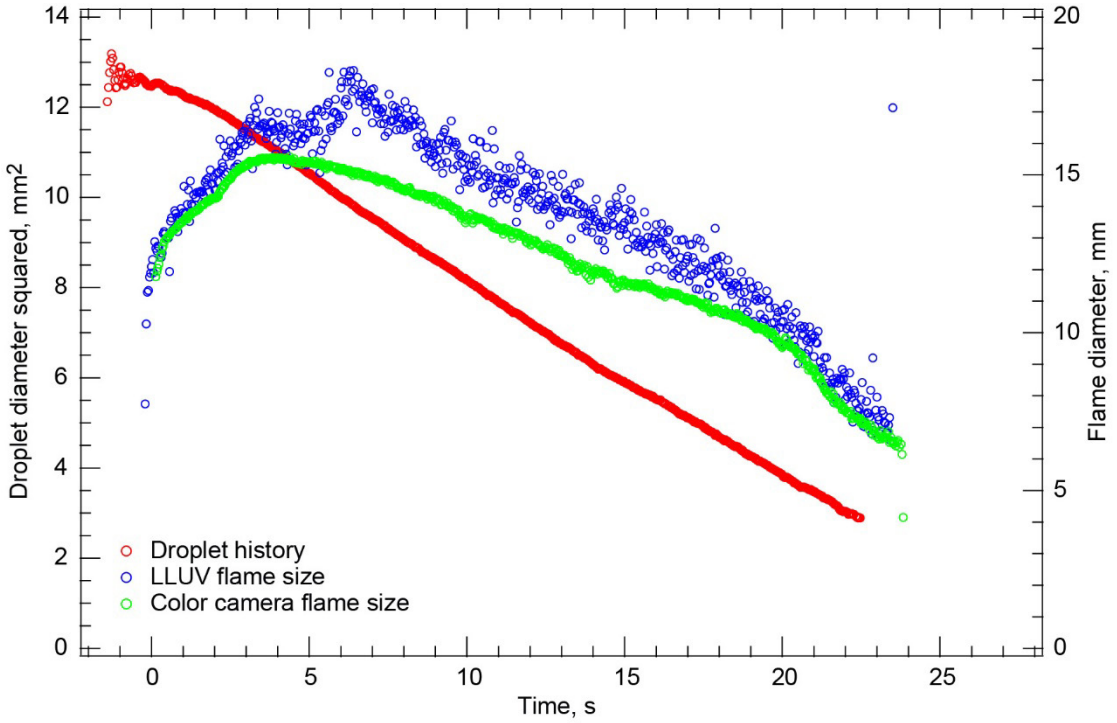

Figure 148.—Test FLEX–144. Free-floating methanol droplet burning in a 0.20/0.75/0.05 $O_2/N_2/CO_2$, 1.0-atm ambient environment. The droplet was nearly motionless after deployment and ignition. Halfway through the burn, the droplet drifted south. It left the High-Bit-Depth Multispectral (HiBMs) field of view (FOV) just before the flame extinguished, but it remained in the FOVs of the Low Light Level Ultra-Violet (LLUV) and color camera. The burning rate constant measured near the end of the time when the droplet was in the HiBMs FOV was used to extrapolate the extinction droplet diameter from the droplet history from when the droplet left the HiBMs FOV until the flame extinguished.

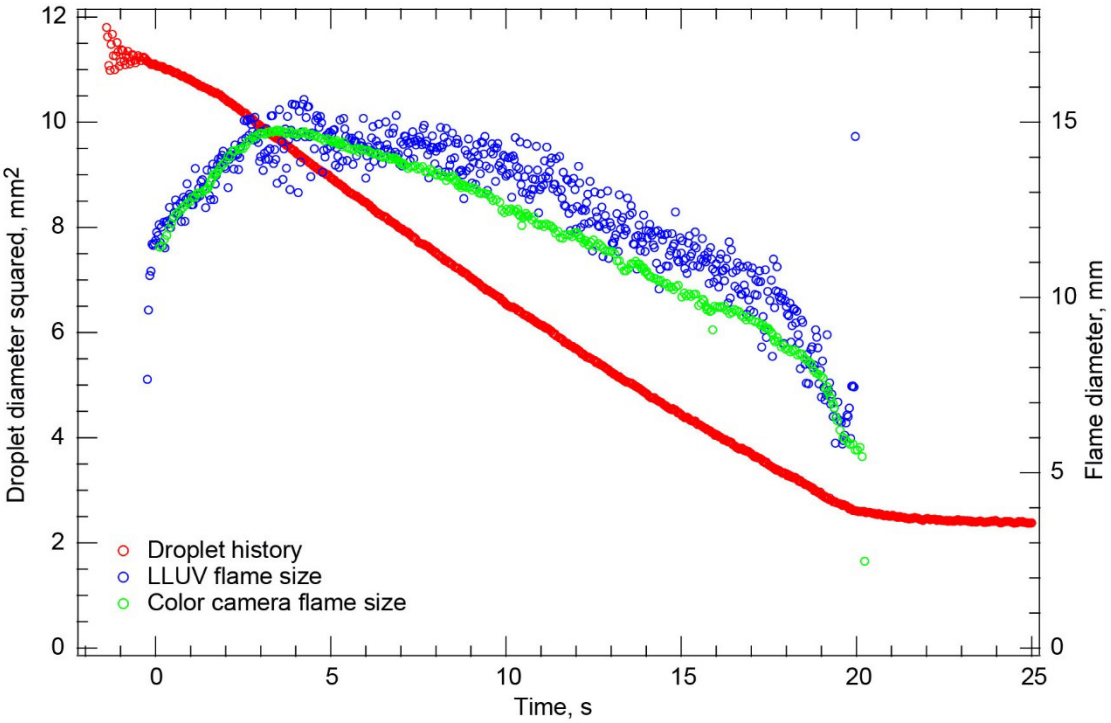

Figure 149.—Test FLEX−145. Free-floating methanol droplet burning in a 0.20/0.75/0.05 $O_2/N_2/CO_2$, 1.0-atm ambient environment. The droplet remained in the fields of view (FOVs) of all the cameras during the entire burn.

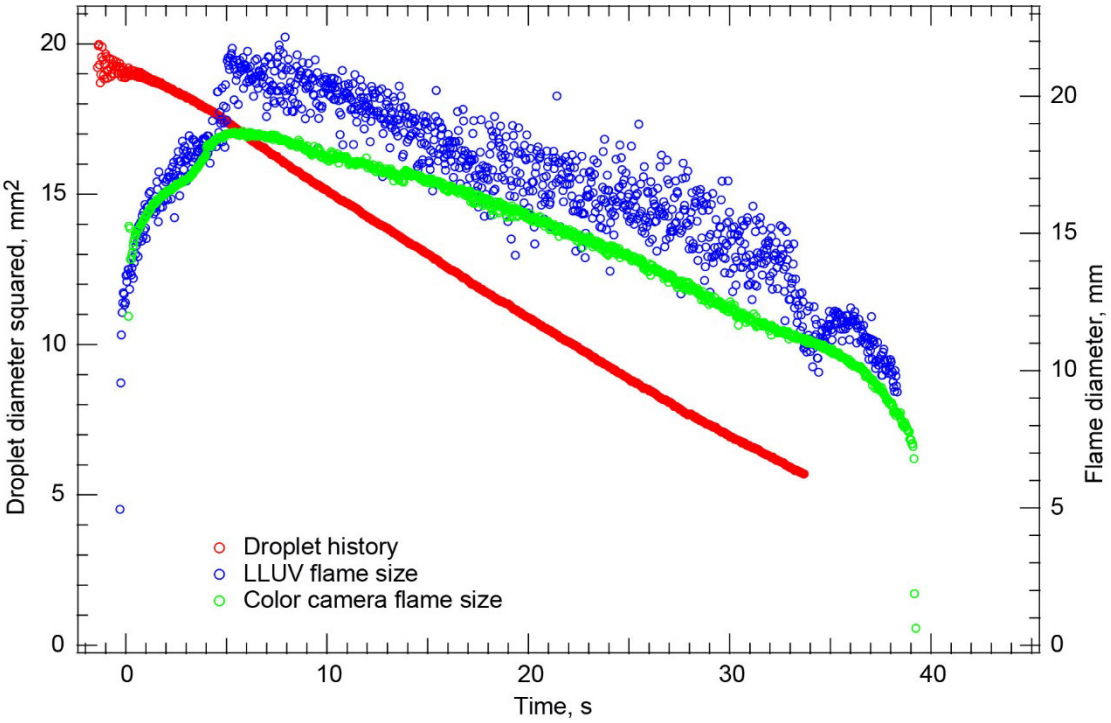

Figure 150.—Test FLEX−146. Free-floating methanol droplet burning in a 0.20/0.75/0.05 $O_2/N_2/CO_2$, 1.0-atm ambient environment. This very large droplet was nearly motionless after deployment and ignition. The droplet eventually drifted south in the High-Bit-Depth Multispectral (HiBMs) field of view (FOV) and left the FOV a short time before the flame extinguished. Because the flame was very dim and there was contamination on the Combustion Integrated Rack (CIR) LLUV viewing window, the flame size from the color camera was a bit more reliable than that from the Low Light Level Ultra-Violet (LLUV). The burning rate constant measured near the end of the time that the droplet was in the High-Bit-Depth Multispectral (HiBMs) FOV was used to extrapolate the extinction droplet diameter from the droplet history from when the droplet left the HiBMs FOV until the flame extinguished.

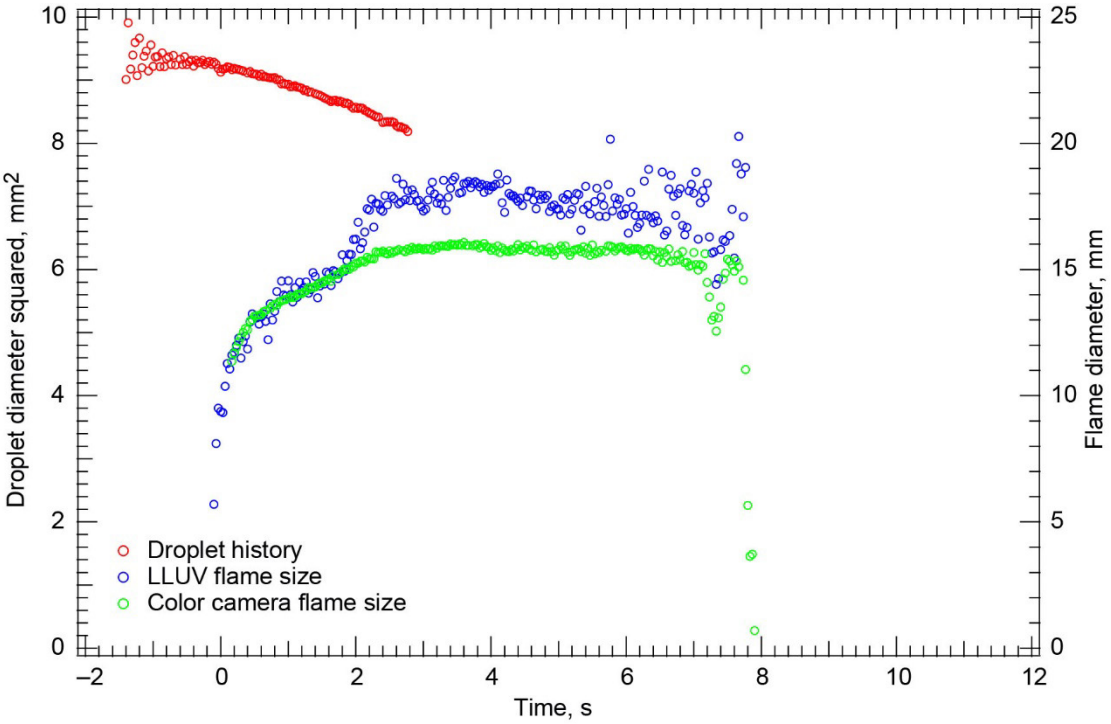

Figure 151.—Test FLEX−147. Free-floating methanol droplet burning in a 0.17/0.38/0.45 $O_2/N_2/CO_2$, 0.70-atm ambient environment. The droplet drifted southeast at approximately 4 to 5 mm/s (deployment-induced change of direction at ignition) and out of the High-Bit-Depth Multispectral (HiBMs) field of view (FOV) after a few seconds. The droplet remained in the FOVs of the Low Light Level Ultra-Violet (LLUV) and color camera for the entire test, but it was at the very edge of the FOVs of both cameras. The flame dimmed increasingly throughout the test. Because the droplet was in the HiBMs FOV for only a small fraction of the burn, no extinction droplet diameter is reported.

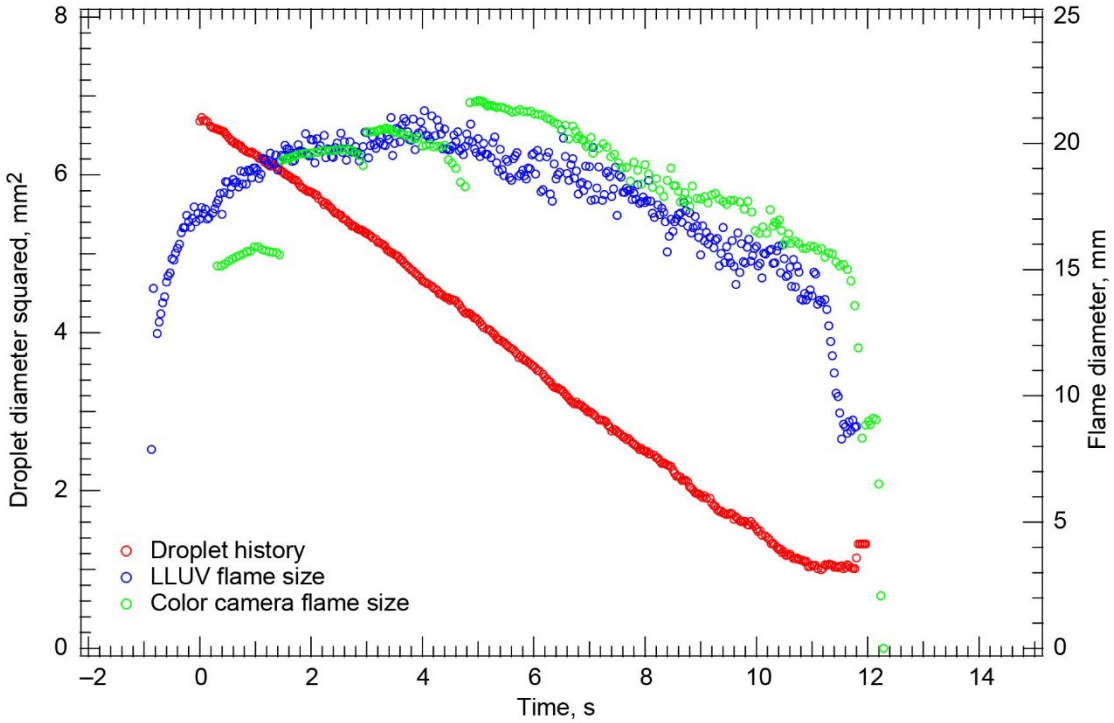

Figure 152.—Test FLEX–148. Free-floating heptane droplet burning in a 0.20/0.75/0.05 $O_2/N_2/CO_2$, 1.0-atm ambient environment. There was very little residual motion after deployment and ignition. The droplet remained in the fields of view (FOVs) of all the cameras for the entire test. It burned cleanly to small size, then it disrupted coincident with when the flame extinguished. The extinction droplet size is the size when the droplet disrupted. The High-Bit-Depth Multispectral (HiBMs) Image Processing and Storage Unit (IPSU) stopped recording data sometime before deployment to part way through the burn. The plotted data used the first measured droplet as time zero even though the droplet had been burning for some time before that point.

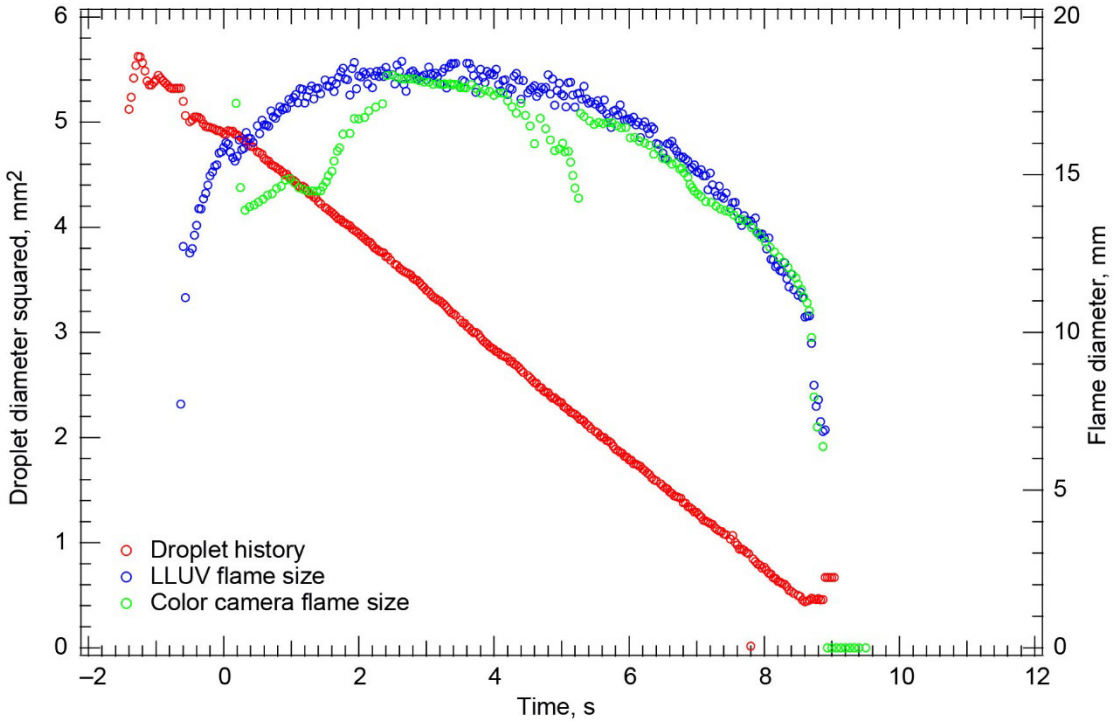

Figure 153—Test FLEX–149. Free-floating heptane droplet burning in a 0.20/0.75/0.05 $O_2/N_2/CO_2$, 1.0-atm ambient environment. The deployment was excellent with almost no residual motion after deployment and ignition. The droplet drifted a little south in the High-Bit-Depth Multispectral (HiBMs) field of view (FOV), but it remained in the FOVs of all cameras for the entire test. The droplet burned cleanly down to a small size then disrupted coincident with flame extinction. The extinction droplet size is the size when the disruption occurred.

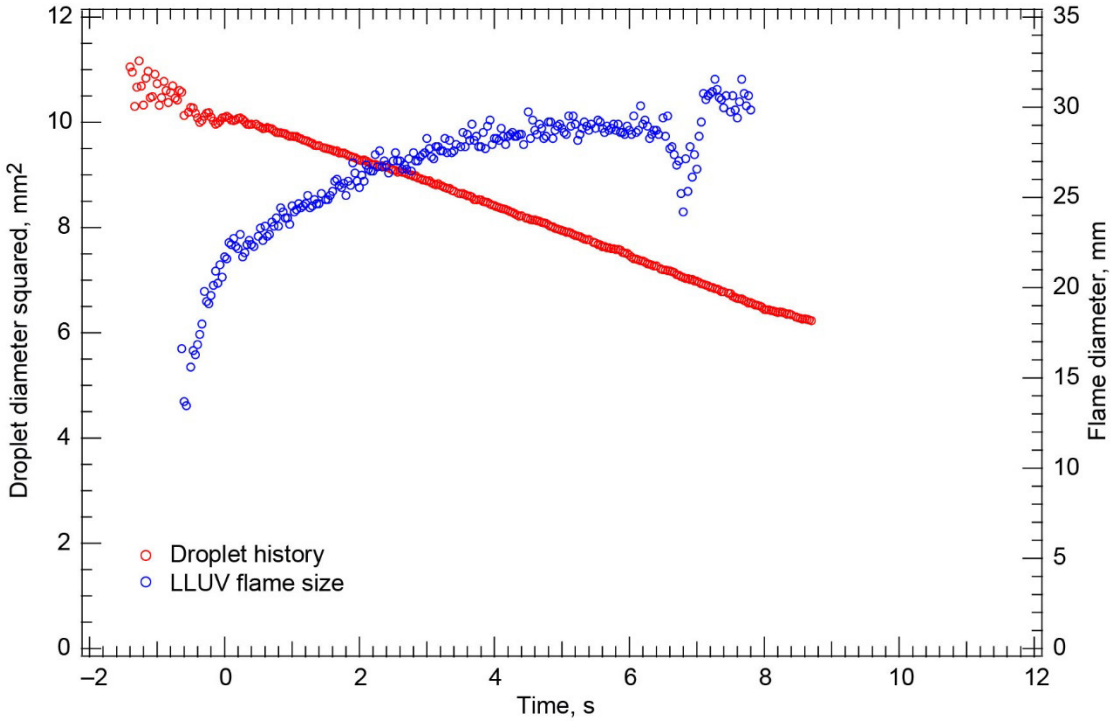

Figure 154.—Test FLEX–150. Free-floating heptane droplet burning in a 0.20/0.75/0.05 $O_2/N_2/CO_2$, 1.0-atm ambient environment. The droplet drifted northwest in the High-Bit-Depth Multispectral (HiBMs) field of view (FOV) after deployment and ignition, remained in the FOV for the entire burn, and left the FOV shortly after the visible flame extinguished. The flame oscillated a few times before it extinguished radiatively. A vapor cloud formed approximately 20 sec after the visible flame extinguished, indicating cool flame burning and extinction after visible flame extinction. The color camera Image Processing and Storage Unit (IPSU) did not record any images after deployment.

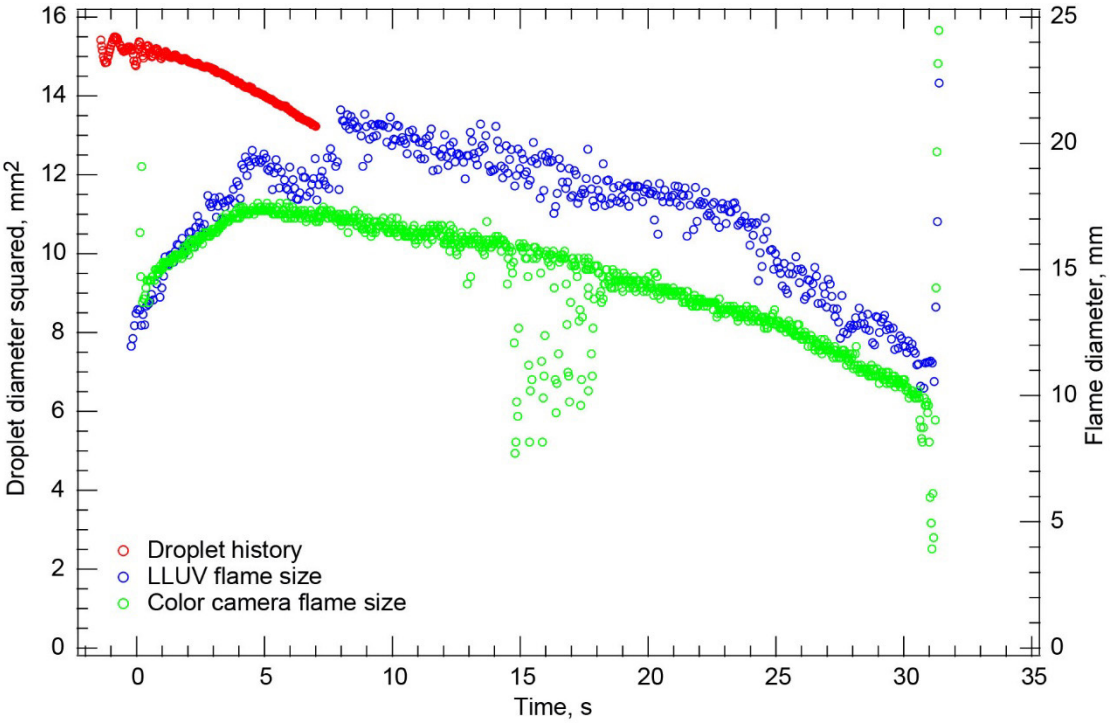

Figure 155.—Test FLEX−151. Free-floating methanol droplet burning in a 0.18/0.67/0.15 $O_2/N_2/CO_2$, 1.0-atm ambient environment. The droplet drifted northeast and out of the High-Bit-Depth Multispectral (HiBMs) field of view (FOV) about one-fourth of the way through the burn. The droplet burned for a very long time, but the flame was very dim and difficult to see, with significant noise in the Low Light Level Ultra-Violet (LLUV) when automated analysis was used and a very low threshold when manual analysis was used. The droplet oscillated for a few seconds halfway through the burn, then it burned with a steady flame until it oscillated again right before the flame extinguished. Because the droplet was in the HiBMs FOV for only a short time, no extinction droplet diameter is reported.

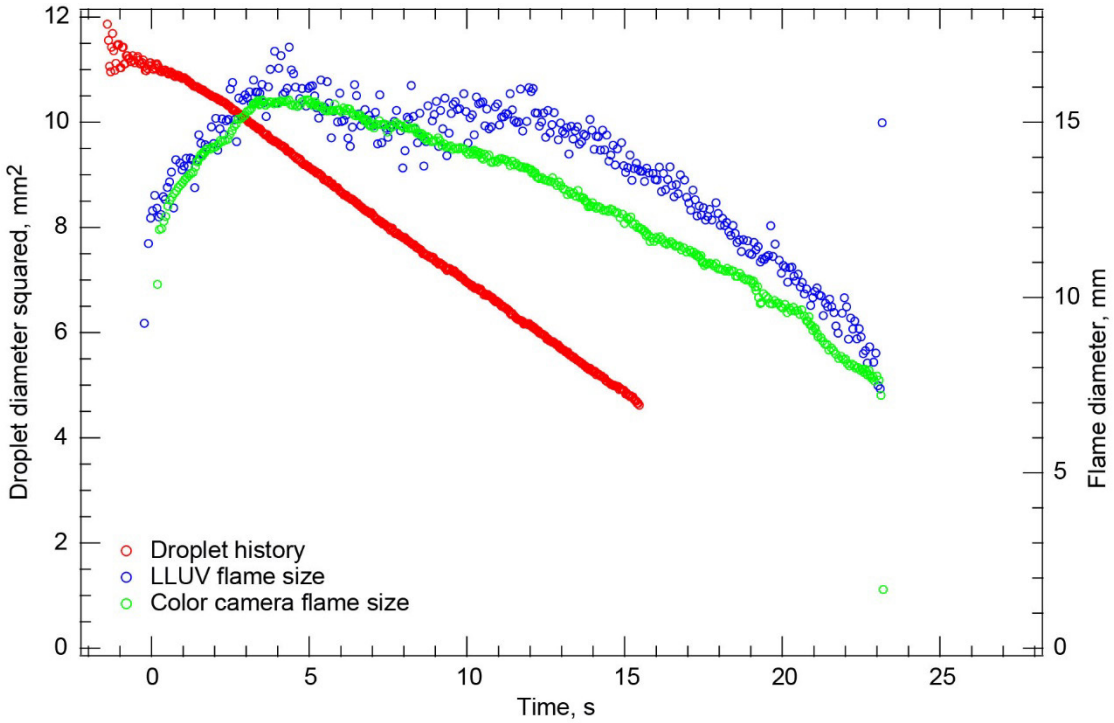

Figure 156.—Test FLEX–152. Free-floating methanol droplet burning in a 0.18/0.67/0.15 $O_2/N_2/CO_2$, 1.0-atm ambient environment. The droplet drifted south in the High-Bit-Depth Multispectral (HiBMs) field of view (FOV), and it left the FOV about two-thirds of the way through the burn. The burning rate constant from the droplet history for a short period of time before the droplet left the HiBMs FOV was used to extrapolate the extinction droplet diameter from the droplet history from when the droplet left the HiBMs FOV until the flame extinguished.

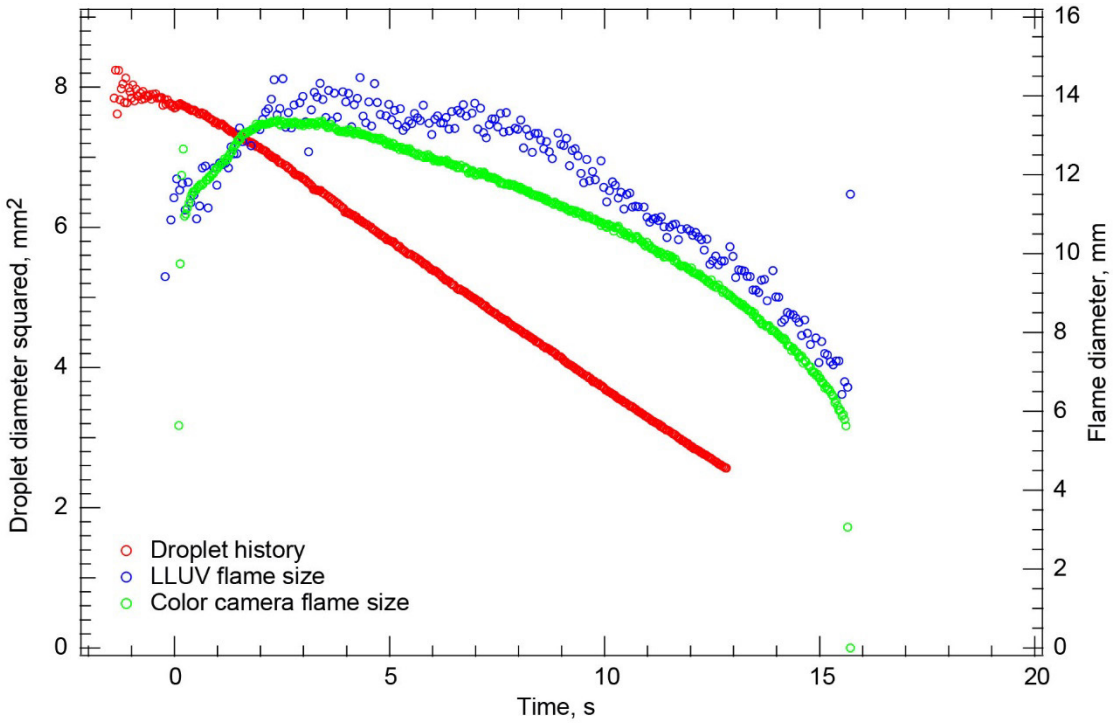

Figure 157.—Test FLEX–153. Free-floating methanol droplet burning in a 0.18/0.67/0.15 $O_2/N_2/CO_2$, 1.0-atm ambient environment. The droplet drifted north after deployment and ignition; then it began to drift back to the center. It remained in the High-Bit-Depth Multispectral (HiBMs) field of view (FOV) until four-fifths of the way through the burn when the HiBMs stopped recording data for about 5 s. The HiBMs did not record data when the flame extinguished. It was a long burn, and the measured burning rate constant for a short time right before recording stopped was used to extrapolate the extinction diameter from the droplet history until the visible flame extinguished.

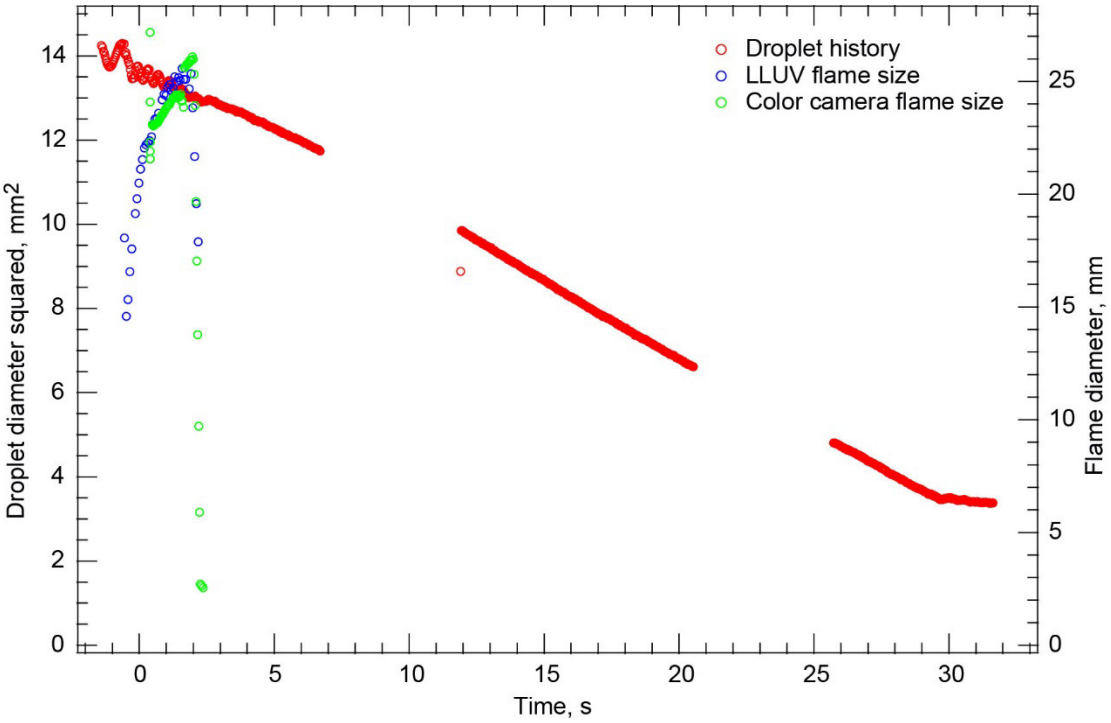

Figure 158.—Test FLEX–154. Free-floating heptane droplet burning in a 0.18/0.67/0.15 $O_2/N_2/CO_2$, 1.0-atm ambient environment. The droplet had almost no residual motion after deployment and ignition. This relatively large droplet remained in the High-Bit-Depth Multispectral (HiBMs) field of view (FOV) for the entire (short) burn and for the entire recording time of the HiBMs Image Processing and Storage Unit (IPSU). The droplet extinguished radiatively after a short burn with no flame oscillations. Late in the recording time, there was significant post-visible-flame-extinction vaporization and a large vapor cloud formed. The post-visible-flame-extinction behavior is indicative of cool flame burning and extinction.

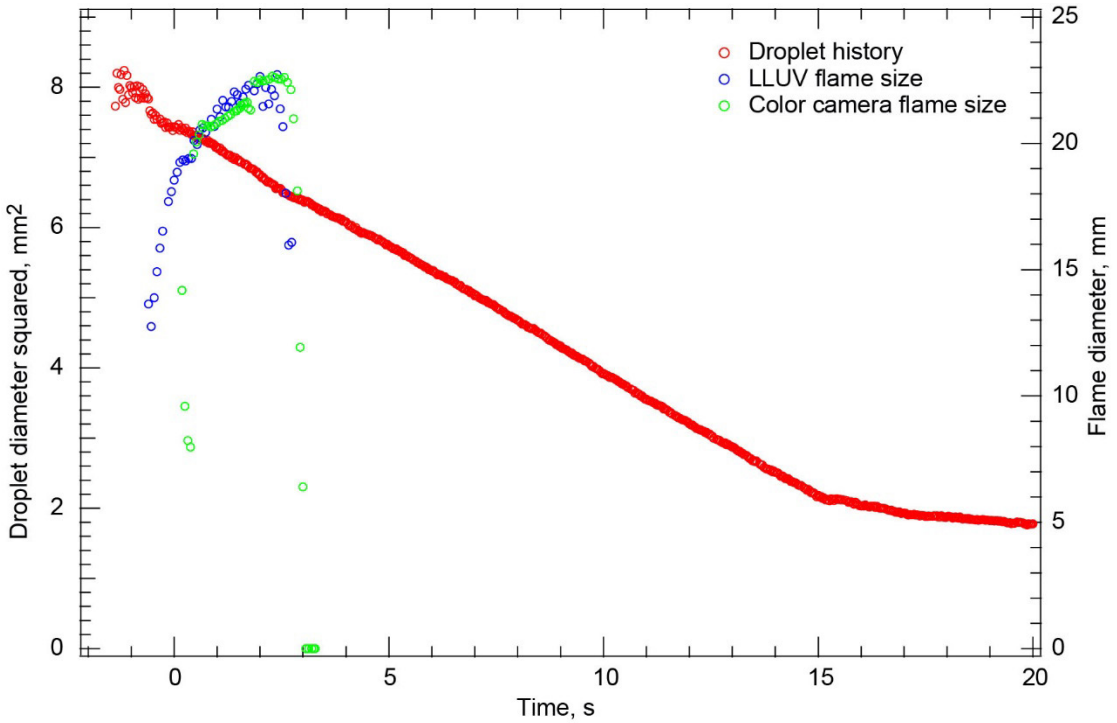

Figure 159.—Test FLEX–155. Free-floating heptane droplet burning in a 0.18/0.67/0.15 $O_2/N_2/CO_2$, 1.0-atm ambient environment. The droplet had almost no residual motion after deployment and ignition, and it remained in the High-Bit-Depth Multispectral (HiBMs) field of view (FOV) for the entire time that images were recorded. The flame had a very short burn time and probably extinguished radiatively. The vaporization rate was high after the visible flame extinguished, and there was an eventual plateau late in the HiBMs Image Processing and Storage Unit (IPSU) recording time coincident with the formation of a large vapor cloud. The post-visible-flame-extinction behavior is indicative of cool flame burning and extinction.

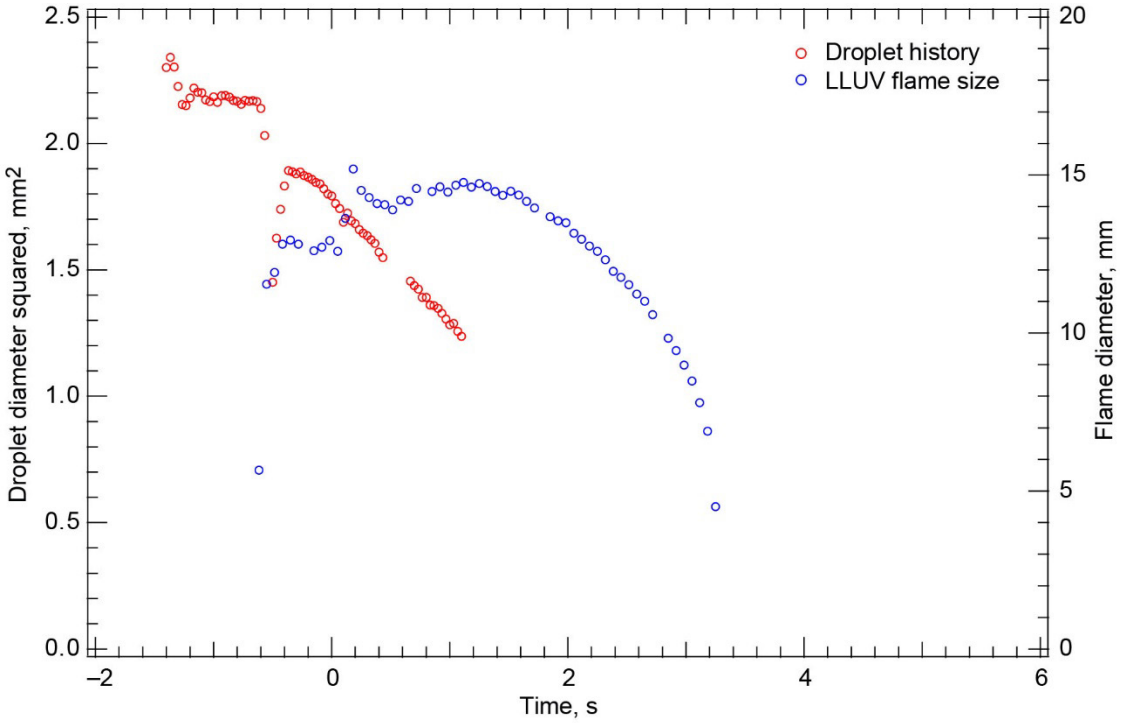

Figure 160.—Test FLEX–157. Free-floating heptane droplet burning in a 0.18/0.67/0.15 $O_2/N_2/CO_2$, 1.0-atm ambient environment. This very small droplet had a high northwest drift velocity in the High-Bit-Depth Multispectral (HiBMs) field of view (FOV). The droplet left the HiBMs FOV about one-third of the way through the test, and it moved past the northwest igniter before the igniter began to withdraw. The color camera Image Processing and Storage Unit (IPSU) failed to record any frames after deployment. Because the droplet was in the HiBMs FOV for only a short fraction of the entire test, no extinction diameter is reported.

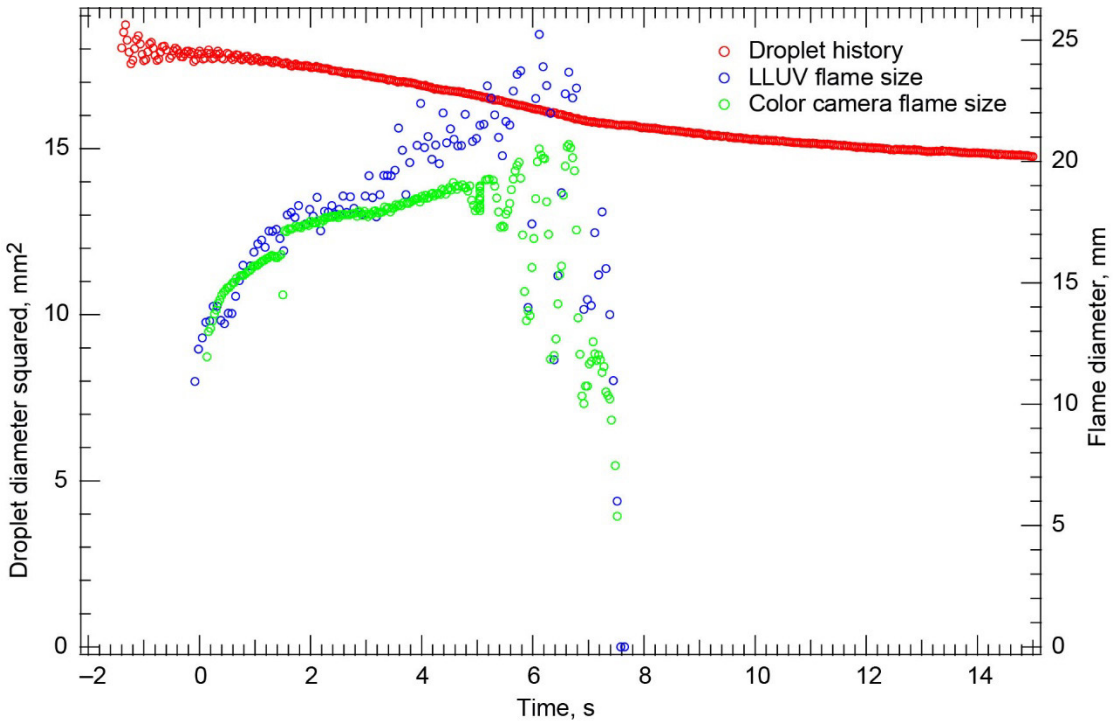

Figure 161.—Test FLEX–158. Free-floating methanol droplet burning in a 0.18/0.67/0.15 $O_2/N_2/CO_2$, 1.0-atm ambient environment. This relatively large droplet was nearly motionless after deployment and ignition, and it remained in the fields of view (FOVs) of all the cameras. The flame oscillated for a few cycles (increasing in magnitude with time) until it extinguished radiatively. Because the flame was dim and there was contamination on the Low Light Level Ultra-Violet (LLUV) viewing window, the flame was difficult to see with the LLUV.

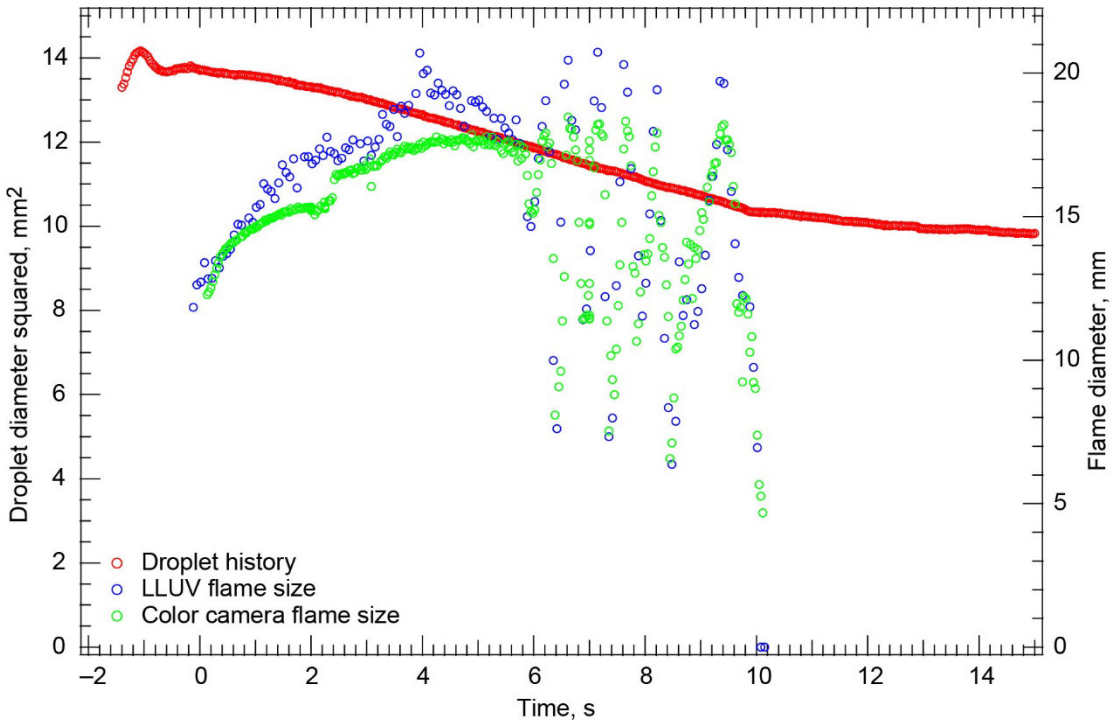

Figure 162.—Test FLEX–159. Free-floating methanol droplet burning in a 0.18/0.67/0.15 $O_2/N_2/CO_2$, 1.0-atm ambient environment. The droplet was nearly motionless after deployment and ignition, and it remained near the center of the fields of view (FOVs) for the entire test. The flame oscillated for several cycles before extinguishing radiatively. Because the flame was very dim and there was contamination on the Combustion Integrated Rack (CIR) LLUV viewing window, the Low Light Level Ultra-Violet (LLUV) flame diameter data are very noisy.

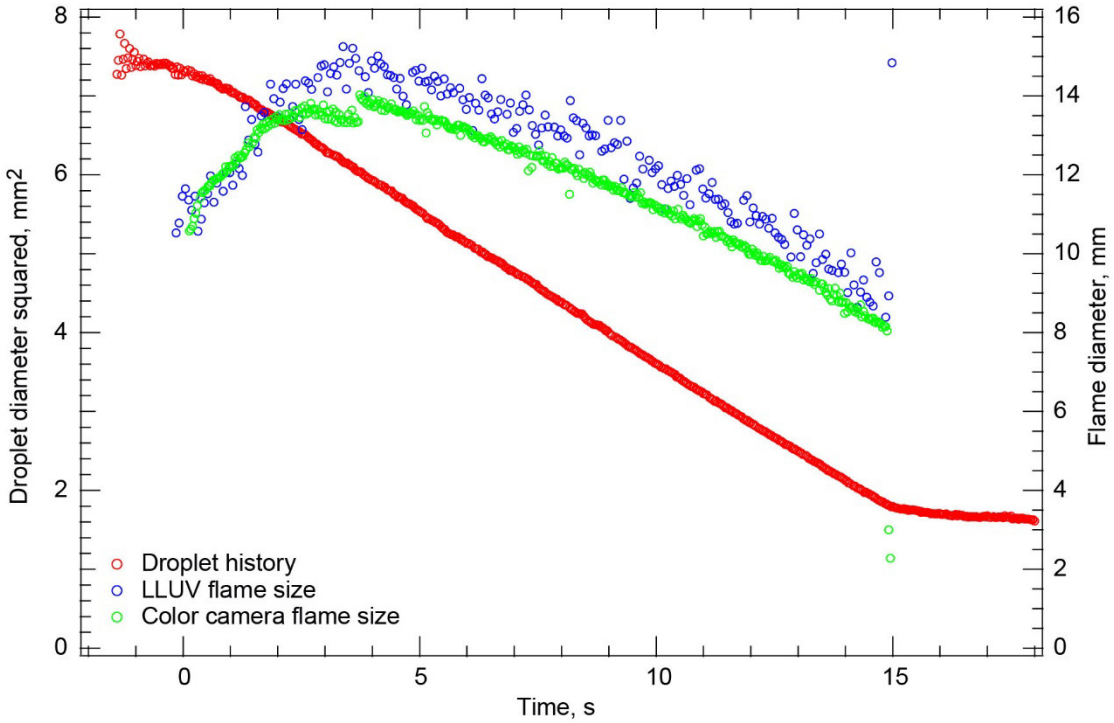

Figure 163.—Test FLEX–160. Free-floating methanol droplet burning in a 0.19/0.59/0.25 $O_2/N_2/CO_2$, 1.0-atm ambient environment. The droplet remained in the fields of view (FOVs) of all the cameras for the entire burn, and the flame extinguished diffusively. Because the Low Light Level Ultra-Violet (LLUV) images were dim and there was contamination on the Combustion Integrated Rack (CIR) LLUV viewing window, the flame size data are a bit noisy but seem to be reasonable.

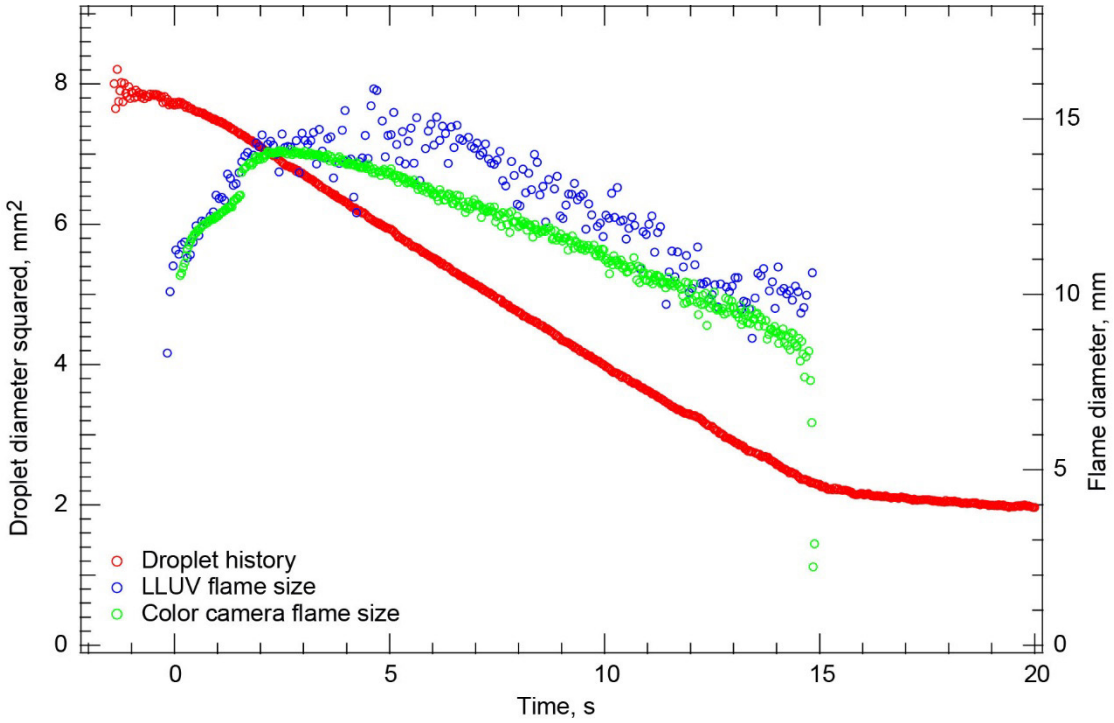

Figure 164.—Test FLEX–161. Free-floating methanol droplet burning in a 0.16/0.59/0.25 $O_2/N_2/CO_2$, 1.0-atm ambient environment. The droplet was nearly motionless after deployment and ignition, and it remained in the fields of view (FOVs) of all the cameras for the entire burn, which was a long burn to diffusive extinction. Because the Low Light Level Ultra-Violet (LLUV) images were dim and there was contamination on the Combustion Integrated Rack (CIR) LLUV viewing window, and the LLUV flame size data are very noisy.

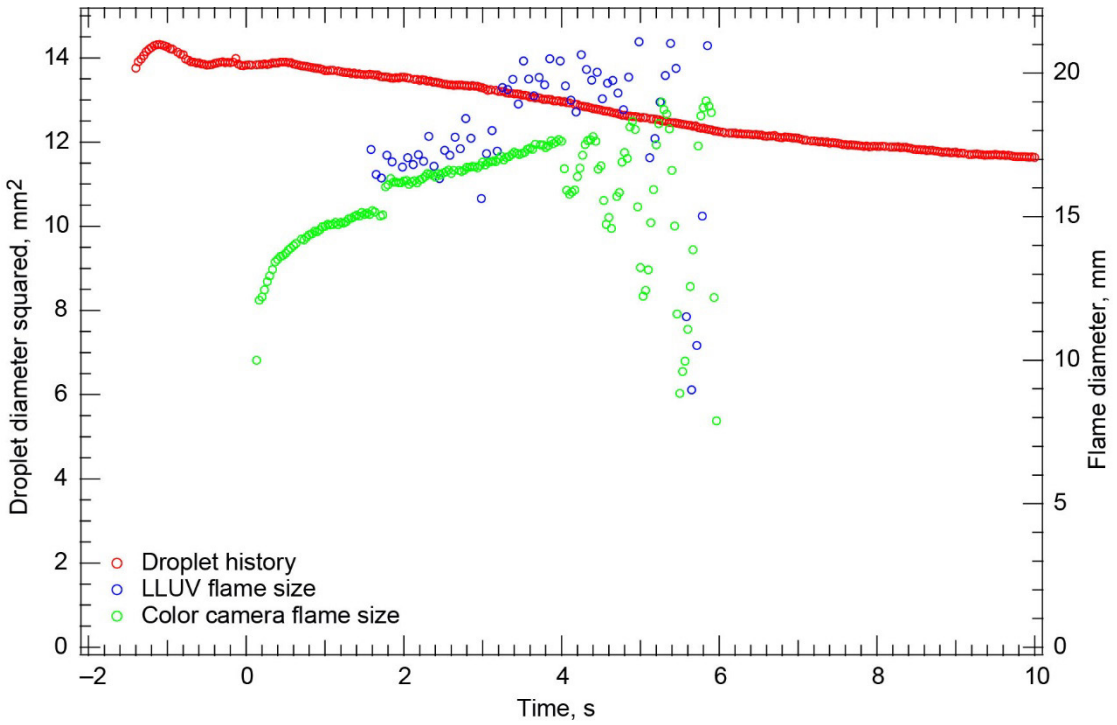

Figure 165.—Test FLEX–162. Free-floating methanol droplet burning in a 0.14/0.54/0.32 $O_2/N_2/CO_2$, 1.0-atm ambient environment. The droplet was nearly motionless after deployment and ignition, and it remained in the fields of view (FOVs) of all the cameras for the duration of the test. The flame oscillated for several seconds with increasing magnitude before extinguishing radiatively. Because the Low Light Level Ultra-Violet (LLUV) images were dim and there was contamination on the Combustion Integrated Rack (CIR) LLUV viewing window, the LLUV flame data are very noisy.

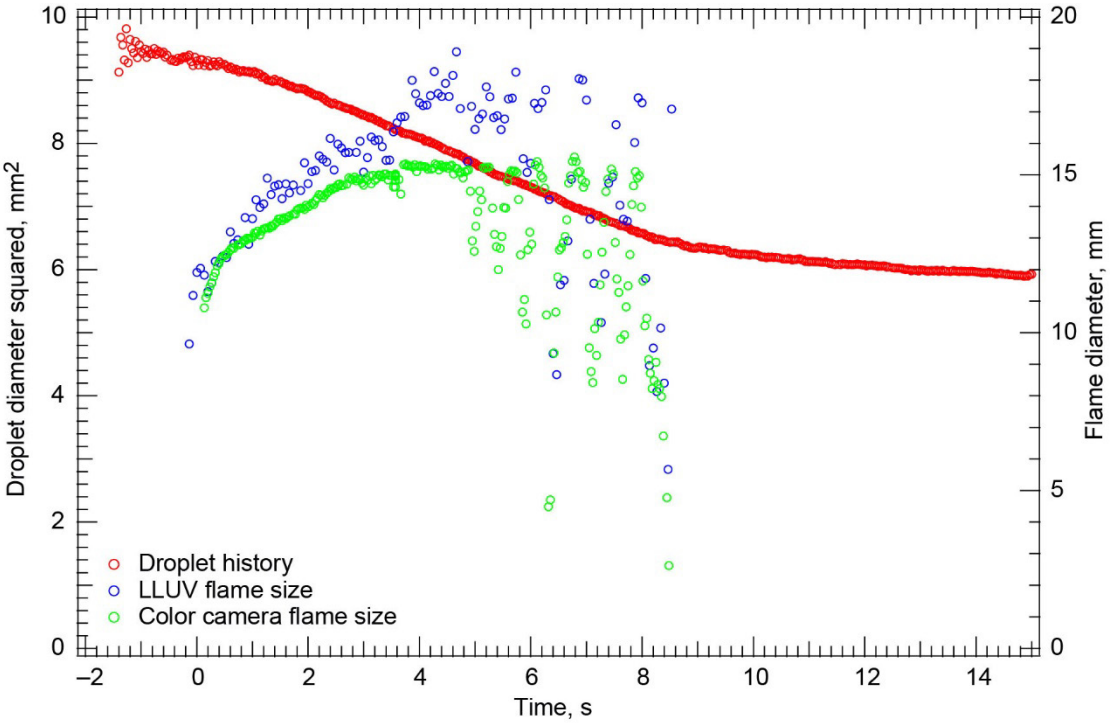

Figure 166.—Test FLEX–163. Free-floating methanol droplet burning in a 0.14/0.54/0.32 $O_2/N_2/CO_2$, 1.0-atm ambient environment. The droplet remained in the fields of view (FOVs) of all the cameras for the entire burn. The flame oscillated for several cycles of increasing magnitude before extinguishing radiatively. Because the Low Light Level Ultra-Violet (LLUV) images were dim and there was contamination on the Combustion Integrated Rack (CIR) LLUV viewing window, the LLUV flame data are very noisy.

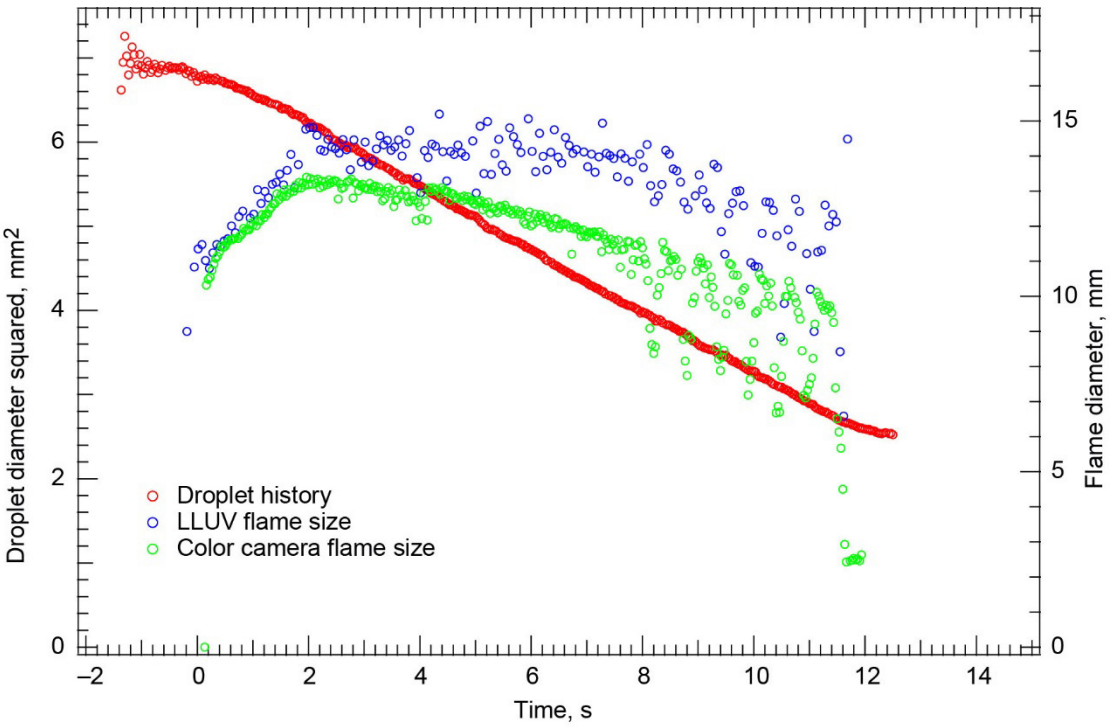

Figure 167.—Test FLEX–164. Free-floating methanol droplet burning in a 0.14/0.54/0.32 $O_2/N_2/CO_2$, 1.0-atm ambient environment. The droplet drifted northwest in the High-Bit-Depth Multispectral (HiBMs) field of view (FOV) after deployment and ignition. It left the FOV just after the visible flame extinguished. The flame oscillated several cycles with a nearly constant amplitude before extinguishing radiatively. Because the Low Light Level Ultra-Violet (LLUV) images were dim and there was contamination of the Combustion Integrated Rack (CIR) LLUV viewing window, the LLUV flame data are noisy.

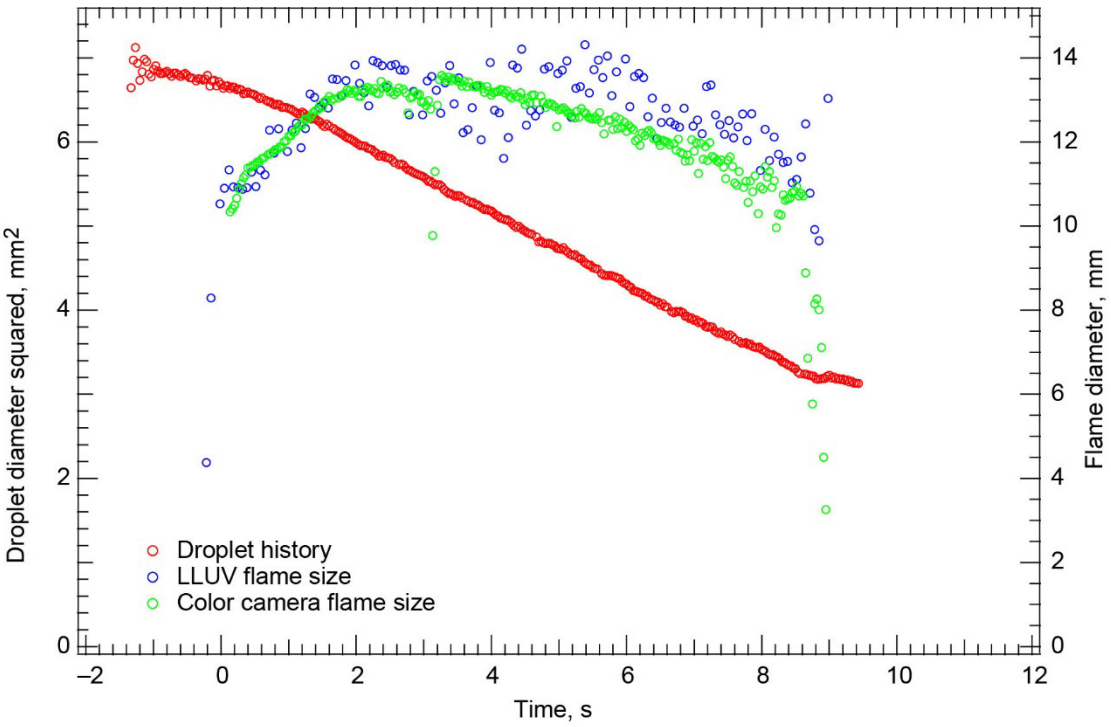

Figure 168.—Test FLEX–165. Free-floating methanol droplet burning in a 0.14/0.54/0.32 $O_2/N_2/CO_2$, 1.0-atm ambient environment. The droplet drifted south in the High-Bit-Depth Multispectral (HiBMs) field of view (FOV) after deployment and ignition, left the FOV shortly after the visible flame extinguished, and then drifted back into the FOV well after extinction near the end of recording. Because this was a very dim flame and there was contamination on the Combustion Integrated Rack (CIR) Low Light Level Ultra-Violet (LLUV) viewing window, the LLUV data are very noisy.

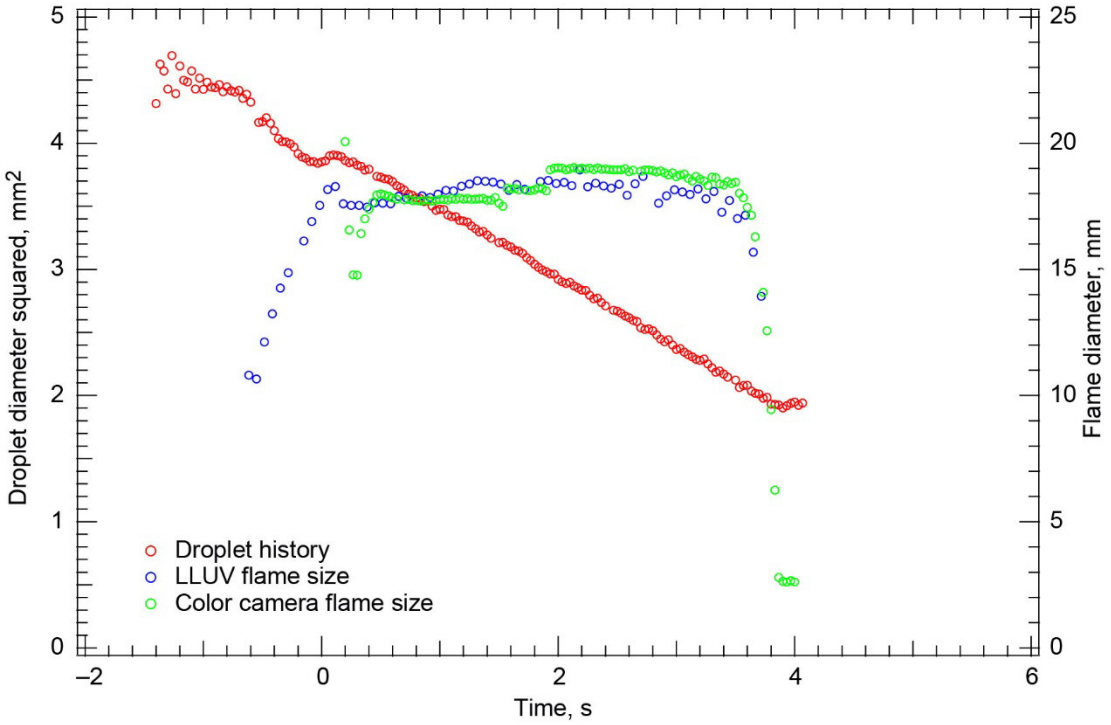

Figure 169.—Test FLEX–166. Free-floating heptane droplet burning in a 0.18/0.670.15 $O_2/N_2/CO_2$, 1.0-atm ambient environment. The droplet drifted southeast in the High-Bit-Depth Multispectral (HiBMs) field of view (FOV), remained in the FOV until the visible flame extinguished, and then drifted out of the FOV. The flame became dimmer as the burn progressed, but it did not oscillate before it extinguished, and no vapor cloud formed after visible flame extinction.

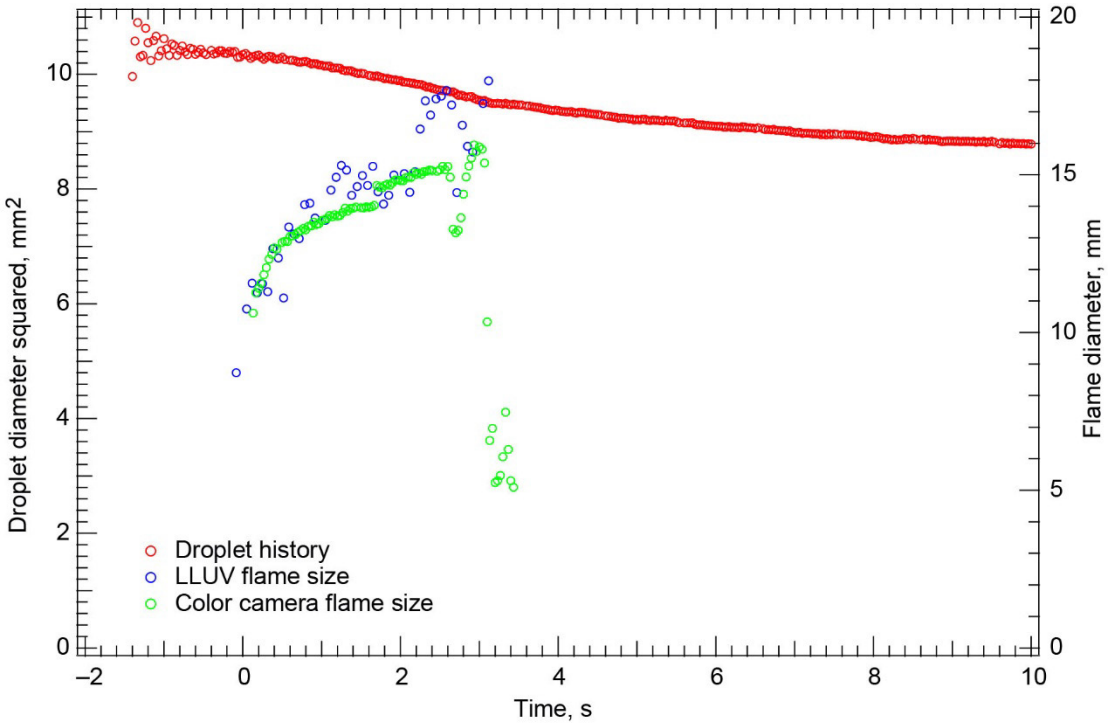

Figure 170.—Test FLEX–167. Free-floating methanol droplet burning in a 0.14/0.50/0.36 $O_2/N_2/CO_2$, 1.0-atm ambient environment. The droplet remained in the fields of view (FOVs) of all cameras. This was a short burn to radiative extinction, and the color camera Image Processing and Storage Unit (IPSU) did not record any images after deployment.

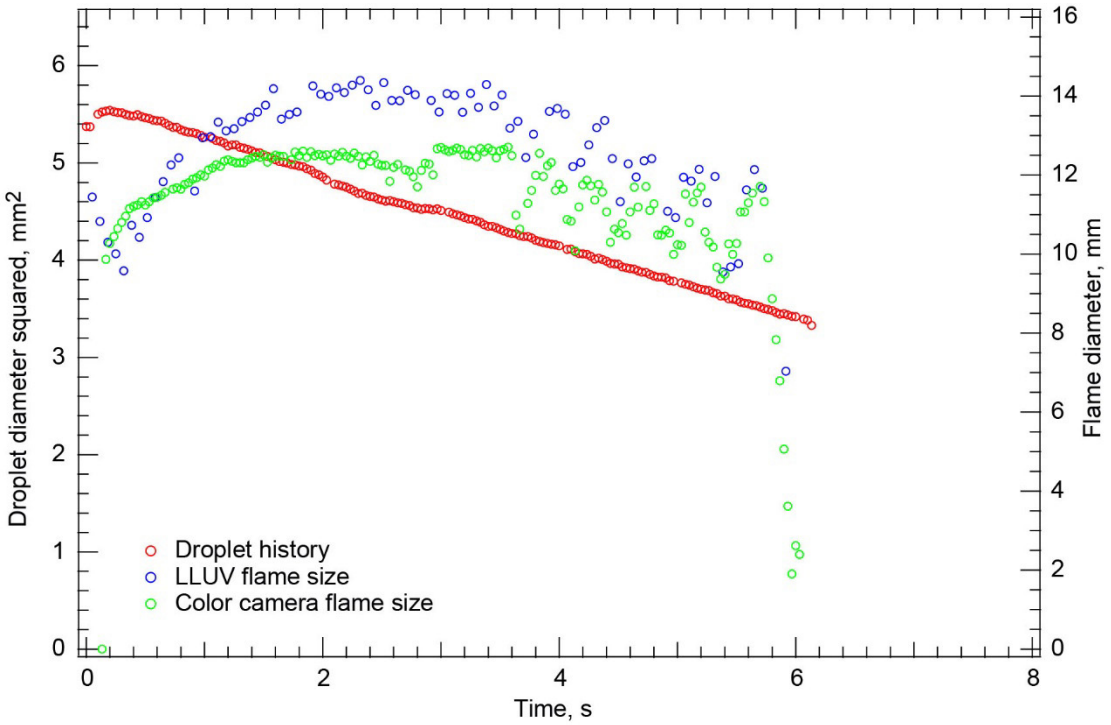

Figure 171.—Test FLEX–168. Free-floating methanol droplet burning in a 0.136/0.50/0.363 $O_2/N_2/CO_2$, 1.0-atm ambient environment. The droplet drifted west in the High-Bit-Depth Multispectral (HiBMs) field of view (FOV) after deployment, hit the igniter, and then drifted slowly east after ignition. It left the HiBMs FOV shortly after the visible flame extinguished. The very dim Low Light Level Ultra-Violet (LLUV) images and the contamination on the Combustion Integrated Rack (CIR) LLUV viewing window resulted in a lot of noise in the data. The flame oscillated for nearly half of its lifetime.

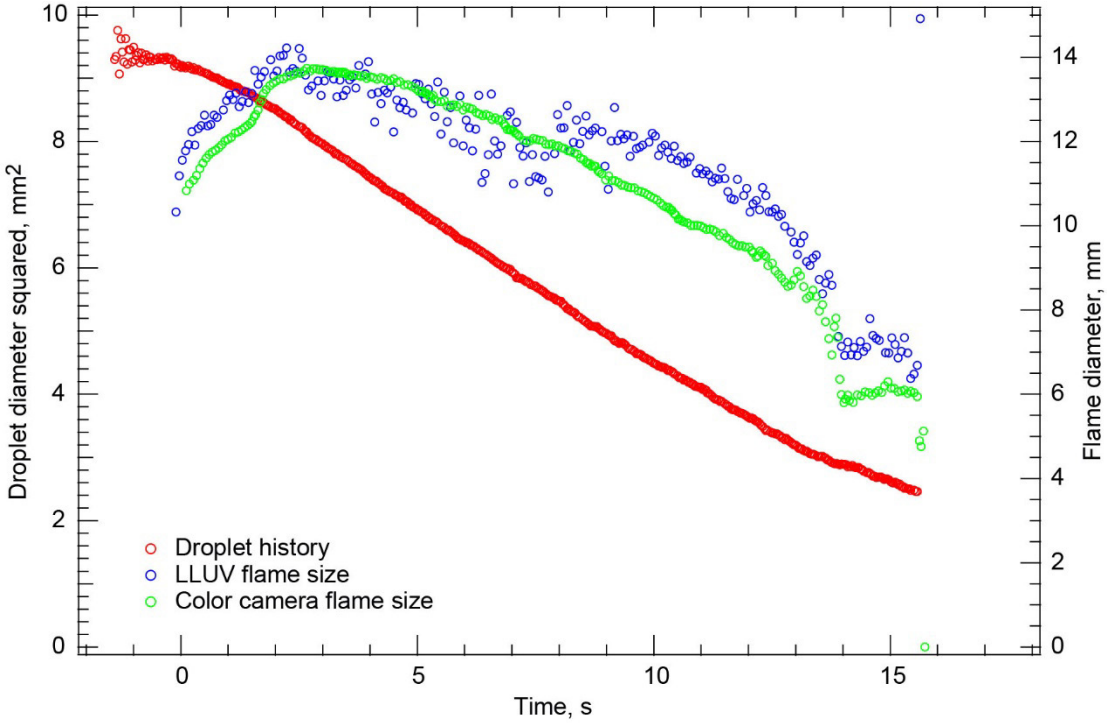

Figure 172.—Test FLEX–169. Free-floating methanol droplet burning in a 0.21/0.64/0.15 $O_2/N_2/CO_2$, 1.0-atm ambient environment. The droplet was nearly motionless after deployment and ignition. It drifted slightly around the High-Bit-Depth Multispectral (HiBMs) field of view (FOV) and then disrupted when the flame extinguished. The extinction droplet diameter is the diameter of the droplet at disruption and not the true extinction droplet diameter.

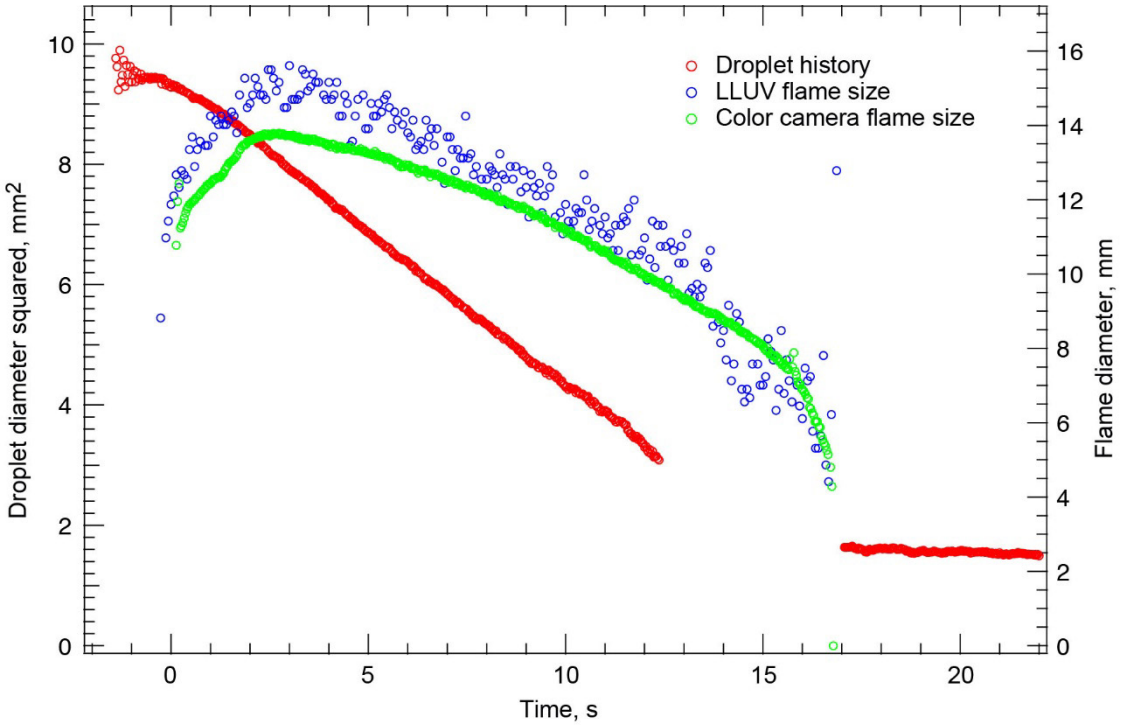

Figure 173.—Test FLEX–170. Free-floating methanol droplet burning in a 0.21/0.64/0.16 $O_2/N_2/CO_2$, 1.0-atm ambient environment. The droplet drifted south in the High-Bit-Depth Multispectral (HiBMs) field of view (FOV) after deployment and ignition. The droplet left the HiBMs FOV three-fourths of the way through the burn; then it drifted back into the FOV just after the visible flame extinguished. The extinction droplet diameter is the diameter of the droplet when it fully reappeared in the FOV. It should be nearly identical to the diameter of the droplet when the visible flame extinguished.

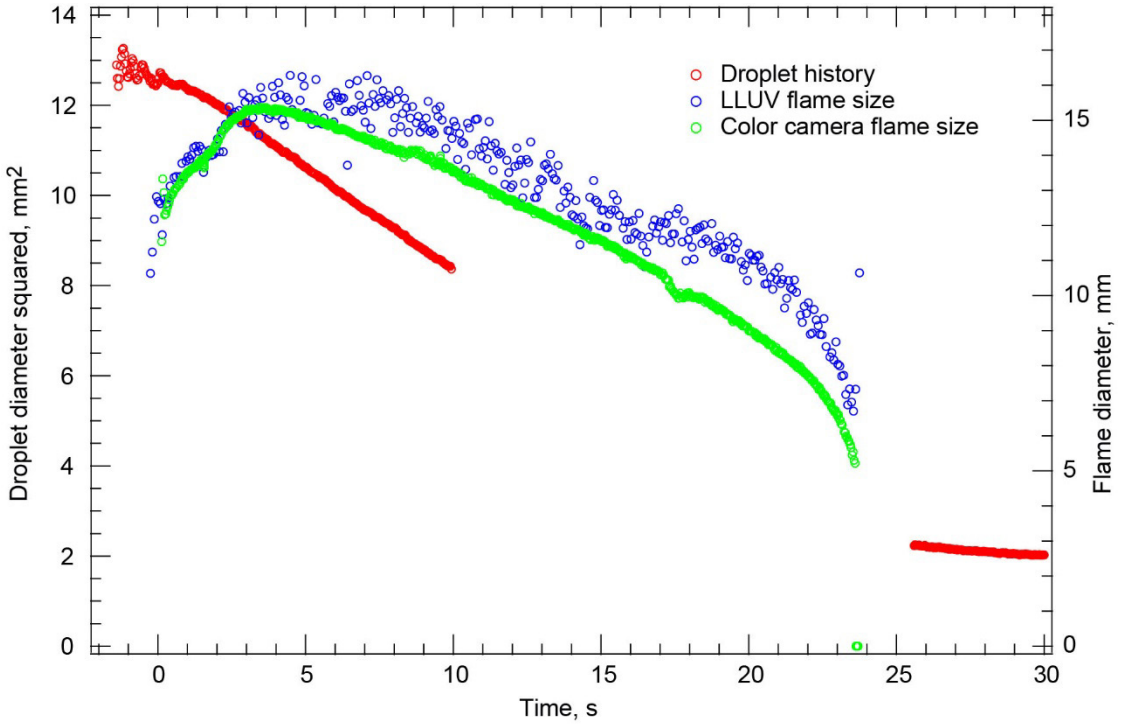

Figure 174.—Test FLEX–171. Free-floating methanol droplet burning in a 0.21/0.64/0.15 $O_2/N_2/CO_2$, 1.0-atm ambient environment. The droplet drifted north in the High-Bit-Depth Multispectral (HiBMs) field of view (FOV) after deployment and ignition, and it drifted out of the HiBMs FOV about halfway through the burn. The droplet then drifted back in shortly after the flame extinguished diffusively. The extinction droplet diameter was determined from a cubic polynomial fit of the droplet history between the two times that the droplet was in the HiBMs FOV (subject to the constraint that the slope of the droplet history of the fit was equal to that of the experiment just before it left and after it returned to the FOV).

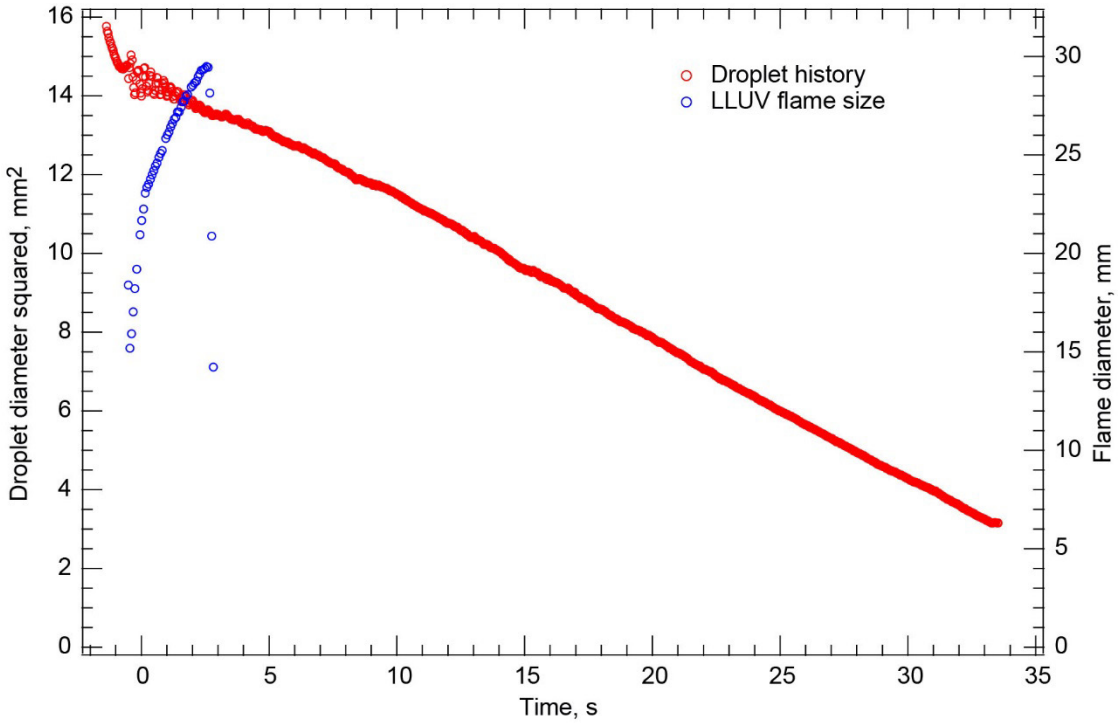

Figure 175.—Test FLEX–172. Free-floating heptane droplet burning in a 0.18/0.67/0.15 $O_2/N_2/CO_2$, 1.0-atm ambient environment. This was the first test after the needle and window were changed out (cleaner window for the Low Light Level Ultra-Violet (LLUV)). The droplet remained in the High-Bit-Depth Multispectral (HiBMs) field of view (FOV) for the entire test with very little residual motion. The LLUV image was very bright with none of the asymmetry observed in the previous tests. The flame extinguished when the droplet was relatively large, and the droplet continued to vaporize at a relatively high and nearly constant rate after the visible flame extinguished—indicating cool flame burning and extinction after visible flame extinction. The color camera Image Processing and Storage Unit (IPSU) did not record any images after deployment.

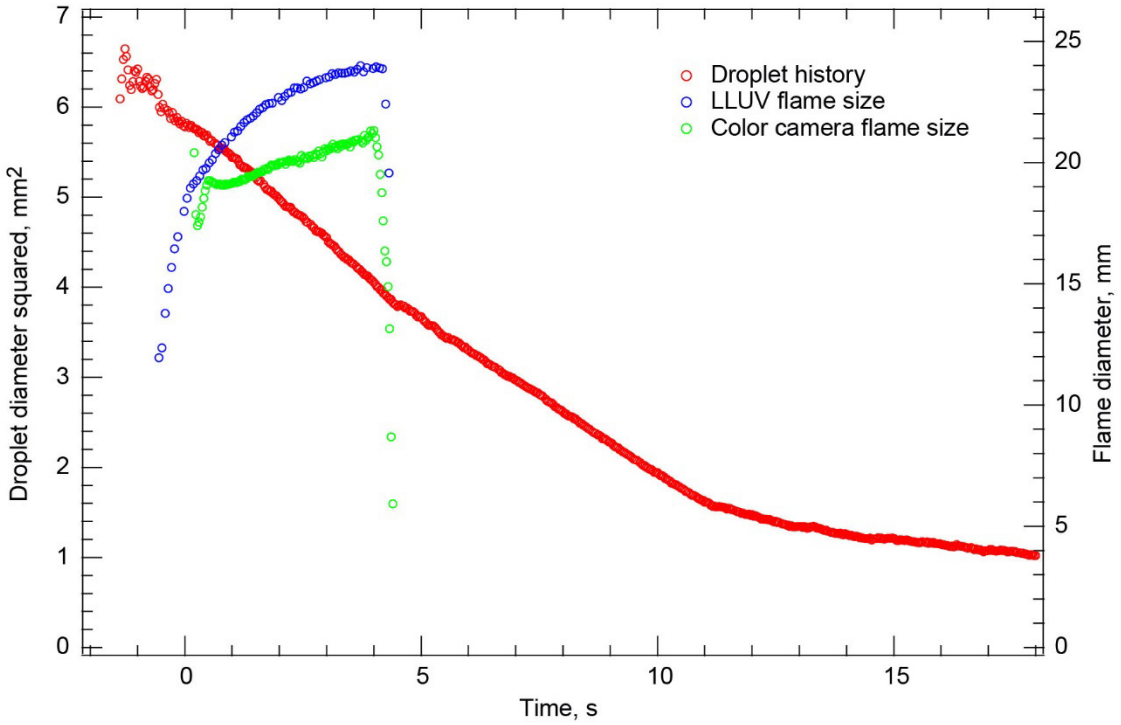

Figure 176.—Test FLEX–173. Free-floating heptane droplet burning in a 0.18/0.67/0.15 $O_2/N_2/CO_2$, 1.0-atm ambient environment. The droplet remained in the High-Bit-Depth Multispectral (HiBMs) field of view (FOV) for the entire test. The Low Light Level Ultra-Violet (LLUV) provided good distortion-free, bright images. The flame extinguished radiatively. The visible flame extinction was followed by rapid vaporization, a plateau when the droplet became quite small, and the formation of a visible vapor cloud late in the recording history. The post-visible-flame-extinction behavior was consistent with cool flame burning and extinction.

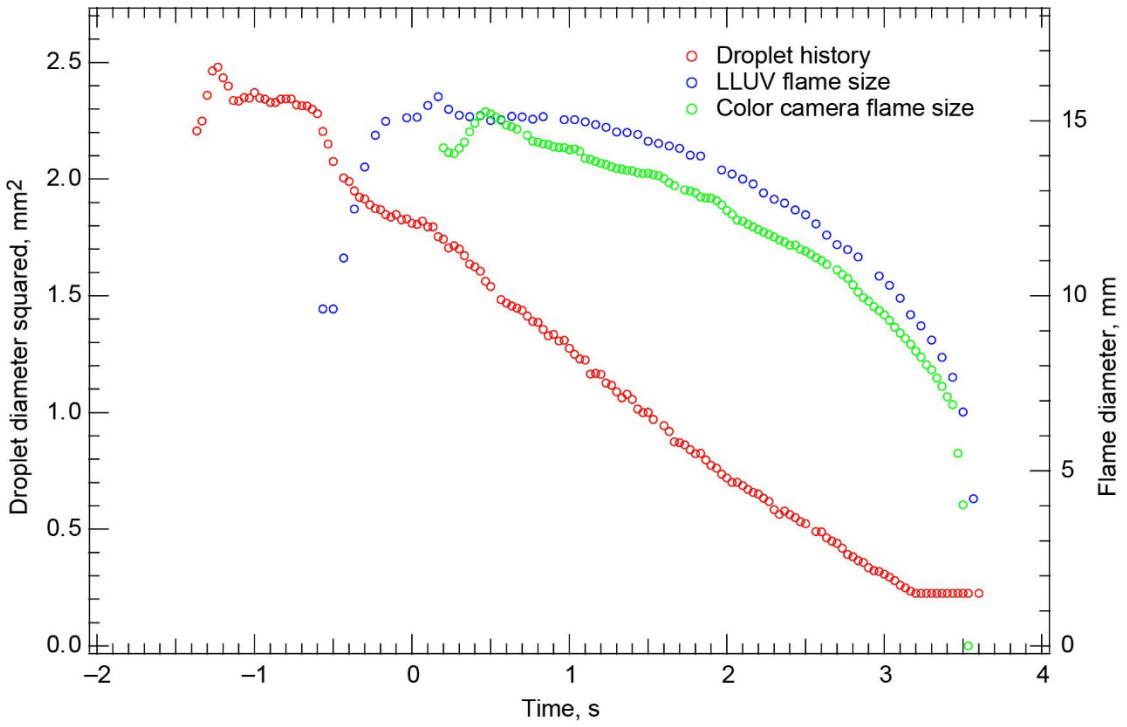

Figure 177.—Test FLEX–174. Free-floating heptane droplet burning in a 0.18/0.67/0.15 $O_2/N_2/CO_2$, 1.0-atm ambient environment. This was a very small heptane droplet. It drifted south in the High-Bit-Depth Multispectral (HiBMs) field of view (FOV) after deployment and ignition, but it remained in the FOV for the entire recording time. The droplet burned with a relatively bright flame to a very small size, at which point there was a small disruption that was coincident with visible flame extinction.

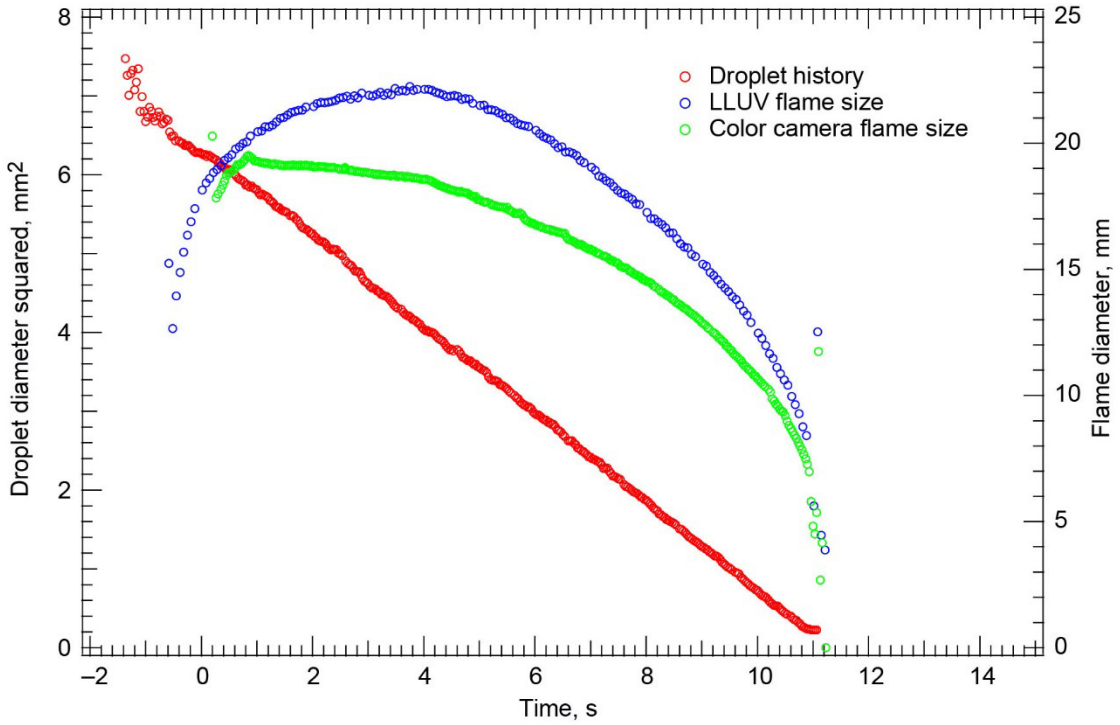

Figure 178.—Test FLEX–175. Free-floating heptane droplet burning in a 0.24/0.56/0.20 $O_2/N_2/CO_2$, 0.70-atm ambient environment. The droplet drifted east, but it remained in the High-Bit-Depth Multispectral (HiBMs) field of view (FOV) for the entire test. The droplet burned linearly to a small size, and it disrupted when the flame extinguished. The droplet size at extinction was an extrapolation of the average burning rate to the time of extinction.

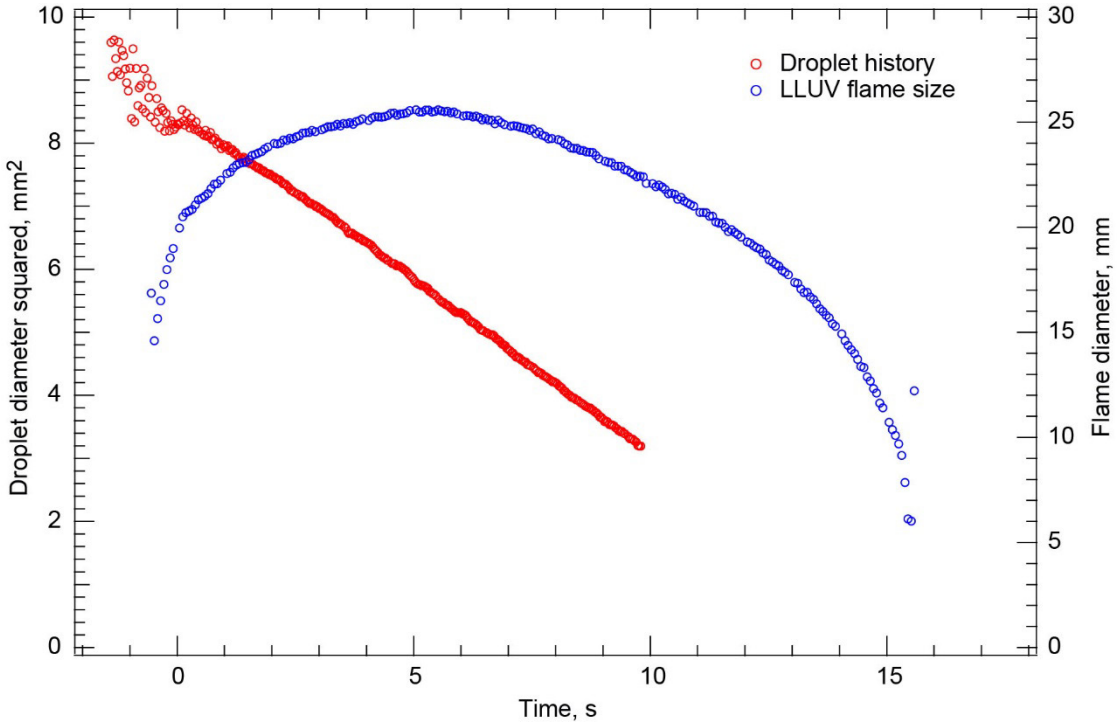

Figure 179.—Test FLEX–176. Free-floating heptane droplet burning in a 0.24/0.56/0.20 $O_2/N_2/CO_2$, 0.70-atm ambient environment. The droplet drifted slowly northeast in the High-Bit-Depth Multispectral (HiBMs) field of view (FOV) after deployment and ignition and out of the FOV a little over halfway through the test. The droplet burned to a small size and then disrupted. An extrapolation of the droplet history to the time when the flame extinguished showed that the droplet had almost completely vaporized when it disrupted and ended the test. The color camera Image Processing and Storage Unit (IPSU) did not record any images after deployment.

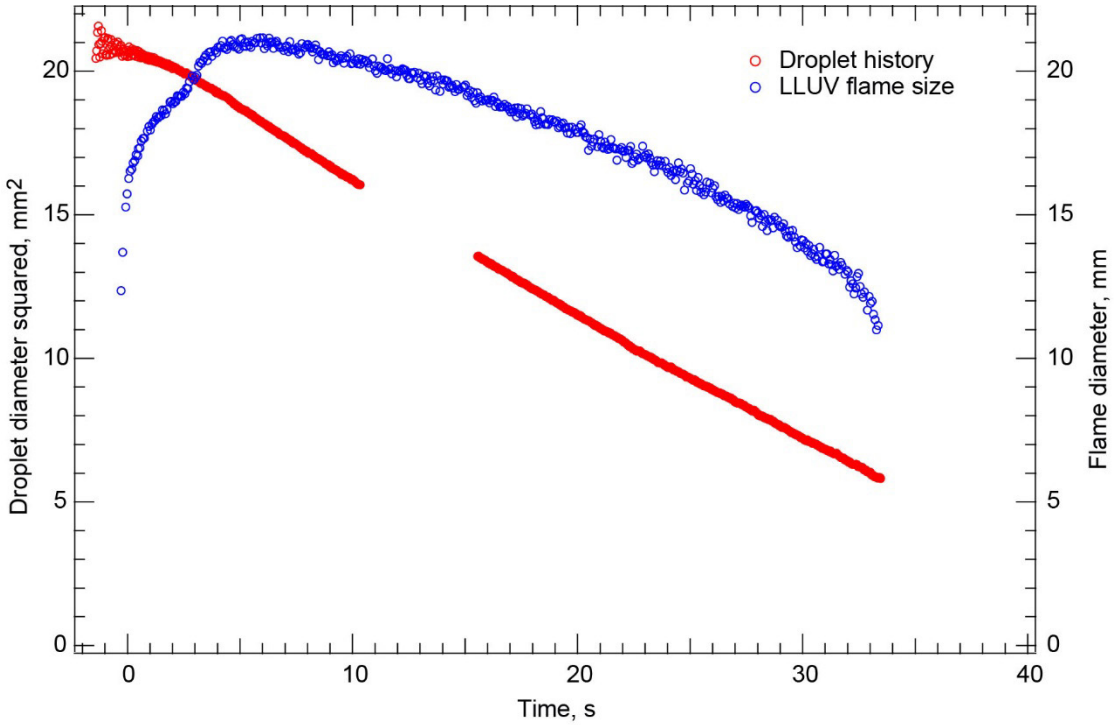

Figure 180.—Test FLEX–177. Free-floating methanol droplet burning in a 0.24/0.56/0.20 $O_2/N_2/CO_2$, 0.7-atm ambient environment. There was almost no drift, and the droplet remained in High-Bit-Depth Multispectral (HiBMs) field of view (FOV) for the entire test. The HiBMs recording stopped before the burn was complete, and the droplet drifted out of the Low Light Level Ultra-Violet (LLUV) FOV before the end of the test. The color camera Image Processing and Storage Unit (IPSU) did not record any images after deployment.

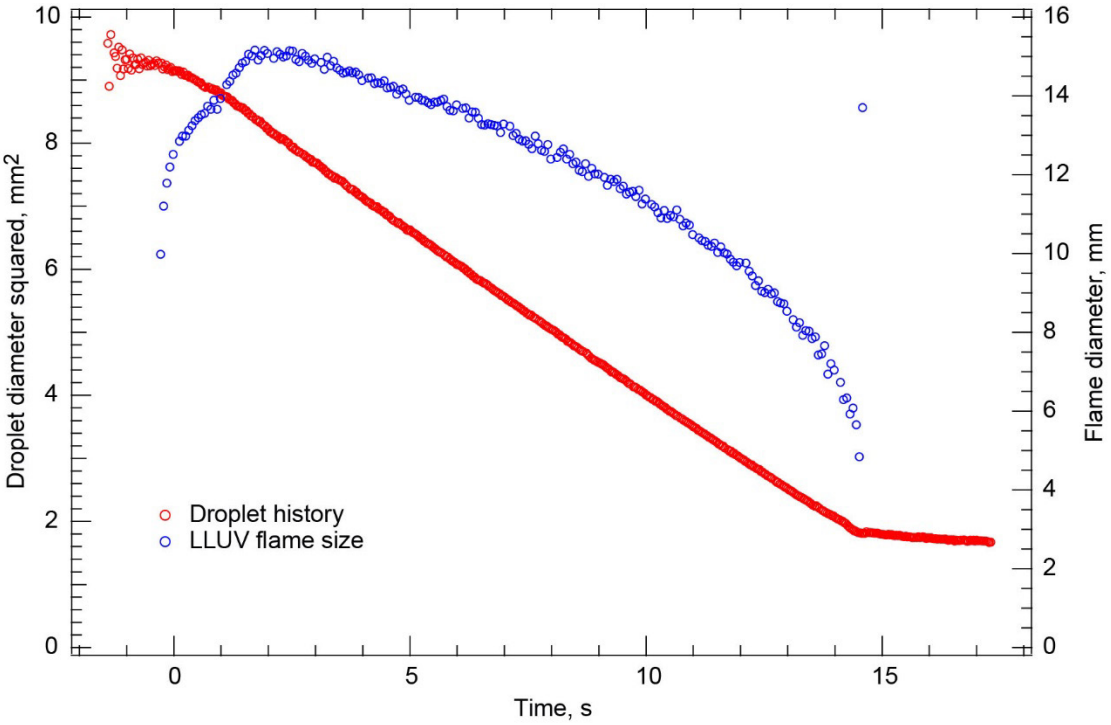

Figure 181.—Test FLEX–178. Free-floating methanol droplet burning in a 0.24/0.56/0.20 $O_2/N_2/CO_2$, 0.70-atm ambient environment. The droplet remained in the High-Bit-Depth Multispectral (HiBMs) and Low Light Level Ultra-Violet (LLUV) fields of view (FOVs) during the entire test. The color camera Image Processing and Storage Unit (IPSU) did not record any images after deployment, and the flame extinguished diffusively with no disruption.

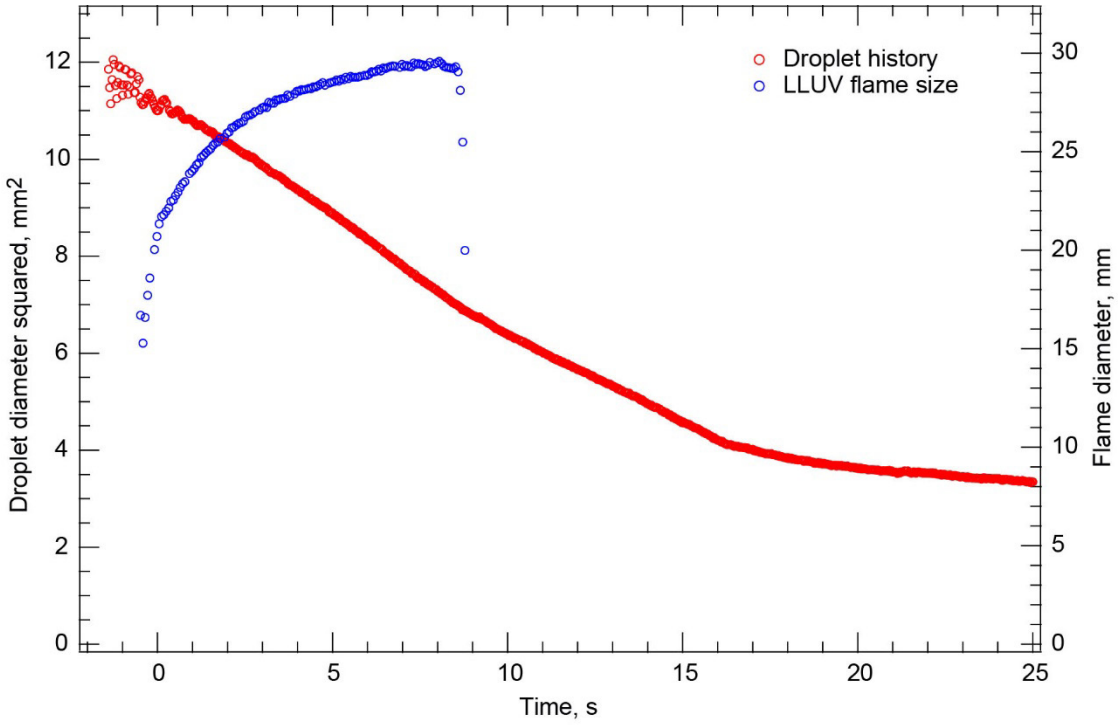

Figure 182.—Test FLEX–179. Free-floating heptane droplet burning in a 0.23/0.52/0.25 $O_2/N_2/CO_2$, 0.7-atm ambient environment. The droplet drifted slowly east in the High-Bit-Depth Multispectral (HiBMs) field of view (FOV), but it remained in the HiBMs FOV for the entire recording time (including after extinction). There was some rapid postextinction vaporization, but it was not as pronounced as in other heptane tests. This was followed by a plateau in the droplet history. The flame extinguished radiatively, and this was probably followed by a cool flame and cool flame extinction. The color camera Image Processing and Storage Unit (IPSU) failed to record any images after deployment.

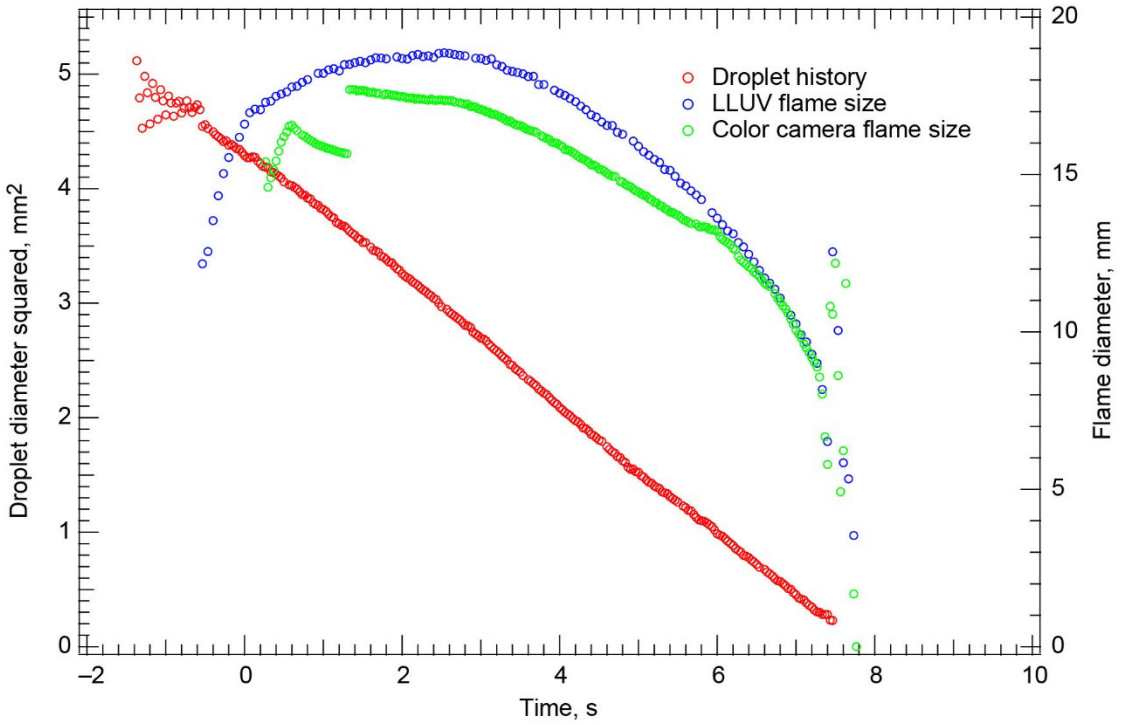

Figure 183.—Test FLEX–180. Free-floating heptane droplet burning in a 0.23/0.52/0.25 $O_2/N_2/CO_2$, 0.7-atm ambient environment. This smaller droplet remained in the High-Bit-Depth Multispectral (HiBMs) field of view (FOV) for the entire test. The droplet disrupted when the droplet was very small—coincident with visible flame extinction. The droplet size at extinction is the size of the droplet just before the disruption.

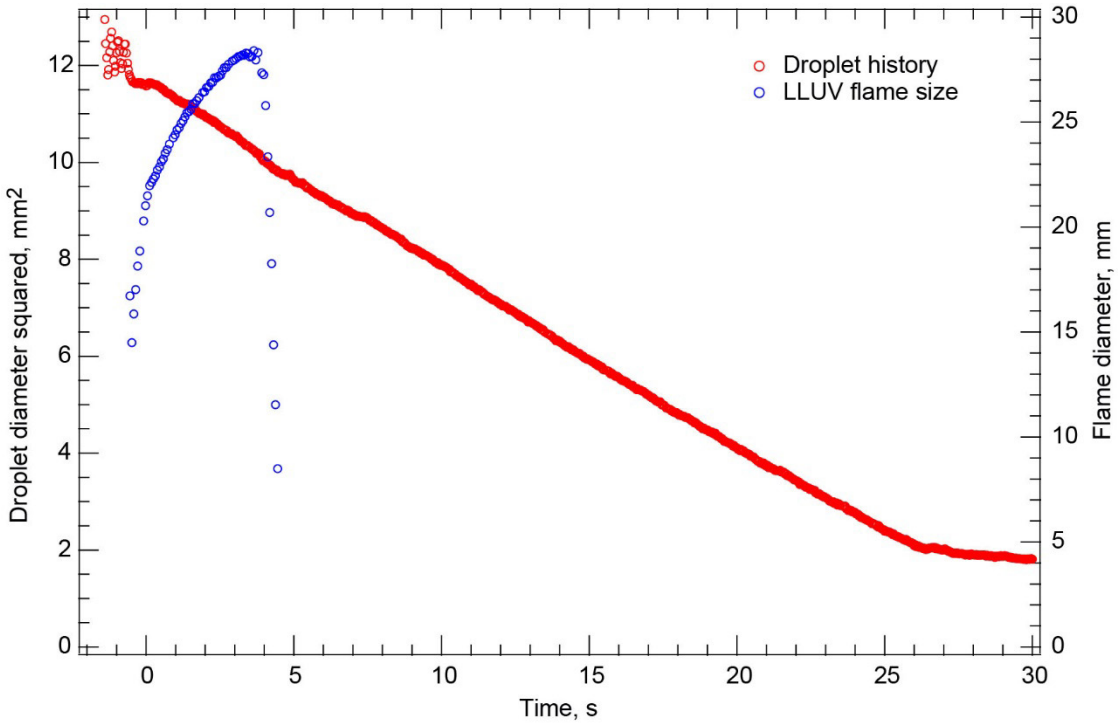

Figure 184.—Test FLEX–181. Free-floating heptane droplet burning in a 0.19/0.71/0.10 $O_2/N_2/CO_2$, 0.7-atm ambient environment. The droplet remained in High-Bit-Depth Multispectral (HiBMs) field of view (FOV) for the entire test, including a long period after the visible flame extinguished. The flame extinguished radiatively when the droplet was relatively large. After the visible flame extinguished, the droplet vaporized rapidly and almost constantly. Then a vapor cloud formed, and there was a plateau in the droplet history. The post-visible-flame vaporization and plateau indicate cool flame burning and extinction, respectively. The color camera Image Processing and Storage Unit (IPSU) did not record any video after deployment.

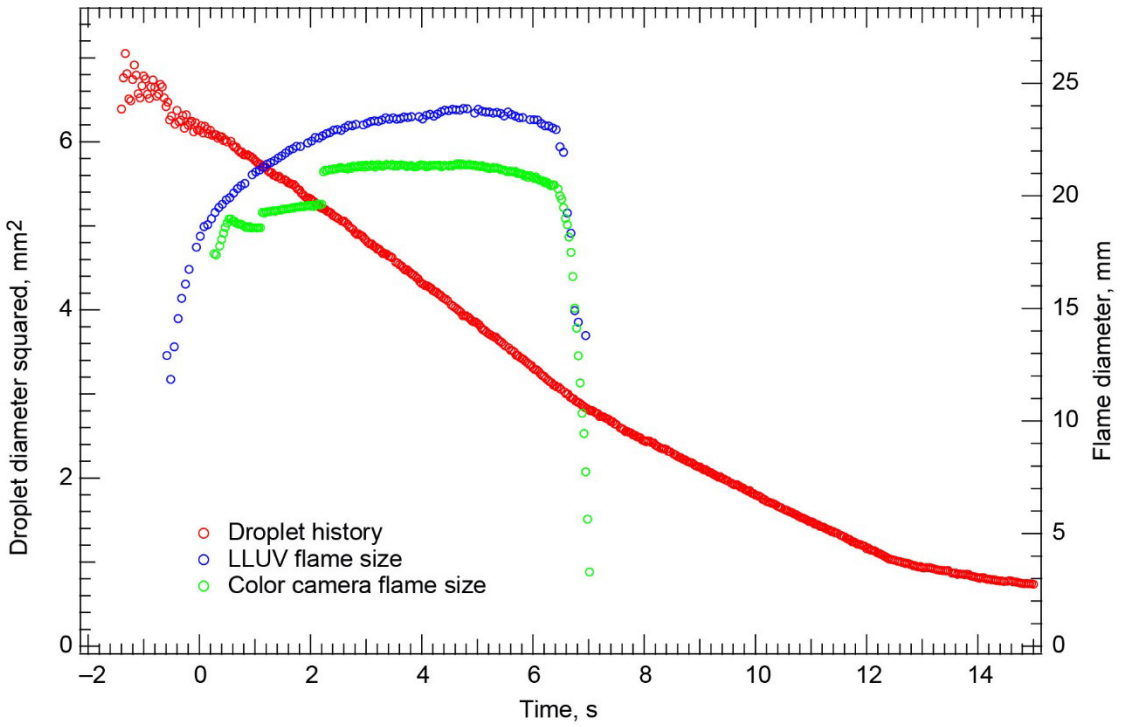

Figure 185.—Test FLEX–182. Free-floating heptane droplet burning in a 0.19/0.71/0.10 $O_2/N_2/CO_2$, 0.7-atm ambient environment. The droplet remained in the High-Bit-Depth Multispectral (HiBMs) field of view (FOV) for the entire test, including after the visible flame extinguished. The flame extinguished radiatively, followed by rapid vaporization and then a plateau late in the test time. The plateau was coincident with the formation of a vapor cloud. The post-visible-flame-extinction behavior and the plateau in the droplet history indicate cool flame burning and extinction, respectively.

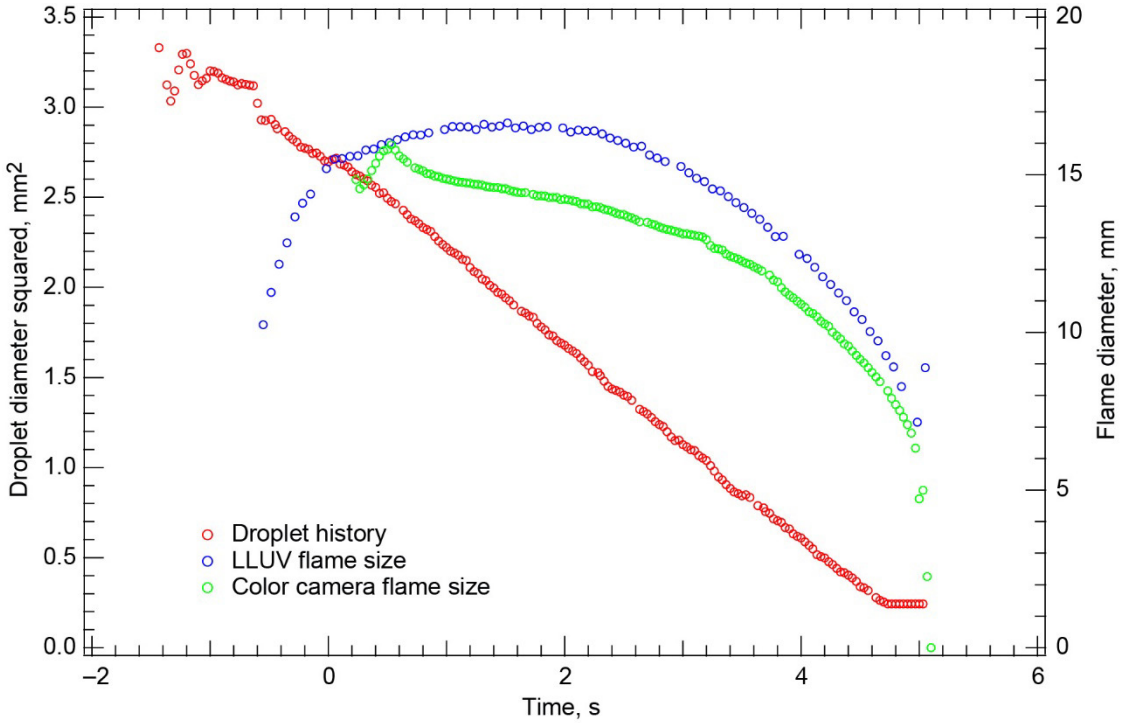

Figure 186.—Test FLEX–183. Free-floating heptane droplet burning in a 0.19/0.71/0.10 $O_2/N_2/CO_2$, 0.7-atm ambient environment. This small droplet remained in the High-Bit-Depth Multispectral (HiBMs) field of view (FOV) for the entire test. The droplet burned to a very small size where it disrupted before the droplet vanished. The extinction droplet diameter is the size of the droplet just prior to the disruption.

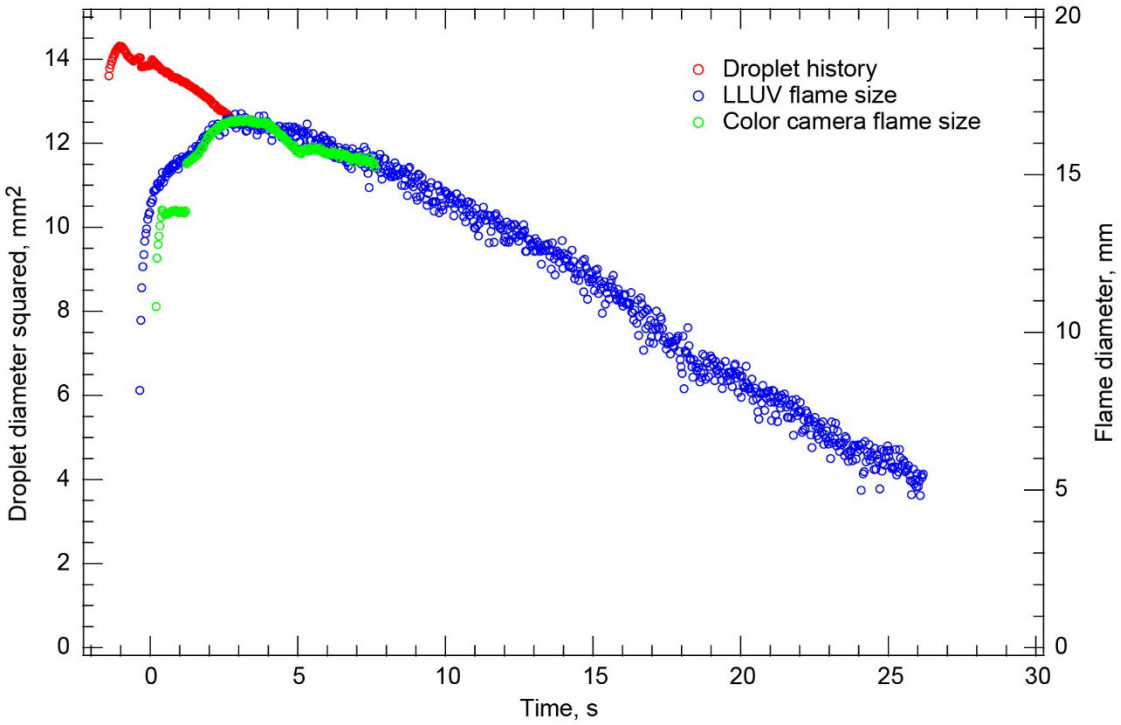

Figure 187.—Test FLEX–184. Free-floating methanol droplet burning in a 0.23/0.52/0.25 $O_2/N_2/CO_2$, 0.70-atm ambient environment. The droplet drifted south and out of the High-Bit-Depth Multispectral (HiBMs) and color camera fields of view (FOVs) relatively quickly after ignition. It remained in the Low Light Level Ultra-Violet (LLUV) FOV for the entire test. The droplet burned for a long time before the flame extinguished diffusively.

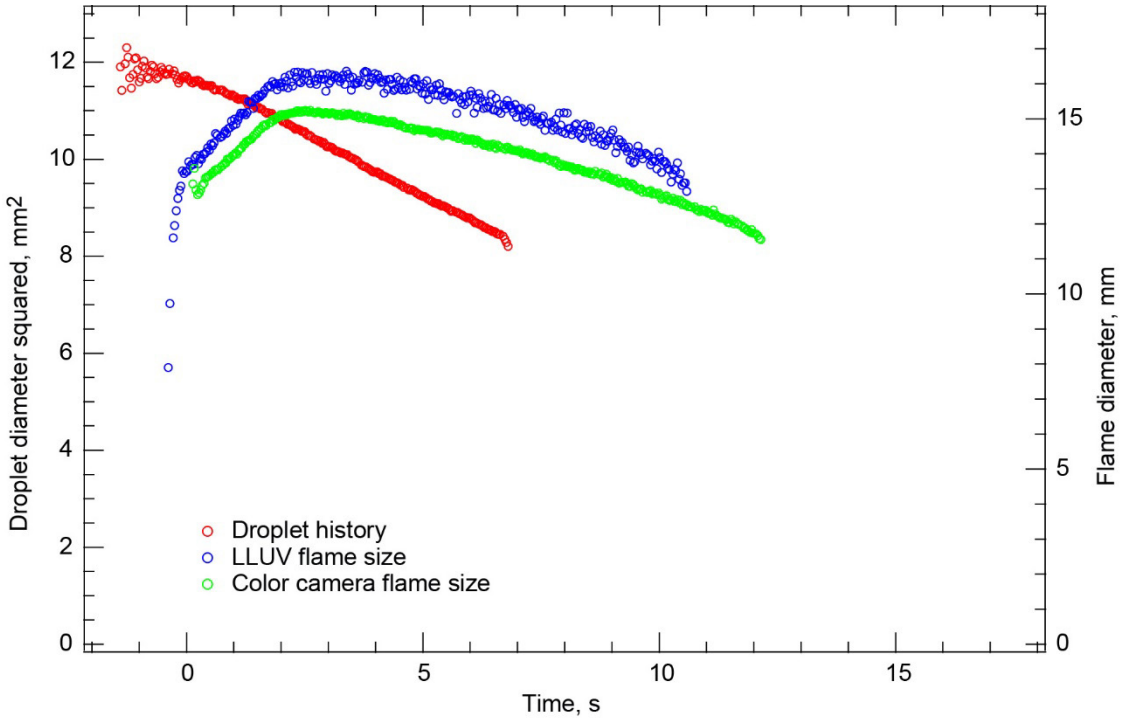

Figure 188.—Test FLEX–185. Free-floating methanol droplet burning in a 0.70/0.52/0.25 $O_2/N_2/CO_2$, 0.70-atm ambient environment. The droplet drifted south after deployment, hit the igniter, and then drifted east slowly. It left fields of view (FOVs) of the High-Bit-Depth Multispectral (HiBMs), Low Light Level Ultra-Violet (LLUV), and color cameras before the flame extinguished.

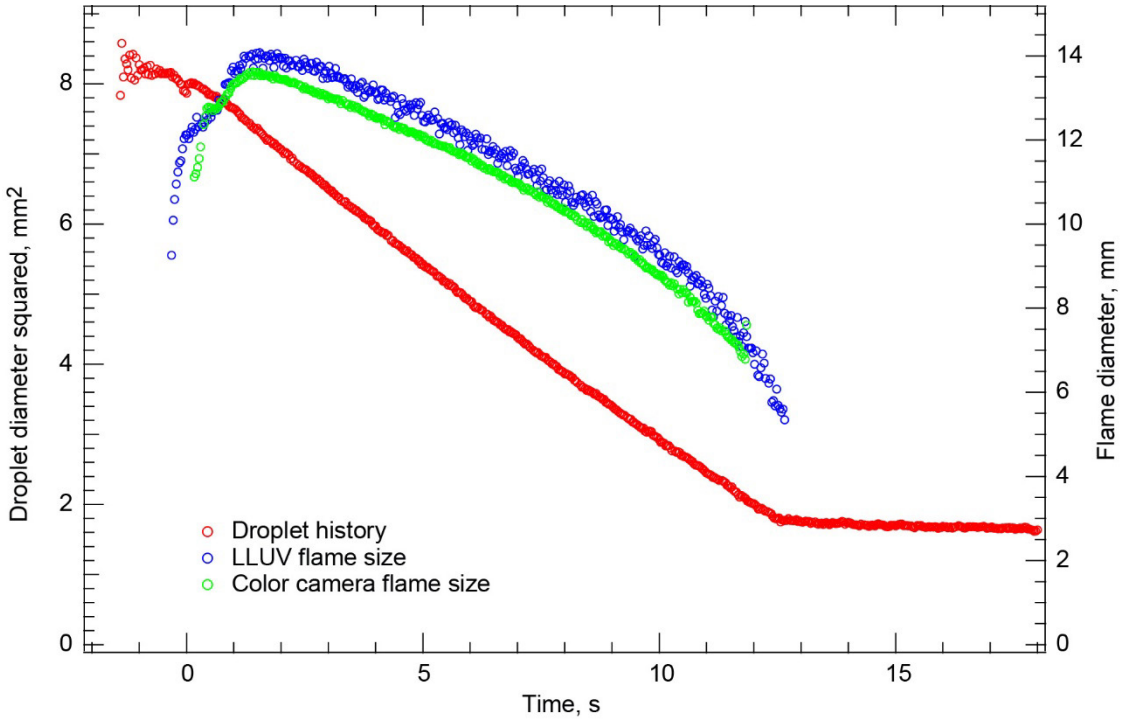

Figure 189.—Test FLEX–186. Free-floating methanol droplet burning in a 0.23/0.52/0.25 $O_2/N_2/CO_2$, 0.70-atm ambient environment. The droplet drifted south in the High-Bit-Depth Multispectral (HiBMs) field of view (FOV) after deployment and ignition, went to the end of the FOV, drifted west briefly, and drifted back north; but it never left the FOVs of any of the cameras. The flame extinguished diffusively.

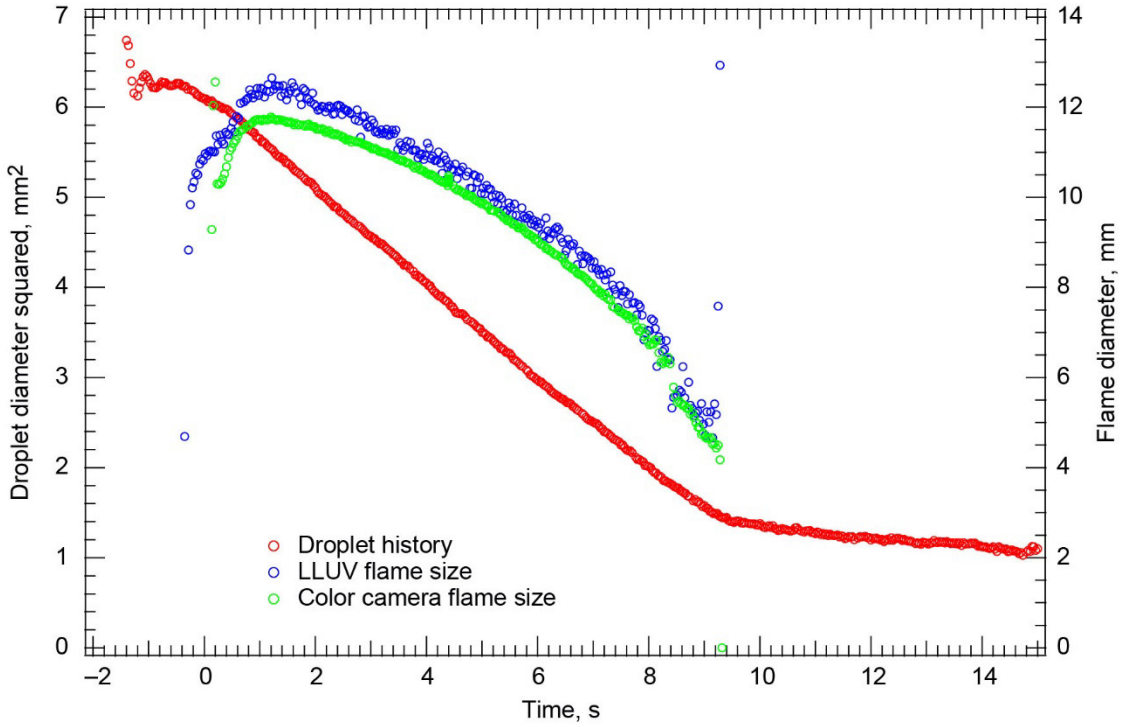

Figure 190.—Test FLEX–187. Free-floating methanol droplet burning in a 0.23/0.52/0.25 $O_2/N_2/CO_2$, 0.70-atm ambient environment. The droplet deployed and ignited with almost no residual motion and remained in the fields of view (FOVs) of all the cameras for the entire test. The flame extinguished diffusively.

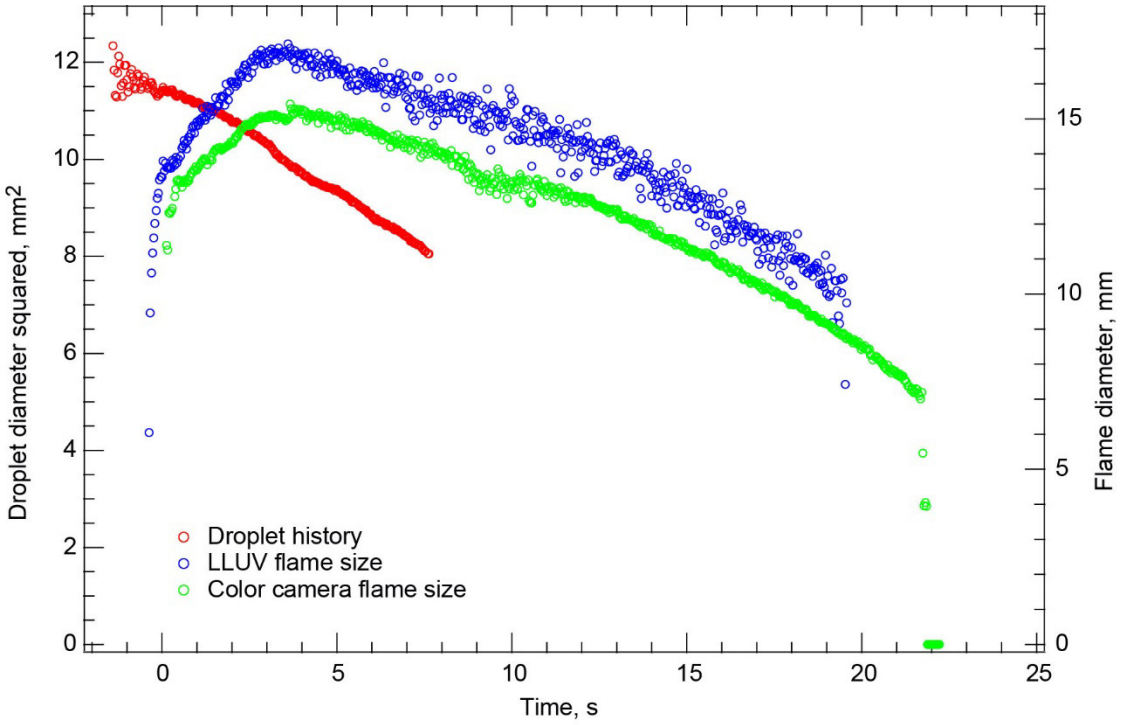

Figure 191.—Test FLEX–188. Free-floating methanol droplet burning in a 0.19/0.71/0.10 $O_2/N_2/CO_2$, 1.0-atm ambient environment. The droplet drifted east and then southeast and out of the High-Bit-Depth Multispectral (HiBMs) field of view (FOV) about one-third of the way through the test. There was no disruption at extinction. This was a very long burn, and the flame probably extinguished diffusively. Because the droplet was in the HiBMs FOV for only a small fraction of the burn, no extinction droplet diameter is reported.

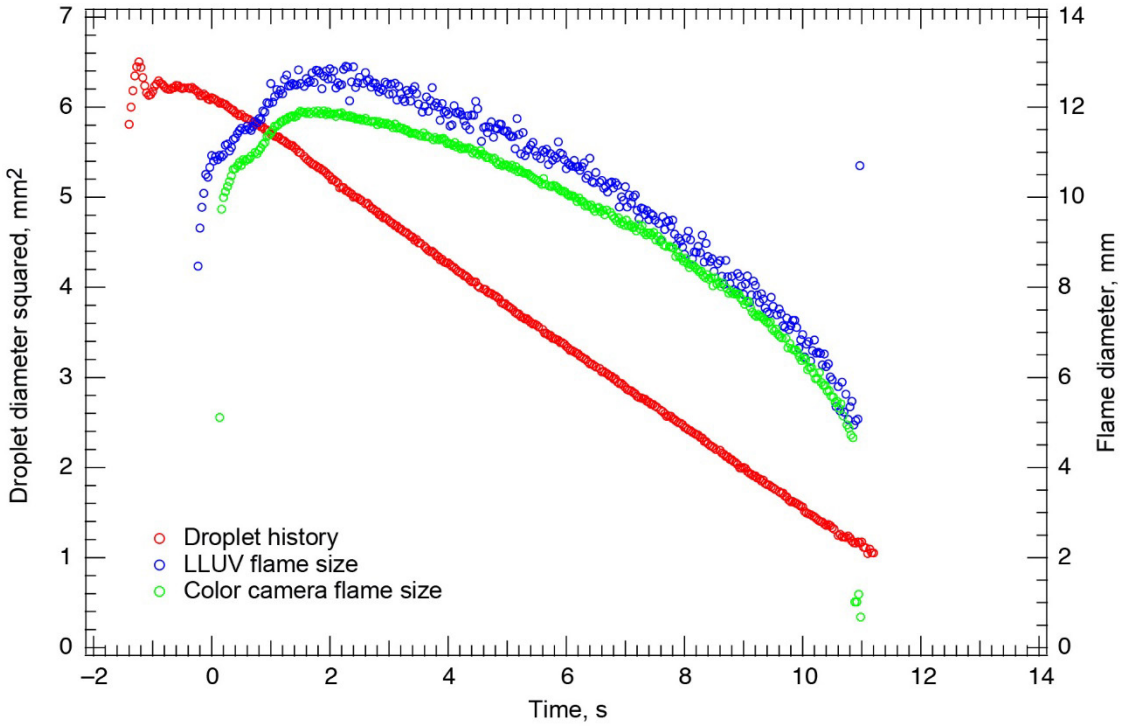

Figure 192.—Test FLEX–189. Free-floating methanol droplet burning in a 0.19/0.71/0.10 $O_2/N_2/CO_2$, 1.0-atm ambient environment. The droplet drifted south in the High-Bit-Depth Multispectral (HiBMs) field of view (FOV) and left the FOV immediately after the visible flame extinguished. It remained in the FOVs of all the cameras for the entire burn, which ended with diffusive extinction.

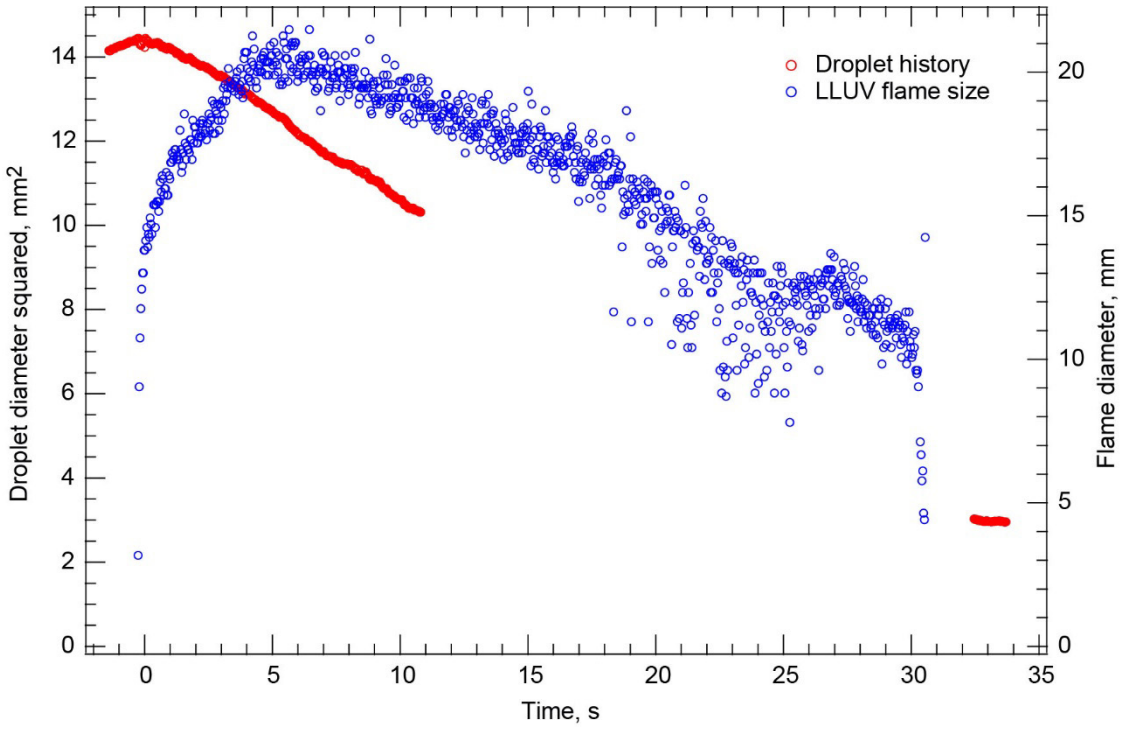

Figure 193.—Test FLEX–190. Free-floating methanol droplet burning in a 0.18/0.67/0.15 $O_2/N_2/CO_2$, 1.0-atm ambient environment. The droplet drifted east after deployment and ignition, and it drifted out of the High-Bit-Depth Multispectral (HiBMs) field of view (FOV) before the flame extinguished. It then drifted briefly back in the HiBMs FOV immediately after the flame extinguished. The color camera Image Processing and Storage Unit (IPSU) did not record any images after deployment. The droplet drifted partially out of the Low Light Level Ultra-Violet (LLUV) FOV for a portion of the burn (resulting in more scatter in the flame size measurement). The extinction droplet diameter was estimated by interpolating the droplet history with a cubic polynomial from the known and measured droplet size and burning rate in the segments of the droplet history just before the droplet left the HiBMs FOV and after it reentered the FOV.

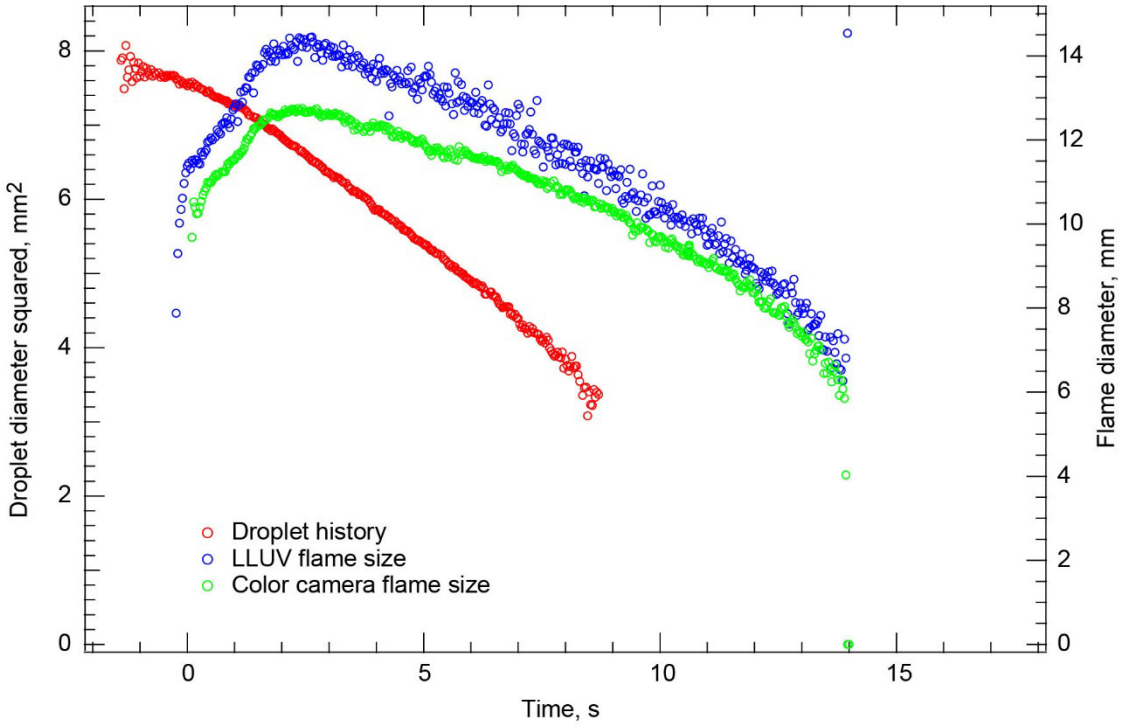

Figure 194.—Test FLEX–191. Free-floating methanol droplet burning in a 0.18/0.67/0.15 $O_2/N_2/CO_2$, 1.0-atm ambient environment. The droplet deployed and ignited with very little residual motion, but it started to drift south in the High-Bit-Depth Multispectral (HiBMs) field of view (FOV) a few seconds after the igniters were withdrawn. The droplet remained in the FOVs of the Low Light Level Ultra-Violet (LLUV) and color camera for the entire burn. The average burning rate constant was used to extrapolate the droplet size at extinction from the droplet history from the time that the droplet left the HiBMs FOV until the flame extinguished as determined by the LLUV and color camera.

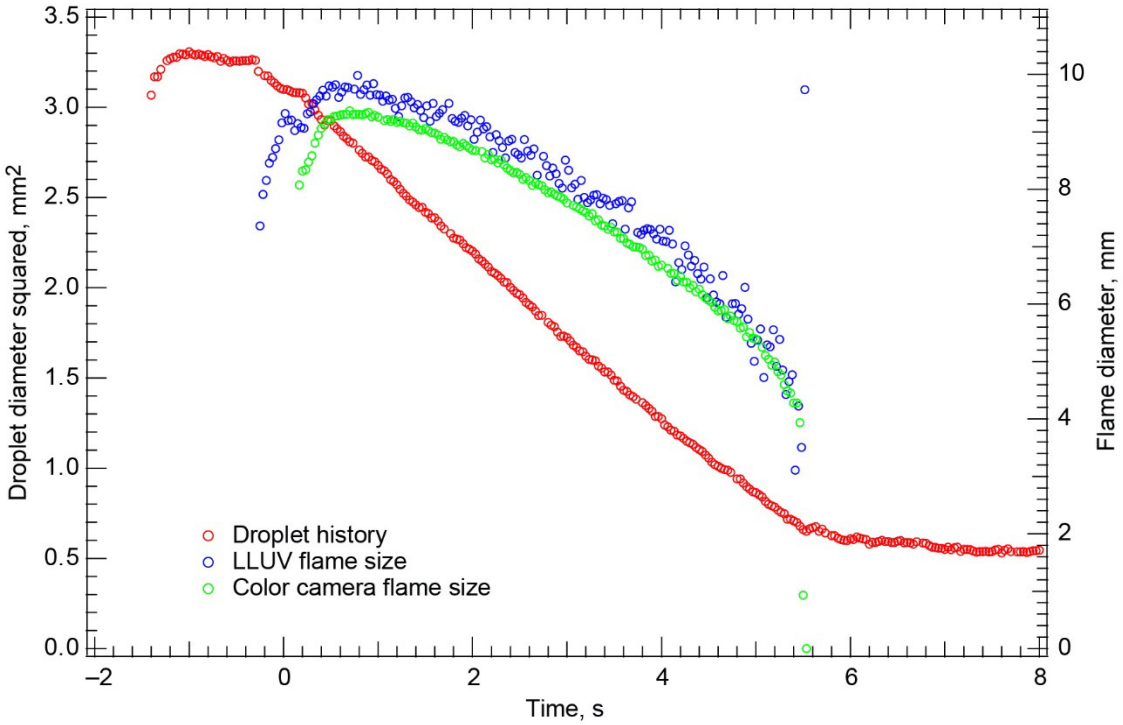

Figure 195.—Test FLEX–192. Free-floating methanol droplet burning in a 0.18/0.67/0.15 $O_2/N_2/CO_2$, 1.0-atm ambient environment. This smaller droplet drifted to the lower igniter after deployment. The igniter seemed to stop the drift, and the droplet remained near the center of the field of view (FOV) for the duration of the entire test. The droplet burned to diffusive extinction.

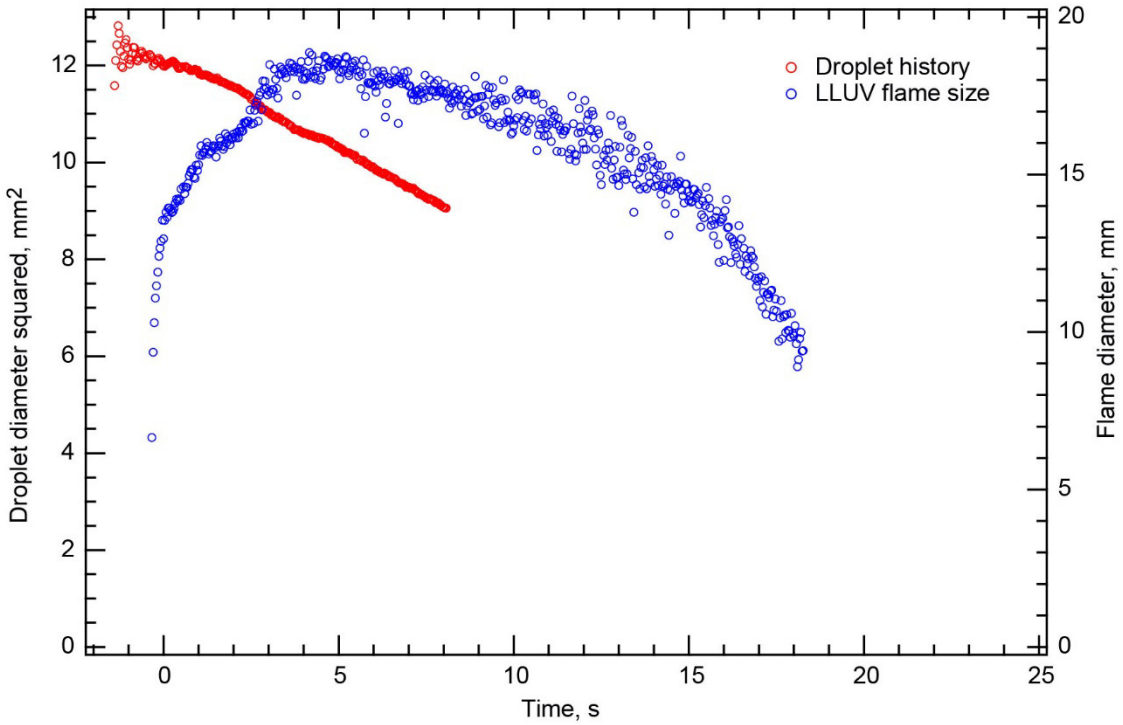

Figure 196.—Test FLEX–193. Free-floating methanol droplet burning in a 0.17/0.63/0.20 $O_2/N_2/CO_2$, 1.0-atm ambient environment. The droplet drifted east and out of the High-Bit-Depth Multispectral (HiBMs) field of view (FOV) after deployment and ignition. The droplet also drifted out of the Low Light Level Ultra-Violet (LLUV) FOV before the flame extinguished. The color camera Image Processing and Storage Unit (IPSU) did not record any images after deployment. The downlink video shows that the flame extinguished diffusively without disruption.

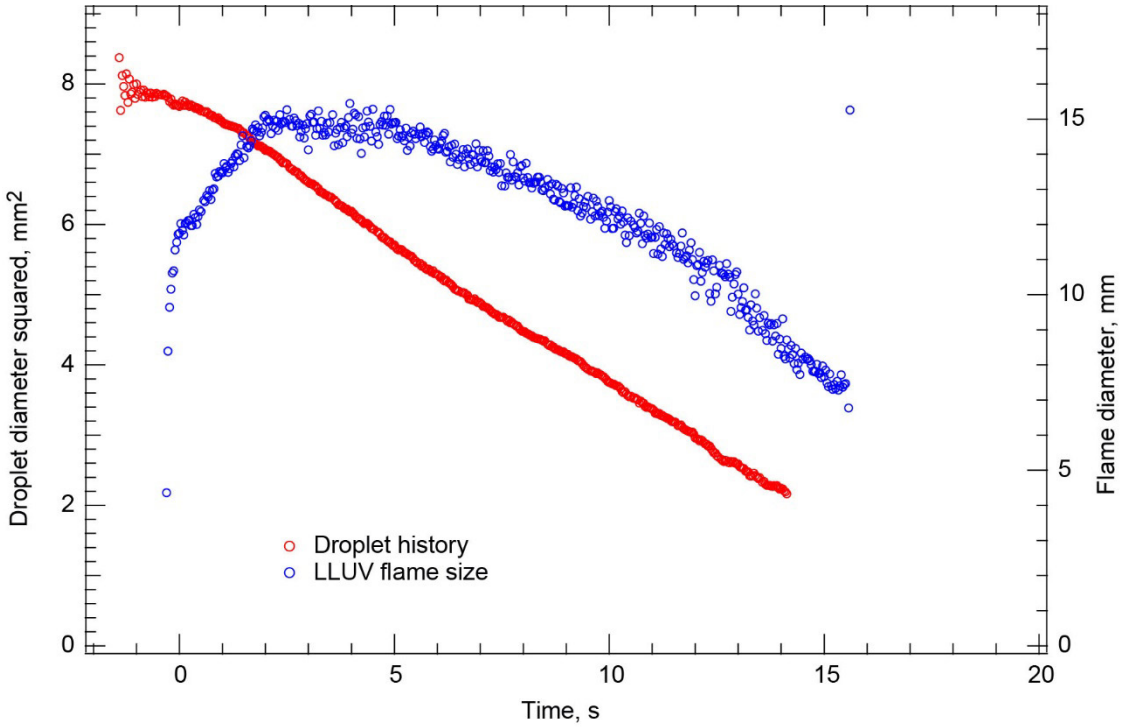

Figure 197.—Test FLEX–194. Free-floating methanol droplet burning in a 0.17/0.63/0.20 $O_2/N_2/CO_2$, 1.0-atm ambient environment. The droplet drifted south in the High-Bit-Depth Multispectral (HiBMs) field of view (FOV) after deployment and ignition, remained in the FOV, briefly drifted north, and then drifted east and out of the HiBMs FOV just before the visible flame extinguished diffusively. The measured burning rate constant from the later part of the burn was used to extrapolate the extinction droplet diameter from the droplet history until the flame extinguished (from the Low Light Level Ultra-Violet (LLUV)). The color camera Image Processing and Storage Unit (IPSU) did not record any images after deployment.

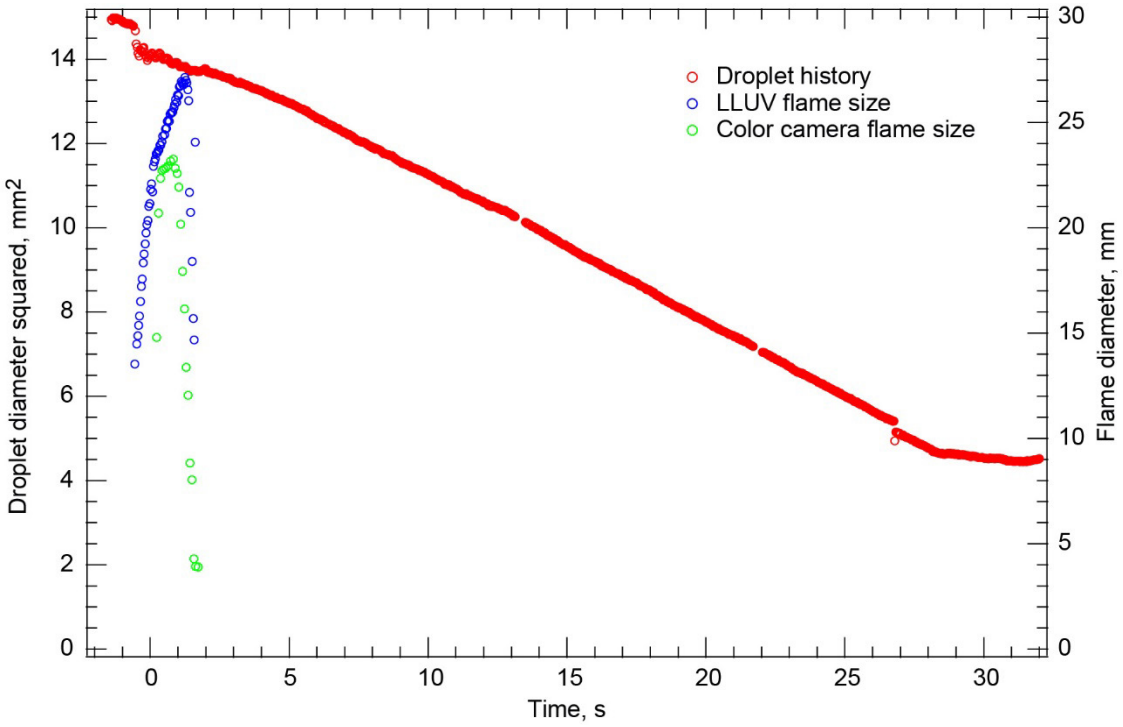

Figure 198.—Test FLEX–195. Free-floating heptane droplet burning in a 0.17/0.63/0.20 $O_2/N_2/CO_2$, 1.0-atm ambient environment. The droplet had almost no drift in the High-Bit-Depth Multispectral (HiBMs) field of view (FOV), and it remained in the FOVs of all cameras for the entire recording time. The flame extinguished radiatively and quickly after ignition. The vaporization rate increased after the visible flame extinguished and then quickly plateaued well after the visible flame extinguished. This is indicative of cool flame burning and extinction. The HiBMs view became extremely dark when a vapor cloud formed.

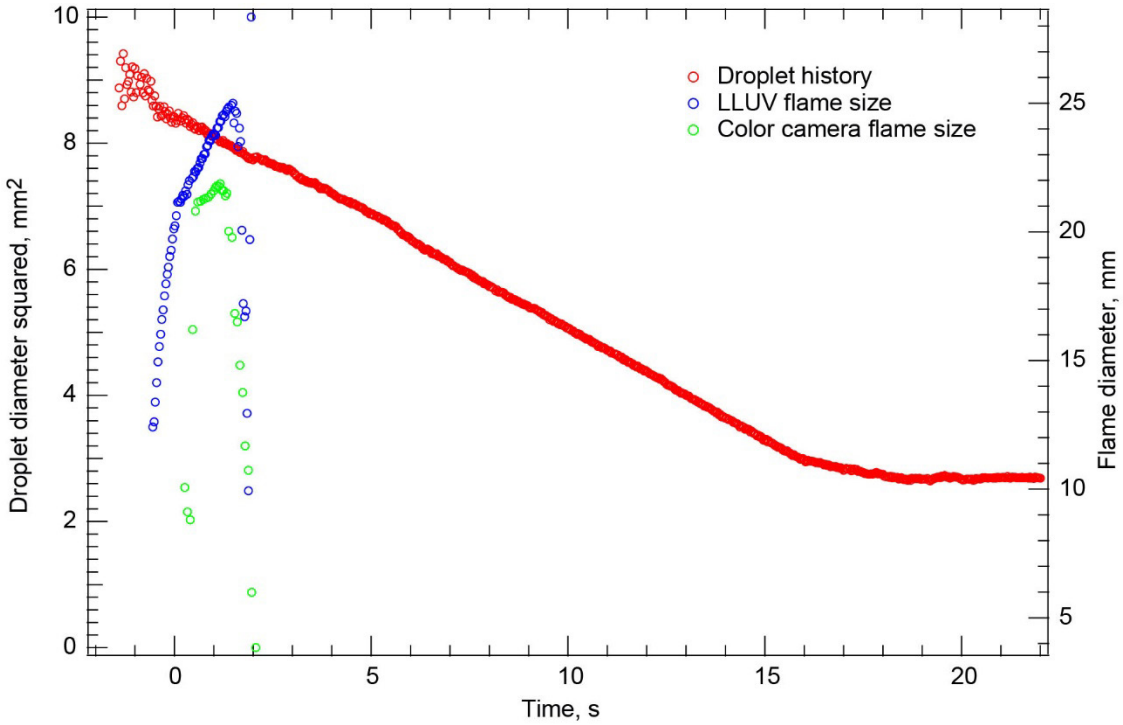

Figure 199.—Test FLEX–196. Free-floating heptane droplet in a 0.20/0.75/0.05 $O_2/N_2/CO_2$, 1.0-atm ambient environment. The droplet remained in the High-Bit-Depth Multispectral (HiBMs) field of view (FOV) with very little residual motion for the entire test. The flame extinguished radiatively and quickly, followed by rapid vaporization and the formation of a large vapor cloud. This indicates that cool flame burning and extinction were likely after the visible flame extinguished. The HiBMs FOV view dimmed when the cloud formed, and this probably caused the droplet to be recorded as being slightly larger at the end of the test (the changing background combined with the fixed segmentation value caused more pixels to be counted as “droplet”).

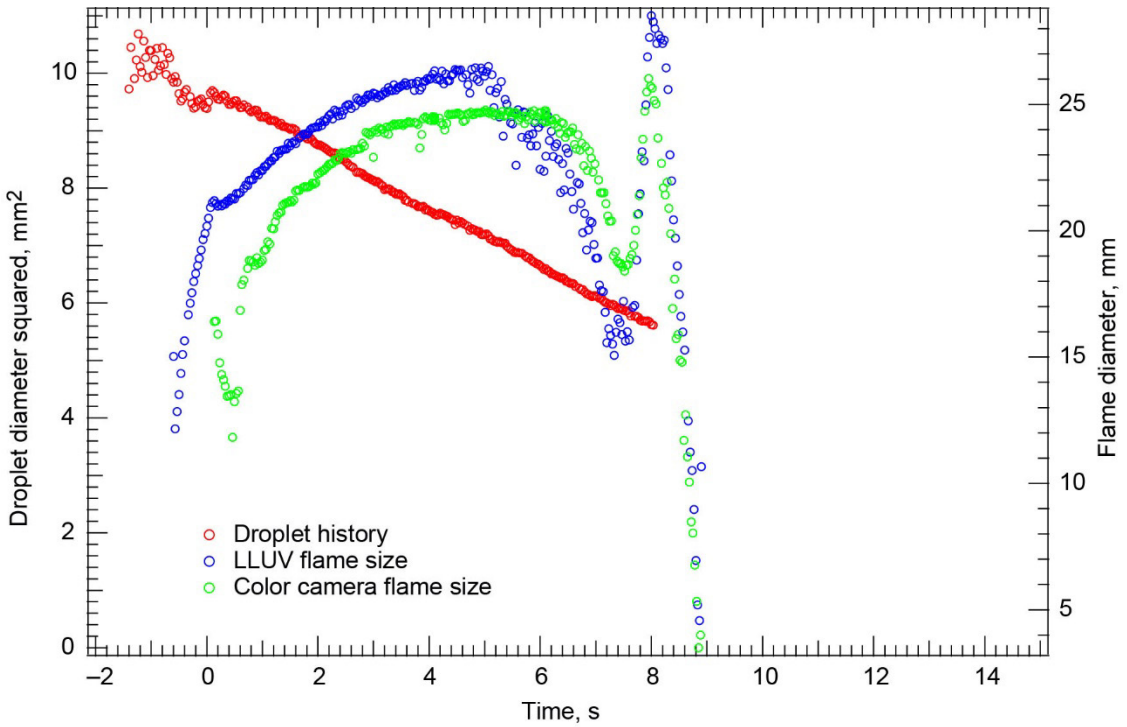

Figure 200.—Test FLEX–197. Free-floating heptane droplet burning in a 0.20/0.75/0.05 $O_2/N_2/CO_2$, 1.0-atm ambient environment. The droplet drifted east out of the High-Bit-Depth Multispectral (HiBMs) field of view (FOV) just before the flame extinguished radiatively. A large vapor cloud formed 15 to 20 s after the visible flame extinguished (visible in the color camera), indicating that cool flame burning and extinction were likely after the visible flame extinguished. The measured burning rate constant (later in the droplet lifetime) was used to extrapolate the extinction droplet diameter from the droplet history, and the Low Light Level Ultra-Violet (LLUV) was used to determine the time of extinction.

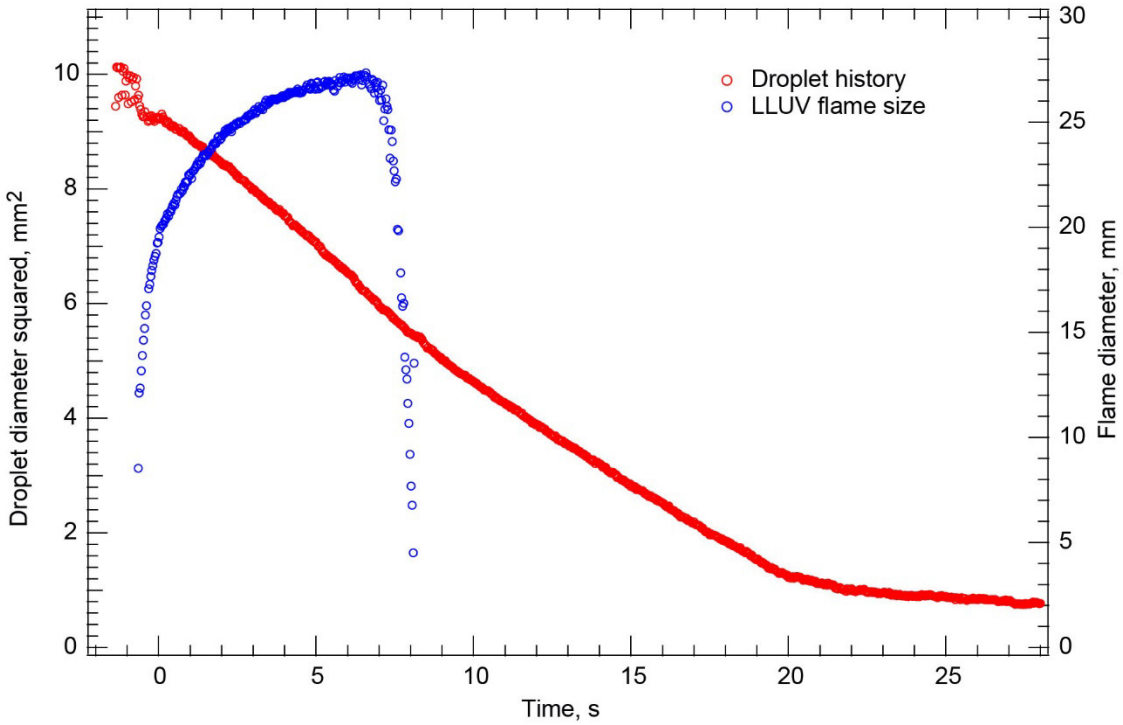

Figure 201.—Test FLEX–198. Free-floating heptane droplet in a 0.20/0.75/0.05 $O_2/N_2/CO_2$, 1.0-atm ambient environment. The droplet remained in the High-Bit-Depth Multispectral (HiBMs) and Low Light Level Ultra-Violet (LLUV) fields of view (FOVs) for the entire recording time. The color camera Image Processing and Storage Unit (IPSU) did not record any images after deployment. The flame extinguished radiatively, and there appeared to be rapid vaporization followed by a plateau late in the recording time after the visible flame extinguished. This is indicative of a cool flame burning and extinction after visible flame extinction.

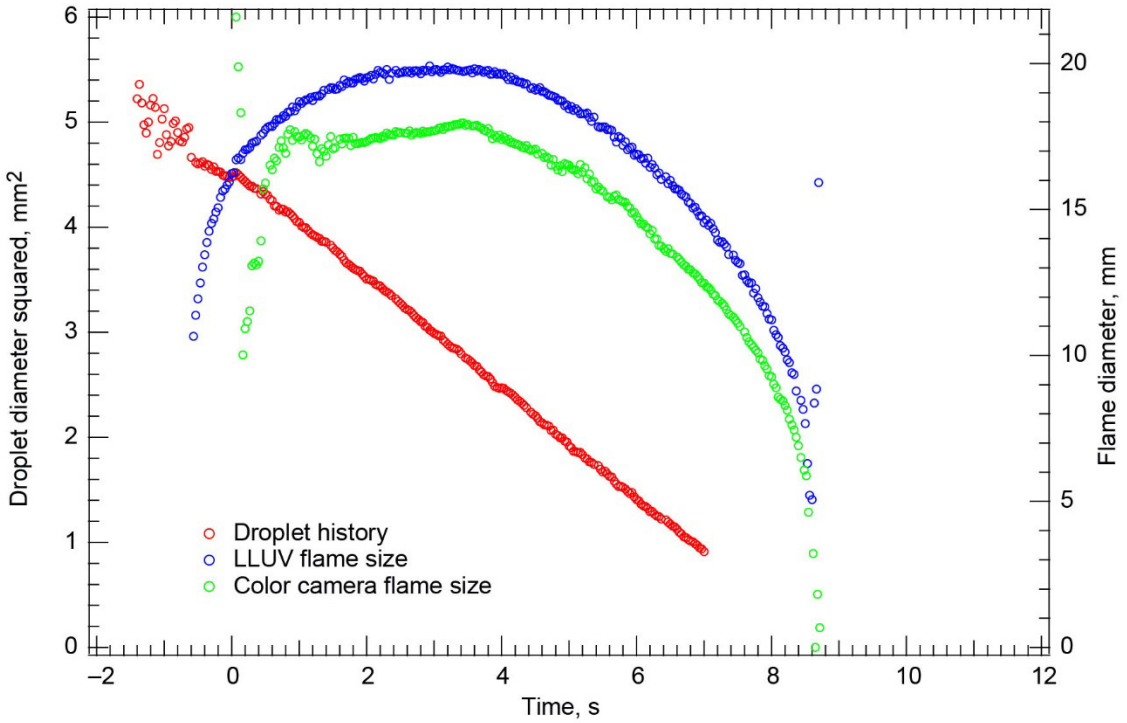

Figure 202.—Test FLEX–199. Free-floating heptane droplet burning in a 0.20/0.75/0.05 $O_2/N_2/CO_2$, 1.0-atm ambient environment. The droplet drifted north after deployment and ignition and out of High-Bit-Depth Multispectral (HiBMs) field of view (FOV). The droplet left the HiBMs FOV before the flame extinguished disruptively when the droplet was very small. The measured burning rate constant was used to extrapolate the extinction droplet diameter from the droplet history until disruption occurred.

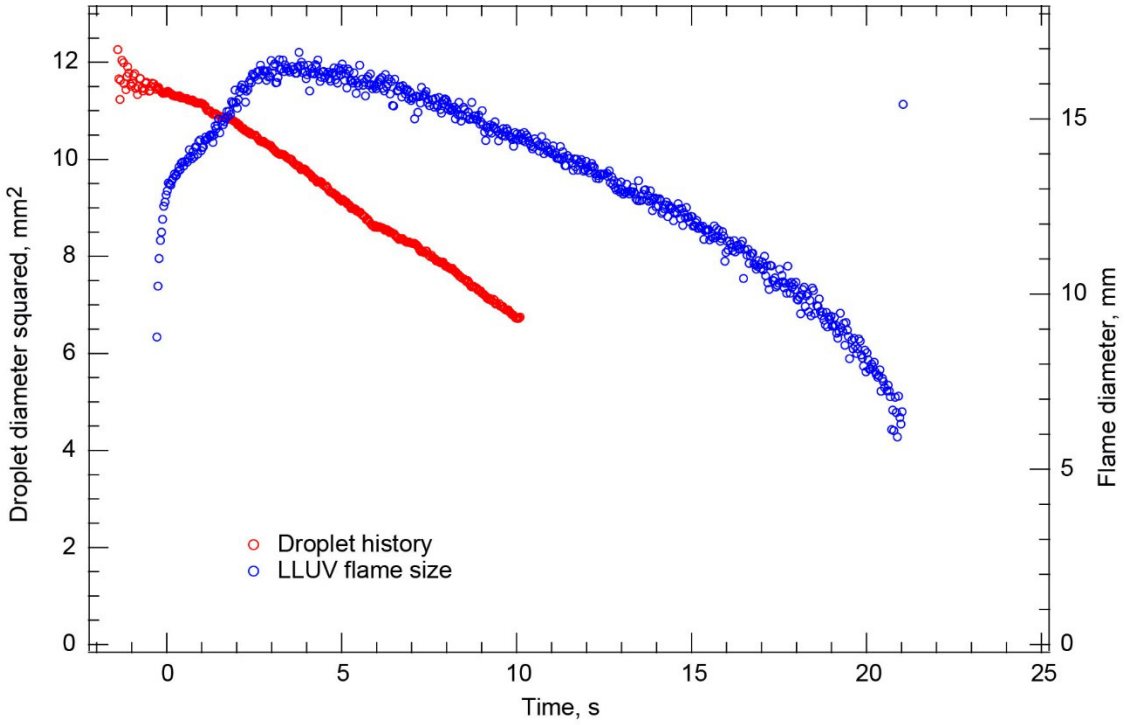

Figure 203.—Test FLEX–200. Free-floating methanol droplet burning in a 0.20/0.75/0.05 $O_2/N_2/CO_2$, 1.0-atm ambient environment. The droplet drifted east and out of the High-Bit-Depth Multispectral (HiBMs) field of view (FOV). After drifting out of the HiBMs FOV, the droplet drifted back in slightly then out again for the rest of the test. The flame extinguished diffusively after a long burn. Because the droplet was in the HiBMs FOV for only a small fraction of the total test, no extinction diameter is reported. The color camera Image Processing and Storage Unit (IPSU) did not record any images after deployment.

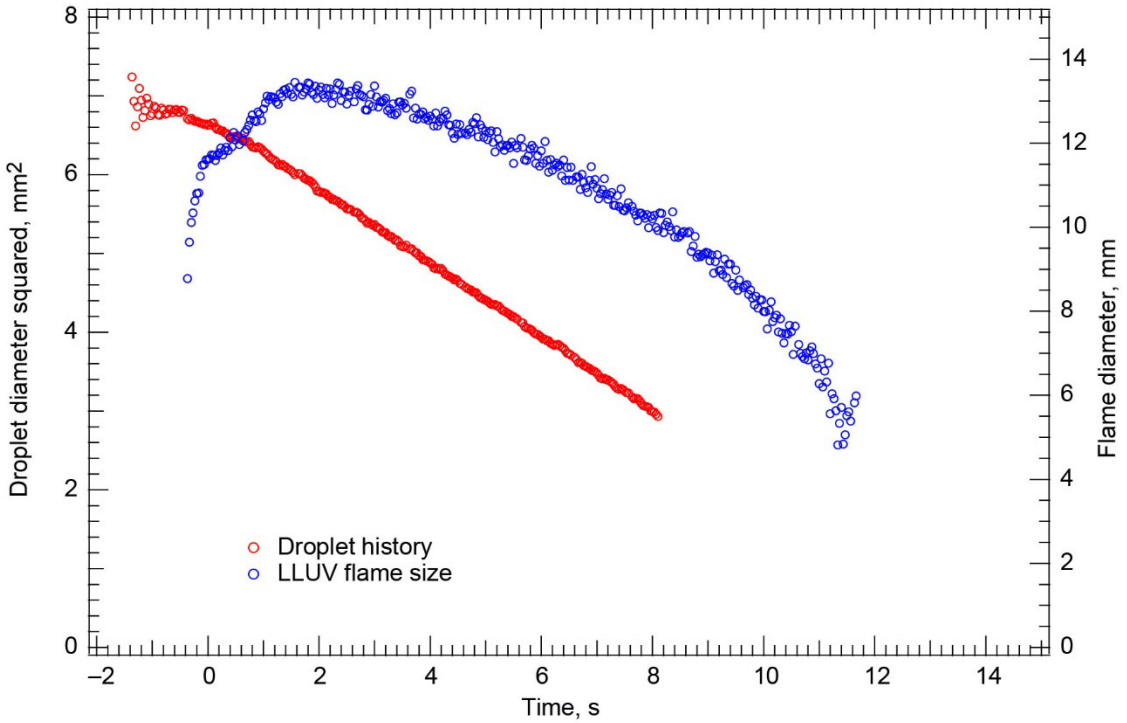

Figure 204.—Test FLEX–201. Free-floating methanol droplet burning in a 0.20/0.75/0.05 $O_2/N_2/CO_2$, 1.0-atm ambient environment. The droplet drifted north in the High-Bit-Depth Multispectral (HiBMs) field of view (FOV) after deployment and ignition. It left the HiBMs FOV approximately two-thirds of the way through the burn, which ended with diffusive extinction. The average burning rate constant from the last half of the time that the droplet was in the HiBMs FOV was used to extrapolate the extinction droplet diameter from the droplet history until the time of extinction. The color camera Image Processing and Storage Unit (IPSU) did not record any images after deployment.

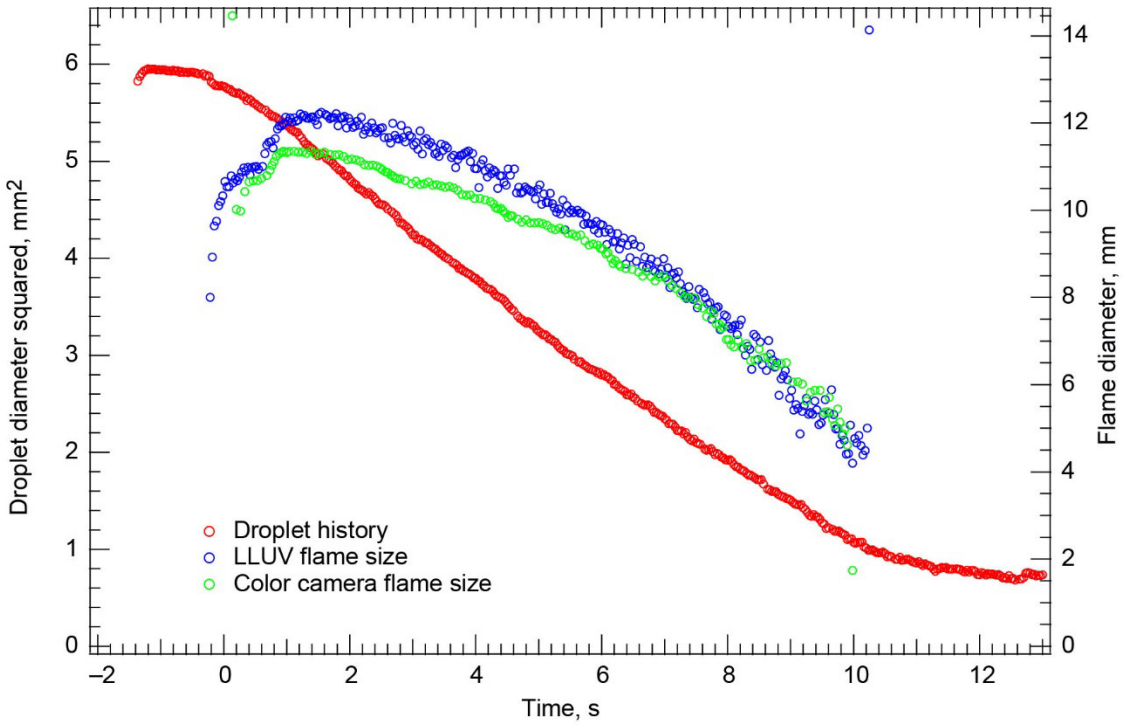

Figure 205.—Test FLEX–202. Free-floating methanol droplet in a 0.20/0.75/0.05 $O_2/N_2/CO_2$, 1.0-atm ambient environment. The droplet had very little residual motion after deployment and ignition, drifting very slowly south in the High-Bit-Depth Multispectral (HiBMs) field of view (FOV). The droplet remained in the FOVs of all the cameras for the entire test.

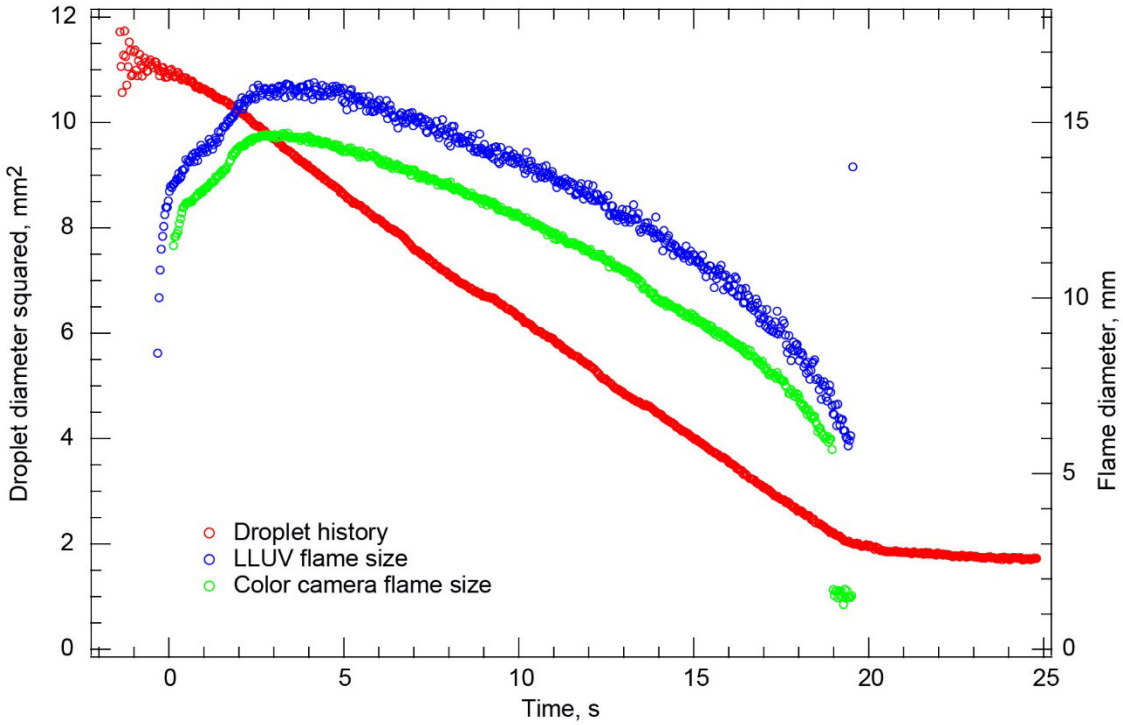

Figure 206.—Test FLEX–203. Free-floating methanol droplet burning in a cabin air (0.21/0.79 O_2/N_2), 1.0-atm ambient environment. The droplet remained in the fields of view (FOVs) of all cameras, and the flame extinguished diffusively.

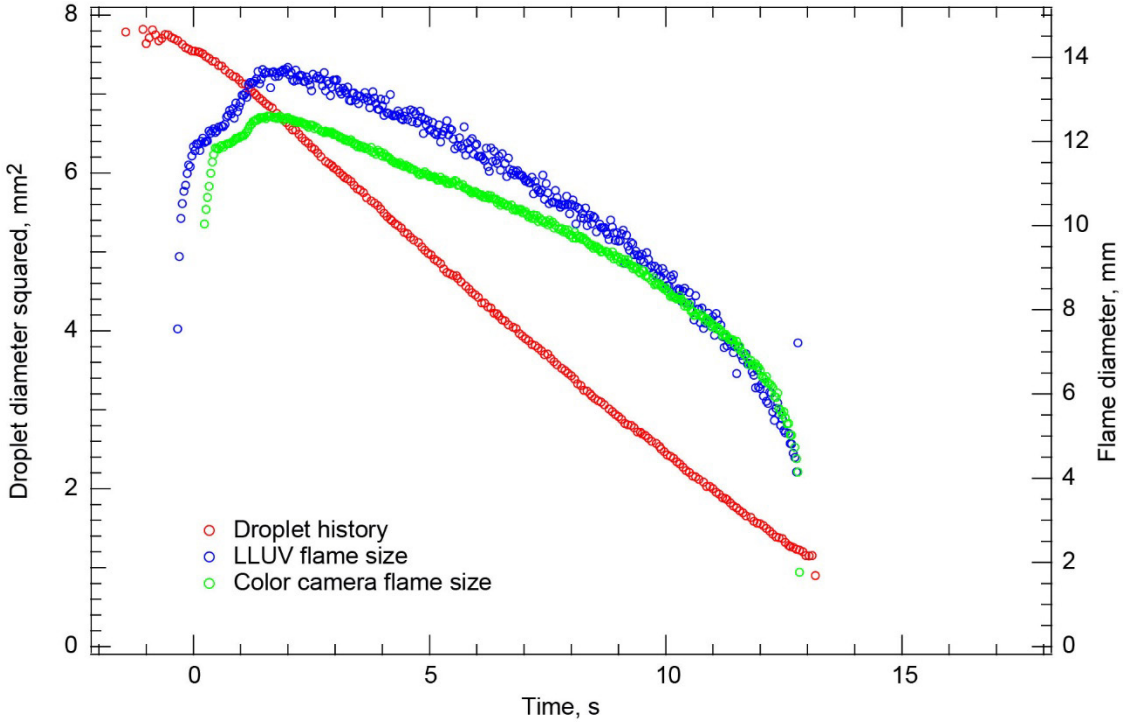

Figure 207.—Test FLEX–204. Free-floating methanol droplet burning in a cabin air (0.21/0.79 O_2/N_2), 1.0-atm ambient environment. The droplet remained in the fields of view (FOVs) of all cameras for the entire burn, but it drifted south and out of the High-Bit-Depth Multispectral (HiBMs) FOV shortly after the flame extinguished diffusively. Image Processing and Storage Unit (IPSU) did not record every frame.

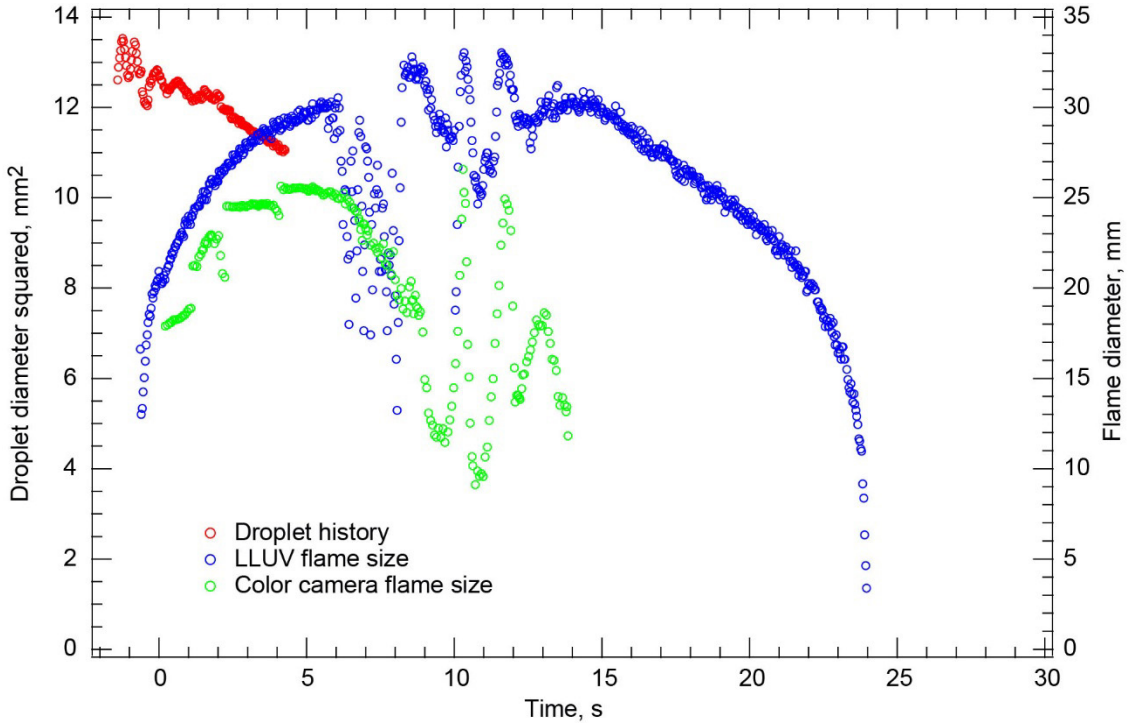

Figure 208.—Test FLEX–206. Free-floating heptane droplet burning in a cabin air (0.21/0.79 O_2/N_2), 1.0-atm ambient environment. The droplet drifted southeast in the High-Bit-Depth Multispectral (HiBMs) field of view (FOV) after deployment; then it hit the igniter and changed direction to the northwest with a relatively high speed. It drifted northwest and out of the HiBMs FOV after a very short time. The droplet also drifted out of the color camera FOV, but it remained in the Low Light Level Ultra-Violet (LLUV) FOV.

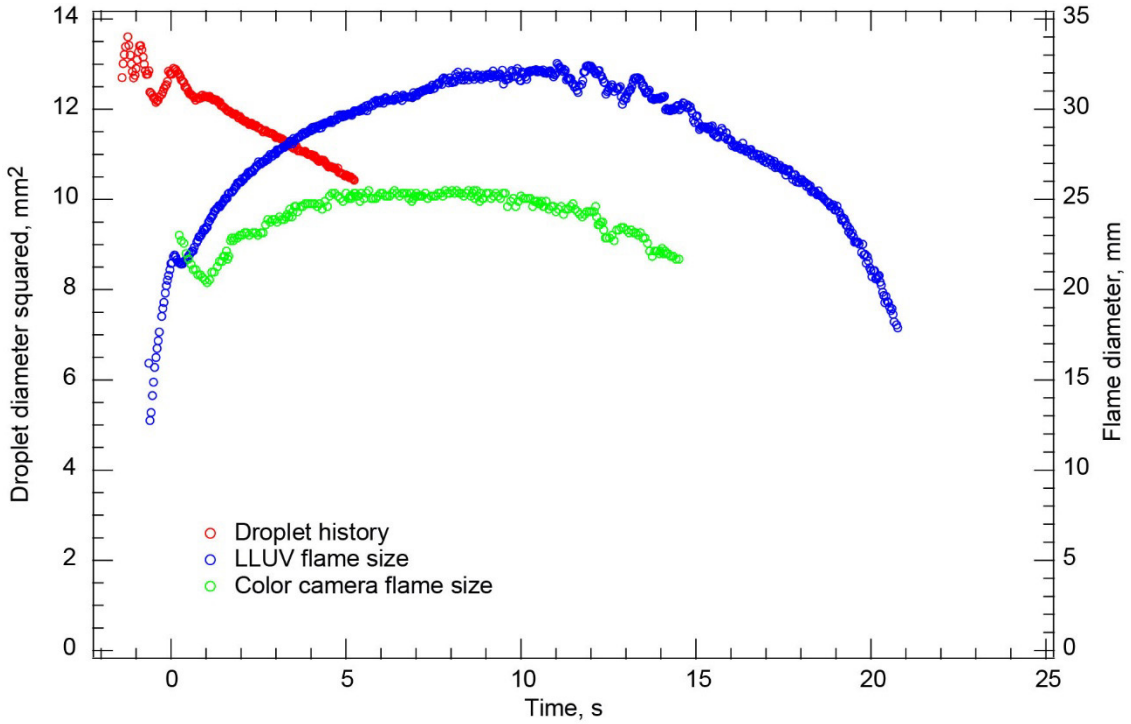

Figure 209.—Test FLEX–207. Free-floating heptane droplet burning in a cabin air (0.21/0.79 O_2/N_2), 1.0-atm ambient environment. The droplet drifted southeast in the High-Bit-Depth Multispectral (HiBMs) field of view (FOV) after deployment; then it hit the igniter and began to drift north. The drift velocity was relatively high, and the droplet drifted out of the HiBMs FOV relatively quickly after ignition. It also drifted out of the Low Light Level Ultra-Violet (LLUV) and color camera FOVs before the end of the test. The flame oscillated briefly in the middle of the burn and then became steady and burned to a disruptive extinction. The flame was very dim in the color camera FOV, with the leading edge of the flame (in the direction of the droplet drift) much brighter than the trailing edge.

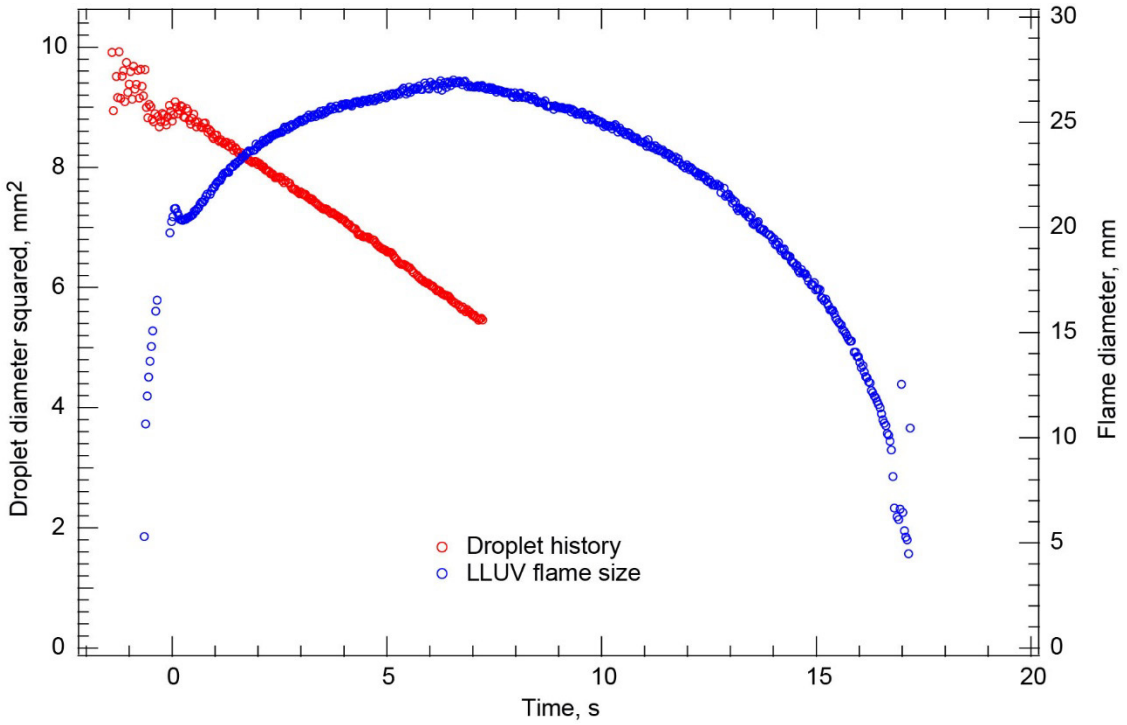

Figure 210.—Test FLEX–208. Free-floating heptane droplet burning in a cabin air (0.21/0.79 O_2/N_2), 1.0-atm ambient environment. The droplet drifted southeast after deployment, drifted into the igniter, and changed direction to the north after the igniter was withdrawn. The droplet drifted north during the burn and out of the High-Bit-Depth Multispectral (HiBMs) field of view (FOV). The flame grew, remained stable (no oscillations), and then shrank to a disruptive extinction at a relatively small size. The droplet remained in the Low Light Level Ultra-Violet (LLUV) FOV for the entire test, but the Multi-User Droplet Combustion Apparatus (MDCA) color camera did not record images onboard for this test (the downlinked video is available).

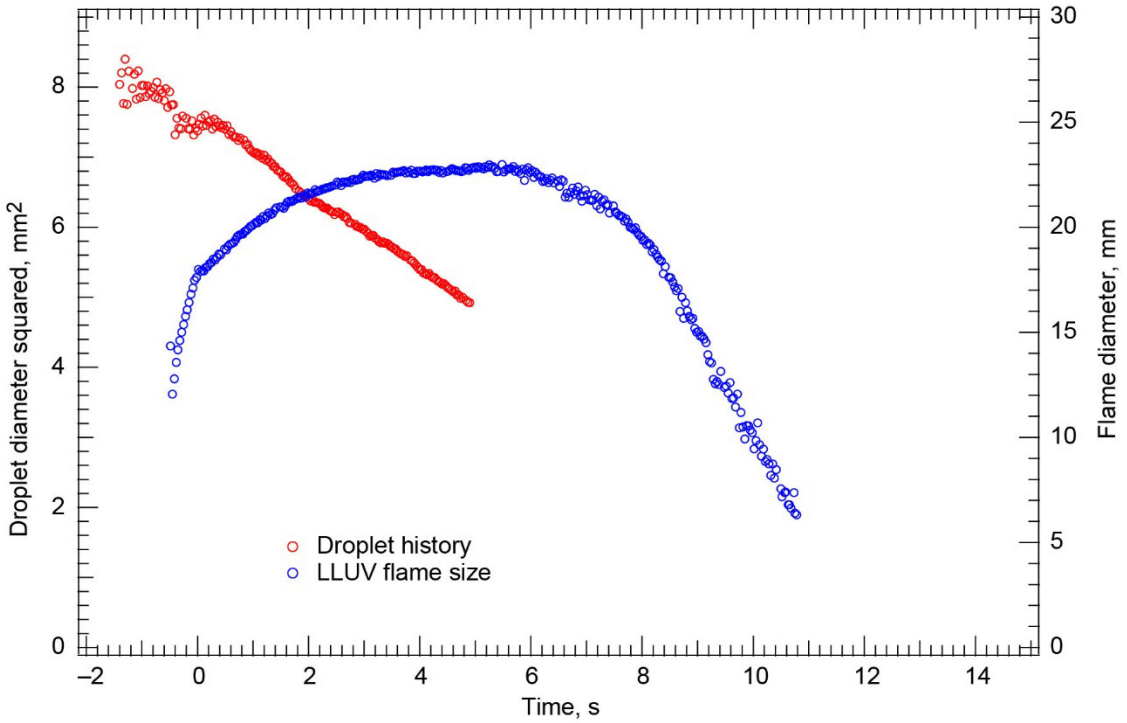

Figure 211.—Test FLEX–209. Free-floating heptane droplet burning in a cabin air (0.21/0.79 O_2/N_2), 1.0-atm ambient environment. The droplet drifted southeast after deployment, did not touch the igniter, and continued to drift southeast in the High-Bit-Depth Multispectral (HiBMs) field of view (FOV) and out of the FOV. The droplet also drifted south and out of the Low Light Level Ultra-Violet (LLUV) FOV. The color camera Image Processing and Storage Unit (IPSU) did not record color camera data. It is not clear whether disruption occurred.

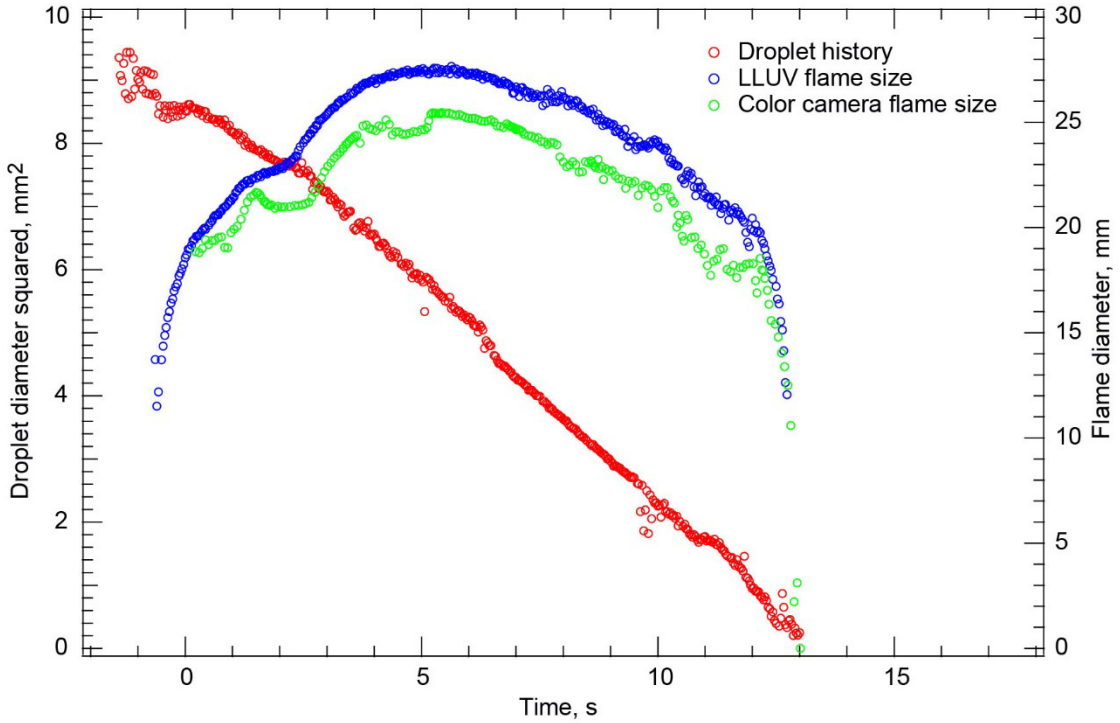

Figure 212.—Test FLEX–210. Fiber-supported heptane droplet in a cabin air (0.21/0.79 O_2/N_2), 1.0-atm ambient environment. The droplet drifted east some on the fiber after ignition and early in the droplet lifetime. The soot agglomerates that were near the droplet created a lot of noise in the droplet measurement for the first half of the burn. The droplet also moved significantly on the fiber late in the droplet lifetime. There was evidence of some unusual soot dynamics—large soot particles moving slowly toward the droplet and then being more rapidly pushed away (presumably by the Stefan flow). The droplet burned to completion.

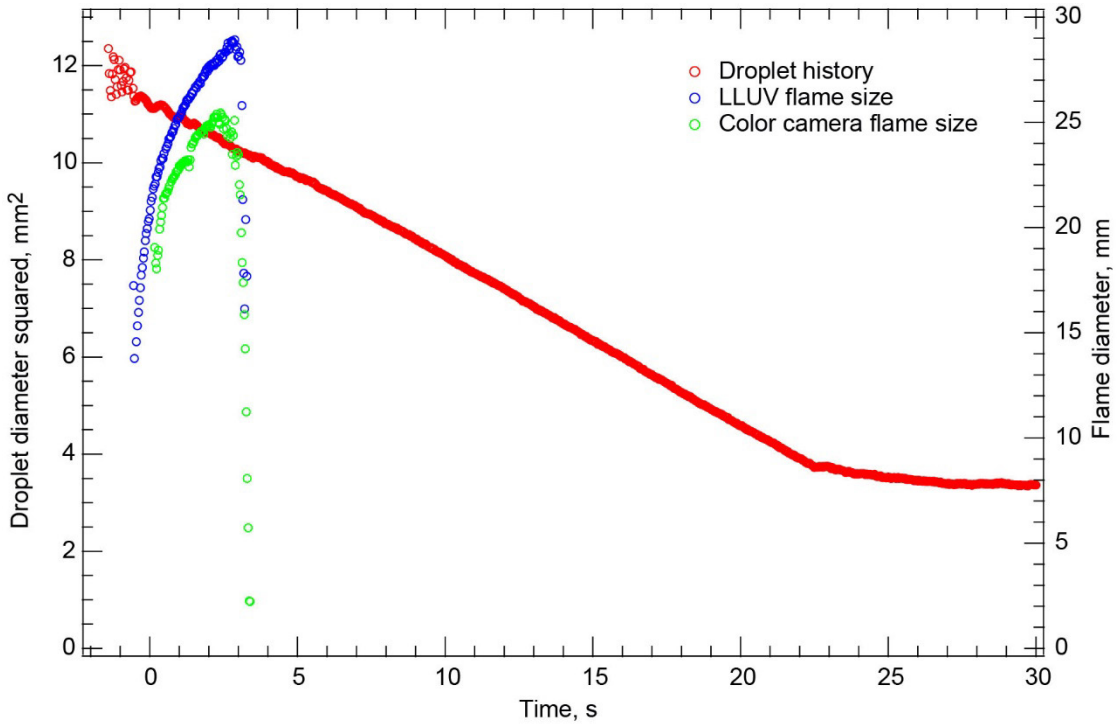

Figure 213.—Test FLEX–211. Free-floating heptane droplet burning in a 0.16/0.84 O_2/N_2, 1.0-atm ambient environment. The droplet was nearly motionless after deployment and ignition and remained in the fields of view (FOVs) of all the cameras throughout the entire recording time of the Image Processing and Storage Units (IPSUs). The visible flame grew then extinguished radiatively. This was followed by rapid vaporization. The vaporization rate of the droplet actually increased after the visible flame extinguished and then rapidly decreased when a vapor cloud formed. This behavior is indicative of cool flame burning and extinction.

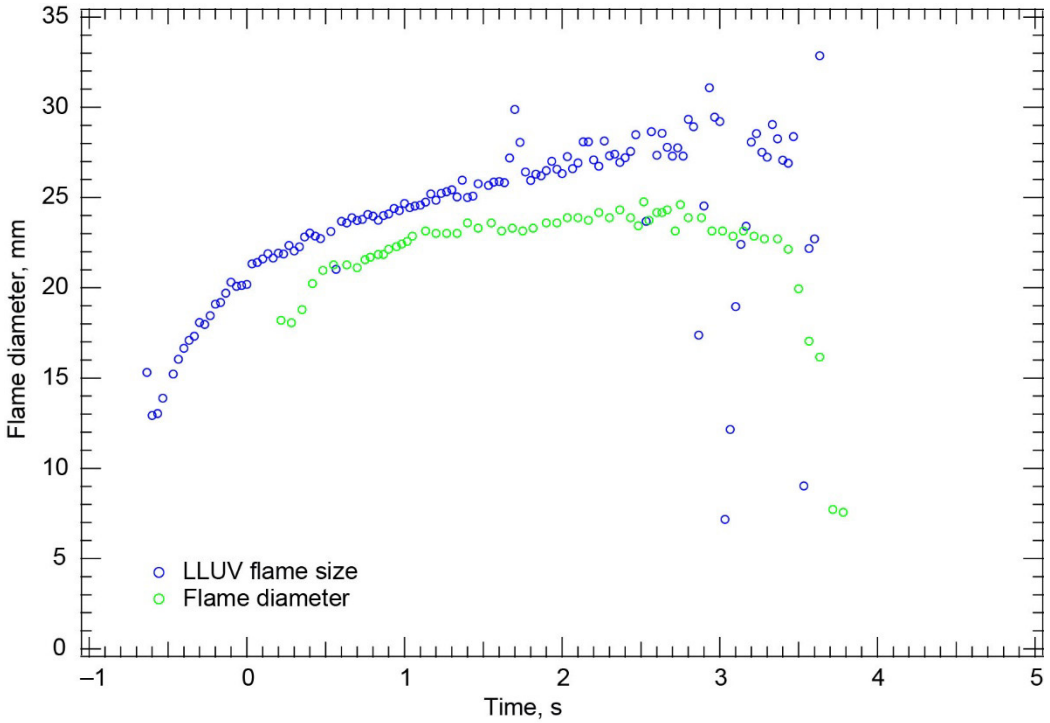

Figure 214.—Test FLEX−212. Free-floating heptane droplet burning in a 0.16/0.84 O_2/N_2, 1.0-atm ambient environment. The droplet drifted north in the color camera field of view (FOV). The High-Bit-Depth Multispectral (HiBMs) Image Processing and Storage Unit (IPSU) did not record any images for this test, but the droplet remained in the FOVs of the Low Light Level Ultra-Violet (LLUV) and color camera. The flame burned for a short time to radiative extinction. This was probably followed by cool flame burning and extinction. The color camera showed that a large vapor cloud formed sometime after the visible flame extinguished.

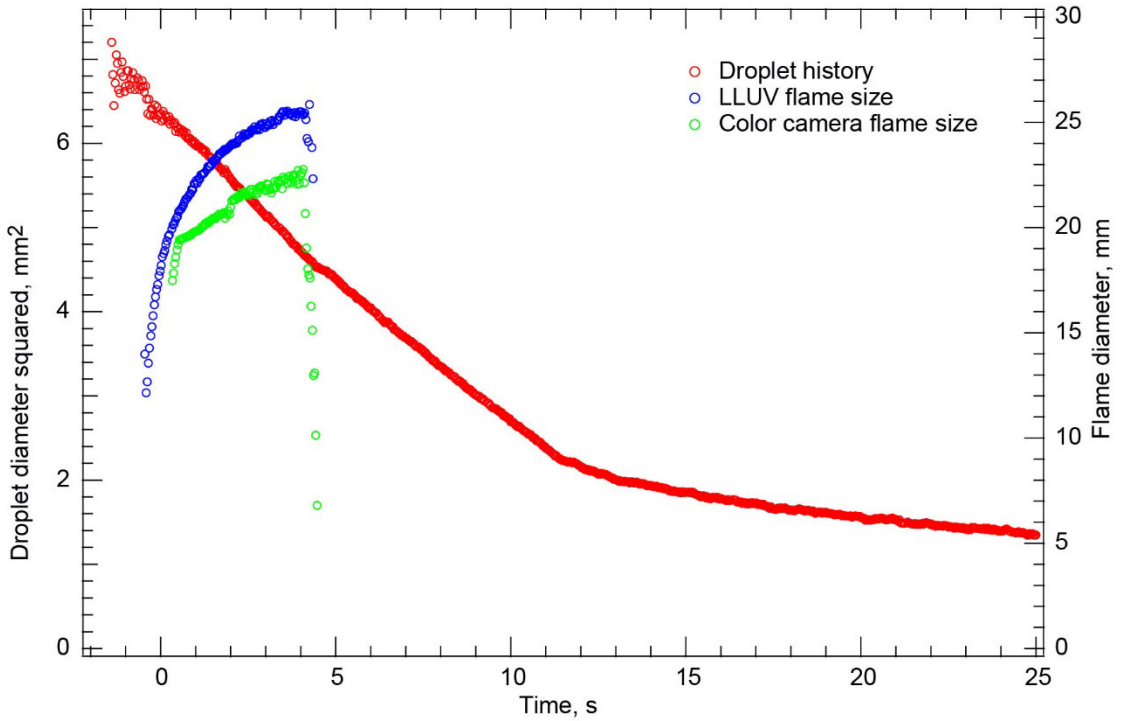

Figure 215.—Test FLEX–214. Free-floating heptane droplet burning in a 0.16/0.84 O_2/N_2, 1.0-atm ambient environment. The droplet remained in the fields of view (FOVs) of all cameras for the entire recording time of the Image Processing and Storage Units (IPSUs). The flame grew and extinguished radiatively shortly after ignition. A period of rapid post visible flame extinction vaporization was followed by a plateau in the droplet history coincident with the appearance of a vapor cloud. Both indicate cool flame burning and extinction following visible flame extinction.

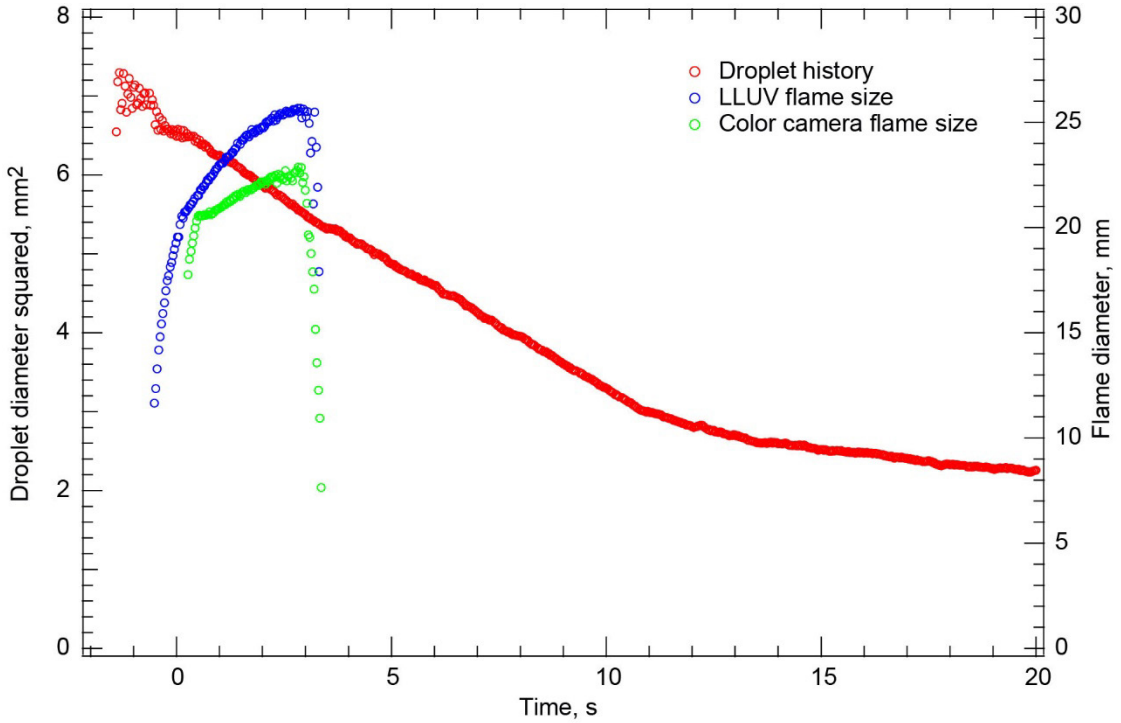

Figure 216.—Test FLEX–215. Free-floating heptane droplet burning in a 0.15/0.85 O_2/N_2, 1.0-atm ambient environment. The droplet had very little residual motion after deployment and ignition with only a very small drift north in the High-Bit-Depth Multispectral (HiBMs) field of view (FOV). The droplet remained in the FOVs of all cameras throughout the recording time of the Image Processing and Storage Units (IPSUs). After ignition, the flame grew but became dimmer, and it extinguished radiatively shortly after ignition. This was followed by a period of rapid vaporization and a quick plateau in the droplet history coincident with the formation of a vapor cloud. Both of these are evidence of cool flame burning and extinction after visible flame extinction.

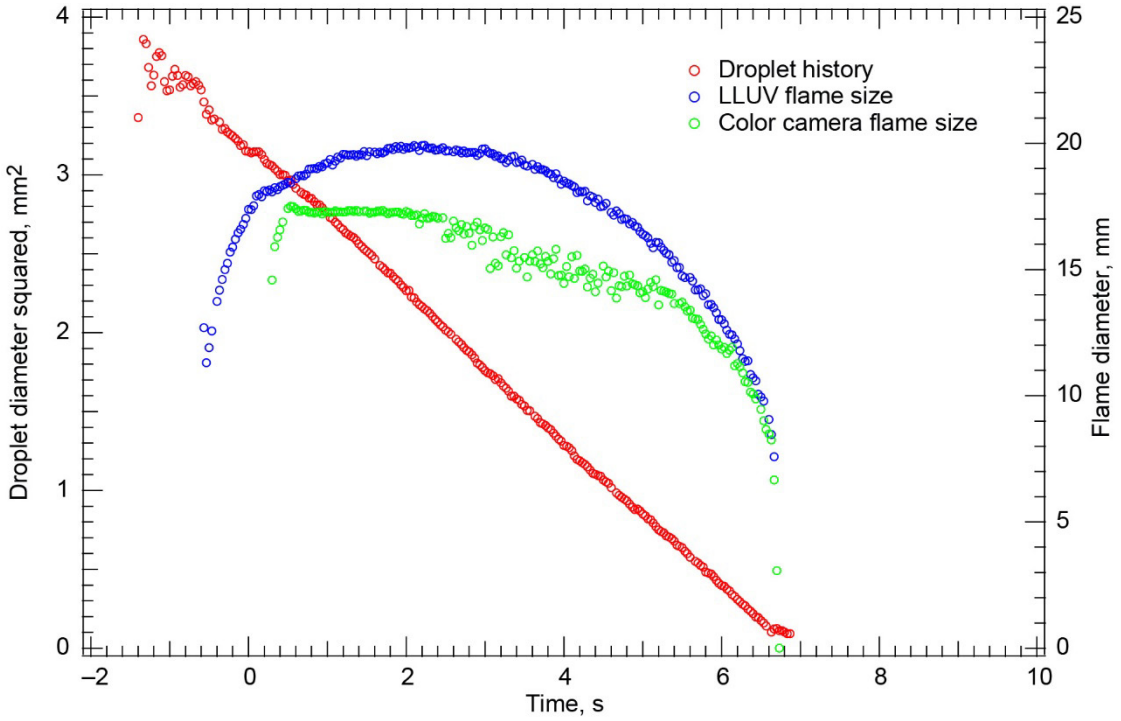

Figure 217.—Test FLEX–216. Free-floating heptane droplet burning in a 0.15/0.84 O_2/N_2, 1.0-atm ambient environment. The droplet remained in the fields of view (FOVs) of all the cameras throughout the entire burn and during the recording time of the Image Processing and Storage Unit (IPSUs). Either the droplet burned to completion or the flame extinguished when the droplet was very small. There was no disruption when the flame extinguished.

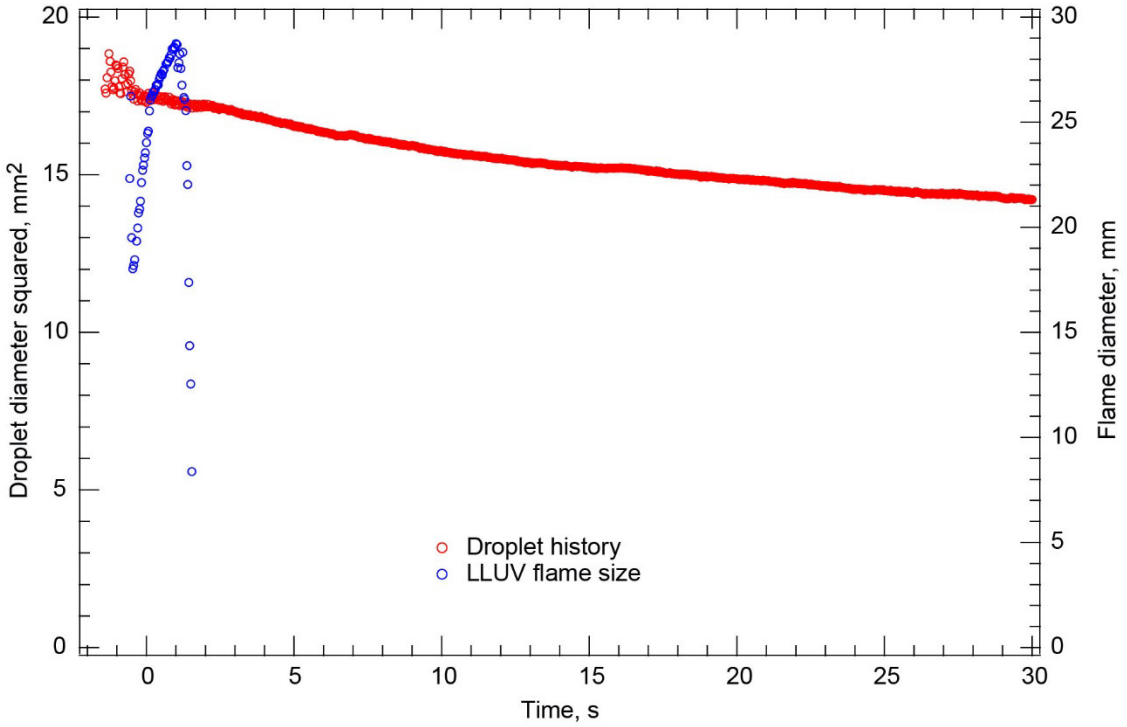

Figure 218.—Test FLEX–217. Free-floating heptane droplet burning in a 0.14/0.86 O_2/N_2, 1.0-atm ambient environment. The droplet remained in the fields of view (FOVs) of all cameras for the entire recording time of all the Image Processing and Storage Units (IPSUs). The droplet did drift east to the edge of the High-Bit-Depth Multispectral (HiBMs) FOV and then south to the corner of the HiBMs FOV, but it never left the HiBMs FOV. The flame had a very quick radiative extinction. The vaporization rate did not change after extinction, and a small vapor cloud formed, indicating that there may have been a cool flame, although the extinction of the cool flame was not pronounced.

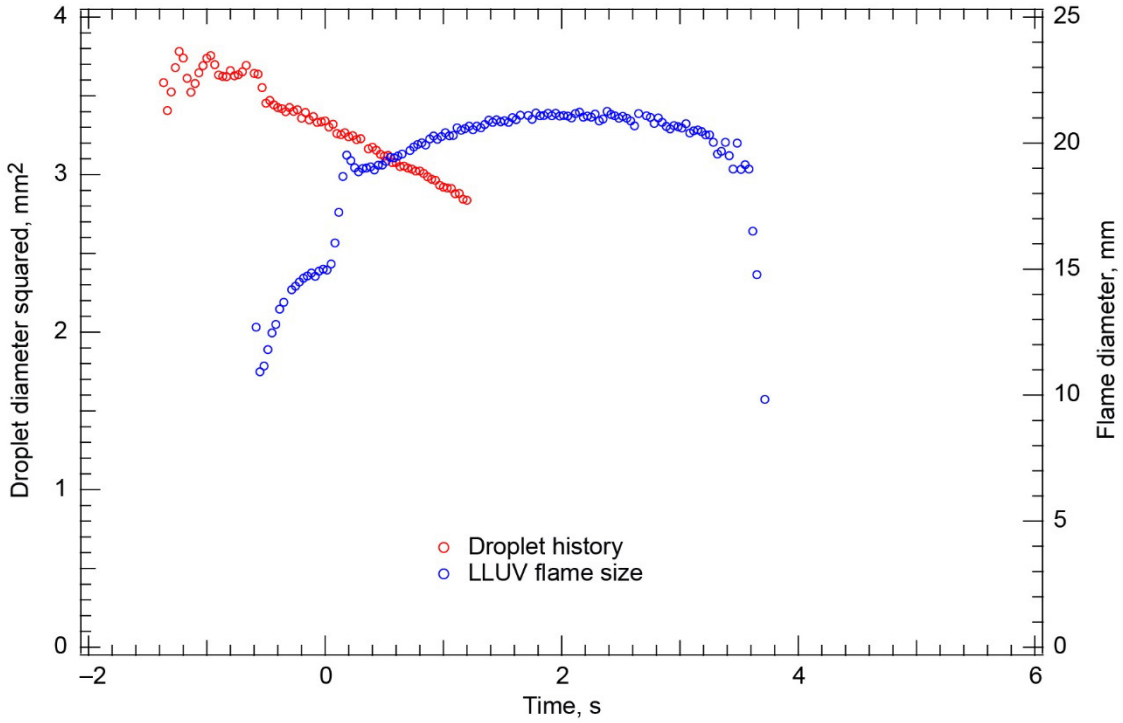

Figure 219.—Test FLEX–218. Free-floating heptane droplet burning in a 0.14/0.86 O_2/N_2, 1.0-atm ambient environment. This small droplet drifted quickly northwest in the High-Bit-Depth Multispectral (HiBMs) field of view (FOV) after deployment and ignition. It drifted out of the FOV a short time after the igniter was withdrawn. The droplet appeared to extinguish radiatively, even at this relatively small size. Because the droplet was in the HiBMs FOV for only a small fraction of the entire test, no extinction droplet diameter is reported. The color camera Image Processing and Storage Unit (IPSU) did not record any images after deployment.

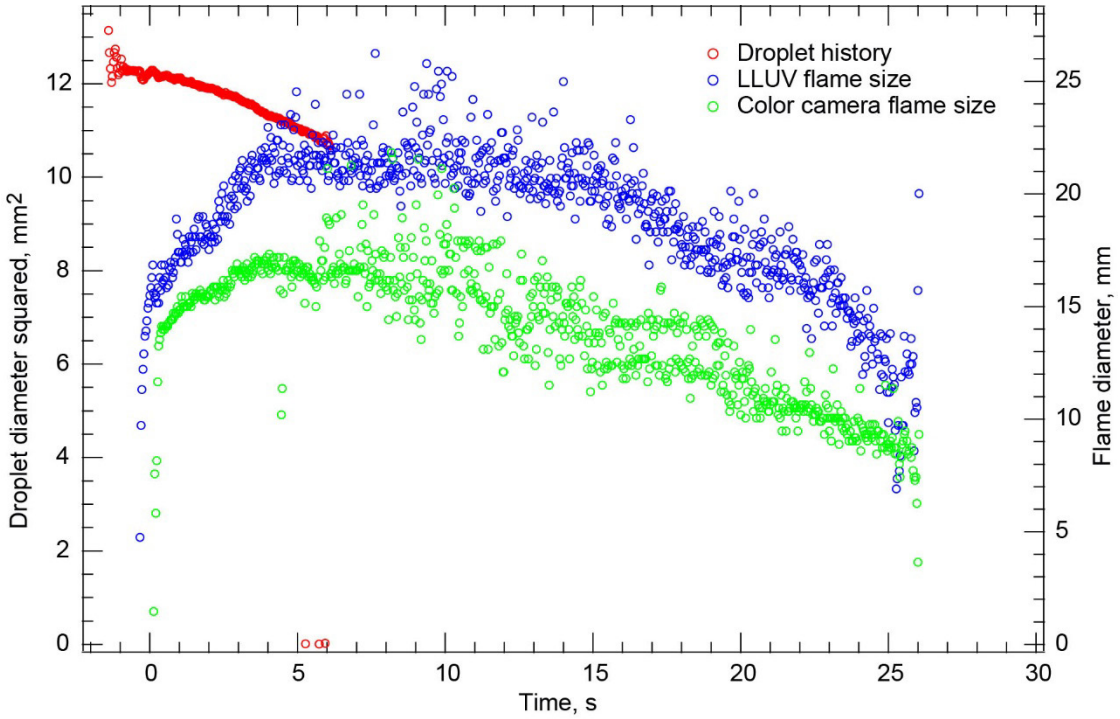

Figure 220.—Test FLEX–219. Free-floating methanol droplet burning in a 0.14/0.86 O_2/N_2, 1.0-atm ambient environment. The droplet drifted north and out of High-Bit-Depth Multispectral (HiBMs) field of view (FOV) about one-fourth of the way through a very long burn that appeared to end in a diffusive extinction. The droplet drifted east and partially out of the Low Light Level Ultra-Violet (LLUV) FOV, but it remained in the color camera FOV. This was a very weak flame, barely visible on both the LLUV and color cameras. Because the droplet was only in the HiBMs FOV for a small fraction of the flame lifetime, no extinction droplet diameter is reported.

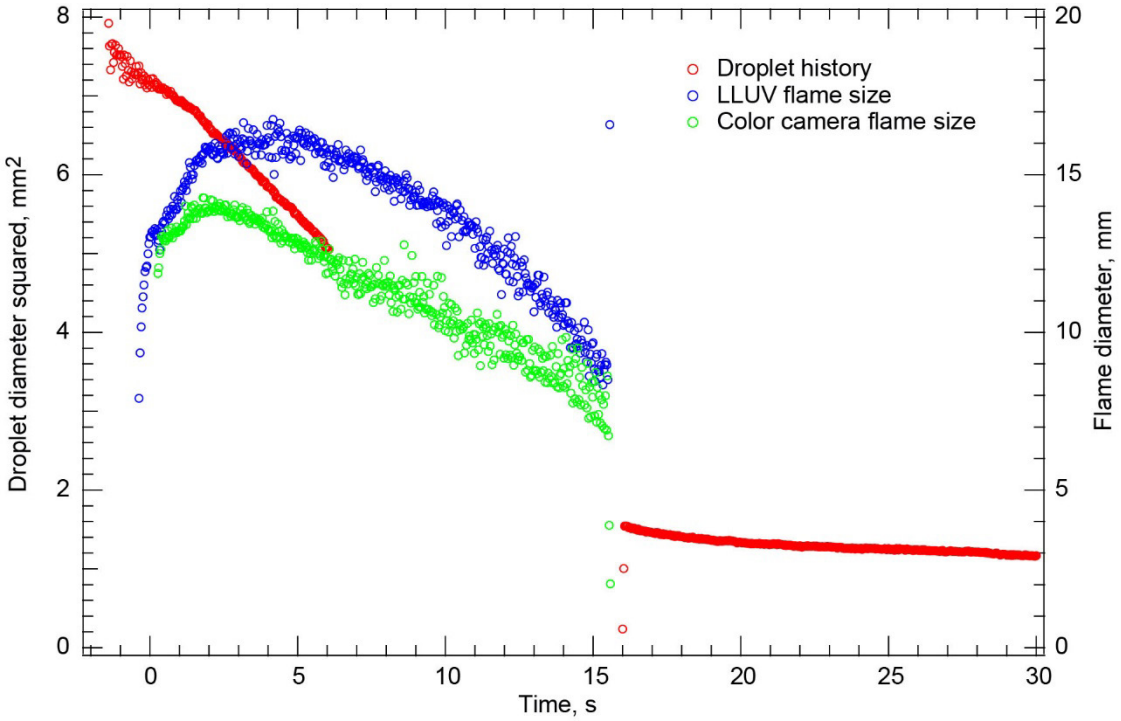

Figure 221.—Test FLEX–220. Free-floating methanol droplet in a 0.14/0.86 O_2/N_2, 1.0-atm ambient environment. The droplet drifted north after deployment and ignition and then out of High-Bit-Depth Multispectral (HiBMs) field of view (FOV). Just after the visible flame extinguished, the droplet drifted back into the HiBMs FOV. This was a weak flame with a long burn to diffusive extinction. The extinction droplet diameter was derived from a spline fit between the periods of time when the droplet was in the HiBMs FOV.

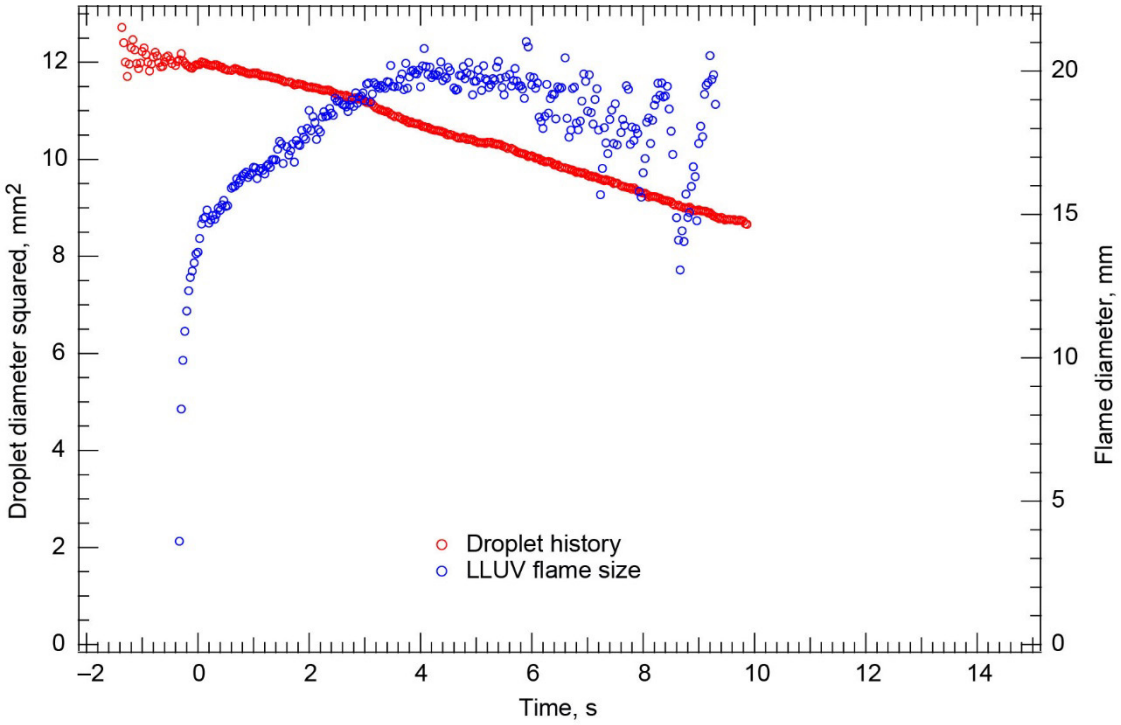

Figure 222.—Test FLEX–221. Free-floating methanol droplet burning in a 0.13/0.87 O_2/N_2, 1.0-atm ambient environment. The droplet drifted east; then just after the visible flame extinguished, it drifted south and out of the southeast corner of the High-Bit-Depth Multispectral (HiBMs) field of view (FOV). The flame oscillated for several seconds before it extinguished radiatively. The flame oscillations are very difficult to discern in the Low Light Level Ultra-Violet (LLUV) view because the flame luminosity barely registered on the LLUV. The color camera Image Processing and Storage Unit (IPSU) did not record any images for this test.

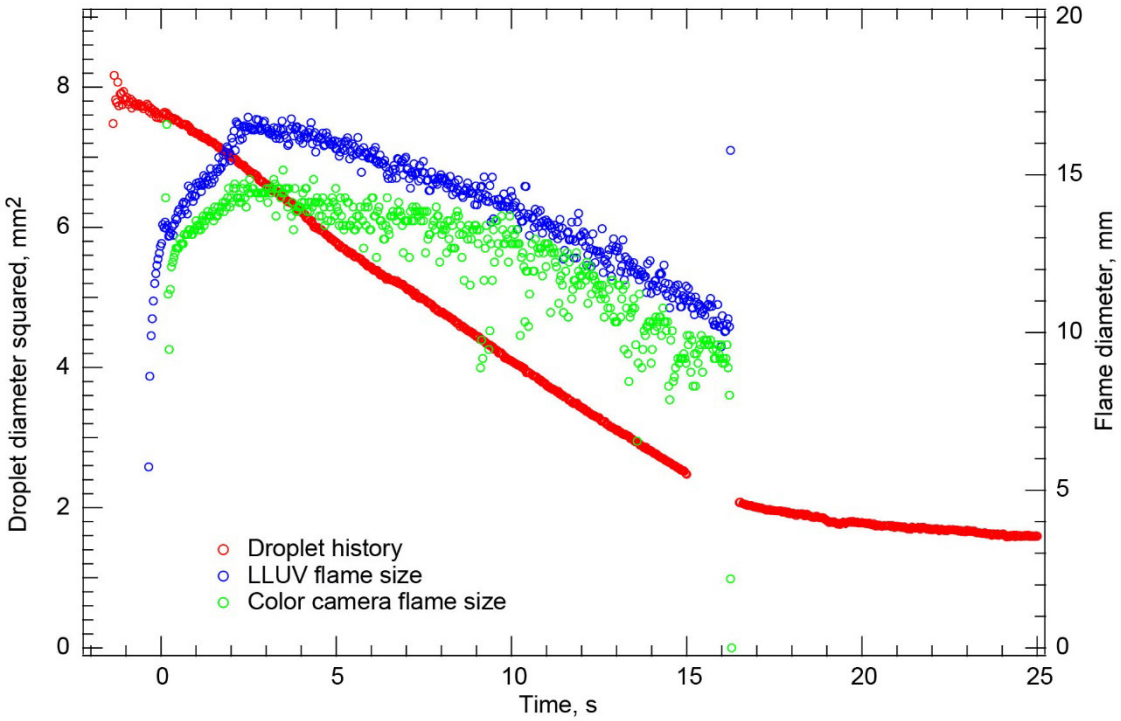

Figure 223.—Test FLEX–222. Free-floating methanol droplet burning in a 0.13/0.87 O_2/N_2, 1.0-atm ambient environment. The droplet remained in the High-Bit-Depth Multispectral (HiBMs) field of view (FOV) for most of the test. For a short period near visible flame extinction, the droplet drifted partially out of the FOV. It drifted back into the HiBMs FOV for the remainder of the HiBMs Image Processing and Storage Unit (IPSU) recording time. The flame was very dim, barely above the background level, in both the Low Light Level Ultra-Violet (LLUV) and color cameras. The extinction droplet diameter was interpolated from the droplet history from when the droplet left the HiBMs FOV to when it reentered a short time after the visible flame extinguished. The interpolation polynomial is a fourth-order polynomial with the constraint that the values and burning rate constants at both ends match the experimental values.

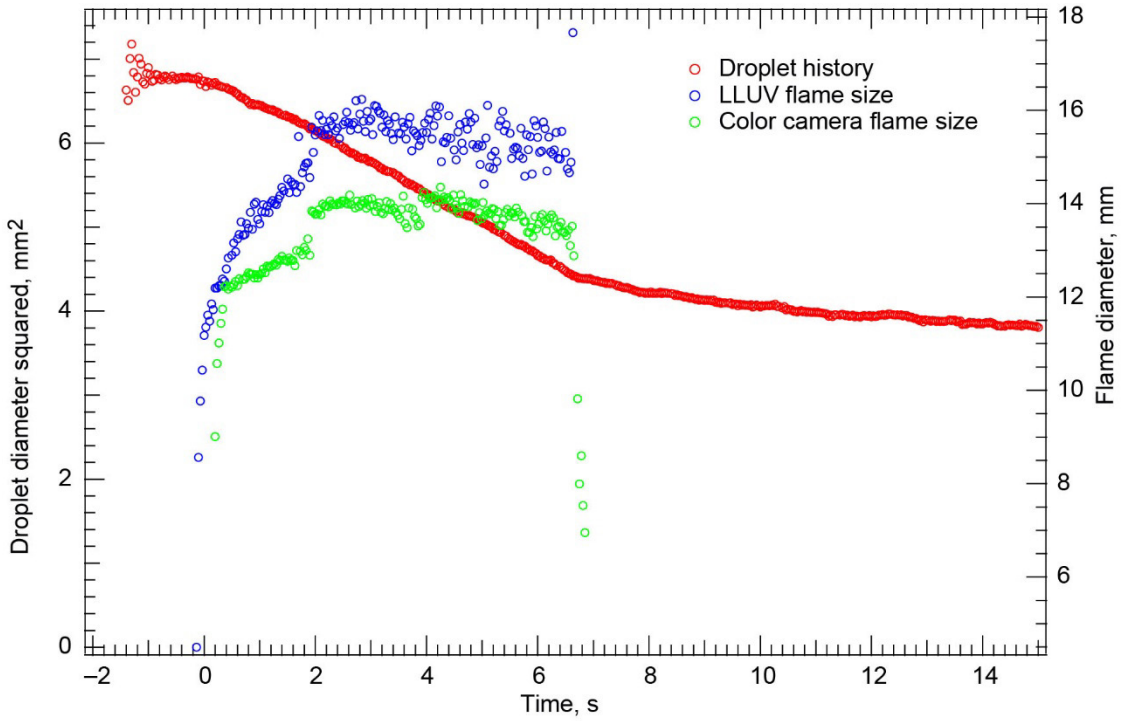

Figure 224.—Test FLEX–223. Free-floating methanol droplet burning in a 0.12/0.88 O_2/N_2, 1.0-atm ambient environment. The droplet deployed and ignited with almost no residual motion. The droplet drifted a little south and then east in the High-Bit-Depth Multispectral (HiBMs) field of view (FOV), but it remained in the FOVs of the HiBMs, Low Light Level Ultra-Violet (LLUV), and color cameras for the entire recording time.

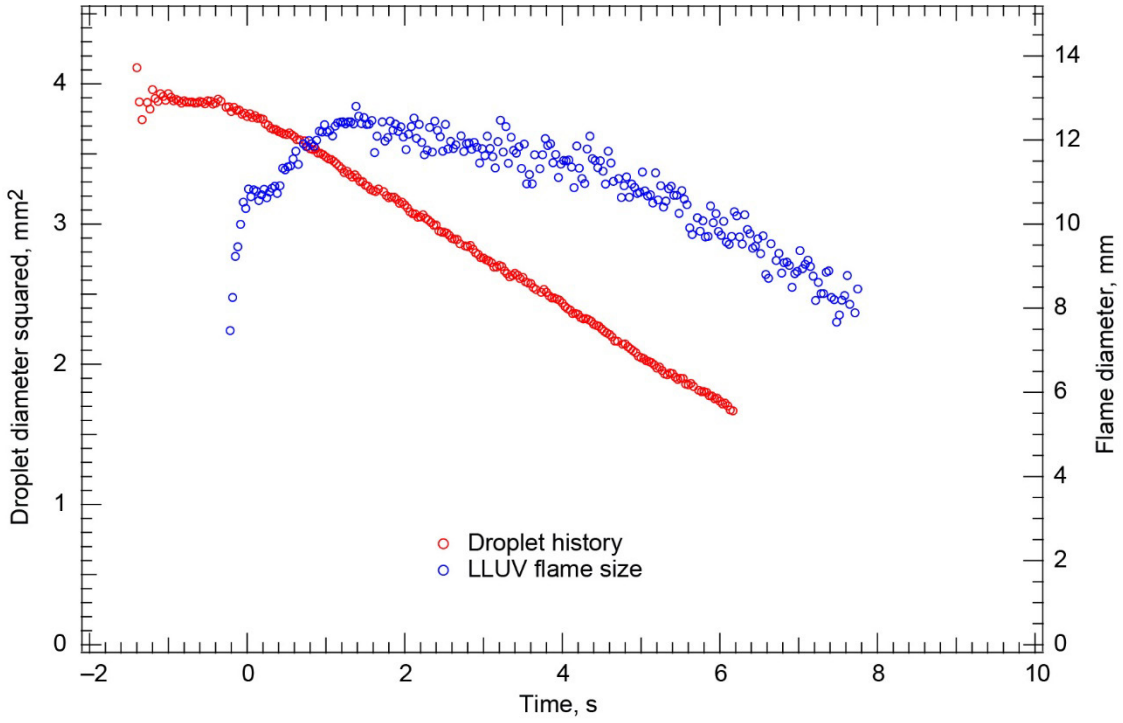

Figure 225.—Test FLEX–224. Free-floating methanol droplet burning in a 0.12/0.88 O_2/N_2, 1.0-atm ambient environment. The droplet drifted north after deployment and ignition and out of the High-Bit-Depth Multispectral (HiBMs) field of view (FOV) about three-fourths of the way through the burn. The flame grew and then shrank in response to the shrinking droplet. The flame was very dim and difficult to see in the Low Light Level Ultra-Violet (LLUV). The flame probably extinguished diffusively. The measured burning rate constant while the droplet was in the FOV was used to extrapolate the extinction droplet diameter from the droplet history to flame extinction.

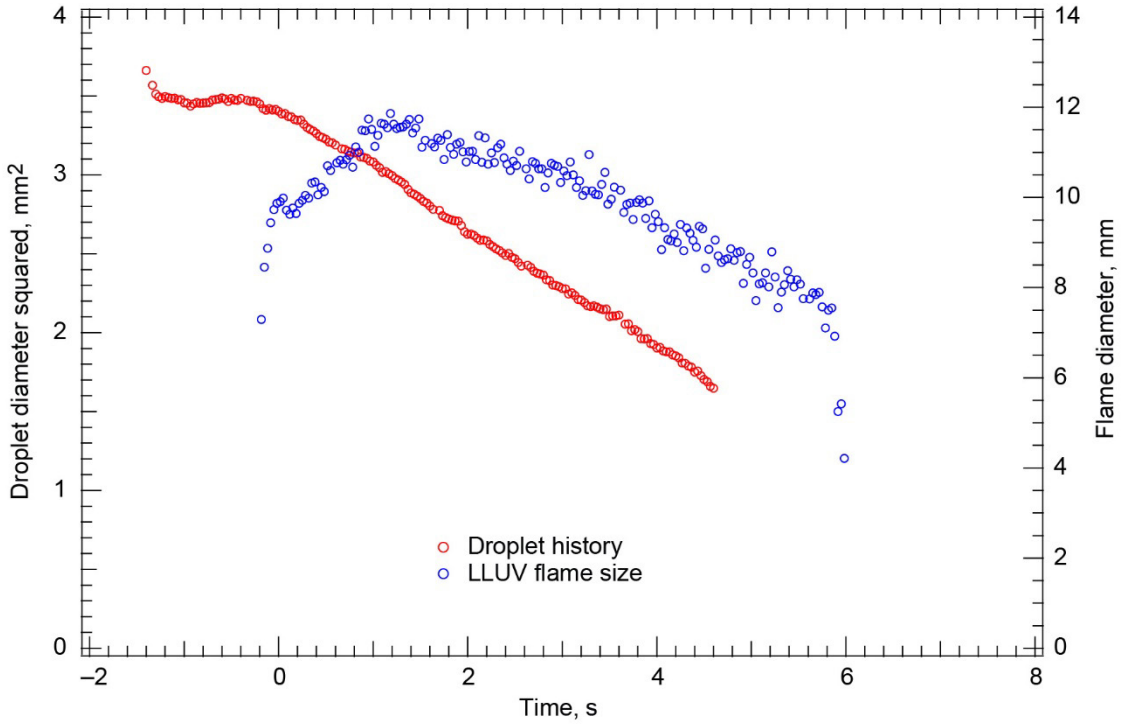

Figure 226.—Test FLEX–225. Free-floating methanol droplet burning in a 0.12/0.88 O_2/N_2, 1.0-atm ambient environment. The droplet was nearly motionless after deployment and ignition. Then it started to drift slowly east, but it changed direction and quickly drifted west in the High-Bit-Depth Multispectral (HiBMs) field of view (FOV). The droplet left the HiBMs FOV about three-fourths of the way through the burn. The flame was very dim, but it did appear to grow, reach a maximum, and then decrease in size in response to the shrinking droplet. The burning rate constant measured from the last part of the droplet history while the droplet was still in the HiBMs FOV was used to extrapolate the extinction droplet diameter from the droplet history to when the flame extinguished (as measured by the Low Light Level Ultra-Violet (LLUV)). The flame probably extinguished diffusively with a significant contribution from radiative loss. The color camera Image Processing and Storage Unit (IPSU) did not record any images after deployment.

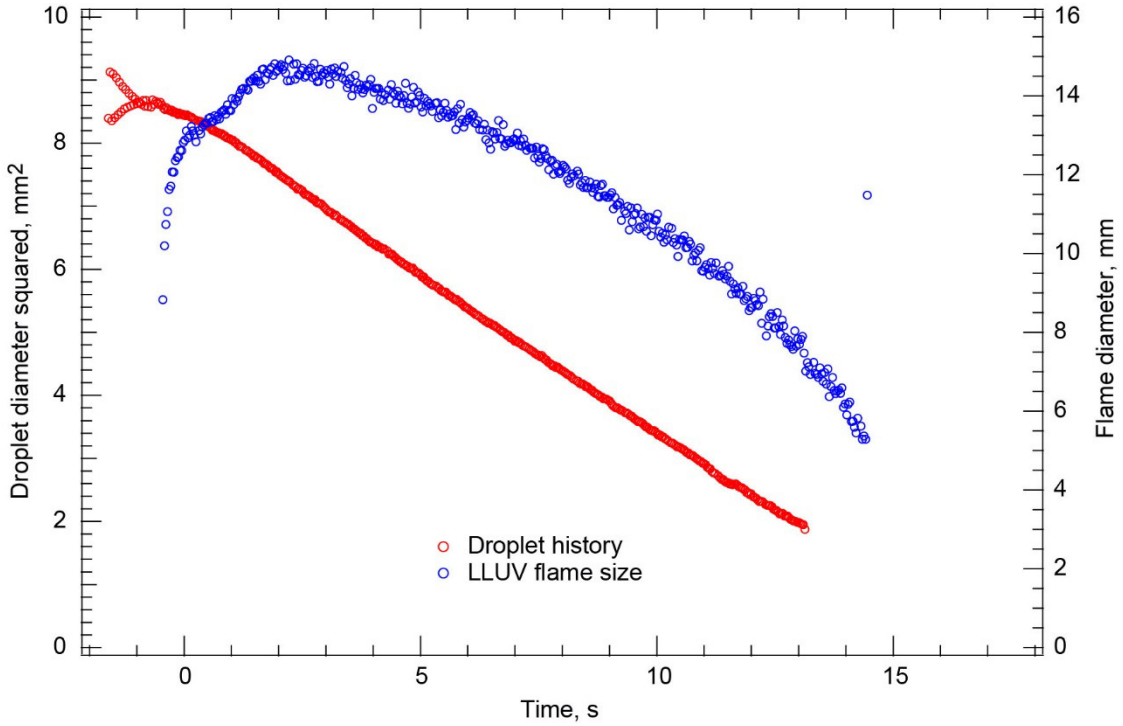

Figure 227.—Test FLEX–226. Free-floating methanol droplet burning in a 0.20/0.75/0.05 O_2/N_2/He, 1.0-atm ambient environment. The droplet was nearly motionless after deployment and ignition, but it began to drift southeast in the High-Bit-Depth Multispectral (HiBMs) field of view (FOV) a few seconds after ignition. The droplet drifted out of the HiBMs field of view (FOV), but it remained in the FOVs of the Low Light Level Ultra-Violet (LLUV) and color cameras. The color camera Image Processing and Storage Unit (IPSU) failed to record any images after deployment. The droplet burned for a relatively long time before the flame extinguished diffusively. The burning rate constant from a short period just prior to the droplet leaving the HiBMs FOV was used to extrapolate the extinction droplet diameter from the droplet history from the time that the droplet left the HiBMs FOV until the flame extinguished.

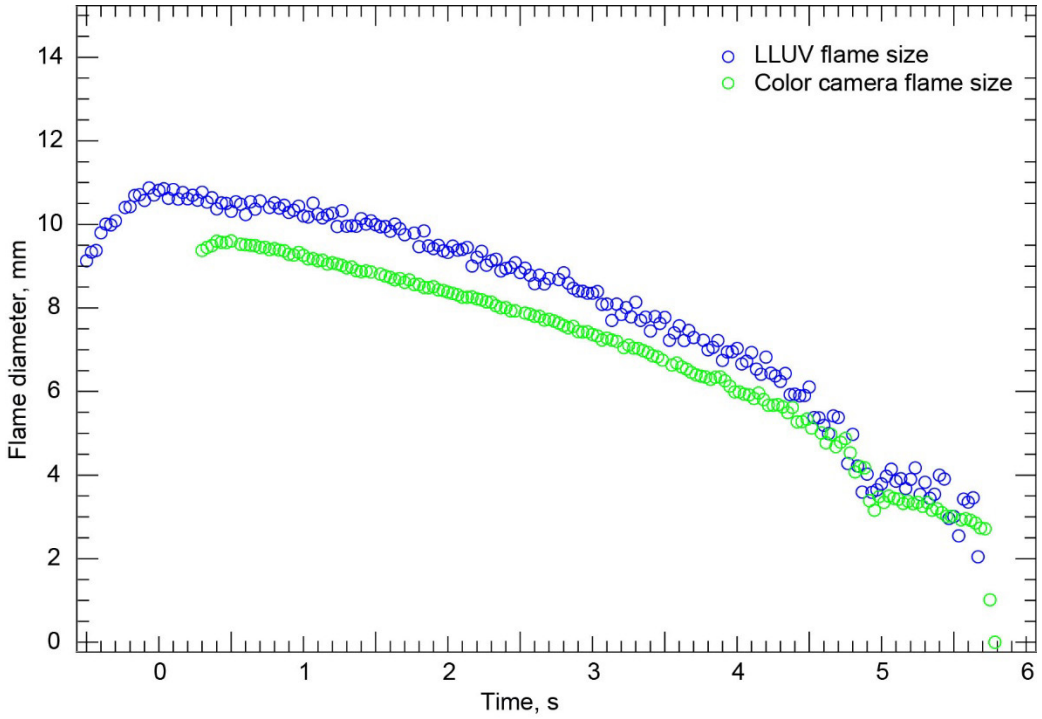

Figure 228.—Test FLEX–227. Free-floating methanol droplet in a 0.20/0.75.0.05 O_2/N_2/He, 1.0-atm ambient environment. The High-Bit-Depth Multispectral (HiBMs) Image Processing and Storage Unit (IPSU) failed to start, so no droplet data were recorded. The flame was bright and burned for over 5 s until it (presumably) extinguished diffusively.

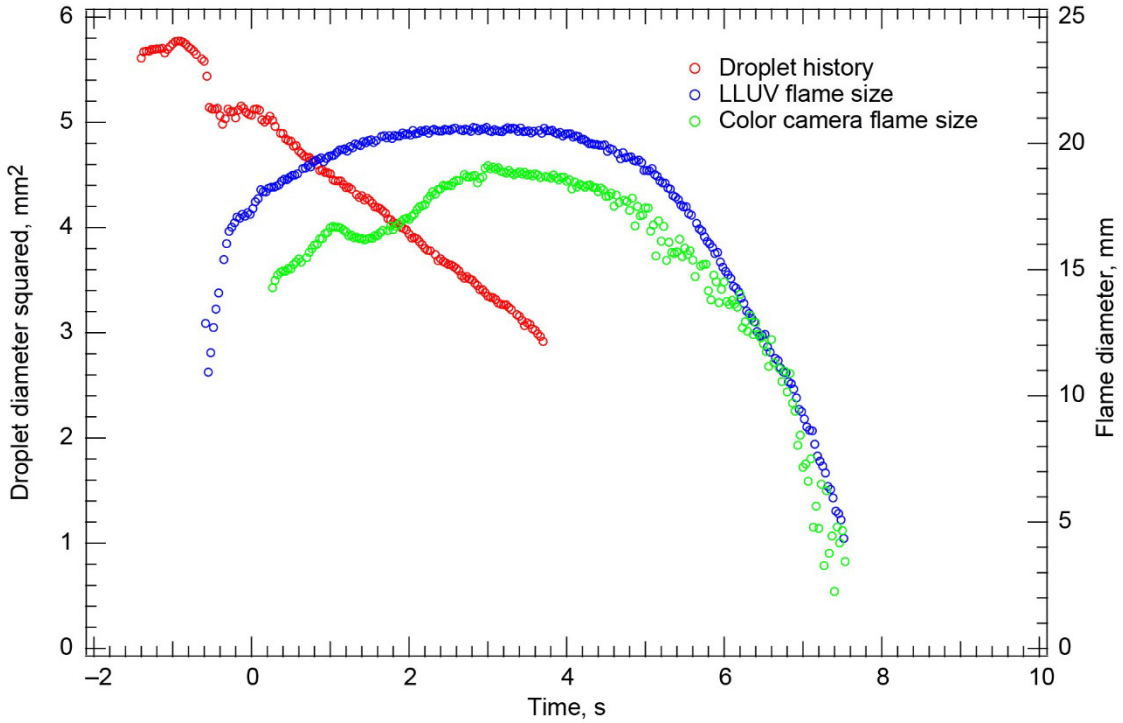

Figure 229.—Test FLEX–229. Free-floating heptane droplet burning in a 0.20/0.75.0.05 O_2/N_2/He, 1.0-atm ambient environment. The droplet drifted southeast after deployment in the High-Bit-Depth Multispectral (HiBMs) field of view (FOV), hit the igniter, and developed a large drift velocity to the east. The droplet drifted out of the FOV of the HiBMs and then out of the FOVs of the Low Light Level Ultra-Violet (LLUV) and color cameras before the flame either extinguished or burned out.

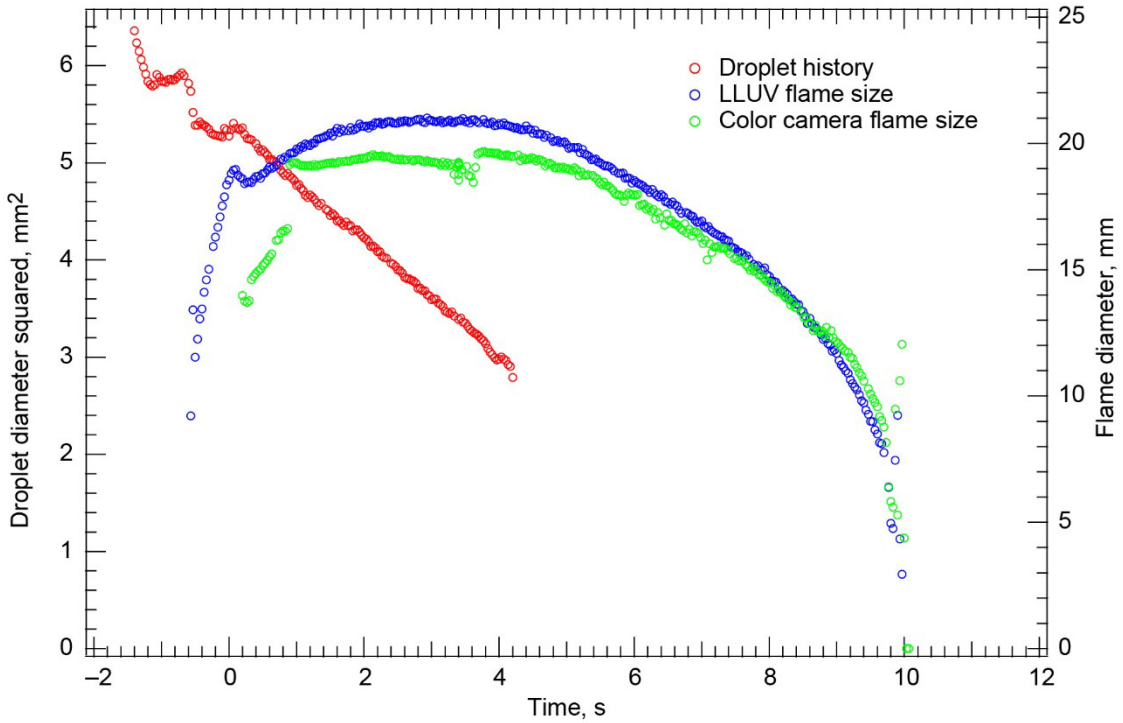

Figure 230.—Test FLEX–230. Free-floating heptane droplet burning in a 0.20/0375/0.05 O_2/N_2/He, 1.0-atm ambient environment. The droplet drifted southwest after deployment then hit the igniter and moved southwest in the High-Bit-Depth Multispectral (HiBMs) field of view (FOV). It left the HiBMs FOV about halfway through the burn. Because of soot, the droplet burned very brightly with a lot of luminosity. The soot diminished, and the flame burned with a dim blue flame that got brighter near the end of the burn. The droplet burned to a very small size and disrupted coincident with flame extinction.

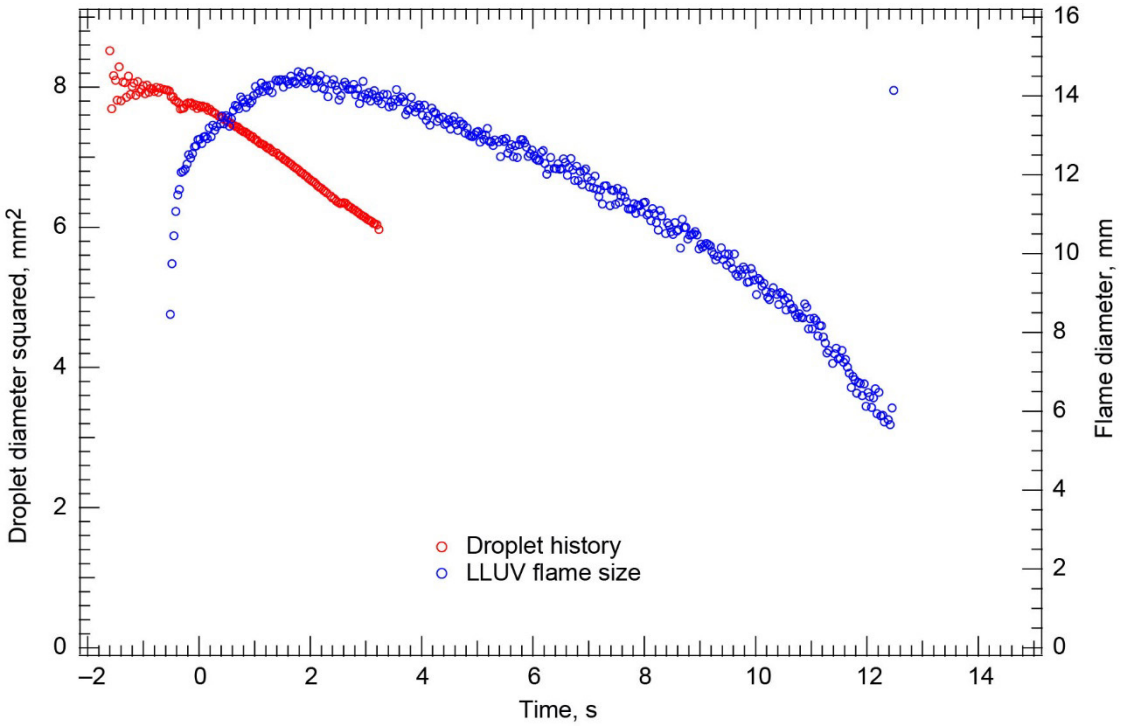

Figure 231.—Test FLEX–231. Free-floating methanol droplet burning in a 0.19/0.71/0.10 O_2/N_2/He, 1.0-atm ambient environment. The droplet had a pronounced drift south in the High-Bit-Depth Multispectral (HiBMs) field of view (FOV) after deployment; then it struck the igniter and continued to drift south and out of the HiBMs FOV about one-third of the way through the burn. The droplet burned for a relatively long time before the flame extinguished diffusively. The color camera Image Processing and Storage Unit (IPSU) did not record any images after deployment for this test. Also, because the droplet was in the HiBMs FOV for only a short fraction of the total test, no extinction droplet diameter is reported for this test.

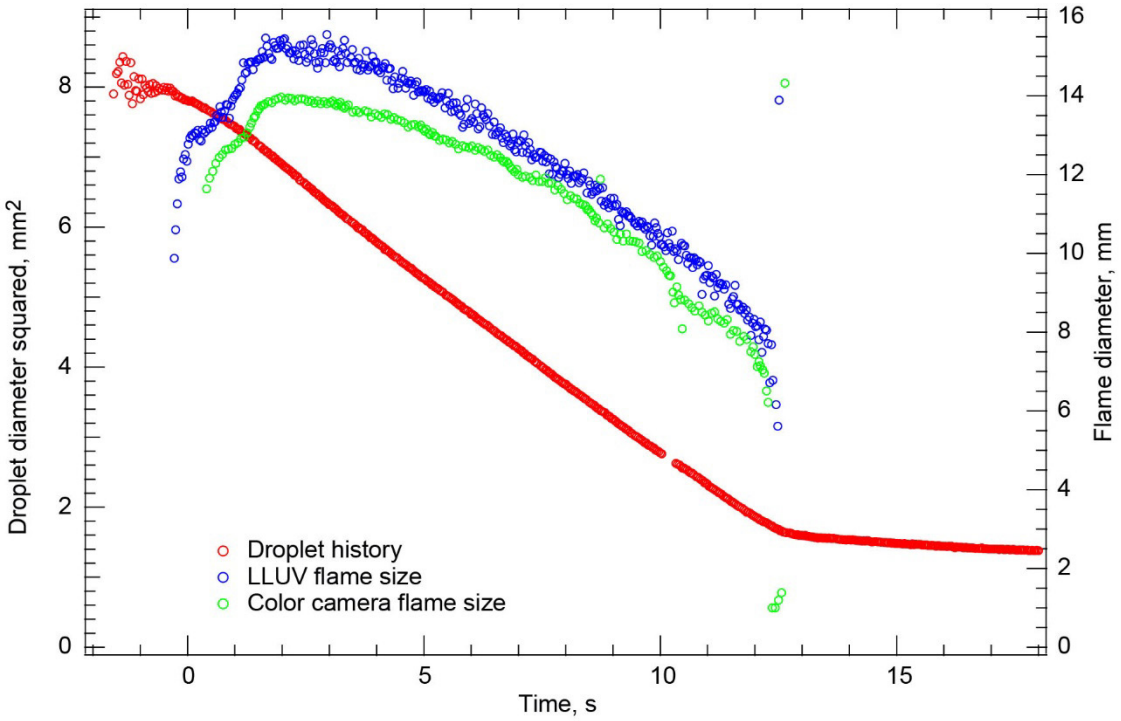

Figure 232.—Test FLEX–232. Free-floating methanol droplet burning in a 0.18/0.67/0.15 O_2/N_2/He, 1.0-atm ambient environment. The droplet slowly drifted south after deployment and ignition in the High-Bit-Depth Multispectral (HiBMs) field of view (FOV), but it never left the FOV. The flame extinguished diffusively with no disruption.

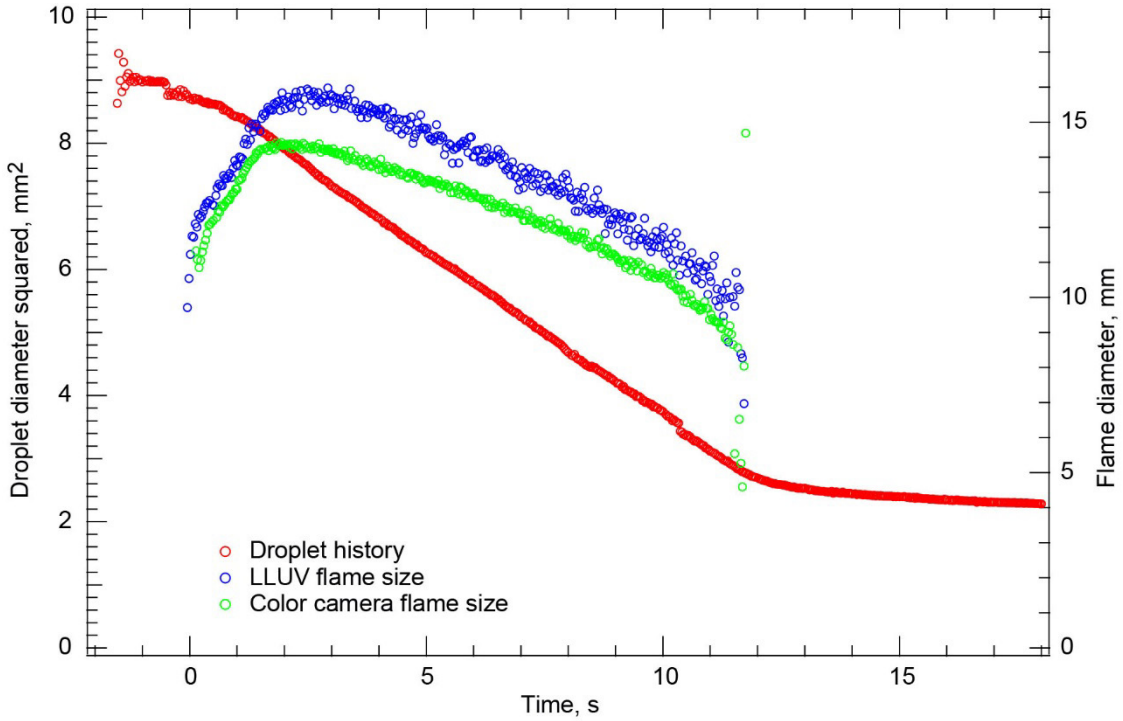

Figure 233.—Test FLEX–233. Fiber-supported methanol droplet burning in a 0.18/0.67/0.15 O_2/N_2/He, 1.0-atm ambient environment. After ignition, the droplet moved slowly and smoothly west on the fiber in the High-Bit-Depth Multispectral (HiBMs) field of view (FOV). The droplet drifted to the edge of the HiBMs FOV, but it remained in the FOV. There was some small oscillatory motion on the fiber, but the burn was relatively clean until the flame extinguished diffusively.

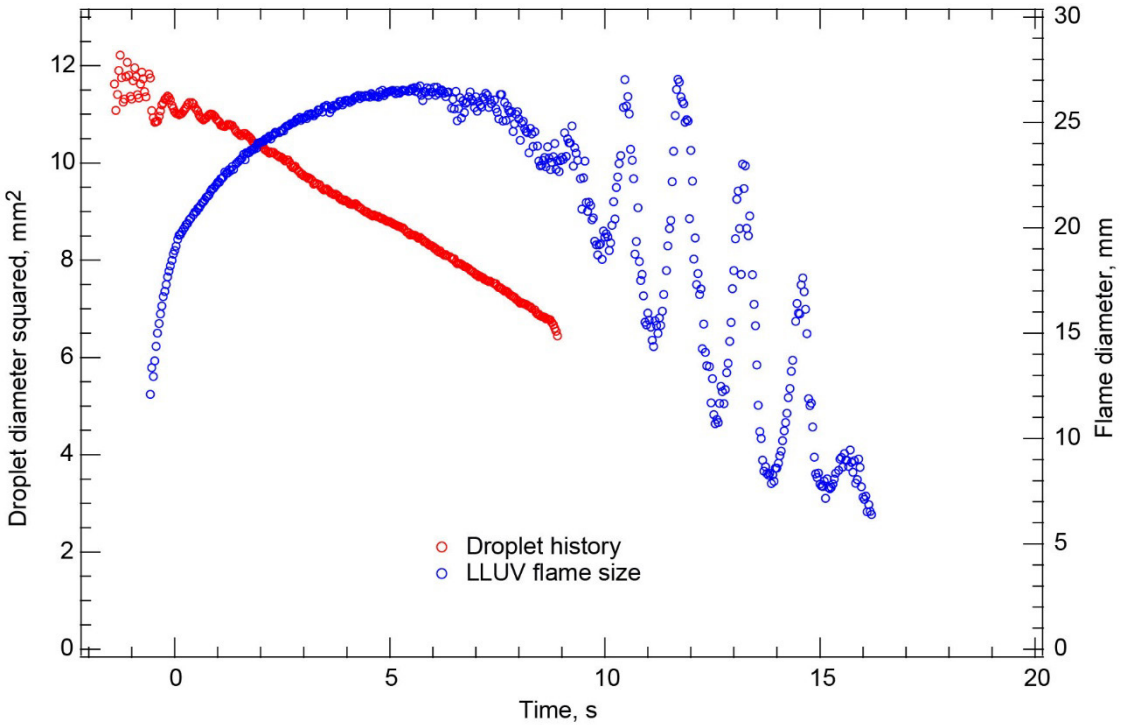

Figure 234.—Test FLEX–234. Free-floating heptane droplet burning in a cabin air (0.21/0.79 O_2/N_2), 1.0-atm ambient environment. The droplet drifted southeast and out of the High-Bit-Depth Multispectral (HiBMs) field of view (FOV) about halfway through the burn. The flame began to oscillate and then drifted south and out of the Low Light Level Ultra-Violet (LLUV) FOV before the flame extinguished. The color camera Image Processing and Storage Unit (IPSU) did not record any images during the burn. It is not clear whether the droplet continued to burn in the LLUV FOV or for how long it burned if it continued to burn. The oscillations were significant, but the flame appeared to decrease in size. From the radiometer, it appears that the droplet burned with a stable flame after the flame oscillations stopped.

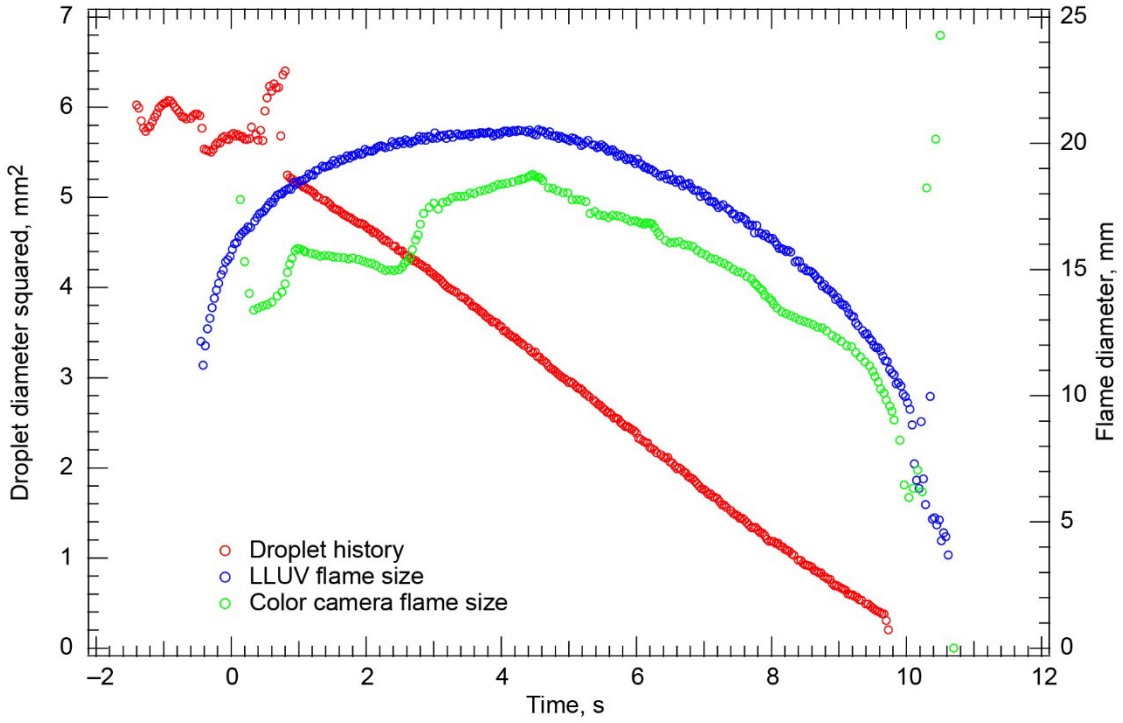

Figure 235.—Test FLEX–235. Free-floating heptane droplet burning in a cabin air (0.21/0.79 O_2/N_2), 1.0-atm ambient environment. The droplet remained in the High-Bit-Depth Multispectral (HiBMs) field of view (FOV) for most of its lifetime. The droplet burned to a very small size, with a small disruption coincident with visible flame extinction.

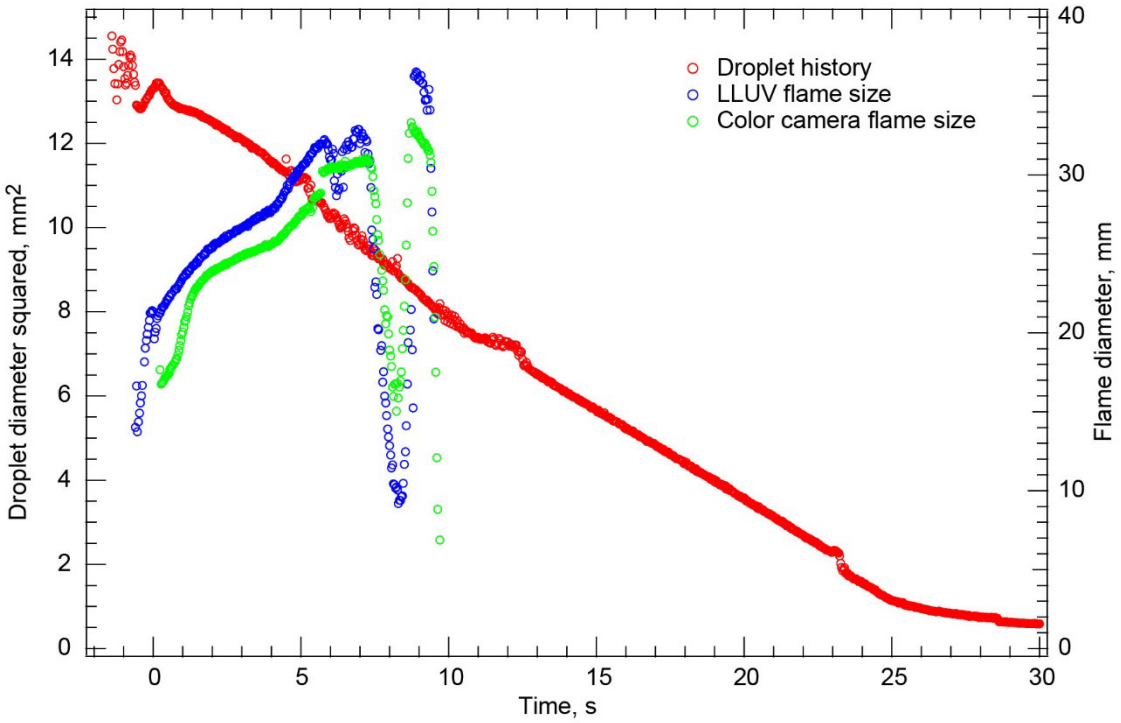

Figure 236.—Test FLEX–236. Fiber-supported heptane droplet burning in a cabin air (0.21/0.79 O_2/N_2), 1.0-atm ambient environment. The droplet oscillated on the fiber throughout the burn, but it remained in the High-Bit-Depth Multispectral (HiBMs) field of view (FOV). Large soot agglomerates interfered with the measurement of droplet size for a portion of the burn. The flame extinguished radiatively after a very long, slow, high-amplitude oscillation. This was followed by rapid vaporization and the formation of a vapor cloud coincident with the plateau. The droplet moved during the vaporization, but this did not seem to impact the size measurement significantly. There was a small disruption near the end of the vaporization and a small jump in droplet size—maybe a gas bubble that burst. A cool flame and cool flame extinction probably followed the visible flame extinction.

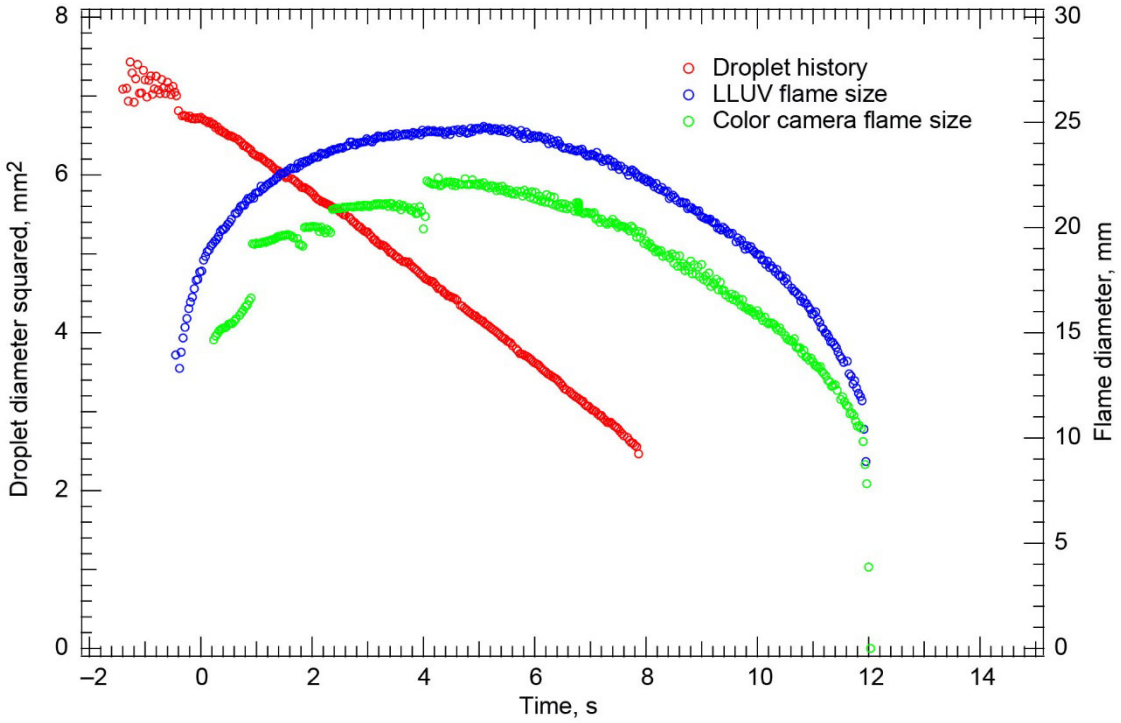

Figure 237.—Test FLEX–237. Free-floating heptane droplet burning in a 0.19/0.71/0.10 O_2/N_2/He, 1.0-atm ambient environment. The droplet drifted north in the High-Bit-Depth Multispectral (HiBMs) field of view (FOV) after deployment and ignition and just out of the FOV before the flame extinguished and disrupted. There may have been a disruption coincident with when the flame extinguished.

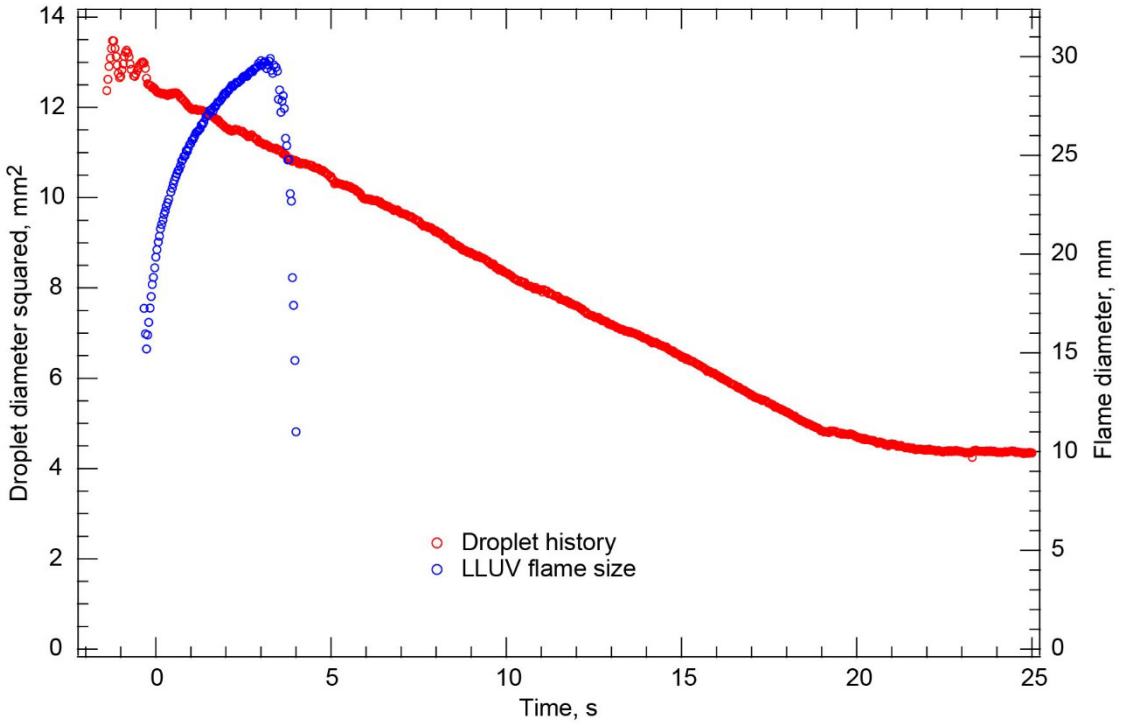

Figure 238.—Test FLEX–238. Free-floating heptane droplet burning in a 0.18/0.67/0.15 O_2/N_2/He, 1.0-atm ambient environment. The droplet was almost motionless after deployment and ignition. This was a large droplet, and it remained in High-Bit-Depth Multispectral (HiBMs) field of view (FOV) for the entire test. After ignition, the flame grew but became increasingly dimmer, and it quickly extinguished because of radiative loss. After the visible flame extinguished, the droplet continued to vaporize at almost the same rate well after the flame extinguished when a plateau occurred coincident with the formation of a large vapor cloud. Both phenomena indicate cool flame burning and extinction after visible flame extinction. The color camera Image Processing and Storage Unit (IPSU) did not record any images after deployment.

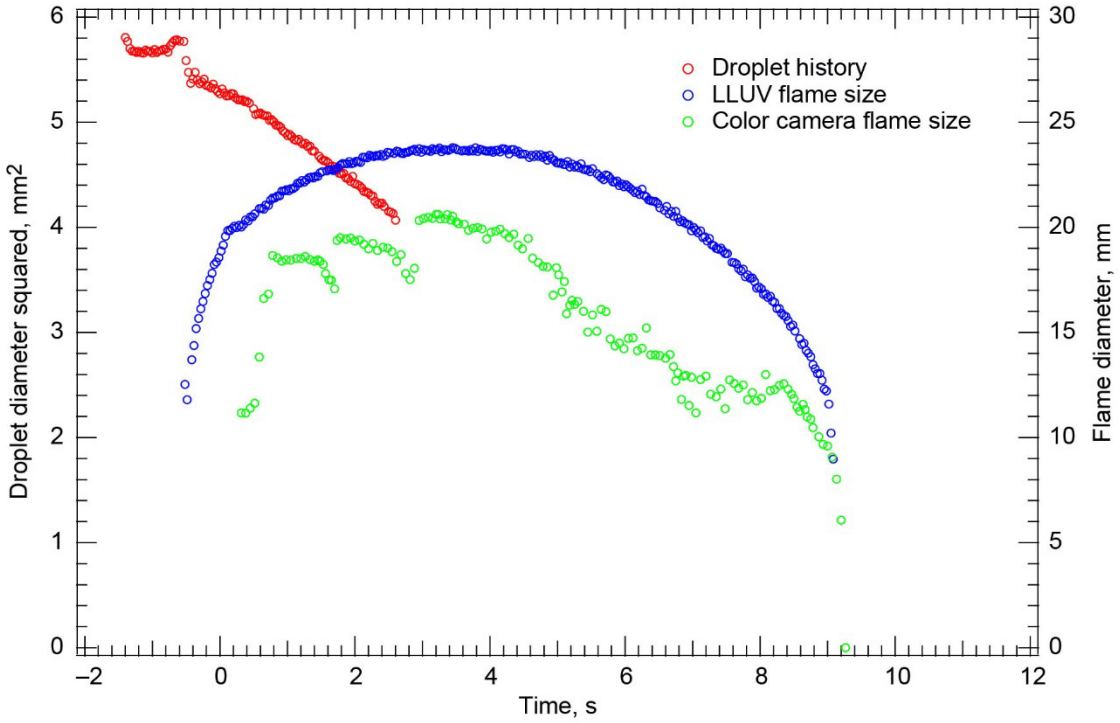

Figure 239.—Test FLEX–239. Free-floating heptane droplet burning in a 0.18/0.67/0.15 O_2/N_2/He, 1.0-atm ambient environment. The droplet drifted north after deployment and ignition and out of the High-Bit-Depth Multispectral (HiBMs) field of view (FOV) one-third of the way through the burn. The flame remained in the FOV of both the Low Light Level Ultra-Violet (LLUV) and color camera for the duration of the burn. Initially, soot oxidation caused the flame to be bright and very luminous, but quickly the flame became a dimmer blue. The luminosity increased slightly as the flame approached extinction. Because the droplet was out of the HiBMs FOV for the majority of the test, no extinction diameter is reported.

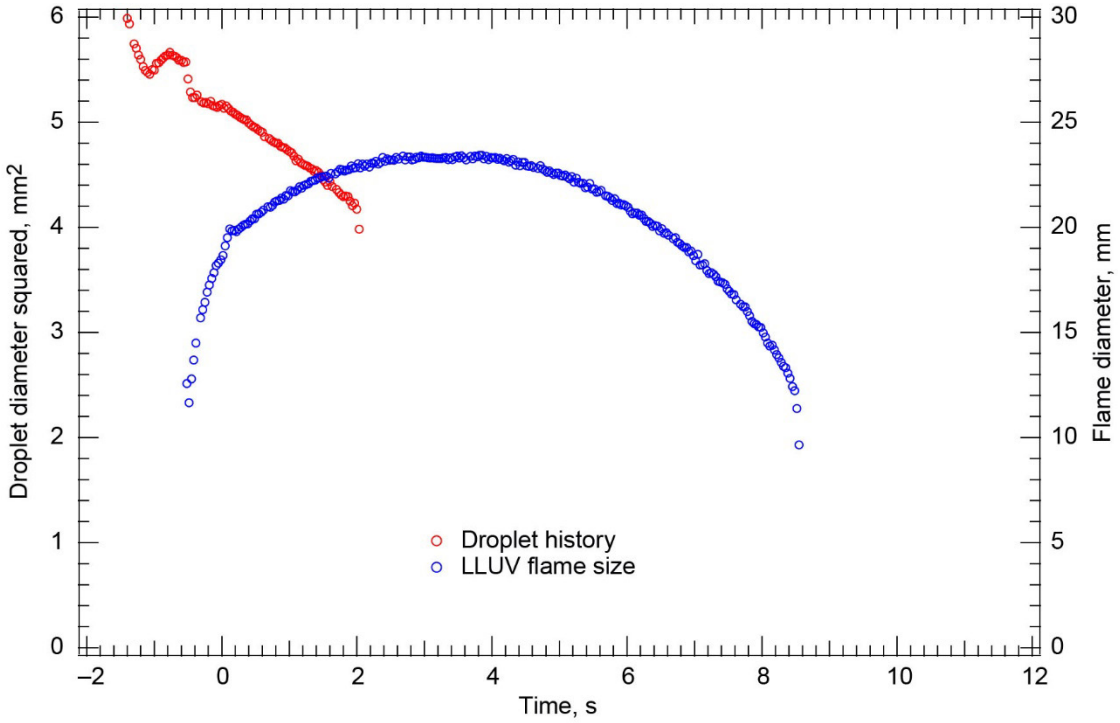

Figure 240—Test FLEX–240. Free-floating heptane droplet burning in a 0.18/0.67/0.15 O_2/N_2/He, 1.0-atm ambient environment. The droplet drifted north after deployment and ignition and out of the High-Bit-Depth Multispectral (HiBMs) field of view (FOV) about one-fourth of the way through the burn. The drift velocity was relatively high, and the flame was brighter on the leading edge in the direction of the drift. The droplet did remain in the FOVs of the Low Light Level Ultra-Violet (LLUV) and color camera. Because the droplet was in the HiBMs FOV for only a small fraction of the burn, no extinction diameter is reported for this test. The color camera Image Processing and Storage Unit (IPSU) did not record any images after deployment for this test.

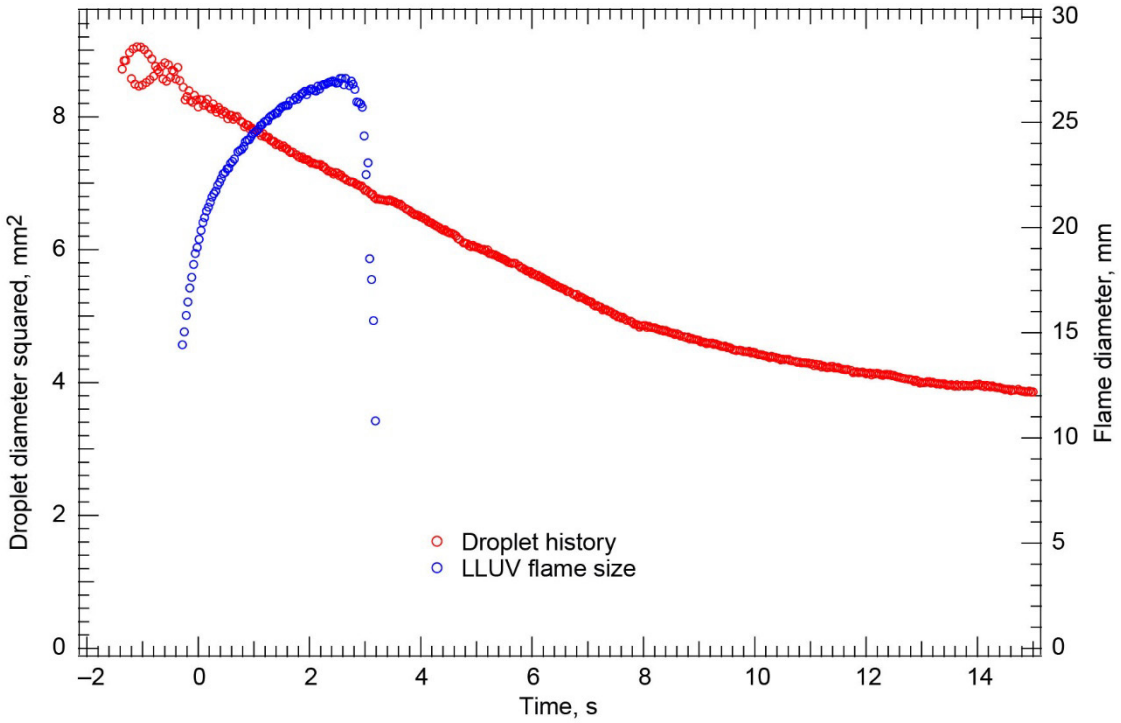

Figure 241.—Test FLEX–241. Free-floating heptane droplet burning in a 0.17/0.63/0.20 O_2/N_2/He, 1.0-atm ambient environment. The droplet had almost no drift after deployment and ignition, and it remained in the High-Bit-Depth Multispectral (HiBMs), Low Light Level Ultra-Violet (LLUV), and color camera fields of view (FOVs) with little motion throughout the Image Processing and Storage Unit (IPSU) recording time. The flame extinguished radiatively, and there was a brief period after the visible flame extinguished in which the droplet continued to vaporize at a nearly constant rate, indicating that there was a cool flame after the visible flame extinguished. The color camera IPSU did not record any images after deployment.

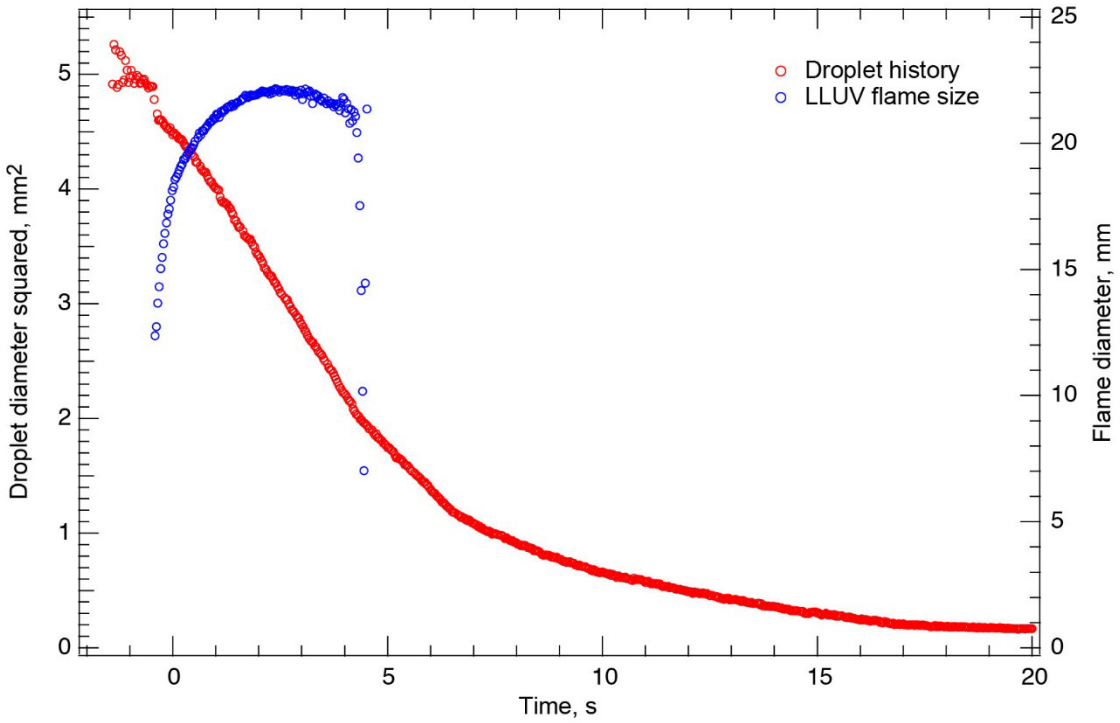

Figure 242.—Test FLEX−242. Free-floating heptane droplet burning in a 0.17/0.63/0.20 O_2/N_2/He, 1.0-atm ambient environment. The droplet had almost no drift after deployment and ignition, moving slightly to the southeast in the High-Bit-Depth Multispectral (HiBMs) field of view (FOV) but remaining in the FOV of all the cameras for the entire test. The color camera Image Processing and Storage Unit (IPSU) failed to record any images after deployment. The flame extinguished after approximately 5 s, and extinction was probably followed by cool flame burning and extinction.

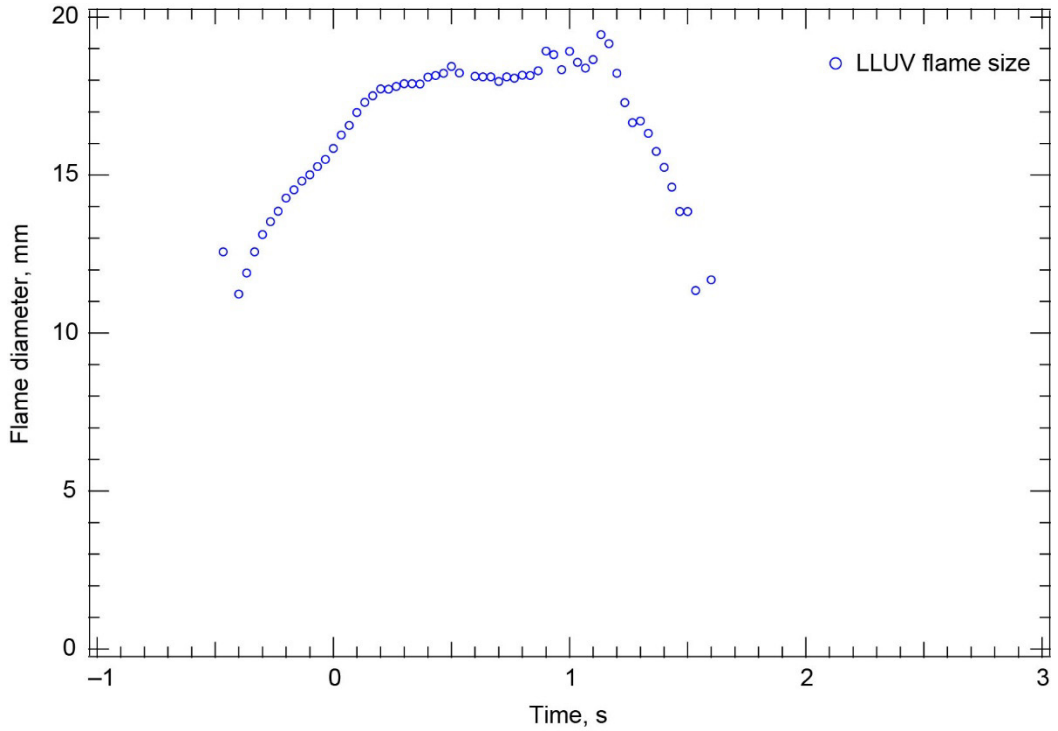

Figure 243.—Test FLEX−243. Fiber-supported heptane droplet burning in a 0.17/0.63 O_2/N_2, 1.0-atm ambient environment. Neither the High-Bit-Depth Multispectral (HiBMs) or color camera Image Processing and Storage Units (IPSUs) recorded any images for this test. The droplet burned for a short time to disruption.

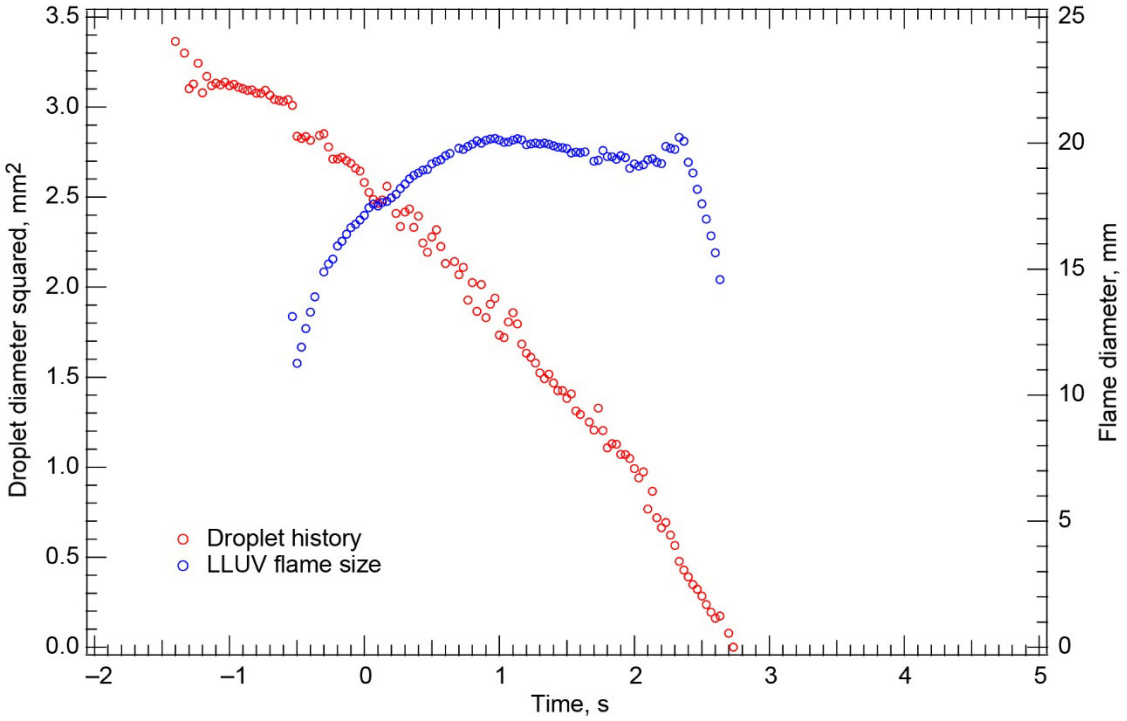

Figure 244.—Test FLEX–244. Fiber-supported heptane droplet burning in a 0.17/0.63/0.20 O_2/N_2/He, 1.0-atm ambient environment. This was a smaller droplet. After ignition, there was a lot of motion on the fiber. It was not really disruptive burning, in which the droplet becomes dislodged from the fiber, but the motion clearly influenced the burning history. The droplet burned to completion, and the color camera did not record to the onboard Image Processing and Storage Unit (IPSU) for this test.

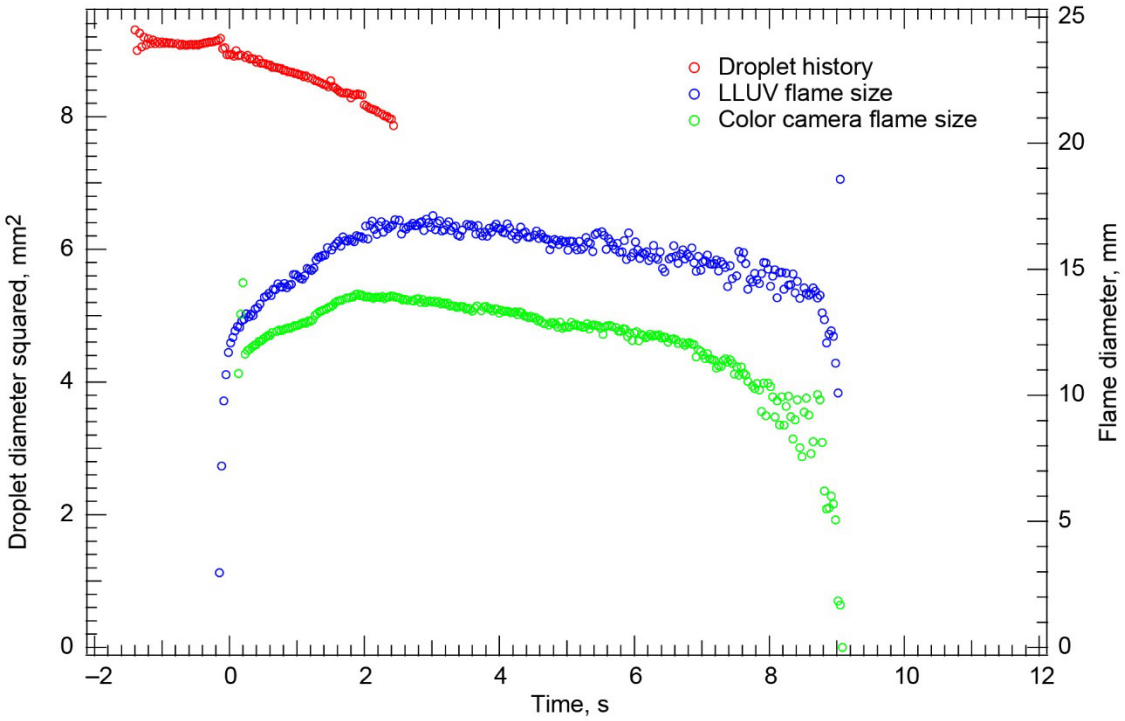

Figure 245.—Test FLEX–245. Free-floating methanol droplet in a 0.17/0.63/0.20 O_2/N_2/He, 1.0-atm ambient environment. The droplet had a strong north to northeast drift after deployment, nearly hitting the igniter before it withdrew. The droplet had a relatively high drift velocity after ignition and only remained in the High-Bit-Depth Multispectral (HiBMs) field of view (FOV) for one-fourth of the burn. Because the droplet was in the FOV for only a short time, no extinction diameter is reported. The flame extinguished diffusively.

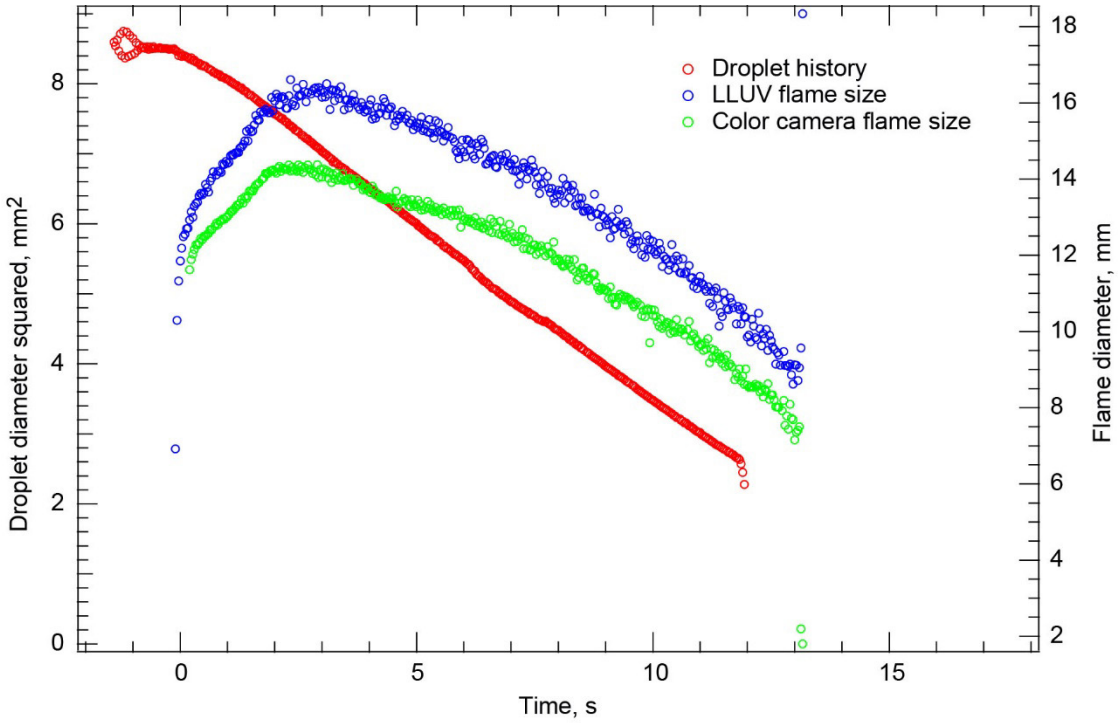

Figure 246.—Test FLEX–246. Free-floating methanol droplet burning in a 0.17/0.63/0.20 O_2/N_2/He, 1.0-atm ambient environment. The droplet had almost no drift after deployment and ignition, but shortly into the burn it developed a slow drift northeast then east in the color camera field of view (FOV). The droplet left the High-Bit-Depth Multispectral (HiBMs) FOV near diffusive flame extinction. The measured burning rate constant while the droplet was in the HiBMs FOV was used to extrapolate the extinction droplet diameter from the droplet history from the time that the droplet left the HiBMs FOV until the flame extinguished. The diameter should be reasonably accurate because the flame extinguished only a short time after it left the HiBMs FOV.

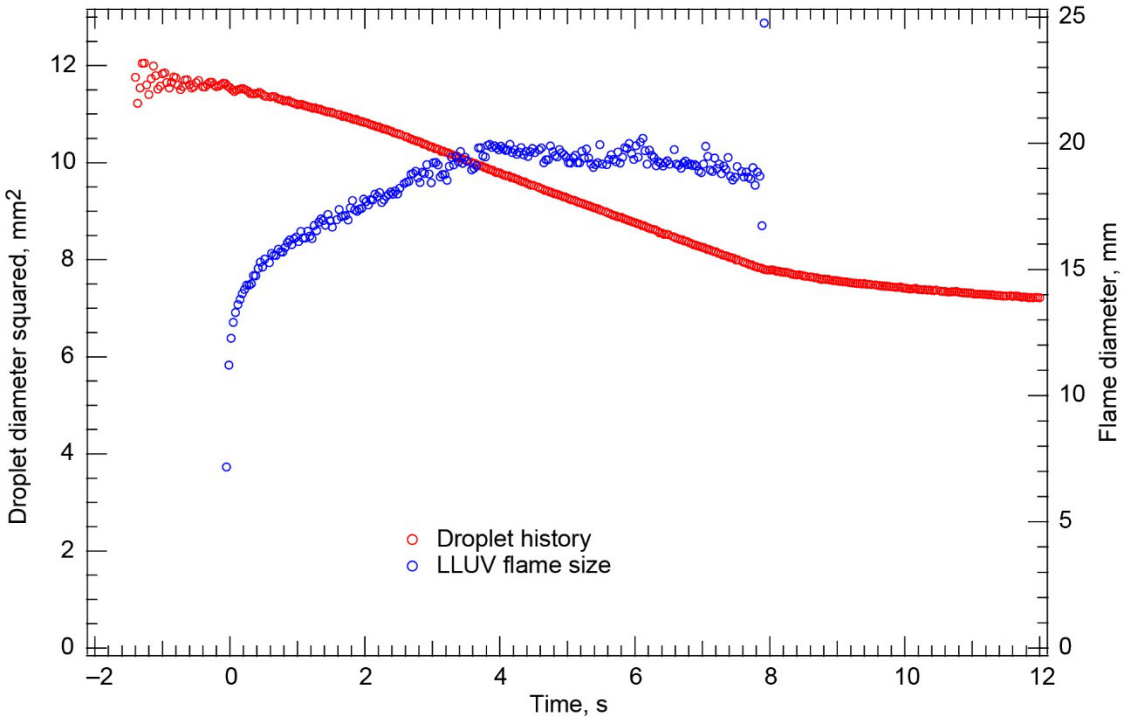

Figure 247.—Test FLEX–247. Free-floating methanol droplet burning in a 0.16/0.59/0.25 O_2/N_2/He, 1.0-atm ambient environment. The droplet was nearly motionless after deployment and ignition, and it remained in the fields of view (FOVs) of all the cameras for the entire recording time. It is difficult to say whether the flame extinguished diffusively or radiatively. It was probably near the flammability boundary. The color camera Image Processing and Storage Unit (IPSU) failed to record any images after deployment.

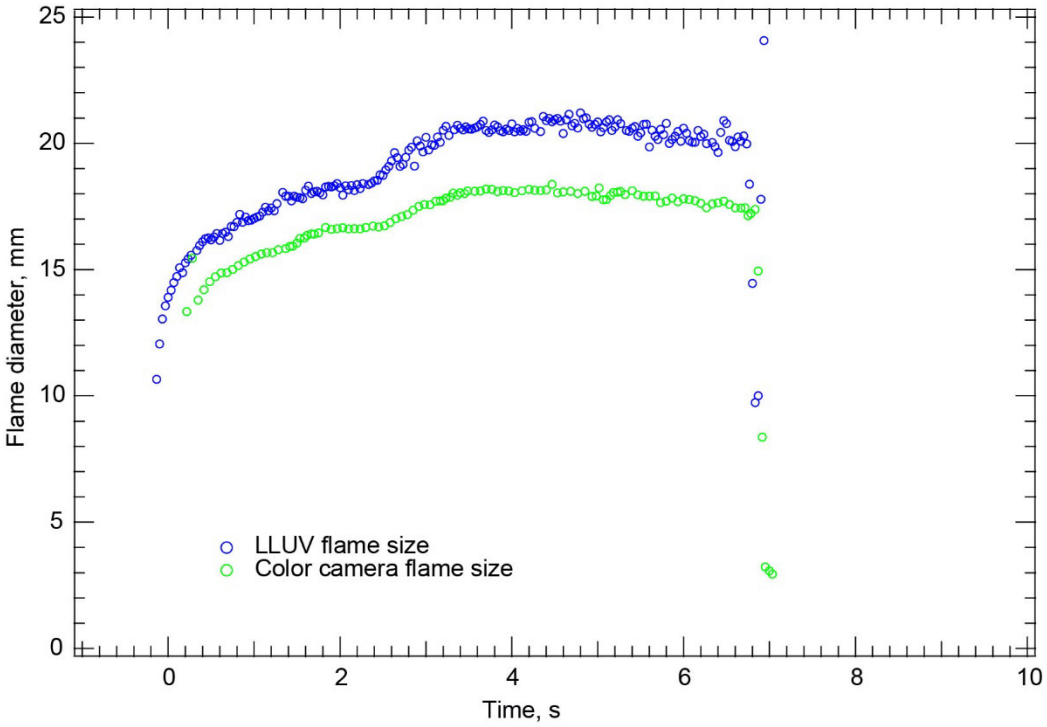

Figure 248.—Test FLEX−248. Free-floating methanol droplet burning in a 0.16/0.59/0.25 O_2/N_2/He, 1.0-atm ambient environment. The High-Bit-Depth Multispectral (HiBMs) Image Processing and Storage Unit (IPSU) did not record any images for this test. There was only a very small drift south in color camera field of view (FOV), but the droplet remained in the FOV for the entire test (as well as the Low Light Level Ultra-Violet (LLUV) FOV). The droplet burned to extinction.

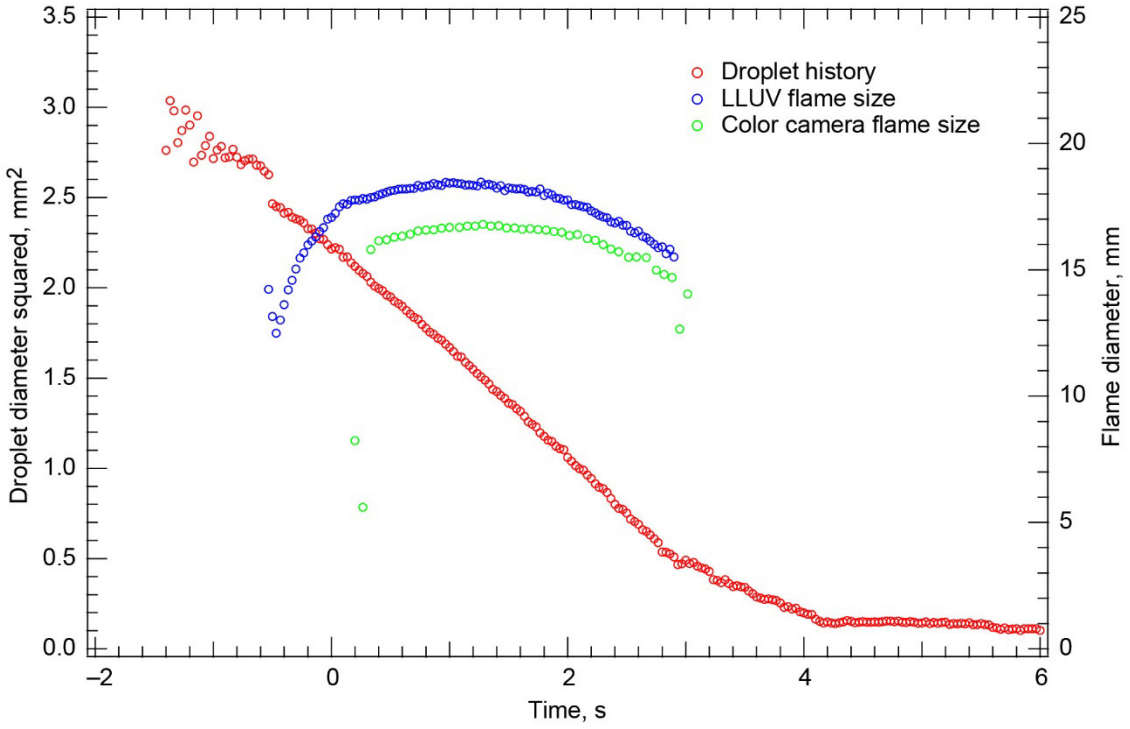

Figure 249.—Test FLEX–249. Free-floating heptane droplet burning in a 0.16/0.59/0.25 O_2/N_2/He, 1.0-atm ambient environment. This smaller droplet was nearly motionless after deployment and ignition, and it remained in the fields of view (FOVs) of all the cameras. The flame surrounding the droplet extinguished at a very small size, near the limit of what we can reasonably measure. The flame size was nearly constant throughout the burn, decreasing only slightly toward the end of the burn after increasing only slightly in size initially. The flame standoff increased linearly throughout the burn.

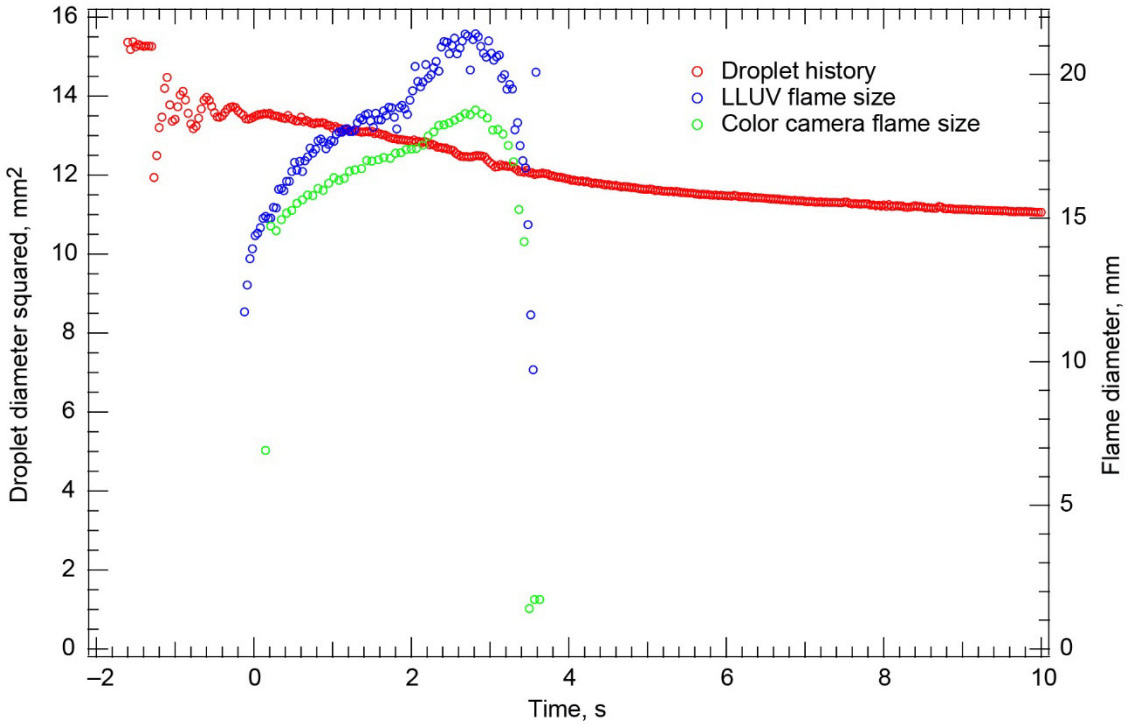

Figure 250.—Test FLEX–250. Fiber-supported methanol droplet burning in a 0.15/0.55/0.30 O_2/N_2/He, 1.0-atm ambient environment. There was a small amount of axial motion on the fiber, but it did not seem to influence the burning behavior to a large degree. This was a relatively short, transient burn, and the flame probably extinguished radiatively.

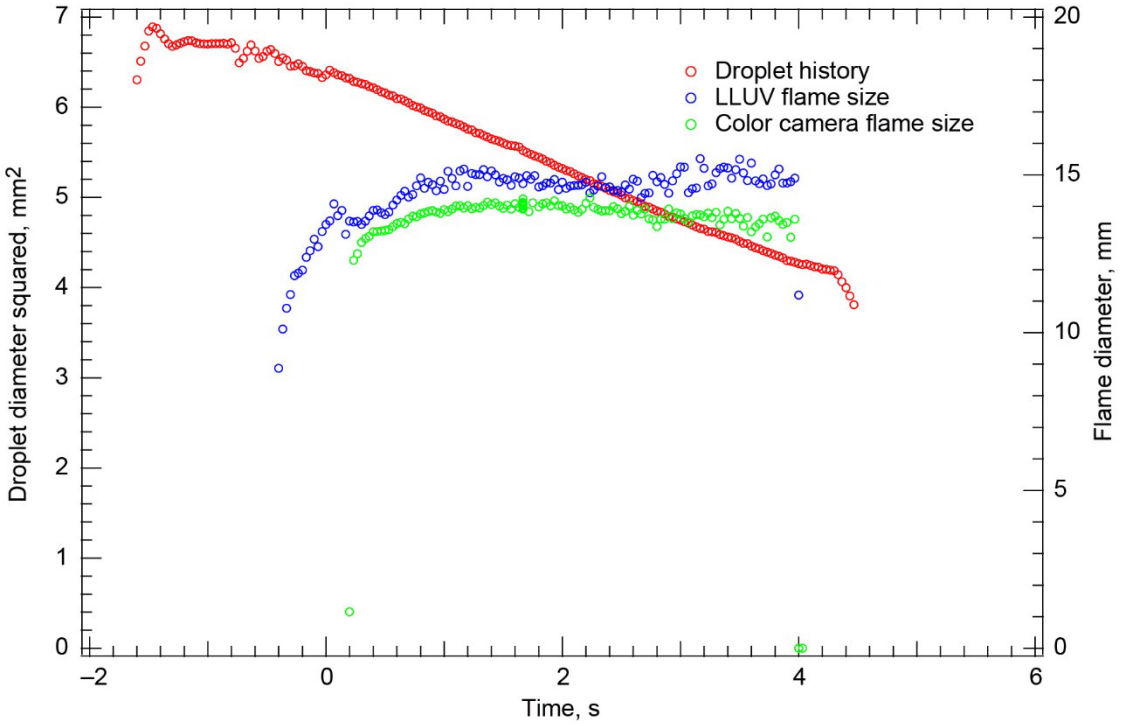

Figure 251.—Test FLEX–251. Free-floating methanol droplet burning in a 0.15/0.55/0.30 O_2/N_2/He, 1.0-atm ambient environment. The droplet drifted south in the High-Bit-Depth Multispectral (HiBMs) field of view (FOV) after deployment and ignition. It remained in the FOV for the duration of the burn, leaving shortly after the visible flame extinguished. This ambient environment was probably near the flammability boundary, so it is difficult to determine whether the flame extinguished diffusively or radiatively.

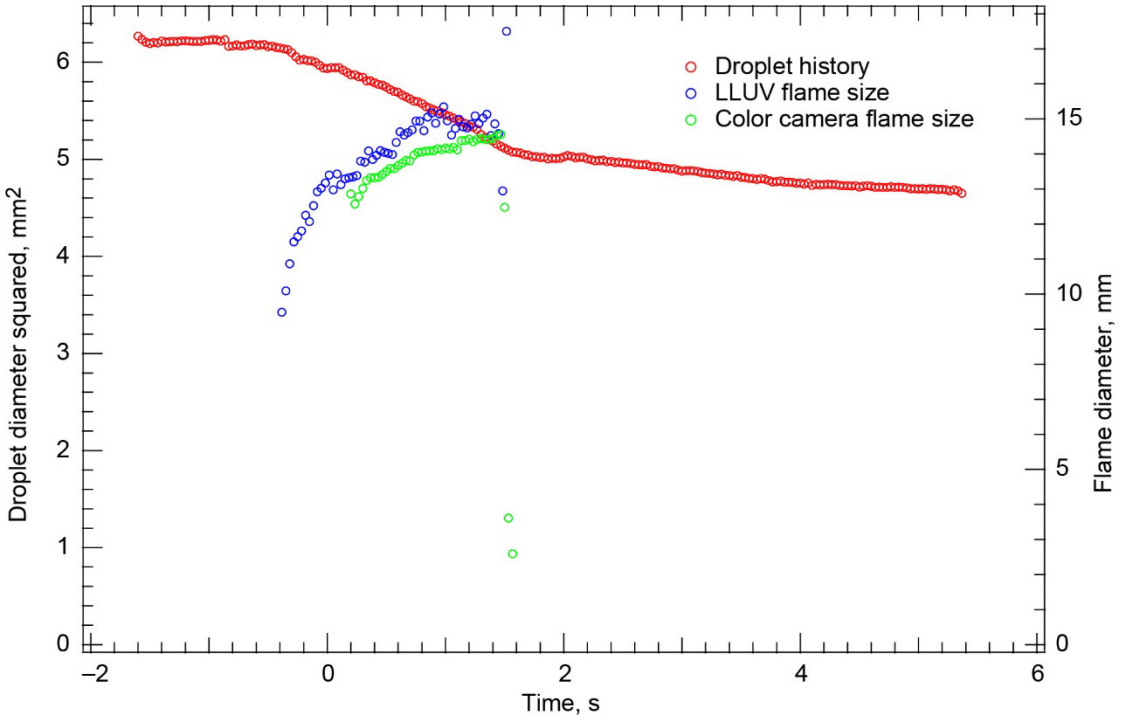

Figure 252.—Test FLEX−252. Free-floating methanol droplet burning in a 0.14/0.51/0.35 O_2/N_2/He, 1.0-atm ambient environment. After deployment and ignition, the droplet had a slow southeast drift in the High-Bit-Depth Multispectral (HiBMs) field of view (FOV). It left the HiBMs FOV well after the visible flame extinguished, but it drifted back into the HiBMs FOV before the end of the recording period. The droplet burned for a short time before the flame extinguished.

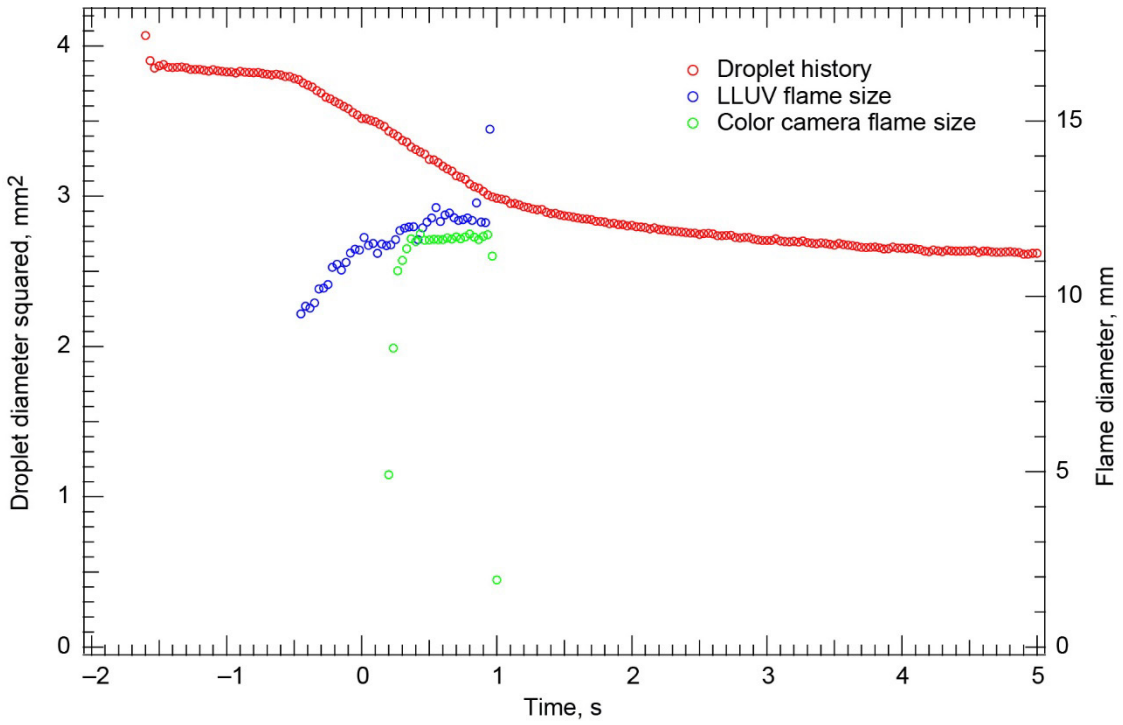

Figure 253.—Test FLEX–253. Free-floating methanol droplet burning in a 0.14/0.51/0.35 O_2/N_2/He, 1.0-atm ambient environment. The droplet was nearly motionless after deployment and ignition in the High-Bit-Depth Multispectral (HiBMs) field of view (FOV). It started to drift south as it burned, and it left the FOV well after the visible flame extinguished. The droplet burned for only a very short time, and the flame was very dim, almost undetectable in both the Low Light Level Ultra-Violet (LLUV) and color camera. The droplet was very near or even below the flammability limit.

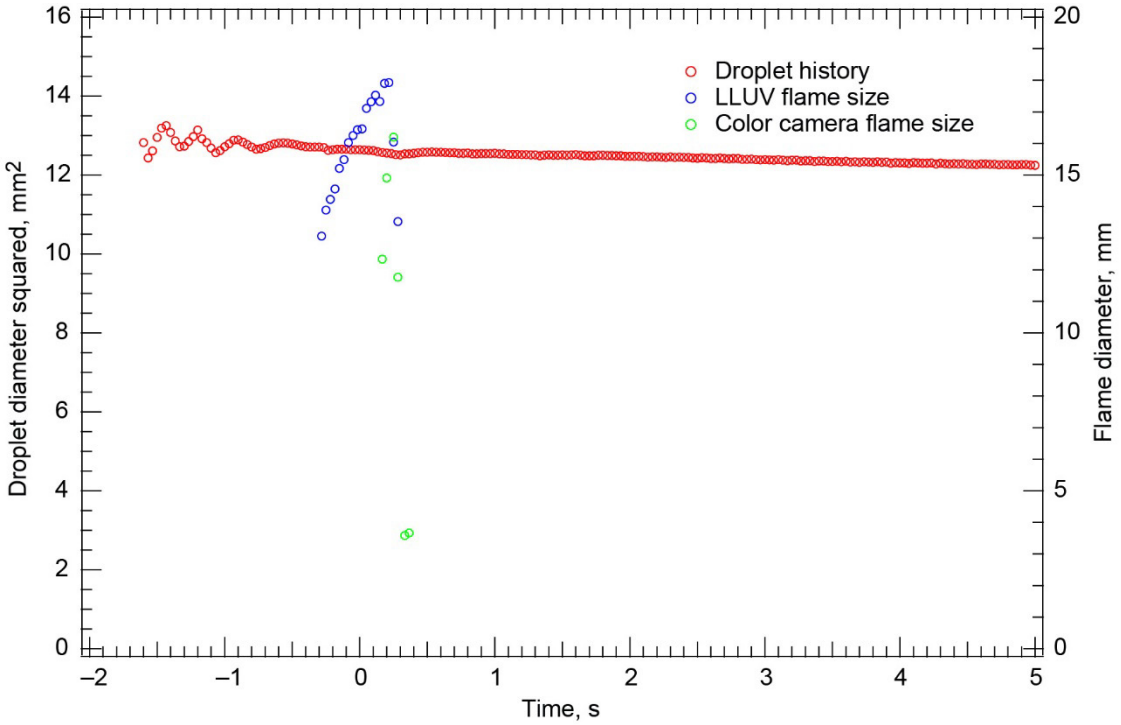

Figure 254.—Test FLEX–254. Free-floating methanol droplet burning in a 0.13/0.47/0.40 O_2/N_2/He, 1.0-atm ambient environment. The droplet remained in the High-Bit-Depth Multispectral (HiBMs) field of view (FOV) for the entire recording period. It had a very short burn to extinction. This was probably below the flammability limit.

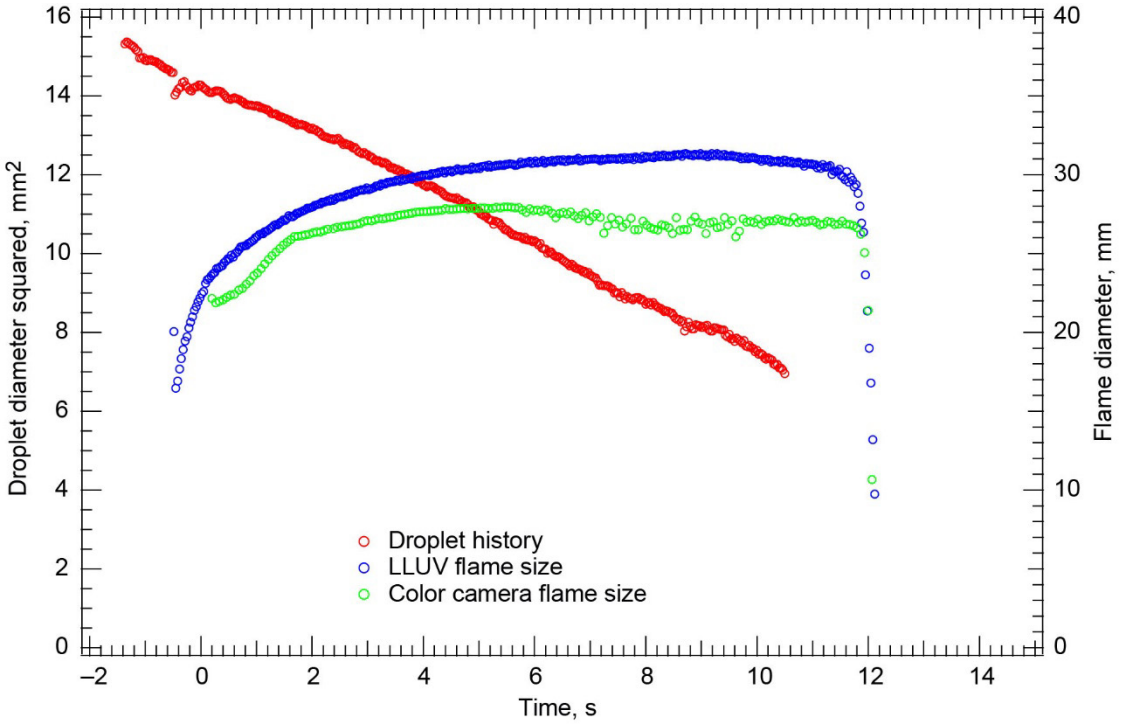

Figure 255.—Test FLEX–255. Free-floating heptane droplet burning in a 0.24/0.56/0.20 O_2/N_2/He, 0.70-atm ambient environment. The droplet drifted out of the High-Bit-Depth Multispectral (HiBMs) field of view (FOV) close to extinction, but it remained in the FOV of the Low Light Level Ultra-Violet (LLUV) and color camera FOVs. A small vapor cloud formed at extinction. There was noise in the analysis of the droplet image because soot particles that formed during combustion interfered with the analysis. It is not clear whether the visible extinction was radiative or diffusive or if there was a cool flame after the visible flame extinguished.

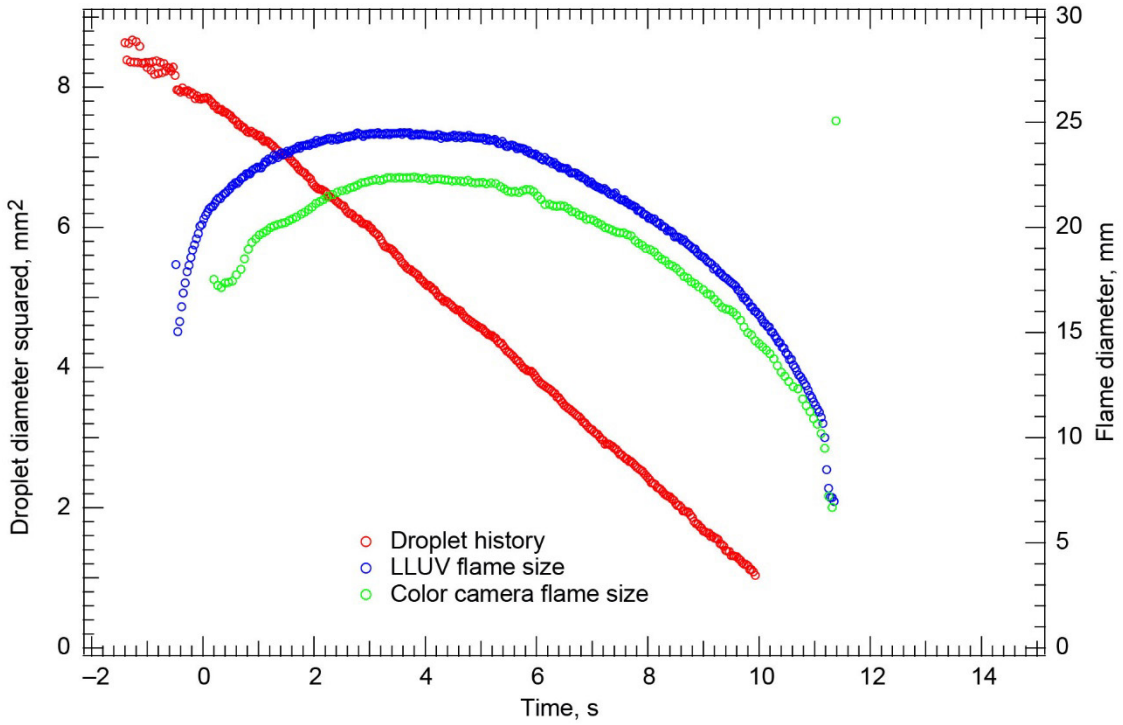

Figure 256.—Test FLEX–256. Free-floating heptane droplet burning in a 0.23/0.52/0.25 O_2/N_2/He, 0.70-atm ambient environment. The droplet drifted east after deployment and ignition in the High-Bit-Depth Multispectral (HiBMs) field of view (FOV), leaving the FOV just prior to extinction or burnout. The droplet burned to a very small size and then appeared to disrupt or rapidly change direction after the droplet left the HiBMs FOV. The measured burning rate constant was used to extrapolate the extinction droplet diameter from the droplet history from the time that the droplet left the FOV until the flame extinguished. The small droplet size at extinction suggests that the droplet burned almost to completion.

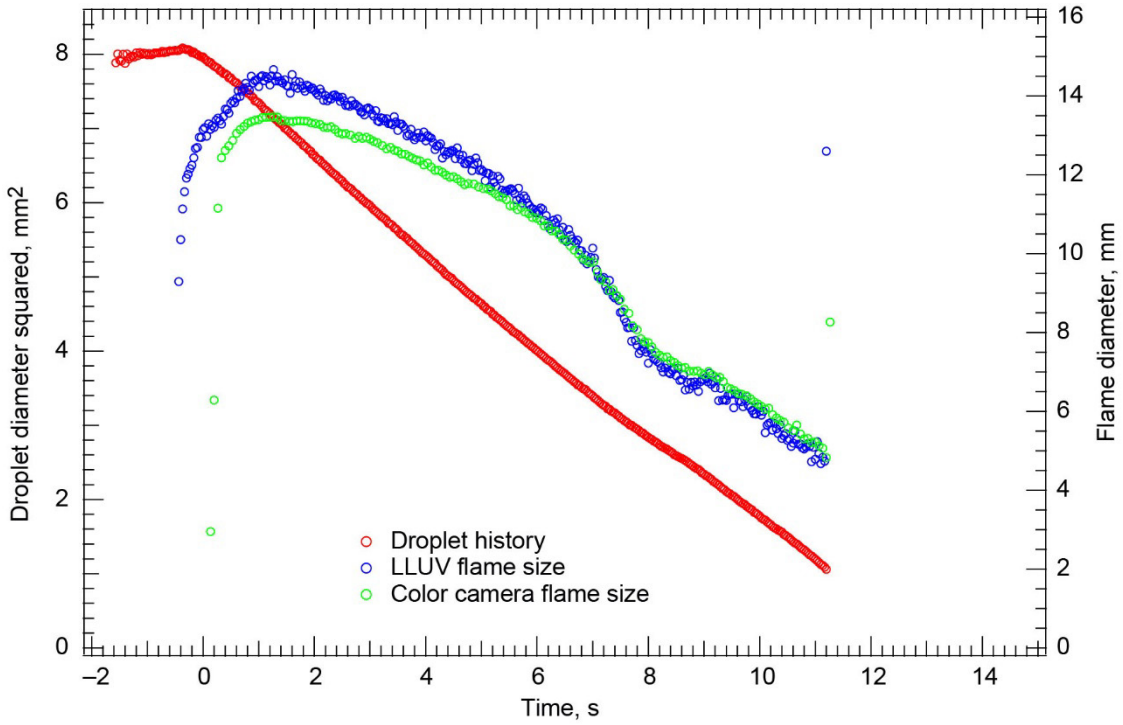

Figure 257.—Test FLEX–257. Free-floating methanol droplet burning in a 0.24/0.56/0.20 O_2/N_2/He, 0.70-atm ambient environment. The droplet drifted southeast in the High-Bit-Depth Multispectral (HiBMs) field of view (FOV) after deployment and ignition. It stopped briefly at the corner of the FOV and then disappeared from the FOV (there one frame, gone the next) at a time coincident with visible flame extinction. The droplet may have moved to just outside of the FOV after the flame extinguished. The droplet burned nicely to a diffusive extinction. The extinction droplet diameter is the droplet diameter in the frame just before the droplet disappeared.

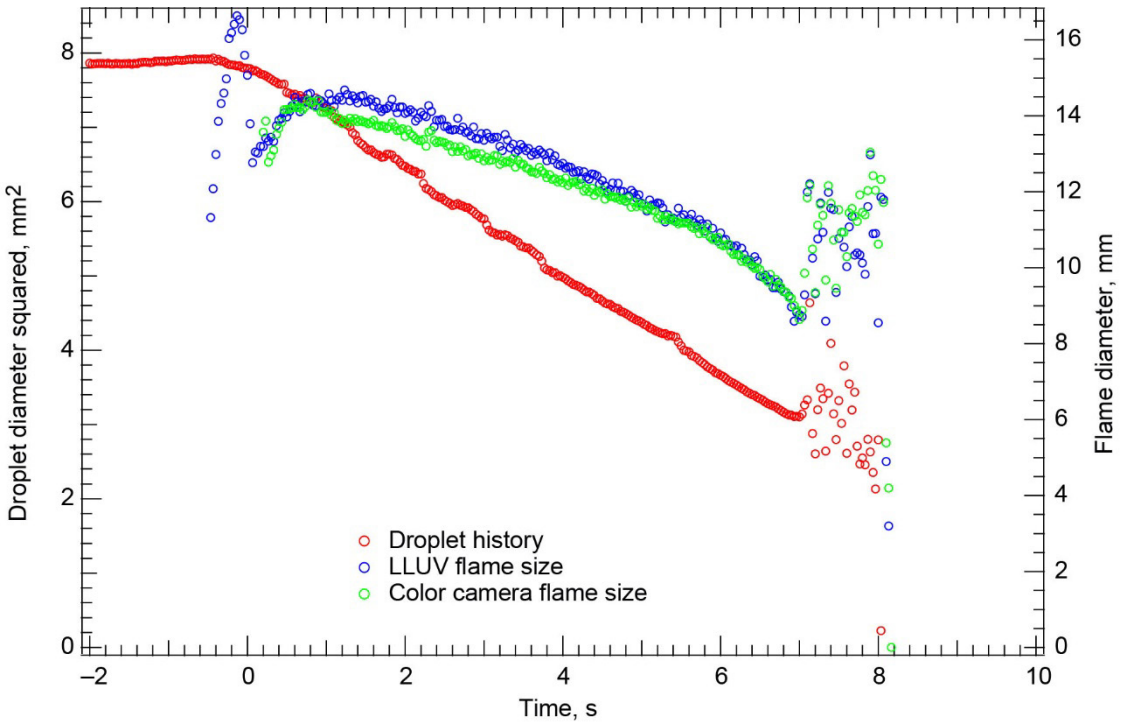

Figure 258.—Test FLEX–258. Fiber-supported methanol droplet burning in a 0.24/0.56/0.20 O_2/N_2/He, 0.70-atm ambient environment. The droplet remained in the High-Bit-Depth Multispectral (HiBMs) field of view (FOV), but there was a lot of motion on the fiber. Eventually the droplet disrupted and dislodged from the fiber. Because of the disruption, no extinction droplet diameter is reported.

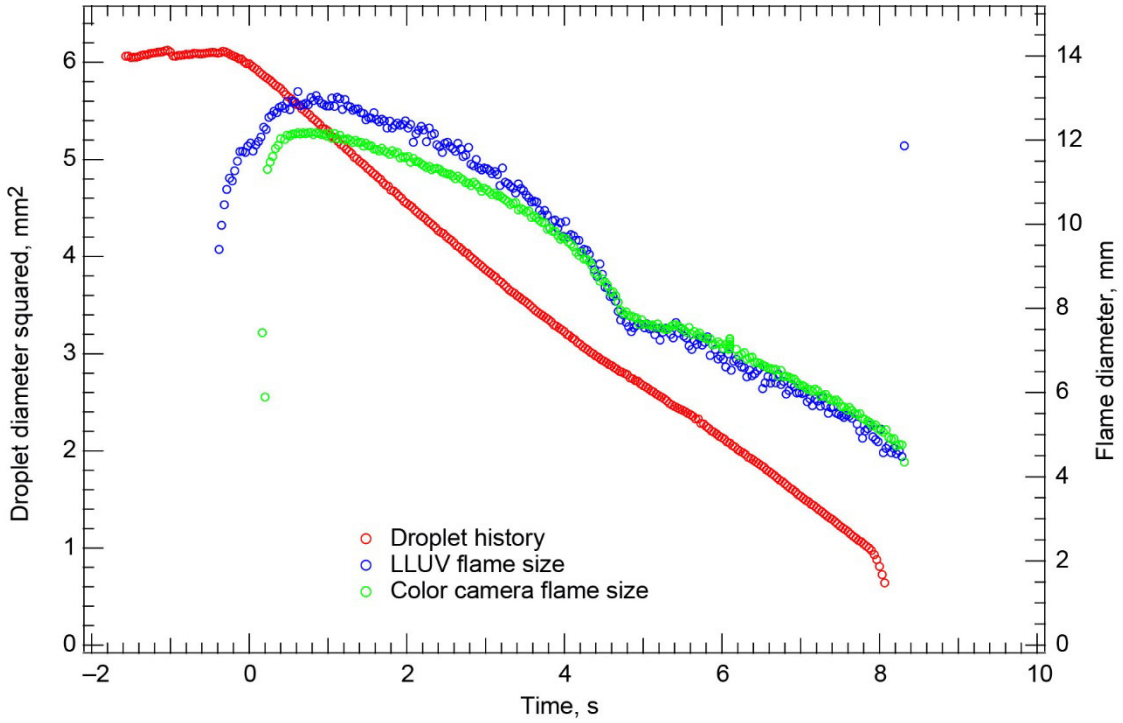

Figure 259.—Test FLEX–259. Free-floating methanol droplet in a 0.23/0.52/0.25 O_2/N_2/He, 0.70-atm ambient environment. The droplet drifted southeast in the High-Bit-Depth Multispectral (HiBMs) field of view (FOV) after ignition and out of the FOV near diffusive extinction. The burning rate constant from the last part of the burn while the droplet was in the FOV was used to extrapolate the extinction droplet diameter from the droplet history from the time that the droplet left the HiBMs FOV until the visible flame extinguished.

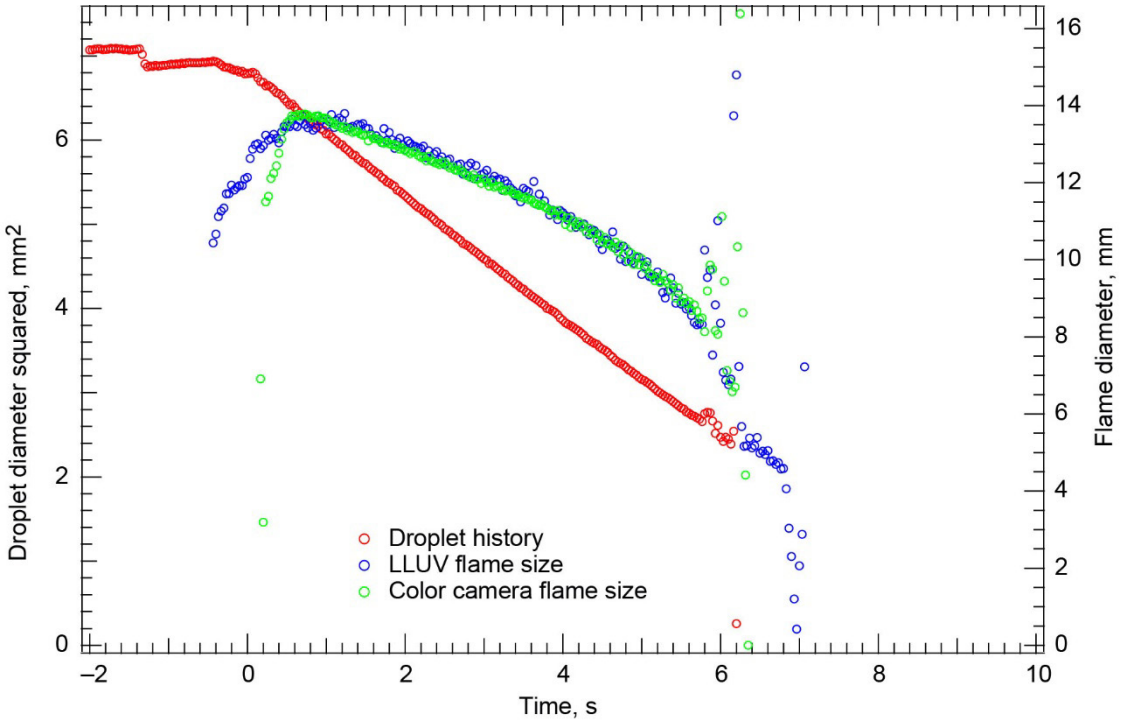

Figure 260.—Test FLEX–260. Fiber-supported methanol droplet burning in a 0.23/0.52/0.25 O_2/N_2/He, 0.70-atm ambient environment. The droplet remained in the High-Bit-Depth Multispectral (HiBMs) field of view (FOV), and there was very little motion on the fiber until very close to visible flame extinction when the droplet dislodged from the fiber. Because the flame extinguished when the droplet disrupted off of the fiber, no extinction droplet diameter is reported.

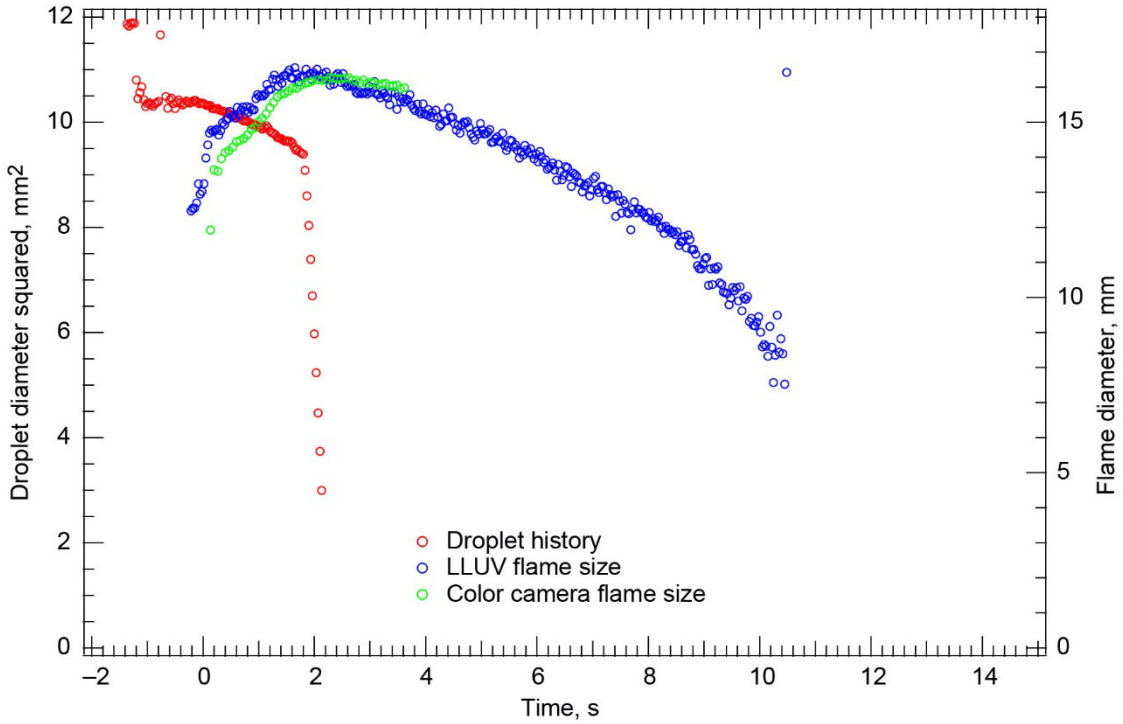

Figure 261.—Test FLEX–261. Free-floating methanol droplet in a 0.21/0.49/0.30 O_2/N_2/He, 0.70-atm ambient environment. The droplet drifted northwest in the High-Bit-Depth Multispectral (HiBMs) field of view (FOV) after deployment, hit the igniter, and then drifted quickly south after ignition. Because the droplet left the HiBMs FOV shortly after ignition, only a small portion of the droplet burning history was captured. The droplet also left the color camera FOV. Because only a short part of the burning history was captured, no extinction droplet diameter is reported and the burning rate constant is probably inaccurate.

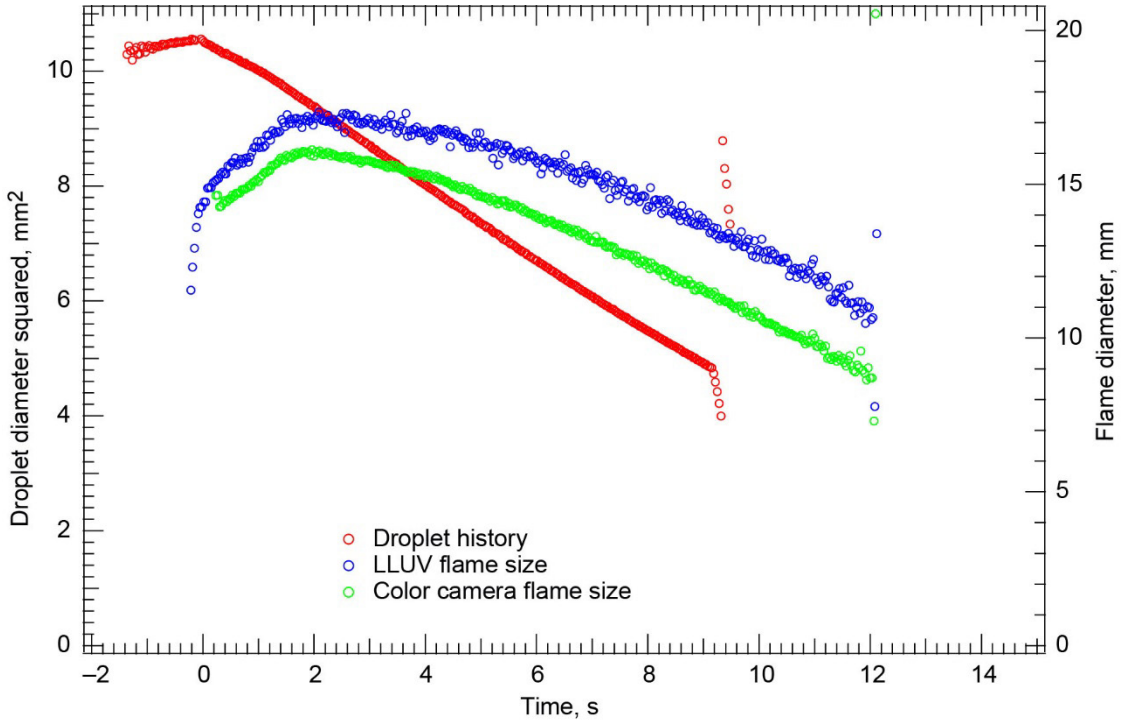

Figure 262.—Test FLEX–262. Free-floating methanol droplet in a 0.21/0.49/0.30 O_2/N_2/He, 0.70-atm ambient environment. The droplet drifted southeast in the High-Bit-Depth Multispectral (HiBMs) field of view (FOV) after deployment, hit the igniter, and then began to drift slowly northwest after ignition. The droplet left the HiBMs FOV before extinction, but most of the burning history was captured by the HiBMs. The droplet burned for a long time before the flame extinguished diffusively. The measured burning rate constant from just before the droplet left the HiBMs FOV was used to extrapolate the extinction droplet diameter from the droplet size history from the time that the droplet left the HiBMs FOV until the visible flame extinguished.

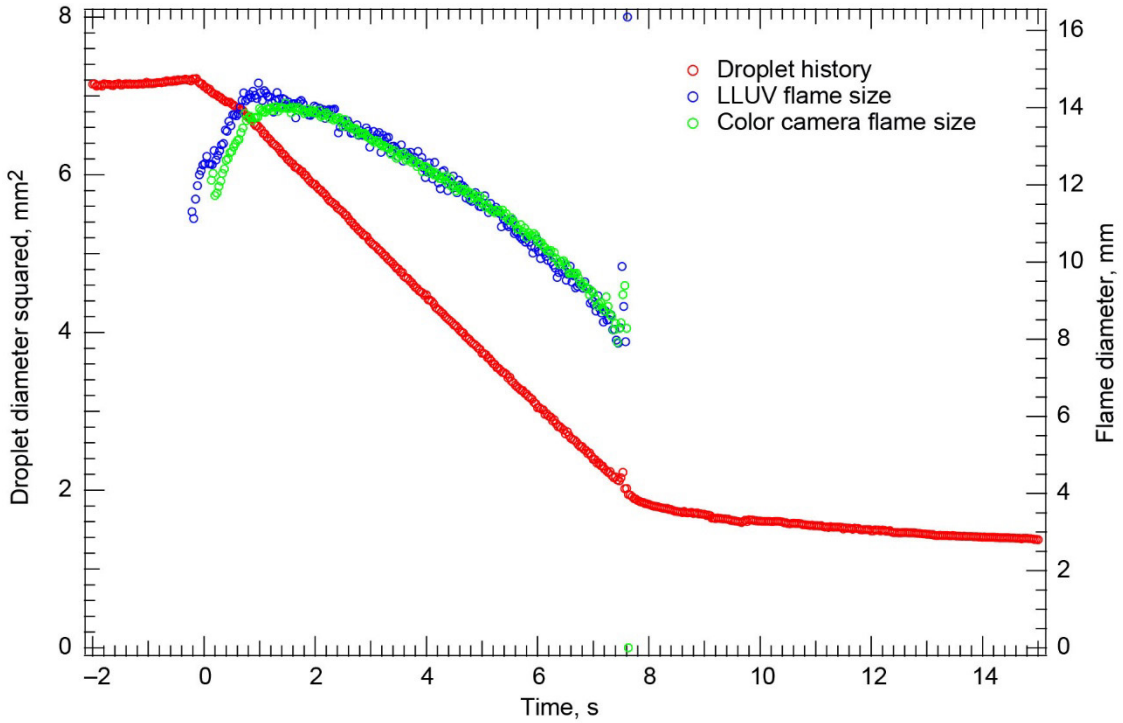

Figure 263.—Test FLEX–263. Fiber-supported methanol droplet burning in a 0.21/0.49/0.30 O_2/N_2/He, 0.70-atm ambient environment. The droplet drifted slowly east along the fiber in the High-Bit-Depth Multispectral (HiBMs) field of view (FOV) after deployment and ignition. There was a little disruptive motion on the fiber during the burning history. The flame extinguished diffusively.

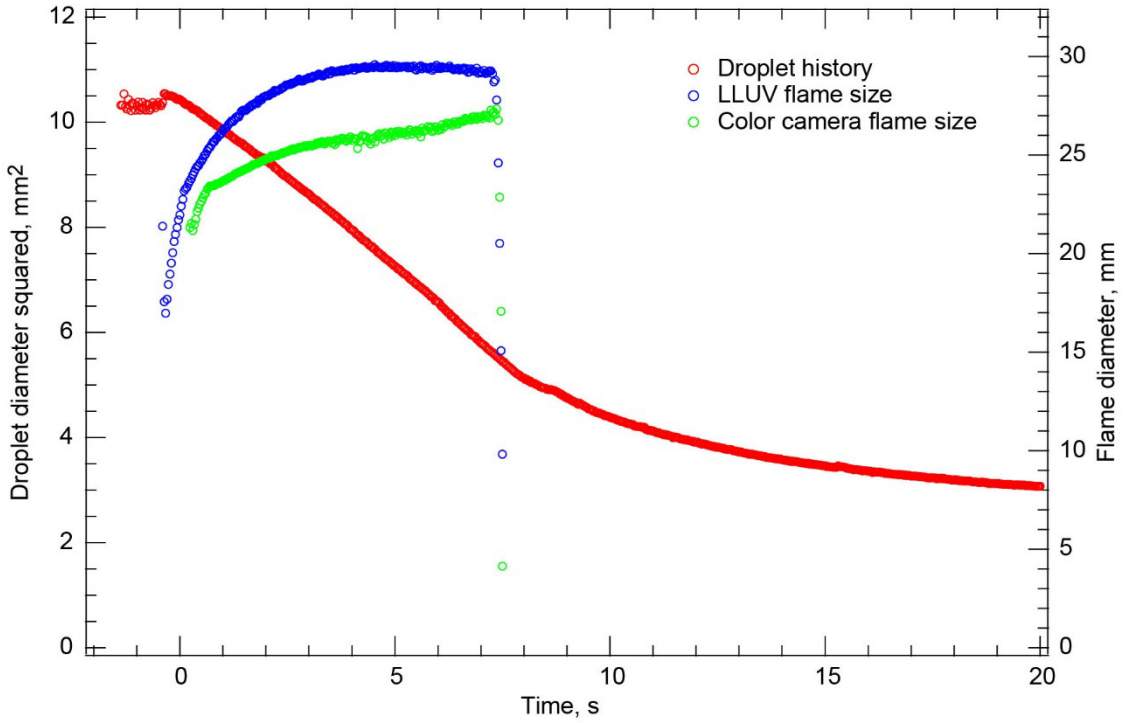

Figure 264.—Test FLEX–264. Free-floating heptane droplet in a 0.21/.0.49/0.30 O_2/N_2/He, 0.7-atm ambient environment. The droplet remained in the High-Bit-Depth Multispectral (HiBMs) field of view (FOV) for the entire test. The flame grew to a maximum size shortly after ignition, then remained at a constant size until extinction. It is not clear whether the flame extinguished diffusively or radiatively. There was no evidence of prolonged cool flame burning after the visible flame extinguished; there was no rapid vaporization after extinction and no vapor cloud formed in the color camera view.

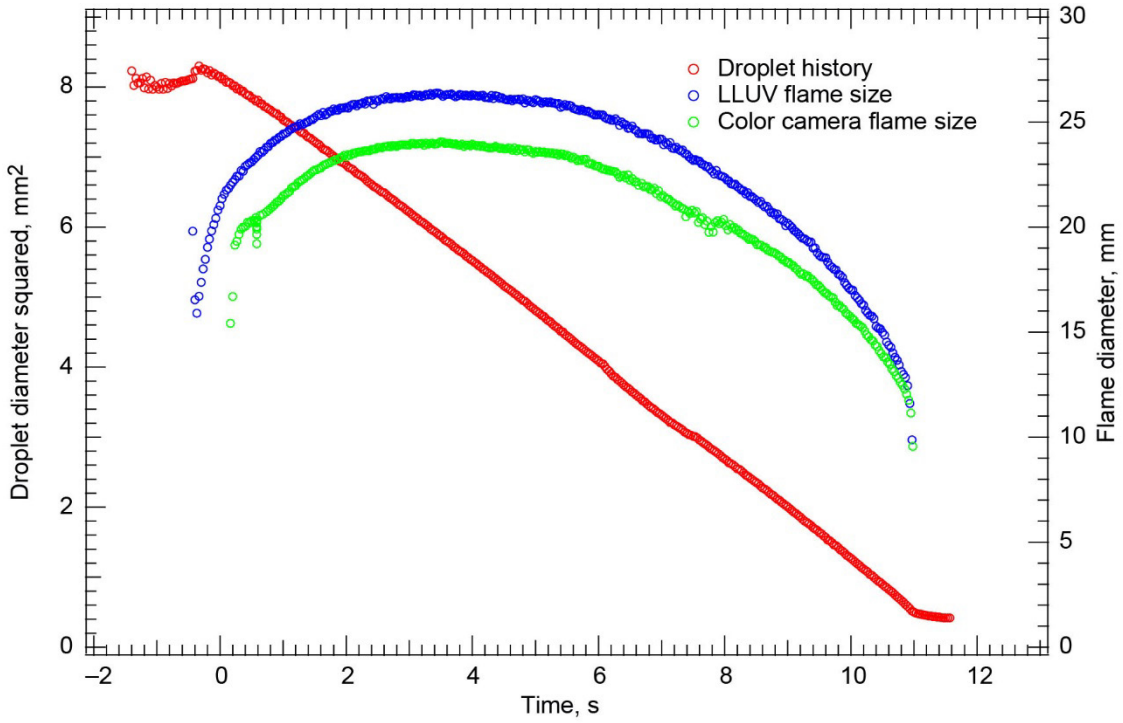

Figure 265.—Test FLEX–265. Free-floating heptane droplet burning in a 0.21/0.49/0.30 O_2/N_2/He, 0.70-atm ambient environment. The droplet remained in the fields of view (FOVs) of all the cameras for the entire test. The flame grew, reached a maximum size, and then decreased in size until it extinguished diffusively at a very small size. Shortly after extinction, the droplet appeared to disrupt and disappeared from the High-Bit-Depth Multispectral (HiBMs) FOV.

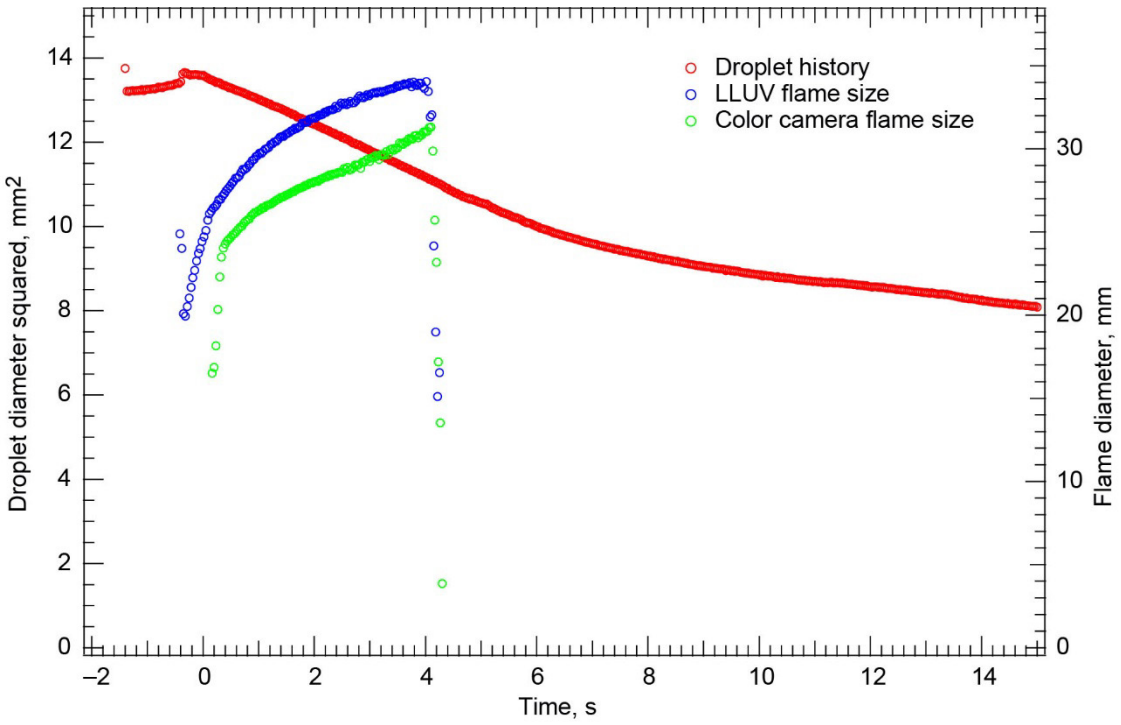

Figure 266.—Test FLEX–266. Free-floating heptane droplet burning in a 0.20/0.45/0.35 O_2/N_2/He, 0.70-atm ambient environment. The droplet remained in the High-Bit-Depth Multispectral (HiBMs) field of view (FOV) (and the FOVs of all cameras) for the entire test. The flame grew continuously after ignition, extinguishing radiatively after approximately 5 s. There appears to be no cool flame or only a very brief one—there was no significant vaporization after extinction and no vapor cloud formed in the color camera view.

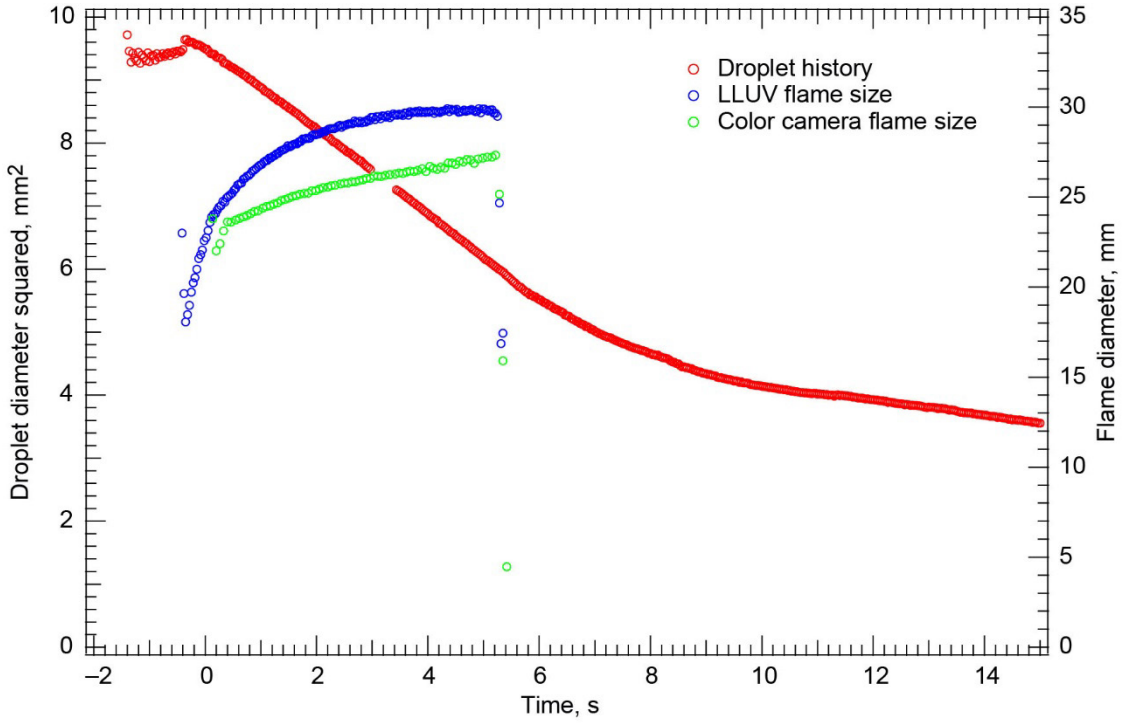

Figure 267.—Test FLEX–267. Free-floating heptane droplet burning in a 0.20/0.45/0.35 O_2/N_2/He, 0.70-atm ambient environment. The droplet remained in the High-Bit-Depth Multispectral (HiBMs) field of view (FOV) (and the FOVs of all the cameras) for the entire test. The flame grew throughout the test and became dimmer until it extinguished radiatively after approximately 5 s. There appeared to be no evidence of cool flame formation—there was no rapid vaporization after the visible flame extinguished and no vapor cloud formed in the color camera view.

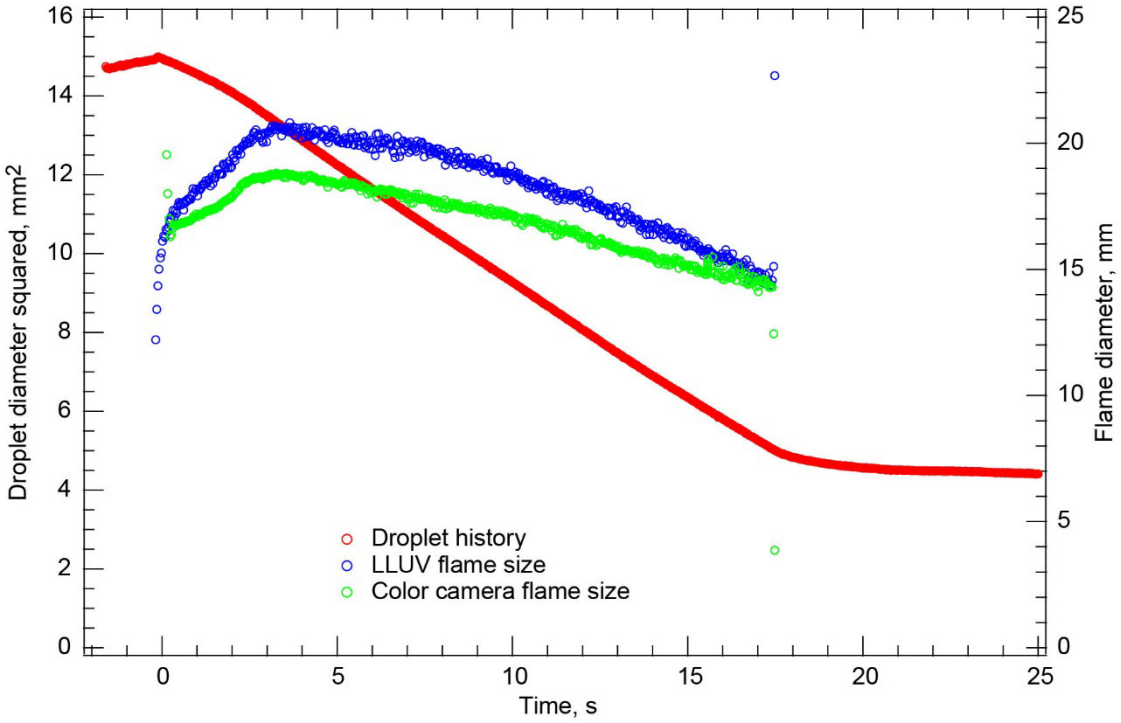

Figure 268.—Test FLEX–268. Free-floating methanol droplet burning in a 0.20/0.45/0.35 O_2/N_2/He, 0.70-atm ambient environment. The droplet drifted south in the High-Bit-Depth Multispectral (HiBMs) field of view (FOV) after deployment and ignition, but it remained in the FOV for the entire test. The flame was very dim and barely detectable in the color camera. The very long burn resulted in diffusive extinction, although the flame standoff grew throughout the test.

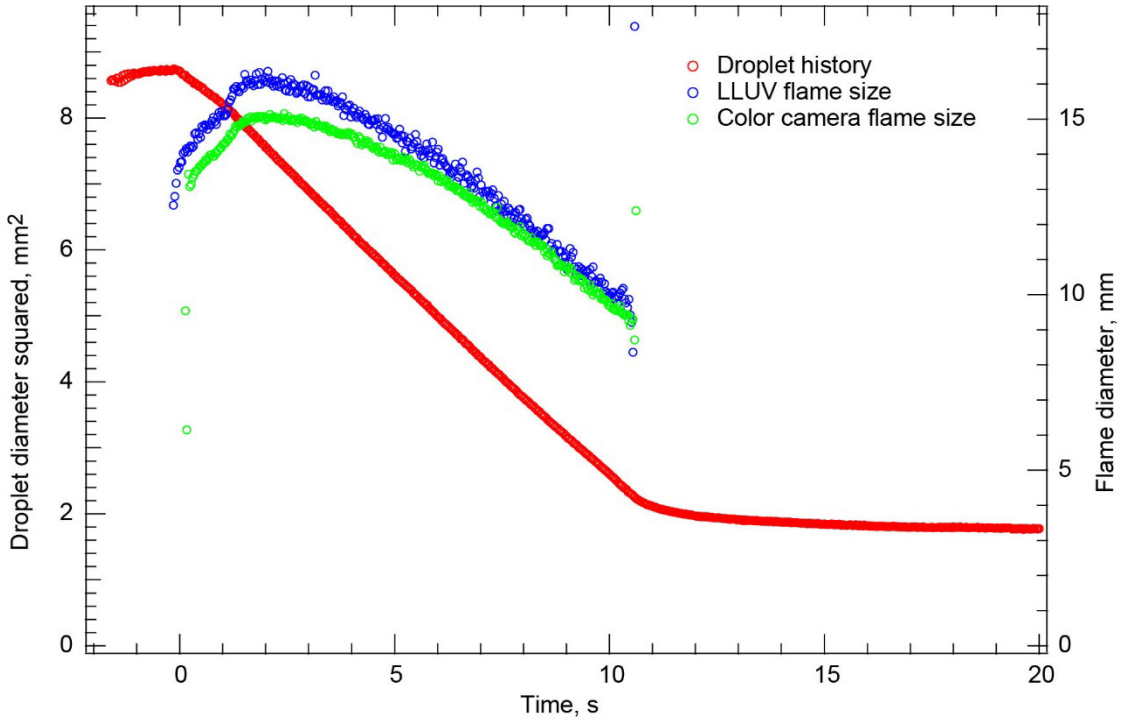

Figure 269.—Test FLEX–269. Free-floating methanol droplet burning in a 0.20/0.45/0.35 O_2/N_2/He, 0.70-atm ambient environment. The droplet was nearly motionless after deployment and ignition, and it drifted around the High-Bit-Depth Multispectral (HiBMs) field of view (FOV). However, it remained in the FOV for the entire burn and well after the visible flame extinguished.

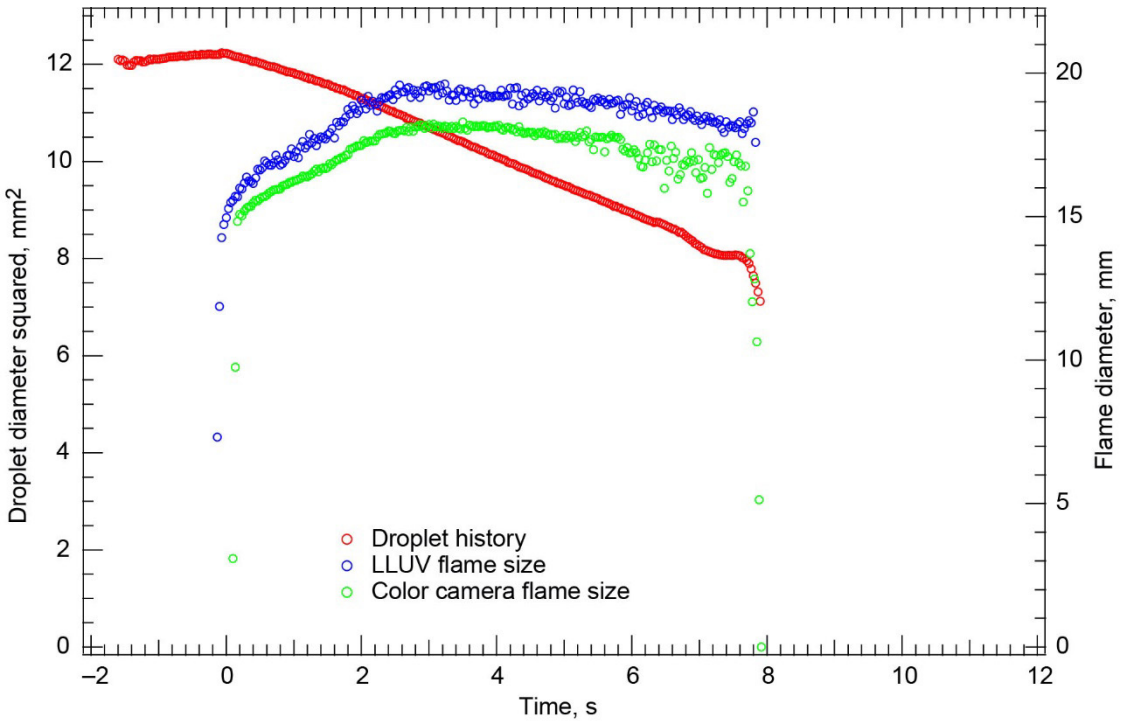

Figure 270.—Test FLEX–270. Free-floating methanol droplet burning in a 0.18/0.42/0.40 O_2/N_2/He, 0.70-atm ambient environment. The droplet drifted south in the High-Bit-Depth Multispectral (HiBMs) field of view (FOV) after deployment and ignition, leaving the FOV when the visible flame extinguished. This was a large droplet, and it probably extinguished radiatively.

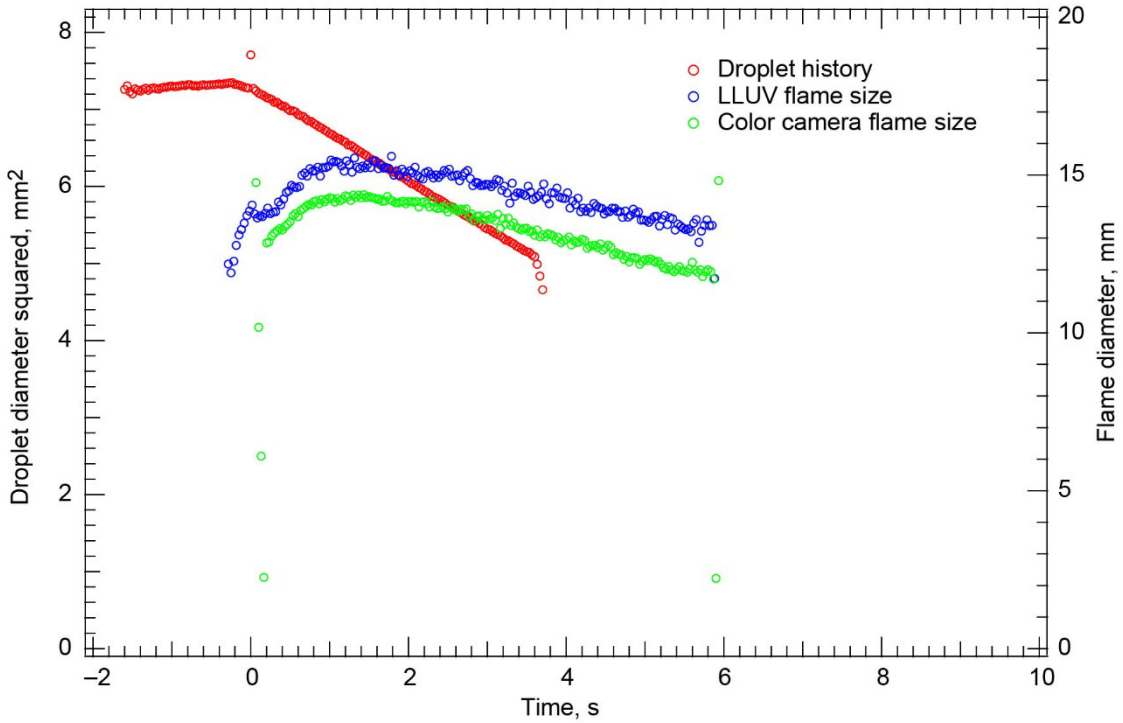

Figure 271.—Test FLEX–271. Free-floating methanol droplet burning in a 0.18/0.42/0.40 O_2/N_2/He, 0.70-atm ambient environment. The droplet drifted north in the High-Bit-Depth Multispectral (HiBMs) field of view (FOV) after deployment; then it hit the igniter and drifted east and out of the FOV before extinction. The burning rate constant measured during the later period while the droplet was in the HiBMs FOV was used to extrapolate the extinction droplet diameter from the droplet history from the time that the droplet left the HiBMs FOV until the visible flame extinguished.

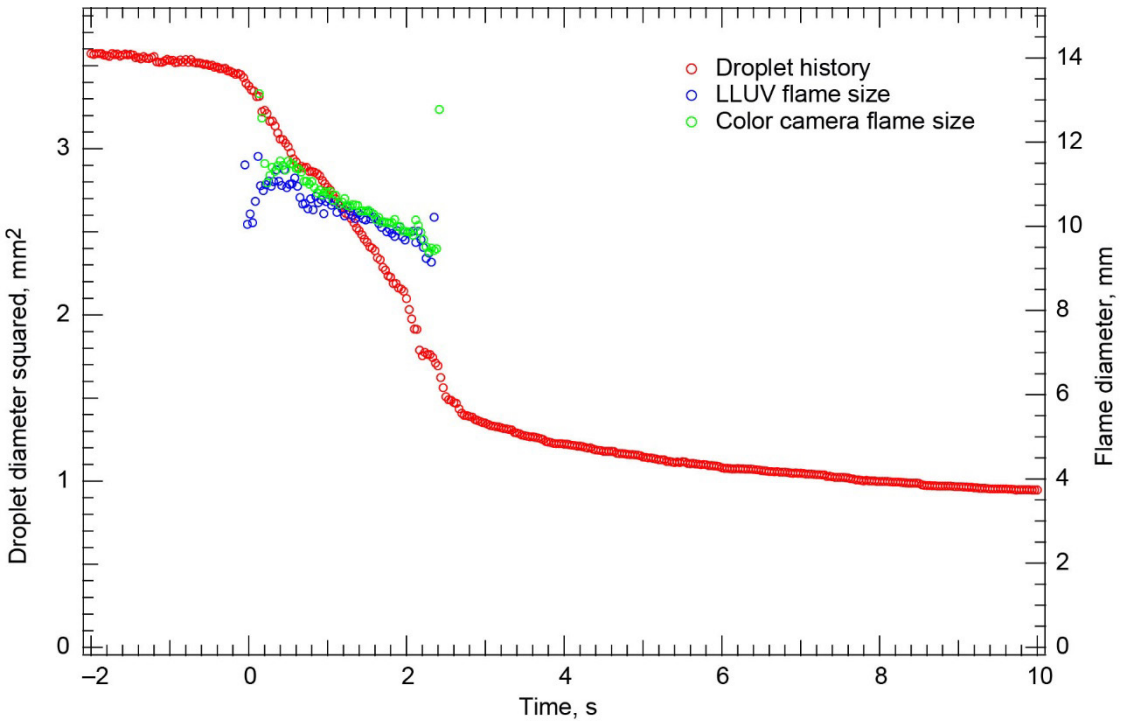

Figure 272.—Test FLEX–272. Fiber-supported methanol droplet burning in a 0.18/0.42/0.40 O_2/N_2/He, 0.70-atm ambient environment. There was almost no axial motion of the droplet relative to the fiber, but the droplet oscillated radially on the fiber, causing minor disruptions in the flame and creating some scatter in the droplet history.

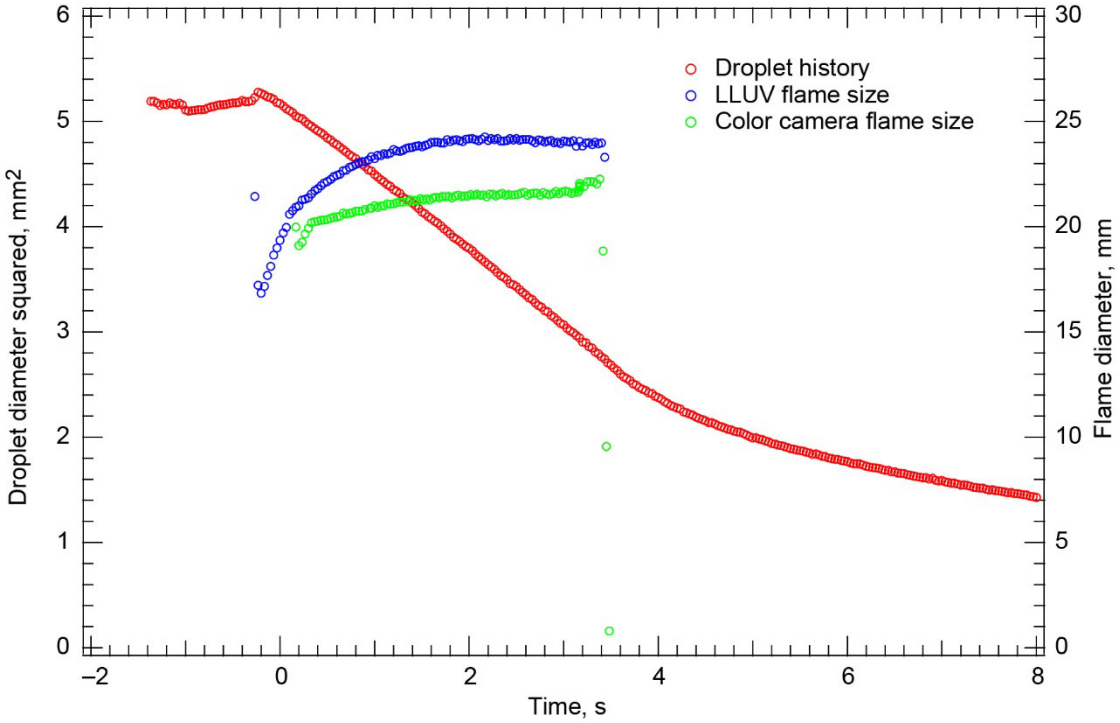

Figure 273.—Test FLEX–273. Free-floating heptane droplet burning in a 0.18/0.42/0.40 O_2/N_2/He, 0.70-atm ambient environment. The droplet drifted northeast in the High-Bit-Depth Multispectral (HiBMs) field of view (FOV) after deployment and ignition, but it remained in the FOVs of all cameras for the entire test. The droplet burned for several seconds, and the flame grew, reached a maximum size, and remained nearly constant for the entire test. The luminosity of the flame continuously decreased as the droplet burned. This was probably near the flammability limit. There was no evidence of cool flame formation (no rapid vaporization or vapor cloud formation).

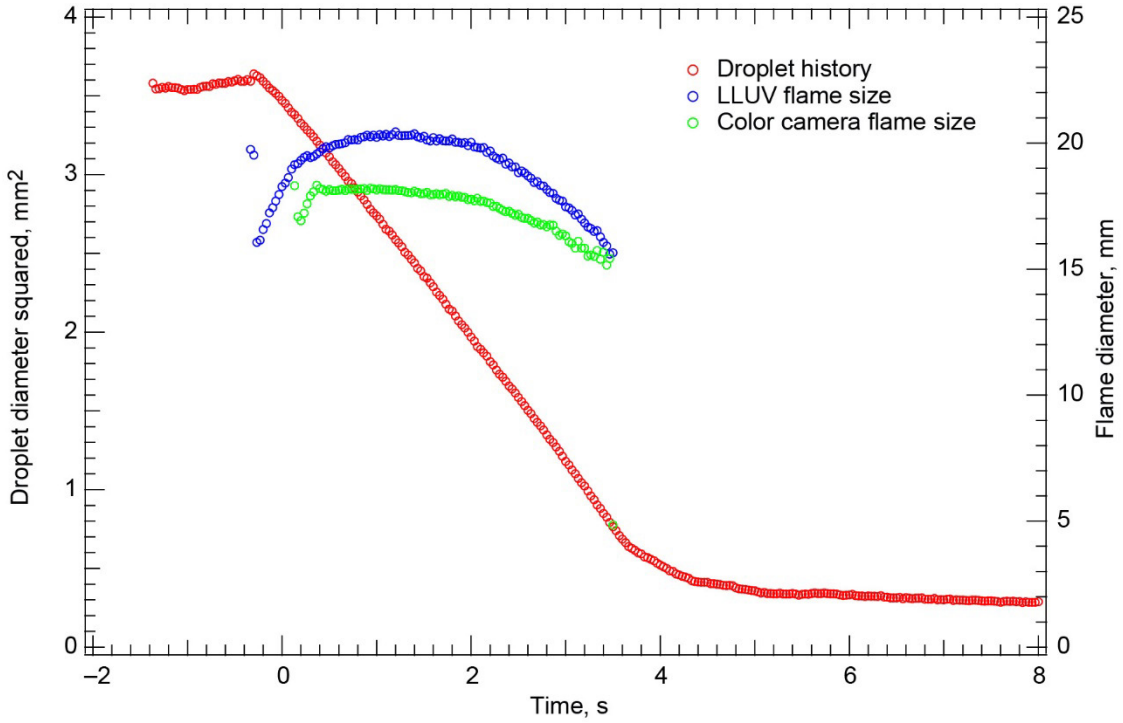

Figure 274.—Test FLEX–274. Free-floating heptane droplet burning in a 0.18/0.42/0.40 O_2/N_2/He, 0.70-atm ambient environment. The droplet drifted northeast after deployment and ignition, but it remained in the High-Bit-Depth Multispectral (HiBMs) field of view (FOV) for the entire burn and for several seconds after the flame extinguished (long enough to observe the vaporization history). The flame grew slightly and reached a maximum size one-third of the way through the burn. It then decreased in size in response to the shrinking droplet. The flame probably extinguished diffusively, but it was very close to the flammability limit. There was no evidence of a cool flame; that is, there was no rapid vaporization after the visible flame extinguished and no vapor cloud formed.

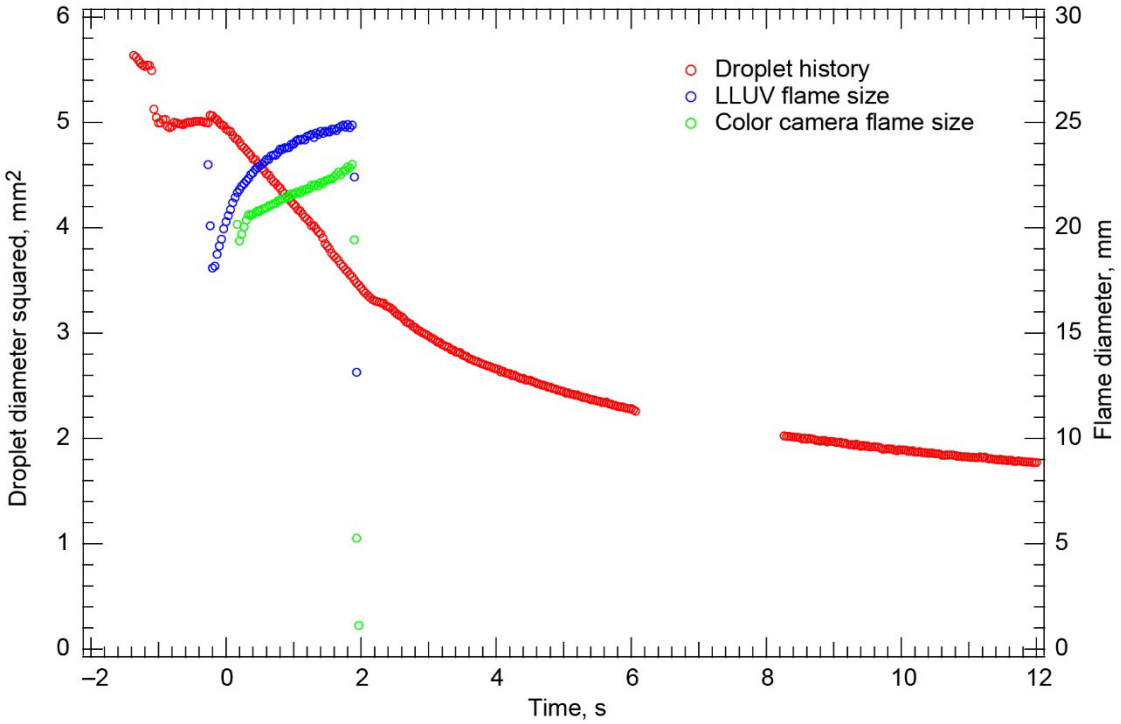

Figure 275.—Test FLEX–275. Free-floating heptane droplet burning in a 0.17/0.38/0.45 O_2/N_2/He, 0.70-atm ambient environment. The droplet drifted northeast in the High-Bit-Depth Multispectral (HiBMs) field of view (FOV), but it remained in the FOV for the entire test. Well after the flame extinguished, the droplet drifted partially out of the HiBMs FOV and then back in for the remainder of the recording time. The flame grew continuously throughout the test, getting dimmer until the flame extinguished. There was no evidence of a cool flame (continued vaporization or vapor cloud).

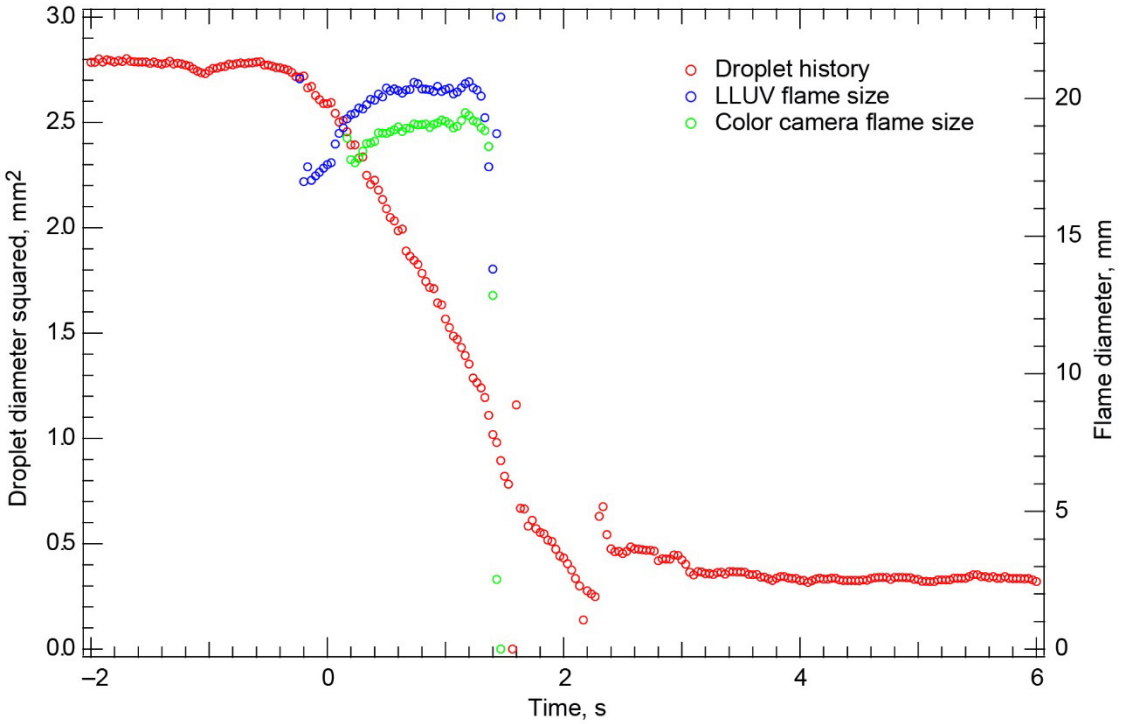

Figure 276.—Test FLEX–276. Fiber-supported heptane droplet burning in a 0.17/0.38/0.45 O_2/N_2/He, 0.70-atm ambient environment. The droplet exhibited significant axial and radial oscillations throughout the test, and the burning rate and extinction diameter data were strongly influenced by this motion. The residual droplet on the fiber had a large gas bubble that resulted in the size jump after the visible flame extinguished.

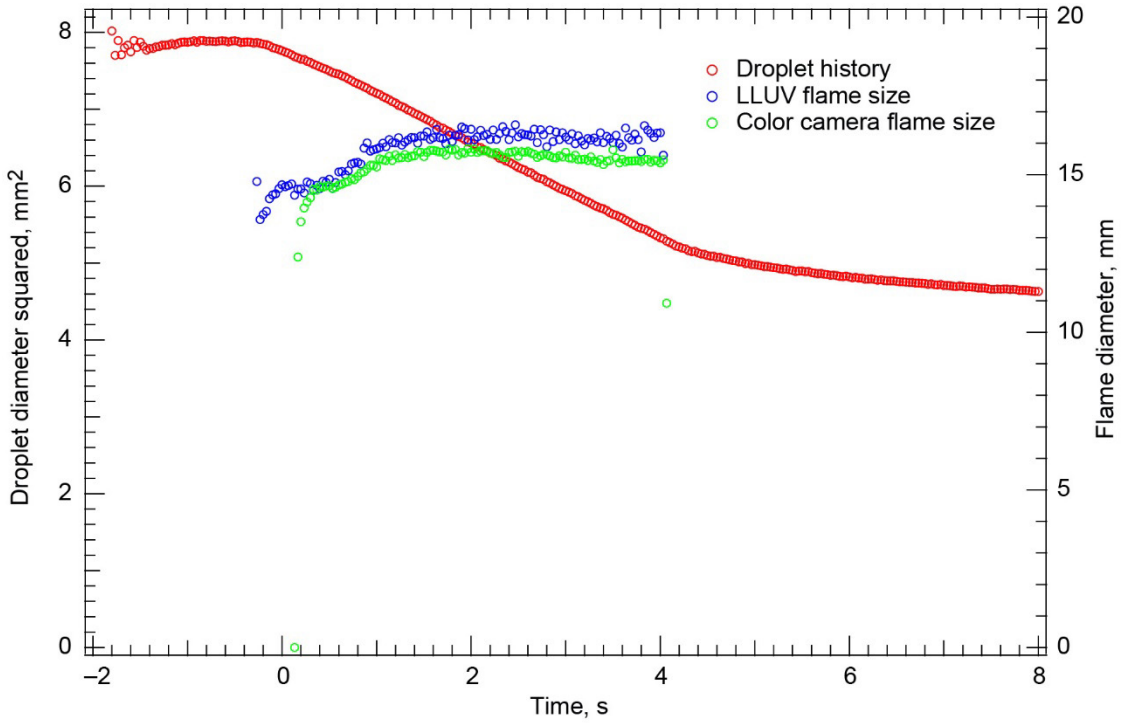

Figure 277.—Test FLEX–277. Free-floating methanol droplet burning in a 0.17/0.38/0.45 O_2/N_2/He, 0.70-atm ambient environment. The droplet drifted south in High-Bit-Depth Multispectral (HiBMs) field of view (FOV) after deployment and ignition. Well after extinction, the droplet drifted out of the FOV.

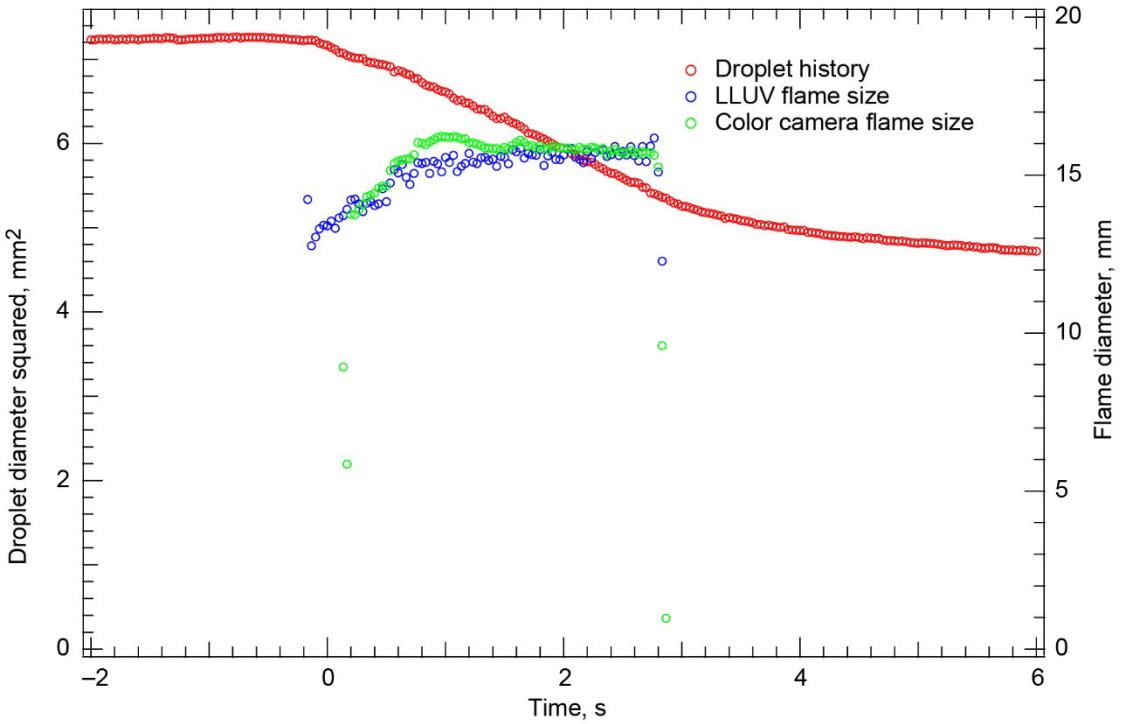

Figure 278.—Test FLEX–278. Fiber-supported methanol droplet burning in a 0.17/0.38/0.45 O_2/N_2/He, 0.70-atm ambient environment. The droplet migrated slowly west in the High-Bit-Depth Multispectral (HiBMs) field of view (FOV) after ignition, but it remained in the FOV the entire test. There was a small spot on the fiber that burned off early in the burn, which was a short burn to extinction. This was near the limiting oxygen index (LOI) in this ambient mixture.

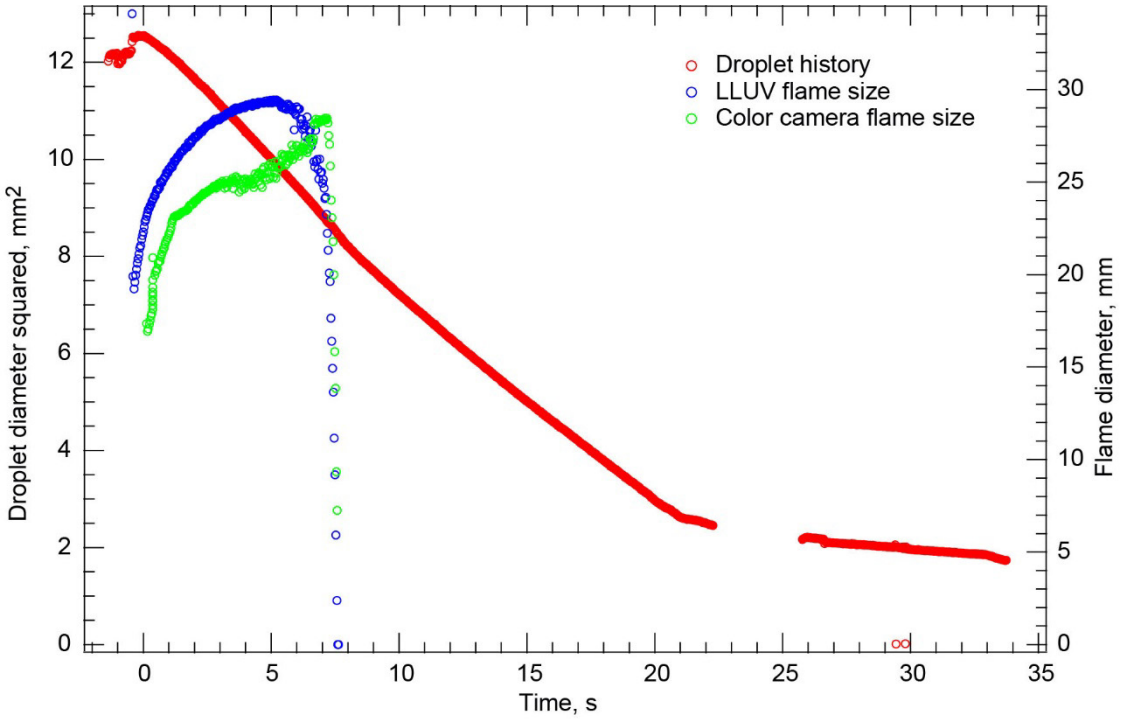

Figure 279.—Test FLEX–279. Free-floating heptane droplet burning in a 0.21/0.64/0.15 O_2/N_2/He, 1.0-atm ambient environment. The droplet remained in High-Bit-Depth Multispectral (HiBMs) field of view (FOV) for the entire test (it briefly drifted out well after the visible flame extinguished). A large vapor cloud formed at the end of the test, indicating that a cool flame probably followed visible flame extinction.

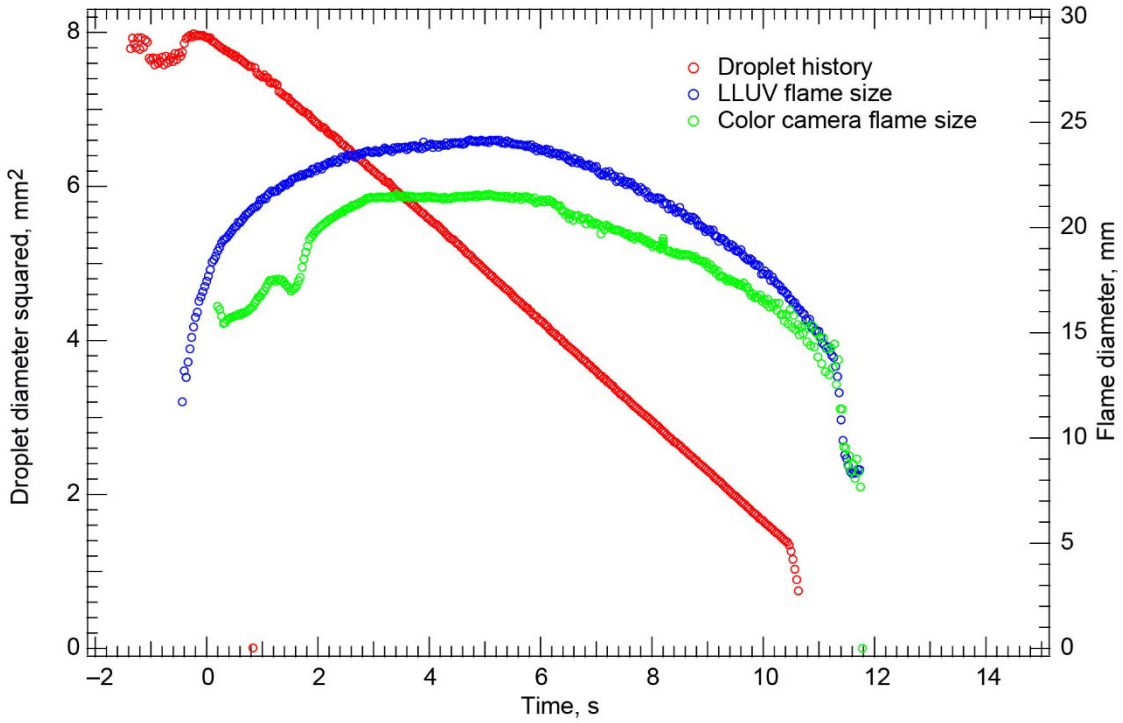

Figure 280.—Test FLEX–280. Free-floating heptane droplet burning in a 0.21/0.15/0.64 O_2/N_2/He, 1.0-atm ambient environment. The droplet drifted east in the High-Bit-Depth Multispectral (HiBMs) field of view (FOV) after deployment and ignition, and it drifted out of the FOV right before the flame extinguished diffusively. The measured burning rate constant from the last part of the burn was used to extrapolate the extinction droplet diameter from the droplet history from the time that the droplet left the FOV until the visible flame extinguished.

References

Banu, Bilkis: Fluids and Combustion Facility (FCF)—Combustion Integrated Rack (CIR). Payload Accommodations Handbook, NASA CIR–DOC–4064, 2008. Available from the NASA Center for AeroSpace Information.

Choi, M.Y.; and Dryer, F.L.: Microgravity Droplet Combustion. Microgravity Combustion: Fire in Free Fall, Howard D. Ross, ed., ch. 4, Academic Press, San Diego, CA, 2001, pp. 183–297.

Dietrich, D.L., et al.: Droplet Combustion Experiments in Spacelab. Proceedings of the 1996 26th International Symposium on Combustion, vol. 1, 1996, pp. 1201–1207.

Faeth, G.M.: Current Status of Droplet and Liquid Combustion. Prog. Energy Combust. Sci., vol. 3, no. 4, 1977, pp. 191–224.

Godsave, G.A.E.: Studies of the Combustion of Drops in a Fuel Spray: The Burning of Single Drops of Fuel. Proceedings of the Fourth Symposium (International) on Combustion, Combustion Institute, 1952, pp. 818–830.

Goldsmith, M.: Experiments on the Burning of Single Drops of Fuel. Jet Propulsion, vol. 26, no. 3, 1956, pp. 172–178.

Hall, A.R.; and Diederichsen, J.: An Experimental Study of the Burning of Single Drops of Fuel in Air at Pressures up to Twenty Atmospheres. Proceedings of the Fourth Symposium (International) on Combustion, 1953, pp. 837–846.

Kumagai, Seiichiro; and Isoda, Hiroshi: Combustion of Fuel Droplets in a Falling Chamber. Proceedings of the Sixth Symposium (International) on Combustion, 1956, pp. 726–731.

Law, C.K.: Recent Advances in Droplet Vaporization and Combustion. Progress in Energy and Combustion Science, vol. 8, no. 3, 1982, pp. 171–201.

Marchese, A.J., et al.: Hydroxyl Radical Chemiluminescence Imaging and the Structure of Microgravity Droplet Flames. Proceedings of the 1996 26th International Symposium on Combustion, 1996, pp. 1219–1226.

Nayagam, V., et al.: Microgravity n-Heptane Droplet Combustion in Oxygen-Helium Mixtures at Atmospheric Pressure. AIAA J., vol. 36, no. 8, 1998, pp. 1369–1378.

National Institutes of Health: ImageJ, Image Processing and Analysis in Java. 2011. http://rsbweb.nih.gov/ij/ Accessed Dec. 11, 2012.

Robbins, Jesse; and Shinn, Clarise: Multi-user Droplet Combustion Apparatus FLEX2. Reflight Safety Data Package, NASA MDC–DOC–1790A, Rev. A, 2010. Available from the NASA Center for AeroSpace Information.

Sirignano, William A.: Fuel Droplet Vaporization and Spray Combustion Theory. Prog. Energy Combust. Sci., vol. 9, no. 4, 1983, pp. 291–322.

Spalding, D.B.: The Combustion of Liquid Fuels. Proceedings of the Fourth Symposium (International) on Combustion, 1952, pp. 847–864.

Spalding, D.B.: Experiments on the Burning and Extinction of Liquid Fuel Spheres. Fuel, Vol. XXXII, 1953, pp. 169–185.

Suh, H.K.; Choi, M.Y.; and Ferkul, P.V.: New Observations of Sooting Behavior of Isolated Droplets of n-Heptane in Microgravity Conditions. Proceedings of the 7th U.S. National Combustion Meeting, Atlanta, GA, 2011.

Williams, Alan: Combustion of Droplets of Liquid Fuels: A Review. Combust. Flame, vol. 21, no. 1, 1973, pp. 1–31.

Williams, Forman A.: Droplet Burning. Combustion Experiments in a Zero-Gravity Laboratory, Thomas H. Cochran, ed., vol. 73, ch. 2, 1981, pp. 31–60.

Wise, Henry; and Agoston, George A.: Burning of a Liquid Droplet. Adv. Chem., ch. 10, vol. 20, 1958, pp. 116–135.